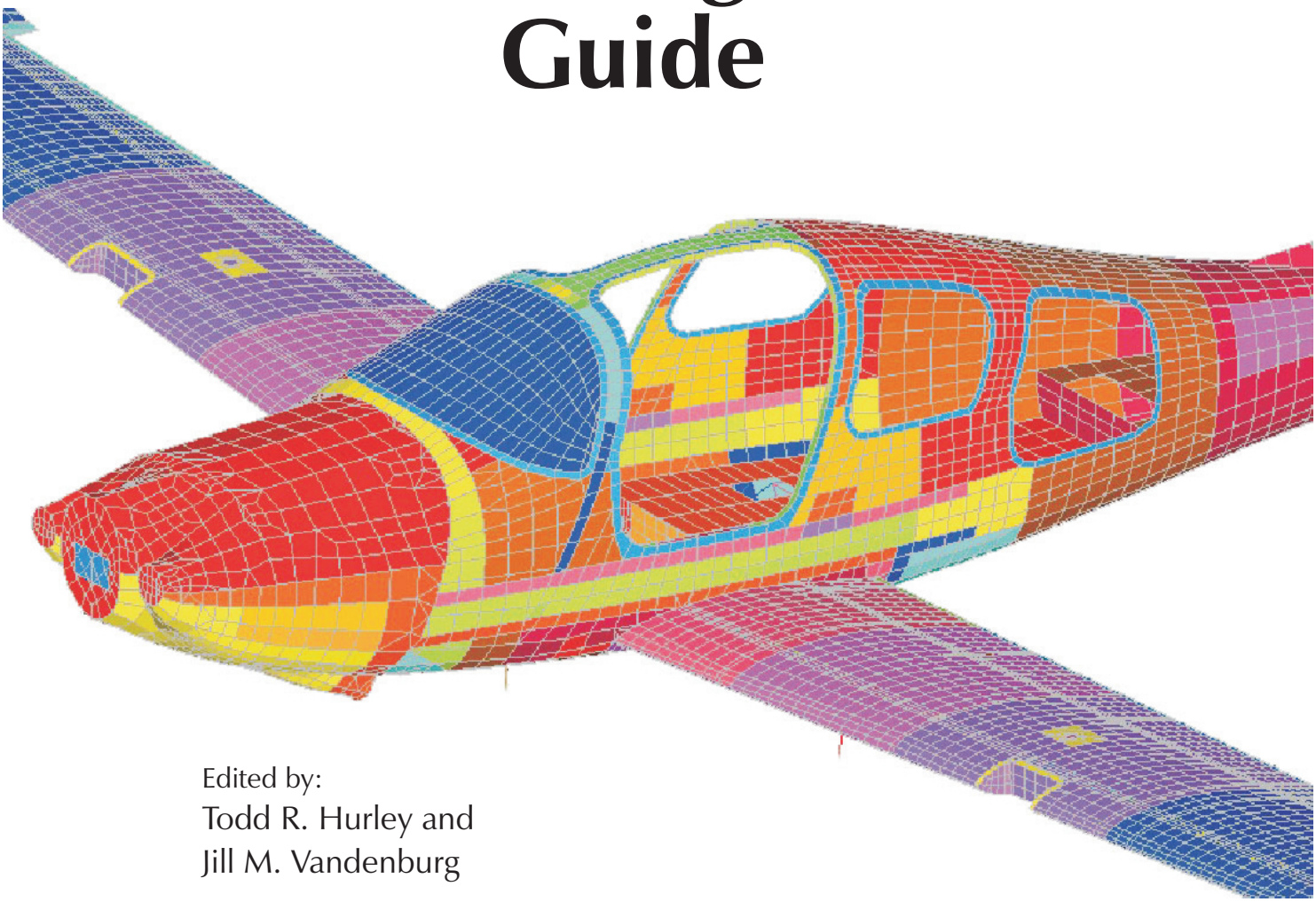
This Document Provided by the Abbott Aerospace
Technical Library
abbottaerospace.com

Small Airplane

Crashworthiness Design Guide



Edited by:
Todd R. Hurley and
Jill M. Vandenburg

SIMULA

AGATE
NASA INDUSTRY FAA
ADVANCED GENERAL AVIATION TRANSPORT EXPERIMENTS

Report Reference Number: AGATE-WP3.4-034043-036
Work Package Title: WBS3.0 Integrated Design and Manufacturing
Date of General Release: April 12, 2002

This Document Provided by the Abbott Aerospace
Technical Library
abbottaerospace.com

This Document Provided by the Abbott Aerospace
Technical Library
abbottaerospace.com

Small Airplane Crashworthiness Design Guide

Todd R. Hurley
Jill M. Vandenburg
editors

Prepared for:
The NASA Langley Research Center
General Aviation Program Office
Hampton, VA

and

The AGATE
Integrated Design and Manufacturing
Technical Council

Prepared by:
Simula Technologies, Inc.
10016 South 51st Street
Phoenix, AZ 85044

Simula Technologies Reference Number: TR-98099
AGATE Reference Number: AGATE-WP3.4-034043-036
Work Package Title: WBS 3.0 Integrated Design and Manufacturing (ID&M)
Release Date: April 12, 2002

SIMULA Technologies

AGATE
NASA INDUSTRY FAA

This Document Provided by the Abbott Aerospace
Technical Library
abbottaerospace.com

This Document Provided by the Abbott Aerospace
Technical Library
abbottaerospace.com

Acknowledgements

Many people were involved over the course of writing and editing the Small Airplane Crashworthiness Design Guide. In addition to the chapter authors, credit is due to Barbara Nadolny, who is responsible for most of the illustrations and graphics, and to Mark Ayers, the copy editor.

Special thanks are extended to S. Harry Robertson and Dr. J. W. “Doc” Turnbow for their assistance and contributions to Chapters 2 and 10, and for their permission to reprint the “Fuel System Design Checklist” and “Hazard Level Rating System” papers found in Appendices C and D, respectively.

Credit is also due to the authors, companies and organizations listed in the Reference sections of each chapter, and to the authors of the many editions of the U.S. Army Aircraft Crash Survival Design Guide, for their contributions to the field.

Simula prepared the Small Airplane Crashworthiness Design Guide for the Integrated Design and Manufacturing (ID&M) Technical Council of the Advanced General Aviation Transport Experiments (AGATE) Alliance, and for the National Aeronautics and Space Administration (NASA) Langley Research Center, Hampton, Virginia, under NASA cooperative agreements NCA1-137 and NCA1-167, for Program Years 1997 through 2001. Funding was provided by the NASA AGATE Program, the NASA Aviation Safety Program, and Simula.

This Document Provided by the Abbott Aerospace
Technical Library
abbottaerospace.com

This Document Provided by the Abbott Aerospace
TECHNICAL LIBRARY
ABBOTTAEROSPACE.COM

Table of Contents

Acknowledgements i

Foreword v

Chapter 1 - Introduction to Crashworthiness 1-1

Chapter 2 - Crash Physics 2-1

Chapter 3 - Aircraft Design Crash Impact Conditions 3-1

Chapter 4 - Biometrics 4-1

Chapter 5 - Modeling 5-1

Chapter 6 - Airframe Structural Crash Resistance 6-1

Chapter 7 - Seats 7-1

Chapter 8 - Personnel Restraint Systems 8-1

Chapter 9 - Delethalizing Aircraft Interiors 9-1

Chapter 10 - Post-Crash Factors 10-1

Appendix A - Definitions A-1

Appendix B - General Aviation Crashworthiness Design Evaluation B-1

Appendix C - Design Checklist C-1

Appendix D - Hazard level Rating System D-1

This Document Provided by the Abbott Aerospace
Technical Library
abbottaerospace.com

This Document Provided by the Abbott Aerospace
Technical Library
abbottaerospace.com

Foreword

The Small Airplane Crashworthiness Design Guide was created to assist aircraft designers in understanding the design considerations associated with the development of crashworthy General Aviation (GA) aircraft. The document was originally conceived as a condensed, single-volume version of the five-volume U.S. Army Aircraft Crash Survival Design Guide. In fact, certain sections of this work are direct excerpts from the U.S. Army Design Guide. However, the U.S. Army Design Guide focused primarily on the crashworthiness of rotorcraft and, as a result, was lacking information that related directly to the design of GA aircraft. Also, various groups, such as the Advanced Crashworthiness Group of the AGATE Alliance, have conducted many research programs on the crashworthiness of GA aircraft since the last revision of the U.S. Army Design Guide was published in 1989. Some of the information obtained from these research endeavors has been incorporated into this document along with information pertaining to the GA crashworthiness information that was missing from the U.S. Army Design Guide. The Small Airplane Crashworthiness Design Guide goes well beyond the original concept to include current state-of-the-art crashworthiness technologies applicable to civil GA aircraft.

The scope of this design guide focuses on the crashworthiness of the so-called “AGATE-class” airplane, but also covers most other light airplanes. An AGATE-class airplane was defined as an all-composite, single-engine, single-pilot, fixed-wing airplane holding 2 to 6 occupants with a maximum gross weight of 6,000 lb. While “all-composite” was part of the AGATE definition, this work also includes guidance for small airplanes constructed of other materials. The principles and guidance are also appropriate for larger airplanes up to the size covered by Part 23 of the Federal Aviation Regulations (14 CFR Part 23). The terms “small airplane” and “light airplane” are used interchangeably throughout and are meant to describe all airplanes that fit the scope of the document.

The Small Airplane Crashworthiness Design Guide is divided into 10 chapters and 4 appendices. The first five chapters lay the foundation of aircraft crashworthiness. Chapter 1 introduces the principles of crashworthiness and briefly discusses the history of occupant protection in small airplanes. Chapter 2 is a brief review of the physics involved in impact dynamics. The physical principles of deceleration distance and the absorption of kinetic energy by performing work presented in Chapter 2 are fundamental to successful crashworthy designs. Chapter 3 presents design impact conditions, both the regulatory seat test conditions and the AGATE-developed whole-airplane conditions. Chapter 4 covers the human aspects of crashworthiness design including discussions on human anthropometry, occupant motion and flail envelopes, injury tolerance criteria, and anthropometric test devices (ATD’s) or crash test dummies. Finally, Chapter 5 outlines some of the general computer modeling practices that are used to simulate the response of the occupant and aircraft structure in crash events.

The next five chapters, Chapters 6 through 10, address the crashworthiness of specific areas of the airplane. Chapter 6 covers the structural aspects of crashworthy design. The chapter begins with a description of the general requirements and considerations for structural design. The chapter then proceeds to define more detailed design considerations for strength, controlled crush, analysis, and testing of the airframe. Chapter 6 also presents a simplified analysis to estimate firewall crash loads that was used by the AGATE Advanced Crashworthiness Group in the design of a small airplane full-scale test article crash tested at NASA Langley in July of 2001. Chapter 7 provides design specifications for aircraft seating

This Document Provided by the Abbott Aerospace
Technical Library
abbottaerospace.com

systems, which are the last line of protection for the occupant in crashes with a severe vertical component. Chapter 8 describes conventional occupant restraints and how to design their installation into the aircraft. This chapter goes on to describe more advanced restraint concepts including inflatable systems such as air bags and air belts. Chapter 9 outlines several techniques for designing the interior of the aircraft to minimize secondary impact injuries. Finally, Chapter 10 focuses on design methodologies used to prevent post-crash fire and to facilitate occupant egress following a crash.

Appendix A provides definitions of crashworthiness and crash survival terminology. Appendix B presents a GA crashworthiness design evaluation tool first used at the AGATE Small Airplane Crashworthiness Design Seminar held in October of 2000. This evaluation can be used as a design checklist, used during design trade studies to compare one concept to another, and/or used to evaluate the crashworthiness of existing designs. Appendices C and D are reprints of papers that contain detailed evaluation checklists for the crashworthiness of fuel systems.

One major difference of this work from the U.S. Army Design Guide is the inclusion of guidance pertaining to the regulations. Where possible, this guidance comes from the real-world crashworthiness certification experience of the members of the AGATE Advanced Crashworthiness Group. While the guidance is considered to be accurate, nothing in the Small Airplane Crashworthiness Design Guide supercedes applicable laws and regulations unless a specific exemption has been obtained from the appropriate regulatory agency. For consistency, we have chosen the abbreviation 14 CFR Part 23, or sometimes just 14 CFR 23, to indicate the Code of Federal Regulations, Title 14 Part 23, "Airworthiness Standards: Normal, Utility, Acrobatic, and Commuter Category Airplanes". This is synonymous with the Federal Aviation Regulations, or FAR, Part 23. Other Federal regulations are abbreviated in the same way.

The Small Airplane Crashworthiness Design Guide is intended to be the first, best source of information on crashworthiness design of light airplanes. The information that is provided in this document represents the current knowledge for aircraft design in this field. It is our hope that this research will continue and be incorporated in future revisions of the document.

Todd R. Hurley and Jill M. Vandenburg, Editors

December 2001

THIS DOCUMENT PROVIDED BY THE ABBOTT AEROSPACE
TECHNICAL LIBRARY
ABBOTTAEROSPACE.COM

Chapter 1

Introduction to Crashworthiness

Todd R. Hurley
Jill M. Vandenburg
Lance C. Labun

In a 1995 aircraft market survey, analysts discovered that safety was the primary concern among pilots and passengers of General Aviation (GA) aircraft (Reference 1-1). For pilots, the level of safety offered by the aircraft was said to be the primary decision factor when purchasing a light airplane. For potential pilots (the "latent market" for airplanes and flight services), a lack of safety was the primary reason for not piloting light airplanes. And for potential passengers, a lack of safety was the primary reason for not wanting to travel in light airplanes.

The respondents of this survey were not given a definition of the term safety; they were allowed used their own definition in formulating their response. Even though there were probably nearly as many concepts of what defines safety as there were people surveyed, safety can be broadly categorized into two areas. The first is the control and minimization of the factors that cause accidents, or accident prevention. The second area is the control and minimization of the factors that cause injury once an accident occurs, or injury mitigation. Designing for crashworthiness addresses this second category of safety.

Customer concern over the safety of GA aircraft is somewhat warranted. Although declining, the accident rate of GA aircraft remains relatively high (Table 1-1) and the average number of GA-accident-related fatalities remain significantly higher than other forms of air transportation (Table 1-2).

Table 1-1.
U.S. General Aviation safety data (References 1-2 and 1-3)

	1975	1980	1985	1990	1995	2000[c]
Total accidents[a]	3,995	3,590	2,739	2,215	2,053	1,835
Total fatal accidents	633	618	498	443	412	341
Total fatalities	1,252	1,239	956	767	734	592
Total seriously injured persons	769	681	483	402	395	N/A
Flight hours (in thousands)[b]	28,799	36,402	28,322	28,510	24,906	30,800

[a] Since April of 1995, the National Transportation Safety Board (NTSB) has been required by law to investigate all public-use accidents, thereby increasing the number of NTSB-reported GA accidents by approximately 1.75 pct.
[b] Flight hours are estimated by the Federal Aviation Administration.
[c] Data is preliminary.
N/A - not available.
Note: Not all data is available for 2000.

This Document Provided by the Abbott Aerospace
TECHNICAL LIBRARY
ABBOTTAEROSPACE.COM

Table 1-2. Average annual U.S. aviation fatalities 1990-1999 (Reference 1-2)		
Mode	**Fatalities**	**Percentage of Total**
General Aviation	713	80
Commercial transport	94	11
Commuter	26	3
Air taxis	54	6
TOTAL	887	

Aviation, as a whole, has historically devoted much more energy to accident prevention. While this approach has been very effective in the commercial and business jet aviation sectors, accident prevention has not been as successful in GA. Based on the number of flight hours, GA has an accident rate approximately 20 times that of the scheduled airlines (Table 1-3, Reference 1-2).

Table 1-3.
Accidents, fatalities, and rates, 2000 preliminary statistics for U.S. Aviation (Reference 1-2)

	Accidents		**Fatalities**			**Accidents per 100,000 Flight Hours**	
	All	**Fatal**	**Total**	**Aboard**	**Flight Hours**	**All**	**Fatal**
U.S. air carriers operating under 14 CFR 121							
Scheduled	49	3	92	92	17,170,000	0.285	0.017
Nonscheduled	5	-	-	-	870,000	0.575	-
U.S. air carriers operating under 14 CFR 135							
Scheduled	12	1	5	5	550,000	2.182	0.182
Nonscheduled	80	22	71	68	2,430,000	3.29	0.91
U.S. General Aviation	1,835	341	592	582	30,800,000	5.96	1.11
U.S. civil aviation	1,975	365	748	747			

Notes: All data are preliminary.
Flight hours and departures are compiled and estimated by the Federal Aviation Administration (FAA).
Accidents and fatalities in the categories do not necessarily sum to the figures in U.S. civil aviation because of collisions involving aircraft in different categories.

If GA is to grow significantly and become the alternative to the hub and spoke air transportation system that the National Aeronautics and Space Administration (NASA) envisions, perceived and real safety must improve. The latent market (people interested in GA, but not currently using it) will not participate without a stronger perception of safety. The general public has come to expect crash safety in their cars, and will likely demand the same from light airplanes. Furthermore, crash safety at aviation velocities has been demonstrated in racecars and in small airplane and helicopter full-scale tests. While many of the improvements in overall safety should come from accident prevention through such areas as enhancements in the airspace

This Document Provided by the Abbott Aerospace
TECHNICAL LIBRARY
ABBOTTAEROSPACE.COM

infrastructure, flight systems, training, etc., the automotive experience has shown that privately owned and operated vehicles will continue to crash. A zero accident rate is not likely. The automotive industry has accepted this reality and designed crashworthiness into its cars, and consequently thousands of lives are saved each year. By designing crashworthiness into light airplanes, GA can see similar results.

1.1 Principles of Crashworthiness

The concept of crashworthiness refers to those vehicle design characteristics that protect the occupant from injury or death during a crash event. Specifically, the designer strives to (1) eliminate injuries and fatalities in relatively mild impacts, (2) minimize injuries and fatalities in all severe but survivable crashes, and (3) minimize the damage to the aircraft structure in all crash events (Reference 1-4). The fundamental principles of crashworthiness can be described using the acronym CREEP (Reference 1-5):

- **C**ontainer (fuselage structure)
- **R**estraint (restraint system, seats, and attachments)
- **E**nergy Management (seats, restraints, fuselage, and engine mounts)
- **E**nvironment (items within the occupants' strike zone)
- **P**ost-crash Factors (fuel system, fire, and egress)

The most critical consideration for crashworthiness concerns the container, or the occupant compartment. A strong, enclosed container must be maintained around the occupants in order to create a survivable volume. Protection provided by the other four principles is of no value if the cabin volume is compromised.

Restraining the occupants within the container is the next-most-important consideration. The key issues in restraint design are the placement of the restraints and the attachment strength. The restraints should transfer the inertial loads from the occupants out through the body's strong skeletal structure rather than through soft tissue or vital organs. Restraints are also used to control the occupant's motion to prevent striking the interior of the airplane, or to allow interaction with secondary restraints such as airbags.

Controlling the peak decelerations and maximum forces applied during the crash is perhaps the most sophisticated and complex aspect of crashworthy design. Energy-absorbing technologies incorporated into the fuselage structure, landing gear, seats, and restraints can be used to effectively control these decelerations and forces.

Proper design of the cabin interior is required to minimize occupant injury. From an aircraft designer's perspective, the risk of injury can be reduced by understanding the types of injury mechanisms that can occur, limiting the size of the occupant's flail envelope, and eliminating, relocating, or delethalizing all potential strike hazards.

The final task is to minimize the post-crash hazards and ensure safe egress for the occupants. This requires the prevention of post-crash fire and the accessibility of functional egress pathways and exits. Fire prevention can be achieved by eliminating the spillage of flammable fluids and by controlling hazardous ignition sources. Exits should be clearly identified, accessible in a rolled and/or deformed aircraft, easy to use, and reliable.

Substantially increasing the level of crashworthiness offered by GA aircraft requires addressing all five principles as a system. Using a "systems approach" to crashworthiness design offers the maximum level of protection to the occupants. In a systems approach, the designer ensures that all of the separate safety systems in the aircraft work together to absorb the aircraft's kinetic energy and to decelerate the occupants to rest without causing injurious loading. This is

This Document Provided by the Abbott Aerospace
Technical Library
abbottaerospace.com

accomplished by designing individual crashworthy components and then evaluating the performance of these components as a whole system. Continual evaluation and design iteration of the components occurs until the desired level of safety performance of the whole system is achieved.

For example, the landing gear, aircraft structure, and occupant seats must all be designed to work together as a vertical-energy-management system to absorb kinetic energy and slow the occupant to rest without injuries (Reference 1-6). Figure 1-1 depicts these three contributors to energy absorption in a fixed-wing aircraft. The landing gear is capable of absorbing energy to reduce the impact velocity to the fuselage. The subfloor structure provides additional deceleration distance. The seat completes the energy-management system by helping to protect the occupant from high decelerations and absorbing energy during the crushing process. By absorbing energy with the landing gear and subfloor structure, the occupant compartment is protected from excessive loads, so that the survivable volume is maintained. The occupant compartment structure also does not have to be as heavy as it would need to be and still maintain survivable space without these energy-absorbing mechanisms. Furthermore, by optimizing the location of energy-absorbing structures in the subfloor area of composite airframes, the loads transmitted to the stroking seat, occupant, and airframe can be minimized, which helps reduce occupant injury and structural damage. This type of systems approach to crashworthy design can easily be incorporated into the design process for GA aircraft.

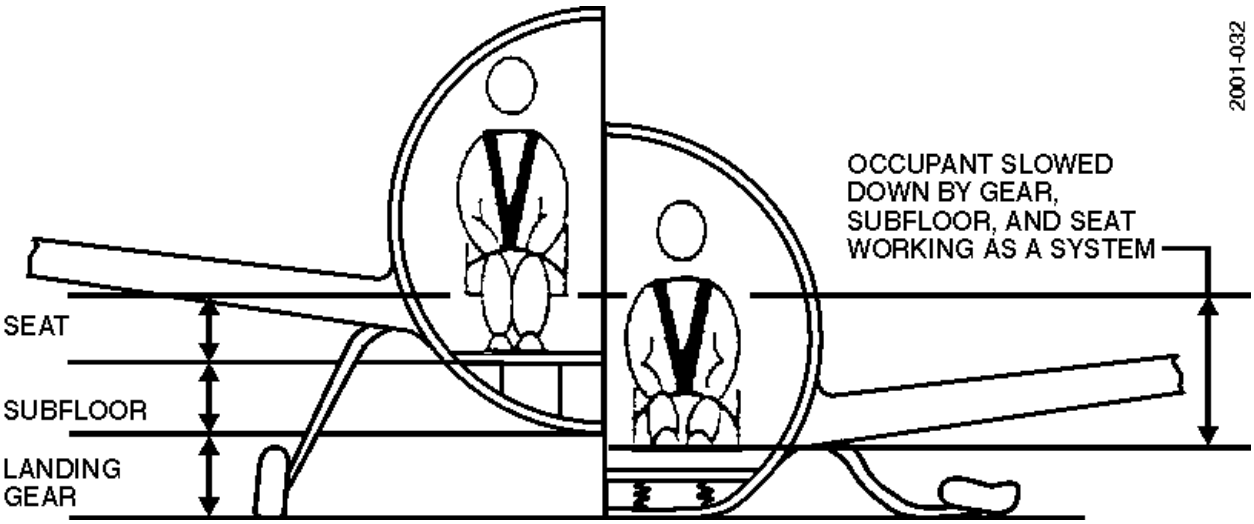


Figure 1-1.
Energy management system for a typical airplane (adapted from Reference 1-6).

It is important to note that the majority of the critical crashworthy design considerations are inherent to the general layout and structure of the aircraft. As a result, a designer must integrate crashworthiness technologies into the design from the inception of the aircraft. This Design Guide will provide the tools to achieve such a design.

This Document Provided by the Abbott Aerospace
TECHNICAL LIBRARY
ABBOTTAEROSPACE.COM

1.2 Development of Light Airplane Crashworthiness

Hugh DeHaven

Some of the most significant work in the area of aviation crashworthiness and occupant survivability began in the 1920's with the research efforts of Hugh DeHaven (Reference 1-7). Deemed the "father of aviation crashworthiness," DeHaven's interest in aircraft impact survival began shortly after his own brush with death in 1917. While training to be a pilot for the Canadian Royal Flying Corps during World War I, DeHaven's aircraft was involved in a mid-air collision during a training exercise. DeHaven suffered multiple limb fractures, as well as ruptures of the spleen, liver, and pancreas. Despite his near-fatal injuries, De-Haven was the only person out of both airplanes to survive the accident.

After a 6-month recovery period, he went to work as an accident investigator with the aim of understanding how and why people were injured during traumatic events including crashes and falls. His research efforts and conclusions caught the attention of the National Research Council and the Office of Naval Research. These two organizations provided funding for DeHaven to continue his research investigations at the Cornell University Medical College. The funding allowed for the establishment of the Crash Injury Research (CIR) program, which was officially established as the Aviation Crash Injury Research (AvCIR) program in 1950.

One of DeHaven's most significant achievements was his application of freight shipping principles to aircraft crashworthiness. Recognizing that delicate cargo could be transported and delivered undamaged, DeHaven surmised that the same principles used to protect cargo could be used to protect people in aircraft. He developed the "Four Principles of Packaging for Accident Survival" and first published his theories in a 1952 Society of Automotive Engineers (SAE) paper entitled *Accident Survival – Airplane and Passenger Car* (Reference 1-8). His four principles were as follows:

1. "The package should not open up and spill its contents and should not collapse under expected conditions of force and thereby expose objects inside it to damage."
2. "The packaging structures which shield the inner container must not be made of brittle or frail materials; they should resist force by yielding and absorbing energy applied to the outer container so as to cushion and distribute impact forces and thereby protect the inner container."
3. "Articles contained in the package should be held and immobilized inside the outer structure by what packaging engineers call interior packaging. This interior packaging is an extremely important part of the overall design, for it prevents movement and resultant damage from impact against the inside of the package itself."
4. "The means for holding an object inside a shipping container must transmit the forces applied to the container to the strongest parts of the contained objects."

In this analogy, the container represents the occupant compartment, the interior packaging represents the seat and restraint system, and the objects contained in the package represent the occupants. Over the years, these fundamental crashworthiness principles have been described in many different ways. For example, one particular description, identified by the acronym CREEP, was described in Section 1.1. Although each of these definitions is slightly different, the same core principles are always represented.

Ag-1 Aircraft

In the late 1940's and early 1950's, Fred Weick at Texas A & M designed and built the first airplane using DeHaven's recommendations (Reference 1-7). The Ag-1 agricultural (crop-duster) aircraft was designed with a 40-G cockpit structure, provided a large amount of energy-absorbing structure in front of the pilot, and located the pilot as far aft as possible. The structures in front of the cockpit, specifically the engine mount and agricultural chemical hopper,

This Document Provided by the Abbott Aerospace
TECHNICAL LIBRARY
ABBOTTAEROSPACE.COM

were designed to be weaker than the occupant compartment and fail progressively. The cockpit structure was composed of a tubular steel structure surrounding the pilot with a roll cage positioned above to offer extra protection in the event that the aircraft inverted during an impact. In addition to the reinforced cockpit structure, the aircraft incorporated a military-style seat belt and shoulder harness. The restraint system included inertia reels, which locked automatically under 3-G loads. Most so-called "modern," purpose-built agricultural application airplanes—the Piper Pawnee, Cessna AgWagon, Grumman AgCat, and Rockwell/Ayres Thrush, to name a few—all used the same basic layout and crashworthy design as the Ag-1 (Reference 1-9). The design appeared to have worked quite well; the only Ag-1 prototype built actually crashed and the pilot walked away with only minor injuries. In addition, a study of agricultural plane accidents by Swearingen showed that this class of airplanes generally does a good job of protecting the pilots in the event of a crash (Reference 1-10).

Beechcraft Bonanza

With the design of the Bonanza aircraft in the early 1950's, the Beechcraft Company was the first major aircraft manufacturer to integrate crashworthiness directly into the design of an aircraft (Reference 1-7). The design incorporated a long nose section to allow gradual impact deceleration of the occupants. It possessed a reinforced keel section in the fuselage, as well as a reinforced cockpit area to provide a "cocoon" around the occupants. The structure was designed not only to provide a strong, protective envelope, but the strong floor consisted of longerons (longitudinal beams) to encourage sliding over the impact surface rather than digging into it (Reference 1-11). Although very rigid, the structure was not designed to be energy absorbing. The wing design of the Bonanza was intended to attenuate energy during an impact and the seats in the aircraft were hard-mounted to the spar truss (Reference 1-7). The aircraft also incorporated a breakaway instrument panel and yoke to reduce occupant head trauma. Interestingly enough, torso restraints (in the form of three-point restraints) were offered as an option on this aircraft, but were later discontinued due to lack of customer interest (Reference 1-11). Shoulder restraints were not required by regulation in light airplanes until the late 1970's.

The Bonanza aircraft was truly ahead of its time (Reference 1-7). Beechcraft's marketing campaign highlighted the "survivability" features of the aircraft. However, in the mind of the consumer of the 1950's, advertising survivability admitted that aircraft crashes were possible. This marketing approach was a huge failure, since the GA community was not ready to hear about anything suggesting the possibility that an airplane might crash.

Helioplane Courier (HelioCourier)

In the early 1950's, another aircraft, the Helioplane Courier (HelioCourier), was designed based on the recommendations of the Crash Injury Research program (Reference 1-7). The HelioCourier incorporated a tubular-steel frame, which was designed to maintain the occupiable space around the occupants. The aircraft was also equipped with large, shock-absorbing landing gear, a 15-G floor and seat system, and lap belts and shoulder harnesses in all seats. The HelioCourier proved to be very useful in rough terrain and in jungle environments due to its ruggedness and its ability to protect its occupants.

Federal Aviation Administration

Through the 1970's and 1980's, the FAA made a series of amendments to the Federal Aviation Regulations (14 CFR Part 23, Reference 1-12) that were intended to improve the crashworthiness of light airplanes. All of the amendments focused primarily on crashworthiness afforded by restraints and seats. The first, Amendment 23-19 (1977), required shoulder harnesses for the front-row seats in newly certified light airplanes. Existing type-certified airplanes were not affected by this amendment. In 1985, Amendment 23-32 updated 23-19 by requiring shoulder harnesses in all seat positions for light airplanes of nine passengers or less

This Document Provided by the ABBOTT Aerospace
TECHNICAL LIBRARY
ABBOTTAEROSPACE.COM

(excluding crew) manufactured one year after the effective date of the amendment. Amendment 23-32 affected all new or existing type-certified airplanes in production, but not those that had already been manufactured. The reason behind these amendments was that shoulder harnesses have repeatedly been shown to improve the survivability in airplanes that are equipped with them and when they are used (Reference 1-13).

The biggest change occurred with Amendment 23-36 (1988). This amendment added two dynamic tests of the seat and restraint system: one that represents a primarily vertical impact, and one that represents a primarily longitudinal impact. The amendment also added "pass-fail" criteria for these dynamic tests that included, for the first time, injury criteria as measured by standardized anthropomorphic test devices (ATD's). The tests and criteria were added based on a recommendation of the General Aviation Safety Panel (GASP), which was a group of aviation industry representatives convened by the FAA in the mid-1980's to look at ways to improve the crash survivability of light airplanes (Reference 1-14). This amendment affected only newly type-certified light airplanes; the retrofit of the existing fleet or of existing type-certified airplanes in production was not required. Even after being in effect for more than a decade, as of this writing only a few light airplanes have been fully certified (that is, with no exemptions) to Amendment 23-36. These airplanes—the Lancair Columbia 300, and the Cirrus Designs SR-20 and its derivative, the SR-22—have only been in production for a few years. It will be a few years more before the efficacy of the improvements imposed by Amendment 23-36 can be fully ascertained with field data.

Terry Engineering

In 1997, Terry Engineering conducted four full-scale crash tests of small composite airframes at the NASA Langley Research Center Impact Dynamics Research Facility (Reference 1-15). Two of the tests were conducted onto a concrete surface and two were onto soil. The test impact conditions used by Terry were similar to some of the earlier NASA tests of production, metallic GA aircraft (Reference 1-16). A comparison of the Terry tests with the earlier NASA tests confirmed the improvement in crashworthiness of the Terry-designed airplanes. No single feature was identified as being responsible for the improvement in crashworthiness. The combination of an energy-absorbing engine mount, an engine cowling and lower firewall designed to prevent earth scooping, a stronger cabin structure, energy-absorbing foams in the sub-floor, and the proper combination of restraints and energy-absorbing seats, limited the occupant loads to within human tolerance. The duration of the deceleration was longer, allowing more time and distance for the occupants to come to rest. The stronger cabin structure maintained the needed occupant space for survival.

While the Terry airplanes were not certified production aircraft, per se, the tests conclusively showed that small airplanes could be designed so the occupants would survive a relatively severe accident near stall speed.

AGATE Advanced Crashworthiness Group

From 1995-2001, the AGATE Advanced Crashworthiness Group (ACG) worked to substantially improve the crash safety of small airplanes (to levels seen in modern automobiles), while minimizing the cost of improvements. The charter of the ACG was to (1) develop a set of design and certification guidelines, (2) demonstrate crashworthy technologies and design processes, and (3) educate the designers and the public. This Design Guide is a product of the ACG that addressed their charter.

THIS DOCUMENT PROVIDED BY THE ABBOTT AEROSPACE
TECHNICAL LIBRARY
ABBOTTAEROSPACE.COM

References

1-1. Single-Pilot GA Aircraft Market Study, conducted for NASA by Wichita State University, July 1995.

1-2. National Transportation Safety Board, http://www.ntsb.gov/aviation/Stats.htm, site accessed on December 12, 2001.

1-3. Bureau of Transportation Statistics, National Transportation Statistics 2000, http://www.bts.gov/btsprod/nts/, site accessed on September 6, 2001.

1-4. Zimmerman, R. E., and Merritt N. A., Aircraft Crash Survival Design Guide, Volume I–Design Criteria and Checklists, Simula, Inc., Phoenix, Arizona; USAAVSCOM TR 89-D-22D, Aviation Applied Technology Directorate, U.S. Army Aviation Research and Technology Activity (AVSCOM), Fort Eustis, Virginia, December 1989.

1-5. International Center for Safety Education, Crash Survival Investigation School: Basic Course Notebook, Section B-10, Course 95-2, Robertson, S. H., contributing author, Simula, Inc., Phoenix, Arizona, September 1995.

1-6. Mason-Reyes, M., "Summary of a Small Business Innovation Research Program: Thermoplastic Energy-Absorbing Subfloor Structures," Simula Government Products, Phoenix, Arizona, August 27, 1997.

1-7. Waldock, W. D., "A Brief History of Crashworthiness," Embry-Riddle Aeronautical University, no date provided.

1-8. DeHaven, H., "Accident Survival – Airplane and Passenger Car," SAE 520016, Society of Automotive Engineers, Inc., Warrendale, Pennsylvania, January 1952.

1-9. Bruggink, G. M., Barnes, A. C., and Gregg, L. W., "Injury Reduction Trends in Agricultural Aviation," Aerospace Medicine, May 1964, pp. 472-475.

1-10. Swearingen, J. J., Wallance, T. F., Blethrow, J. G., et al., "Crash Survival Analysis of 16 Agricultural Aircraft Accidents," Federal Aviation Administration Civil Aeromedical Institute, Washington, D.C., April 1972.

1-11. Snyder, R. G., "Civil Aircraft Restraint Systems: State of the Art Evaluation of Standards, Experimental Data, and Accident Experience," SAE 770154, in Aircraft Crashworthiness, PT-50, R. F. Chandler, ed., Society of Automotive Engineers, Warrendale, Pennsylvania, 1995.

1-12. "Federal Aviation Regulations, Part 23, Airworthiness Standards: Normal, Utility, Acrobatic, and Commuter Category Airplanes," 14 CFR 23, Federal Aviation Administration, Washington, D.C.

1-13. Clark, J. C., "Summary Report on the National Transportation Safety Board's General Aviation Crashworthiness Project Finding," SAE 871006, Society of Automotive Engineers, Warrendale, Pennsylvania, April 1987.

1-14. Soltis, S. J., and Olcott, J. W., "The Development of Dynamic Performance Standards for General Aviation Aircraft Seats," SAE 850853, Society of Automotive Engineers, Warrendale, Pennsylvania, April 1985.

1-15. Terry, J. E., Hooper, S. J., "Design and Test of an Improved Crashworthiness Small Composite Airframe," Phase II Report, NASA SBIR Contract NAS1-20427, October 1997.

THIS DOCUMENT PROVIDED BY THE ABBOTT AEROSPACE
TECHNICAL LIBRARY
ABBOTTAEROSPACE.COM

1-16. Castle, C. B., Alfaro-Bou, E., “Crash Tests of Three Identical Low-Wing Single-Engine Airplanes,” NASA Technical Paper No. 2190, 1983.

This Document Provided by the Abbott Aerospace
Technical Library
abbottaerospace.com

THIS DOCUMENT PROVIDED BY THE ABBOTT AEROSPACE
TECHNICAL LIBRARY
ABBOTTAEROSPACE.COM

Chapter 2

Physics

Lance C. Labun
Jill M. Vandenburg

This chapter will review the basic principles of crash physics. Descriptions of crash kinematics, as well as work-energy relationships, will be discussed. It is important to note that although this particular chapter will describe a work-energy approach to crash analysis, an impulse-momentum approach can also be used. In general, work-energy is more useful for crashworthy design, whereas impulse-momentum is more useful for accident reconstruction.

The majority of the information presented in this chapter was taken from Dr. James Turnbow's section of the International Center for Safety Education (ICSE) Crash Survival Investigation School Basic Course Notebook (Reference 2-1). Definitions and conventions for the algebraic signs of various quantities can be found in Appendix A.

2.1 KINEMATICS

A large volume of data associated with vehicle accident studies and human tolerance to decelerative loads is presented in the form of time plots of displacement, velocity, and acceleration. The following section will provide an explanation of the invariant relationships between these four quantities.

Consider an aircraft impacting a vertical wall as shown in Figure 2-1.

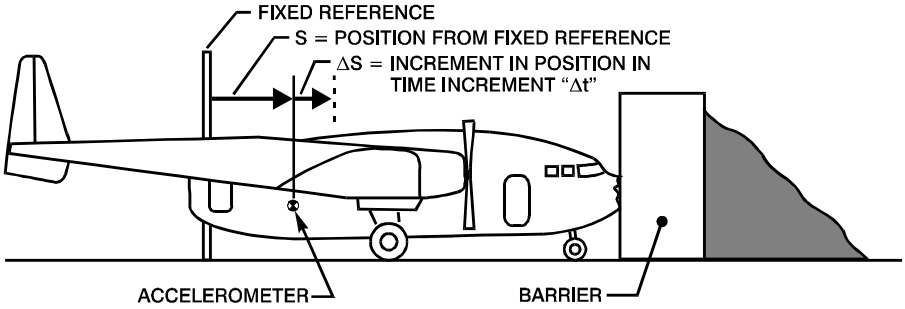


Figure 2-1.
A schematic of an aircraft impacting a vertical wall.

If ΔS is the infinitesimal displacement, which occurs in the infinitesimal time interval Δt, then we say by definition that the velocity at the beginning of the time interval is:

$$V = \frac{\Delta S}{\Delta t} \tag{1}$$

THIS DOCUMENT PROVIDED BY THE ABBOTT AEROSPACE
TECHNICAL LIBRARY
ABBOTTAEROSPACE.COM

Note that the velocity is an instantaneous quantity and has the units of length per unit of time. Similarly, if ΔV is the change in velocity, which occurred in the time interval Δt, then the acceleration at the beginning of the time interval is defined by:

$$a = \frac{\Delta V}{\Delta t} \tag{2}$$

Acceleration is also an instantaneous quantity and has the unit of velocity per unit time.

Unfortunately, these mathematical expressions leave much to be desired in the practical interpretation and understanding of these basic quantities. An excellent visual aid to better understanding these quantities is the velocity-time diagram (Figure 2-2). This diagram consists of three plots: (1) acceleration versus time, (2) velocity versus time, and (3) displacement versus time.

Observation of Figure 2-2 reveals that the "a" in Equation 2 is the height of the a-t curve and $\Delta V/\Delta t$ is the slope of the V-t curve. Therefore, the height of the a-t curve is numerically equal to the slope of the V-t curve:

$$a = \frac{\Delta V}{\Delta t}$$

Height of the a-t curve = Slope of V-t Curve (3)

This is an invariant relationship and any data, whether experimental or theoretical, must meet this criterion to be valid.

Similarly, Equation 1 and Figure 2-2 illustrate that the height of the V-t curve is equal to the slope of the S-t curve:

$$V = \frac{\Delta S}{\Delta t}$$

Height of the V-t curve = Slope of the S-t curve (4)

Through basic algebraic manipulation, two additional invariant relationships can be obtained among these three curves. By rearranging Equation 2, we obtain:

$$\Sigma \Delta V = \Sigma a \bullet \Delta t \tag{5}$$

Total change in velocity = Area under the a-t curve (6)

In this expression, $\Sigma a \bullet \Delta t$ represents the area of the horizontally shaded strip in the a-t curve (see Figure 2-2). The sum of these areas in any time interval is the total area under the a-t curve in the interval. The term $\Sigma \Delta V$ is the sum of the successive changes in velocity, which is the total change in velocity in a given interval. Thus, Equation 5, which states that the total change in velocity in a given interval is equal to the area under the a-t curve in the interval, is valid for all situations.

This same condition exists between the V-t and S-t curves. By rearranging Equation (1), we obtain:

$$\Sigma \Delta S = \Sigma V \bullet \Delta t \tag{7}$$

Total change in velocity = Area under the V-t curve (8)

This expression indicates that the maximum vehicle travel, as shown on the lower curve of Figure 2-2, would have to be equal to the shaded area under the V-t curve.

THIS DOCUMENT PROVIDED BY THE ABBOTT AEROSPACE
TECHNICAL LIBRARY
ABBOTTAEROSPACE.COM

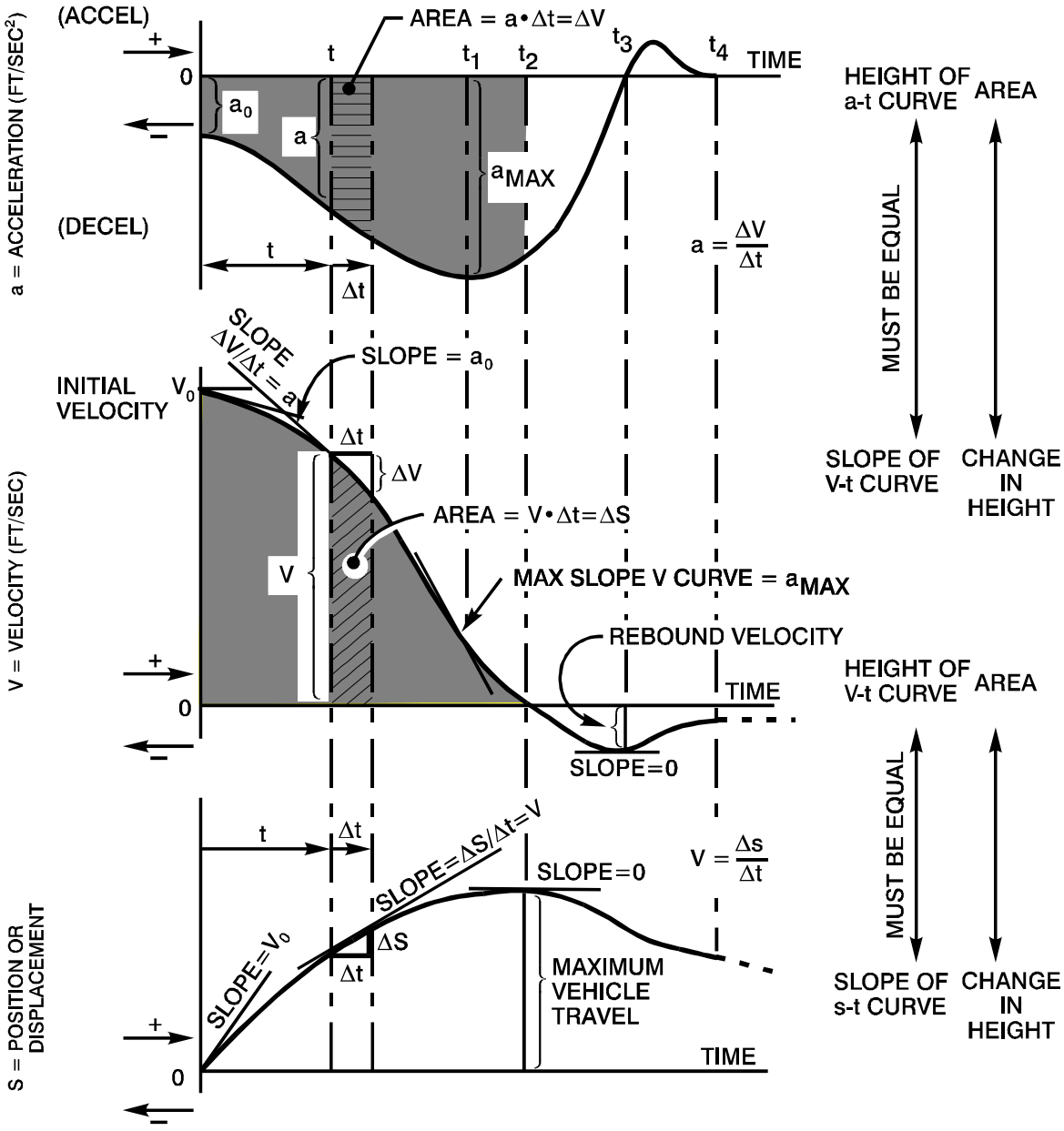


Figure 2-2.
The velocity-time diagram.

Other important relationships to note from Figure 2-2 include:

1. The areas below the t axis must be considered to be negative (deceleration), thus giving negative velocity changes or reductions in velocity. When the curve lies above the "t" axis, the area under the axis is positive (acceleration), giving an increase in velocity.
2. The velocity is changing at the most rapid rate when the acceleration (or deceleration) is maximum, time "t_1".
3. The displacement reaches a maximum when the velocity becomes zero, time "t_2".
4. The velocity need not necessarily be zero (time t_2) when the acceleration is maximum (time t_1).

THIS DOCUMENT PROVIDED BY THE ABBOTT AEROSPACE
TECHNICAL LIBRARY
ABBOTTAEROSPACE.COM

5. The area under the deceleration pulse (from t_0 to t_3) is equal to the initial velocity plus the rebound velocity or the total algebraic change in velocity.
6. The area under the deceleration curve between t_2 and t_3 is equal to the rebound velocity.

These same relationships can be determined for any set of displacement, velocity, and acceleration curves.

2.2 DECELERATION PULSES

In a crash event, the acceleration pulse is usually a complex function of time. Fortunately for design engineers, the crash pulse can often be simplified into an easily managed analytic form. The following section will describe the use of basic pulse shapes, including rectangular and triangular, for calculating the key variables for different types of crash events.

2.2.1 Rectangular Deceleration Pulse

As previously mentioned, acceleration is the instantaneous change of the velocity with respect to time. Integrating the acceleration over time gives the instantaneous velocity and integrating the velocity over time gives the instantaneous distance traveled during the event. The acceleration-velocity-displacement relationships for a rectangular pulse are illustrated in Figure 2-3.

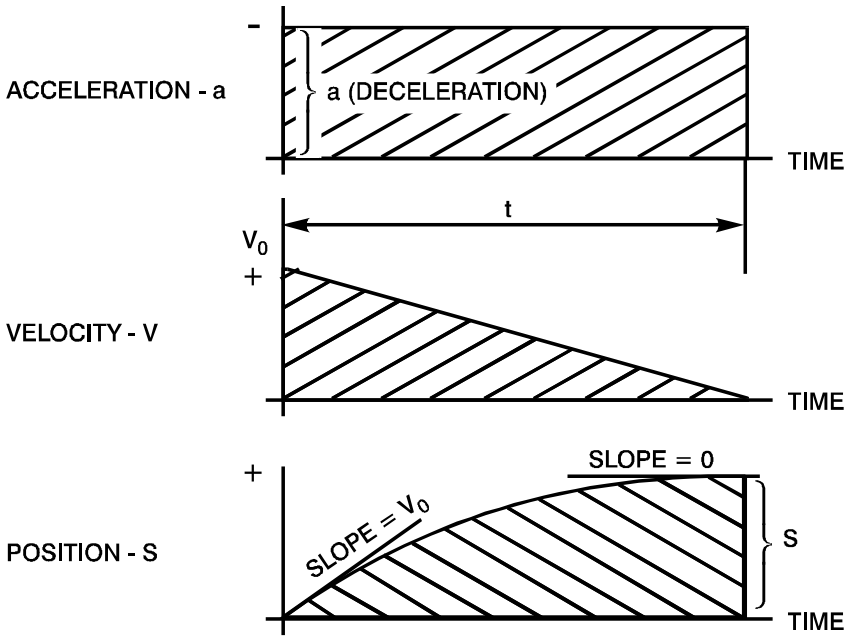


Figure 2-3.
Constant deceleration pulse (rectangular pulse).

The constant acceleration case is the simplest analytically. The integration of the acceleration and velocity curves leads to an expression for stopping distance. The stopping distance can be expressed as a function of the initial velocity by:

$$S = \frac{1}{2}\frac{V_0^2}{a} \tag{9}$$

THIS DOCUMENT PROVIDED BY THE ABBOTT AEROSPACE
TECHNICAL LIBRARY
ABBOTTAEROSPACE.COM

As shown in Equation 9, a large velocity, V_0, will require a very large stopping distance. A large stopping distance will also be required if the acceleration, a, was small.

Horizontal slide out can be treated as a constant acceleration event, where the acceleration is determined by the coefficient of sliding friction. The constant-acceleration idealization is also used where energy absorption is incorporated into the design in items such as an energy-absorbing landing gear, an energy-absorbing stroking seat, or energy-absorbing structure with a uniform crush strength.

2.2.2 Symmetrical Triangular Pulse

In practice, the symmetrical triangular pulse is often used to simulate the crushing of structure. Thus, the pulse generated by an aircraft striking a barrier horizontally or vertically and crushing the fuselage would be approximated by a triangular pulse. The stopping distance for this pulse is given by:

$$S = \frac{V_o^{\,2}}{a} \tag{10}$$

The acceleration-velocity-displacement relationships for a symmetrical triangular pulse are illustrated in Figure 2-4.

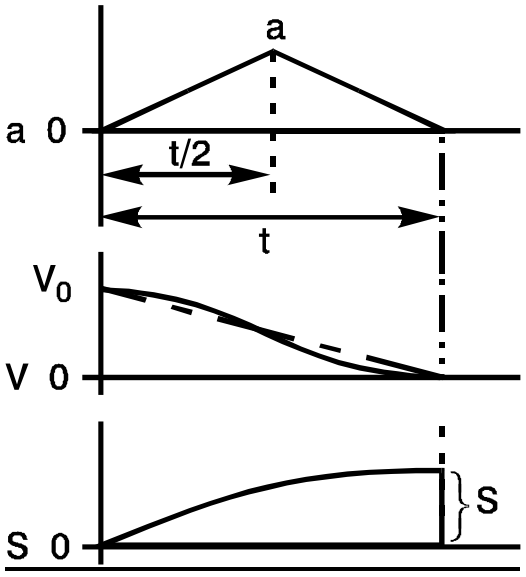


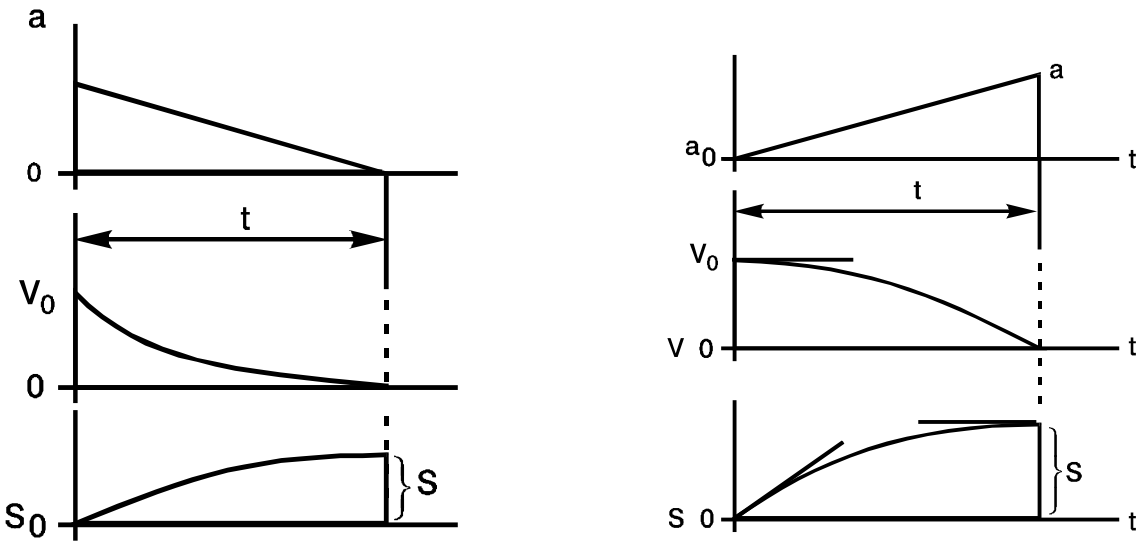
Figure 2-4.
The symmetrical triangular pulse.

2.2.3 Asymmetrical Triangular Pulses

As illustrated in Figure 2-5, asymmetrical triangular pulses can be divided into two extreme categories: zero rise time pulse and zero offset pulse. These two pulse approximations are used less often, but reviewing their behavior is useful for demonstrating the effect of shifting the peak acceleration from the midpoint of the event as in the symmetrical pulse to either earlier or later in the event. Figure 2-5 reveals that although the stopping time for the two pulses is identical, the stopping distance for the zero-offset pulse is twice the stopping distance for the zero-rise-time pulse with the symmetrical pulse midway between the two pulses. In an event

THIS DOCUMENT PROVIDED BY THE ABBOTT AEROSPACE
TECHNICAL LIBRARY
ABBOTTAEROSPACE.COM

where a relatively rigid structure is presented in the crash, the peak acceleration will shift to an earlier time in the pulse. This phenomenon tends to occur in vertical water impacts, where the aircraft's belly skin fails and the water meets the relatively stiff floor structure without crushing the subfloor structure. The peak might occur late in the pulse in a case where the aircraft struck a soft surface at a small angle and began to plow up material relatively slowly, thus gradually increasing the mass to be accelerated.



(a) **(b)**

$$S = \frac{2}{3}\frac{V_o^2}{a} \qquad S = \frac{4}{3}\frac{V_o^2}{a}$$

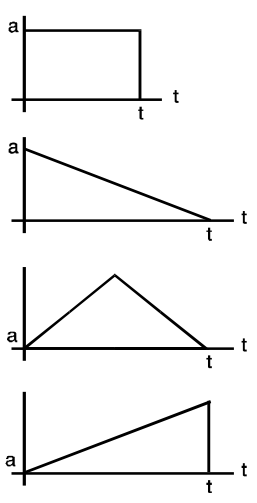
Figure 2-5.
Comparison of two asymmetrical pulses: (a) zero-rise-time pulse and (b) zero-offset-time pulse.

2.2.4 Comparison of Deceleration Pulse Characteristics

Figures 2-6 and 2-7 display a summary of the pulse shapes and formulas for the four deceleration pulse types described in this chapter. As an example of the difference in magnitude of these pulses, imagine a decelerating aircraft at three different velocities: 50, 100, and 150 mph (73, 147, and 220 ft/sec) with a constant acceleration. If the stopping distance is held constant at 20 ft., then the deceleration rates are 4.25 G, 12.5 G, and 20.8 G, respectively. The deceleration rate for a 150-mph crash is almost 5 times the deceleration rate for the 50-mph crash.

The stopping time is of less significance to the designer than the stopping distance (Figure 2-7). The time to stop for the three triangular pulses is equal; however, the stopping distances are most emphatically not equal. The shortest stopping distance is achieved with the constant acceleration pulse. Thus, constant acceleration is the preferred pulse to achieve the maximum velocity change in the least distance for a given acceleration level.

THIS DOCUMENT PROVIDED BY THE ABBOTT AEROSPACE
TECHNICAL LIBRARY
ABBOTTAEROSPACE.COM



$$S = \frac{V_o^2}{2a}, \qquad t = \frac{V_o}{a}$$

$$S = \frac{2}{3}\frac{V_o^2}{a}, \qquad t = \frac{2V_o}{a}$$

$$S = 1.000\frac{V_o^2}{a}, \qquad t = \frac{2V_o}{a}$$

$$S = \frac{4}{3}\frac{V_o^2}{a}, \qquad t = \frac{2V_o}{a}$$

Figure 2-6.
Summary of stopping distance and stopping time equations for various crash pulses where $V_f = 0$.

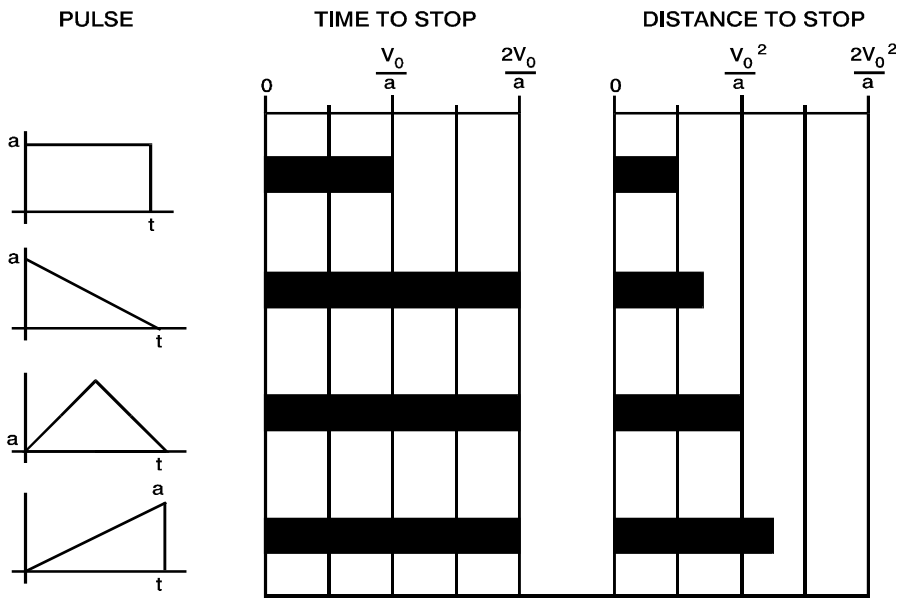


Figure 2-7.
Relative times and stopping distances for various deceleration pulses.

2.3 WORK-ENERGY RELATIONSHIP

Designing crashworthy aircraft involves finding ways to absorb the kinetic crash energy within tolerable acceleration levels. Applications include seats, restraint systems, landing gear, and in the aircraft structure itself. As a result, aircraft designers need a thorough understanding of the concepts of energy and energy-absorbing principles. This section will briefly discuss some of the key principles related to work and energy in crash scenarios.

THIS DOCUMENT PROVIDED BY THE ABBOTT AEROSPACE
TECHNICAL LIBRARY
ABBOTTAEROSPACE.COM

The concept of energy arises in the work-energy principle, which is derived from Newton's Second Law. If the resultant force applied to the mass is "F", as shown in Figure 2-8, then the force, the mass, and the acceleration are related by Equation 11.

$$F = ma = m\frac{\Delta V}{\Delta t} = m\frac{\Delta V}{\Delta t} \bullet \frac{\Delta S}{\Delta S} = mV \bullet \frac{\Delta V}{\Delta S} \tag{11}$$

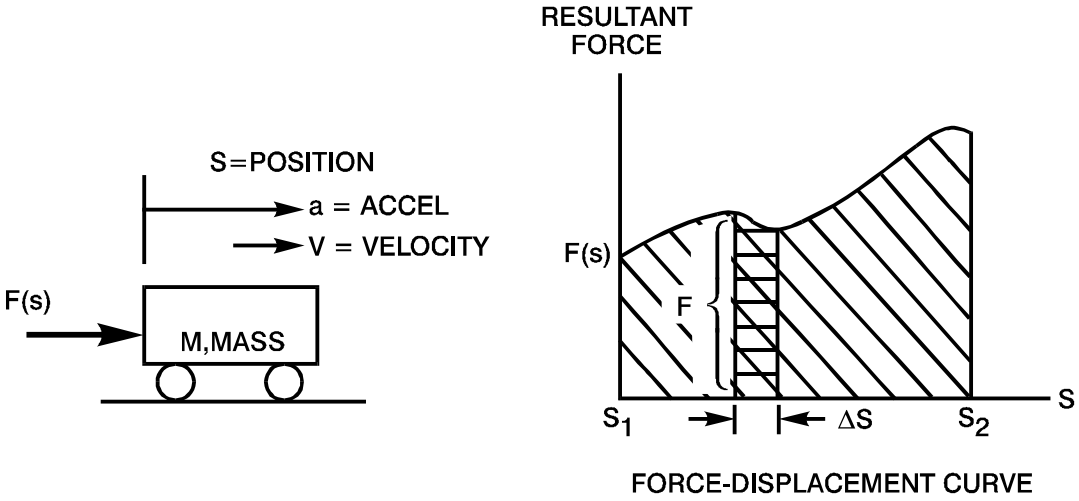


Figure 2-8.
The work-energy principle.

Further manipulation of Equation 10 yields an expression for the area under the F-S curve in Figure 2-8. The area under the F-S curve is referred to as the system's kinetic energy and is expressed as:

$$\Delta KE = \frac{1}{2}mV_2^{\,2} - \frac{1}{2}mV_1^{\,2} \tag{12}$$

The square dependence in Equation 12 is a very powerful consideration in designing for crashworthiness. It indicates that doubling the velocity of a mass quadruples its kinetic energy. But, more subtly, the square dependence indicates that the increase in kinetic energy that is due to an incremental change in velocity depends very strongly on the original velocity to which the increment is added.

The change in kinetic energy, as described by Equation 13, is equivalent to the amount of work done on the mass.

$$Work = \Delta KE \tag{13}$$

Work can also be expressed as:

$$W = \Sigma F \bullet \Delta S = area\ under\ F - S\ curve \tag{14}$$

THIS DOCUMENT PROVIDED BY THE ABBOTT AEROSPACE
TECHNICAL LIBRARY
ABBOTTAEROSPACE.COM

2.4 ENERGY ABSORPTION

The area under the F-S curve in Figure 2-8 represents the amount of energy absorbed. Equations 13 and 14 indicate that the only way in which energy can be removed from a body (i.e., reducing a body's velocity) is to hold a force on the body as the body moves (Figure 2-9a). This can be accomplished by the use of a crushable structure or material that maintains a constant force as the mass travels through a certain distance (Figure 2-9b). A device or system that achieves this objective is referred to as an energy absorber.

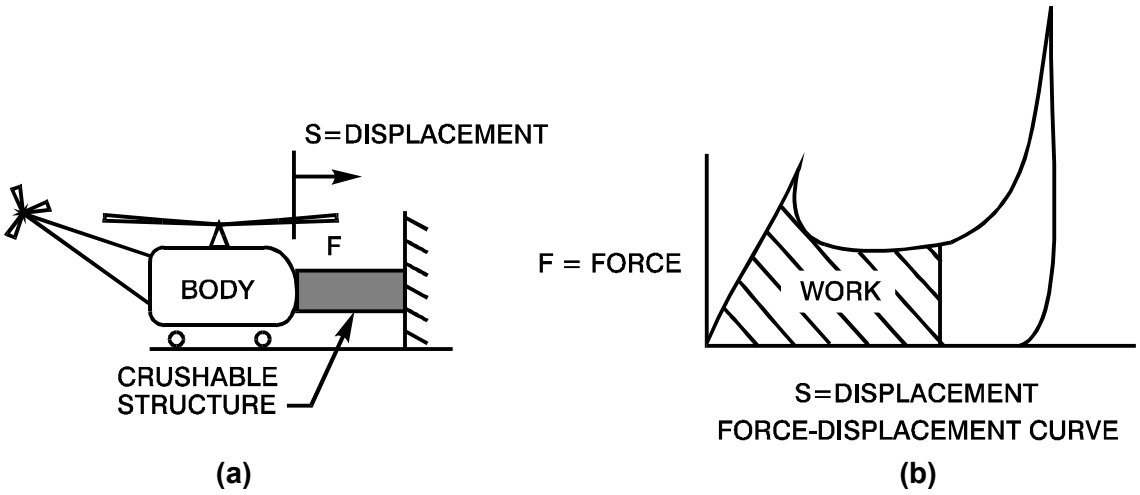


Figure 2-9.
Use of an energy absorber.

The generation of an "ideal energy absorber" is shown in Figures 2-10 and 2-11. As shown in Figure 2-10, if "a" is constant, the F=ma is also constant. The F-S curve for the energy absorber is represented by Figure 2-11. Certain foamed materials and honeycomb materials approach this ideal force-displacement curve to the extent shown in Figure 2-12.

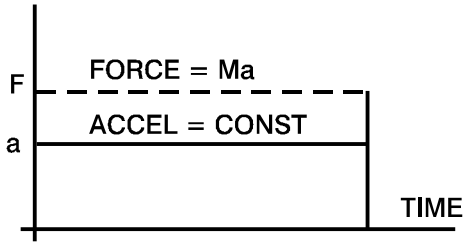


Figure 2-10.
Relationship between constant acceleration and constant force.

THIS DOCUMENT PROVIDED BY THE ABBOTT AEROSPACE
TECHNICAL LIBRARY
ABBOTTAEROSPACE.COM

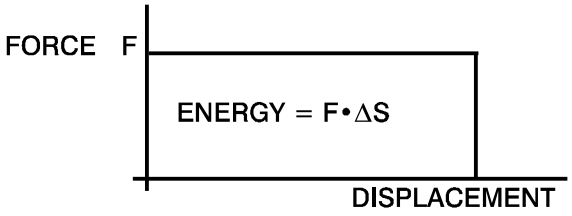


Figure 2-11.
Ideal energy absorber.

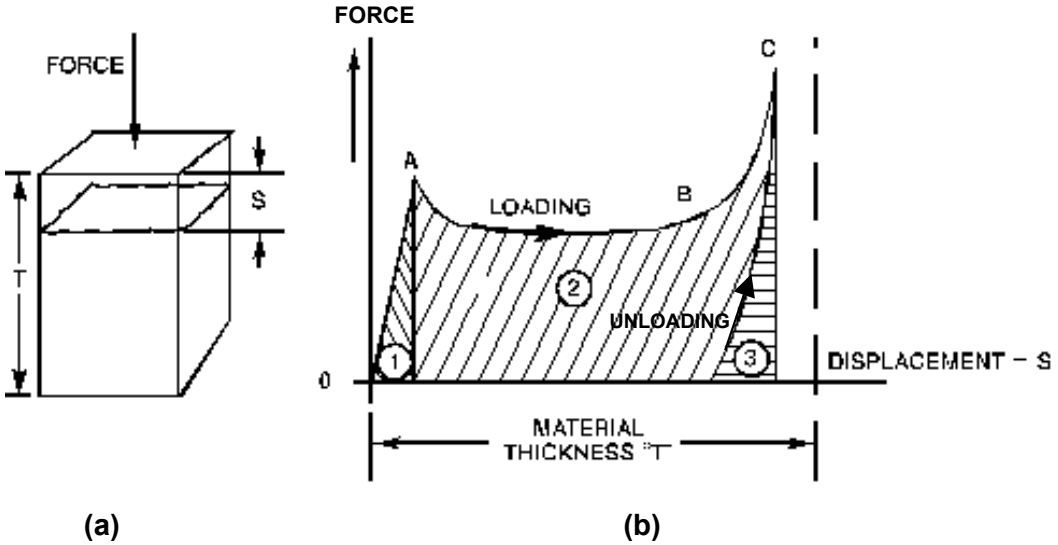


Figure 2-12.
Force-displacement curve for honeycomb materials.

As previously mentioned, the area under the force-displacement curve (Figure 2-12b) represents the amount of energy absorbed. This area can be divided into three separate regions: elastic, plastic, and rebound. If loading increases only up to Point A in Figure 2-12b, then unloading generally occurs along the elastic curve 0A, and the energy indicated by Area "1" is given back, in the same manner as a spring gives back its energy when it is unloaded. Area "2" represents plastic energy absorption. If loading reaches Point C in the figure, the energy corresponding to Areas "1" and "2" plus Area "3" is absorbed. However, as unloading occurs, the energy of Area "3" is given back in the form of rebound. Loading in the region from B to C in the figure is often referred to as "bottoming out," a condition wherein the deforming structure or material has become completely compacted and the load increases rapidly with very little increased deformation.

2.5 EXAMPLE SCENARIO

The following is an example of the calculations required to design the stroking force for a seat intended to stroke under the decelerative load imposed by a 50th-percentile male occupant (adapted from Reference 2-2). The stroking load is calculated using the equation

THIS DOCUMENT PROVIDED BY THE ABBOTT AEROSPACE
TECHNICAL LIBRARY
ABBOTTAEROSPACE.COM

$$L_{Stroke} = G_L W_{Eff} \tag{15}$$

where:

L_{Stroke} = stroking load of the seat (lb)

G_L = limit load (G)

W_{Eff} = effective weight of the 50th-percentile occupant (lb)

Based on Equation 15, two parameters need to be determined in order to calculate the stroking load: the limit load, G_L, and the effective weight of the 50th-percentile occupant, W_{Eff}. Assuming that the limit load is approximately 12 G, Table 2-1 can be used to determine the effective occupant weight, W_{Eff} using the equation

$$\begin{aligned} W_{Eff} &= W_{50eff} + W_{Ceff} + W_{Beff} \\ W_{Eff} &= 136\ lbs + 2.4\ lbs + 2\ lbs \\ W_{Eff} &= 140.4\ lbs \end{aligned} \tag{16}$$

Table 2-1.
Weight parameters

Parameter	Actual Weight (lb)	Effective Weight (lb)	Symbol
Nude weight of the 50th-percentile male occupant	170	136	W_{50eff}
Weight of clothes (less shoes)	3	2.4	W_{Ceff}
Seat stroking weight (weight of seat bucket)	2	--	W_B
*Effective weight in the vertical direction represents 80 pct of the actual weight, since the occupant's lower extremities are partially supported by the floor of the aircraft.			

Using this information, the stroking load can be calculated as:

$$\begin{aligned} L_{Stroke} &= G_L W_{Eff} \\ L_{Stroke} &= (12\ G)(140.4\ lbs) \\ L_{Stroke} &= 1684.8\ lbs \end{aligned} \tag{16}$$

THIS DOCUMENT PROVIDED BY THE ABBOTT AEROSPACE
TECHNICAL LIBRARY
ABBOTTAEROSPACE.COM

References

2-1. International Center for Safety Education, Aircraft Crash Survival Investigation Basic Course Manual, Course 99-3, Turnbow, J. W., contributing author, Simula, Inc., Phoenix, Arizona, September 1999, Section B-15.

2-2. Desjardins, S. P., Zimmermann, R. E., Bolukbasi, A. O., et al., Aircraft Crash Survival Design Guide, Volume IV, Aircraft Seats, Restraints, Litters, and Cockpit/Cabin Delethatlization, TR- 87442, Simula Inc., Tempe, Arizona; USARTL TR-89-D-22D, Applied Technology Laboratory, U.S. Army Research and Technology Laboratories, (AVRADCOM), Fort Eustis, Virginia, December 1989.

This Document Provided by the Abbott Aerospace
TECHNICAL LIBRARY
ABBOTTAEROSPACE.COM

Chapter 3

Design Crash Impact Conditions

Todd R. Hurley
Darrel Noland

This chapter presents the impact conditions that should be used in the design of AGATE-class airplanes. The first section of this chapter presents the regulatory impact conditions of FAR Part 23 (14 CFR Part 23, Reference 3-1). The second section presents the AGATE-developed, whole-airplane impact conditions that, if used for design, may provide a higher level of occupant protection than provided by the current regulations. The third section presents background information that may be useful to the reader who wants to understand where the impact conditions originated.

The focus of this chapter is only on the impact conditions and impact-related load factors used in design. The purpose this focus is two-fold: (1) to provide an easily referenced location for impact information that is used in the design of the protection systems covered in this book; and (2) to illustrate the differences between the regulatory and AGATE impact conditions. The other requirements needed in the design of occupant protection systems are more completely presented in subsequent chapters.

3.1 CURRENT FAA IMPACT CONDITIONS

The current requirements for the impact conditions used to design aircraft occupant protection systems are located in 14 CFR Part 23, Subpart C - Structure; specifically, in Section 23.561 “General” and in Section 23.562 “Emergency Landing Dynamic Conditions.” The regulations mainly address the strength and performance of seat/restraint systems, although some consideration is given to the occupant’s immediate surroundings and to the strength of the fuselage.

The impact conditions in the regulations are based on crash research and accident investigation studies conducted by the FAA, NASA, and the NTSB from as far back as the 1950’s. In the mid-1980’s, the General Aviation Safety Panel (GASP) distilled this impact information into a recommendation that later became the basis for the dynamic test conditions that are cited in Section 23.562. Designers should note that, except for adjustments in the static loads and vertical dynamic test conditions for airplanes with stall speeds greater than 61 kts, the static and dynamic regulatory impact conditions assume that all airplanes respond similarly in a crash. In other words, the current regulations presume all airplanes crash such that the loads, accelerations, and velocity changes are the same. This assumption is clearly a simplification and emphasizes that the CFR’s are minimum performance standards.

3.1.1 14 CFR 23.561 “General”

This regulatory section states that each occupant must be protected in an emergency landing, and that the structure must be designed to provide each occupant with a reasonable chance of escaping serious injury. The 23.561 section also presents the ultimate load factors that must be

THIS DOCUMENT PROVIDED BY THE ABBOTT AEROSPACE
TECHNICAL LIBRARY
ABBOTTAEROSPACE.COM

designed into the seat, restraint, and aircraft structure. The section further states that the occupant will experience static inertia forces corresponding to these stated loads if proper seats, safety belts, and shoulder harnesses are provided by the designer and used by the occupants. The ultimate load factors that must met for restraining items of mass and cargo are also presented. The load factors specified in 23.561 are shown in Table 3-1.

Table 3-1.
Load factors specified in 14 CFR 23.561

Load Direction	Category		
	Normal, Utility, and Commuter Airplanes (G)	Acrobatic Airplanes (G)	Items of Mass (G)
Upward	3.0	4.5	3.0
Forward	9.0	9.0	18.0
Sideward	1.5	1.5	4.5
Downward	6.0	6.0	N/A

The designer must increase these load factors by a formula found in Paragraph 23.562(d) of the regulation if the stall speed of the airplane at maximum take-off weight (MTOW) is greater than 61 kts.

Section 23.561 also specifies design forces and loads to be used when considering gear-up landings by aircraft equipped with retractable gear. This type of airplane is to be designed to protect each occupant during such a landing. The structure must also be designed to protect the occupants if the aircraft is likely to turn over during an emergency landing. The details of these requirements are found in Paragraphs 23.561(c) and (d). These are the only requirements in Part 23 that explicitly address airframe crashworthiness.

3.1.2 14 CFR 23.562 "Emergency Landing Dynamic Conditions"

Section 14 CFR 23.562 in the FAR specifies the impact conditions that are to be used for the design and test of the seat and restraint system. The conditions and test procedures laid out in this section are to be used to demonstrate that the occupant will be protected during an emergency landing. Human injury tolerance criteria are given that must not be exceeded during these tests. The dynamic tests are conducted with anthropomorphic test devices (ATDs) to simulate the occupant and to measure injury data.

Two tests are required. The first, found in Paragraph (b)(1), and commonly referred to as "Test 1," is a dynamic test that simulates an emergency landing with a primarily vertical impact. The seat/restraint system and occupant are oriented in their normal position with respect to the airplane, and then rotated on the test apparatus so the aircraft coordinates are 30-deg nose-down with respect to the vertical impact vector. This test may appear to simulate a nose-down accident, but is actually devised to simulate an essentially flat, high sink-rate impact onto a surface that has a 0.5 coefficient of friction. The test orientation of the aircraft coordinates depends on the test apparatus: 30-deg nose-down on a drop tower (vertical impact vector) or 60-deg nose-up on a sled (horizontal impact vector). Consequently, this test condition is also referred to as the 30-deg down test or the 60-deg pitch-up test, depending on the test facility. Like the static load factors in 23.561, the crash pulse of Test 1 is modified by 23.562(d) for airplanes with a V_{so} of more that 61 kts at MTOW.

THIS DOCUMENT PROVIDED BY THE ABBOTT AEROSPACE
TECHNICAL LIBRARY
ABBOTTAEROSPACE.COM

The second test, described in Paragraph (b)(2), and commonly referred to as "Test 2," simulates an emergency landing with a primarily horizontal impact. The seat/restraint system and occupant are again oriented in their normal position with respect to the airplane, and rotated with a 10-deg yaw, but no pitch, relative to the horizontal impact vector. This test condition simulates an accident with a large longitudinal component (relative to the airplane) such as a nose-down impact into dirt, or a flat, sliding impact in which the aircraft hits an obstacle such as a berm or tree. The 10-deg yaw is supposed to be oriented to produce the greatest load in the shoulder harness, but is often oriented to produce the highest likelihood of headstrike. Floor warpage must be taken into account in Test 2 by pitching one of the floor mounting rails 10 deg out of alignment with the other floor mounting rail. In addition, one of the rails must be rolled 10 deg. The crash pulse of Test 2 is not modified by 23.562(d) for airplanes with a V_{so} greater than 61 kts. The designer should always reference the appropriate FAA regulations and guidance when designing an aircraft or seating/restraint system. Both the Test 1 and Test 2 impact conditions are shown in Table 3-2.

Table 3-2.
FAA crash impact design standards

	14 CFR 23.562(b)(1) "Test 1"		**14 CFR 23.562(b)(2) "Test 2"**	
	Front Row	**All Other Rows**	**Front Row**	**All Other Rows**
Velocity Change (ft/sec)	NLT 31	NLT 31	NLT 42	NLT 42
Rise Time to Peak (sec)	0.05	0.06	0.05	0.06
Peak Acceleration (G)	19	15	26	21
Seat/Restraint Position	60-deg Pitch Up No Yaw	60-deg Pitch Up No Yaw	10-deg yaw No Pitch Floor Warpage	10-deg yaw No Pitch Floor warpage

One aspect of the regulations unique to light airplanes is that the magnitude and rise time of the pulse used to test the front row seat/restraint system differs from the pulse used for all seats behind the front row. Justification for this difference came from the NASA full-scale crash test data of 1970's-era metal monocoque light airplanes that showed the magnitude of the deceleration pulse decreased and the duration of the deceleration increased the further aft the measurement was taken (Reference 3-2). This was due to load attenuation by local deformation of the airframe and cabin structure. In other words, the front seat occupants had a shorter distance to decelerate than did the occupants in the rear. Different crew-versus-passenger-seat test pulses are not found in the regulations for any other aircraft category (i.e., Part 25, Transport Category Airplanes, and Parts 27 and 29, Rotorcraft).

More recent NASA full-scale tests of composite light airplanes that are designed to be crashworthy show little difference between the pulses measured at the pilot position versus the pulses at the passenger positions (Reference 3-3). Crashworthy airframes are designed so that the majority of deformation and energy attenuation occurs outside of the occupant compartment. This design strategy reduces the attenuation that occurs within the cabin area and, therefore, little difference is observed in the acceleration pulses between the different cabin positions. Composite airframe structures also tend to be stiffer than metal airframe structures, even when they are not designed for crashworthiness. Moving the deformation and energy-absorption zones outside of the cabin has other effects. In the 30-deg nose-down tests done

THIS DOCUMENT PROVIDED BY THE ABBOTT AEROSPACE
TECHNICAL LIBRARY
ABBOTTAEROSPACE.COM

onto a hard surface, the rear-seat position actually saw higher vertical acceleration pulses due to a rapid whole-airplane rotation and a secondary impact referred to as “tail slap.” The engine mount, rather than the cabin structure, absorbed the impact energy; thus, the ground reaction load occurs further forward from the aircraft's center of gravity, causing the rapid rotation.

The regulations also allow the front and rear seat/restraint systems to be dynamically tested with different pulses. In real-world practice, the airplane designer needs to decide if the additional testing is justified in terms of cost and airframe response. Often, the front and rear seat/restraint systems are designed to use the same or virtually the same structure, cushions, energy absorbers, and restraints to reduce the cost of design and manufacturing. In systems with a great deal of commonality between the crew and passenger seats, one seat/restraint system (either the crew or passenger, depending on a rational justification of which is worst-case) can be tested to the front seat conditions and then the other positions certified by similarity. This approach has the potential to halve the number of tests and test articles required. For airframes designed to be crashworthy, the authors of this Design Guide recommend that all the seat/restraint systems for that aircraft be designed and tested to the front-row conditions, regardless of seat commonality, for the reasons described above. This recommendation is also appropriate for many composite airframes, due to their stiffness.

3.2 AGATE IMPACT CONDITIONS

The Advanced Crashworthiness Group (ACG) was a subset of the Integrated Design and Manufacturing (ID&M) Work Package in the AGATE Alliance whose task was to develop guidelines and standards to substantially improve the crashworthiness of light airplanes while minimizing the additional cost of these improvements. Like all of AGATE, the members of the ACG represented a broad cross-section of the GA industry and university researchers, in partnership with members from the FAA and NASA. One thrust of the ACG was to develop a simple design and certification methodology for whole-airplane crashworthiness focusing on airframe energy absorption and occupant compartment integrity. While the ACG had not come to a consensus on simplified occupant compartment load factors or the airframe certification methodology by the end of the AGATE program in 2001, they had agreed on the research design approach, the design features of the test airplane, and the design and test impact conditions. These impact conditions are presented here in Table 3-3 and Figure 3-1, and were used in the design of a crashworthy test airplane and in the full-scale crash test of that airplane conducted by the AGATE ACG in the summer of 2001 (References 3-4 and 3-5).

Table 3-3.
AGATE-determined impact conditions

Impact Velocity	V_{so}
Impact Angle	-30 deg (down)
Attitude	-30-deg pitch (nose down)
Weight	MTOW consisting of: • A 170-lb occupant in each seat • Fuel up to MTOW or capacity • Baggage up to MTOW, if fuel is at capacity (Other scenarios may be used if they can be justified, e.g., seats designed with restricted occupant weight should be tested at the maximum restricted weight)
Impact Surfaces	Hard (concrete) Soil (Defining parameters TBD)

THIS DOCUMENT PROVIDED BY THE ABBOTT AEROSPACE
TECHNICAL LIBRARY
ABBOTTAEROSPACE.COM

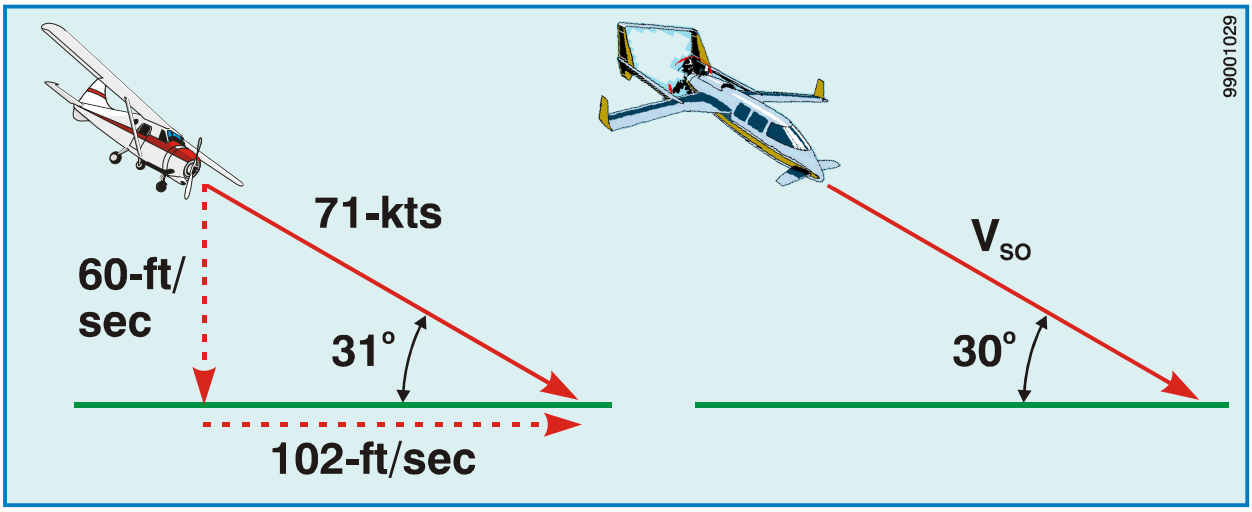


Figure 3-1.
AGATE-determined impact conditions.

It should be noted that the AGATE impact conditions are for the whole airplane and take into account the stall speed (that is, the vehicle's minimum operating speed) and weight of the airplane. These whole-airplane conditions acknowledge that different airplane designs will have different initial crash conditions based on the performance and size of the airplane. These conditions also do not presume the structural response of the airplane; the structural response is defined by the crashworthiness of the design and the ingenuity of the designer. The two different impact surfaces specified recognize that the impact surface also influences the airplane response. At 30 deg nose down, the hard-surface impact typically produces sliding impact with deformation in the lower nose structure and sometimes the front-seat footwells, a whole-airplane pitch-up rotation that aligns the airplane with the impact surface, and a higher vertical (relative to the airplane) component of acceleration. The hard-surface condition forces the designer to address energy absorption primarily in the subfloor structures and also, to a certain extent, in the nose of the airplane; the designer is also induced to address the strength of the lower forward occupant compartment, and the bending strength of the fuselage. An impact on soil at 30 deg nose down produces a very different response. For airplanes that are not designed to be crashworthy, the airplane structure will typically dig into the soil, stopping abruptly, thereby producing a very high longitudinal (relative to the airplane) deceleration. The soil-impact condition forces the designer to address energy absorption primarily in the nose or engine mount, the longitudinal strength of the occupant compartment and firewall, and the use of anti-plowing features. Properly designed, a crashworthy airplane will tend to pitch up out of the crater and thus extend the stopping distance many times over compared to an airplane that digs in (Reference 3-3). The properties of the impact test soil had not been determined by the ACG by the end of the AGATE program in 2001.

3.2.1 Justification

Members of the ACG examined the research discussed in Section 3.4 during an AGATE study of accident impact conditions to determine the design and test impact conditions. Based on the data compiled during the AGATE study, the average impact velocity and the angle at which at least one occupant survived and at least one occupant was fatally injured was 71 kts and 31 deg (Reference 3-6). Comparing the results from the AGATE study to the design pulses

This Document Provided by the Abbott Aerospace
TECHNICAL LIBRARY
ABBOTTAEROSPACE.COM

recommended in the 1967 Crash Survival Design Guide (Reference 3-7) required calculating the longitudinal and vertical changes in velocities from the average impact conditions of 71 kts and 31 deg. Four accidents from the database that had very similar impact velocities and angles to the AGATE study average were selected for further analysis. After accounting for slide-out and a range of surface coefficients of friction, the average change in velocity in the longitudinal direction from the AGATE study was shown to be 58 to 69 ft/sec, which correlates well with the 60 ft/sec change in velocity recommended in the Crash Survival Design Guide. The average vertical velocity change from the study was approximately 61 ft/sec, which is larger than the 42-ft/sec change in velocity recommended in the Crash Survival Design Guide. The actual change in vertical velocity in the AGATE study is probably conservative, since the assessment assumed no airframe crushing or ground compaction.

The velocity changes in the AGATE study also compared well with those determined in the NTSB studies of survivable GA accidents. The NTSB studies suggested that longitudinal velocity changes of 60 to 70 ft/sec (with accelerations of 30 to 35 G) were survivable (Reference 3-8). The survivable vertical velocity changes were calculated to be 50 to 60 ft/sec (with 25 to 30 G). The NTSB studies also developed a "survivable envelope" that plotted impact velocity versus impact angle. The impact velocity of the NTSB survivable envelope at 30 deg is approximately 70 kts, which is almost the same as the AGATE study impact conditions. The findings of these studies and the FAA seat test pulse are summarized in Table 3-4.

Table 3-4.
A comparison of industry standards and past studies
(Adapted from Reference 3-6)

	Crash Survival Design Guide 1967 (Reference 3-7)	**NTSB Study 1985 (Reference 3-8)**	**GASP 1984 FAA 1988: Amendment 23-36 (References 3-9 & 3-2)**	**AGATE Study Findings 1999 (Reference 3-6)**
Velocity Change	**Vertical:** 42 ft/sec **Longitudinal:** 60 ft/sec	**Vertical:** 50-60 ft/sec **Longitudinal:** 60-70 ft/sec	**Vertical:** 31 ft/sec **Longitudinal:** 42 ft/sec	**Vertical:** 60 ft/sec **Longitudinal:** 58-69 ft/sec
Acceleration Load	**Vertical:** 48 G **Longitudinal:** 34 G	**Vertical:** 25-30 G **Longitudinal:** 30-35 G	**Vertical:** 19 G (15 G*) **Longitudinal:** 26 G (21 G*)	Data was inconclusive. Insufficient data to determine the acceleration loads.

*Peak G for seats behind the front row.

The FAA and GASP conditions are intended for evaluating the performance of airplane seats and restraint systems. These conditions take into account aircraft deformation, based on metal alloy aircraft, which absorbs energy and reduces the loads that are transmitted to the seats and occupants during a crash. At present, the majority of aircraft are constructed out of light metal alloys; however, as more composite aircraft enter the market, the energy-absorbing characteristics of the population of aircraft will change. Evidence of differences in energy-absorbing characteristics has already been demonstrated and was seen in the Terry Engineering and, later, in the AGATE ACG full-scale crash tests (References 3-3 and 3-5).

A comparison of the accelerations at the seat locations between the AGATE study and the FAA and GASP conditions was not possible because the data did not provide enough information on seat floor and cabin deformation to conduct a proper crash analysis. However, the initial impact

THIS DOCUMENT PROVIDED BY THE ABBOTT AEROSPACE
TECHNICAL LIBRARY
ABBOTTAEROSPACE.COM

conditions in some of the full-scale tests on which the FAA and GASP condition were based were approximately 50 kts and 30 deg (References 3-2 and 3-10). The initial impact conditions are less severe than the findings from the AGATE study, the NTSB recommendations, and the Crash Survival Design Guide recommendations.

The determination of an "average" survivable impact condition of 71 kts and 31 deg is an artificial simplification, as airplanes can crash at any angle and attitude and at a wide range of speeds. In fact, the AGATE study contained accidents that met the study criteria of at least one fatality and at least one survivor that had impact velocities ranging from less than 15 kts to greater than 120 kts. However, designing for all orientations and velocities would be very difficult, so some simplification is justified. In addition, having some minimum performance standard tends to improve survivability across a wide range of accidents. For example, the automobile industry primarily uses a few crash tests to demonstrate their crashworthiness performance [Federal Motor Vehicle Safety Standards (FMVSS) 208 and 214, and the New Car Assessment Program (NCAP), References 3-11, 3-12, and 3-13]. The frontal crash tests are conducted into a rigid barrier at 30 and 35 mph, and the side-impact tests are conducted with a movable barrier at 33.5 and 38.5 mph. These are minimum standards, but the field data indicate improved survivability in cars at accident speeds and crash angles much different than those that just replicate the tests.

For the following reasons, several ACG members believed that 71 kts was too high for a design and test impact condition. One member thought was that the range assigned for each of the impact velocity "check boxes" on the NTSB accident investigation report form could have skewed the average velocity of the accident studies. These ranges are smaller (15 kts range) at impact speeds below 90 kts and larger (30 kts) above. Also, the ACG was developing a minimum standard—that is, a condition at which there is a high probability of survival—whereas the AGATE study average represented a velocity at which the airplanes apparently failed to protect roughly half their occupants. Another concern was that the NASA Langley Research Center Impact Dynamics Research Facility (IDRF), the location the ACG crash test was to take place, could not reach that impact velocity without augmentation. Finally, there was a precedence of using stall speed to modify the test condition already in the regulations (14 CFR 23.562(d)). Several members of the ACG re-evaluated some of the original AGATE study database and noted that the impact speed range checked in the NTSB accident report contained or was just above the airplane's published stall speed. As a consequence, the ACG chose V_{so} (stall speed) at the MTOW.

The MTOW was selected simply to produce the maximum loads on the cabin structure. The order in which weight is added to meet the MTOW—occupants first, then fuel, then baggage—reflects the group's emphasis on cabin integrity and occupant safety.

The ACG generally supported the 30-deg impact angle with a 30-deg nose-down attitude as an appropriate choice. The two surface conditions produce essentially two different loading cases on the occupant compartment. Many other tests had also been conducted at the IDRF at this angle and attitude (References 3-3 and 3-10), thus providing a generous supply of data for comparison.

By choosing whole-airplane impact conditions, members of the ACG were not advocating widespread, full-scale crash testing of airplanes as a means of certification. The ACG recognized that full-scale testing, at current light-airplane production volumes, would be an undue economic burden to the industry. Instead, the ACG needed the crash-impact conditions and full-scale testing in order to develop a simplified means of designing and demonstrating occupant compartment integrity and airframe energy absorption.

THIS DOCUMENT PROVIDED BY THE ABBOTT AEROSPACE
TECHNICAL LIBRARY
ABBOTTAEROSPACE.COM

3.3 CRASH CONDITION BACKGROUND

Crash data for GA has been collected and analyzed in studies going back over 30 years. A brief review of the previous studies is discussed below. Much of this section comes directly from Reference 3-6.

3.3.1 1967 Crash Survival Design Guide

Early experimental data collected from full-scale crashes of light fixed-wing aircraft and helicopters were organized and presented in the U.S. Army's 1967 Crash Survival Design Guide (Reference 3-7). The information in the 1967 Design Guide has been used as a reference in many airplane and helicopter designs, and has been revised a number of times, most recently in 1989. The experimental data were presented as triangular design crash pulses corresponding to the 95th-percentile accident for light fixed-wing aircraft and helicopters. The values for the light fixed-wing pulses are shown in Table 3-4.

3.3.2 NTSB Three Phase Study

Several years later, from 1981 to 1985, the NTSB conducted a three-phase study on GA crashworthiness and occupant protection (References 3-8, 3-14, 3-15, and 3-16). In part, the NTSB performed very detailed accident reconstructions to determine the accelerations and changes in velocity for what were to be considered "survivable" accidents. These survivable crash pulse ranges are shown in Table 3-4. The NTSB noted that even though the vertical accelerations were survivable, the loads were likely to produce crippling injuries to the back and neck. According to the study findings, the then-current FAA static seat requirements of 9 G longitudinal and 3 to 6 G downward were insufficient (dynamic tests of the seat/restraint system were not required at that time). The NTSB recommended torso harnesses (shoulder belts) and vertical energy-attenuating seats as the two changes that would be most effective to protect the occupants.

3.3.3 GASP FAA Study

During the same period as the NTSB studies, the FAA requested that an independent panel be formed to recommend ways in which the FAA could promote GA safety. The General Aviation Safety Panel (GASP) was composed of a partnership of various representatives from the GA community. The panel reviewed and analyzed NTSB, NACA, and NASA accident and full-scale test data for both light airplanes and helicopters, as well as dynamic seat test data conducted by the FAA, to determine realistic dynamic performance standards for GA seat/restraint systems. The panel made its recommendation for dynamic seat testing for GA airplanes to the FAA in May 1984 (References 3-2 and 3-9). The recommendation described a dynamic seat test standard that would result in a high-strength seat that would provide occupant protection in severe, but survivable, crashes. The test conditions are described more thoroughly in Section 3.1.2 and summarized in Table 3-4. The panel also recommended including upper-torso restraint systems as mandatory equipment in all newly manufactured GA aircraft and

promoted the installation of shoulder harness on all older GA aircraft. The GASP panel reported that the use of upper-torso restraints could provide the most effective method of reducing fatal and serious injuries in GA accidents.

The FAA incorporated the GASP recommendations in two amendments to 14 CFR Part 23: Amendment 23-32 required shoulder belts for all passengers in light airplanes manufactured after December 12, 1985 (Reference 3-17); and Amendment 23-36 adopted dynamic seat/restraint system testing for airplanes certified after September 14, 1988 (Reference 3-2).

This Document Provided by the Abbott Aerospace
TECHNICAL LIBRARY
ABBOTTAEROSPACE.COM

3.3.4 AGATE Crash Conditions Study

To design a crashworthy aircraft, criteria had to be selected to produce the most crashworthy airplane while taking into consideration other constraints such as costs, manufacturing, availability of materials, and public acceptance. The test criteria called out by the FAA to certify the seat/restraint system is not necessarily the impact criteria that will afford the most occupant protection. To determine the most effective criteria, three members of the AGATE ACG conducted a study of real-world accident data in 1996 and 1997 (Reference 3-6).

The purpose of the research was two-fold:

1. Provide a crash condition or multiple crash conditions representative of “real-world” GA accidents that could then be used in the design and testing of crashworthiness systems in AGATE aircraft.
2. Identify the injuries and the injury mechanisms that occur in “real-world” GA accidents so the best combination of crashworthiness technologies could be selected for AGATE aircraft.

The study focused on current GA aircraft that are representative of what will be the AGATE aircraft. The AGATE-class airplane was defined as an all-composite, single-engine, single-pilot, fixed-wing airplane holding 2 to 6 occupants with a maximum gross weight of 6,000 lb. Only a few current GA airplanes are constructed from composites, with the majority of aircraft constructed from lightweight metals. Since the accident database for the composite aircraft is so small, aircraft constructed from all materials were included, in order to obtain a significant sample size for the database. The current fleet of airplanes is likely to represent the same pre-impact conditions as composite aircraft. However, it is likely that the composite aircraft will respond differently to an impact as compared to metal aircraft.

Cases that met the criteria of at least one fatality and at least one survivor were selected in order to avoid reviewing data that involved minor accidents and data involving catastrophic accidents that are outside the limit of survivability. From this database, the results were compared to the limits of survivability that are discussed in John Clark’s NTSB report (Reference 3-8) to see if there were any significant differences between the database results and previous GA crash studies (specifically, the GASP recommendations and the NTSB crashworthiness reports). Also, the study was conducted to find out if the previous studies were still valid with the current fleet and with AGATE-class airplanes.

This approach does not include accident data for single-occupant crashes. However, the information in the database still provided insight into the limits of survivable airplane accidents. The database selected only a sub-set of all aircraft accidents. The intent of the selected database was to be an accurate representation of aircraft accidents pertaining to AGATE-class aircraft.

The results from the AGATE study were compared to previous GA crashworthiness studies and shown to be similar. The more pertinent results of the AGATE study were presented in Section 3.3.1.

THIS DOCUMENT PROVIDED BY THE ABBOTT AEROSPACE
TECHNICAL LIBRARY
ABBOTTAEROSPACE.COM

References

3-1. Federal Aviation Regulations, Part 23, Airworthiness Standards: Normal, Utility, Acrobatic, and Commuter Category Airplanes, 14 CFR 23, Federal Aviation Administration, Washington, D.C.

3-2. 14 CFR Part 23, Amendment 23-36, "Small Airplane Crashworthiness Review Program, Amendment 1," Published in 53 FR 30802, August 15, 1988.

3-3. Terry, J. E., Hooper, S. J., and Nicholson, M., "Design and Test of an Improved Crashworthiness Small Composite Airframe," Phase II Report, Terry Engineering, Andover, Kansas; NAS1-20427, NASA Langley Research Center, Hampton, Virginia. October 1997.

3-4. Hooper, S. J., Henderson, M. J., and Seneviratne, W. P., "Design and Construction of a Crashworthy Composite Airframe," National Institute for Aviation Research - Wichita State University, Wichita, Kansas, August 9, 2001.

3-5. Henderson, M. J. and Hooper, S. J., "AGATE Composite Airframe Impact Test Results," National Institute for Aviation Research - Wichita State University, Wichita, Kansas, October 31, 2001.

3-6. Grace, G. B., Hurley, T. R., and Labun, L., "General Aviation Crash Safety Analysis and Crash Test Conditions: A Study of Accident Data from 1988 to 1995," TR-98002, Simula Technologies, Inc., Phoenix, Arizona, February 15, 1998.

3-7. Turnbow, J. W., Carroll, D. F., et al., Crash Survival Design Guide, Aviation Safety Engineering and Research, July 1967 (Revised January 1969).

3-8. Clark, J. C., "Summary Report on the National Transportation Safety Board's General Aviation Crashworthiness Project Finding," SAE 871006, Society of Automotive Engineers, Warrendale, Pennsylvania, April 1987.

3-9. Soltis, S. J., and Olcott, J. W., "The Development of Dynamic Performance Standards for General Aviation Aircraft Seats," SAE 850853, Society of Automotive Engineers, Warrendale, Pennsylvania, April 1985.

3-10. Castle, C. B., and Alfaro-bou, E., "Crash Tests of Three Identical Low-Wing Single-Engine Airplanes," NASA Technical Paper 2190, NASA Langley Research Center, Hampton, Virginia, 1983.

3-11. 49 CFR Part 571, Federal Motor Vehicle Safety Standards, Subpart 208, Occupant Crash Protection, National Highway Traffic Safety Administration, Department of Transportation, Washington, D.C., October 1, 2001.

3-12. 49 CFR Part 571, Federal Motor Vehicle Safety Standards, Subpart 214, Side Impact Protection, National Highway Traffic Safety Administration, Department of Transportation, Washington, D.C., October 1, 2001.

3-13. National Highway Traffic Safety Administration web site, http://www.nhtsa.gov, site accessed December 14, 2001.

3-14. "General Aviation Crashworthiness Project, Phase One," NTSB/SR-83/01, National Transportation Safety Board, Washington, D.C., June 27, 1983.

3-15. "General Aviation Crashworthiness Project, Phase Two – Impact Severity and Potential Injury Prevention in General Aviation Accidents," NTSB/SR-85/01, National Transportation Safety Board, Washington, D.C., March 5, 1985.

This Document Provided by the Abbott Aerospace
Technical Library
abbottaerospace.com

3-16. "General Aviation Crashworthiness Project, Phase Three – Acceleration Loads and Velocity Changes of Survivable General Aviation Accidents," NTSB/SR-85/02, National Transportation Safety Board, Washington, D.C., September 4, 1985.

3-17. 14 CFR Part 23, Amendment 23-32, "Shoulder Harnesses in Normal, Utility, and Acrobatic Category Airplanes," Published in 50 FR 46872, November 13, 1985.

This Document Provided by the ABBOTT AEROSPACE
TECHNICAL LIBRARY
ABBOTTAEROSPACE.COM

THIS DOCUMENT PROVIDED BY THE ABBOTT AEROSPACE
TECHNICAL LIBRARY
ABBOTTAEROSPACE.COM

Chapter 4
Biometrics

Jill M. Vandenburg
Anita E. Grierson

The primary objectives of crashworthy aircraft design are to prevent occupant fatalities and minimize injury during crash scenarios. To meet these objectives, aircraft designers need to have an understanding of the human body and how it responds to trauma. General knowledge of human anthropometry (Section 4.1), occupant flail envelopes (Section 4.2), and human injury tolerance (Section 4.3) will prove to be a tremendous asset to the aircraft designer during the design process. In addition, aircraft designers should also have an understanding of the types of anthropometric test devices (ATDs) that can be used to represent the human body during the design, testing, and certification of aircraft safety systems and components (Section 4.4).

4.1 HUMAN BODY ANTHROPOMETRY AND ITS APPLICATION TO AIRCRAFT DESIGN

The discipline of anthropometry is concerned with the measurement of the human body and its biomechanical characteristics. Scientific measurement techniques are used to measure body dimensions, mass properties, and joint range of motion of human volunteer subjects within a particular population. In the design of General Aviation (GA) aircraft, anthropometric measurements are used to create a comfortable, safe, and functional environment for the pilots, passengers, and crew of the aircraft. Specifically, anthropometric measurements define the dimensions of those aircraft components that directly interact with the human body, including:

- **Crew stations** - Functional reach, instrument panel design, location of primary flight controls, crew seat dimensions and comfort, seatback height, seat pan and seat cushion length and width, seat adjustment range, seat restraint system anchor locations, design eye view, etc.
- **Passenger seats** - Functional reach, seatback height, seat pan and seat cushion length and width, view of exterior, seat adjustment range, restraint system anchor locations, comfort, seat pitch, egress issues, etc.

These measurements are also used to design human and ATD computer models for aircraft simulation and analysis purposes. In addition, the anthropometric measurements are used to assess the accessibility and functionality of components related to the maintenance, repair, and overhaul of the aircraft.

Overall, the discipline of anthropometry enables aircraft designers to accommodate the wide variability in demographics that exists within the GA population of pilots, passengers, and crew. Across this population, individuals may vary in terms of age, gender, ethnicity, and health, as well as body size, shape, mass, and joint range of motion. Proper accommodation for these variable characteristics in aircraft design is imperative to enhancing the aircraft's comfort, safety, and functionality. Inadequacies in the physical dimensions of the aircraft design can lead to discomfort, fatigue, and human error.

THIS DOCUMENT PROVIDED BY THE ABBOTT AEROSPACE
TECHNICAL LIBRARY
ABBOTTAEROSPACE.COM

This section of the Design Guide will further define the role of anthropometry in GA aircraft design by discussing the:

- Structure and motion of the human body
- Sources of anthropometric differentiation
- Types of anthropometric measurements
- Presentation of anthropometric data
- Anthropometric data resources and databases.

4.1.1 Describing the Structure and Motion of the Human Body

In anthropometry, the human body is described by referencing three primary anatomical planes, several different anatomical orientations and landmarks, and the joint ranges of motion (Reference 4-1). These common references help to standardize the terminology that is used during anthropometric surveys. Figure 4-1 illustrates the three primary anatomical planes that are defined for the human body, which include:

1. Sagittal plane: partitions the body into right and left halves.
2. Coronal plane: partitions the body into front and back halves.
3. Transverse plane: partitions the body into upper and lower halves.

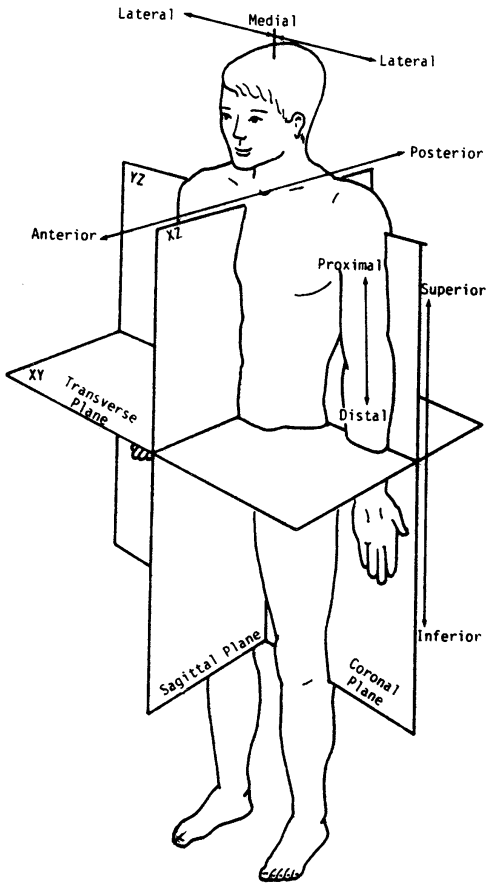


Figure 4-1.
Anatomical planes and orientations of the human body (Reference 4-1).

THIS DOCUMENT PROVIDED BY THE ABBOTT AEROSPACE
TECHNICAL LIBRARY
ABBOTTAEROSPACE.COM

Figure 4-1 also displays several common anatomical orientations for the human body that are described using directional arrows. For example, the directional arrow labeled *anterior* refers to the front side of the body, whereas the directional arrow labeled *posterior* refers to the backside of the body.

Figures 4-2 and 4-3 illustrate several common anatomical landmarks that are used to define various anthropometric measurements. For example, Figure 4-3 includes the phalange and metacarpal bones of the human hand. These bones form the metacarpal-phalangeal joints of the fingers. In order to measure the breadth of the human hand, as shown in Figure 4-4, standard anthropometric procedures state that the hand breadth should be measured between the metacarpal-phalangeal joints of the second and fifth fingers. The metacarpal-phalangeal joints of these two fingers serve as anatomical landmarks for this particular type of anthropometric measurement.

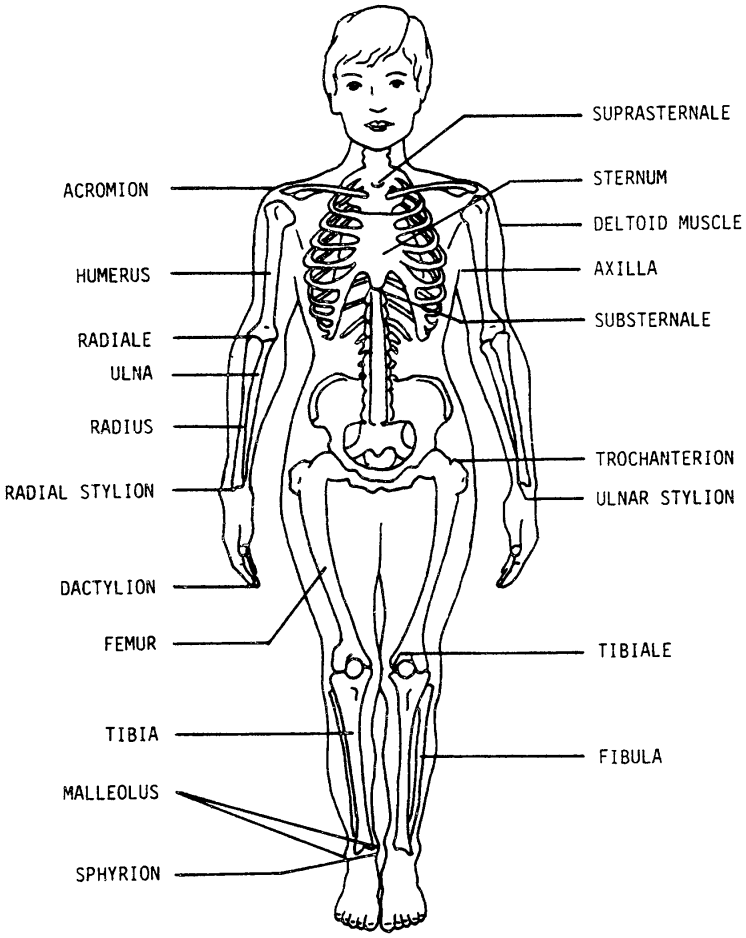


Figure 4-2.
Selected anthropometric landmarks of the human body – anterior view (Reference 4-1).

THIS DOCUMENT PROVIDED BY THE ABBOTT AEROSPACE
TECHNICAL LIBRARY
ABBOTTAEROSPACE.COM

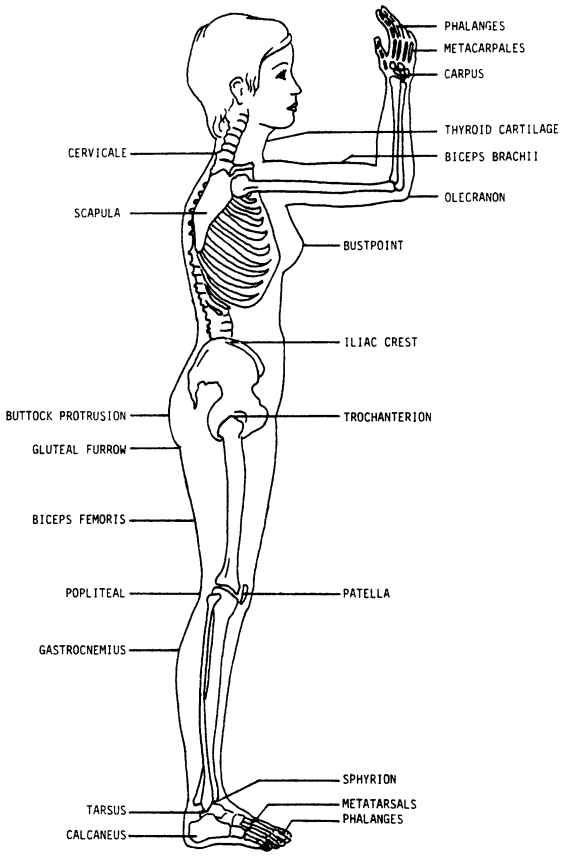


Figure 4-3.
Selected anthropometric landmarks of the human body – lateral view (Reference 4-1).

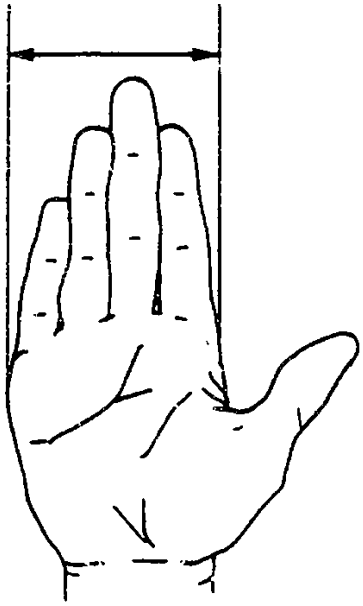


Figure 4-4.
Anthropometric measurement of the breadth of the hand (Reference 4-1).

THIS DOCUMENT PROVIDED BY THE ABBOTT AEROSPACE
TECHNICAL LIBRARY
ABBOTTAEROSPACE.COM

Finally, Figure 4-5 and Table 4-1 describe the range of motion for several different human body joints. Understanding the range of motion for all major joints in the human body is essential in the assessment of body mobility within any given environment.

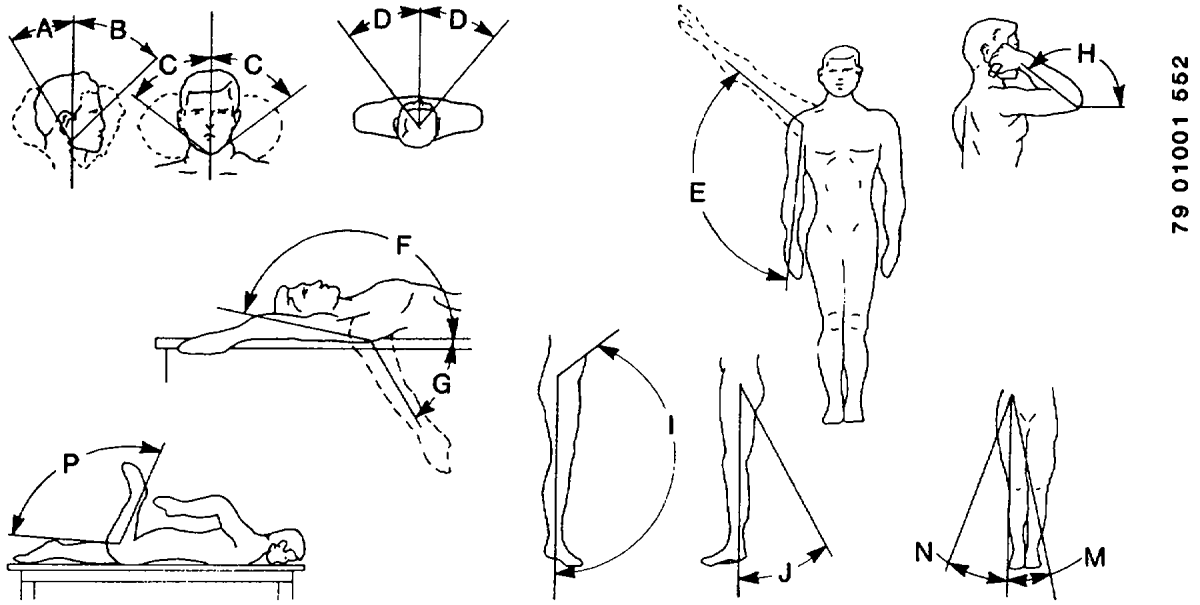


Figure 4-5.
Joint ranges of motion for various joints on the human body (Reference 4-2).

Table 4-1.
Joint ranges of motion for the human body (Reference 4-2)

Body Component Motion	Figure 4-5 Symbol	Joint Motion Description	Measured Voluntary Rotation (Deg)	Measured Forced Rotation (Deg)
Head with respect to the torso	A	Dorsiflexion	61	77
	B	Ventriflexion	60	76
	C	Lateral flexion	41	63
	D	Rotation	78	83
Upper arm at the shoulder	E	Abduction (coronal plane)	130	137
	F	Flexion	180	185
	G	Hyperextension	58	69
Forearm at the elbow	H	Flexion	141	146
Thigh at the hip	I	Flexion	102	112
	J	Hyperextension	45	54
	M	Adduction	--	--
	N	Abduction	71	79
Lower leg at the knee	P	Flexion	125	138

THIS DOCUMENT PROVIDED BY THE ABBOTT AEROSPACE
TECHNICAL LIBRARY
ABBOTTAEROSPACE.COM

4.1.2 Sources of Anthropometric Differentiation

Numerous factors contribute to the anthropometric variability within a given population. As shown in Figure 4-6, these factors can be classified into three separate categories: biological factors, environmental factors, and procedural factors (Reference 4-3). Biological factors are considered to be intrinsic to the individual and are typically genetic in nature, whereas environmental factors are considered to be extrinsic to the individual. Procedural factors involve the methods used to acquire and analyze the anthropometric data.

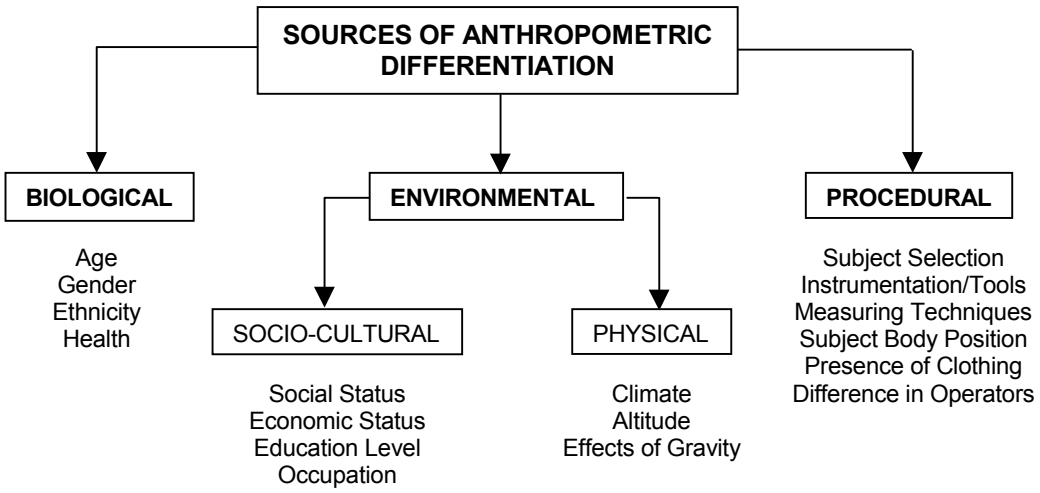


Figure 4-6.
Sources of anthropometric differentiation (Reference 4-3).

Each of the examples listed under the category headings can have a significant effect on the anthropometric characteristics of any individual within a population (Reference 4-3). For example, gender is listed as a biological factor. In the United States, on average, men are typically slightly taller and heavier than women, and generally have larger absolute body segment measurements. Common exceptions include hip breadth and circumference measurements, as well as thigh circumference measurements, which are typically larger in women. Body segment proportions also vary according to gender. For example, on average, males' arms and legs are longer than females' limbs. In addition, male arms and legs are longer in relation to stature and sitting height. Aircraft designers should recognize that these sources of anthropometric differentiation exist within any given population. As a result, it is essential for designers to be able to identify these factors and understand how they affect the population of interest. This task is accomplished by conducting an anthropometric survey of the population or using data from existing surveys.

In an anthropometric survey, a random sample of individuals is selected from the population of interest. In most cases, the selection process is not completely randomized, since the human test subjects must volunteer to participate in the study. Researchers identify potential sources of anthropometric differentiation by recording a series of pre-defined anthropometric measurements for each individual within the sample population. The measurements are selected based on the overall objectives of the anthropometric study.

THIS DOCUMENT PROVIDED BY THE ABBOTT AEROSPACE
TECHNICAL LIBRARY
ABBOTTAEROSPACE.COM

4.1.3 Types of Anthropometric Measurements

There are two different types of measurements that can be recorded during an anthropometric survey of a particular population: static measurements and dynamic measurements (Reference 4-3). Static anthropometric data consists of passive measurements of the human body including heights, lengths, circumferences, breadths, and depths. These measurements are traditionally recorded while the subject is in either a seated or standing position. For example, Figure 4-7 illustrates the conventional static measurements recorded for an individual in a seated position. Static anthropometric measurements are used to determine size and spacing requirements for the design of equipment, vehicles, aircraft, workspace layout, clothing, and computer models of the human body (Reference 4-1). Dynamic anthropometric measurements are used to describe human body movement (Reference 4-3), and measure muscular strength, joint range of motion, inertial properties of body segments, and the speed and accuracy of segment motion.

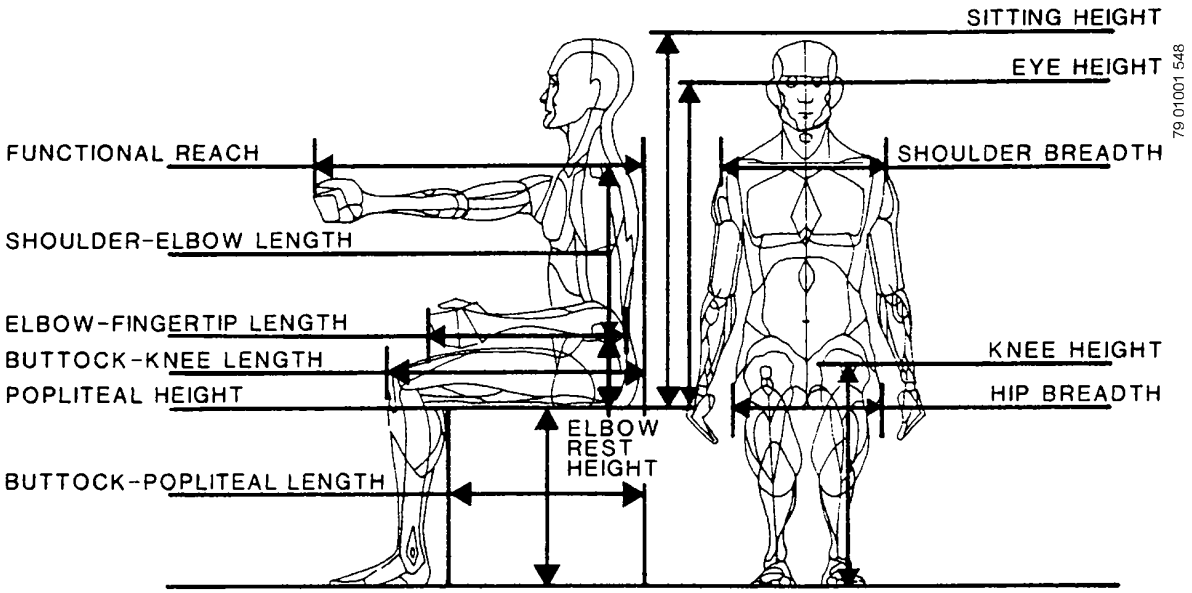


Figure 4-7.
Conventional seated anthropometric measurements (Reference 4-2).

The dynamic anthropomorphic measurements may be defined in the following manner:

- Muscular Strength Measurements: These are used to predict the ability of a human operator to perform dynamic strength tasks (Reference 4-4).
- Joint Range of Motion Measurements: Understanding the range, speed, and accuracy of motion for all major joints and segments in the human body is essential in the assessment of body mobility (Reference 4-5).
- Measurement of Inertial Properties: Inertial properties, including segment mass, volume, center of mass, and moment of inertia aid in the assessment of body mobility (Reference 4-6).

All static and dynamic anthropometric measurements are selected based on the overall objectives of the anthropometric survey.

This Document Provided by the Abbott Aerospace
TECHNICAL LIBRARY
ABBOTTAEROSPACE.COM

4.1.4 Presentation of Anthropometric Data

Anthropometric data are generally analyzed in the form of a statistical distribution. The normal, or Gaussian distribution (bell-shaped curve) is the most frequently used distribution for approximating anthropometric data such as stature, body weight, sitting height, design eye height, etc. Descriptive statistics, including mean and standard deviations, are used to further describe the distribution of anthropometric data.

Current anthropometric databases and literature references typically describe anthropometric dimensions in terms of percentiles; i.e., 5th-percentile, 50th-percentile, 95th-percentile, etc. The definition of percentile states, "A percentile value of an anthropometric dimension represents the percentage of the population with a body dimension of a certain size or smaller (Reference 4-8)." The following example illustrates the use of percentiles in presenting anthropometric data.

Example:

An aircraft designer is designing the pilot seat for an aircraft. One of the most important occupant dimensions needed for the design of the seat is the eye height of the pilot. The designer's objective is to design a seat that will accommodate a range of different design eye heights to allow different-sized pilots to efficiently fly the aircraft. To obtain this dimension, the aircraft designer locates a current anthropometric data reference or database that contains a distribution for pilot eye height. The eye height data values should be based on measurements recorded for a population that is representative of the GA population of pilots.

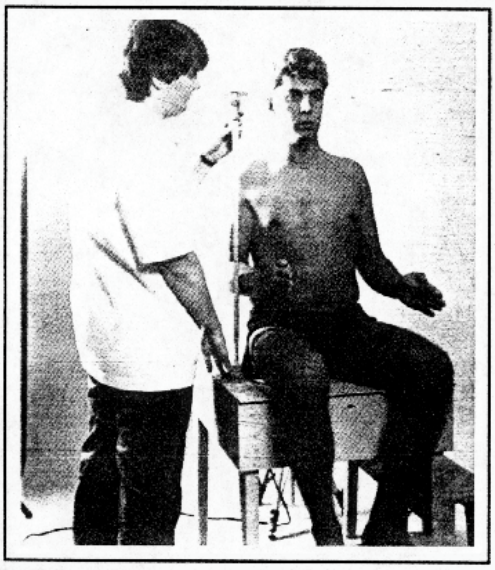
Figure 4-8 displays the format of the data that would be provided in a standard anthropometric reference text (Reference 4-9). As shown, the eye height measurements are presented in terms of a range of percentiles. For example, the 25th-percentile mark indicates that approximately 25 pct of the sample population of male pilots have an eye height less than or equal 76.88 cm (30.27 in). On the other hand, the 25th-percentile mark also indicates that approximately 75 pct of the sample population of male pilots have an eye height greater than or equal to 76.88 cm (30.27 in). It would appear desirable to design aircraft or other vehicles to accommodate the extremes of a population (1st- and 100th-percentile occupants). Unfortunately, due to space constraints and cost issues, this can become a tremendous design challenge. As a result, most engineers elect to use the 5th- and 95th-percentiles to define the range of design dimensions. This percentile range ensures that at least 90 pct of the population will be accommodated by the design.

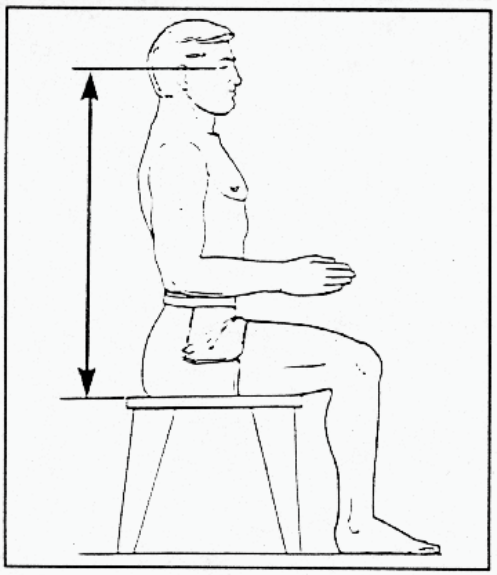
In this example, the use of percentiles for the presentation of anthropometric data allows aircraft designers to select an appropriate range for design eye height that will effectively accommodate the population of pilots that will fly the aircraft. This same methodology can be applied for all required anthropometric dimensions.

4.1.5 Anthropometric Data Resources and Databases

Anthropometric data can be obtained from a variety of sources. Resource texts and computer databases may serve as a quick and simple reference for aircraft designers. In those situations where the current anthropometric literature or databases do not provide the information required for the design, the aircraft designer can conduct his/her own anthropometric survey. The designer can also hire an outside company or organization to conduct a survey.

THIS DOCUMENT PROVIDED BY THE ABBOTT AEROSPACE
TECHNICAL LIBRARY
ABBOTTAEROSPACE.COM





THE PERCENTILES

FEMALES CM	FEMALES INCHES		MALES CM	MALES INCHES
66.40	26.14	1ST	71.18	28.02
67.21	26.46	2ND	72.11	28.39
67.74	26.67	3RD	72.70	28.62
68.46	26.95	5TH	73.50	28.94
69.60	27.40	10TH	74.76	29.43
70.38	27.71	15TH	75.61	29.77
71.01	27.96	20TH	76.29	30.04
71.56	28.17	25TH	76.88	30.27
72.06	28.37	30TH	77.40	30.47
72.52	28.55	35TH	77.88	30.66
72.96	28.72	40TH	78.34	30.84
73.39	28.89	45TH	78.79	31.02
73.82	29.06	50TH	79.23	31.19
74.25	29.23	55TH	79.66	31.36
74.68	29.40	60TH	80.10	31.54
75.13	29.58	65TH	80.56	31.72
75.61	29.77	70TH	81.04	31.90
76.13	29.97	75TH	81.55	32.11
76.71	30.20	80TH	82.13	32.33
77.37	30.46	85TH	82.78	32.59
78.21	30.79	90TH	83.61	32.92
79.43	31.27	95TH	84.80	33.39
80.20	31.57	97TH	85.56	33.68
80.75	31.79	98TH	86.10	33.90
81.59	32.12	99TH	86.93	34.23

Figure 4-8.
Design eye height for male and female U.S. Army personnel (Reference 4-9).

When searching for anthropometric data, it is important to remember to obtain the most recent data available. The more recent the data, the more accurate it will be in defining the proper dimensions for the product. The majority of the currently available anthropometric data was recorded prior to the 1980's. As a result, the data that is currently available in anthropometric literature may not be exactly representative of the United States civilian and/or military populations of today. Anthropometric data that is used for the design of newly developed GA aircraft should take into account the changes in population anthropometry.

Anthropometric surveys frequently record measurements that are required for use in a specific application (Reference 4-1). As a result, aircraft designers should verify that the selected population and the anthropometric measurements taken for the survey are applicable to their

THIS DOCUMENT PROVIDED BY THE ABBOTT AEROSPACE
TECHNICAL LIBRARY
ABBOTTAEROSPACE.COM

design needs. In addition, anthropometric data should be extracted from those surveys that have standardized and/or clearly defined the subject selection criteria and measuring techniques used during the survey. Standardization allows the anthropometric data to be compared effectively from survey to survey. This is especially true for designers who utilize CAD and CAM programs that provide anthropometric models for use in design and analysis. If the anthropometric model is not based on published anthropometric data, then the final CAD or CAM design may be inadequate for the selected population. The designer should know the source dimensions, mass properties, and joint range of motion of the CAD or CAM anthropometric model, and the model should be based on published anthropometric data that has been clearly defined for a particular population.

While there are several sources for civilian anthropometry available, the most detailed data pertains to the anthropometry of military personnel. Table 4-2 lists several useful anthropometric references for both civilian and military populations. It is important to recognize that Table 4-2 is not a complete listing of anthropometric resources, and that numerous other resource texts and computer databases are available for use in aircraft design applications.

In an effort to expand on the currently available anthropometric data, researchers at the Computerized Anthropometric Research and Design (CARD) Laboratory at Wright-Patterson Air Force Base in Dayton, Ohio, in cooperation with NATO and numerous industrial partners, are conducting a large-scale anthropometric survey of civilian populations worldwide (References 4-10 - 4-12). The anthropometric data collected from this survey will be included in a state-of-the-art database called the Civilian American and European Surface Anthropometric Resource, or CAESAR.

The primary objective of this initiative is to document the anthropometric variability of American and European adult civilians (Reference 4-11). Three-dimensional digital surface anthropometry technology will be used to measure the three-dimensional size and shape of approximately 4,000 American and 4,000 European males and females of various weights and ranging in age from 18 to 65. Using a Cyberware WB4 Whole Body Scanner, researchers will be able to generate high-resolution data of the human body's surface (Reference 4-12). The anthropometric data acquired from these 3-D whole-body digital images will be easily transferred to CAD or CAM tools to be used for applications involving the design of industrial workstation layouts, automobiles, aircraft, apparel, and protective equipment.

The three populations (United States, Italy, and the Netherlands) were selected for the large-scale anthropometric survey based on their unique anthropometric characteristics (Reference 4-11):

- The United States represents the NATO nation with the largest population.
- Italy represents the NATO nation with the shortest population.
- The Netherlands represents the NATO nations with the tallest populations.

The sample populations that are selected from the three larger populations will be comprised of individuals representing a wide variety of ethnic groups, socio-economic classes, and geographic regions. The data collection methods will be standardized in order to continually update the database with the data recorded from future anthropometric surveys. Future surveys plan to target additional age groups and populations in other European countries. The project was scheduled to be completed by the end of 2000 (Reference 4-1).

THIS DOCUMENT PROVIDED BY THE ABBOTT AEROSPACE
TECHNICAL LIBRARY
ABBOTTAEROSPACE.COM

Table 4-2.
Examples of anthropometric data references

YEAR	AUTHOR(S) AND AFFILIATION	TITLE AND DESCRIPTION	REF NO.
1991	Donelson, S. M., and Gordon, C. C., U.S. Army Natick Research, Development, and Engineering Center	**1988 Anthropometric Survey of U.S. Army Personnel: Pilot Summary Statistics**	4-9
1993	Tilley, A. R., Henry Dreyfuss Associates	**The Measure of Man and Woman, Human Factors in Design** Data for children through elderly; contains 1st- through 99.5th-percentile dimensions	4-13
1990	Griener, T. M., and Gordon, C. C., U.S. Army Natick Research, Development, and Engineering Center	**An Assessment of Long-term Changes in Anthropometric Dimensions: Secular Trends of U.S. Army Males**	4-14
1989	Gordon, C. C., Bradtmiller, B., and Churchill, T., et al., U.S. Army Natick Research, Development, and Engineering Center	**1988 Anthropometric Survey of U.S. Army Personnel: Methods and Summary Statistics** Data for U.S. Army men and women; contains 1st- through 99th-percentile dimensions for both females and males	4-15
1988	Robinette, K., Fowler, J., Wright-Patterson Air Force Base	**An Annotated Bibliography of the United States Air Force Engineering Anthropometry, 1946-1988**	4-16
1987	Harry G. Armstrong Aerospace Medical Research Laboratory at Wright-Patterson AFB	**Anthropometry and Mass Distribution for Human Analogues, Vol. 1: Male Military Aviators**	4-17
1987	Salvendy, G.	**Handbook of Human Factors** Fundamentals of human factors and design	4-18
1983	Young, J. W., Chandler, R. F., and Snow, C. C., Civil Aeromedical Institute	**Anthropometric and Mass Distribution Characteristics of the Adult Female**	4-19
1983	Reynolds, H. M., and Leung, S. C., Aerospace Medical Research Laboratory at Wright-Patterson Air Force Base	**A Foundation for Systems Anthropometry: Lumbar/Pelvic Kinematics**	4-20
1983	Schneider, L. W., et al., University of Michigan	**Development of Anthropometrically Based Design Specifications for an Advanced Adult Anthropomorphic Dummy Family, Volume 1** Data for adult ATDs used to test automobiles and aircraft	4-21
1982	Easterby, R., Kroemer, K. H. E., Chaffin, D. B.	**Anthropometry and Biomechanics: Theory and Application** Collection and application of anthropometric principles	4-22
1982	Reynolds, H. M., Snow, C. C., and Young, J. W., Civil Aeromedical Institute	**Spatial Geometry of the Human Pelvis**	4-23
1982	Vaughn, C. L., Andrews, J. G., and Hay, J. G.	**Selection of Body Segment Parameters by Optimization**	4-24
1981	Chandler, R. F., and Young, J., Civil Aeromedical Institute	**Uniform Mass Distribution Properties and Body Size Appropriate for the 50 Percentile Male Aircrewmember During 1980-1990**	4-25
1981	Gregoire, H. G., and Slobodnik, B., Naval Air Test Center	**The 1981 Naval and Marine Corps Aviation Anthropometric Survey**	4-26
1980	McConville, J. T., et al., AFAMRL	**Anthropometric Relationships of Body and Body Segment Moments of Inertia** Volume, center of volume, and principal moments of inertia for 31 male subjects	4-27

THIS DOCUMENT PROVIDED BY THE ABBOTT AEROSPACE
TECHNICAL LIBRARY
ABBOTTAEROSPACE.COM

Table 4-2. (continued)
Examples of anthropometric data references

YEAR	AUTHOR(S)	TITLE/DESCRIPTION	REF NO.
1978	Laubach, L. L., McConville, J. T., and Tebbetts, I., Webb Associates	**Anthropometric Source Book, Volumes 1, 2, And 3** Comprehensive handbook of anthropometric data and applications of the data; also provides an annotated bibliography of 236 references covering topics in physical anthropology, anthropometry, and applications of anthropometric data in sizing and design	4-28
1977	Churchill, E., et al.	**Anthropometry of Women in the U.S. Army**	4-29
1977	Snyder, R. G., Schneider, L. W., and Owings, C. L.	**Anthropometry of Infants, Children, and Youths to Age 18 for Product Safety Design** Data for 2-18 year-olds	4-30
1976	Atkins, E. R., Dauber, R. L., Karas, J. N., and Pfaff, T. A., Vought Corporation	**Study to Determine the Impact of Aircrew Anthropometry on Airframe Configuration**	4-31
1975	Chandler, R. F., et al.	**Investigation of Inertial Properties of the Human Body** Moments of inertia with respect to six axes for fourteen segments of six cadavers; principal moments of inertia	4-32
1975	Reynolds, H. M., Clauser, C. E., and McConville, J.	**Mass Distribution Properties of the Male Cadaver**	4-33
1974	Kroemer, K. H. E., Aerospace Medical Research Laboratory at Wright-Patterson, Air Force Base	**Designing for the Muscular Strength of Various Populations**	4-34
1973	Walker, L. B., Harris, E. H., and Pointius, U. R.	**Mass, Volume, Center of Mass, and Moment of Inertia of Head and Head and Neck of the Human Body** Male cadaver data	4-35
1972	Becker, E. B.	**Measurement of Mass Distribution Parameters of Anatomical Segments**	4-36
1972	Clauser, C. E., et al., Wright-Patterson Air Force Base	**Anthropometry of Air Force Women**	4-37
1971	Churchill, E., et al., U.S. Army Natick Laboratories	**Anthropometry of U.S. Army Aviators - 1970** U.S. Army male aviators	4-38
1971	White, R. M., and Churchill, E., U.S. Army Natick Laboratories	**The Body Size of Soldiers – U.S. Army Anthropometry – 1966** U.S. Army male non-aviators	4-39
1970	Kroemer, K. H. E., Aerospace Medical Research Laboratory at Wright-Patterson, Air Force Base	**Human Strength: Terminology, Measurement, and Interpretation of Data**	4-40
1969	Clauser, C. E., McConville, J. T., and Young, J. W.	**Weight, Volume, and Center of Mass of Segments of the Human Body** Center of mass locations for cadaver body segments; developed regression equations	4-41
1969	Laubach, L. L., Aerospace Medical Research Laboratory at Wright-Patterson Air Force Base	**Body Composition in Relation to Muscle Strength and Range of Joint Motion**	4-42
1968	Singley and Haley	**Models and Analogues for the Evaluation of Human Biodynamic Response, Performance, and Protection** Segment mass, center of mass, and skeletal joint locations for a 50th-percentile U.S. Army male aviator	4-43
1967	Dempster, W. T., Wright Air Development Center	**Space Requirements for the Seat Operator** Moments of inertia, mass, and center of mass locations measured on cadaver body segments; link lengths between effective joint centers for major body parts	4-44

THIS DOCUMENT PROVIDED BY THE ABBOTT AEROSPACE
TECHNICAL LIBRARY
ABBOTTAEROSPACE.COM

Table 4-2. (continued)
Examples of anthropometric data references

YEAR	AUTHOR(S)	TITLE/DESCRIPTION	REF NO.
1967, 1955	Dempster, W. T., and Gaughran, G. R. L.	**Properties of Body Segments Based on Size And Weights** Moments of inertia, mass, and center of mass locations measured on cadaver body segments; link lengths between effective joint centers for major body parts	4-45
1966	Laubach, L. L., Aerospace Medical Research Laboratory at Wright-Patterson Air Force Base	**Muscle Strength, Flexibility, and Body Size of Adult Males**	4-46
1965	Gifford, E. C., Provost, J. R., and Lazo, J., Aerospace Crew Equipment Lab, Department of the Navy	**Anthropometry of Naval Aviators – 1964**	4-47
1963	Santschi, W. R., DuBois, J., and Ornoto, C.	**Moments of Inertia and Centers of Gravity of the Living Human Body** Moments of inertia of live human subjects in a seated position	4-48
1962	Swearingen, J. J., Civil Aeromedical Research Institute	**Determination of Centers of Gravity of Man** Centers of gravity for adult males	4-49
1959	Buck, C. A., et al.	**Study of Normal Range of Motion in the Neck Utilizing a Bubble Goniometer** Range of motion of the head-neck complex	4-50
1937	Glanville, A. D., and Kreezer, G.	**The Maximum Amplitude and Velocity of Joint Movements in Normal Male Human Adults** Joint angles of motion for the movements illustrated in Figure 4-5	4-51

4.2 OCCUPANT FLAIL ENVELOPES

The available flail volume surrounding the occupant in an aircraft is typically referred to as the occupant's flail envelope. The occupant flail envelope can vary significantly depending on several factors, including, but not limited to, the type of torso restraint, the restraint anchorage points, the magnitude and direction of the crash deceleration, the initial slack and initial position of the restraint webbing on the occupant, the amount of webbing stored on the inertia reel spool, the occupant's size/weight, the deformation of the cabin interior, etc. Because of these variables, it is not possible to fully predict the occupant flail envelope in an actual crash, or even to predict the ATD response during seat qualification testing. Therefore, the flail envelopes provided in this section are recommended for use only for the initial design trade studies. Detailed computer simulation and/or dynamic testing will ultimately be required to fully define the occupant flail envelope for each unique aircraft/restraint configuration.
Figures 4-9 through 4-11 illustrate occupant flail envelopes for a 95th-percentile male ATD with a five-point restraint (Reference 4-52). The restraint consists of a lap belt, lap belt tie-down strap, and two shoulder straps. The motions shown are based on test data obtained during a 30-G forward impact test pulse with a velocity change of 50 ft/sec. Even though this test pulse is more severe than the current GA test requirements, it is recommended that all aircraft interior components within the extremity flail envelopes shown be designed to minimize impact injuries.

The flail envelope of the head is the primary concern when designing an aircraft's interior. If at all possible, there should be no aircraft components within the occupant's head flail envelope. Therefore, the aircraft designer must have information on the anticipated head flail envelope early in the design process.

THIS DOCUMENT PROVIDED BY THE ABBOTT AEROSPACE
TECHNICAL LIBRARY
ABBOTTAEROSPACE.COM

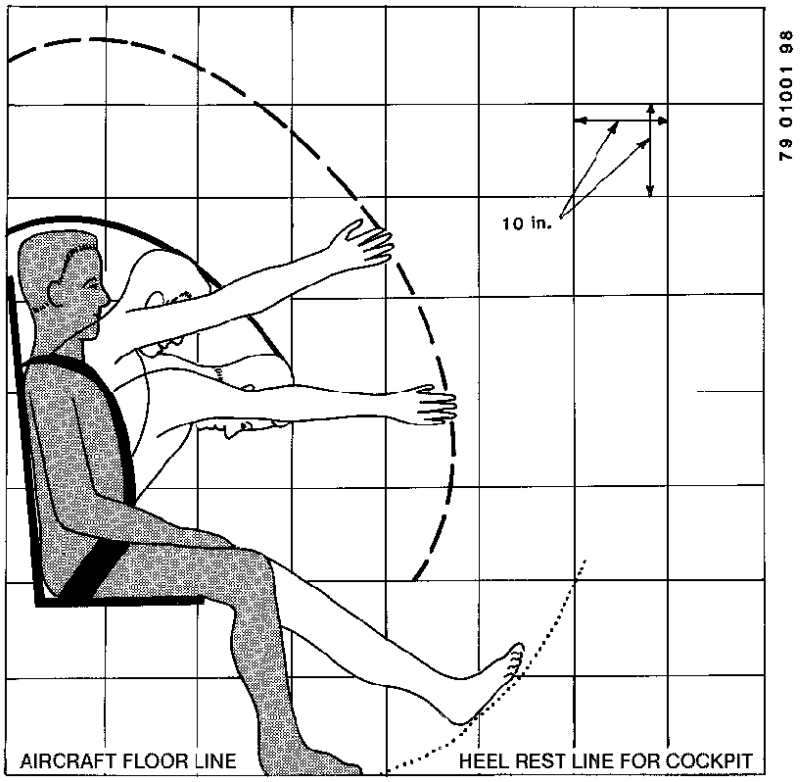


Figure 4-9.
Flail envelope for the 95th-percentile ATD wearing a five-point restraint - side view.

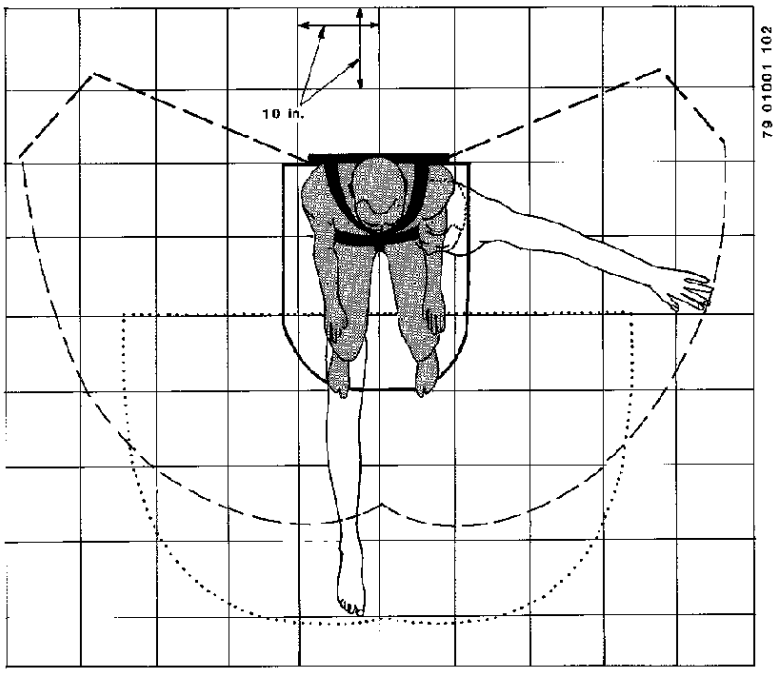


Figure 4-10.
Flail envelope for the 95th-percentile ATD wearing a five-point restraint - top view.

THIS DOCUMENT PROVIDED BY THE ABBOTT AEROSPACE
TECHNICAL LIBRARY
ABBOTTAEROSPACE.COM

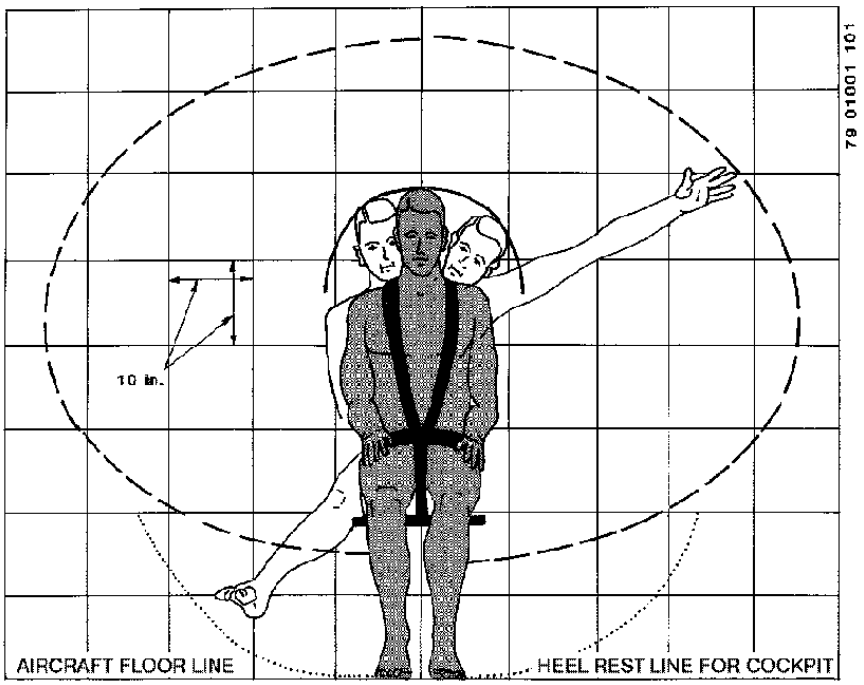


Figure 4-11.
Flail envelope for the 95th-percentile ATD wearing a five-point restraint - front view.

As previously mentioned, the occupant's flail envelope can be influenced by a number of factors, but the most influential factor is the type of occupant restraint used. To show some of the effects of restraint configuration, a series of sled tests were recently conducted to evaluate alternative restraint types for use in AGATE aircraft (References 4-53 and 4-54).

Four restraint types were evaluated using the standard FAA forward-impact test pulse (a nominal 26-G triangle pulse with a 42-ft/sec velocity change), except there was no yaw angle. A 50th-percentile male ATD was utilized. The restraint types evaluated were a conventional three-point harness (baseline), a three-point harness with a shoulder belt pre-tensioner, a three-point harness with a buckle pre-tensioner, and the three-point Inflatable Tubular Torso Restraint (ITTR™) currently in development at Simula Inc. The seat back recline angle was 20 deg from vertical.

Figures 4-12 and 4-13 show the trajectories of the ATD head center of gravity (c.g.) from the initial head position. Markers are shown at 10-msec intervals for reference. The ITTR provided significant improvement over the baseline restraint in terms of peak head excursion. The shoulder belt pre-tensioner also reduced the forward displacement, and the buckle pre-tensioner reduced the vertical displacement. More details and other benefits of the alternate restraints are discussed in Chapter 8.

™ITTR is a registered trademark of Simula, Inc.

THIS DOCUMENT PROVIDED BY THE ABBOTT AEROSPACE
TECHNICAL LIBRARY
ABBOTTAEROSPACE.COM

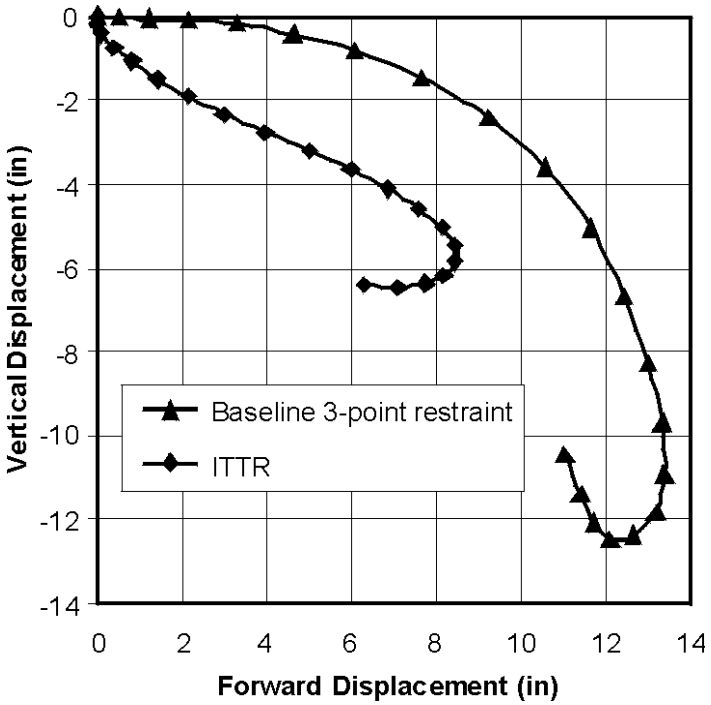


Figure 4-12.
Relative head displacement for the 50th-percentile ATD; three-point restraint and ITTR.

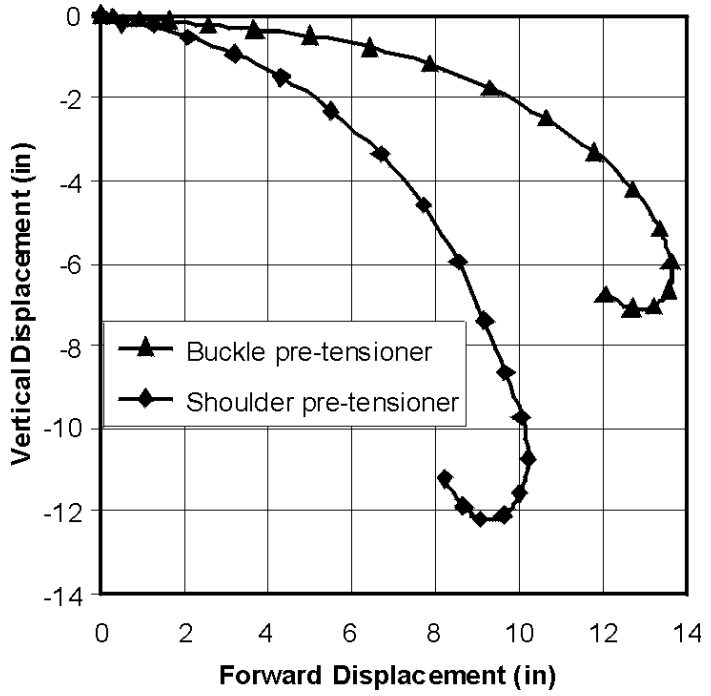


Figure 4-13.
Relative head displacement for the 50th-percentile ATD; three-point restraint with buckle pre-tensioner and shoulder belt pre-tensioner.

THIS DOCUMENT PROVIDED BY THE ABBOTT AEROSPACE
TECHNICAL LIBRARY
ABBOTTAEROSPACE.COM

Note that the graphs show the head c.g. displacement and not the head flail envelope. The head flail envelope can be estimated by adding a radius of approximately 4.0 in. to the envelopes shown. Another important consideration is that the envelopes do not include the effects of seat stroke. A combined vertical/longitudinal crash will increase the vertical displacement relative to the cabin by approximately the same magnitude of the seat stroke. Depending on the seat design, this will typically be approximately 4.0 in.

Again, it should be noted that even though the previously shown flail envelopes are based on the current FAA seat qualification test pulse, the results are recommended to be used only for initial design trade studies and to show the relative performance of alternate restraint systems.

4.3 HUMAN TOLERANCE TO INJURY

The objective of this section is to provide the designers and regulators of GA aircraft systems with information on human tolerance to injury. In the dynamic impact environment, several factors can affect the human body's response to impact. Specifically, it is important to characterize the accelerative conditions and the direction, duration, rate, and distribution of loading on the occupant. Limiting the accelerations and applied loads to levels that are tolerable by the human body will help to reduce the overall risk of occupant injury. Knowledge in this area is an integral part of the design process of crashworthy aircraft.

Considerable research has been conducted in the area of biodynamics and human tolerance to injury. Unfortunately, the body of research is not complete, and many areas of uncertainty remain. Some of the research has led to the establishment of human tolerance guidelines for the design of GA aircraft. These guidelines are specified in FAR 23.562, and provide detailed tolerance requirements for the head, chest, and lumbar spine. In addition, guidelines for the abdominal region are defined in terms of lap belt requirements.

The information presented in this section is intended to provide aircraft designers with a broader perspective of the crashworthy design process as it relates to human injury tolerance and occupant protection. Topics that will be focused on include:

- Factors that affect the application of human tolerance criteria
- Injury mechanisms, tolerances, and regulations that are related to various segments of the human body
- Types of injury scales that are employed in injury tolerance research.

4.3.1 Factors Affecting Application of Human Tolerance

Human tolerance to impact is dependent upon a number of factors; specifically, load direction, load duration, load rate, the types of physiological structures loaded, load distribution, and previous loading history. In the dynamic impact environment, there are a number of factors that will determine the human tolerance to injury and the subsequent injury criteria that is utilized. These conditions can be separated into three distinct categories: biological variability, restraint conditions, and crash conditions.

4.3.1.1 Biological Variability

Human tolerance values are determined through experimentation with whole cadavers, tissue specimens, and animals, and through computational analyses. The tolerance of the body to impact can vary greatly among individuals. Human tolerance values also generally vary with

This Document Provided by the Abbott Aerospace
TECHNICAL LIBRARY
ABBOTTAEROSPACE.COM

age, gender, size, and physical condition. It should be noted that human tolerance values are often determined from cadaveric specimens that are older and, prior to their death, were in relatively poor physical health.

4.3.1.2 Restraint System

The type of restraint system utilized will influence the loading that the occupant experiences. Common restraints vary from the two-point lap belts used in commercial large aircraft transportation, to the three-point lap and shoulder belts used in automobiles and some GA aircraft, and the four- and five-point harness restraints used in some military aircraft.

Two-Point Lap Belt

When restrained only by a two-point lap belt, the occupant's tolerance to abrupt acceleration is relatively low. Laananen has provided a complete analysis of the effects of lap-belt-only restraint on human tolerance (Reference 4-55). Laananen reviewed all available existing data from dynamic testing of volunteer human subjects applicable to transport aircraft crash conditions and established minimum human tolerance levels for transport aircraft seat design. Since the data were acquired in human subject testing, the tolerance levels are only minimum levels and survivable tolerance levels may be substantially higher.

In forward-facing seats, a longitudinal impact will cause a rotation of the upper torso over the belt, a whipping action of the head, and often the impact of the upper torso or head on interior components or upon the occupant's legs, resulting in chest, head, and neck injuries. Head injuries due to impacts with the surrounding environment are very common for occupants restrained only with lap belts. When longitudinal forces are combined with a vertical component, there is a tendency for the occupant to slip under the belt to some degree. This motion, often referred to as submarining, can shift the belt up over the abdomen. The longitudinal component of the pulse then causes the upper torso to flex over the belt, with the restraining force concentrated at some point on the spine and not on the pelvic girdle. In this configuration, tolerance to acceleration is extremely low and internal injury is likely.

Three- and Five-Point Restraint Systems

The addition of a shoulder harness greatly reduces the potential for injury from head and chest impacts and helps to maintain proper spinal alignment for strictly vertical impact forces. However, this three-point configuration may not be optimal for impacts with both vertical and longitudinal components. Pressure by the upper torso against the shoulder straps causes these straps to pull the lap belt up into the abdomen and against the lower margin of the rib cage. This movement of the lap belt allows the pelvis to move forward under the lap belt, causing severe flexing of the spinal column, as shown in Figure 4-14.

In this flexed position, the vertebrae are very susceptible to anterior compression fracture and, if the lap belt slips off the top of the pelvic bone structure (over the top of the iliac crests), severe injury can occur as a result of crushing of the viscera. A lap belt tiedown strap, similar to that used in five-point restraint systems, prevents the raising of the lap belt by the shoulder harness and may nearly double the tolerance to impact forces. However, five-point restraint systems are typically only used in military aircraft crewseats. This type of restraint system consists of a lap belt tiedown strap, left- and right-side lap belts, and left-and right-side shoulder straps connected by a single-point release buckle.

THIS DOCUMENT PROVIDED BY THE ABBOTT AEROSPACE
TECHNICAL LIBRARY
ABBOTTAEROSPACE.COM

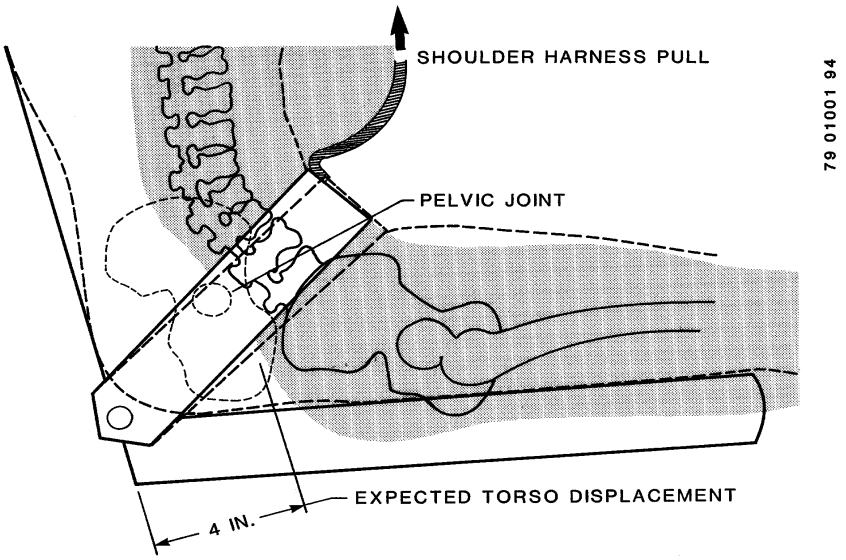


Figure 4-14.
Movement of the lap belt into the soft tissue of the abdomen and resultant spinal flexing.

The amount of slack and the load-elongation characteristics of a restraint system can affect the human survivability with a given acceleration pulse. For instance, a restraint system with no slack but with high-elongation webbing would tend to load the belt and occupant early in the crash pulse, but would also stretch more, thereby increasing the opportunity for the occupant to be injured by a secondary impact with the airplane interior. On the other hand, a restraint system with low-elongation webbing but with slack in the system can also affect survivability. In this case, the inertia of the occupant will cause him/her to maintain a near-constant velocity, independent of the decreasing velocity of the seat and vehicle, until the slack in the restraint system is taken up. As this point is reached, the velocity of the occupant is abruptly changed to match that of the seat, resulting in high G levels. This is often referred to as dynamic overshoot. Specifically, dynamic overshoot is a complex phenomenon involving the elasticity, geometry, mass distribution, and thus the natural frequency of the occupant, and the restraint and seat systems. Ultimately, it would be ideal to design a stiff restraint system with little slack that will load early. However, even in the ideal situation, the loads and accelerations may become too high for the tolerance levels of the occupant. These problems can be overcome through the use of pre-tensioners and load-limiters, as discussed in Chapter 8.

4.3.1.3 Crash Conditions

Much of what is known about human tolerance to injury is based upon controlled experiments in which only one direction or one type of loading is applied to the occupant. Specifically, the majority of the human tolerance values that have been obtained have been determined from uni-axial loading. However, “real-world” crashes are not as simple as experimental procedures. They often involve multi-axis loading and multiple impacts in which a subsequent impact may be more severe than the initial impact (e.g., an initial impact with a tree and a subsequent impact on the ground). Following the initial impact, the occupant may sustain certain types of injuries, thereby increasing his/her susceptibility to further injuries during any secondary impacts.

This Document Provided by the Abbott Aerospace
TECHNICAL LIBRARY
ABBOTTAEROSPACE.COM

4.3.2 Use of Anthropomorphic Test Devices (ATDs)

In determining the injury potential in a crash event or dynamic test situation, the design engineer is often limited to the use of ATDs to simulate the response of a human. The ATDs are designed to represent a certain size of individual; for example, the 5th-percentile female, 50th-percentile male, or 95th-percentile male. These test devices do not seek to represent the whole population, nor are they able to fully represent all of the features of a living human. For example, muscles and soft tissue are not represented in the ATD. When used in research and testing environments, the ATD can limit the accuracy of the human tolerance data that is collected.

4.3.3 Whole-Body Acceleration Tolerance

The tolerance to whole-body acceleration is dependent upon the direction of loading. In general, whole-body acceleration is not used as a tolerance criteria in GA design regulations. This results from the differences in the performance of typical seats and restraint systems. However, evaluation of whole-body acceleration can be useful when making general estimations during the initial phase of aircraft design. Therefore, the following section will discuss spineward, sternumward, headward, tailward, and lateral accelerations. It will also introduce the theory behind the Eiband curve and the concept of injury tolerance as a function of acceleration duration.

4.3.3.1 Spineward Acceleration

The magnitude and duration of the applied accelerative force have definite effects on human tolerance, as shown in Figure 4-15 (Reference 4-56). As indicated by this curve, a spineward chest-to-back accelerative force of 45 G has been tolerated voluntarily by some subjects when the pulse duration is less than 0.044 sec. Under similar conditions, when the duration is increased to 0.2 sec, the tolerable magnitude is reduced to about 25 G. Accordingly, Figure 4-15 shows that the tolerable limits on acceleration loading are a function of duration.

Note: The whole-body tolerance data displayed in Figure 4-15 were collected for a variety of full-torso restraints and, in some cases, head restraints. With less-than-optimum restraints, the tolerable level will be significantly reduced, and some debilitation and injury will occur.

With respect to whole-body deceleration, the rate of onset of the applied force also has a definite, although not yet well understood, effect on human tolerance. Under some impact conditions, the rate of onset appears to be a determining factor, as indicated by the diagram in Figure 4-16 (Reference 4-56). Lower rates of onset were more tolerable than higher rates under the test conditions present. Under other impact conditions, such as the extremely short duration that occurs in impacts from free falls, rates of onset as high as 28,000 G/sec were survivable and appeared to have little effect on human tolerance (Reference 4-57). It appears that in certain ranges, the effects of the rate of onset are related to the natural frequencies of the body and of the various body organs (Reference 4-58).

4.3.3.2 Sternumward Acceleration

The human tolerance limit for sternumward (back to chest, eyeballs in), $+G_X$ acceleration has not yet been accurately established. Due to the high degree of restraint provided by a full-length seat back in this configuration, it can be safely assumed that maximum tolerated acceleration is greater than for spineward acceleration. A maximum of 83 G measured on the chest with a base duration of 0.04 sec was experienced during one run in a backward-facing seat. However, the subject was extremely debilitated, went into shock following the test, and

THIS DOCUMENT PROVIDED BY THE ABBOTT AEROSPACE
TECHNICAL LIBRARY
ABBOTTAEROSPACE.COM

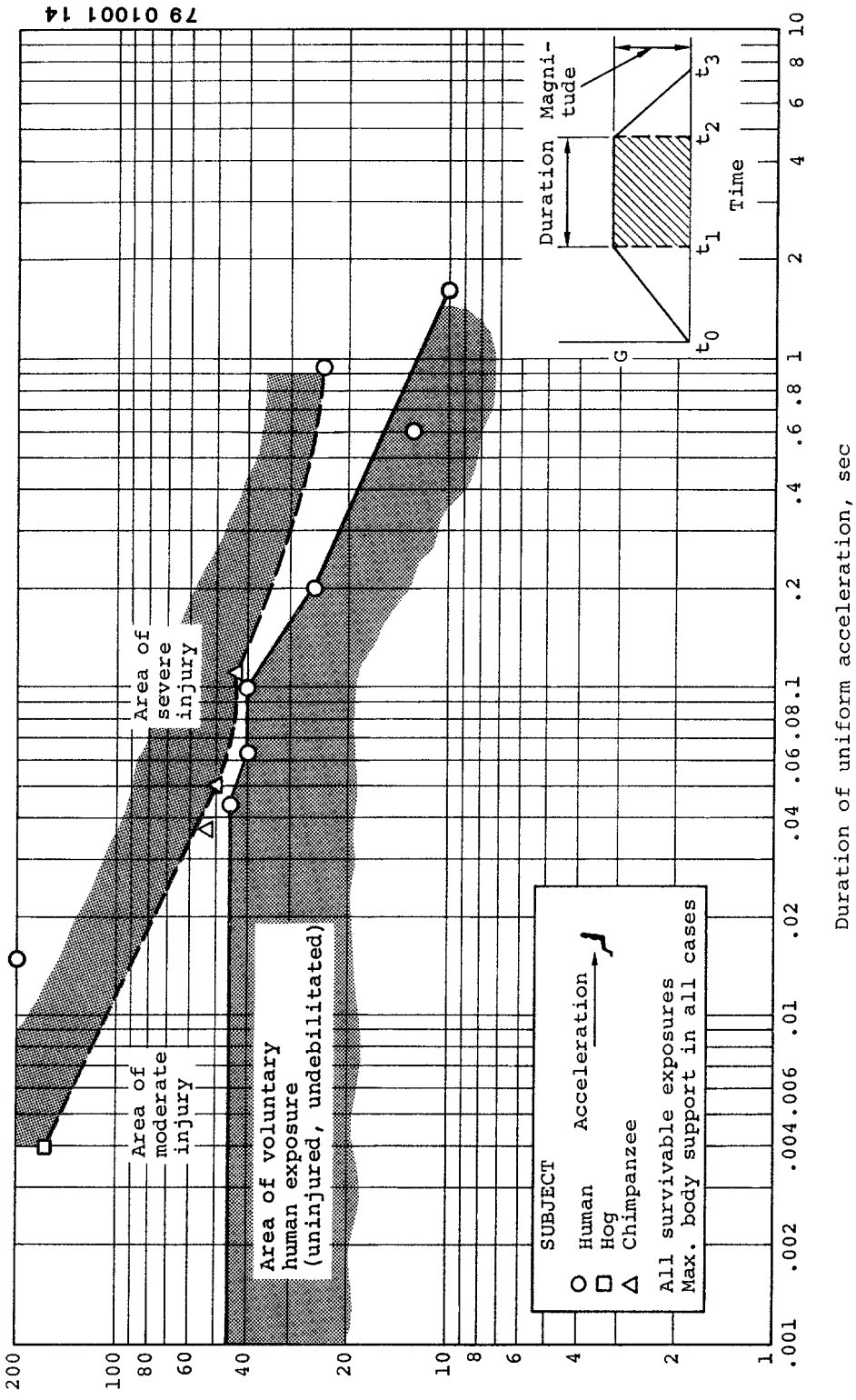


Figure 4-15.
Spineward (chest-to-back) accelerative forces.

THIS DOCUMENT PROVIDED BY THE ABBOTT AEROSPACE
TECHNICAL LIBRARY
ABBOTTAEROSPACE.COM

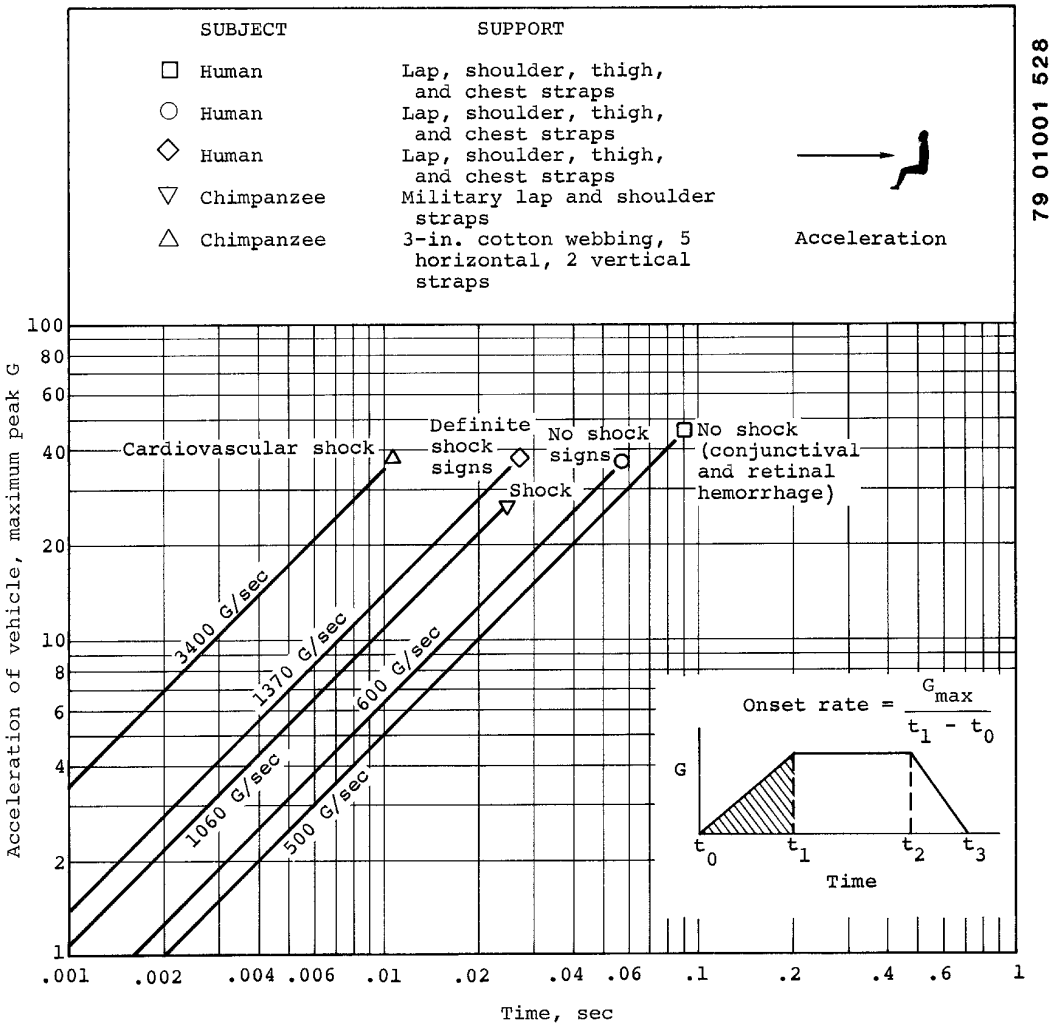


Figure 4-16.
Spineward (chest-to-back) accelerative forces.

required on-the-scene-medical treatment (Reference 4-57). Human tolerance to sternumward acceleration, therefore, probably falls somewhere between this figure of 83 G for 0.04 sec and 45 G for 0.1 sec, which is the accepted end point for the $-G_X$ (eyeballs-out) case.

4.3.3.3 Headward Acceleration

The human body is able to withstand a much greater force when the force is applied perpendicular to the long axis of the body in a forward or backward direction (G_X) than when applied parallel to the long axis (G_Z). This is shown by a comparison of the curves in Figures 4-15 and 4-17. A primary reason for the significantly lower tolerance to headward ($+G_Z$) loading is the susceptibility of the lumbar vertebrae, which must support most of the upper torso load, to compression fracture. Spinal alignment is a significant consideration in the determination of the human tolerance value.

THIS DOCUMENT PROVIDED BY THE ABBOTT AEROSPACE
TECHNICAL LIBRARY
ABBOTTAEROSPACE.COM

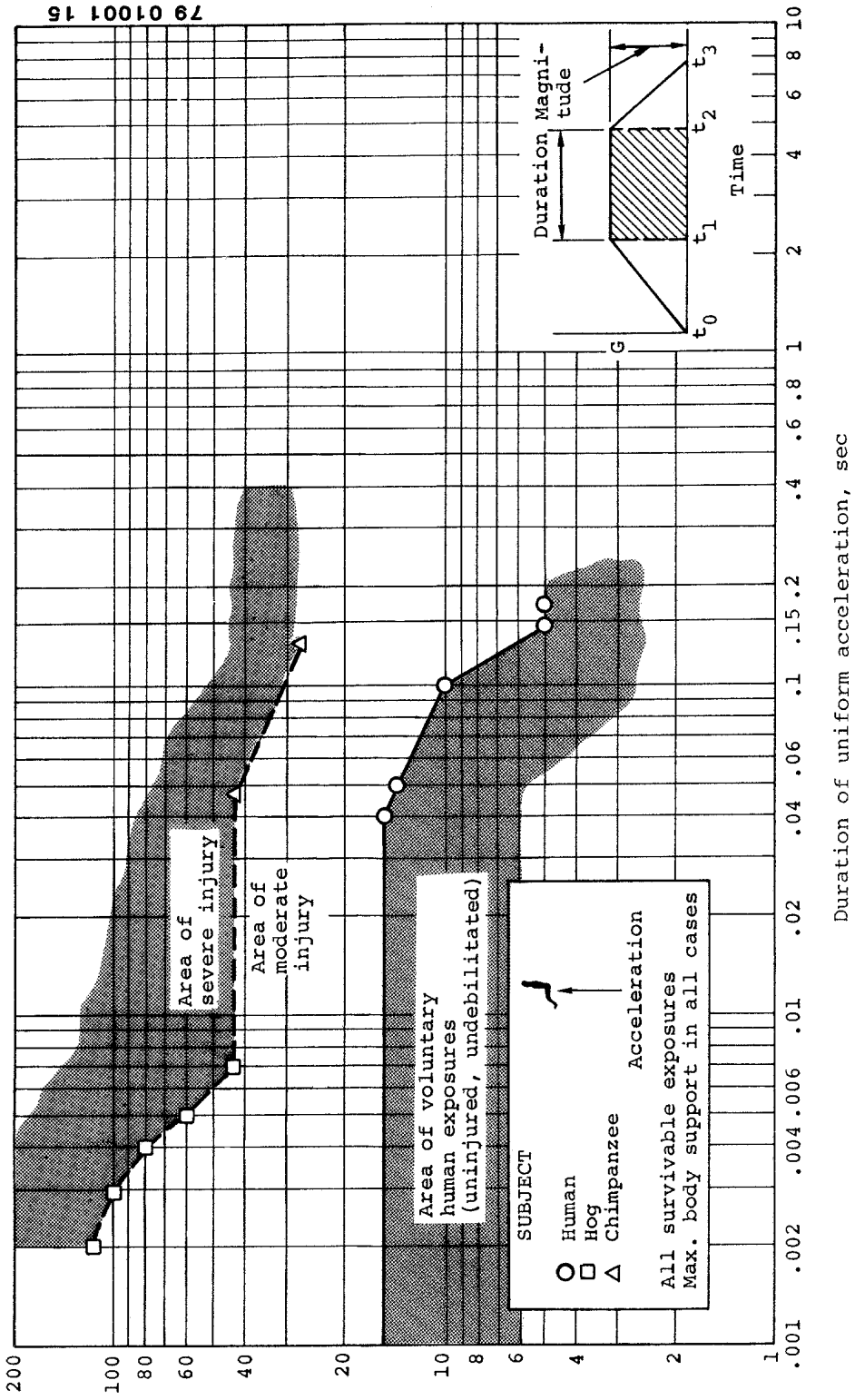


Figure 4-17.
Headward accelerative forces.

THIS DOCUMENT PROVIDED BY THE ABBOTT AEROSPACE
TECHNICAL LIBRARY
ABBOTTAEROSPACE.COM

The skeletal configuration and mass distribution of the body are such that vertical loads cannot be distributed over as large an area as can loads applied forward or aft (G_X). These vertical loads, therefore, result in greater stress per unit area than do sternumward or spineward loads. Finally, along the direction of the long axis, the body configuration allows for greater displacement of the viscera within the body cavity. Forces applied parallel to the long axis of the body, headward or tailward (G_Z), place greater stain on the suspension system of the viscera than do forces applied sternumward or spineward (G_X), thereby increasing the susceptibility of the viscera to injuries.

As in the case of the longitudinal direction (Figure 4-16), rate of onset also affects the tolerance to vertical accelerative loads; however, insufficient data were available to establish the limits. Figure 4-18 presents one set of available data.

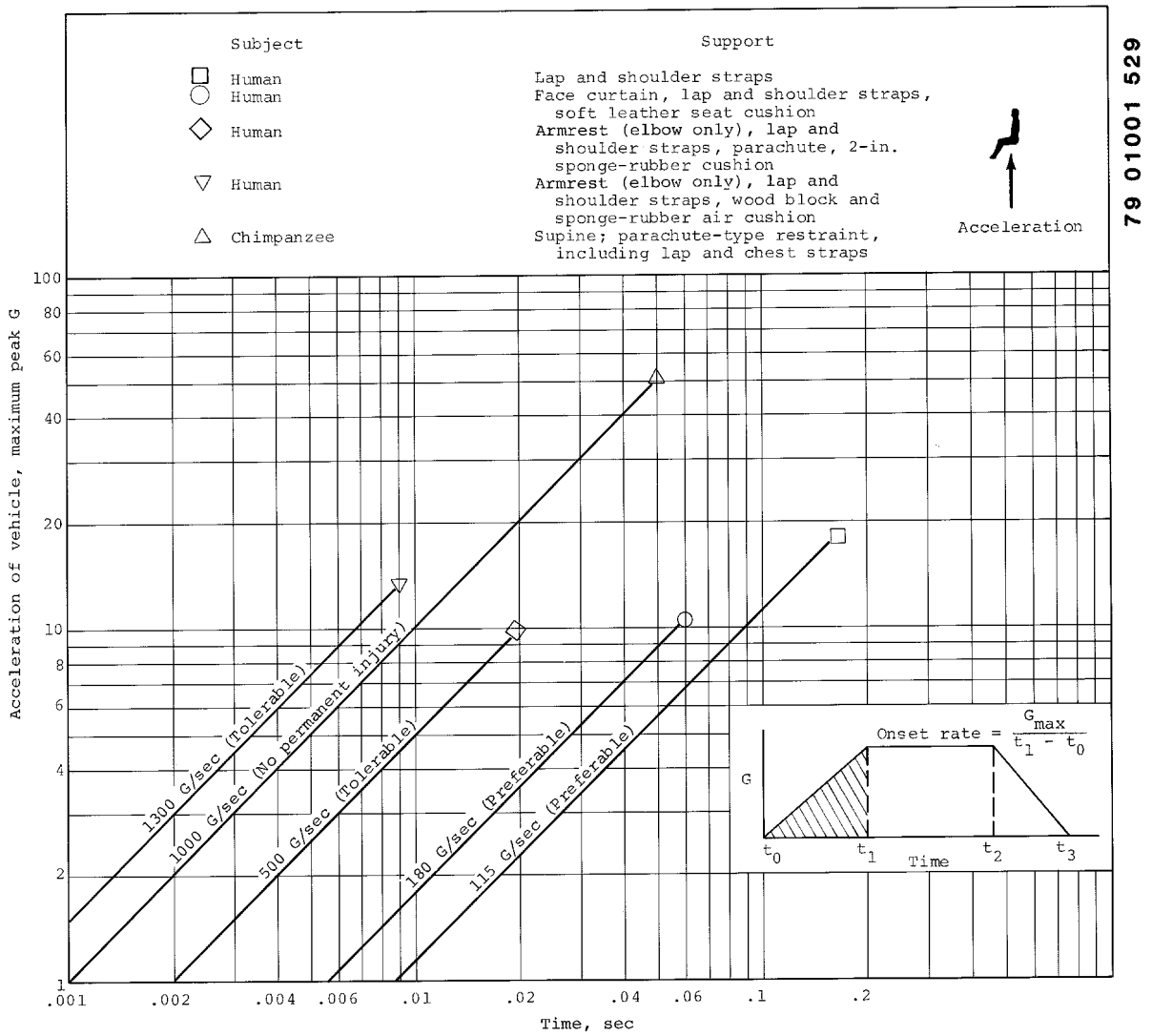


Figure 4-18.
Headward accelerative forces.

This Document Provided by the Abbott Aerospace
TECHNICAL LIBRARY
ABBOTTAEROSPACE.COM

4.3.3.4 Tailward Acceleration

The human tolerance limit for tailward (eyeballs-up), $-G_Z$, acceleration, is approximately 15 G for a duration of 0.1 sec. The shoulder harness/lap belt restraint has been used in all human testing with tailward accelerations. Most experiments also have included a lap belt tiedown strap (five-point harness), and the 15-G tolerance limit is based on this latter configuration.

4.3.3.5 Lateral Acceleration

Very little research has been conducted on whole-body human tolerance to lateral (G_Y) accelerations. Two studies, one involving restraint by a lap belt alone (Reference 4-59) and another involving restraint by the lap belt/shoulder harness configuration (Reference 4-60), provide the principal available data. In both cases, a side panel provided additional restraint. With restraint by the lap belt alone, volunteers were able to withstand a pulse with an average peak of approximately 9 G for a duration of approximately 0.1 sec. At this level, the tests were discontinued due to increasing concern about lateral spinal flexion. In the experiments with restraint by lap belt and shoulder harness, volunteers were able to withstand a pulse with an average acceleration of approximately 11.5 G for a duration of approximately 0.1 sec with no permanent physiological changes. Tests were discontinued at this level due to possible cardiovascular involvement experienced by one of the two subjects tested. No end points for human tolerance to lateral impacts were proposed in the reports of these experiments. The only reasonable conclusions determined from these data at this time are that a pulse of 11.5 G with a duration of 0.1 sec is readily sustained by subjects restrained by a lap belt and shoulder harness and that the human survival limit is at some point beyond this level, probably at least 20 G for 0.1 sec.

The above values are supported by a series of human volunteer experiments conducted to measure the inertial response of the head and neck to $+G_Y$ whole-body acceleration (Reference 4-61). Acceleration inputs ranged from long-duration pulses with magnitudes of 2.0 to 7.5 G to short duration pulses of 5.0 to 11.0 G.

4.3.4 Head Impact Tolerance

4.3.4.1 Head Injury Mechanisms

In the design of GA aircraft, one of the most significant concerns regarding occupant injury prevention is the protection of the occupant's head during crash scenarios. Within the dynamic impact environment, head injury mechanisms are classified into two different categories: contact and non-contact injury mechanisms (Reference 4-62).

4.3.4.1.1 Contact Injuries of the Head

Contact injuries of the head result from deformation of the skull due to a direct blow to the head (Reference 4-62). They do not, however, result from motion of the head following the head impact. Contact injuries can be described as local deformations, distant deformations, or traveling wave injuries, as follows.

1. Local deformations of the skull result from localized forces at the point of contact. Injuries to the head are sustained at or near the point of contact. For example, a head strike on the instrument panel or a high-mass projectile striking the occupant's head may produce local skull deformation injuries such as skull fracture, extradural hematoma (a localized swelling in the tissue resulting from a collection of blood released from damaged blood vessels; this type of injury is located above the layer of dura matter surrounding the brain), or coup contusion (a bruise, or damaged blood vessels located below the unbroken skin near the

This Document Provided by the Abbott Aerospace
TECHNICAL LIBRARY
ABBOTTAEROSPACE.COM

impact site). High localized forces can also induce penetrating contact injuries. Penetrating contract injuries occur when an intruding structure is driven into the occupant. The localized forces at the point of contact force the object to penetrate the occupant's skin and enter his/her body. The severity of injuries can range from skin and tissue lacerations to serious internal organ damage. A sharp object piercing an occupant's body is an example of a penetrating contact injury.

2. Distant deformations of the skull result from distributive forces that are applied over a region of the occupant's head. In general, the localized contact forces are not high enough to cause serious local head injury. However, the summation of the localized contact forces may be high enough to induce serious injury in another area in the head or body, far from the region of contact. Examples of distant deformation head injuries include distant vault fractures (fractures of the cranial bones that cover the upper regions of the brain) and basilar fractures (fractures of the cranial bones that surround the underside, or base, of the brain). Fracture of the occupant's neck due to head impact on a bulkhead is also an example of a distant deformation injury.

3. Head contact with a barrier can also produce "traveling wave" injuries. These injuries result from a "shock wave" of energy traveling through the occupant's head. Examples of traveling wave injuries include contracoup contusions (a bruise, or damaged blood vessels located below unbroken skin far from the impact site) and intracerebral hematoma (a localized swelling in the tissue resulting from a collection of blood released from damaged blood vessels; this type of injury is located within the cerebral portion of the brain).

4.3.4.1.2 Non-contact Injuries of the Head

Non-contact injuries of the head are defined as injuries to the brain that occur as a result of tissue deformation, or strain, produced by the head's inertial response to an acceleration (Reference 4-62). Non-contact injuries are typically the result of the occupant's torso being restrained, accompanied by an extreme forward rotational or whipping motion of the head. The rotational acceleration of the head can force the brain to impact the interior walls of the skull, generating two different types of strain within the brain: surface strain and deep strain. Surface strains can produce subdural hematoma (a localized swelling in the tissue resulting from a collection of blood released from damaged blood vessels; this type of injury is located beneath the layer of dura mater that surrounds the brain) while deep strains can induce concussion syndromes (movement of the brain inside the skull) or diffuse axonal injuries (mechanical disruption of numerous neurons, or brain cells). Non-contact injuries can be extremely serious; however, they do not occur as often as contact injuries. Non-contact injuries usually result from severe crash conditions and the extreme rotational acceleration of the head.

4.3.4.2 The Head Injury Criterion (HIC)

Presently, the potential risk for occupant head injury in dynamic impact events is predicted using the Head Injury Criterion (HIC). This section describes the historical development of the HIC, delineates the controversial issues surrounding the interpretation and application of the HIC, and identifies present and future research objectives aimed to develop a more accurate and consistent HIC.

4.3.4.2.1 Historical Development of the HIC

The evolution of the HIC began in 1960 with the development of the Wayne State Tolerance Curve (WSTC) by Lissner, et al., at Wayne State University (WSU) located in Detroit, Michigan (References 4-63 – 4-67). The WSTC is an acceleration-time history that was generated in an

THIS DOCUMENT PROVIDED BY THE ABBOTT AEROSPACE
TECHNICAL LIBRARY
ABBOTTAEROSPACE.COM

effort to define a tolerance boundary for cerebral concussion. The curve was constructed using head injury data collected from human cadavers, human volunteer subjects, and animals. Embalmed human cadavers were subjected to impact tests against rigid surfaces in order to produce contact head injuries (i.e., skull fractures). Restrained human volunteers and animals were subjected to high-speed sled tests in order to determine the human tolerance to non-contact injuries (i.e., concussion, hematoma, etc.).

Lissner, et al., discovered that the contact head injuries were typically generated by short-duration, high-magnitude accelerations, whereas the non-contact head injuries were generated by long-duration, low-magnitude accelerations (Reference 4-63). As illustrated in Figure 4-19, Lissner, et al., used the contact-based injury data to construct the initial portion of the WSTC and the non-contact-based injury data to construct the final portion of the WSTC. It is important to recognize that the most clearly defined portion of the curve was created using the contact-based injury data. This region of the curve contains a greater number of data points and extends up to approximately 15 msec in duration. As a result, researchers have traditionally been more confident in using the initial portion of the acceleration-time history as an indicator of skull fracture.

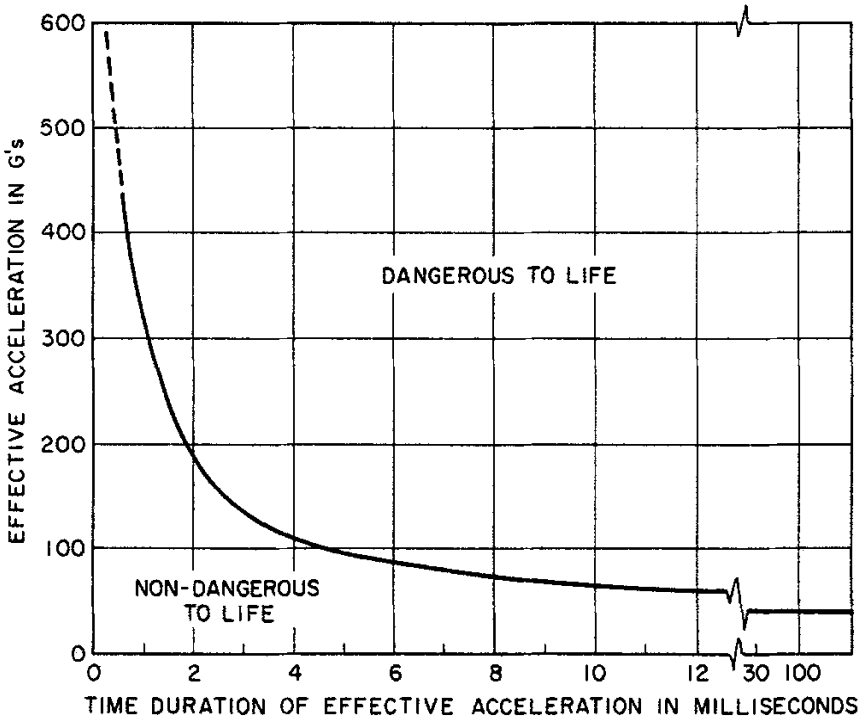


Figure 4-19.
The Wayne State Tolerance Curve (WSTC) (Reference 4-62).

In order to compare the severity of head impacts, Gadd used the WSTC to develop a weighted impulse criterion called the Severity Index (SI) (References 4-65 – 4-69). As illustrated in Figure 4-20, Gadd was able to generate a straight-line approximation of the WSTC by plotting the curve on a logarithmic scale (References 4-68, 4-69).

THIS DOCUMENT PROVIDED BY THE ABBOTT AEROSPACE
TECHNICAL LIBRARY
ABBOTTAEROSPACE.COM

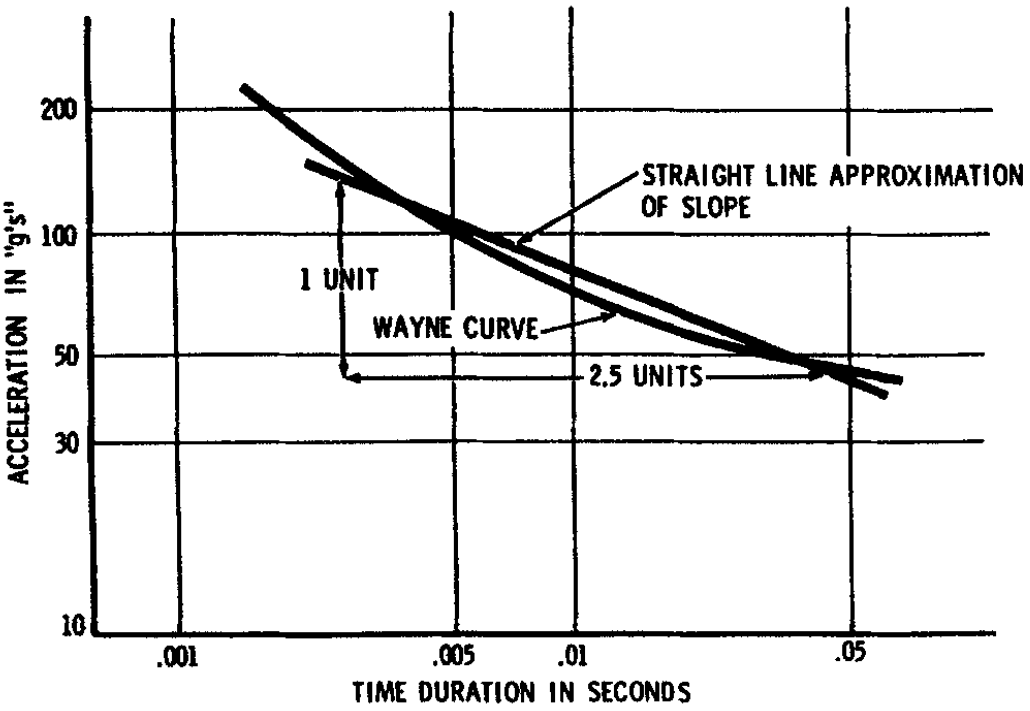


Figure 4-20.
Gadd's linear approximation of the log-log plot of the WSTC (References 4-68, 4-69).

On the log-log scale, a straight line is described by the following expression (Reference 4-69):

$$\log A = m \log T + \log k$$

where: A = acceleration in G's
m = slope of line
T = time in seconds
k = intercept of line.

Gadd determined that the best-fitting line for the log-log plot of the WSTC had a slope equal to -0.4. Using this value and a single coordinate from the WSTC, Gadd was able to solve for the intercept value, *k*. In order to simplify the calculation, Gadd defined *T* = 1 sec, which allowed the value of log*T* to equal zero. The value *T* = 1 sec, corresponded to an acceleration value of 15.85 G's. Substituting these coordinates (1, 15.85) into the above equation yielded the following value for the intercept, *k*:

$$\log(15.85) = -0.4(\log 1) + \log k$$
$$k = 15.85$$

Substituting the values *k* = 15.85 and *m* = -0.4 back into the original linear equation and rearranging the variables yielded the following:

THIS DOCUMENT PROVIDED BY THE ABBOTT AEROSPACE
TECHNICAL LIBRARY
ABBOTTAEROSPACE.COM

$$\log A = -0.4 \log T + \log 15.85$$
$$\log A = \log T^{-0.4} + \log 15.85$$
$$\log A = \log\left(15.85 \times T^{-0.4}\right)$$
$$A = 15.85 \times T^{-0.4}$$
$$TA^{2.5} = 15.85^{2.5}$$
$$TA^{2.5} = 1{,}000$$

The final equation represents the straight-line approximation for the WSTC. Using the weighting factor of 2.5 and the boundary value of 1,000, Gadd proposed the following Severity Index:

$$Severity\ \ Index = \int_0^t a^n\, dt < 1{,}000 \qquad (1)$$

where: a = instantaneous acceleration in G's
n = weighting factor (2.5)
t = time in seconds.

According to Gadd's Severity Index, values greater than 1,000 indicated that the acceleration profile would most likely induce injury.

In 1971, the National Highway Transportation Safety Administration (NHTSA) accepted the SI as the first head injury tolerance criterion. However, numerous discrepancies in the development of the SI encouraged many researchers to question its validity. To address the objections of the research community, Versace investigated the development of the SI. He recognized that the SI did not provide an adequate fit for the WSTC at very short and very long acceleration durations. The SI also did not provide a basis for defining a consistent measure of acceleration regardless of the waveform, nor did it provide a means for scaling injury severity.

As a result of these and other issues, Versace developed an alternative head injury criterion that was referred to as the HIC (Reference 4-67). In its present form, the HIC is defined as:

$$HIC = \left\{ \left[\frac{1}{t_2 - t_1} \int_{t_1}^{t_2} a(t)\, dt \right]^{2.5} \left(t_2 - t_1\right) \right\}_{\max} \qquad (2)$$

where: a(t) = resultant acceleration of the head's center of gravity during the t_2-t_1 time interval; recorded in G's
t_2-t_1 = time interval during which a(t) attains a maximum value; recorded in msec (HIC time interval).

The resultant linear acceleration at the center of gravity of the ATD's head is measured using an accelerometer. In order to determine the HIC value for a head acceleration-time history, the HIC equation is applied over every possible time interval combination within the acceleration profile. The reported HIC value is the maximum value calculated from all of the time interval combinations. The time interval associated with this maximum HIC value is referred to as the

This Document Provided by the Abbott Aerospace
Technical Library
abbottaerospace.com

"HIC time interval." It is standard practice to define the minimum duration for the HIC time interval as 1 msec. The maximum duration is usually defined within the occupant protection regulations for each transportation industry (see Section 4.3.4.2.2.3).

As a result of Versace's work, NHTSA repealed the SI and adopted the HIC in March of 1972 (References 4-64, 4-65, 4-70). The new standard required the HIC to be calculated for contact and non-contact cases over the entire duration of the crash. In terms of Pass/Fail criteria for the standard, the original boundary value of 1,000, taken from Gadd's straight-line approximation of the WSTC, was defined as the maximum acceptable HIC value. As illustrated in Figures 4-21 and 4-22, it was later determined that the maximum HIC value represents a 16-pct risk of serious head injury (References 4-71 and 4-72). In 1986, the automotive industry revised the HIC calculation by restricting the HIC time interval (t_2-t_1) to a maximum duration of 36 msec (References 4-72 and 4-73). The 36-msec time interval corresponds to the maximum HIC tolerance value of 1,000 at a constant head acceleration of 60 G's (Reference 4-70). The 60-G acceleration limit was defined by the creators of the WSTC as a reasonable threshold for head injury.

4.3.4.2.2 Issues Surrounding the Interpretation and Application of the HIC

Following the introduction and adoption of the HIC, further research revealed that there were still numerous limitations to the WSTC, the SI, and the HIC (Reference 4-74). For example, none of these criteria are able to distinguish between skull fracture and brain injury. In addition, these three criteria do not account for the location and direction of head impact forces. As a result, several issues surround the interpretation and application of the HIC as a predictor of head injury potential. In an effort to delineate some of these issues, three of them will be addressed in the following sections. These three issues are:

- The use of the WSTC in the development of the HIC,
- The interpretation of HIC in contact-versus-non-contact impact scenarios,
- The selection of an appropriate HIC time interval.

4.3.4.2.2.1 Use of the WSTC in the Development of the HIC

As discussed in Section 4.3.4.1, the origin of the HIC was based on the development of the WSTC. However, many current researchers question the methods and procedures employed during the development of the WSTC (Reference 4-65). They point out that the curve was created using data from a variety of completely different experimental procedures. For example, data was collected from frontal-impact cadaver tests, exposed animal brains subjected to bursts of air, and human volunteers subjected to non-injurious decelerations. The researchers at WSU also made two assumptions during the analysis of the test data. They assumed that the data from these different experimental procedures could be analyzed as a single dataset. In using this combined dataset, the WSU researchers also assumed that the different test subjects all possessed the same tolerance to head injury. Finally, current researchers have proposed that the effective acceleration used in the plots was poorly defined, and a portion of the original data was not plotted correctly, while other data points were completely omitted from the acceleration-time curve.

Overall, these complex issues have led current researchers to question the validity of the WSTC and the subsequent development of the HIC. As a result, the general consensus in the industry is that the HIC does not serve as a complete measure of head injury risk.

THIS DOCUMENT PROVIDED BY THE ABBOTT AEROSPACE
TECHNICAL LIBRARY
ABBOTTAEROSPACE.COM

4.3.4.2.2.2 Interpretation of the HIC in Contact Versus Non-contact Impact Scenarios

Another issue surrounding the HIC concerns whether it can be used to interpret both contact and non-contact impact scenarios (Reference 4-71). Since the HIC's conception, researchers have applied the HIC to contact and non-contact impact scenarios as an indicator of both skull fracture and brain injury. However, as noted previously, the HIC was formulated based on the WSTC, which represented a tolerance to skull fracture, and not brain injury. In addition, the HIC assumes that head injury potential can be measured by evaluating only the translational acceleration of the head. Contrary to this argument, recent head trauma research has demonstrated that rotational acceleration plays a major role in producing brain injuries, thereby suggesting that the HIC is not an appropriate measure of head injury in non-contact impact scenarios (Reference 4-75).

4.3.4.2.2.3 Selection of an Appropriate HIC Time Interval

As mentioned in Section 4.3.4.2.1, the time interval associated with the maximum HIC value is referred to as the HIC time interval. Most transportation regulations define a minimum and maximum length for the HIC time interval. It is standard practice to define the minimum duration for the HIC time interval as 1 msec. The maximum duration is usually defined within the occupant protection regulations for each transportation industry. The GA industry defines the HIC time interval as "the time duration of the major head impact, expressed in seconds" (Reference 4-76).

4.3.5 Facial Impact Tolerance

Presently, the FAA has not specified any requirements for facial impact tolerance in FAR Part 23. However, in the design of a crashworthy aircraft, it is still important to understand the anatomy of the human facial structure and what types of injuries can result from facial impacts.

The anatomy of the human face is extremely complex. The facial structure is composed of numerous bones that possess unique biomechanical properties, varying in size, shape, thickness, rigidity, and composition. These facial bones are covered by thin layers of soft tissue that provide little protection during impact. Figures 4-21 and 4-22 illustrate the anterior and lateral views of the facial bones in the human skull.

The fracture patterns generated by an impact to the skull are a function of the magnitude and direction of the applied load on the bone as well as the resistance to the load produced by the bone (Reference 4-77). Injuries can occur to both the soft and hard facial tissues that may result in permanent facial deformity, disability, and/or brain injury.

Within the general population, facial fractures typically result from motor vehicle accidents, impacts incurred while participating in athletics, and interpersonal violence (Reference 4-64). Little research has been conducted to determine the forces that cause facial bones to fracture. The facial bones receiving the most attention by researchers are the mandible, maxilla, zygoma, and nasion. Through a limited number of experiments using human cadavers, the fracture tolerance of these facial bones has been determined. It is important to recognize the non-uniformity of the test conditions defined in these experiments. Variable factors included impactor size, velocity, and mass, sample size, and the number of impacts applied per test subject. Table 4-3 displays the fracture forces of various facial bones with respect to sample size and impactor area. The following summary describes some of the results listed in the table.

THIS DOCUMENT PROVIDED BY THE ABBOTT AEROSPACE
TECHNICAL LIBRARY
ABBOTTAEROSPACE.COM

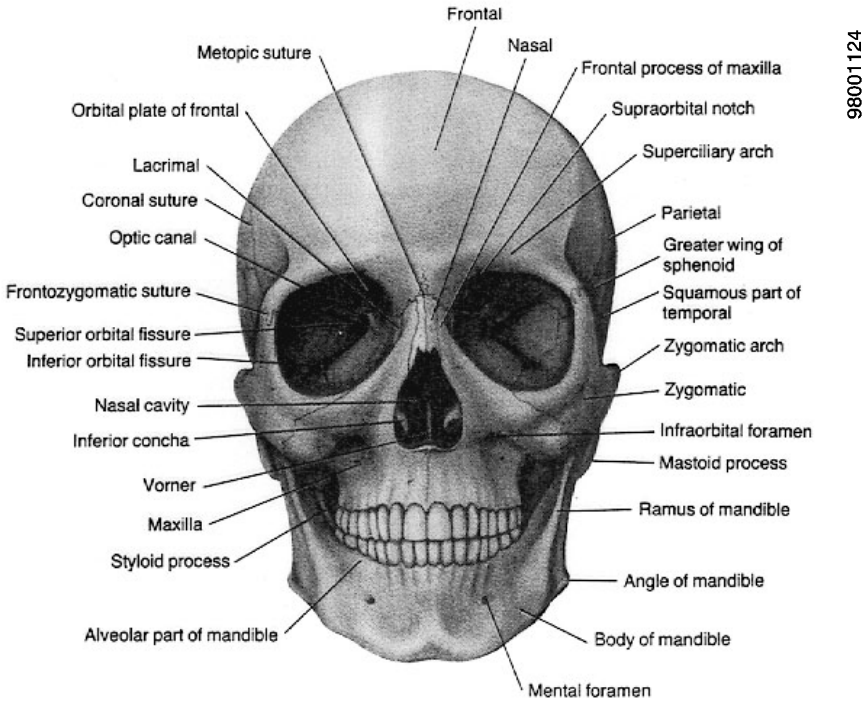


Figure 4-21.
Anterior view of the skull (Reference 4-64).

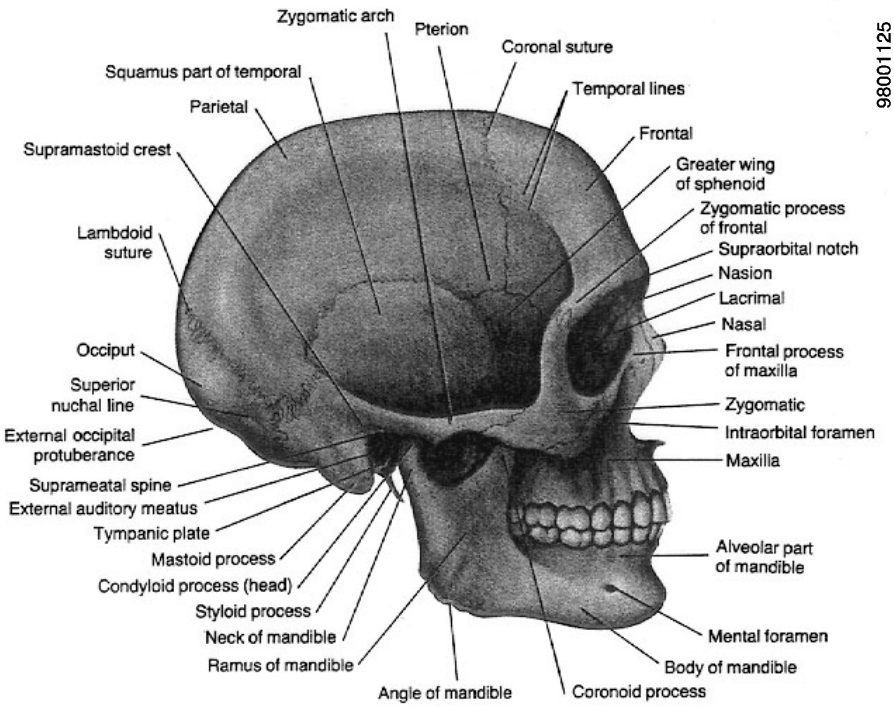


Figure 4-22.
Lateral view of the skull (Reference 4-64).

THIS DOCUMENT PROVIDED BY THE ABBOTT AEROSPACE
TECHNICAL LIBRARY
ABBOTTAEROSPACE.COM

Table 4-3.
Fracture Force of Facial Bones (Reference 4-64)

Bone	Force - Range (N)	Force - Mean (N)	Sample Size	Impactor Area (cm^2)	Author (Reference)
Mandible					
Midsymphysis	1,890-4,110	2,840	6	6.5	Schneider (32)
Lateral	818-2,600	1,570	6	25.8	Schneider (32)
Maxilla	623-1,980	1,150	11	6.5	Schneider (32)
Maxilla	1,100-1,1800	1,350	6	20-mm-dia bar	Allsop (20)
Maxilla	788	788	1	25-mm-dia bar	Welbourne (36)
Zygoma	970-2,850	1,680	6	6.5	Schneider (32)
Zygoma	910-3,470	1,770	18	6.5	Nahum (31)
Zygoma[a]	1,120-1,660	1,360	4	6.5	Hodgson (28)
Zygoma[a]	1,600-3,360	2,320	6	33.2	Hodgson (28)
Zygoma[b]	2,010-3,890	3,065	4	25-mm-dia bar	Nyquist (19)
Zygoma[b]	900-2,400	1,740	8	20-mm-dia bar	Allsop (20)
Zygoma	1,499-4,604	2,390	13	Approx. 25-mm-dia bar (steering wheel)	Yoganandan (34)
Nasion	1,875-3,760	2,630	5	25-mm-dia bar	Welbourne (36)
Full face[c]	--	>6,300	5	181.0	Melvin (41)

[a]Multiple impacts prior to fracture.
[b]Both zygomas below the suborbital ridges.
[c]Greater than 6300 N for fractures other than nasal.

Hodgson is credited with performing the majority of the early research regarding the examination of facial fracture forces. Using a multiple impact technique, he discovered that the fracture force was proportional to the impactor surface area. In other words, as the impactor surface area increased, the force required to produce a fracture also increased (Reference 4-78).

Schneider and Nahum investigated the fracture forces of the maxilla and mandible. They used their data to suggest minimal fracture forces for these regions of the face, including 670 N for the maxilla, 1,780 N for the anterior-posterior mandible, and 890 N for the lateral mandible (Reference 4-79).

Yoganandan investigated the fracture forces of the zygoma during impact. He recorded forces in the range of 1,499 - 4,604 N with an average force of 2,390 N. In addition, he investigated the relationships between fracture strength, bone mineral content, and HIC. Results of his tests indicate that both mineral content and HIC do not correlate with fracture strength (References 4-80 and 4-81).

Welbourne investigated the fracture forces of the maxilla and nasion. During tests conducted on the maxilla, a range of 516 - 1,362 N was applied. Only one fracture occurred in the region of the subnasal maxilla at 788 N. These results led Welbourne to conclude that impact energy was not an effective indicator of fracture potential in this region of the face. In the tests performed to the nasion, Welbourne observed that fracture severity increased with an increase in the maximum applied force (Reference 4-82).

THIS DOCUMENT PROVIDED BY THE ABBOTT AEROSPACE
TECHNICAL LIBRARY
ABBOTTAEROSPACE.COM

Melvin and Shee examined the fracture forces of the entire facial structure. Using a flat plate to impact the face, only nasal fractures were observed at forces less than 6.3 kN. They used their results to propose a force-time corridor for a full-facial rigid impact. This response corridor, illustrated in Figure 4-23, was used in the design of their deformable Hybrid III ATD face (Reference 4-83).

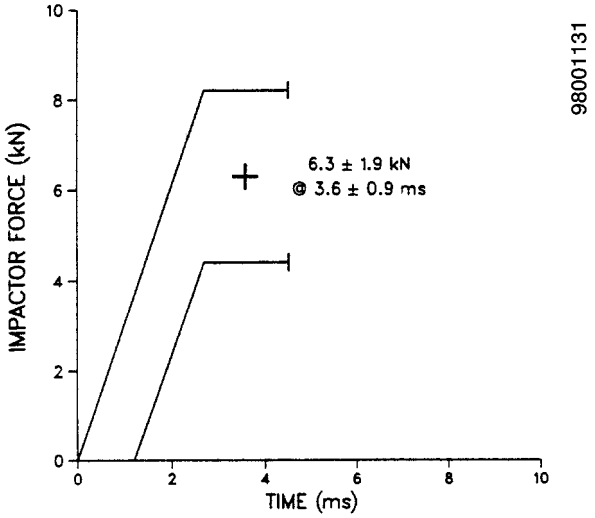


Figure 4-23.
Preliminary force-time response corridor at 6.7 msec for full-face rigid impact (Reference 4-64).

4.3.6 Neck Impact Tolerance

Currently, the FAA has not specified any requirements for neck impact tolerance in FAR Part 23. However, there is a great deal of interest in defining neck impact tolerances for transport category aircraft. The NHTSA recently added neck injury criteria to the Federal Motor Vehicle Safety Standard (FMVSS) (Reference 4-84). Initially, the NHTSA established injury tolerance criteria for the neck by conducting impact experiments using the Hybrid III ATD. The following neck injury tolerance values were adopted into the FMVSS 208 in 1998:

Neck Flexion Moment	190 Nm (SAE Class 600 filter)
Neck Extension Moment	57 Nm (SAE Class 600 filter)
Neck Axial Tension	3,300 N peak (SAE Class 1,000 filter)
Neck Axial Compression	4,000 N peak (SAE Class 1,000 filter)
Neck Fore-Aft Shear	3,100 N peak (SAE Class 1,000 filter)

In October 2000, the NHTSA adopted the N_{ij} criterion into FMVSS 208. The N_{ij} criterion evaluates the axial forces and fore/aft bending moments applied to the occupant's head and neck. The criterion defines four classifications of combined neck loading modes: tension-extension, tension-flexion, compression-extension, and compression-flexion. These modes are referred to as "N_{ij}" or N_{TE}, N_{TF}, N_{CE}, and N_{CF}, where the first index represents the axial load, while the second index represents the bending moment within the sagittal plane. A linear combination of the axial loads and fore/aft bending moments is determined using the equation:

THIS DOCUMENT PROVIDED BY THE ABBOTT AEROSPACE
TECHNICAL LIBRARY
ABBOTTAEROSPACE.COM

$$Nij = \left(\frac{F_z}{F_{\text{int}}}\right) + \left(\frac{M_y}{M_{\text{int}}}\right) \quad (3)$$

where: F_z = axial force
F_{int} = critical axial force intercept value
M_y = fore/aft bending moment
M_{int} = critical fore/aft bending moment intercept value.

An Nij equal to 1.0 is equivalent to a 22-pct risk of an AIS-3 neck injury.

If similar tolerance specifications are eventually added to FAR Part 25, it is possible that the specifications may also be added to FAR Part 23. Therefore, it is important to understand the anatomy of the human neck structure as well as the neck injury mechanisms and injuries that can result from an impact scenario.

The internal structure of the human neck is composed of seven vertebrae and their surrounding soft tissues. Figure 4-24 illustrates the arrangement of these vertebrae. Injury to the neck can occur from direct contact and inertial loading, and may occur at any location along the cervical spine, affecting the hard and/or soft tissue.

4.3.6.1 Injury Mechanisms

Traditionally, neck injuries are categorized by the primary direction of loading (Reference 4-64). The five basic engineering descriptions of neck loading (bending, compression, tension, torque, and shear) are shown in Figure 4-25. The neck loading mechanisms can be further defined by describing the head motion that occurs under a load with respect to a fixed location. However, the general motion of the head does not necessarily represent the actual loading mechanisms that occur at the vertebral level. The head motions illustrated in Figure 4-26 occur about the craniocervical junction.

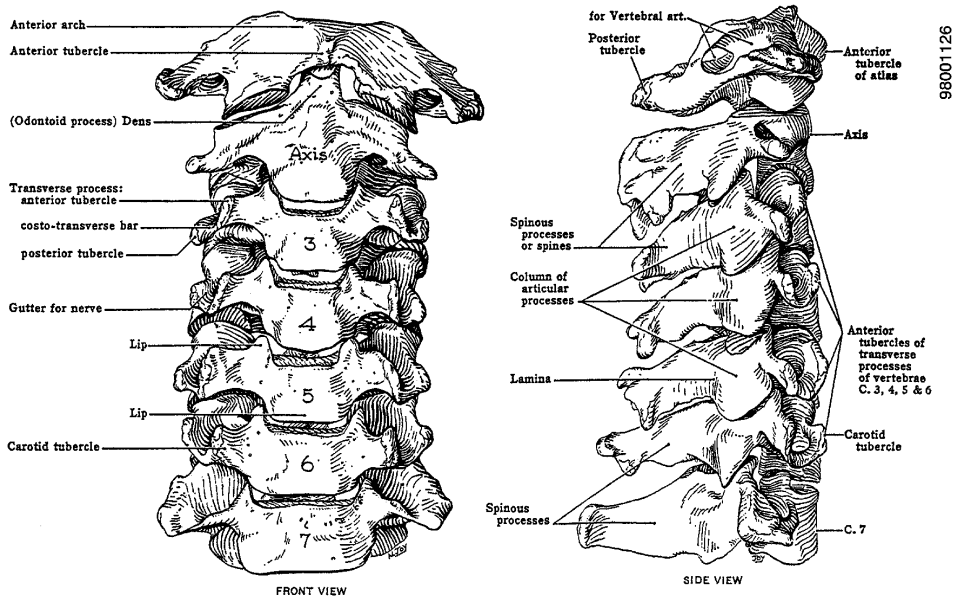


Figure 4-24.
Frontal and side view of the human cervical vertebral column (Reference 4-64).

THIS DOCUMENT PROVIDED BY THE ABBOTT AEROSPACE
TECHNICAL LIBRARY
ABBOTTAEROSPACE.COM

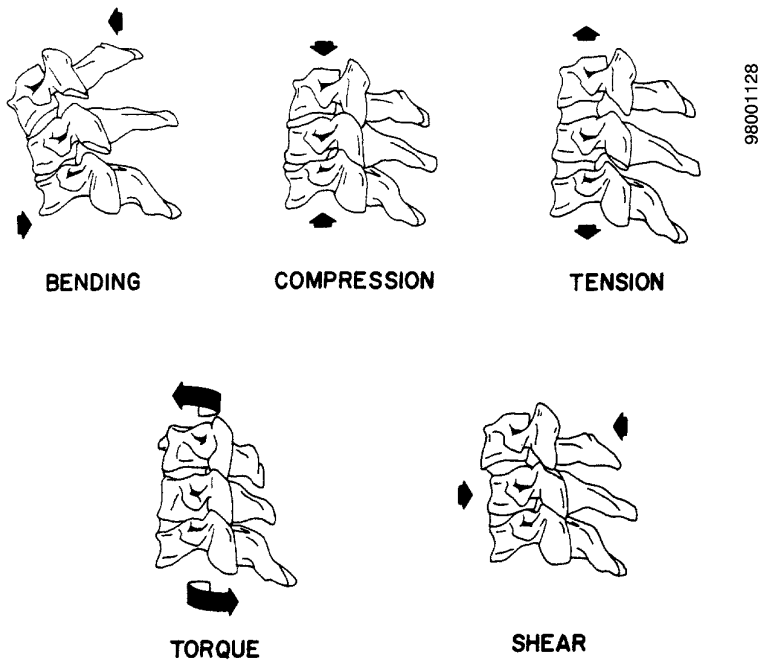


Figure 4-25.
Neck loading mechanisms (Reference 4-64).

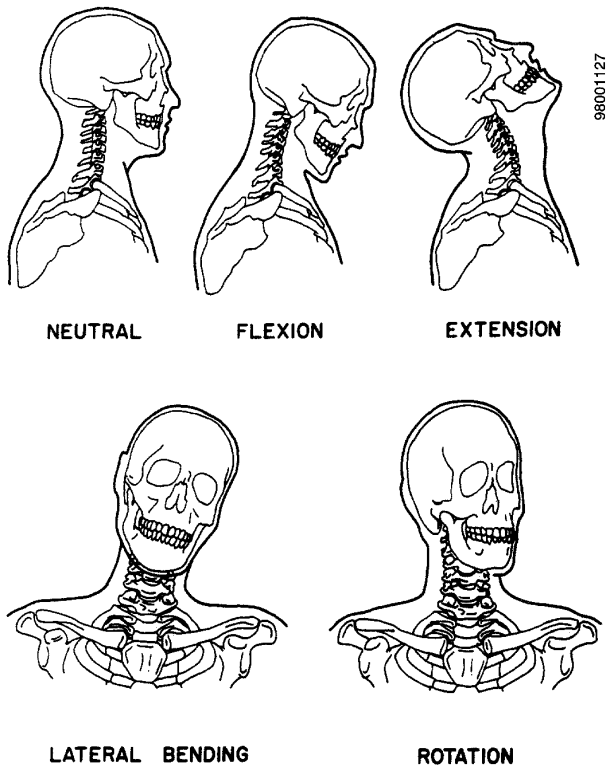


Figure 4-26.
Motion of the head/neck complex (Reference 4-64).

THIS DOCUMENT PROVIDED BY THE ABBOTT AEROSPACE
TECHNICAL LIBRARY
ABBOTTAEROSPACE.COM

To evaluate human tolerance to injury, neck injury studies are conducted to measure and analyze the affects of various loading mechanisms on the neck. These loads are measured using ATD's, whole cadavers, individual spinal motion segments, and individual vertebrae. It is difficult to associate the cause of an injury with only one type of loading mechanism, since it is very common for injuries to result from a combination of loading conditions. The loading required to produce injury will vary substantially with the boundary conditions defined for the experiment, including the type of test specimen used, the initial positioning of the specimen, and the degree of fixation. In terms of the positioning of the specimen, a few degrees of variation can influence the difference between a flexion or extension injury. The following information describes the five loading mechanisms that have the potential to cause injury to the human neck.

Axial Compression

As a result of the complexity of the cervical spinal structure, purely compressive loading rarely occurs (Reference 4-64). However, many loading situations are considered to be predominantly compressive. In the upper cervical spine, multi-part fractures of the atlas originate from compressive forces. In the lower cervical spine, simple compressive fractures of the vertebral body occurring at the C4, C5, and C6 vertebrae are the most common sites of compressive injury. Ligamentous damage to the cervical spine is unlikely to occur under purely compressive loads

Compression-Flexion

The combination of a compressive load and a flexion bending moment results in increased compressive stresses in the anterior portion of the vertebral bodies and increased tension in the posterior portion (References 4-64 and 4-85). The high compressive forces typically cause failure of the anterior structures of the vertebral bodies. However, failure can also occur in the posterior portion of the vertebral bodies as a result of the high tensile stresses placed on the ligaments. Compression-flexion injuries of the spine include burst fractures, wedge compression fractures, hyperflexion sprains, unilateral and bilateral facet dislocations, "clay shoveler's" fractures, teardrop fractures, and soft tissue injuries.

Compression-Extension

The combination of a compressive load and an extension bending moment results in increased compressive stresses in the posterior portion of the vertebral bodies and increased tensile stresses in the anterior portion of the vertebral bodies (Reference 4-85). Compression-extension forces are believed to cause injuries throughout the entire cervical spine. The type of injuries produced are greatly dependent on the boundary conditions that are defined for the experiment. Fractures tend to occur in the spinous processes and in the vertebral bones surrounding the spinal canal. Rupturing of the anterior disc and anterior longitudinal ligament, horizontal vertebral body fractures, and "clay-shoveler's" fractures have been observed in experimental studies. In addition, "hangman's" fractures, which are traditionally associated with tension-extension mechanisms, have also been produced.

Axial Tension

Pure tensile loading is not a common neck loading mechanism (Reference 4-85). During motor vehicle accidents, rapid decelerative conditions produce inertial forces that act through the head's center of gravity, creating both shear and tensile loading of the neck. Ultimately, injury is caused by the loading of the ligamentous structures of the neck and is restricted to the upper

This Document Provided by the Abbott Aerospace
TECHNICAL LIBRARY
ABBOTTAEROSPACE.COM

cervical spine. For example, this type of loading can generate occipitoatlantal distraction with unilateral or bilateral dislocation of the occipital condyles. This can produce ligamentous injuries without fracturing the hard tissue.

Tension-Extension

The combination of tension-extension loading is a common injury mechanism. Neck injuries resulting from tension-extension loading include "whiplash", "hangman's" fractures, horizontal fractures of the vertebral body, teardrop fractures, and structural injury to the anterior column of the spine (References 4-64 and 4-85). Large accelerations may injure the anterior longitudinal ligament and intervertebral disk or produce horizontal vertebral fractures. Tension-extension injuries typically occur via one of three methods (Reference 4-64):

1. Constraint of the head with continued forward motion of the torso. (diving accidents, falls, or unbelted occupant contacting windshield)
2. Abrupt forward acceleration of the torso producing inertial neck loading. ("whiplash")
3. Forceful loading below the chin directed in a posterosuperiorly direction (judicial hanging or air bag deployment at an out-of-position occupant).

Tension-Flexion

The combination of a tensile load and a flexion bending moment results in increased tensile stresses in the posterior portion of the vertebral bodies and increased compressive stresses in the anterior portion (Reference 4-85). Various experimental studies have suggested that tension-flexion loading produces injuries similar to compression-flexion loading, including bilateral facet dislocations, unilateral facet dislocations, and hyperextension sprains. These results indicate that the flexion bending moment is the primary factor generating the injuries.

Axial Rotation/Torsion

Torsional loading is thought to play a role in both upper and lower cervical spinal injuries (Reference 4-64). Injuries to the atlantoaxial joint, including rotary atlantoaxial dislocation with or without tearing of the alar ligaments, unilateral anterior and posterior subluxations, and bilateral anterior and posterior subluxations, are common to the upper cervical spine. These injuries may result from a combination of shear and torsional loading and typically include the dislocation of one or both of the surfaces of the atlas facets on the axis facet joint surface. In the lower cervical spine, the contribution of torsional loading to injuries is debatable. It has been demonstrated that the lower cervical spine is stronger in torsion that the atlantoaxial joint of the upper cervical spine, implying that torsional loading affects the lower cervical spine to a lesser degree. In addition, it is believed that torsional loading may produce unilateral facet dislocations in the lower cervical spine; however, this has not been demonstrated experimentally (Reference 4-85).

Fore-Aft (Horizontal) Shear, Lateral Shear, and Lateral Bending

Horizontal shear can produce anterior and posterior atlantoaxial subluxations resulting from transverse ligament failure or fracture of the odontoid process (Reference 4-64). These injuries can induce spinal cord impingement and make surgical repair procedures extremely challenging. Lateral shear and lateral bending are injury mechanisms that occur within the coronal plane of the body and are generally produced during side-impact collisions. Lateral shear loading produces nerve-root avulsion injuries and may also contribute to the type of odontoid fractures that occur from trauma. Forced lateral bending can generate radicular symptoms and bracheal plexus injuries. These loading mechanisms, in combination with other

This Document Provided by the Abbott Aerospace
TECHNICAL LIBRARY
ABBOTTAEROSPACE.COM

loads, have been shown to produce hemorrhagic lesions in the C4-C5 and C6-C7 disc spaces of human cadavers. They can also initiate unilateral wedging and/or produce simple unilateral fractures of the cervical vertebrae (Reference 4-85).

4.3.6.2 Injury Tolerance

Numerous studies have been conducted to determine human tolerance levels for the cervical spine (Reference 4-85). Studies include the use of human volunteers, whole cadavers, isolated head and cervical spines, isolated cervical spine motion segments, animals, anthropomorphic test devices, and analytical techniques. However, several limitations exist which make it difficult to accurately define the injury tolerance criteria, including:

- Pure loading of the spine is rare.
- The observed motions and forces of the head do not necessarily reflect the motions or true injury mechanism of the cervical spine.
- Neck loading is strongly influenced by the inertial behavior of the head.
- Changes in the initial position of the spine, the end condition, and the eccentricity of the applied force have been shown to change the injury produced.
- Variation in the selection of test subjects, boundary conditions, restraint systems, and testing environments.

These limitations exist in both the automotive and aviation testing communities. However, the aviation industry has an additional limitation involving the selection of the ATDs used during testing. Presently, the aviation community uses the Hybrid II ATD, which lacks sufficient instrumentation and biofidelic characteristics in the neck region of the ATD body. Improved instrumentation and biofidelity initiated the design of the Hybrid III ATD, which is currently used by the automotive industry (Reference 4-86). The Hybrid III ATD features the Denton six-axis upper neck load cell for measurement of neck forces and moments during impact conditions. The Hybrid III ATD also possesses an articulated neck structure that is comparable to the human neck.

4.3.7 Spinal Injury Tolerance

Presently, the FAA specifies a single loading requirement for the spinal column during impact testing. FAR Part 23.563(c)(7) states that the “compression load measured between the pelvis and the lumbar spine of the ATD may not exceed 1,500 pounds” (Reference 4-76).

The human spinal column serves numerous functions in the human body. It is responsible for protecting the spinal cord, providing support and structure for the body, and enabling movement of the head, neck, and torso (Reference 4-64). The human spinal column is comprised of 24 individual vertebrate and 2 groupings of fused vertebrae. The 24 individual vertebrae create the flexible portion of the spine that is divided into 3 different sections: cervical (7 vertebrae), thoracic (12 vertebrate) and lumbar (5 vertebrae). The hard tissue vertebrae are connected by several different types of soft tissue, including ligaments, skeletal muscles, and intervertebral discs. The two fused groupings, the sacrum and coccyx, are situated beneath the lumbar vertebrae and form the rear wall of the pelvic girdle. The vertebral structures that form the sacrum and coccyx do not possess the same features as the individual vertebrae. For example, the fused vertebrae do not possess the posterior structures of the individual vertebrae. The anatomy of the spinal column is illustrated in Figure 4-27.

THIS DOCUMENT PROVIDED BY THE ABBOTT AEROSPACE
TECHNICAL LIBRARY
ABBOTTAEROSPACE.COM

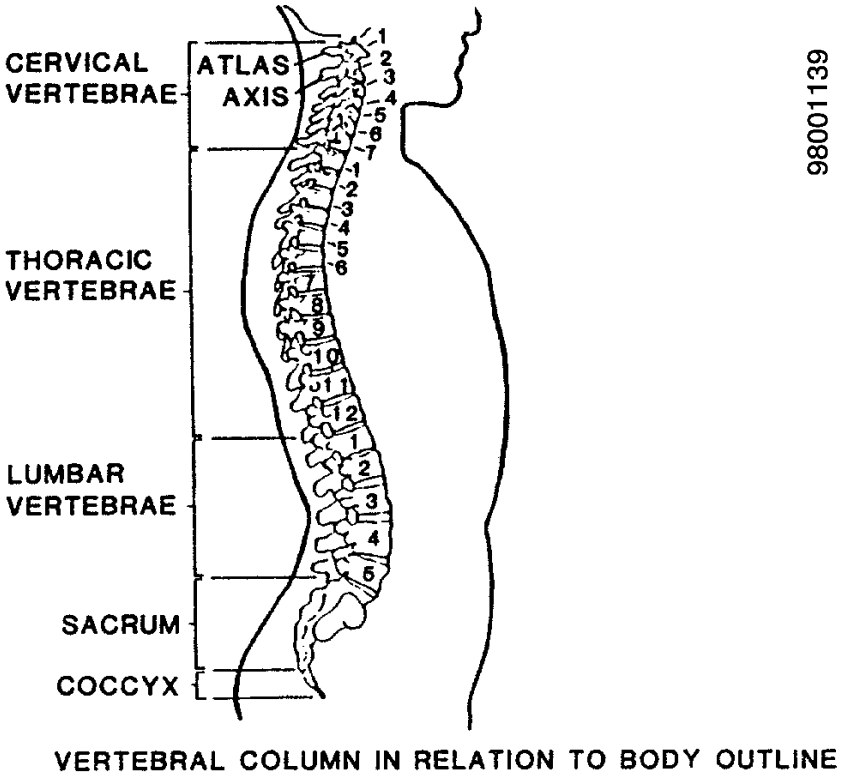


Figure 4-27.
Anatomy of the spinal column (Reference 4-2).

4.3.7.1 Injury Mechanisms

Injuries to the spinal column are categorized by the primary direction of loading (Reference 4-64). The five basic engineering descriptions of spinal loading (bending, compression, tension, torque, and shear) are shown in Figure 4-25 in Section 4.3.6.1. Spinal injuries can be attributed to combinations of these loading mechanisms.

To evaluate human tolerance to injury, studies are conducted to measure and analyze the affects of various loading mechanisms on the spine. The loading required to produce injury will vary substantially with the boundary conditions defined for the experiment, including the type of test specimen used, the initial positioning of the specimen, and the degree of fixation. In terms of the positioning of the specimen, a few degrees of variation can influence the difference between a flexion or extension injury. The following information describes the loading mechanisms that have the potential to cause injury to the human spinal column.

Axial Compression

Axial compressive forces generally produce fracture-type injuries to the vertebral bodies of the spinal column. In light aircraft and helicopter accidents, the most common sites of compressive injury are T10-L2 (Reference 4-87). In combined loading situations involving flexion and compression, common injuries include anterior wedge fractures and burst fractures (Reference 4-64). These injuries usually occur in the C5-T1 and T11-L12 regions (Reference 4-88).

This Document Provided by the Abbott Aerospace
TECHNICAL LIBRARY
ABBOTTAEROSPACE.COM

Axial Tension

Pure tensile loading is not a common spinal loading mechanism (Reference 4-85). During motor vehicle accidents, rapid decelerative conditions produce inertial forces that act through the head's center of gravity, creating both shear and tensile loading of the cervical portion of the spine. Ultimately, injury is caused by the loading of the ligamentous structures of the neck and is restricted to the upper cervical spine. For example, this type of loading can generate occipitoatlantal distraction with unilateral or bilateral dislocation of the occipital condyles. This can produce ligamentous injuries without fracturing the hard tissue.

Axial Rotation/Torsion

The rotation of the spinal column about its longitudinal axis in combination with axial and/or shear loads can create several different hard tissue injuries of the spine (Reference 4-64). Injuries include lateral wedge fractures, uniform compression of the vertebral bodies, and fracture of the articular facets and lamina. These injuries have the potential to cause neurological deficit, including paraplegia. In addition, injuries to the intervertebral discs, joints, and ligaments of the spinal column often result from torsional loads (Reference 4-89).

Fore-Aft (Horizontal) Shear

Horizontal shear in combination with flexion and rotation of the spine can produce both unilateral and bilateral dislocations of the thoracolumbar vertebrae (Reference 4-64). In the cervical spine, horizontal shear loads can produce anterior and posterior atlantoaxial subluxations resulting from transverse ligament failure or fracture of the odontoid process. These injuries can induce spinal cord impingement and make surgical repair procedures extremely challenging.

Spinal Flexion

During flexion of the spinal column, the anterior portions of the spine endure compressive loads, while the posterior portions endure tensile loads (Reference 4-64). As mentioned previously, flexion of the spinal column in combination with other injury mechanisms can produce a variety of injuries to the vertebrae, including unilateral and bilateral dislocations, anterior wedge fractures, and burst fractures. "Chance" fractures are also related to the flexion of the spinal column. These fractures occur when the lumbar spine flexes over the lap belt, separating the posterior components of the vertebral bodies.

Spinal Extension

During extension of the spinal column, the anterior portions of the spine experience tensile loading, while the posterior portions experience compressive loading (Reference 4-64). Extension injuries tend to produce teardrop fractures in the cervical spine. They have also been associated with a loss of posterior vertebral height that, in turn, can cause injury to the articular facets, pedicles, and laminae of the vertebrae. In the thoracolumbar spine, injuries may include fractures to the posterior components of the vertebrae and distraction fractures of the vertebral bodies (Reference 4-90). During ejection from F/FB-118 aircraft, extension of the spinal column has ruptured the anterior longitudinal ligament in the thoracic spine (Reference 4-64).

This Document Provided by the Abbott Aerospace
TECHNICAL LIBRARY
ABBOTTAEROSPACE.COM

4.3.7.2 Injury Tolerance

The quantity of reported spinal injury tolerance data is extremely limited. The spinal column is not injured as frequently as other body regions including the head and the thorax, and, therefore, it has not been studied to the same degree (Reference 4-64). In addition, several limitations exist in both the automotive and aviation research communities that make it difficult to accurately define injury tolerance criteria, including:

- Pure loading of the spinal column is rare; injuries typically result from a combination of loading mechanisms.
- The overall configuration of the spinal column plays a large role in defining the injury pattern.
- It is difficult to develop explicit injury criteria for the spinal column, since the failure of the spinal components includes both the hard and soft tissues.
- Neck loading is strongly influenced by the inertial behavior of the head.
- The observed motions and forces of the head do not necessarily reflect the motions or true injury mechanism of the cervical spine.
- Changes in the initial position of the spine, the end condition, and the eccentricity of the applied force have been shown to change the injury produced.
- Variation in the selection of test subjects, boundary conditions, restraint systems, and testing environments.

Presently, injury tolerance data is collected from instrumented human volunteers, whole cadavers, isolated head and cervical spines, isolated cervical spine motion segments, animals, and ATDs. In terms of the ATDs, the aviation community utilizes the Hybrid II ATD that is capable of measuring the compressive loads in the lumbar spine (Reference 4-86). The Hybrid II has a non-articulating pelvis and a straight spinal column, and can only be positioned in a reclined or seated position. The automotive industry uses a version of the Hybrid III ATD referred to as the “automotive" ATD. This particular ATD has a curved spinal column, but does not possess the instrumentation required to measure the lumbar loads in the spine. Similar to the Hybrid II, the automotive ATD can only be positioned in a reclined or seated position and has a non-articulating pelvis. The military uses another version of the Hybrid III ATD referred to as the "pedestrian" ATD. This ATD has an articulating pelvis, a straight spinal column, and is instrumented to measure the spinal compressive loads in the lumbar spine. In addition, the pedestrian ATD is not limited to a reclined or seated position, but instead has the ability to stand. As a result of the differences among these three types of ATDs, it is difficult to compare the collected data from the related impact tests that are conducted within these communities.

4.3.8 Upper-Extremity Injury Tolerance

In GA accidents, injuries to the upper extremity may result from contact with the aircraft interior and/or from flailing of the arm. The types of injuries sustained may include damage to both the hard and soft tissues of the arm. A study conducted by researchers from the Department of Emergency Medicine at Johns Hopkins University School of Medicine compared the autopsy data from aviation crashes that occurred in both 1980 and 1990. The data revealed that upper-extremity fractures comprised only 0.6 pct of the total injuries received by aircraft occupants during both 1980 and 1990 (Reference 4-91). In comparison with the injury tolerance of other body regions, this data suggests that the evaluation of upper-extremity injury tolerance may not be a current priority for the GA community.

THIS DOCUMENT PROVIDED BY THE ABBOTT AEROSPACE
TECHNICAL LIBRARY
ABBOTTAEROSPACE.COM

Presently, with the exception of specific ejection ATDs, standard ATDs are not capable of measuring upper-extremity loading. However, an increase in upper-extremity injuries related to air bag deployments in automobile accidents has heightened interest in assessing upper-extremity injury. Recently, the Research Arm Injury Device (RAID) was introduced and is being used to examine the interaction between the upper extremities and automobile air bags. Prior to the development of the RAID, a limited number of research studies were conducted to investigate upper-extremity injury mechanisms and to develop human tolerance injury values for the arm (Reference 4-64). The human tolerance values for the hard tissue components of the arm that have been reported in the literature are listed in Table 4-4.

Table 4-4.
Upper-extremity bone tolerance values

Upper-Extremity Bone	Gender / Notes	Torque (N-m)	Bending (kN)	Average Max. Moment (N-m)	Long-Axis Compression (kN)
Clavicle	Male*	15	0.98	30	1.89
	Female*	10	0.60	17	1.24
Humerus	Male*	70	2.71	151	4.98
	Female*	55	1.71	85	3.61
Radius	Male*	22	1.20	48	3.28
	Female*	17	0.67	23	2.16
Radius	27 cm support**			35	
	14 cm support**			18	
	**		0.52		
Ulna	Male*	14	1.23	49	4.98
	Female*	11	0.81	28	3.61
Ulna	27 cm support**			42	
	14 cm support**			22	
	**		0.627		

* Messerer
** Yamada - Japanese male bones

4.3.9 Chest Impact Tolerance

In FAR Part 23.562(c)(6), the FAA has specified requirements for chest impact tolerance in terms of the loads exerted by the individual shoulder harness straps. For a single strap, the loads may not exceed 1,750 lb. If dual straps are used, the total strap loads may not exceed 2,000 lb.

In the automotive industry, injuries to the thorax typically result from interaction with the steering column, restraint system, instrument panel, or deploying air bag (Reference 4-64). Similar interactions with interior structures can also occur in GA accidents. To evaluate the potential for thoracic injury in frontal impacts, the automotive community utilizes Hybrid II and Hybrid III ATDs to examine the peak longitudinal spinal acceleration and maximum chest deflection experienced during impact. In lateral impacts, the Side Impact Dummy (SID) is used to record the peak lateral spinal acceleration. The following sections briefly describe the acquisition, analysis, and application of these measurements.

4.3.9.1 Acceleration Criterion

Peak spinal acceleration provides a general indication of the “overall severity of whole-body impact” (Reference 4-64) and is used to evaluate the potential for thoracic injury in the human body. This acceleration is measured using a triaxial accelerometer that is positioned at the center of gravity of the thoracic spine (Reference 4-86). Both the Hybrid II and Hybrid III ATDs

THIS DOCUMENT PROVIDED BY THE ABBOTT AEROSPACE
TECHNICAL LIBRARY
ABBOTTAEROSPACE.COM

are capable of measuring this acceleration. For frontal motor vehicle collisions, the Code of Federal Regulations 571.208 (Reference 4-84) specifies that the peak spinal acceleration can not exceed 60 G during a period of 3 msec or longer. This data is displayed in Table 4-5. Use of the acceleration criterion is limited to predicting the severity of human skeletal injury (Reference 4-92). Note: All experiments discussed in Table 4-5 utilized human cadavers as test subjects, unless otherwise specified.

Table 4-5.
Frontal impact injury tolerances (Reference 4-64).

Tolerance Level	Injury Level	Reference
Force		
3.3 kN to sternum	Minor Injury	Patrick, et al. (1969)
8.8 kN to chest and shoulders	Minor Injury	Patrick, et al. (1969)
Acceleration		
60 G	3-msec limit for Hybrid II and III	FMVSS 208
Deflection		
58 mm	No rib fracture	Stalnaker and Mohan (1974)
76 mm	Limit for Hybrid III	FMVSS 208
Compression		
20 pct	Onset of rib fracture	Kroell, et al. (1971, 1974)
32 pct	Flail chest	Kroell, et al. (1971, 1974)
40 pct	Tolerance for rib cage stability	Viano (1978)
VC_{max}		
1.0 m/sec	25 pct probability of AIS >3 (anesthetized rabbits)	Viano and Lau (1985)
1.3 m/sec	50 pct probability of AIS >3 (anesthetized rabbits)	Viano and Lau (1985)

4.3.9.2 Compression Criterion

Another predictor of thoracic trauma is the magnitude of chest compression, or deflection, that occurs during the impact of the chest with an external object. The Hybrid III is the only ATD capable of measuring chest compression (Reference 4-93). The thoracic region of the Hybrid III is comprised of three components: spine, rib cage, and a removable chest jacket. Six steel ribs are attached to the rear portion of the welded steel spinal column. The inside surface of each rib is covered with a polyviscous damping material that helps to generate the appropriate chest response to blunt trauma. The removable chest jacket is composed of urethane and is used to distribute loads during frontal impact. Chest compression is measured using a chest deformation transducer located within the thoracic region of the Hybrid III ATD. The transducer is comprised of a potentiometer that is positioned on top of a bracket that extends over the lumbar spine. Input to the potentiometer travels from the sternum via a rod and sliding mechanism. The amount of compression is determined by recording the instantaneous displacement of the ATD's sternum relative to its thoracic spine. The Hybrid III chest structure is capable of recording deflections up to 90 mm in depth. As indicated in Table 4-5, FMVSS 208 specifies a maximum chest compression of 76 mm for the 50th-percentile Hybrid III ATD.

THIS DOCUMENT PROVIDED BY THE ABBOTT AEROSPACE
TECHNICAL LIBRARY
ABBOTTAEROSPACE.COM

Kroell, et al., discovered that the degree of chest compression correlated well with the Abbreviated Injury Scale (AIS) (References 4-94 and 4-95). The following linear equation was developed to represent the relationship between chest compression and AIS:

$$AIS = -3.78 + 19.56C \quad (4)$$

The variable *C* represents the deformation of the chest divided by the chest depth. Research conducted by Viano demonstrated that an average maximum compression (C_{max}) of 40 pct can produce severe injuries to internal organs. To better protect these internal organs, Viano has proposed a C_{max} of 32 pct that will help to maintain sufficient rib cage stability.

In automotive accidents, compression of the chest typically results from interaction with the steering wheel, air bag, or shoulder belt. The load applied from the interaction with the steering wheel or air bag tends to produce a distributed deformation across the chest, whereas the load applied by the shoulder belt results in a localized chest deformation. Unfortunately, the majority of the chest compression tolerance data that is provided in the literature reflects only the effects of distributed loads. However, the GA community utilizes three-point restraint systems that may induce localized chest deformation, suggesting that localized chest deformation data will need to be collected to accurately evaluate the injury tolerance of the chest in aviation-related accidents.

4.3.9.3 Viscous Criterion (VC)

In order to define appropriate thoracic injury tolerance criteria, it is necessary to have a thorough understanding of the injury mechanisms that affect the soft tissues in this region. Within this region, injuries to the heart, lungs, and major vessels of the cardiovascular system can occur (Reference 4-64). The heart is subject to contusion and/or laceration resulting from deformation of the chest. High rates of chest loading can disrupt the electromechanical transduction pathways within the heart, inducing fibrillation or cardiac arrest. Within the lungs, high rates of chest loading can damage the alveoli capillary beds in the lung tissue. Fractured ribs can puncture the lung wall, initiating internal bleeding. Internal bleeding can also result from the rupturing of major blood vessels near the heart.

Soft-tissue injuries are dependent on both the degree and the rate of chest deflection (Reference 4-92). These properties are evaluated by a relationship developed by Lau and Viano called the Viscous Criterion. Lau and Viano define the Viscous Criterion as “any generic biomechanical index of injury potential for soft tissue defined by rate-sensitive torso compression” (Reference 4-92). The criterion is based on the viscous response, VC, which is determined by multiplying the velocity of chest deformation and the instantaneous chest compression. The maximum risk of soft tissue injury is defined by the peak viscous response, VC_{max}.

Research conducted by Lau and Viano has demonstrated that this criterion is a reliable indicator of soft tissue injury in certain regions of the body. As illustrated in Figure 4-28, the criterion operates at an optimal level for velocities of deformation between 3 to 30 m/s. As the velocity of deformation falls below 3 m/s, soft tissue injury can be evaluated strictly by the degree of compression. Within this range, crushing injuries are common. However, as the velocity of deformation reaches and exceeds 30 m/s, the rate of compression becomes the primary factor in determining the severity and type of soft tissue injury. Blast injuries are common to this range and initially occur to the lungs and other hollow, thoracic organs.

THIS DOCUMENT PROVIDED BY THE ABBOTT AEROSPACE
TECHNICAL LIBRARY
ABBOTTAEROSPACE.COM

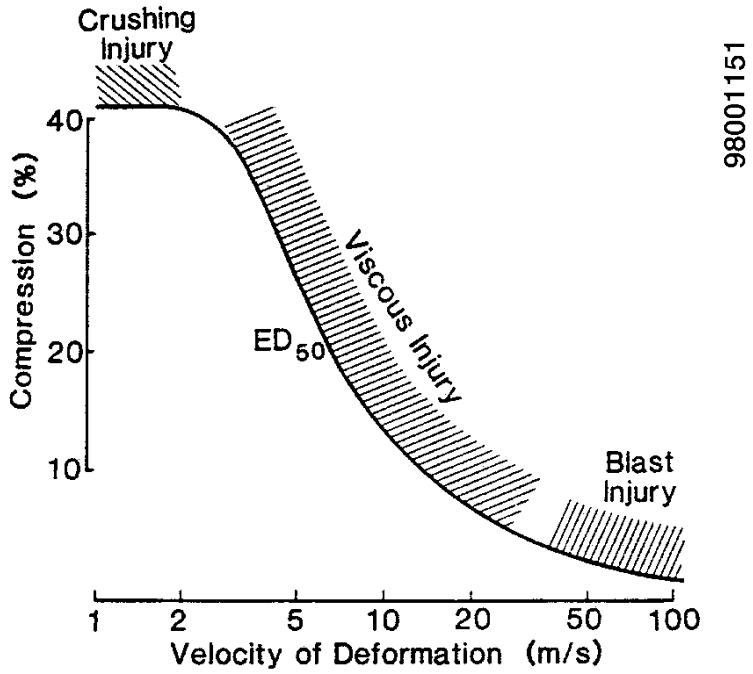


Figure 4-28.
Optimal range for application of the Viscous Criterion (Reference 4-92).

4.3.9.4 Thoracic Trauma Index (TTI)

In 1979, the SID was created to evaluate the potential for human injury during side-impact collisions (Reference 4-86). In the SID's thoracic region, injury potential is monitored by a measurement of the peak lateral spinal acceleration. An array of 12 accelerometers is used to record the response of the sternum, ribs, and thoracic spine during impact (Reference 4-64). The acceleration data acquired is evaluated using the Thoracic Trauma Index (TTI). This criterion is based on the age of the test subject, the peak lateral accelerations of either the 4th or 8th rib and the 12th thoracic vertebra, and the subject's mass (Reference 4-96). Specifically, the TTI is represented by the following expression:

$$TTI = \left(1.4 \times Age\right) + \tfrac{1}{2}\left(Rib_y + T12_y\right)\left(\frac{Mass}{Mass_{st}}\right) \qquad (5)$$

where: Rib_y = average acceleration of the 4th struck-side rib
$T12_y$ = average acceleration of the 12th thoracic vertebra acceleration
Mass = subject mass
$Mass_{st}$ = standard mass of 75 kg

For measurements recorded using the SID, the TTI expression is altered by the removal of the age factor and the mass ratio.

Investigations by Morgan, et al., have shown that the TTI is an accurate predictor of thoracic injury level resulting from a lateral impact (Reference 4-97). Table 4-6 displays TTI values for automotive side impacts. Note: All experiments discussed in Table 4-6 utilized human

THIS DOCUMENT PROVIDED BY THE ABBOTT AEROSPACE
TECHNICAL LIBRARY
ABBOTTAEROSPACE.COM

cadavers as test subjects, unless otherwise specified. In terms of the use of the TTI in evaluating thoracic injuries in aviation crashes, current research projects are being conducted at the Civil Aerospace Medical Institute and Wichita State to investigate the accuracy of the TTI over non-impulse, longer term G loads.

Table 4-6.
Lateral impact injury tolerances (Reference 4-64)

Tolerance Level	Injury Level	Reference
Force		
7.4 kN (drop test)	AIS 0	Tarrierre, et al. (1979)
10.2 kN (drop test)	AIS 3	Tarrierre, et al. (1979)
5.5 kN (pendulum impact)	25-pct probability of AIS 4	Viano (1989)
Acceleration		
45.2 G $T8_Y$	25-pct probability of AIS 4	Viano (1989)
31.6 G $T12_Y$	25-pct probability of AIS 4	Viano (1989)
27.7 G Upper sternum-X	25-pct probability of AIS 4	Cavanaugh, et al. (1990)
TTI		
85 G	Max in SID for four-door cars	FMVSS214
90 G	Max in SID for two-door cars	FMVSS214
Compression to half thorax		
35 pct	AIS 3	Stalnaker, et al. (1979)
35 pct	AIS 3	Tarrierre, et al. (1979)
31 pct (includes arms)	25-pct probability of AIS 4	Cavanaugh, et al. (1990)
Compression to whole thorax		
38.4 pct	25-pct probability of AIS 4	Viano (1989)
VC_{max} to half thorax		
< 1.0 m/sec	AIS 0-2	Cavanaugh, et al. (1990) and unpublished data
>1.0 m/sec	AIS 4-5	
VC_{max} to whole thorax		
1.47 m/sec	25-pct probability of AIS 4	Viano (1989)

4.3.10 Abdominal Impact Tolerance

Presently, the FAA specifies the abdominal impact tolerance requirement in terms of the position of the lap belt during impact testing. FAR Part 23.563(c)(4) states that the "safety belt must remain on the ATD's pelvis during the impact" (Reference 4-76).

The abdomen of the human body is a large cavity located below the diaphragm and above the pelvic girdle. The abdominal cavity is filled with numerous organs, each of which respond differently to mechanical loading. Figure 4-29 illustrates the positioning of these organs within the abdominal cavity.

4.3.10.1 Influential Factors

There are several factors that influence the mechanical properties, injury mechanisms, and injury tolerances of the abdominal region (Reference 4-64). These factors can be described as being either external or internal to the abdominal cavity. External factors include:

- Rate of impact loading
- Impact force
- Energy input at impact
- Rapid deceleration of the occupant's body.

THIS DOCUMENT PROVIDED BY THE ABBOTT AEROSPACE
TECHNICAL LIBRARY
ABBOTTAEROSPACE.COM

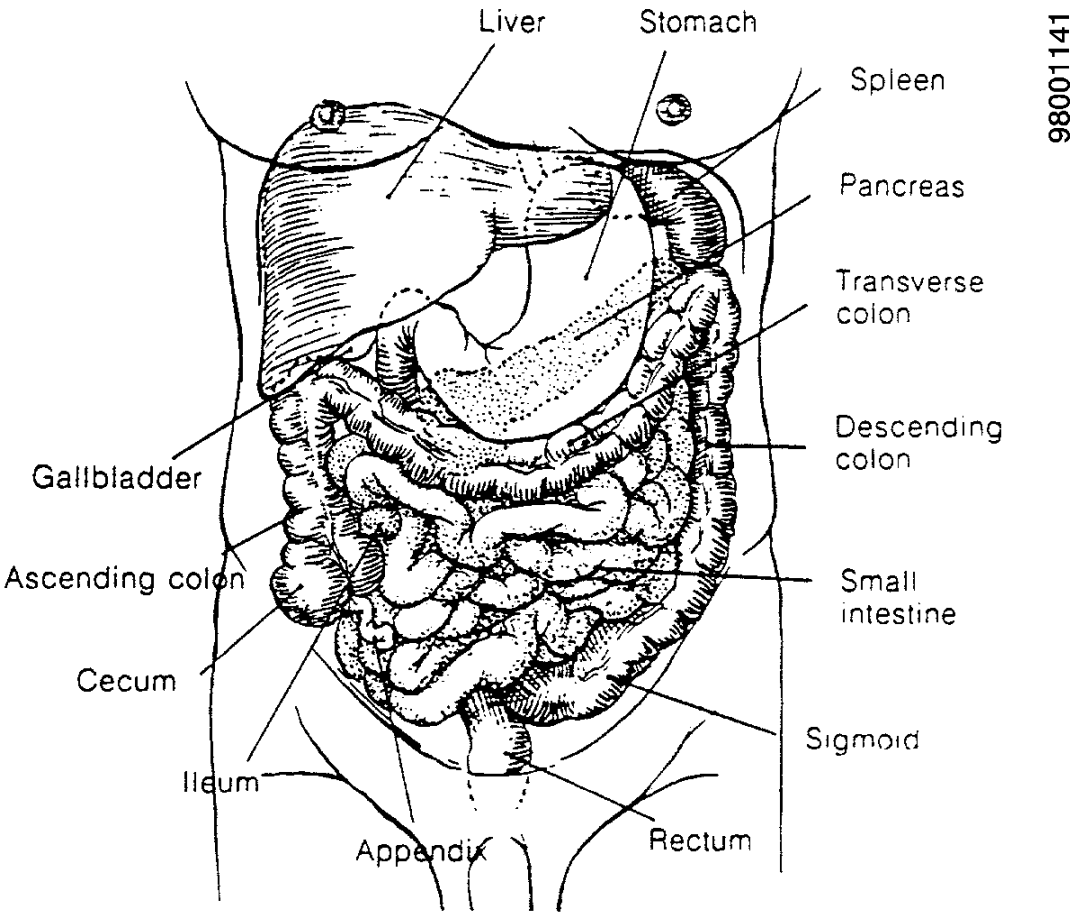


Figure 4-29.
Organs of the abdomen (Reference 4-64).

The internal factors that influence the mechanical characteristics exhibited by a particular abdominal organ include:

- Location of the organs within the cavity
- High mobility of the organs
- Gross density
- Age
- Pathological state.

The location of the organs in the abdomen dictates whether they will be injured by mechanical loading. Certain organs are positioned behind the lower rib cage and may receive more protection than other abdominal organs. Organ location becomes increasingly important in experiments that are conducted using animals as human surrogates. The organs of these animals tend to have a different geometry than human organs, and may be located in different positions within the abdominal cavity. This makes it challenging to generate worthwhile comparisons between animals and humans.

This Document Provided by the Abbott Aerospace
TECHNICAL LIBRARY
ABBOTTAEROSPACE.COM

The organs of the abdomen are also highly mobile. Many of the organs are not rigidly fixed within the abdominal cavity, which allows the organs to change their position in response to changes in overall body posture and orientation (References 4-98 and 4-99). The peritoneum membrane that covers the organs and the inner cavity of the abdomen also creates a low-friction interface between the organs and the cavity walls that increases organ mobility (Reference 4-64). These properties alter the repeatability of injuries that are sustained under similar types of mechanical loading.

The gross density of the abdominal organs causes each individual organ to behave differently under mechanical loading. Abdominal organs can be separated into two different categories: solid organs and hollow organs. The liver and the spleen are examples of solid organs that are characterized by their fluid-filled vessels and dense composition. The stomach and intestines are examples of hollow organs. Hollow organs are less dense than the solid organs, as a result of the presence of a large cavity within the organ. In addition, the age and pathological state of the organs may also affect the organs' response to mechanical loading. These physical properties vary among the abdominal organs, making the force and injury analysis process extremely difficult.

4.3.10.2 Injury Mechanisms

Trauma to the abdomen may occur by penetration of objects into the abdomen or from blunt impact to the region. Injuries resulting from blunt impact are usually more difficult to diagnose. In addition, the mortality rate associated with blunt trauma to the abdomen is significantly higher than the rate associated with penetrating trauma (Reference 4-64). The following injury mechanisms have been associated with blunt trauma:

Compression

Compression injuries to the abdomen typically result from blunt impacts to the abdominal surface. During impact, the outer surface of the abdominal region deforms, pressing the superficial organs against other internal organs and surfaces. Several impact studies have demonstrated a relationship between maximum abdominal wall compression and abdominal injury severity (Reference 4-100). This relationship may be a function of the type of collision used to produce the injuries.

Wave Motion

Injuries to the abdominal region can occur to areas that are remote from the site of the blunt impact. These injuries may be attributed to stress and shear waves which propagate through the organs and tissues of the abdominal cavity (References 4-101 and 4-102). The magnitude of the wave is primarily defined by the velocity of deformation. For high-velocity deformations (>50 m/sec), the waves originate at the impact site and propagate through the abdominal tissues at the speed of sound. Injuries to the tissues occur between the boundaries of differing tissue types (Reference 4-64). Three different injury mechanisms have been suggested for high-velocity deformations including:

- Stress-wave-induced compression and re-expansion of the stressed abdominal wall
- Production of a pressure differential across the boundary
- "Spalling" – as the wave travels from a dense to a much-less-dense medium, energy is released.

This Document Provided by the Abbott Aerospace
TECHNICAL LIBRARY
ABBOTTAEROSPACE.COM

In lower-velocity deformations (<15 m/sec), injuries occur from the propagation of a shear waves which move transversely through the abdominal tissues for a long duration of time. The three injury mechanisms proposed include:

- Differential motion of connected adjacent structures
- Strain at the attachment sites
- Collision of the viscera with stiffer structures.

Submarining

In the automotive industry, several studies have been conducted to examine the interaction of the abdominal region with the vehicle restraint system (Reference 4-64). Accident investigations and experimental studies have revealed that high lap belt loads can cause injuries to both the pelvic and abdominal region of the human body. These injuries generally result from misplacement of the restraint system and/or "submarining". The term "submarining" was introduced to describe the movement of the occupant's body with respect to the lap belt portion of a restraint system. Submarining occurs when the iliac crests of the pelvis slide below the lap belt, thereby loading the abdomen. Currently, the presence of submarining is detected by changes in lap belt loading; otherwise, must be observed visually. Improvements in restraint systems have helped to decrease the occurrence of submarining injuries when the lap belt is worn in the correct position. Specifically, the automotive industry has changed from a two-point restraint to a three-point restraint, while the military has changed from a four-point restraint to a five-point restraint.

Pressure

High rates of loading generate an increase of the internal fluid pressure of the abdomen (Reference 4-64). This increased pressure can produce viscous injuries including tensile or shear strains in the liver, tears at the pedicle or hilar regions of the spleen, or avulsion of the blood vessels in the abdominal region.

4.3.10.3 Injury Tolerance

In the aviation industry, studies were conducted by DeHaven and by Windquist, et al., to investigate abdominal injuries in light plane accidents. In a study conducted in 1944, DeHaven observed that the abdominal wall could resist an impact of approximately 2,200 lb (Reference 4-103). A second study, performed by Windquist, et al., in 1953, examined the injuries sustained from blunt abdominal trauma relative to objects within an aircraft cockpit (Reference 4-104). Results from the study indicated that the following forces were survivable: a force of 1,080 lb against a 10 $in.^2$ area, a force of 893 lb against a protruding pin, and a force of 750 lb through the abdominal belt.

Regarding the issue of submarining, Walfisch, et al., subjected 14 belted cadavers to a series of sled impacts (Reference 4-105). Initially, a lap belt load of 450 lb per side was recommended as the appropriate abdominal tolerance limit. This tolerance limit was later increased to an average lap belt tension of 790 lb per side, with a belt penetration of 1.5 in.

Presently, the aviation industry uses the Hybrid II ATD to evaluate the potential for injury during impact tests. In terms of abdominal injury, the Hybrid II ATD does not possess the instrumentation required to measure abdominal loads (Reference 4-86). In addition, the structure of the ATD abdominal region lacks biofidelic properties. To improve this process, researchers within the automotive industry are trying to develop quality ATD abdominal instrumentation and to enhance the biofidelity of the ATD abdominal structure.

This Document Provided by the Abbott Aerospace
TECHNICAL LIBRARY
ABBOTTAEROSPACE.COM

4.3.11 Lower-Extremity Impact Tolerance

To date, the FAA has not specified any requirements for lower-extremity impact tolerance in FAR Part 23. However, in the design of a crashworthy aircraft, it is still important to understand the injury mechanisms that occur from impact to the lower extremities. It is also important to recognize the problems that can arise during egress from an aircraft when the occupant has sustained minor to serious lower-extremity injuries. Entrapment can occur if the occupant's injuries are so severe that he/she is unable to egress effectively.

In GA accidents, the types of injuries sustained by the lower extremities may include damage to both the hard and soft tissues. A study conducted by researchers from the Department of Emergency Medicine at Johns Hopkins University School of Medicine compared the autopsy data from aviation crashes that occurred in both 1980 and 1990 (Reference 4-91). The data revealed that lower-extremity fractures comprised 4.0 pct of the total injuries received by aircraft occupants during 1980 and 3.5 pct in 1990.

Injuries to the lower extremities depend on the type of impact sustained by the occupant (Reference 4-106). Fractures to the femur typically occur indirectly through the knee. In frontal-impact automotive accidents, loading of the femur occurs when the knee strikes the dashboard of the vehicle (Reference 4-64). This loading situation can also occur in aviation accidents when the knee impacts the instrument panel or the bulkhead of the plane's interior.

To investigate the injury tolerance of the femur, researchers in the automotive industry have conducted a variety of impact studies using Hybrid-III-type adult ATDs. From these studies, injury-assessment curves were developed to describe the axial compressive femur force as a function of the duration of loading (Reference 4-107). These curves are illustrated in Figure 4-30. If the value of the axial compressive femur load is above the time-dependent curve, distributed loads applied to the knee may cause fractures of the femur.

Figure 4-30 also describes the potential for fracture of the patella and pelvis as a result of distributed loads applied to the knee. These distributed loads can originate from direct contact with the vehicle or aircraft's interior (Reference 4-64). The patella can also be injured indirectly from contraction of the quadriceps muscle while in a sitting position with the knee partially flexed.

Other lower extremity injuries involve the tibia, fibula, and ankle. Fractures to the tibia and fibula typically occur from direct contact with the aircraft's interior. Ankle injuries, including hard tissue fractures and tearing of the soft tissues, are produced from pure vertical loading or combined loads resulting from supination or pronation and internal or external rotation of the ankle. Human tolerance values for the tibia and fibula are described in Table 4-7.

Presently, the aviation community uses the Hybrid II ATD to monitor the response of the lower extremities in impact tests. However, the Hybrid II is only instrumented to record the forces and moments of the lower femur (Reference 4-64). The automotive industry utilizes the Hybrid III ATD that contains more sophisticated lower-extremity instrumentation. The Hybrid III is capable of measuring both upper and lower femur forces and moments, knee position, knee-tibia displacement, knee-clevis forces, upper tibia moments, lower tibia forces and moments, and foot/ankle/toe forces and moments.

THIS DOCUMENT PROVIDED BY THE ABBOTT AEROSPACE
TECHNICAL LIBRARY
ABBOTTAEROSPACE.COM

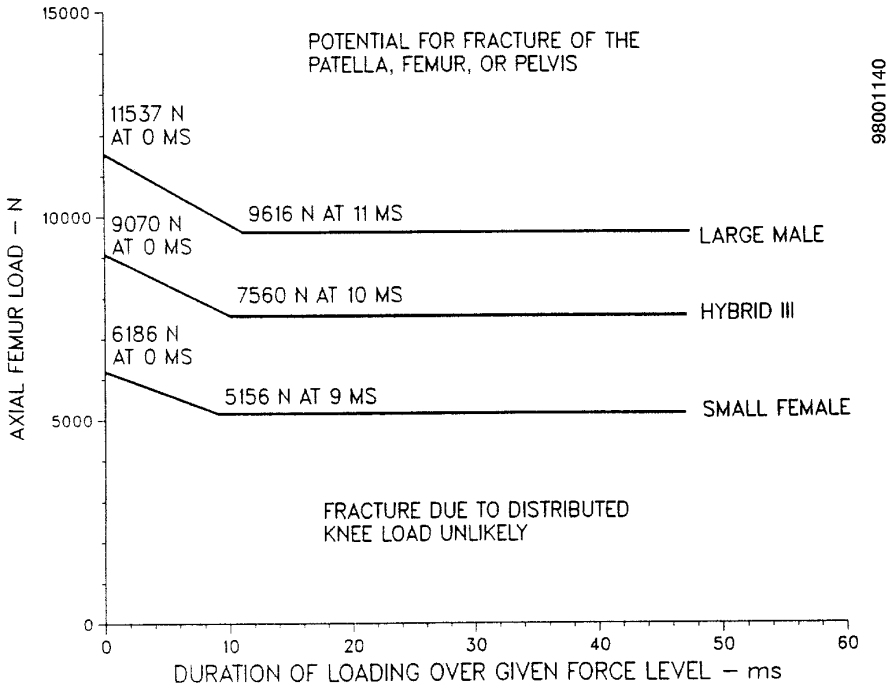


Figure 4-30.
Injury-assessment curves for axial compressive femur force measured with Hybrid III-type ATDs (Reference 4-107).

Table 4-7.
Strength of lower extremity bones (Reference 4-64)

Lower Extremity Bone	Gender	Torque (N-m)	Bending (kN)	Average Max. Moment (N-m)	Long-Axis Compression (kN)
Femur	Male	175	3.92	310	7.72
	Female	136	2.58	180	7.11
Tibia	Male	89	3.36	207	10.36
	Female	56	2.24	124	7.49
Fibula	Male	9	0.44	27	0.60
	Female	10	0.30	17	0.48

4.3.12 Injury Scales

The study of injury etiology requires the development and application of standard injury classification systems. In general, there are two types of scales used to categorize injuries: (1) scales which evaluate the physiological status of a patient before and during the treatment period for the injury, and (2) scales which describe the severity of an injury in terms of its anatomical location and specific wound type (Reference 4-108). The following scales represent the most popular classification systems within the injury assessment community.

4.3.12.1 Abbreviated Injury Scale

The Abbreviated Injury Scale (AIS), first published in 1971, was developed as a comprehensive system for rating injuries by type and severity (Reference 4-108). The goal was to create a system that would be acceptable to physicians, engineers, and researchers working in automotive crash investigation. Over the last decade, the AIS has evolved as the universal

THIS DOCUMENT PROVIDED BY THE ABBOTT AEROSPACE
TECHNICAL LIBRARY
ABBOTTAEROSPACE.COM

system of choice for assessing impact injury severity. As the sophistication in injury assessment capabilities has improved, particularly among emergency room trauma specialists, the AIS has undergone several revisions. The latest revision was published in 1990.

As displayed in Table 4-8, the AIS classifies injuries by body region on a 7-point scale. The AIS numbers 1 - 6 indicate increases in injury severity ranging from minor to maximum injury severities. AIS number 9 represents those injury cases where trauma did occur, but no assessment information was provided to allow an AIS number to be assigned. The numbers in the AIS coding system do not indicate a relative weight. For example, AIS 2 is more severe than AIS 1, however, AIS 2 is not twice as severe as AIS 1. Additionally, two AIS 1 injuries are not equivalent to one AIS 2 injury. The AIS also divides the body into 9 major regions that provide a total of 1,320 injury descriptions. To determine the AIS number assigned to a particular injury, one would use the AIS dictionary to locate the specific body region and injury type in question.

Table 4-8.
Severity codes and corresponding descriptions for the AIS (Reference 4-108).

AIS No.	Severity Code
1	Minor
2	Moderate
3	Serious
4	Severe
5	Critical
6	Maximum Injury, Virtually Un-survivable
9	Unknown

4.3.12.2 Injury Severity Score

The Injury Severity Score (ISS) expands the AIS to consider the effects of injury to multiple body segments (Reference 4-109). The ISS defines six body regions: (1) head and neck, (2) face, (3) chest, (4) abdomen or pelvic contents, (5) extremities or pelvic girdle, and (6) external. As shown in Equation 6, the overall score is based on a mathematically derived code number determined from the highest AIS codes in each of the three most severely injured body regions.

$$ISS = (AIS_1)^2 + (AIS_2)^2 + (AIS_3)^2 \quad (6)$$

where: AIS_1 = Highest AIS anywhere in the body
AIS_2 = Highest AIS anywhere in the body except body region of AIS_1
AIS_3 = Highest AIS anywhere in the body except body region of AIS_1 or AIS_2

4.3.12.3 Injury Impairment Scale

The purpose of the Injury Impairment Scale (IIS) is to assess the level of impairment suffered as a result of the injury received by the victim (Reference 4-110). The IIS code numbers and their corresponding descriptions are provided in Table 4-9. Impairment is assigned in cases where whole-body dysfunction exists. The IIS is not used to assess the impairment of individual

THIS DOCUMENT PROVIDED BY THE ABBOTT AEROSPACE
TECHNICAL LIBRARY
ABBOTTAEROSPACE.COM

body organs or body systems. When impairment levels are defined, they are based on the original injury sustained by the victim and are assessed one year following the occurrence of the injury.

Table 4-9.
Injury Impairment Scale (Reference 4-110)

IIS Code	Level of Impairment
0	No impairment, normal function
1	Impairment detectable, but does not limit normal function
2	Impairment level compatible with most, but not all, normal function
3	Impairment level compatible with some normal function
4	Impairment level significantly impedes some normal function
5	Impairment level precludes most useful function
6	Impairment level precludes any useful function

4.3.12.4 Glasgow Coma Scale

The Glasgow Coma Scale (GCS) is used to quickly and concisely quantify a complex head injury (Reference 4-111). The GCS provides a method for evaluating changes in the level of consciousness of a victim and is based on a functional assessment of eye opening, verbal response, and motor response. The observed function in each of these three categories is assigned a numerical value.. The numerical scores for the three assessment categories are added together to obtain a total score within a range from 3 (no response) to 15 (no impairment).

4.3.12.5 Concept of "Harm"

"Harm" is a measure of the economic cost associated with an injury. It is defined as the "sum of all injured people (fatalities and injured survivors), each weighted in proportion to the outcome, as represented by the cost of the person's most severe injury" (Reference 4-77). For example, in terms of cost, an AIS 5 injury has a higher cost than an AIS 6 injury. Overall, the concept of harm can be useful in identifying opportunities for reducing trauma-related injuries.

4.4 ANTHROPOMORPHIC TEST DEVICES (ATDS)

An anthropomorphic test device (ATD) is an instrumented mechanical device that is used to mimic the response of the human body under various loading and accelerative conditions. ATDs are commonly referred to as "crash test dummies" or "manikins". They can be designed to represent an entire human body or an individual body segment. Various ATDs have been created for the automotive industry, the aviation industry, and for various branches of the military. Initially, the primary function of the ATD was to represent the approximate size and weight of a human during dynamic loading of a test vehicle. Today, ATDs are also used to:

- Serve as a measurement device in the assessment of occupant injury protection in dynamic crash events
- Assist in the research, development, and certification of new or improved vehicles and safety systems
- Assist in the testing and certification of personal safety equipment (i.e., helmets, parachutes, flotation devices, etc.).

This Document Provided by the Abbott Aerospace
TECHNICAL LIBRARY
ABBOTTAEROSPACE.COM

4.4.1 Design Characteristics

In order for an ATD to serve as an effective human surrogate, the design of each individual ATD should address seven distinct issues, including (Reference 4-86):

- Biofidelity
- Anthropometry
- Measurement Capability
- Repeatability and Reproducibility
- Durability
- Sensitivity
- Ease of Use

The following sections provide a brief description of the relevance of each of these issues.

4.4.1.1 Biofidelity

In order to accurately mimic the response behavior of a live human being, ATDs must be designed with a high level of biofidelity (References 4-86 - 4-114). Biofidelity refers to the "degree to which pertinent human physical characteristics are incorporated in the ATD design (Reference 4-86)." A high level of biofidelity is achieved through the use of:

- Anthropometric measurements that define the size, shape, and mass characteristics of the ATD
- Special materials which can approximate the stiffness, flexibility, and energy-absorption characteristics of the human body.

By employing these specifications, the ATD can be designed to simulate human responses including body segment trajectory, velocity, articulation, and deformation under applied loads and accelerations.

Current regulatory ATDs are designed to be biofidelic in only one direction (i.e., either forward or sideways). It is important to note that even in the primary biofidelic design direction, **no** ATDs are perfectly biofidelic. This lack of fidelity results from design compromises that must be made in order to ensure that the ATD will incorporate the other basic design characteristics listed in 4.4.1.1.

4.4.1.2 Anthropometry

In an effort to maintain a high degree of biofidelity, ATDs have traditionally been custom-designed to serve a specific purpose and to represent a particular population (References 4-86 and 4-112). This is accomplished by designing the ATD to represent the general anthropometric characteristics of an average person within the selected population or to represent extreme characteristics of certain individuals within a given population. However, the majority of the current ATDs were designed using data from anthropometric studies conducted in the 1950's and 1960's (Reference 4-86). As a result, the anthropometry of current ATDs may not be exactly representative of the United States civilian and/or military populations of today. New ATD designs should account for changes in population anthropometry. (Refer to Section 4.1 for a detailed description on human anthropometry.)

THIS DOCUMENT PROVIDED BY THE ABBOTT AEROSPACE
TECHNICAL LIBRARY
ABBOTTAEROSPACE.COM

4.4.1.3 Measurement Capability

The ATDs in use today are specially designed to house numerous types of instrumentation including linear and angular accelerometers, linear and rotary potentiometers, and axial, shear, and torsional load cells (References 4-86 – 4-114). When selecting ATD instrumentation, it is critical to select the standard sensors that have been designed to fit the particular ATD. In many cases, certain sensors are made by more than one manufacturer, suggesting that the general characteristics may vary from sensor to sensor. For example, certain sensors have a different mass, shape, size, and response that could potentially influence the overall response characteristics of the ATD. Therefore, it is worthwhile to ensure that the selected sensors are compatible with the particular ATD.

The types of instrumentation used should correspond to the types of measurements that are desired within a test environment. For example, the BioSID ATD was specifically designed to evaluate automotive side-impact collisions and is capable of recording the forces and accelerations experienced by the shoulder as well as the displacement of the shoulder (References 4-86 and 4-112). Similarly, the Hybrid II and Hybrid III ATDs were designed to evaluate frontal automotive and aircraft collisions and are not instrumented to record shoulder responses.

In order to utilize the data recorded by the ATD's instrumentation, a data acquisition system is required. Most modern data acquisition systems are digital. Analog systems are still used; however, the analog system usually serves as back-up data acquisition system for the digital devices. Currently, there are three different types of data acquisition systems available for use (Reference 4-86):

1. Off-Board the Sled or Test Vehicle – Typically used when the laboratory equipment is too large to fit safely on the sled, or when the test vehicle transducer cables are used and are connected to the recording equipment through junction boxes and/or umbilical cables.
2. On-Board the Sled or Test Vehicle – No umbilical cord is needed, as the system package is relatively light and small and is placed directly on the sled or test vehicle. The ATD's transducers are connected to the system through cables that remain in the vehicle or sled. This system provides signal conditioning, anti-aliasing filtering, digitizing, data scaling, and data storage in one package.
3. On-Board the ATD – This system that is incorporated directly into the ATD, thereby eliminating the need for transducer umbilical cables. This system provides signal conditioning, anti-aliasing filtering, digitizing, data scaling and data storage. An example of an "on-board-the-ATD" data acquisition system is the battery-operated Intelligent Dummy Data Acquisition System (IDDAS) developed by Robert A. Denton, Inc. (Reference 4-114). The IDDAS unit is currently available for use with the Hybrid III 50th-percentile male ATD.

4.4.1.4 Repeatability and Reproducibility

Additional areas of concern regard the repeatability and reproducibility of the ATD (References 4-86, 4-112, 4-115). The property of repeatability suggests that in repeated impact tests under the same input conditions, an individual ATD should be capable of yielding the same response, or output, each time. The repeatability of an ATD is affected by several different factors including temperature, humidity, the age of the ATD, the degree of "wear and tear", the duration of time between impact tests, and the instrumentation calibration. In order to verify the repeatability of an ATD, repeated impact tests are conducted using the same ATD. Peak responses recorded during each test are used to calculate a mean response and standard

This Document Provided by the ABBOTT Aerospace
TECHNICAL LIBRARY
ABBOTTAEROSPACE.COM

deviation. A Coefficient of Variation is determined for the ATD using the following expression (Reference 4-86):

$$\textit{Coefficient of Variation} = \textit{standard deviation/mean response} \quad (7)$$

An acceptable Coefficient of Variation value is approximately 10 pct.

Reproducibility concerns the efficiency of different ATDs of the exact same design. For example, all 50th-percentile Hybrid III male ATDs should be capable of yielding identical responses for similar impact test environments and conditions. Compliance with this specification will allow the data from similar impact tests, using two separate 50th-percentile Hybrid III male ATDs, to be compared effectively. The factors affecting the reproducibility of an ATD include manufacturing tolerances, material property variation, and instrumentation calibration.

4.4.1.5 Durability

One of the most challenging aspects in ATD design is in creating a strong, durable ATD that is able to maintain its structure and biofidelic characteristics under repeated impact tests (References 4-86, 4-112, 4-115). To accomplish this task, designers often have to accept design tradeoffs between strength and biofidelic characteristics. For example, the majority of the ATD's skeletal system is composed of steel. Steel was selected for its relatively high strength properties and, as a result, it is expected to remain intact and undamaged after repeated impact tests. However, using steel also presents a disadvantage in that it does not accurately represent the properties of human bone.

4.4.1.6 Sensitivity

The issue of sensitivity is primarily concerned with how factors such as temperature and humidity affect the performance of the ATD (Reference 4-86). The ATDs should be composed of materials that are insensitive to these extraneous conditions. This characteristic becomes especially important for those ATDs that are used in outdoor test facilities. Outdoor test facilities are unable to maintain control over these conditions, whereas most indoor facilities have this capability.

4.4.1.7 Ease of Use

The ATDs should be easy to use in a variety of testing environments (Reference 4-86). The ATD's components should be easy to repair or replace with readily available replacement parts, the instrumentation should be easy to calibrate, and any additional support equipment external to the ATD itself should be kept to a minimum to increase the ATD's maneuvering and positioning capabilities before and after each test.

4.4.2 Historical Development of ATDs

In 1949, the Sierra Engineering Company was employed by the United States Air Force (USAF) to design and manufacture the first whole-body ATD, which was called Sierra Sam (Reference 4-86). Sierra Sam was developed to evaluate the safety of aircraft ejection seats. Its exterior shape and body weight depicted human-like qualities, including articulating limb joints.

This Document Provided by the Abbott Aerospace
Technical Library
abbottaerospace.com

Unfortunately, Sierra Sam had limited instrumentation, and was not capable of withstanding repeated ejection seat tests without damage.

Following the introduction of Sierra Sam, the development of new and improved instrumentation and biofidelic materials allowed for significant advances in ATD technology. The majority of the currently available ATDs have been designed primarily for use in automotive impact testing. Automotive impacts primarily occur within a two-dimensional, planar space, since roll over or vertical landing scenarios are not as common in automobiles as they are in airplanes. This allows the principal direction of force in an automotive crash to be described as a two-component vector. As a result, most ATDs were designed specifically to evaluate occupant injury risk in planar surface frontal and side impacts.

However, there were some ATDs that were designed for use as test devices in the aviation industry. For example, in 1986, Systems Research Laboratories (SRL) developed the Advanced Dynamic Anthropomorphic Manikin (ADAM) for the Armstrong Aerospace Medical Research Laboratory (AAMRL) at the Wright-Patterson Air Force Base in Ohio. The ADAM was designed to be used in impact tests that assessed the capabilities of the Crew Escape Systems Technologies (CREST) ejection seat. The ADAM was also used to mimic the response of the human body during parachute and helicopter seat tests.
Aircraft impacts occur in a three-dimensional space, where a third vector component (vertical component) is added. This allows the principal direction of force in aircraft crashes to be described as a three-component vector. Therefore, ATDs that are designed for use in aircraft crash simulations must be able to withstand impact crash forces from potentially three different directions.

In general, currently available ATDs can be divided into two distinctly different categories: frontal-impact ATDs and side-impact ATDs. Presently, GA regulations only require the use of a single ATD in the evaluation of aircraft systems and components: the Hybrid II frontal-impact ATD (Reference 4-116). However, with advancements in ATD technology and aircraft design, additional ATDs will be employed to accurately assess the occupant injury protection capabilities of different aircraft. The following two sections briefly describe the characteristics of the frontal- and side-impact ATDs that are currently available in the transportation industry today.

4.4.3 Frontal Impact ATDs

Presently, there are four different frontal-impact ATDs available for impact testing in the automotive and aviation industries: Hybrid II, Hybrid III, FAA-Hybrid III, and THOR. The following sections will describe the injury-predictive measurement capabilities, as well as the biofidelic attributes and deficiencies, of each frontal-impact ATD.

4.4.3.1 Hybrid II Frontal Impact ATD

In 1972, General Motors introduced the Hybrid II 50th-percentile adult male ATD (References 4-113 and 4-114). Figure 4-31 illustrates the exterior structure of the Hybrid II ATD. The Hybrid II ATD was designed and manufactured for the purpose of evaluating the reliability of lap/shoulder belt restraint systems in frontal automotive impacts. In 1973, the Department of Transportation required the use of the Hybrid II ATD for the impact testing of all vehicles equipped with passive restraint systems (References 4-86 – 4-113). This requirement is specified in 49 CFR Parts 571.208 and 572, Subpart B (References 4-116 and 4-119).

THIS DOCUMENT PROVIDED BY THE ABBOTT AEROSPACE
TECHNICAL LIBRARY
ABBOTTAEROSPACE.COM



Figure 4-31.
General Motors' Hybrid II 50th-percentile adult male ATD (Reference 4-86).

The Hybrid II ATD demonstrates an adequate degree of repeatability, durability, and serviceability during impact testing (Reference 4-114). However, the Hybrid II ATD's limited biofidelity and injury measurement capability have prevented it from obtaining accurate assessments of restraint system effectiveness. A thorough description of the Hybrid II ATD's attributes, deficiencies, and anthropometric characteristics is provided in Tables 4-10 – 4-14 and Figure 4-32.

THIS DOCUMENT PROVIDED BY THE ABBOTT AEROSPACE
TECHNICAL LIBRARY
ABBOTTAEROSPACE.COM

Table 4-10.
Design Characteristics for the Hybrid II ATD (References 4-86 – 4-113)

Body Segment	Structure and *Instrumentation*	Biofidelic Attributes	Biofidelic Deficiencies	Injury-Predictive Measurements
Head	Adapted from the Sierra Engineering 292-1050 ATD design; aluminum shell covered by vinyl skin with facial features; *triaxial accelerometer located at c.g.; angular accelerometer*	Exterior size and shape of 50th-percentile adult male	Head-to-neck attachment location, mass distribution, c.g. location, and hard-surface impact response are not humanlike	Facial laceration prediction is possible if a chamois covering is used; brain injury and/or skull fracture predictions are based on linear acceleration measurements and are poor for hard-surface impact, due to non-humanlike impact response
Neck	Monolithic butyl rubber cylinder with braided wire cable through center and attached to endplates	None	Bending response is not humanlike	None
Thorax	Adapted from the Alderson VIP-50A ATD; six steel ribs connected to rigid steel spine and leather sternum; damping material attached to ribs; rib cage covered by vinyl skin; *triaxial accelerometer located in thoracic spine*	Exterior size and shape of 50th-percentile adult male	Rib cage not humanlike in shape; mass distribution and force deflection response not humanlike	Thoracic injuries related to gross thoracic acceleration
Lumbar Spine	Circular cylinder composed of rubber with braided steel cable passing through the axis and attached to circular aluminum endplates; *lumbar spine load cell*	None	Bending response not humanlike; does not provide humanlike sitting posture	Forces and moments exerted on lumbar spine (Lumbar load cell is not a standard feature, but is recommended for use in aviation applications)
Abdomen	Polyurethane foam-filled rubber bladder	None	Force-penetration response is not humanlike	None
Pelvis	Aluminum casting of human pelvis shape covered with vinyl skin; *triaxial accelerometer*	Humanlike pelvis shape	Mass and mass distribution are not humanlike	Injuries to the pelvis due to gross pelvic acceleration
Lower Extremity	Steel shafts used for femur and leg structures covered with vinyl skin; limited rotation ball joint at hip and pin joints at knee and ankle; twist joint in femur shaft; adjustable friction joints; *axial sensitive load cell in femoral shaft*	Humanlike ranges of motion, except the ankle joint	Ankle joint cannot bend sideways; mass distribution, joint resistances, and knee impact response characteristics are not humanlike	Axial compressive femur load used to predict injuries to the femur
Shoulder	Aluminum casting pin-jointed to spine; fore/aft range of motion controlled by rubber resistor	Geometry of clavicle simulated in area where the shoulder belt would load the clavicle	Mass distribution and load-deflection responses are not humanlike	None
Arm	Steel shafts used for upper and lower arms; frictional pin joint at shoulder, elbow, and wrist; shafts covered with vinyl skin	Humanlike ranges of motion	Mass distribution and joint resistance are not humanlike	None

This Document Provided by the Abbott Aerospace
TECHNICAL LIBRARY
ABBOTTAEROSPACE.COM

Table 4-11.
External anthropometric measurements for the Hybrid II ATD (References 4-2 and 4-116)

Measurement	Figure 4-32 Code	Dimension (in.)
Seated height	A	35.7 ± 0.1
Shoulder pivot height	B	22.1 ± 0.3
Hip pivot height	C	3.9
Hip pivot from back line	D	4.8
Knee pivot from back line	E	20.4 ± 0.3
Knee pivot from floor	F	19.6 ± 0.3
Head back from back line	G	1.7
Chest depth	H	9.3 ± 0.2
Shoulder width	I	18.1 ± 0.3
Chest circumference over nipples	K	37.4 ± 0.6
Waist circumference at minimum girth	L	32.0 ± 0.6
Hip width	M	14.7 ± 0.7
Politeal height	N*	17.3 ± 0.2
Shoulder-elbow length	Q*	14.1 ± 0.3
Elbow rest height	R*	9.5 ± 0.5
Head width	S*	6.1 ± 0.2
Head length	T*	7.7 ± 0.2
Head segment line	AA	9.3
Shoulder-thorax segment line	BB	25.1

*Measurements not included in Part 572 anthropometric data

Table 4-12.
Segment mass measurements for the Hybrid II ATD (References 4-2 and 4-116)

Body Segment	Mass (lb)
Head	11.2 ± 0.1
Upper torso (including lumbar spine)	41.5 ± 1.6
Lower torso (including visceral sac and upper thighs)	37.5 ±1.5
Upper arm	4.8 ± 0.2
Lower arm	3.4 ± 0.1
Hand	1.4 ± 0.1
Upper leg	17.6 ± 0.7
Lower leg	6.9 ± 0.3
Foot	2.8 ± 0.1
Total (including instrumentation in head, torso, and femurs)	164.0 ± 3.0

Table 4-13.
Center-of-gravity locations for the Hybrid II ATD (References 4-2 and 4-116)

Segment	X and Z Reference Origin*	X (in.)*	Z (in.)*
Head	Back and top of head	+4.0 ± 0.2	-4.7 ± 0.1
Upper torso	Backline and top of head	+4.1 ± 0.3	-17.2 ± 0.3
Lower torso and upper thigh	Backline and top of head	+4.9 ± 0.5	-31.0 ± 0.5
Upper arm	Shoulder pivot	+0.0 ± 0.3	-5.0 ± 0.3
Lower arm	Elbow pivot	+4.2 ± 0.3	0.0 ± 0.3
Hand	Wrist pivot	+2.2 ± 0.3	0.0 ± 0.3
Upper leg	Knee pivot to upper leg rotation center	-6.7 ± 0.3	0.0 ± 0.3
Lower leg	Knee pivot to ankle pivot	0.0 ± 0.3	-8.0 ± 0.3
Foot	Ankle pivot	+ 2.2 ± 0.3	-1.7 ± 0.3

*Coordinate system is defined in Figure 4-32 (+x forward and +z up).

THIS DOCUMENT PROVIDED BY THE ABBOTT AEROSPACE
TECHNICAL LIBRARY
ABBOTTAEROSPACE.COM

Table 4-14. Hybrid II ATD mass moments of inertia (Reference 4-118)			
Body Segment	**Mass Moments of Inertia ($in.\text{-}lb\text{-}sec^2$)**		
	I_X	I_Y	I_Z
Head	0.266	0.275	--
Head/neck	0.310	0.367	0.233
Upper torso (includes lumbar spine)	2.18	1.79	--
Lower abdomen, pelvis, and visceral sac	2.32*	1.73*	--
Right upper arm	0.134	0.132	0.022
Right forearm (no hand)	0.012	0.068	0.071
Right upper leg	0.127	0.873	0.890
Right lower leg (no foot)	0.599	0.575	0.359

*Includes lumbar spine section.
NOTES:
1. Instrumentation was installed in the head, chest, and femurs during the measurements.
2. Estimated accuracy of measurements: ± 3 pct.

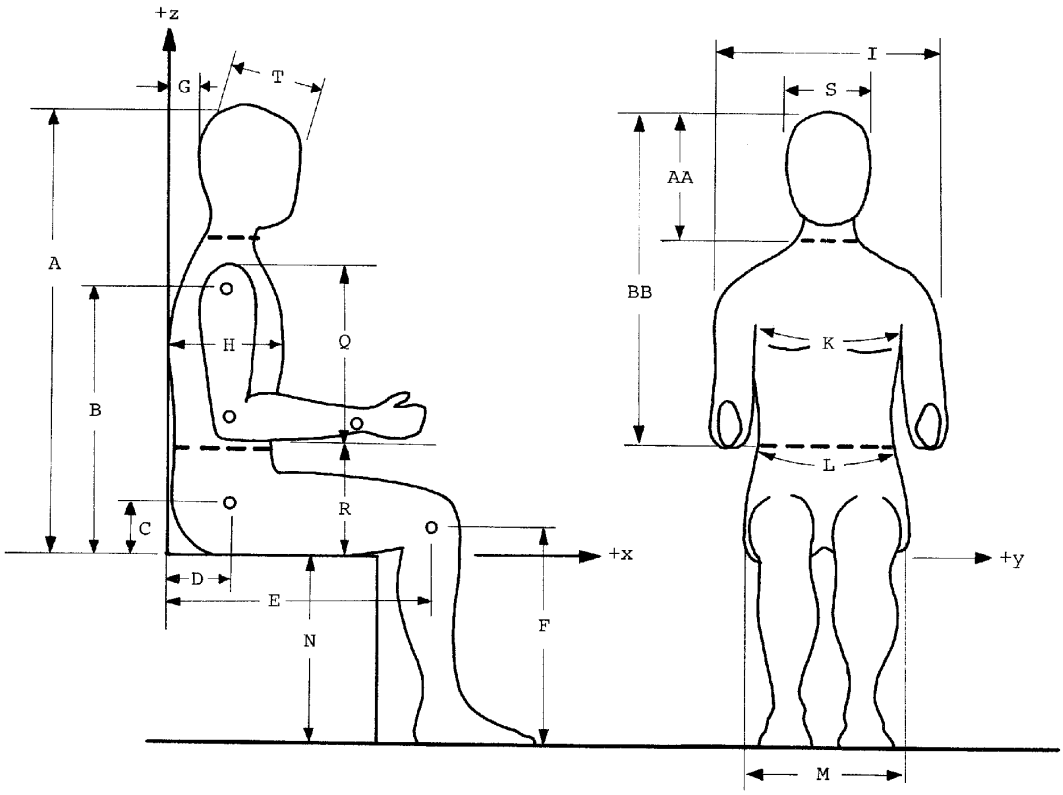


Figure 4-32.
External anthropomorphic measurements for the Hybrid II ATD (Reference 4-2).

4.4.3.1.1 Impact Protection Requirements for GA Aircraft

In 1988, the Federal Aviation Administration (FAA) imposed additional stringent impact protection requirements for certification of GA aircraft (Reference 4-119). Two dynamic impact tests were added to assess the crashworthiness of each aircraft in emergency landing conditions (Reference 4-120). As described in 14 CFR 23.562(b), each impact test must utilize

THIS DOCUMENT PROVIDED BY THE ABBOTT AEROSPACE
TECHNICAL LIBRARY
ABBOTTAEROSPACE.COM

an instrumented Hybrid II ATD to measure the loads and accelerations applied to the ATD's body during impact. Specifically, 14 CFR 23.562(b) states that "these tests must be conducted with an occupant simulated by an anthropomorphic test device (ATD) defined by 49 CFR Part 572, Subpart B, or an FAA-approved equivalent, with a nominal weight of 170 pounds and seated in the normal upright position." The FAA Advisory Circular 23.562-1 indicates that ATDs will be deemed equivalent if "…(i) they are fabricated in accordance with design and production specifications established and published by a regulatory agency which is responsible for crash injury protection systems; (ii) they are capable of providing data for the measurements discussed in this AC or of being readily altered to provide data; (iii) they have been evaluated by comparison with the Part 572(b) ATD; (iv) any deviations for the Part 572(b) ATD configuration or performance are representative of the occupant of a civil airplane in the impact environment discussed in this AC" (Reference 4-121).

As previously mentioned, the Hybrid II ATD is required to measure specific parameters during Test 1 and Test 2 in order to evaluate the potential risk for occupant injury. Table 4-15 describes the instrumentation that is required for each test, the parameters that are measured, and the tolerance limits defined for each measurement.

Table 4-15.
Instrumentation, measurements, and tolerance limits required for compliance with 14 CFR 23.562 (Reference 4-120)

Required Instrumentation	Location	Parameter Measured	Tolerance Limit (lb)
Triaxial accelerometer	Located at the c.g. of the head	Head Injury Criterion (HIC)	1,000
Load cell	Inserted between the pelvis and the lumbar spine	Compressive load between pelvis and lumbar spine	1,500
Load cell	Attached to the shoulder harness strap(s)	Load exerted on the harness strap(s)	Individual strap - 1,750 Dual straps - 2,000

4.4.3.1.2 Acceptable Modifications to the Hybrid II ATD for Aircraft Testing

In order to use the Hybrid II ATD to effectively evaluate occupant injury in aircraft crash scenarios, Advisory Circular 23.562-1 recommends that the following modifications be made to the instrumentation and structure of the ATD (Reference 4-121):

1. Lumbar Load Cell - The lumbar load cell is not a standard component of the Hybrid II ATD. As a result, a lumbar load cell should be added to monitor compressive load between the lumbar spinal column and the pelvis in those situations where a vertical loading component was present and/or a downward load was exerted on the shoulders by the restraint system.
2. Stronger Clavicles - Flailing of the Hybrid II ATD's arms during an aircraft impact test typically causes the original, aluminum Hybrid II clavicles to break. As a result, clavicles that are identical in shape but are made of a stronger material (typically manganese-bronze) should replace the aluminum clavicles.
3. Submarining Indicators - Electronic transducers should be attached to the anterior surface of the ATD's ilium in order to track the position of the lap belt as it loads the pelvis.

This Document Provided by the Abbott Aerospace
TECHNICAL LIBRARY
ABBOTTAEROSPACE.COM

4.4.3.2 Hybrid III Frontal-Impact ATD

The Hybrid III frontal-impact test ATD was introduced by General Motors in 1976 (Reference 4-86). The Hybrid III has proven to be a durable, repeatable, reproducible, and serviceable test instrument (References 4-86, 4-112, 4-115, 4-121). Figure 4-33 illustrates the Hybrid III 50th-percentile male with and without its skin, while Table 4-16 lists the standard anthropometric dimensions of the Hybrid III ATD. In addition, a thorough description of the Hybrid III ATD's attributes, deficiencies, and anthropometric characteristics is provided in Table 4-17. The Hybrid III has markedly improved component biofidelity, particularly in the head and neck system, thorax, and re-distributed lower torso weight. It also possesses additional injury predictive measurement capabilities, including transducers for assessing neck and lower-extremity injuries.

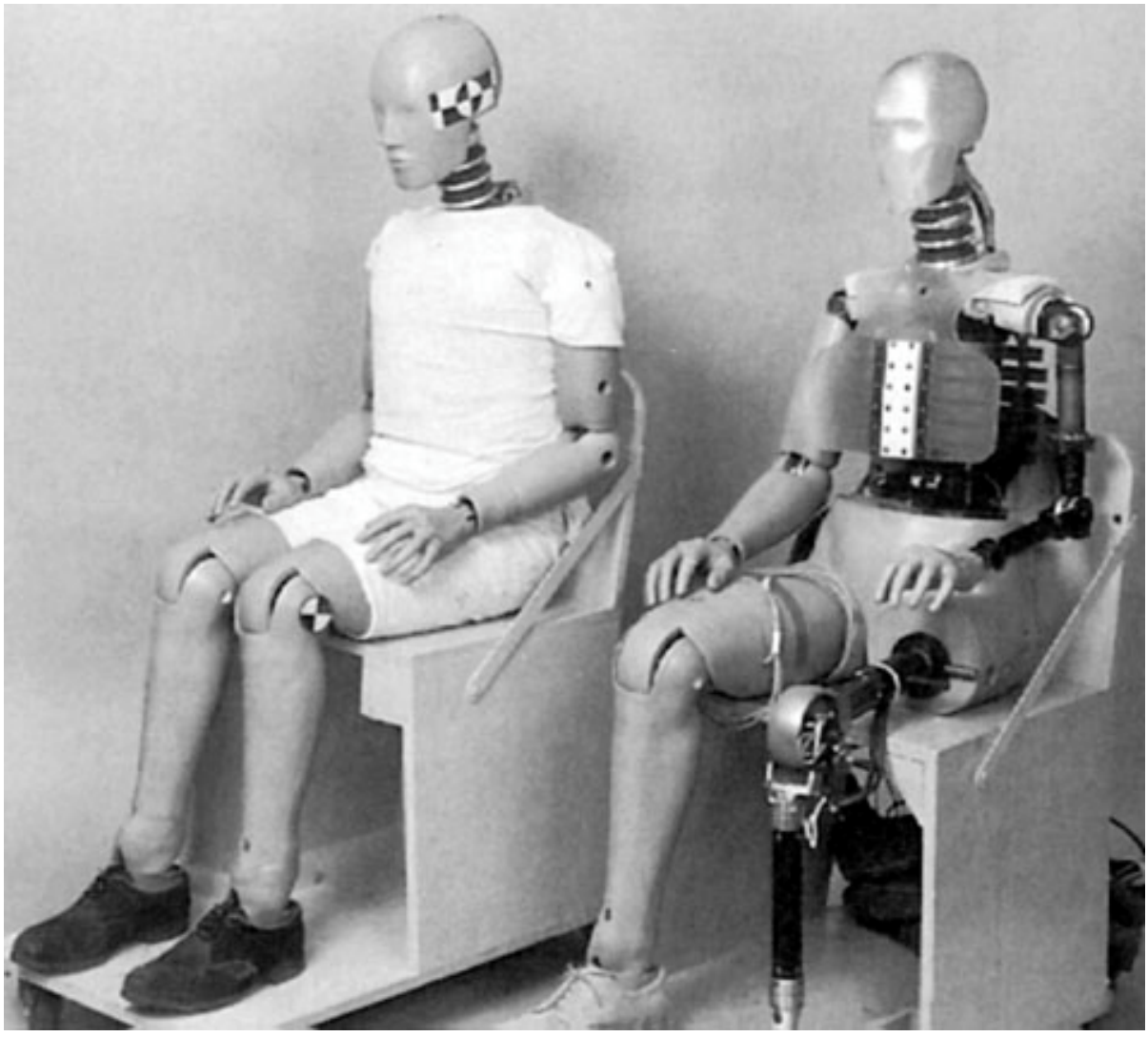


Figure 4-33.
Hybrid III 50th-percentile adult male with and without its skin (Reference 4-112).

This Document Provided by the Abbott Aerospace
TECHNICAL LIBRARY
ABBOTTAEROSPACE.COM

Table 4-16.
Standard anthropometric dimensions for various ATDs (References 4-86, 4-122)

Type of ATD	Mass (kg)	Sitting Height (m)	Buttock to Knee Length (m)	Knee Height Sitting (m)	Shoulder Height Sitting (m)
Hybrid III					
5th Female	48.7	0.790	0.521	0.457	0.442[c]
50th Male	78.2	0.884	0.592	0.493[b]	0.513[c]
95th Male	101.1	0.935	0.633	0.594	0.549[c]
SID					
50th Male	76.5	0.899	0.592	0.544	N/A
SIDIIs					
5th Female	44.52	0.790	0.521	0.457	0.422[c]
BioSID					
50th Male	76.2	0.884	0.592	0.493[b]	0.513
EuroSID-1					
50th Male	72.0	0.904	0.610	0.544	0.557[c]

a – Total mass includes with mass of ATD and the mass of the on-board data acquisition system.
b – Knee pivot height.
c – Shoulder pivot height, sitting.

Table 4-17.
Design characteristics for the Hybrid III ATD (References 4-86 – 4-114)

Body Segment	Structure and *Instrumentation*	Biofidelic Attributes	Biofidelic Deficiencies	Injury-Predictive Measurements
Head	Aluminum shell covered by a constant-thickness vinyl skin over cranium; vinyl facial features*; triaxial accelerometer located at c.g.; sagittal plane angular accelerometer*	Exterior size and shape of a 50th-percentile adult male; humanlike head-to-neck attachment location, mass and sagittal plane mass moment of inertia, response for deforming-surface impacts, and response for hard-surface forehead impacts	Mass moment of inertia may not be humanlike for other than sagittal pane; hard-surface impact response may not be humanlike for side, top, and rear of head	Facial laceration prediction possible if chamois covering is used; brain injury and/or skull fracture predictions based on linear acceleration measurements possible for deforming-surface impacts to front, top, back, and side of head and for hard-surface impacts to the forehead.
Neck	One-piece structure comprised of four asymmetric butyl rubber segments bonded to thin aluminum disks and two endplates; braided wire cable passes through the center of the neck and attaches to the endplates; top endplate is a single-pivot nodding joint; *upper and lower neck load cells*	Humanlike fore/aft bending response	Lateral bending response may not be humanlike; neck is too stiff in axial compression	Forces and moments measured at the upper and lower portions of the neck provide a basis for predicting neck injuries
Thorax	Similar to Hybrid II ATD, except the rib size and the damping material selected give a more humanlike force deflection response for distributed sternal loading; *triaxial accelerometer located in thoracic spine; transducer to measure sternal-to-spine motion; sternal accelerometer*	Exterior size and shape of 50th-percentile adult male; humanlike mass and impact response for fore/aft compression due to distributed sternal impacts	Rib cage geometry, mass distribution, lateral impact response, and concentrated load impact response not humanlike	Thoracic injuries related to gross thoracic acceleration, sternal displacement and acceleration, and forces and moments exerted on the thorax

THIS DOCUMENT PROVIDED BY THE ABBOTT AEROSPACE
TECHNICAL LIBRARY
ABBOTTAEROSPACE.COM

Table 4-17. (continued)
Design characteristics for the Hybrid III ATD (References 4-86 – 4-114)

Body Segment	Structure and *Instrumentation*	Biofidelic Attributes	Biofidelic Deficiencies	Injury-Predictive Measurements
Lumbar Spine	Circular rubber segment with two braided steel cables attached to endplates to provide lateral bending stability	Provides humanlike sitting posture in automobiles	Bending response is not humanlike	None
Pelvis	Aluminum casting of human pelvis shape covered with vinyl skin; *three load transducers on each iliac sarorius; triaxial accelerometer*	Humanlike pelvis shape	Mass and mass distribution not humanlike	Load transducers measure lap belt loading of pelvis; accelerometer to measure the acceleration of the pelvis
Lower Extremity	Steel shafts used for femur and leg shafts covered with vinyl skin; knee area has butyl rubber pad inserted beneath vinyl skin; ball joints at hip and ankle; knee joint allows leg to rotate and translate relative to femur in sagittal plane; adjustable frictional rotational joints; *load cells in femur and leg shafts, ankle, and knee joints; displacement transducer at knee joints*	Humanlike ranges of motion and knee impact response	Mass distribution and joint resistances not humanlike	Axial compressive femur load; leg relative to femur translation; sagittal and lateral tibial bending moments; medial and lateral tibial plateau compressive loads; Fore/aft ankle bending moment and shear load or lateral bending moment and shear load, depending on transducer orientation; knee laceration potential using chamois technique
Shoulder	Aluminum casting pin-jointed to spine; broad area provided for shoulder belt loading	None	Mass distribution and load-deflection responses not humanlike	None
Arm	Steel shafts used for upper and lower arms; frictional pin joints at shoulder, elbow, and wrist; shafts covered with vinyl skin; *bending moment transducer located in lower arm*	Humanlike range of motion	Mass distribution and joint resistances not humanlike	Fore/aft and lateral bending moments

As a result of these enhanced features, the Hybrid III ATD was incorporated into the Code of Federal Regulations standard 49 CFR 572(e) in 1986 (Reference 4-123). After the incorporation date of October 23, 1986, manufacturers had the option of using either the Hybrid II ATD or the Hybrid III for compliance testing until August 31, 1991. As of September 1, 1991, the Hybrid III completely replaced the Hybrid II ATD for use during occupant injury compliance testing in the automotive industry. Today, the Hybrid III ATD is still used as the exclusive means of determining a motor vehicle's compliance with the occupant injury protection requirements specified in 49 CFR 571.208 (References 4-86 – 4-113, 4-115, 4-117).

4.4.3.3 FAA-Hybrid III ATD

One of the significant differences between the design of the Hybrid II and Hybrid III ATDs concerns the design of the lumbar spine (Reference 4-124). The Hybrid II is equipped with a straight lumbar spine that allows for the measurement of axial compressive loads between the lumbar spine and the pelvis. The Hybrid III is equipped with a curved lumbar spine that is not capable of measuring lumbar spinal loads. The curved lumbar spine was specially designed to

THIS DOCUMENT PROVIDED BY THE ABBOTT AEROSPACE
TECHNICAL LIBRARY
ABBOTTAEROSPACE.COM

better represent the automotive seating posture that is typically used by most drivers. Unfortunately, this feature of the Hybrid III ATD excludes it from being used to assess occupant injury in aircraft crash scenarios. Aircraft crashes typically experience a vertical loading component that can cause severe compression injuries in the lumbar spine. The curved lumbar spine of the Hybrid III does not provide an accurate measurement of the axial compressive loads experienced within the lumbar spine.

However, researchers in the aviation industry wanted to take advantage of the additional biofidelic features offered by the Hybrid III ATD during aircraft seat certification testing and other aviation-related research activities. For example, use of the Hybrid III biofidelic neck and instrumentation would allow aviation researchers to assess the potential risk for occupant neck injury in aircraft crash simulations. In order to address the requests of the aviation research and testing community, a cooperative research initiative was established among the Federal Aviation Administration (FAA) Civil Aeromedical Institute (CAMI), Applied Safety Technologies Corporation (ASTC), and Robert A. Denton, Inc. These three organizations worked to develop potential modifications to the Hybrid III lumbar spine and pelvis that would enable the ATD to:

- Maintain an erect seating posture
- Accurately measure the loads between the lumbar spine and pelvis
- Produce biodynamic responses that were similar to those produced by the Hybrid II ATD.

The modified version of the standard Hybrid III ATD, referred to as the FAA Hybrid III, was evaluated along with the standard Hybrid II and Hybrid III ATDs in dynamic impact tests representative of the Test 1 and Test 2 testing requirements specified in the transport-category regulation FAR 25.562 (Reference 4-125). These dynamic tests were conducted to compare the compressive lumbar loads measured by the lumbar spine, the loads imparted to the aircraft seat, the lap belt loads, and the head motion kinematics of each of the three ATDs. Testing results indicated a good correlation in all areas between the Hybrid II and FAA Hybrid III. Recently, additional tests were conducted at CAMI to compare the biodynamic response of all three ATDs using the Test 1 and Test 2 requirements specified for the GA and rotorcraft categories of aircraft. The results from these tests are currently awaiting publication.

4.4.3.4 Test Device for Human Occupant Restraint (THOR)

Advances in ATD technology and instrumentation have encouraged the development of an advanced frontal ATD called the Test Device for Human Occupant Restraint (THOR) (References 4-126,4-127). With funding from the NHTSA, GESAC, Inc., began development of the THOR in 1994. This advanced frontal ATD was designed to demonstrate increased sensitivity to current and future automotive restraint systems including both safety belts and air bag technologies. The THOR features enhanced biofidelity and extensive instrumentation in almost every region of the body. A unique feature of the THOR is the THOR-LX lower limb assembly. Designed by GESAC, Inc., the NHTSA Vehicle Research and Test Center (VRTC), and the ASTC, the THOR-LX assembly is capable of measuring loads in the upper and lower tibia, Achilles tendon, and in the heel and ball of the foot. The THOR-LX can also measure rotation of the individual ankle joints, as well as acceleration of the tibia and foot. The first THOR prototypes were designed using the anthropometric characteristics representative of a 50th-percentile male.

This Document Provided by the Abbott Aerospace
Technical Library
abbottaerospace.com

Research is currently underway to develop a second THOR ATD with anthropometric characteristics representative of a 5th-percentile female. The overall objective is to eventually incorporate the THOR into the federal vehicle dynamic impact testing regulations.

4.4.4 Side-Impact ATDs

Presently, four different side-impact ATDs are commercially available for use in lateral impact testing: the Side Impact Dummy (SID), the Side Impact Dummy IIs (SIDIIs), the European Side Impact Dummy (EuroSID-1), and the Biofidelic Side Impact Dummy (BioSID) (References 4-86 - 4-113, 4-122). Table 4-16 lists the standard anthropometric dimensions of each side-impact ATD. Three of these side-impact ATDs possess the body size and shape characteristics of a 50th-percentile adult male (SID, BioSID, and EuroSID) while the fourth ATD possesses the body size and shape characteristics of a 5th-percentile adult female (SIDIIs).

Each of these ATDs was specifically designed to assess occupant injury protection in automotive lateral collisions. However, the aviation community also uses them to assess the performance of side-facing aircraft seats during frontal collisions. Research efforts are currently underway in the aviation community to develop an official impact test standard and a set of occupant injury tolerance criteria for the performance evaluation and certification of side-facing aircraft seats. In addition, the aviation community is trying to determine which side-impact ATD to use during these impact tests.

The following sections provide a brief description of the biofidelic attributes of each side-impact ATD, including a section discussing the characteristics of the newest automotive side-impact ATD, the World Side-Impact Dummy (WorldSID). The section concludes with a discussion of the results obtained from recent aviation-related side-impact ATD dynamic impact tests conducted at CAMI.

4.4.4.1 Side-Impact Dummy (SID)

From 1979-1982, the University of Michigan Transportation Research Institute (UMTRI), in cooperation with the NHTSA, developed the Side-Impact Dummy (SID) (References 4-112, 4-113, 4-119, 4-122). The SID is a modified version of the Hybrid II 50th-percentile adult male ATD. As illustrated in Figure 4-34, the head and neck complex of the SID are identical to the Hybrid II head and neck design. However, several other modifications have been made to the basic design of the Hybrid II ATD. For example, the thorax and knees of the Hybrid II were redesigned to produce more human-like acceleration responses in the lateral directions. A hydraulic damper was added to the SID torso to control the displacement of the ribs relative to the spine. Accelerometers were inserted in the ribs, spine, and pelvis to monitor the linear acceleration of each of these body segments. The shoulders and arms of the Hybrid II were removed for the design of the SID and were replaced with soft foam. Cadaver tests revealed that these body segments did not significantly contribute to transmitting the loads exerted during a lateral impact and that they prevented the ATD instrumentation from obtaining repeatable responses (Reference 4-113). However, removing the arms of the ATD decreased its overall mass. Therefore, to account for the change in mass of the ATD, additional mass was incorporated into the thoracic region of the ATD.

This Document Provided by the Abbott Aerospace
TECHNICAL LIBRARY
ABBOTTAEROSPACE.COM

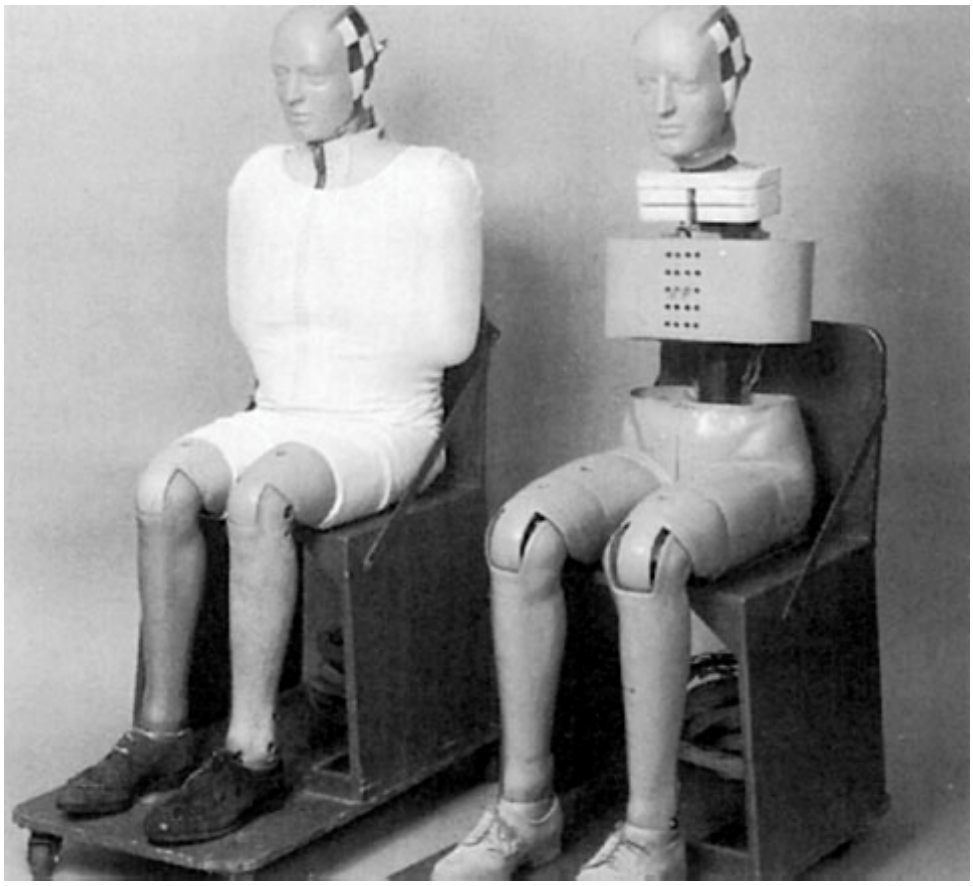


Figure 4-34.
Side Impact Dummy (SID) shown with and without its torso skin. (2)

In the late 1980's, the International Standards Organization (ISO) subjected the SID to full-scale lateral impact tests in order to evaluate the biofidelity of the ATD (Reference 4-113). The ISO concluded that the SID did not possess an acceptable level of biofidelity for the assessment of occupant injury in automotive lateral collisions. For example, the SID chest possesses no lateral elastic stiffness and, as a result, the SID's chest compliance doesn't consistently mimic the human chest response. The soft foam structure that replaced the shoulders does not mimic the lateral load-carrying capacity of the human shoulder. In addition, the SID is not capable of assessing the body-armrest interaction during lateral impacts. This results from the lack of an instrumented, biofidelic abdomen. Unfortunately, the interaction between the human body and the armrest is needed to properly assess the occupant protection in lateral impacts. This particular interaction has been the source of serious liver and spleen injuries in lateral collisions. Despite the ISO's recommendation, the Department of Transportation decided to adopt the SID into the side-impact testing regulations, 49 CFR 571.214 and 49 CFR 572(f), for use in the lateral-impact testing of all automotive vehicles (References 4-112, 4-128, 4-129).

4.4.4.2 Side-Impact Dummy IIs (SIDIIs)

In 1994 and 1995, the Side Impact Dummy IIs (SIDIIs) was developed by First Technology Safety Systems (FTSS) and the Occupant Safety Research Partnership (OSRP) (Reference 4-122). The SIDIIs represents the anthropometry of a 5th-percentile female and is

This Document Provided by the Abbott Aerospace
Technical Library
abbottaerospace.com

based on the design of the Hybrid III 5th-percentile female ATD. The anthropometry of the SIDIIs also closely represents the size and weight of a 12-13 year old child. Figure 4-35 illustrates the external and internal structure of the SIDIIs. The SIDIIs is equipped with instrumentation for assessing injury to the head, neck, arm, thorax, abdomen, pelvis, and leg.

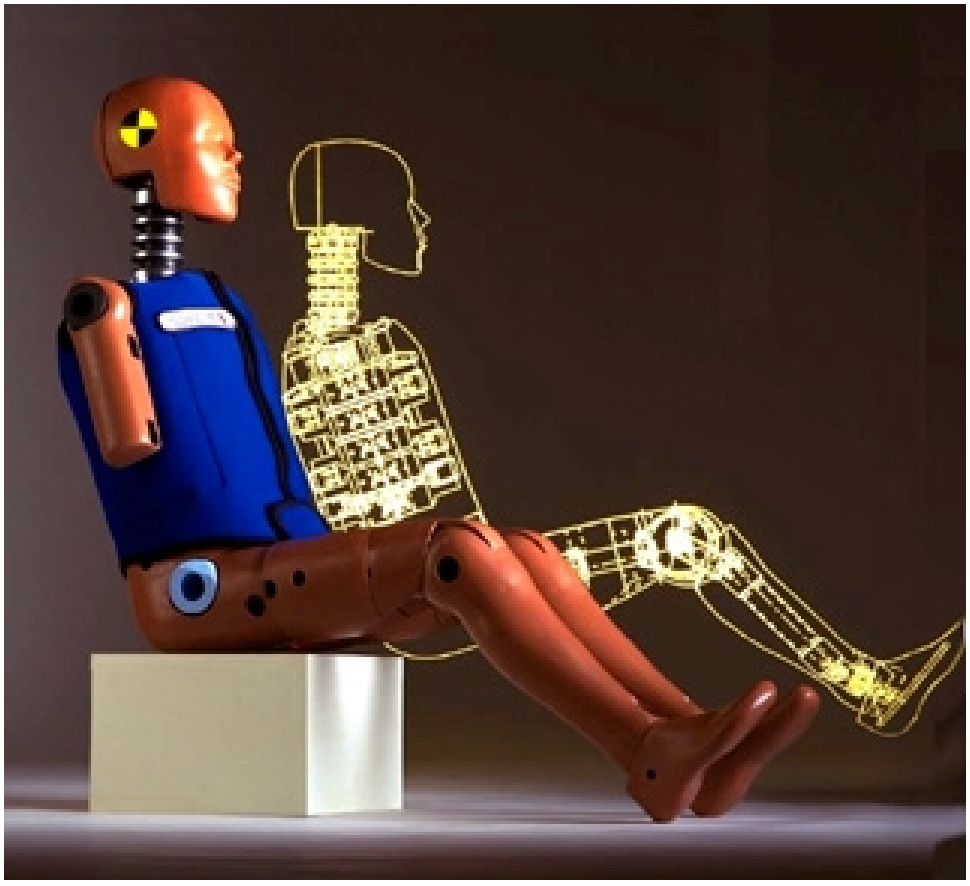


Figure 4-35.
The external and internal structure of the Side-Impact Dummy IIs (SIDIIs) (Reference 4-122).

4.4.4.3 European Side Impact Dummy (EuroSID-1)

From 1983-1985, the European Experimental Vehicle Committee (EEVC) sponsored the development of the first European side-impact ATD called EuroSID (References 4-86, 4-119, and 4-130). Figure 4-36 illustrates the EuroSID without its torso skin. In order to assess the biofidelity of the EuroSID, the ISO subjected the EuroSID to full-scale side-impact tests (Reference 4-112). The ISO concluded that the EuroSID did not demonstrate sufficient biofidelity in lateral automotive collisions and, as a result, the EEVC modified the EuroSID design and created the EuroSID-1. The EuroSID-1 was re-evaluated by the ISO and was deemed acceptable in terms of its biofidelic characteristics.

This Document Provided by the Abbott Aerospace
TECHNICAL LIBRARY
ABBOTTAEROSPACE.COM

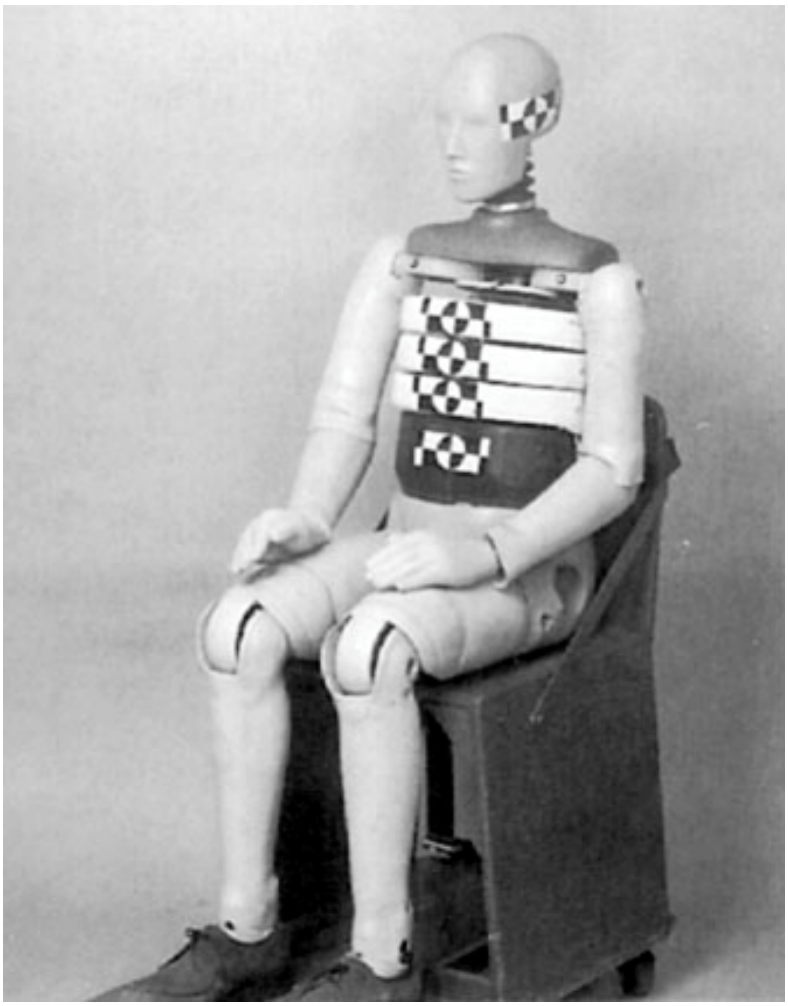


Figure 4-36.
The EuroSID without its torso skin (Reference 4-112).

The EuroSID-1 was designed to represent the anthropometry of a 50th-percentile adult male (Reference 4-86). As illustrated in Figure 4-37, it features a standard Hybrid III head and Hybrid II lower extremities (Reference 4-112, 4-130). The thorax of the EuroSID-1 was designed using hydraulic dampers and springs to allow it to mimic human lateral force-deflection and to measure thoracic injury based on the degree of chest deflection. The shoulder structure of the EuroSID-1 was designed to "roll forward" during impact. The ATD is also equipped with an abdominal insert that provides humanlike abdominal compliance. The EuroSID pelvis is capable of measuring the loads exerted on the pubic symphysis. The deficiencies of the EuroSID ATD include:

- Limited rib-to-spine displacement (50 mm is the maximum possible displacement)
- The shoulder becomes unstable when it is loaded laterally
- The humerus load distribution function is not represented in the arm structure.

This Document Provided by the Abbott Aerospace
Technical Library
abbottaerospace.com

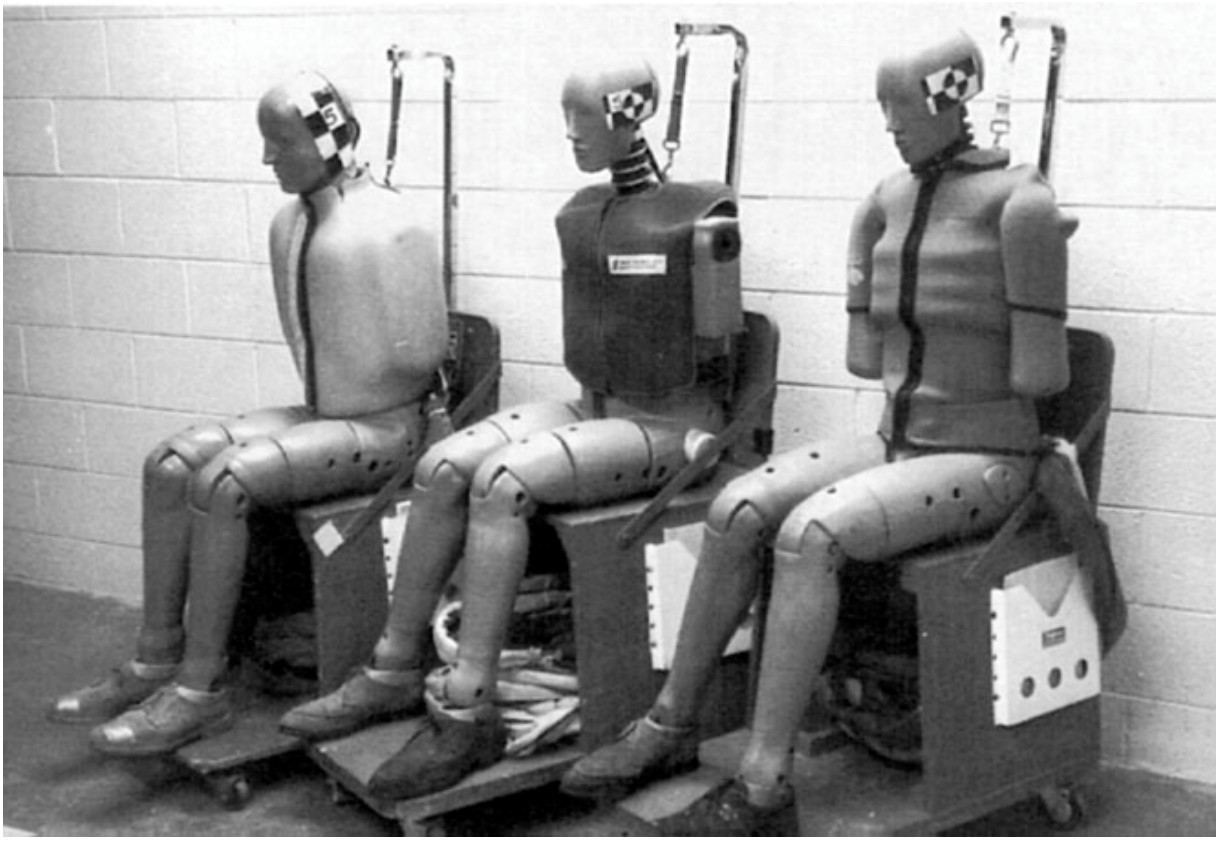


Figure 4-37.
EuroSID with its torso skin (from left to right: SID, BioSID, EuroSID-1) (Reference 4-86).

4.4.4.4 Biofidelic Side-Impact Dummy (BioSID)

In response to the ISO's conclusion regarding the poor biofidelity of the SID and EuroSID, the Society of Automotive Engineers (SAE) task force was convened in the late 1980's to develop a more biofidelic side-impact ATD (References 4-112, 4-119, 4-122). As a result, the SAE Human Biomechanics and Simulation Standards Committee worked in cooperation with General Motors to develop the Biofidelic Side-Impact Dummy (BioSID). Figure 4-38 illustrates the BioSID with and without its torso, pelvic, and leg skins. The BioSID was designed to represent the anthropometry of a 50th-percentile male. It features lateral-impact response biofidelity for the head, neck, shoulder, thorax, abdomen, and pelvis, and has a torso that is capable of rotating 180 deg to convert from a left-side-impact to a right-side-impact ATD. The BioSID is composed of the Hybrid III 50th-percentile male ATD head, neck, upper legs, lower legs, and feet with associated Hybrid III instrumentation. The BioSID pelvis is a modified version of the EuroSID pelvis, and is capable of measuring sacrum, iliac wing, and pubic symphysis loads. In order to adhere to the biofidelic impact requirements for the pelvis, a crushable foam block pelvis insert was designed. This crushable insert must be replaced following each impact test.

This Document Provided by the Abbott Aerospace
TECHNICAL LIBRARY
ABBOTTAEROSPACE.COM

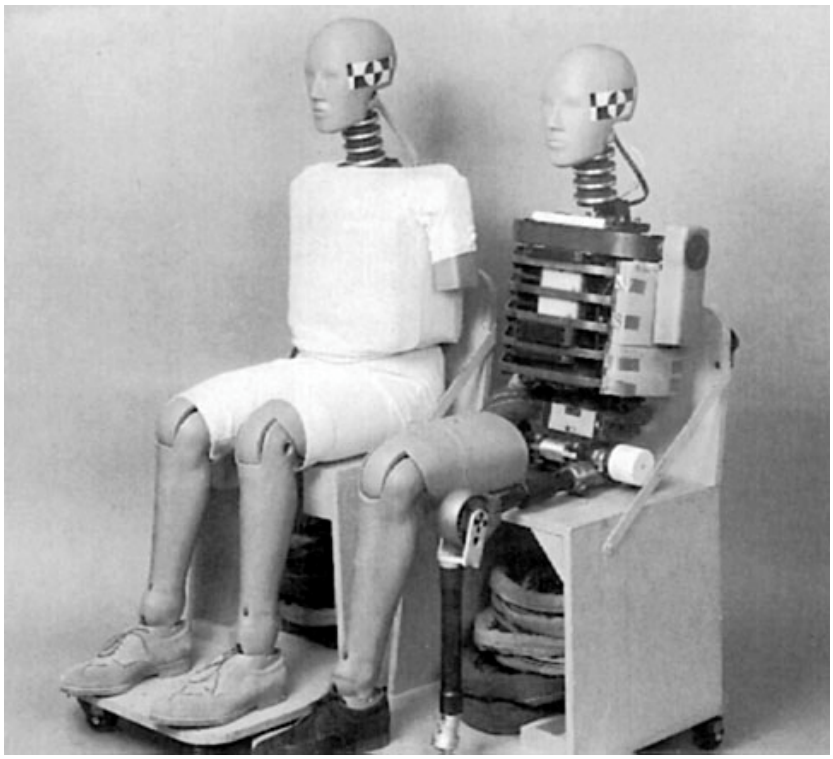


Figure 4-38.
Biofidelic Side Impact Test Dummy (BioSID) illustrated with and without its torso, pelvic, and leg skins (Reference 4-112).

4.4.4.5 Development of the World Side Impact Dummy (WorldSID)

Recently, a worldwide design team was established to develop an internationally accepted automotive side-impact ATD called the World Side Impact Dummy (WorldSID) (Reference 4-131). The WorldSID design team is comprised of representatives from the Americas, Europe, and the Asia/Pacific region. This collaboration represents the first international effort established to standardize ATD design and use worldwide. The primary objectives of the this international design team are to:

- Design and fabricate a single, biofidelic side-impact ATD that will replace all other automotive side-impact ATDs,
- Create a single side-impact test standard that will be included in all automotive side-impact testing regulations worldwide,
- Establish a single set of injury tolerance criteria for the assessment of occupant injury in automotive side-impact tests.

The WorldSID will feature enhanced biofidelity and instrumentation, as well as an “on-board the ATD” data acquisition system. As shown in Figure 4-39, a 50th-percentile WorldSID prototype has been manufactured and is currently undergoing validation impact tests. The design team is scheduled to release the 50th-percentile adult male WorldSID in January of 2005. A 5th-percentile female WorldSID will be released in December 2006. Although the WorldSID is being designed for use in automotive lateral-impact tests, it may also prove to be useful in the performance evaluation of side-facing aircraft seats.

THIS DOCUMENT PROVIDED BY THE ABBOTT AEROSPACE
TECHNICAL LIBRARY
ABBOTTAEROSPACE.COM

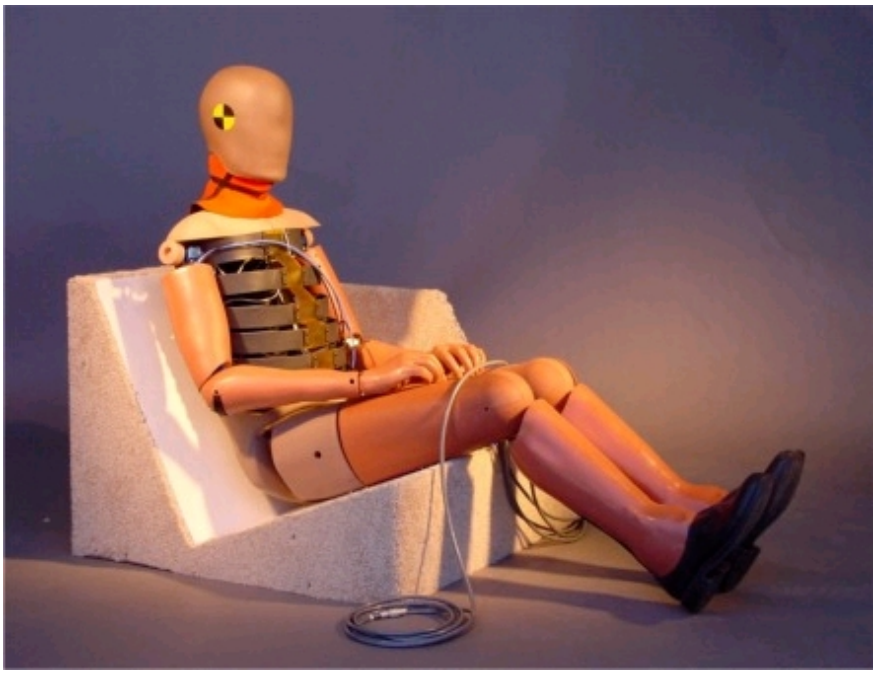


Figure 4-39.
The WorldSID 50th-percentile male prototype (Reference 4-131).

4.4.4.6 Aircraft Side-facing Seat Impact Tests using Side Impact Dummies

In April of 1999, researchers at WSU and CAMI published results from a series of dynamic impact tests that were conducted to assess the biofidelity of the SID, BioSID, and EuroSID in side-facing aircraft seats during frontal collisions (Reference 4-132). A set of potential injury criteria, adopted primarily from the automotive industry, was used to compare the performance of the three side-impact ATDs. The following conclusions were made:

1. The SID is not suitable for reliably measuring the specified injury criteria.
   - The SID is not capable of measuring rib deflection.
   - The lateral flail response of the SID is not accurate. This results from the absence of clavicles in the upper torso. (The clavicles are needed to help position the shoulder belt and to bear a portion of its load).
2. The BioSID is not suitable for reliably measuring the specified injury criteria.
   - The BioSID cannot accurately simulate body-to-body contact.
   - The BioSID is not very durable.
   - Acceleration data collected from the BioSID is usually very "noisy".
3. The EuroSID-1 is reliable in measuring the specified injury criteria.
   - The EuroSID-1 is durable and repeatable.
   - The EuroSID-1 data is well correlated with the other side-impact ATDs.

Although this study indicates that the EuroSID-1 is the most reliable in terms of evaluating occupant injury in side-facing aircraft seats, no official recommendation has been made as to which ATD to use. Presently, these two research teams are working to obtain additional analytical data by running model simulations of the three side-impact ATDs in the MADYMO multi-body analysis modeling program.

THIS DOCUMENT PROVIDED BY THE ABBOTT AEROSPACE
TECHNICAL LIBRARY
ABBOTTAEROSPACE.COM

REFERENCES

4-1. McConville, J. T., and Laubach, L. L., "Chapter III: Anthropometry," Anthropometric Source Book, Volume 1: Anthropometry for Designers, Webb Associates, Yellow Springs, Ohio, July 1978.

4-2. Aircraft Crash Survival Design Guide, Volume II – Aircraft Crash Environment and Human Tolerance, USARTL-TR-79-22B, Simula, Inc., Tempe, Arizona, January 1980.

4-3. Stout, H. W., "Present and Future Needs for Anthropometric Data Bases," Anthropometry and Biomechanics: Theory and Application, ed. Easterby, R., et al., Plenum Press, New York, New York, 1982.

4-4. Laubach, L. L., "Human Muscular Strength," Anthropometric Source Book, Volume 1: Anthropometry for Designers, Webb Associates, Yellow Springs, Ohio, July 1978.

4-5. Laubach, L. L., "Range of Joint Motion," Anthropometric Source Book, Volume 1: Anthropometry for Designers, Webb Associates, Yellow Springs, Ohio, July 1978.

4-6. Reynolds, H. M., Chapter IV, "The Inertial Properties of the Body and its Segments," Anthropometric Source Book, Volume 1: Anthropometry for Designers, Webb Associates, Yellow Springs, Ohio, July 1978.

4-7. Brooks, A., "Statistics and Percentiles in Anthropometry,"Ergonomics in Practice, System Concepts Ltd., London, England, Vol. 3, No. 5, May 1997.

4-8. Wickens, C. D., Gordon, S. E., and Liu, Y., An Introduction to Human Factors Engineering, Addison-Wesley Educational Publishers, New York, New York, 1998, pp.289-318.

4-9. Donelson, S. M., and Gordon, C. C., 1988 Anthropometric Survey of U.S. Army Personnel: Pilot Summary Statistics, Natick/TR-91/040, U.S. Army Natick Research, Development, and Engineering Center, Natick, Massachusetts, July 1991.

4-10. Caesar Fact Sheet," Society of Automotive Engineers Web Site, http://www.sae.org/technicalcommittees/caefact.htm/, site accessed on July 1, 1999.

4-11. "Caesar Scope," Society of Automotive Engineers Web Site, http://www.sae.org/technicalcommittees/caescope.htm/, site accessed on July 1, 1999.

4-12. "Caesar Uses Latest Laser Technology," Society of Automotive Engineers Web Site, http://www.sae.org/technicalcommittees/caelaser.htm/, site accessed on July 1, 1999.

4-13. Tilley, A. R., The Measure of Man and Woman, Human Factors in Design, Henry Dreyfuss Associates, New York, New York,1993.

4-14. Griener, T. M., and Gordon, C. C., An Assessment of Long-term Changes in Anthropometric Dimensions: Secular Trends of U.S. Army Males, Natick/TR-91/006, Natick, Massachusetts: U.S. Army Natick Research, Development, and Engineering Center, Natick, Massachusetts, 1990.

4-15. Gordon, C. C., et al., 1988 Anthropometric Survey of U.S. Army Personnel: Methods and Summary Statistics, Anthropology Research Project, Yellow Springs, Ohio, Natick/TR-89/044, U.S. Army Natick Research, Development, and Engineering Center, Natick, Massachusetts, September 1989.

4-16. Robinette, K., and Fowler, J., An Annotated Bibliography of the United States Air Force Engineering Anthropometry, 1946-1988, Wright-Patterson Air Force Base, Ohio, May 1988.

4-17. Harry, G., Anthropometry and Mass Distribution for Human Analogues, Vol. 1: Military Male Aviators, Armstrong Aerospace Medical Research Laboratory, Wright-Patterson Air Force Base, Ohio, June 1987.

4-18. Salvendy, G., Handbook of Human Factors, John Wiley and Sons: New York, New York, 1987.

THIS DOCUMENT PROVIDED BY THE ABBOTT AEROSPACE
TECHNICAL LIBRARY
ABBOTTAEROSPACE.COM

4-19. Young, J. W., Chandler, R. F., and Snow, C. C., Anthropometric and Mass Distribution Characteristics of the Adult Female, Report No. AD-A143 096, Federal Aviation Administration, Civil Aeromedical Institute, Oklahoma City, Oklahoma, September 1983.
4-20. Reynolds, H. M., and Leung, S. C., A Foundation for Systems Anthropometry: Lumbar/Pelvic Kinematics, Aerospace Medical Research Laboratory at Wright-Patterson Air Force Base, Ohio, May 1983.
4-21. Schneider, L. W., et al., Development of Anthropometrically Based Design Specifications for an Advanced Adult Anthropomorphic Dummy Family, Volume 1, The University of Michigan, UMTRI-83-53-1, U.S. Department of Transportation, December 1983.
4-22. Easterby, R., Kroemer, K. H. E., Chaffin, D. B., Anthropometry and Biomechanics: Theory and Application, Plenum Press: New York, New York, 1982.
4-23. Reynolds, H. M., Snow, C. C., and Young, J. W., Spatial Geometry of the Human Pelvis, Federal Aviation Administration, Civil Aeromedical Institute, Oklahoma City, Oklahoma, March 1982.
4-24. Vaughn, C. L., Andrews, J. G., and Hay, J. G., "Selection of Body Segment Parameters by Optimization," Journal of Biomechanical Engineering, 104, February 1982.
4-25. Chandler, R. F. and Young, J., Uniform Mass Distribution Properties and Body Size Appropriate for the 50th-Percentile Male Aircrewmember During 1980-1990, Report No. AAC-119-91-4, Federal Aviation Administration, Civil Aeromedical Research Institute, Oklahoma City, Oklahoma, 1984.
4-26. Gregoire, H. G. and Slobodnik, B., The 1981 Naval and Marine Corps Aviation Anthropometric Survey, SY-121R-81, Naval Air Test Center, Naval Air Station, Patuxent River, Maryland, November 20, 1981.
4-27. McConville, J. T., Churchill, T. D., Kaleps, I., Clauser, C .E., Cuzzi, J., Anthropometric Relationships of Body and Body Segment Moments of Inertia, Anthropology Research Project, Yellow Springs, Ohio, AFAMRL-TR-80-119, Air Force Aerospace Medical Research Laboratory, December 1980.
4-28. Laubach, L. L., McConville, J. T., and Tebbetts, I., Anthropometric Source Book, Vol. 1: Anthropometry for Designers; Vol. 2: A Handbook of Anthropometric Data, Vol. 3: Annotated Bibliography, Webb Associates, Report No. N79-11734, U.S. Department of Commerce, National Technical Information Service, Springfield, Virginia, July 1978.
4-29. Churchill, E. et al., Anthropometry of Women in the U.S. Army – 1977, Webb Associates, Inc., Yellow Springs, Ohio, Tech., Rep. 77/024, U.S. Army Natick Research and Development Command, Natick, Massachusetts, June 1977.
4-30. Snyder, R. G., Schneider, L. W., and Owings, C. L., Anthropometry of Infants, Children, and Youths to Age 18 for Product Safety Design, SP-450, Final Report, Society of Automotive Engineers, Inc., Warrendale, Pennsylvania, 1977.
4-31. Atkins, E. R., Dauber, R. L., Karas, J. N., and Pfaff, T. A., Study to Determine the Impact of Aircrew Anthropometry on Airframe Configuration, Report No. 2-57110/5R-3244, Vought Corporation, Dallas, Texas, October 31, 1976.
4-32. Chandler, R. F. et al., Investigation of Inertial Properties of the Human Body, Report No. DOT-HS-801-430, U.S. Department of Transportation, Washington, D.C., March 1975.
4-33. Reynolds, H. M., Clauser, C. E., and McConville, J., Mass Distribution Properties of the Male Cadaver, Society of Automotive Engineers, Warrendale, Pennsylvania, 1975.
4-34. Kroemer, K. H. E., Designing for the Muscular Strength of Various Populations, Aerospace Medical Division, Wright-Patterson Air Force Base, Ohio, December 1974.
4-35. Walker, L. B., Harris, E. H., and Pointius, U. R., Mass, Volume, Center of Mass, and Moment of Inertia of Head and Head and Neck of the Human Body, Contract No. N00014-69-A-0248-0001, Final Report to the Department of the Navy, 1973.

THIS DOCUMENT PROVIDED BY THE ABBOTT AEROSPACE
TECHNICAL LIBRARY
ABBOTTAEROSPACE.COM

4-36. Becker, E. B., Measurement of Mass Distribution Parameters of Anatomical Segments, Society of Automotive Engineers, Inc., Warrendale, Pennsylvania, 1972.
4-37. Clauser, C. E., Tucker, P .E., McConville, T. J., Churchill, E., Laubach, L. L., and Reardon, J. A., Anthropometry of Air Force Women, AMRL-TR-70-5, Aerospace Medical Research Labs at Wright-Patterson Air Force Base, Ohio, 1972.
4-38. Churchill, E., et al., Anthropometry of U.S. Army Aviators – 1970, Anthropology Research Project, Yellow Springs, Ohio, Technical Report 72-52-CE, U.S. Army Natick Laboratories, Natick, Massachusetts, AD 94328, December 1971.
4-39. White, R. M., and Churchill, E., The Body Size of Soldiers – U.S. Army Anthropometry – 1966, USANL Technical Report 72-51-CE, U.S. Army Natick Laboratories, Natick, Massachusetts, AD 743465, December 1971.
4-40. Kroemer, K. H. E., Human Strength: Terminology, Measurement, and Interpretation of Data, Aerospace Medical Division, Wright-Patterson Air Force Base, Ohio, May 1970.
4-41. Clauser, C. E., McConville, J. T., and Young, J. W., Weight, Volume, and Center of Mass of Segments of the Human Body, Antioch College, ARML Technical Report 69-70, Aerospace Medical Research Lab, Wright-Patterson Air Force Base, Ohio, AD 710622, August 1969.
4-42. Laubach, L. L., Body Composition in Relation to Muscle Strength and Range of Joint Motion, Aerospace Medical Research Laboratory at Wright-Patterson Air Force Base, Ohio, June 1969.
4-43. Singley and Haley, "Models and Analogues for the Evaluation of Human Biodynamic Response, Performance and Protection," AGARD Conference Proceedings No. 253, NATO Advisory Group for Aerospace Research and Development, Neuilly sur Seine, France, 1968.
4-44. Dempster, W. T., and Gaughran, G. R. L., "Properties of Body Segments Based on Size and Weight," American Journal of Anatomy, Volume 120, 1967, pp. 33-54.
4-45. Dempster, W. T., Space Requirements of the Seat Operator, WADC Technical Report 55-159, Wright Air Development Center, Wright-Patterson Air Force Base, Ohio, AD 087892, 1955.
4-46. Laubach, L. L., Muscle Strength, Flexibility, and Body Size of Adult Males, Aerospace Medical Research Laboratory at Wright-Patterson Air Force Base, Ohio, October 1966.
4-47. Gifford, E. C., Provost, J. R., and Lazo, J., Anthropometry of Naval Aviators – 1964, Aerospace Crew Equipment Lab, Department of the Navy, October 1965.
4-48. Santschi, W. R., DuBois, J., and Ornoto, C., Moments of Inertia and Centers of Gravity of the Living Human Body, AMRL Technical Data Report 63-36, Aerospace Medical Research Lab, Wright-Patterson Air Force Base, Ohio, May 1963.
4-49. Swearingen, J. J., Determination of Centers of Gravity of Man, AOM 62-14, Federal Aviation Agency, Civil Aeromedical Research Institute, Oklahoma City, Oklahoma, 1962.
4-50. Buck, C. A., et al., "Study of Normal Range of Motion in the Neck Utilizing a Bubble Goniometer," Archives of Physical Medicine and Rehabilitation, Volume 40, September 1959.
4-51. Glanville, A. D., and Kreezer, G., "The Maximum Amplitude and Velocity of Joint Movements in Normal Male Human Adults," Human Biology, Volume 9, 1937, pp. 197-211.
4-52. Desjardins, S. P., Zimmermann, R. E., Bolukbasi, A. O., et al., Aircraft Crash Survival Design Guide, Volume IV, Aircraft Seats, Restraints, Litters, and Cockpit/Cabin Delethatlization, TR- 87442, Simula Inc., Tempe, Arizona; USARTL TR-89-D-22D, Applied Technology Laboratory, U.S. Army Research and Technology Laboratories, (AVRADCOM), Fort Eustis, Virginia, December 1989.

This Document Provided by the Abbott Aerospace
TECHNICAL LIBRARY
ABBOTTAEROSPACE.COM

4-53. Manning, J., and Grace, G., "AGATE Alternative Restraint Dynamic Sled Test Report – Evaluation of a Shoulder Belt Pre-tensioner," TR-98109, Simula Technologies, Inc., Phoenix, Arizona, December 31, 1998.
4-54. Grace, G., and Manning, J., "AGATE Alternative Restraint Dynamic Sled Test Report– Evaluation of Inflatable Tubular Torso Restraint (ITTR) and Buckle Pre-tensioner," TR-98110, Simula Technologies, Inc., Phoenix, Arizona, March 19, 1999.
4-55. Laananen, D. H., Whole-Body Human Tolerance to Impact with Lap Belt-Only Restraint, TI-83405, Simula Inc., Phoenix, Arizona, Department of Transportation, FAATC, July 28, 1983.
4-56. Eiband, A. M., Human Tolerance to Rapidly Applied Accelerations: A Summary of the Literature, NASA Memorandum 5-19-59E, National Aeronautics and Space Administration, Washington, D.C., June 1959.
4-57. Beeding, E. L., Jr., and Mosely, J. D., Human Deceleration Tests, Air Force Missile Development Center; AFMDC Technical Note 60-2, AD 23148, Holloman Air Force Base, New Mexico, January 1960.
4-58. Stapp, J. P., Jolt Effects of Impact on Man, Brooks Air Force Base, San Antonio, Texas, November 1961.
4-59. Zaborowhki, A. V., "Human Tolerance to Lateral Impact with Lap Belt Only", Proceedings, Eighth Stapp Car Crash and Field Demonstration Conference, Society of Automotive Engineers, New York, New York, 1964.
4-60. Zaborорwski, A. V., "Lateral Impact Studies - Lap Belt Shoulder Harness Investigations", Proceedings, Ninth Stapp Car Crash Conference, Society of Automotive Engineers, New York, New York, 1965.
4-61. Ewing, C. L., et al., "Dynamic Response of the Human Head and Neck to $+G_y$ Impact Acceleration", Proceedings, Twenty-first Stapp Car Crash Conference, Society of Automotive Engineers, New York, New York, 1977, pp. 547-586.
4-62. Hyde, A. S., Crash Injuries: How and Why They Happen, Hyde Associates, Key Biscayne, Florida, 1992.
4-63. Lissner, H. R., et al., "Experimental Studies on the Relation Between Acceleration and Intercranial Pressure Changes in Man," Surgery, Gynecology, and Obstetrics, 111:329-338, 1960.
4-64. Nahum, A. M., Melvin, J. W., Accidental Injury: Biomechanics and Prevention. Springer-Verlag, New York, New York, 1993.
4-65. Newman, J. A., "Head Injury Criteria in Automotive Crash Testing," Twenty-fourth Stapp Car Crash Conference Proceedings, Society of Automotive Engineers 801317, Troy, Michigan, October 15-17, 1980.
4-66. Hess, R. L., et al., Review of Literature and Regulation Relating to Head Impact Tolerance and Injury Criteria, UM-HSRI-80-52-1, University of Michigan Highway Safety Research Institute, Ann Arbor, Michigan, July 1980.
4-67. Vaughn, A., The Sensitivity of Head Injury Criterion (HIC) to the Impact Surface, Simula Technologies, Inc., Phoenix, Arizona, August 18, 1997.
4-68. Gadd, C. W., "Use of Weighted-Impulse Criterion for Estimating Injury Hazard," Tenth Stapp Car Crash Conference Proceedings, Society of Automotive Engineers 660793, Holloman AFB, New Mexico, November 8-9, 1966.
4-69. Versace, J., "A Review of the Severity Index," Fifteenth Stapp Car Crash Conference Proceedings, Society of Automotive Engineers, 710881, San Diego, California, November 17-19, 1971.
4-70. Department of Transportation, National Highway Transportation Safety Administration, Notice of Proposed Rulemaking, 49 CFR Parts 571 and 585, Docket No. 74-14; Notice 38, 50 FR 14589, Washington, D.C., April 12, 1985.

This Document Provided by the Abbott Aerospace
TECHNICAL LIBRARY
ABBOTTAEROSPACE.COM

4-71. Mertz, H. J., and Prasad, P., "Head Injury Risk Assessments Based on 15 ms HIC and Peak Head Acceleration Criteria," AGARD Conference Proceedings 597, Mescalero, New Mexico, November 7-9, 1997.
4-72. Mertz, H. J., et al., "Injury Risk Curves for Children and Adults in Frontal and Rear Collisions", Society of Automotive Engineers, 973318, Warrendale, Pennsylvania, 1997.
4-73. Pike, J. A., Automotive Safety: Anatomy, Injury, Testing, and Regulation, Society of Automotive Engineers: Warrendale, Pennsylvania, 1990.
4-74. Goldsmith, W., "Meaningful Concepts of Head Injury Criteria," Proceedings from Head Injury Mechanisms: The Need for an Angular Acceleration Criterion, Washington, D.C., October 4, 1989.
4-75. Head Injury Mechanisms: The Need for an Angular Acceleration Criterion, Association for the Advancement of Automotive Medicine, Washington, D.C., October 4, 1989.
4-76. Federal Aviation Regulation Part 23, Airworthiness Standards: Normal, Utility, Acrobatic, and Commuter Category Airplanes, Section 23.562, "Emergency Landing Dynamic Conditions," Washington, D.C., October 22, 2001.
4-77. Levine, R. S., Head and Neck Injury, Society of Automotive Engineers, Warrendale, Pennsylvania, 1994.
4-78. Hodgson, V. R., Thomas L. M., "Comparison of Head Acceleration Injury Indices in Cadaver Skull Fracture", Proceedings from the Fifteenth Stapp Car Crash Conference, No. 710854, 1971.
4-79. Schneider, D. C., Nahum A. M., "Impact Studies of Facial Bones and Skull", Proceedings from the Sixteenth Stapp Car Crash Conference, No. 720965, 1972.
4-80. Yoganandan, N., et al., "Steering Wheel Induced Facial Trauma", Proceedings from the 32nd Stapp Car Crash Conference, No. 881712, 1988.
4-81. Yoganandan, N., et al., Three-dimensional Computerized Tomography Analysis of Steering Wheel, 12th ESV, No. 89-4A-W-020, 1989.
4-82. Welbourne, E. R., et al., A Comparison of Human Facial Fracture Tolerance with the Performance of a Surrogate Test Device, 12th ESV, No. 89-4A-0-004, 1989.
4-83. Melvin, J. W., Shee, T. R., Facial Injury Assessment Techniques, 12th ESV, Volume 1, 1989.
4-84. Code of Federal Regulations Title 49, Part 572, Federal Motor Vehicle Safety Standard 208, October 2000.
4-85. Myers, B. S., Winkelstein, B. A., "Epidemiology, Classification, Mechanism, and Tolerance of Human Cervical Spine Injuries", Critical Reviews in Biomedical Engineering, 23 (5&6): 307 - 409, 1995.
4-86. AGARD Advisory Report, Anthropomorphic Dummies for Crash and Escape System Testing, AGARD-AR-330, North Atlantic Treaty Organization, Neuilly-sur-Seine, France, July 1996.
4-87. Saczalski, K., Singley, G. T., Pilkey, W. D., Huston, R. L., Aircraft Crashworthiness, University Press of Virginia, 1975.
4-88. King, A. I., Prasad P., "Structural Considerations of the Human Vertebral Column", Journal of Aircraft, No. 9, pp. 84-90, January 1972.
4-89. Belytschko, T., Rencis, M., Williams, J., Head-Spine Structure Modeling: Enhancements to Secondary Loading Path Model and Validation of Head-Cervical Spine Model, Aerospace Medical Division No. AAMRL-TR-85-019, July 1985.
4-90. Levy, P. M., "Ejection Seat Design and Vertebral Fractures", Aerospace Medicine, pp. 545-549, June 1964.
4-91. Li, G., Baker, S. P., "Injury Patterns in Aviation-Related Fatalities: Implications for Preventative Strategies", The American Journal of Forensic Medicine Pathology, 18(3), 265 - 270, 1997.

This Document Provided by the Abbott Aerospace
TECHNICAL LIBRARY
ABBOTTAEROSPACE.COM

4-92. Lau, I. V., Viano, D. C., "The Viscous Criterion - Bases and Applications of an Injury Severity Index for Soft Tissues", Proceedings from the 30th Stapp Car Crash Conference. SAE 861882, 1986.
4-93. Foster, K. J., Kortge, J. O., and Wolanin, M. J., "Hybrid III - A Biomechanically Based Crash Test Dummy, SAE 770983, Proceedings from the 21st Stapp Car Crash Conference, New Orleans, Louisiana, 1977.
4-94. Kroell, C. K., et al., "Impact Tolerance and Response to the Human Thorax," Proceedings of the 15th Stapp Car Crash Conference, SAE 710851, pp. 84-134, 1971.
4-95. Kroell, C. K., et al., "Impact Tolerance and Response to the Human Thorax II", Proceedings of the 19th Stapp Car Crash Conference, SAE 741187, pp. 383-457, 1974.
4-96. Viano, D. C., Evaluation of the SID Dummy and TTI Injury Criterion for Side Impact Testing, SAE 872208, 1987.
4-97. Morgan, R. M., et al., "Side Impact – The Biofidelity of NHTSA's Proposed ATD and Efficacy of TTI", 30th Stapp Car Crash Conference, SAE 861877, 1986.
4-98. Hollinshead, W. H., Anatomy for Surgeons: Volume 2 - The Thorax, Abdomen and Pelvis, Harper and Row, New York, New York, 1971.
4-99. Pope, M. E., et al., "Postural Influences on Thoracic Impact", 23rd Stapp Car Crash Conference Proceedings, SAE 791028, 765-795, 1979.
4-100. Stalnaker, R. L., et al., "Side Impact Tolerance to Blunt Trauma", 17th Stapp Car Crash Conference Proceedings, SAE 730979, 377-408, 1973.
4-101. Cooper, G. J., Taylor, D. E. M., Biophysics of Impact Injury to the Chest and Abdomen, JR Army Medical Corps, 135:58-67, 1989.
4-102. Cooper, G. J., et al., "Pearce BP Injury from Blast Loading: Modifications of Stress Transmission by Foams and High-Density Materials" Journal of Biomechanics, 24(5), pp. 273-285, 1991.
4-103. DeHaven, H., Injury in Light Aircraft Accidents, Air Surgeon's Bulletin, 1, 5, July 1944.
4-104. Windquist, P. G., Stumm, P. W., and Hansen R., Crash Injury Experiments with the Monorail Decelerator, AF Technical Report No. AFFTC 53-57, April 1953.
4-105. Walfisch, F., Fayon, A., Leung, Y. C., Tarriere, C., Got, C., Patel, A., "Synthesis of Abdominal Injuries in Frontal Collisions with Belt-Wearing Cadavers Compared with Injuries Sustained by Real-Life Accident Victims", Proceedings of IRCOBI, Goteborg, Sweden, September 1979.
4-106. Pattimore, D., et al., "The Nature and Cause or Lower Limb Injuries in Car Crashes", Proceedings from the 34th Stapp Car Crash Conference, SAE 912901, 1991.
4-107. Mertz, H. J., Injury Assessment Values used to Evaluate Hybrid III Response Measurements, NHTSA Docket 74-14, Notice 32, Enclosure 2 of Attachment I of Part III of General Motors Submission USG2284. March 22, 1984.
4-108. The Abbreviated Injury Scale, 1985 Revision, American Association for Automotive Medicine, Des Plaines, Illinois, 1985.
4-109. The Abbreviated Injury Scale, 1990 Revision, Association for the Advancement of Automotive Medicine, Des Plaines, Illinois, 1990.
4-110. Injury Impairment Scale, American Association for Automotive Medicine, Des Plaines, Illinois, 1994.
4-111. Rimel, R. W., et al., "A Prospective Study of CNS Trauma and Vehicular Accidents", Twenty-sixth Annual Proceedings of the American Association for Automotive Medicine, Ottawa, Ontario, Canada, pp. 1-14, October 1982.
4-112. Mertz, H. J., "Chapter 4: Anthropomorphic Test Devices," from Accidental Injury: Biomechanics and Prevention, Nahum, A. M., and Melvin, J. W., eds., Springer-Verlag, New York, New York, 1993.
4-113. Mertz, H. J. "Chapter 3: Anthropomorphic Models," from Biomechanics of Trauma, Nahum, A. M., and Melvin, J. W., eds., Appleton-Century-Crofts, Norwalk, Connecticut, 1985.

THIS DOCUMENT PROVIDED BY THE ABBOTT AEROSPACE
TECHNICAL LIBRARY
ABBOTTAEROSPACE.COM

4-114. Kelly, J. R., Denton, R. A., Morgan, C. R., "New Developments in Dummy Load Cells", paper presented at the Wayne State University Bioengineering Center 60th Anniversary Impact Biomechanics from Head to Foot Symposium, Novi, Michigan, June 9-11, 1999.
4-115. Foster, J., Kortge, J., Wolanin, M., Hybrid III – A Biomechanically Based Crash Test Dummy, Paper No. 770938, Society of Automotive Engineers, Warrendale, Pennsylvania, 1977.
4-116. Code of Federal Regulations Title 49, Anthropomorphic Test Devices, Part 572, "Subpart B – 50th-Percentile Male," October 1998.
4-117. Code of Federal Regulations Title 49, Federal Motor Vehicle Safety Standards, Part 571.208, "Occupant Crash Protection," October 1997.
4-118. Massing, D. E., Naab, K. N. and Yates, P. E., Performance Evaluation of a New Generation of 50th-Percentile Anthropomorphic Test Devices: Volume 1 – Technical Report, Calspan Corporation; DOT-HS Technical Report 801-431, Department of Transportation, National Highway Traffic Safety Administration, Washington, D.C., PB 240-920, March 1975.
4-119. Marcus, J. H., "Dummy and Injury Criteria for Aircraft Crashworthiness," SAE 951167, paper presented at the Society of Automotive Engineers General, Corporate and Regional Aviation Meeting and Exposition (GCRAM), Wichita, Kansas, May 3-5, 1995.
4-120. Federal Aviation Regulation Part 23, Airworthiness Standards: Normal, Utility, Acrobatic, and Commuter Category Airplanes, Section 23.562, "Emergency Landing Dynamic Conditions," March 26, 98.
4-121. Federal Aviation Administration Advisory Circular 23.562-1, "Dynamic Testing of Part 23 Airplane Seat/Restraint Systems and Occupant Protection," June 22, 1989.
4-122. First Technology Safety Systems, http://www.ftss.com, site accessed on June 15, 1999.
4-123. Code of Federal Regulations Title 49, Anthropomorphic Test Devices, Part 572, "Subpart E – Hybrid III Test Dummy," October 1998.
4-124. Gowdy, V., et al., "A Lumbar Spine Modification to the Hybrid III ATD for Aircraft Seat Tests," presented at the Society of Automotive Engineers General, Corporate, and Regional Aviation Meeting and Exposition (GCRAM), Wichita, Kansas, SAE 1999-01-1609, April 20-22, 1999.
4-125. Federal Aviation Regulation Part 25, Airworthiness Standards: Transport Category Airplanes, Section 25.562, "Emergency Landing Dynamic Conditions," May 27, 1998.
4-126. Beach, D., et al., "THOR Advanced Test Dummy – Biofidelity and Injury Assessment," paper presented at the International Fire and Cabin Safety Research Conference, Atlantic City, New Jersey, November 16-20, 1998.
4-127. White, R. P., Rangarajan, N., and Haffner, M. P., "Development of the THOR Advanced Frontal Crash Test Dummy," paper presented at the 34th Annual SAFE Symposium, 1996.
4-128. Code of Federal Regulations Title 49, Federal Motor Vehicle Safety Standards, Part 571.214, "Side Impact Protection," October 1998.
4-129. Code of Federal Regulations Title 49, Anthropomorphic Test Devices, Part 572, "Subpart F – Side Impact Dummy 50th-Percentile Male," October 1998.
4-130. Neilson, L., et al., "The EuroSID Side Impact Dummy," paper presented at the Tenth International Technical Conference on Experimental Safety Vehicles, National Highway Traffic Safety Administration, Washington, D.C., pp. 153-164, July 1985.
4-131. WorldSID, http://www.worldsid.org, site maintained by Biokinetics and Associates Ltd. and First Technology Safety Systems, site accessed on June 17, 1999.
4-132. Lankarani, H. M., et al., "Compliance Criteria for Side Facing Aircraft Seats", presented at the Society of Automotive Engineers General Corporate and Regional Aviation Meeting and Exposition (GCRAM), SAE Paper No. 199-01-1598, Wichita, Kansas, April 20-22, 1999.

This Document Provided by the Abbott Aerospace
Technical Library
abbottaerospace.com

This Document Provided by the Abbott Aerospace
Technical Library
abbottaerospace.com

Chapter 5
Modeling

Terence Lim
Jill M. Vandenburg

This chapter presents some of the methods used to develop computer models for the evaluation of seating systems, aircraft interiors, and airframes. The information contained in this chapter was provided by Terence Lim of Cessna Aircraft Company and was taken from "Methodology for Seat Design and Certification by Analysis" (Reference 5-1). Please note that the software packages presented in this chapter were selected to serve as examples for the user and their mention does not constitute an endorsement. In addition, the examples described in the text may or may not be applicable to the user's particular version of the software.

When used effectively, computer models can reduce the cost of design and significantly shorten the certification schedule. As an example, consider a seat design process using computer modeling for a GA aircraft seat. In the preliminary design phase of the seat design, a computer model is used to perform numerous parametric studies to investigate different energy-absorbing concepts and establish design parameters to meet the structural and occupant loads. Simple restraint models are generated to predict occupant trajectory, optimize restraint design, and determine the approximate anchor mount positions. Information from the parametric analysis is used to produce the prototype seat design. The prototype seat is then evaluated for fit and function, and modifications are made to refine the design.

As the seat design moves from the prototype phase to the first production concept design, additional detail is added to the computer model. Analysis is performed to obtain an accurate prediction of the structural behavior, occupant response, and occupant loads with respect to the dynamic pass/fail criteria. Interior components such as the glareshield, instrument panels, and side-ledges are added to the model to predict the head injury criteria (HIC). Seat cushions, seat pans, and energy-absorbing devices are modeled to predict the lumbar spinal load in a crash. Floor deformation analysis is performed to determine if the seat structure is able to sustain the induced pre-stress and crash load without failure.

Validation of the model is achieved through a comparison of the modeling results with actual test data. After the basic model has been validated, the design and analysis cycle is iterated until a satisfactory design is attained and the component or structure proceeds to the certification phase.

5.1 UNITS

Finite-element (FE) modeling requires the use of a consistent set of engineering units for the fundamental measures of length (L), time (T), mass (M) and derivative units such as velocity (L/T) and force (ML/T^2). Table 5-1 shows an example of different sets of consistent units. It is

THIS DOCUMENT PROVIDED BY THE ABBOTT AEROSPACE
TECHNICAL LIBRARY
ABBOTTAEROSPACE.COM

good modeling practice to define a specific set of units early in the data deck, as shown in the example MSC/DYTRAN® file in Figure 5-1 (Reference 5-2). Consistent units help the modeler and end users apply the correct input to the model. Certain software packages only recognize a single set of units. For example, the Mathematical Dynamical Model (MADYMO®) software only allows the user to input data and receive output in SI units (References 5-3 and 5-4). The designer should be sure to verify which systems of units their particular software program allows prior to beginning construction of the model.

Table 5-1.
Sets of consistent units

Units	SI	English	mm/kg/msec
Length	Meter (m)	Foot (ft)	Millimeter (mm)
Mass	Kilogram (kg)	Slug (lbf-sec^2/ft)	Kilogram (kg)
Time	Second (sec)	Second (sec)	Millisecond (msec)
Density	kg/m^3	Slug/ft^3	kg/mm^3
Force	kg m/sec^2 = Newton (N)	Slug ft/sec^2 = lbf	kN
Stress	N/m^2 = Pa	(Slug ft/sec^2)/ft^2 =lbf/ft^2	Gpa
Energy	Nm = Joule (J)	(Slug ft/sec^2)ft =lbf-ft	Joules (J)

```
$ SEAT CRASH TEST MODEL
$
$ SI Units: kg - meter - seconds
$ ------------------------------
$  conversion factors
$  lbm/in3 to kg/m3: multiply by 2.767990e+4
START
ENDTIME=150.E-3
PARAM,INISTEP,1.E-6
TLOAD=1
```

Figure 5-1.
Example unit specification data.

5.2 COORDINATE SYSTEM

Ideally, the computer model should be aligned with the aircraft coordinate system and should comply with the coordinate system and sign convention defined in SAE J211 (Reference 5-5). This will facilitate the correlation of the computer modeling results with the dynamic impact test results, which are also based on SAE J211. For example, in a model consisting of a seat and a horizontal test sled, the X-axis should be along the fore-aft (fuselage station) direction of the

® MSC/DYTRAN is a registered trademark of MacNeal-Schwendler Corporation
® MADYMO is a registered trademark of the TNO Road-Vehicles Research Institute

THIS DOCUMENT PROVIDED BY THE ABBOTT AEROSPACE
TECHNICAL LIBRARY
ABBOTTAEROSPACE.COM

aircraft, the Y-axis along the inboard-outboard (buttline) direction, and the Z-axis along the direction of gravity (waterline). Figure 5-2 illustrates a MADYMO model of a forward-facing seat aligned in the aircraft coordinate system.

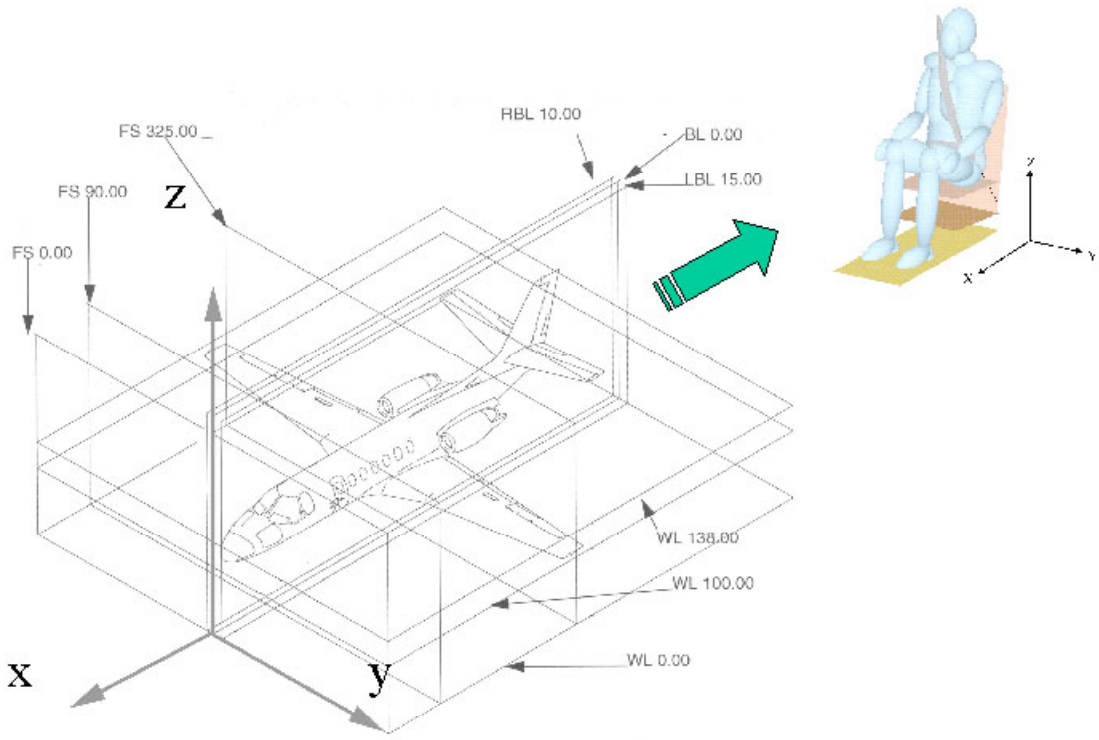


Figure 5-2.
Model coordinate system orientation.

5.3 OCCUPANT MODELS

Validated occupant models are available for use in most software packages. The most widely used occupant model for aircraft applications is the 14 CFR Part 572 Subpart B Hybrid II anthropomorphic test device (ATD) (Reference 5-6). During the AGATE program, Cessna also correlated the response of the Articulated Total Body (ATB®) Hybrid II (Reference 5-7) and MADYMO Hybrid II ATDs using full-scale test data (References 5-8 and 5-9). The test data revealed that both of these occupant models have a response similar to the actual Hybrid II ATD, and are suitable for use in aircraft design and certification.

The ATB Hybrid II occupant is comprised of 17 rigid segments connected by 16 pin and spherical joints (Figure 5-3). The occupant model executes within the ATB crash simulation program. Although the multi-body capabilities of the ATB program can be used to perform crash simulation, the lack of a FE solver makes it impractical for use in complex analysis and certification where stress results are required. As a result, the ATB occupant model is generally coupled with the MSC/DYTRAN FE codes. When coupled with MSC/DYTRAN, the ATB model will appear in the MSC/PATRAN® pre-/post-processor, as shown in Figure 5-4.

® ATB is a public domain code developed and maintained by Wright Patterson Air Force Base
® PATRAN is a registered trademark of MacNeal-Schwendler Corporation

THIS DOCUMENT PROVIDED BY THE ABBOTT AEROSPACE
TECHNICAL LIBRARY
ABBOTTAEROSPACE.COM

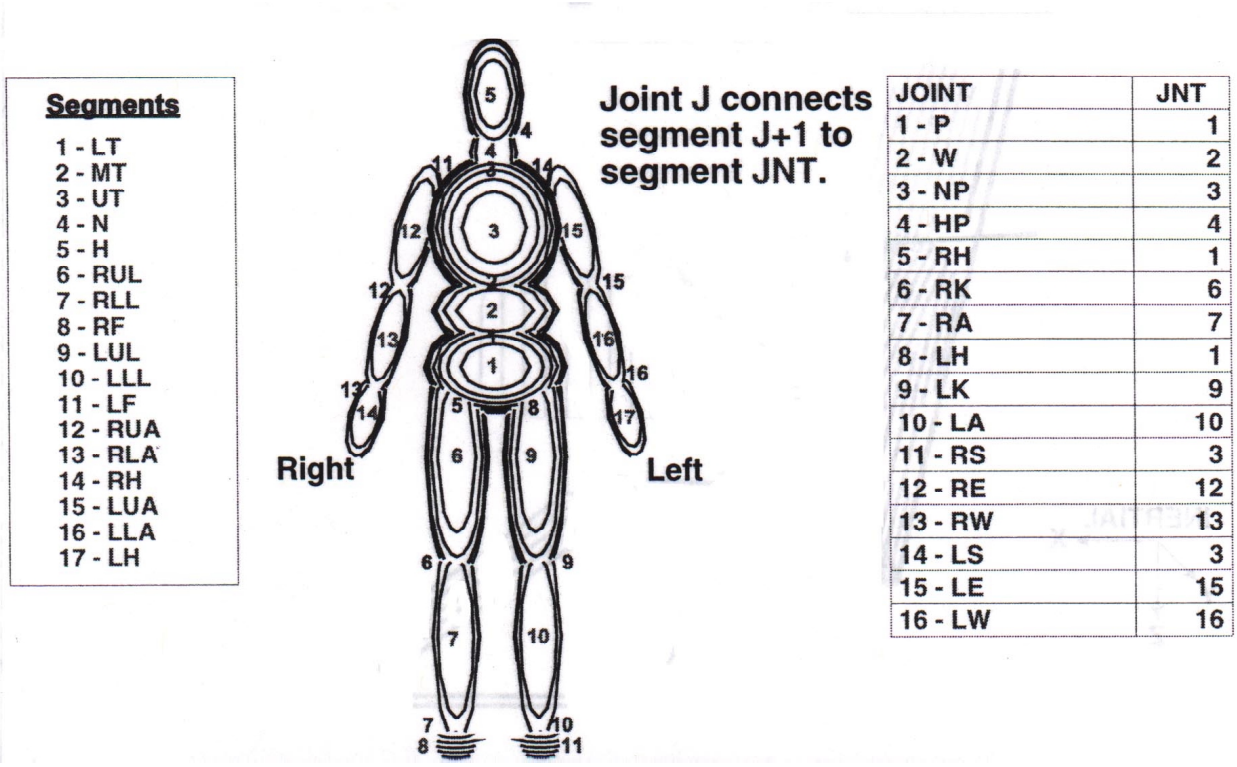


Figure 5-3.
The ATB Hybrid II occupant model.

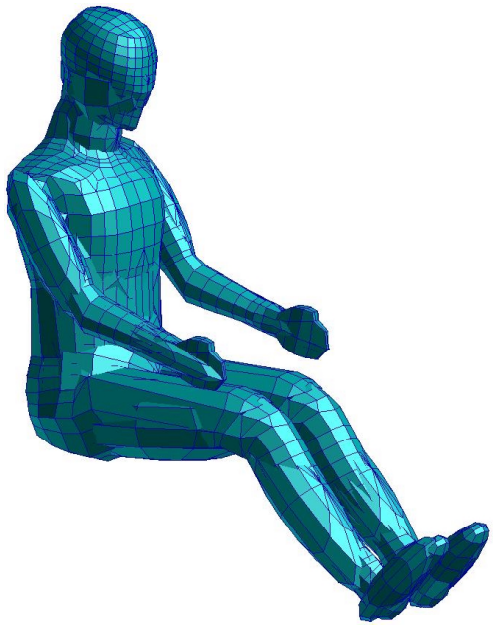


Figure 5-4.
The MSC/DYTRAN representation of the ATB model.

This Document Provided by the Abbott Aerospace
TECHNICAL LIBRARY
ABBOTTAEROSPACE.COM

The MADYMO Part 572 Subpart B Hybrid II ATD is modeled as a system of elliptically shaped masses interconnected by joints (Reference 5-10). It is available in a seated or standing initial position. The MADYMO Hybrid II is comprised of 32 bodies that are connected by a variety of kinematic joints (Figure 5-5 and Table 5-2). The occupant model has been validated for aircraft applications in the vertical and 30-deg nose-down test conditions (Reference 5-11).

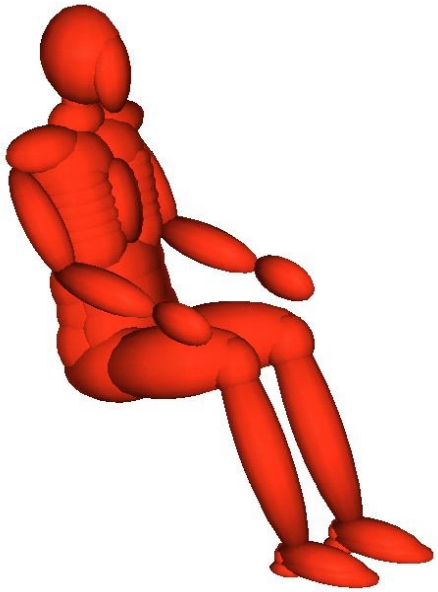


Figure 5-5.
MADYMO Hybrid II (PART 572 Subpart B) ATD model.

5.4 5.5 MODELING STRUCTURAL ELEMENTS

The structural elements that are modeled may consist of the seat structure, fuselage structure, cushions, restraint systems, instrument panels, glareshields, side panels, crash sled, and any other objects that can influence the response of the occupant. There is no ideal method to model structural elements. Generally, each method depends on the capabilities of the software, the information the analyst wants to extract from the model, and the desired accuracy of the analysis. There are three basic methods to model structural elements: multi-body techniques, FE modeling, or the hybrid modeling method.

5.4.1 Method 1 – Multi-body Techniques

The easiest method to model structural objects is through the use of multi-body (a MADYMO definition) or rigid elements. Both MADYMO and ATB possess multi-body modeling capabilities. This includes using combinations of simple planes, cylinders, ellipsoids, and facet surfaces. Multi-body elements are primarily used to simplify the representation of the structure and are utilized in applications where the kinematic response of the structure is desired, but information on stresses and strains is not required. Parts of rigid bodies can be connected together by spring-damper or torsional spring elements to provide resistive force.

This Document Provided by the Abbott Aerospace
TECHNICAL LIBRARY
ABBOTTAEROSPACE.COM

Table 5-2.
Standard MADYMO Part 572 Subpart B ATD definition

NUMBER	NAME	REMARKS
1	LOWER TORSO	REFERENCE BODY OF ATD SYSTEM
2	ABDOMEN	
3	LOWER LUMBAR	
4	UPPER LUMBAR	
5	UPPER TORSO	SPINE BOX AND BACK OF THE RIBS
6	RIBS	FRONTAL AREA OF THE RIB CAGE
7	LOWER NECK BRACKET	FOR NECK ANGLE ADJUSTMENT ONLY
8	LOWER NECK SENSOR	FOR LOAD SENSING ONLY
9	NECK	
10	NODDING PLATE	FOR LOAD SENSING ONLY
11	HEAD	
12	CLAVICLE LEFT	
13	CLAVICLE RIGHT	
14	UPPER ARM LEFT	
15	UPPER ARM RIGHT	
16	LOWER ARM LEFT	
17	HAND LEFT	
18	HAND RIGHT	
19	HAND LEFT	
20	FEMUR LEFT	PROXIMAL OF FEMUR LOAD CELL
21	FEMUR RIGHT	PROXIMAL OF FEMUR LOAD CELL
22	KNEE LEFT	PERIPHERAL OF FEMUR LOAD CELL
23	KNEE RIGHT	PERIPHERAL OF FEMUR LOAD CELL
24	UPPER TIBIA LEFT	ABOVE UPPER LOAD CELL
25	UPPER TIBIA RIGHT	ABOVE UPPER LOAD CELL
26	MIDDLE TIBIA LEFT	IN BETWEEN LOAD CELLS
27	MIDDLE TIBIA RIGHT	IN BETWEEN LOAD CELLS
28	LOWER TIBIA LEFT	BELOW LOWER LOAD CELL
29	LOWER TIBIA RIGHT	BELOW LOWER LOAD CELL
30	FOOT LEFT	
31	FOOT RIGHT	
32	STERNUM	COMPLIANT CENTRAL REGION OF RIB CAGE

Figure 5-6 shows an example of a MADYMO seat model generated using multi-body techniques. This model is particularly useful as a parametric tool because of its simplicity and low computational cost. Changes to the model are easily made, and the next load case can be analyzed. The model in Figure 5-6 represents an over-spar bench seat. Because of the rigidity of the seat, structural deformation and stresses were not required, since there is no significant deformation of the seat. Therefore, a multi-body model was sufficient in determining the response of the occupant.

The seat structure, seat cushion, and crash vehicle were represented by multi-body planes. These planes were positioned to reflect the configuration of the actual seat structure. The planes were fixed to the vehicle inertial system and contacts were defined between the occupant and planes based on the inertial and stiffness properties of the cushions that were obtained from sub-component compression tests.

THIS DOCUMENT PROVIDED BY THE ABBOTT AEROSPACE
TECHNICAL LIBRARY
ABBOTTAEROSPACE.COM

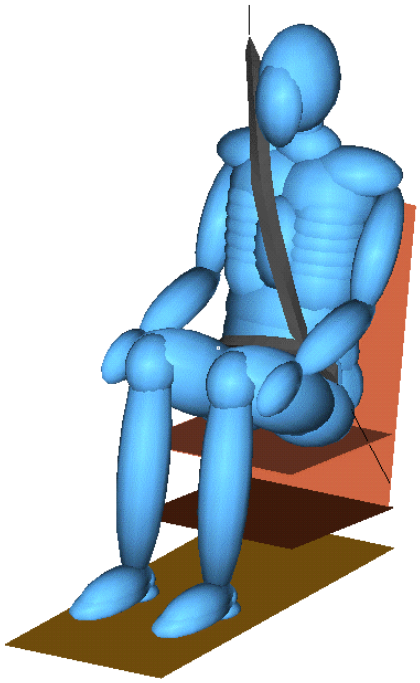


Figure 5-6.
Multi-body MADYMO model.

5.4.2 Method 2 - Finite-Element (FE) Modeling

The most representative technique to model structural objects is to use the finite-element (FE) method. Finite-element models are generated to obtain detailed response of structures and to determine failure modes. The MADYMO and MSC/DYTRAN programs have extensive non-linear FE capabilities. Finite-element models are more difficult to generate than multi-body models; however, FE models are more practical because they predict realistic structural response and offer the capability to output stresses, strains, and internal loads. They can also be utilized to substantiate structural designs. Figure 5-7 shows a process flowchart that is commonly used to generate a FE model.

The precise method on how to generate an efficient FE model of a particular structure will depend on the design of the structure and the desired output of the model. Generally, the first step is to determine the load path of the structure for each load case. Then, lists of the critical load-carrying members within the load path are noted. Engineering judgment will be used to determine the mode of failure for each critical member. This will help determine the choice of elements to represent the structure in the model.

Geometry for the model can either be generated in FE pre-processors or can be imported from a CAD package. If the geometrical data is imported from a CAD package such as CATIA or Pro-Engineer, the data is converted to a format (such as IGES) which can be recognized by the FE pre-processor as surfaces or solids. The imported information is used for generating the FE mesh. Each part of the structure is grouped and meshed independently. Care must be taken to ensure that the shape of each element is not distorted in order to avoid computational problems during the analysis.

THIS DOCUMENT PROVIDED BY THE ABBOTT AEROSPACE
TECHNICAL LIBRARY
ABBOTTAEROSPACE.COM

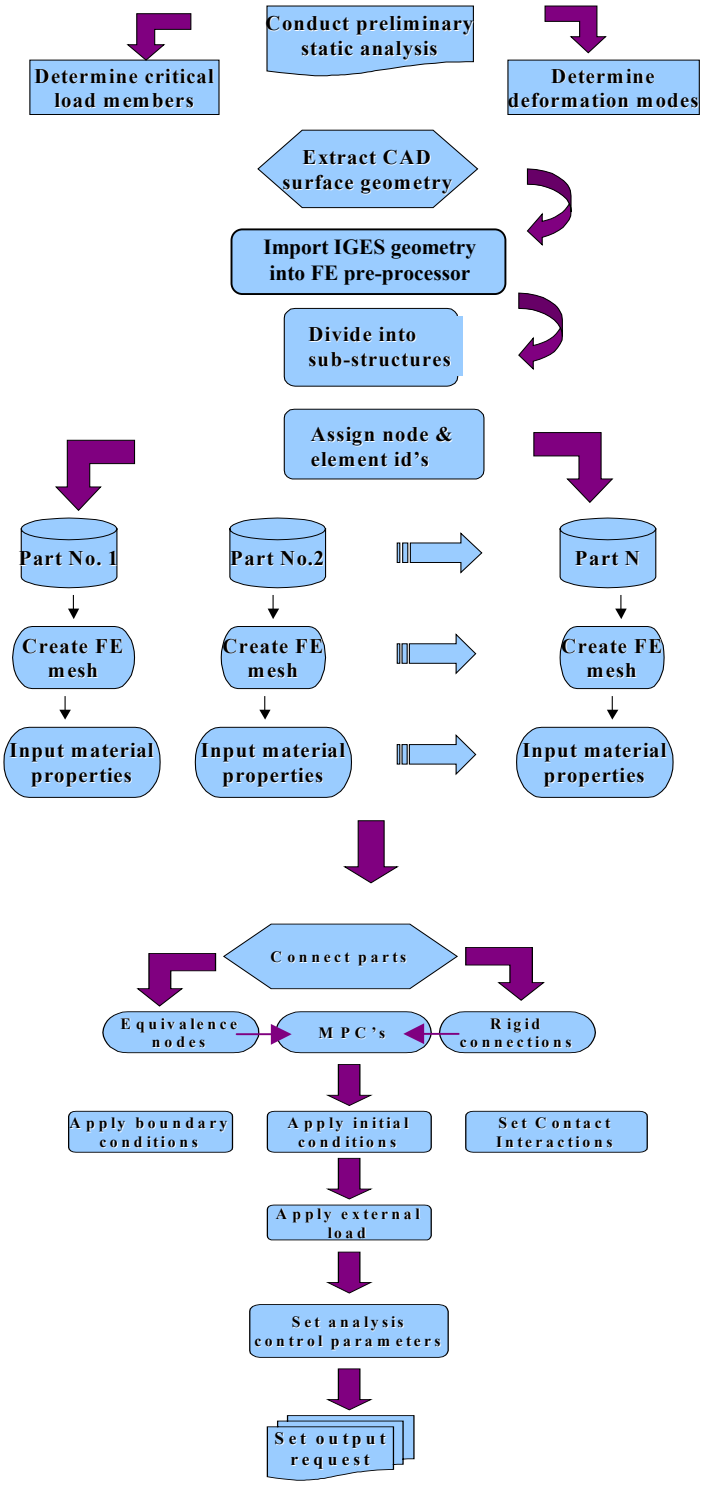


Figure 5-7.
Finite-element modeling flowchart.

THIS DOCUMENT PROVIDED BY THE ABBOTT AEROSPACE
TECHNICAL LIBRARY
ABBOTTAEROSPACE.COM

After all components of the structure are meshed, the individual groups can be merged by equivalencing coincident nodes or by joining the parts together using spot weld elements or rigid elements. Equivalenced nodes fix the components together, whereas spot weld elements allow for the joined parts to separate once the loads have met a user-defined failure criteria. Rigid elements are essentially a multi-point constraint (MPC) and are used to define a set of grid points that forms a rigid element.

The next step is to define the material properties of the entire structure. Pre-processors such as PATRAN and Hypermesh® have capabilities that link CAD geometry to finite elements so that the user can assign properties based on the geometry instead of based on the individual elements in the structure (which tends to be more difficult in complex or large-size models).

After the material properties have been defined, boundary conditions, contact interactions, and external loads can be defined for the model. Boundary conditions are applied to attach the meshed structure to the vehicle by applying a constraint to the translational or rotational degrees of freedom at the juncture of the structure and the vehicle. Contacts are defined between any components that possess the potential to come into contact with each other during the crash event. External loads are applied to the structure in the form of a pre-defined acceleration crash pulse or force.

The final step in the process includes defining a set of analysis control parameters and output parameters (i.e., analysis termination time, integration method, hourglass energy control, mass scaling, loads, accelerations, injury criteria, etc). Execution of the model will reveal any errors in the code and a debugging process can be implemented to identify and correct the errors.

5.4.2.1 Element Types

There are many types of finite elements, and the choice of element selection will depend on the load and deformation characteristics of the actual structure that the FE model will represent. Finite elements are typically grouped in the following categories:

1. Scalar Elements

Scalar elements typically consist of spring, mass, and damper elements. The stiffness properties are usually defined by the user. Scalar masses are commonly used to model a concentrated mass at one location, such as an engine block, fuel tank, or ballast weights. There is no stiffness definition associated with a scalar mass.

As illustrated in Figure 5-8, spring elements connect two grid points and the force acts in the direction of the connecting grid points. Spring elements connect translational and rotational degrees of freedom and may have a linear or non-linear stiffness property. For translational springs, the stiffness is defined in terms of force versus deflection. For rotational springs, the stiffness is defined in terms of moment versus angle of rotation.



Figure 5-8.
Spring element.

® Hypermesh is a registered trademark of Altair Engineering, Inc.

THIS DOCUMENT PROVIDED BY THE ABBOTT AEROSPACE
TECHNICAL LIBRARY
ABBOTTAEROSPACE.COM

2. One-dimensional Elements

One-dimensional elements are used to represent structural members that have stiffness along a line or a curve. Examples of one-dimensional elements are rod and beam elements (Figures 5-9 and 5-10).

Rod elements carry tension and compressive loads only. The mass of the elements are lumped and distributed equally at the nodes. The only geometric property required is the cross-sectional area of the rod.

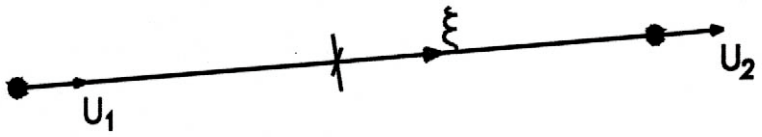


Figure 5-9.
Rod element.

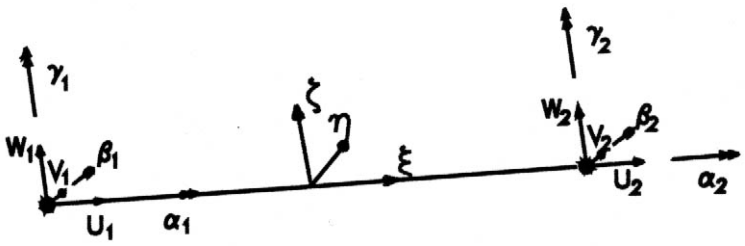


Figure 5-10.
Beam element.

Beam elements carry axial, torsion and bending loads. The mass of the beam is lumped and equally distributed over the two nodes. Unless otherwise stated, the mass, shear center and centroid of the cross-section all coincide. The orientation of the beam should be defined in its element coordinate system. The geometric properties required are the areas and moments of inertia of the beam.

3. Two-dimensional Elements

Two-dimensional elements (Figure 5-11), also known as shell elements, consist of quadrilateral, triangular, and membrane elements. These elements are most widely used because of their versatility and robust formulations. The mass of the two-dimensional elements is lumped and equally distributed over all the nodes.

THIS DOCUMENT PROVIDED BY THE ABBOTT AEROSPACE
TECHNICAL LIBRARY
ABBOTTAEROSPACE.COM

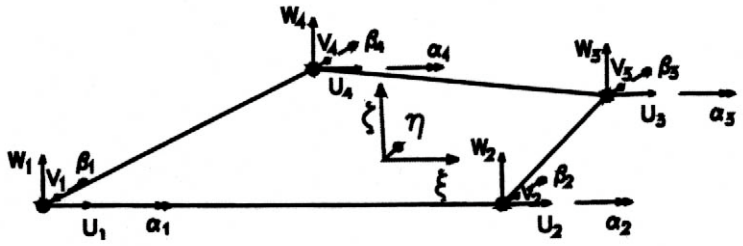


Figure 5-11.
Two-dimensional shell element.

Quadrilateral shell elements are the most widely used type. They carry in-plane as well as bending loads. Quadrilateral shell elements have six degrees of freedom at each node; specifically, three translations and three rotations. Transverse shear stiffness is accounted for by a shear correction factor. The geometric properties required are the shell thickness and the number of integration points through the thickness.

Membrane elements carry in-plane loads and do not have bending stiffness. Membrane elements can be three- or four-node elements with three translation degrees of freedom on each node. The deformation is determined by the translation degrees of freedom on these nodes. Depending on the code, membrane elements can have linear or non-linear properties. Seat belt webbing and seat pans are typically modeled using membrane elements. The geometric property required is the thickness of the membrane.

Triangular elements typically exhibit a stiffer response and are used only as transitional elements and in areas of low stress concentrations. Most codes use a default one-point integration at the center of the element, although there are options to increase the number of integration points; however, this comes at the expense of computational efficiency. Note that when one-point integration is used, the "hourglass" or "zero-energy" modes are generated and have to be suppressed.

Over the years, advanced formulations have allowed for more robust and computationally efficient elements, such as the Belytschko-Tsai, Key-Hoff, and Hughes-Liu shells. The choice of element formulation usage will depend on the need to compromise accuracy with computational speed. In most cases, the Belytschko-Tsai shell formulation is sufficient.

4. Three-dimensional Elements

Three-dimensional elements (Figure 5-12), also known as solid elements, consist of tetra, penta, and hexa elements. These types of elements are capable of carrying tensile, compression, and shear loads. The mass of the solid elements are lumped and equally distributed over all of the nodes.

The most commonly used three-dimensional element is the hexahedral element based on its efficiency and the ease in which the modeler can mesh and interface each element with other elements. The tetra and penta elements are basically degenerated forms of the hexa elements. The grid points of the tetra and penta elements coincide, which ultimately results in a significant reduction in performance.

The solid elements use one-point (or reduced) integration for computational efficiency. However, this also results in twelve "zero-energy" or "hourglass" modes. These modes have to be suppressed using the hourglass energy control parameter that is available in all codes.

THIS DOCUMENT PROVIDED BY THE ABBOTT AEROSPACE
TECHNICAL LIBRARY
ABBOTTAEROSPACE.COM

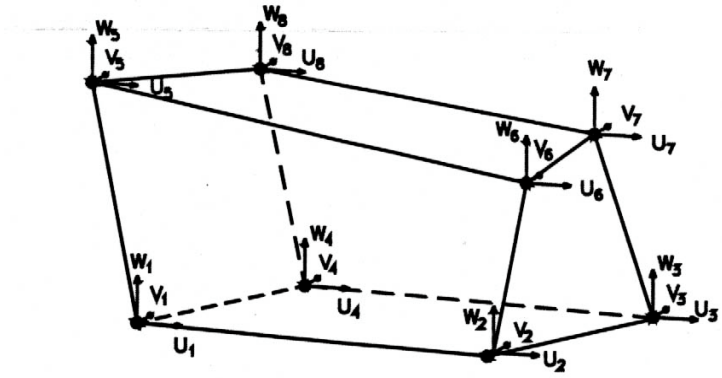


Figure 5-12.
Solid element.

5.4.2.2 Example Finite-Element Model

Figure 5-13 shows an example of a MSC/DYTRAN FE occupant/seat model. The objectives of the model were (1) to obtain an accurate prediction of the structural response, (2) to locate areas of high stress concentrations, and (3) to determine how the seat affects the motion of the occupant.

In the example model, shell elements were the most widely used because of their robust formulation and versatility. The seat assembly consisted of five primary structures: seat back, seat bucket, seat pan, seat base, and seat pivot assembly. The crash load from the occupant is transferred to the seat from the anchor points on the shoulder harness and the lap belt. In a forward impact case, the load is transferred from the seat back down to the pivot mechanism and finally to the diagonal crossmembers on the seat base in the form of compression load.

The majority of the seat structure was modeled using four-noded quadrilateral CQUAD4 (KEYHOFF formulation) shell elements. Triangular CTRIA3 (CO-TRIA formulation) elements were used as transition elements in non-critical stress areas. Seat adjustment mechanisms of structural significance - such as Hydroloks and recline arms - were modeled using non-linear spring and simple beam elements. The seat cushion was modeled using CHEXA solid elements with equivalent cushion thickness. The footrest and sled were modeled using CQUAD4 elements using rigid (MATRIG) material properties. Figure 5-14 shows an exploded view of the FE structure.

5.4.3 Method 3 – Hybrid Modeling Method

Multi-body and FE techniques can be combined to model structures. This is a common method used in MADYMO, although the same method can be applied in MSC/DYTRAN using the rigid ellipsoid capabilities. The hybrid method is used to simplify the FE modeling process, replacing non-critical FE elements with multi-body ellipsoids or planes.

Figure 5-15 shows an example of the hybrid modeling techniques used to model the same seat presented in Section 5.5.2. In this example, the seat frame was modeled using a combination of beam and shell elements. The seat cushion and glareshield were modeled using two ellipsoidal multi-body elements instead of finite elements. A sub-component test was conducted to obtain the load-deflection characteristics of the seat cushion and glareshield to characterize their response during impact.

THIS DOCUMENT PROVIDED BY THE ABBOTT AEROSPACE
TECHNICAL LIBRARY
ABBOTTAEROSPACE.COM

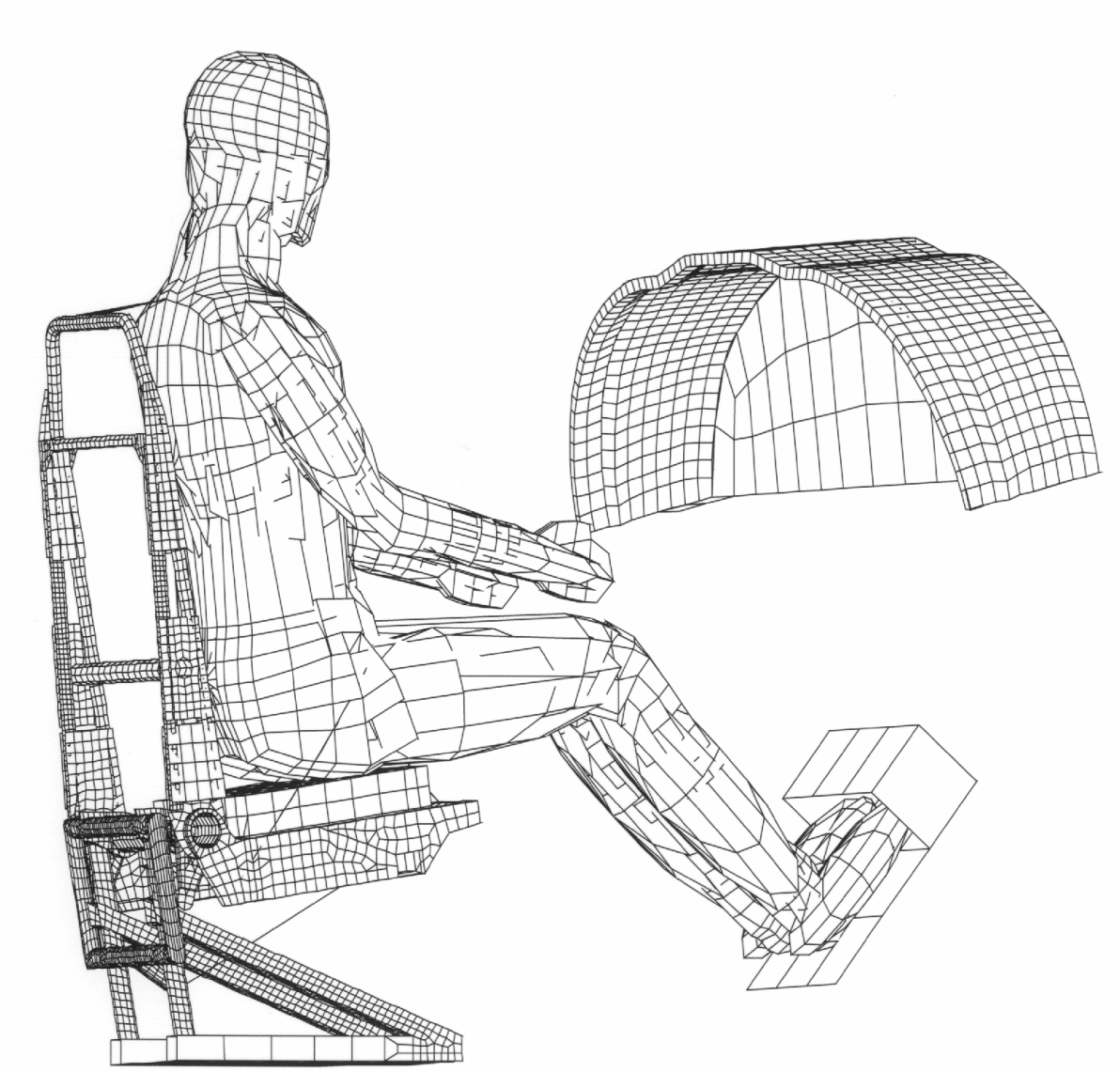


Figure 5-13.
MSC/DYTRAN FE model.

This Document Provided by the Abbott Aerospace
Technical Library
abbottaerospace.com

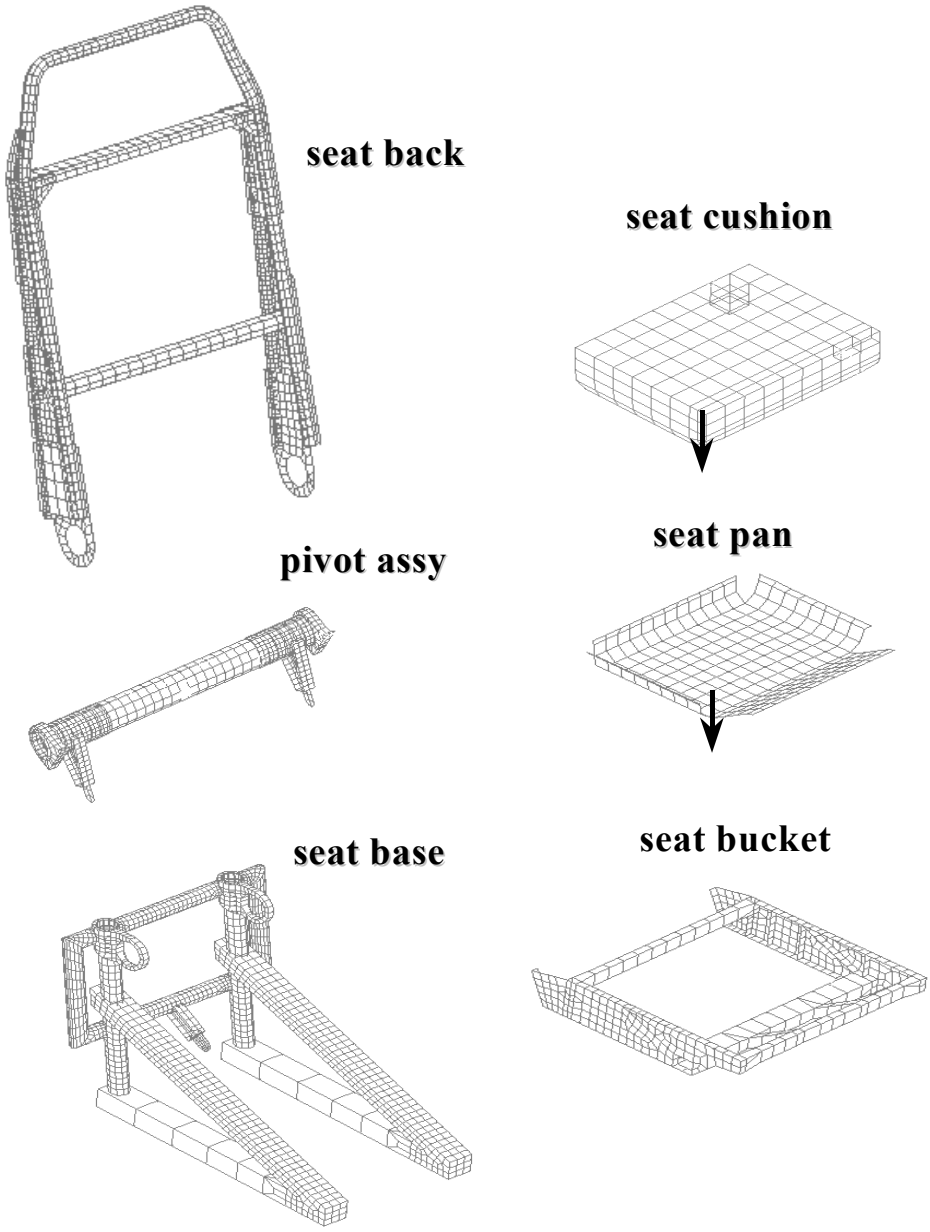


Figure 5-14.
Exploded view of a finite-element seat.

This Document Provided by the Abbott Aerospace
TECHNICAL LIBRARY
ABBOTTAEROSPACE.COM

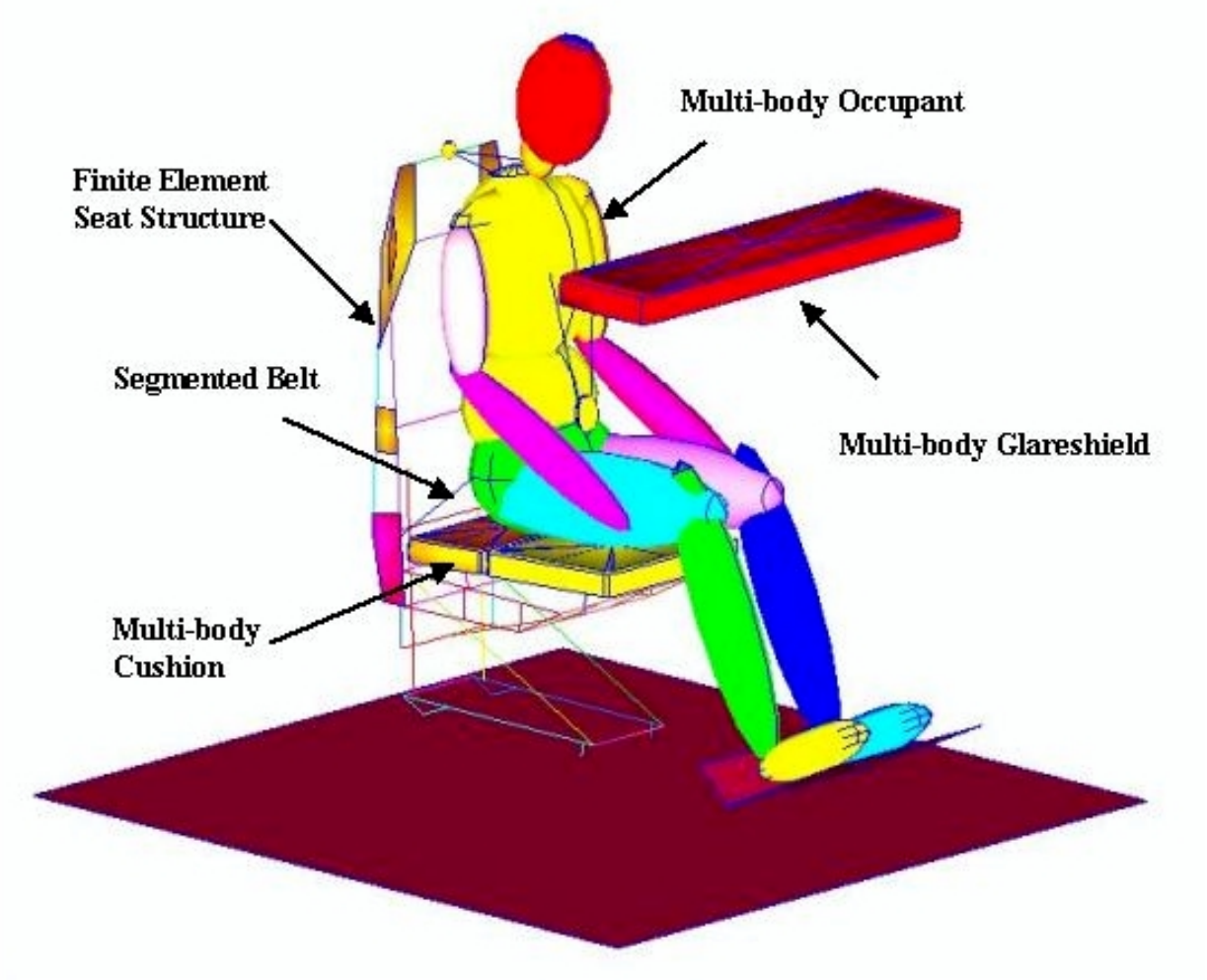


Figure 5-15.
MADYMO hybrid modeling model.

The seat cushion ellipsoids are rigidly connected to the seat bucket at its corner locations using FE-to-multibody constraints. The glareshield is fixed to inertial space. Loads, constaints, and boundary conditions are applied in the same manner as the FE model.

In general, hybrid models are less accurate than FE models. However, the hybrid model uses a smaller amount of CPU resources than a full FE model, and is sufficient to reasonably predict the deformation of the seat structure and the response of the occupant.

5.4.4 Modeling Failure of Joints or Fasteners

There are numerous methods of simulating structural failures in a non-linear FE model. A typical failure mode modeled in seat analysis is failure of rivet and threaded fastener joints. The MADYMO, LS-DYNA3D®, and MSC/DYTRAN programs have capabilities to model simple

® LS_DYNA3D is a registered trademark of the Livermore Software Technology Corporation

THIS DOCUMENT PROVIDED BY THE ABBOTT AEROSPACE
TECHNICAL LIBRARY
ABBOTTAEROSPACE.COM

shear and tensile failure of fasteners. More-complex continuum damage mechanics (CDM) material failure models are available for structures modeled using these codes. As an example, rivet failure can be modeled using MADYMO node-to-node spot weld constraints, as shown below.

```
SPOTWELDS
        NODE-NODE
          MAXFN          300.0
          AN             2.0
          MAXFS          350.0
          AS             2.0
          WINDOW         0.001
          1  743   2  21                FEMHIS
          1  632   2  110               FEMHIS
          1  1219  2  35                FEMHIS
        END NODE-NODE
END SPOTWELDS
```

This example defines three node-node spot welds in a MADYMO 5.4 format. The spot welds are defined as having a maximum allowable normal force of 300.0 and a maximum allowable shear force of 350.0. The failure criteria is defined as follows:

$$\left|\frac{F_{NORM}}{MAXFN}\right|^{AN} + \left|\frac{F_{SHEAR}}{MAXFS}\right|^{AS} < 1$$

The shear and normal failure criteria exponents are set to 2. These exponents determine the rupture criterion shape. The time window (0.001) specifies the time duration that the failure criteria must be violated before the failure initiates. The spot welds created in FE Models 1 and 2 are defined between node pairs 743 and 21, 621 and 110, and 1219 and 35. A vector between the nodes of a spot weld must have a magnitude greater than zero. The optional FEMHIS keyword in the example requests output of the shear and normal forces.

5.5 RESTRAINT MODELING

Restraint modeling techniques are presented for the most common restraint configurations used in FAR Part 23 (Reference 5-12) type aircraft: forward, side, and aft-facing (two- and five-point restraints). These restraints are typically composed of 2-in. nylon or polyester webbing. The belt ends attach to the seat or airframe with a pin joint or an inertia reel / webbing retractor, and are joined together with a metallic buckle on the lap belt.

There are three different methods for modeling these restraint systems:

- A segmented belt model (spring-damper segments)
- An FE model (membrane or truss elements)
- A hybrid model combining segmented belts and finite elements.

The ATB and MADYMO programs offer segmented belt models. The LS-DYNA3D, MADYMO, and MSC/DYTRAN programs have finite elements suitable for restraint modeling. The MADYMO program also has hybrid restraint modeling capability.

THIS DOCUMENT PROVIDED BY THE ABBOTT AEROSPACE
TECHNICAL LIBRARY
ABBOTTAEROSPACE.COM

5.5.1 Segmented Belt Model

The segmented belt (available in ATB and MADYMO) is a simple restraint model represented by linear segments with user-defined non-linear spring-damper characteristics. Initial slack or tension can be assigned to belt segments and the belt ends can be defined as retractors/ pre-tensioners. The belt segments are attached to the occupant at various points. Belt segments allow slip along the length of the belt, but not transversely. The lack of lateral slippage may reduce the accuracy of the simulation and belt loads in some cases. The segmented belt is suitable to simulate occupant restraint and predict tensile loads where there is minimal expected transverse slippage.

The webbing retractor option of the segmented belt model can simulate pay-out, locking, and pre-tension of a production inertia reel or retractor. The MADYMO segmented belt model can be locked based on user-specified sensor signals including vehicle acceleration and belt feed rate. The user must specify the appropriate locking criteria and the force-deflection characteristics of the device being modeled.

5.5.2 Finite-Element (FE) Restraints

A FE restraint offers a more realistic representation by allowing slippage along the length of the belt, as well as in the transverse direction. The model requires the following inputs:

- A discrete mesh of the restraint geometry in the pre-test position
- Material properties appropriate for the magnitude of loads to be applied
- Element properties (cross-sectional area or thickness)
- Boundary conditions (contact interactions, belt connectivity, and support locations)
- Frictional characteristics (static and dynamic coefficients of friction or a friction function).

In MADYMO, the recommended 2-D element for belt webbing is the MEM3NL (plane, constant stress triangular elements with in-plane and no bending stiffness) membrane element with HYSISO material (elastic isotropic material with hysteresis). The recommended 1-D element in MADYMO is the TRUSS2 element (uniaxial with tension and compression stiffness) with HYSISO material definition. For LS-DYNA3D, use the 1-D *ELEMENT_SEATBELT with *MAT_SEATBELT (belt webbing material) and *SECTION_SEATBELT (defines a seatbelt part). The LS-DYNA3D program also has webbing retractor, pre-tensioner, accelerometer, sensor, and slip-ring belt options. In MSC/DYTRAN, use the CROD element with PBELT properties.

It is difficult to manually generate an FE mesh of the belt restraint webbing in contact with the occupant. The FE belt models typically require a pre-simulation analysis to obtain the initial nodal coordinates of the belt positioned on the occupant. For a membrane belt model, the user can create a flat mesh of the belt webbing and position the segments near the target location on the ATD (Figure 5-16). It should use a linear-elastic material with stiffness considerably

higher than the actual belt stiffness. This increased stiffness reduces element distortion during the pre-simulation. The user must define the contact between the belt nodes and the ATD, and lock the joints to prevent the ATD from moving out of the test position.

There are various methods of applying the belt to the occupant in each code. In most FE codes, the user can move the belts into position by specifying a nodal displacement versus time for the belt end nodes. The nodal coordinate output can be extracted from the pre-simulation analysis and used to initialize the positions for the final simulation. Prior to running the impact analysis, the user can replace the pre-simulation material properties with appropriate values,

THIS DOCUMENT PROVIDED BY THE ABBOTT AEROSPACE
TECHNICAL LIBRARY
ABBOTTAEROSPACE.COM

and unlock the ATD joints. In MADYMO, a second method is available. The user can attach belt segments to the end nodes of the belt mesh and apply pre-tensioners to pull the belts into place.

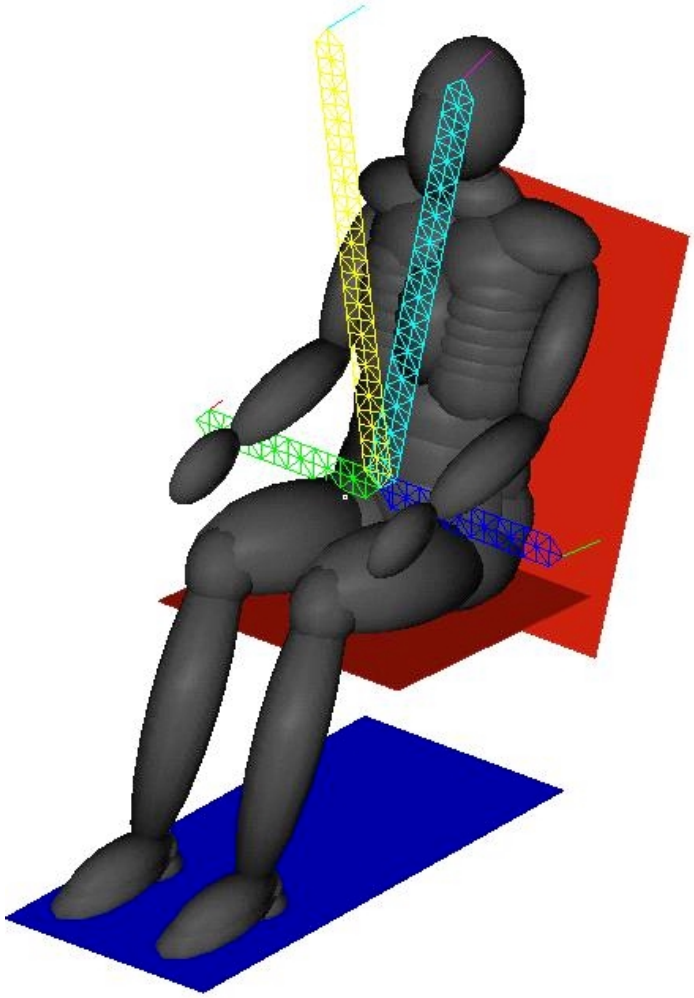


Figure 5-16.
MADYMO four-point restraint before pre-simulation.

5.5.3 Hybrid Belt Model

The MADYMO hybrid belt model is simply a FE belt model combined with segmented belts. The FE part is usually modeled as the portion of the webbing that contacts the occupant. The segmented belts usually connect the end nodes of the FE belt to the airframe or seat (Figure 5-17) and are used to model retractors, pre-tensioners, and slip-rings.

THIS DOCUMENT PROVIDED BY THE ABBOTT AEROSPACE
TECHNICAL LIBRARY
ABBOTTAEROSPACE.COM

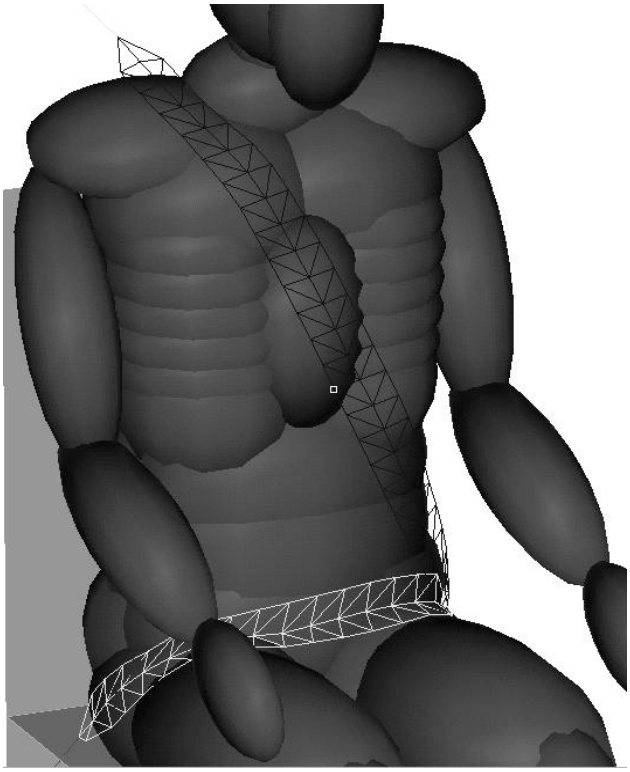


Figure 5-17.
MADYMO hybrid belt after pre-simulation.

5.6 MATERIAL MODELS

The selection and use of appropriate material models is critical to determining the accuracy of the analysis. This section provides some guidance on the selection of material models that have been shown to be effective for the analysis of components that are commonly used in the design of seat and airframe structures. It is important to note that many of the materials described in this section are also used in the design of the airframe and aircraft interior.

It is common practice to initially build the structure using simple material models such as an elastic material model. Simple material models simplify the debugging process and allow the program to execute without introducing additional errors. In addition, the response of simple material models is easier to comprehend, and initial runs using these models can help the analyst determine whether a complex elastic-plastic model is required to improve the accuracy of the analysis.

5.6.1 Metallic Material Models

There are numerous material models, including aluminum and steel, that are associated with aircraft seat metallic structures. The simplest of the metallic material models is the elastic material model. This model describes a linear relationship between the six stress and strain components. Elastic material model input requires only two material constants: Young's modulus E and Poisson's ratio ν. However, most codes will also allow for a failure strain value to be defined. If the material is expected to yield under crash loads, an elasto-plastic model can

THIS DOCUMENT PROVIDED BY THE ABBOTT AEROSPACE
TECHNICAL LIBRARY
ABBOTTAEROSPACE.COM

be used (Figure 5-18). In this case, the material will undergo linear elastic and linear plastic strain (bilinear or piecewise linear). Table 5-3 lists the elastic and elasto-plastic material models for the different codes. These input cards are valid for shell elements and the user should reference the user's manual for the appropriate material card for other element types.

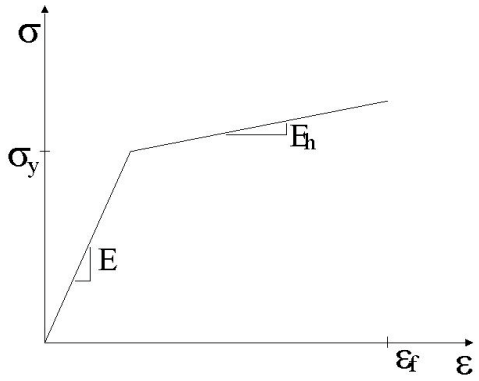


Figure 5-18.
Elasto-plastic material model.

Table 5-3.
Matrix of material models for metallic structures.

Material Model	Analysis Code		
	MSC/DYTRAN	LS-DYNA3D	MADYMO
Elastic	DMATEL	*MAT_ELASTIC	ISOLIN
Elastic-plastic	DMATEP	*MAT_PLASTIC_KINEMATIC	ISOPLA

For some metals, such as mild steel, the material yields at a higher effective stress state at increased strain rates. The strain-rate-sensitive behavior of steel has significant benefits for crashworthiness applications, as it increases the stiffness of the structure under crash loads. The strain-rate hardening law is formulated as:

$$\sigma_d = \sigma_{y_0} g\left(\dot{\varepsilon}\right) + \sigma_{y_1}\left(\varepsilon_p\right)$$

where σ_{y_0} is the initial yield stress, g the strain-rate dependency function, and ε_p is the effective plastic strain. The strain-rate dependency function is treated using the Cowper-Symonds strain-rate empirical function:

$$g\left(\dot{\varepsilon}\right) = 1 + \left(\frac{\dot{\varepsilon}}{c_1}\right)^{\frac{1}{c_2}}$$

where C_1 and C_2 are strain-rate enhancement coefficients. In MSC/DYTRAN, the rate effects are modeled using the DYMAT24 material card. An example input card for 4130 steel (in English units) is shown in Figure 5-19, where the C_1 and C_2 strain rate enhancement coefficients are 40.4 and 5.0, respectively.

THIS DOCUMENT PROVIDED BY THE ABBOTT AEROSPACE
TECHNICAL LIBRARY
ABBOTTAEROSPACE.COM


```
$ -------- Material 4130_steel_solid id =7
DYMAT24         7 .000741 2.9e+07     .32
+A000509
+A000510   75000             0.37    40.4      5.0                          +
+                            DYNA
```

Figure 5-19.
Example MSC/DYTRAN input for strain-rate material.

The rate effects can also be modeled using the MAT_PLASCTIC_KINEMATIC material input card in LS-DYNA3D where the SRC and SRP input card represents the C_1 and C_2 strain-rate enhancement coefficients. An example input deck is provided in Figure 5-20.

```
*MAT_PLASTIC_KINEMATIC
$    MID      RO       E      PR     SIGY     ETAN     BETA
       2 0.000741    2.9+7    0.32    75000   176000        0
$    SRC      SRP       FS
        40.4          5.0          .37
```

Figure 5-20.
Example LS-DYNA3D input for strain-rate material.

In MADYMO, the strain-rate effects for steel can be modeled using the ISOPLA material card. An example input format (in SI units) is shown in Figure 5-21.

```
MATERIALS
*   CollectorName>> 4130N steel
TYPE   ISOPLA
E   2.000E+11
DENSITY   7915
YIELD STR  5.172E+08
RATE DEP  COWPER
DRATE  40.4
PRATE  5.0
```

Figure 5-21.
Example MADYMO input for strain-rate material.

5.6.2 Composite Material Models

Laminated fiber-matrix materials such as fiberglass-epoxy are frequently used in aircraft seats, glareshields, side ledges, cabinets, and tables. Laminated structures with or without a core can be modeled using a shell element mesh. Finite-element codes such as LS-DYNA3D, MSC/DYTRAN, PAMCRASH®, and MADYMO typically include material models for composites.

® PAMCRASH is a registered trademark of ESI Group

THIS DOCUMENT PROVIDED BY THE ABBOTT AEROSPACE
TECHNICAL LIBRARY
ABBOTTAEROSPACE.COM

Techniques for modeling composite structures in LS-DYNA3D are described in the following sections. For information on modeling composite structures in other codes, please refer to the respective user's manuals.

In LS-DYNA3D, there are several options for modeling layered composites with shell elements. The simplest and least general is to use the BETA option of *Section_Shell to define the material direction for each integration point through the element thickness (Figure 5-22). A user-defined integration rule should also be used to control the layer thickness (see IRID of *section_shell, and integration_shell). If a composite is made up of layers of different materials, a more general composite can be modeled by specifying a different part ID for each integration point (see *integration_shell). Each part can refer to a different material model with the restriction that all materials must be of the same type.

For example, you could specify an element with one layer of Material Type 2 using Ea=10, Eb=1, and another layer of Material Type 2 with Ea=3, Eb=3, where Ea and Eb are the Young's modulus in the 'a' and 'b' directions. This method allows different material constants to be used in the different layers, but still does not allow complete general mixing of material types in a single shell element.

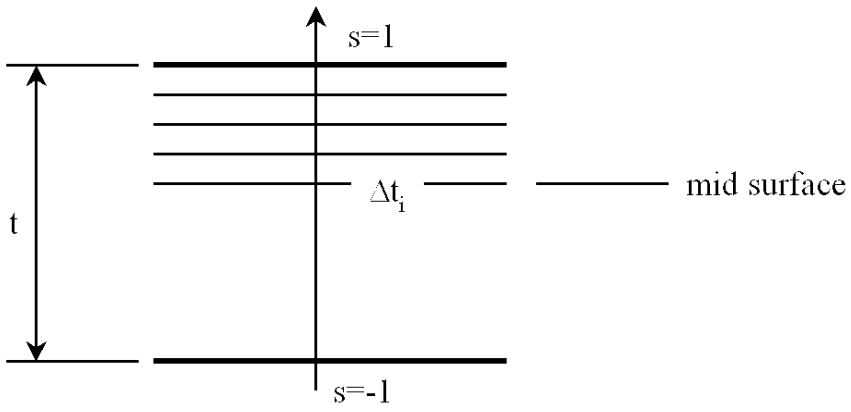


Figure 5-22.
User-defined shell integration points.

Composites with multiple materials can be modeled by defining one element for each material type in the composite. The elements should all be given a thickness equal to the total composite thickness and should all share the same nodes, so they would appear to all lie in the same space when viewed in a pre-processor or post-processor. However, in order to obtain the correct membrane and bending stiffness for the whole composite element, the user should define a separate integration rule for each element in the composite with appropriate weights and through thickness locations.

The following example defines the integration rules for a sandwich-type composite with one material in the middle and another on the top and bottom surfaces. Two integration points could be assigned to the middle material with weight and thickness coordinates of:

Wf1 = 0.25, S1 = -0.25

Wf2 = 0.25, S2 = +0.25

This Document Provided by the Abbott Aerospace
TECHNICAL LIBRARY
ABBOTTAEROSPACE.COM

The surface material could have two integration points with weight and thickness coordinates of:

Wf1 = 0.25, S1 = -0.75

Wf2 = 0.25, S2 = +0.75

In this example, Wf1 is the weight factor for Integration Point 1, and S1 is the thickness direction coordinate of Integration Point 1. The correct stiffness is achieved as long as the total weight of all elements is equal to one. The thickness coordinates are defined such that the integration points are at the middle center of each layer. Theoretically, this method seems feasible. However, LS-DYNA has built-in protection to prevent the input of weights that do not add up to one. If the user attempts to perform the example, LS-DYNA will convert the weights at all integration points to 0.5 so that they add up to one for each element. Fortunately, there is a way to work around this protection. This is accomplished by reducing the thickness of the elements so that the correct membrane stiffness is achieved for each material. In other words, each element should have a thickness equal to the actual summed thickness of layers of that material.

In the example, the element thickness of both elements should be reduced to 1/2 of the total composite thickness. To achieve the correct bending stiffness for the composite, the thickness coordinates for each integration point should be increased accordingly. In the example, since each element has been reduced to half the composite thickness, the thickness coordinates should be doubled, as shown below.

Middle Material: S1=-0.5, S2=+0.5

Surface Material: S1=-1.5, S2=+1.5

Notice that this violates the usual restriction that the thickness coordinates should be in the range of -1 to +1. However, since LS-DYNA does not enforce this rule, the process works.

In this simple example, each of the four material layers has a thickness of 1/4 of the total element thickness. However, there is absolutely no restriction on the number of layers, the thickness of the layers, or the material of the layers using this method. The only rules that should be followed to achieve correct stiffness of the overall composite element are:

1. The sum of the individual element thicknesses should equal the total composite thickness.
2. The thickness coordinates for each integration point should be multiplied by the total composite thickness and divided by the corresponding element thickness.

If the multi-element method is used, care should be taken if the composite is to be checked for contact. Only one of the elements making up the composite should be checked for contact, since all elements share the same nodes. However, the element thickness will be less than the composite thickness, so it may be desirable to directly prescribe the thickness for contact (see SST,MST on *contact) if using a contact type where element thickness is taken into account.

5.6.3 Seat Cushion Foam Material Models

The design of a seat model requires the selection of an appropriate foam material model to represent the seat cushion. This selection is critical toward obtaining an accurate prediction of the lumbar spinal load. Foam models are typically formulated for a particular type of foam behavior. For instance, LS-DYNA3D has different material models for commonly used aircraft

This Document Provided by the Abbott Aerospace
TECHNICAL LIBRARY
ABBOTTAEROSPACE.COM

seat cushion foams such as DAX (polyurethane) and Confor. Other codes, including MADYMO, rely on the user to obtain the specific load-versus-deflection response of the foam from a component-level test as input data for the foam material model.

For example, in MSC/DYTRAN, the seat cushion can be effectively modeled using the FOAM1 material model. The model assumes a crushable material where the Poisson's ratio is effectively zero. The yield behavior of the foam is determined by a stress-strain or crush-strain curve, typically obtained through a uni-axial compression test.

Dynamic crush-stress input data for the FOAM1 material model can be obtained by conducting a high-velocity impact test (Reference 5-13). As illustrated in Figure 5-23, this impact test captures the dynamic response of the seat cushion material. In cases where the foam is not as sensitive to the rate of loading, a comparable static test (Reference 5-13) is sufficient to capture the response of the foam.

Example: An impact test was conducted on HR polyethylene foam of a thickness and build-up that represents the actual seat cushion design. A leather fabric was sewn over the foam to represent the seat cover. A 51-lb/min impactor was dropped on the foam sample at a velocity of 10 ft/sec to obtain the "bottom-out" response of the seat cushion. The data recorded during the test revealed that the stress in the material increases as a function of the percent of crush (Figure 5-24).

Since the MSC/DYTRAN FOAM1 material model does not incorporate hysteresis effects, only the loading function was used for the analysis. The corresponding FOAM1 input deck is shown in Figure 5-25.

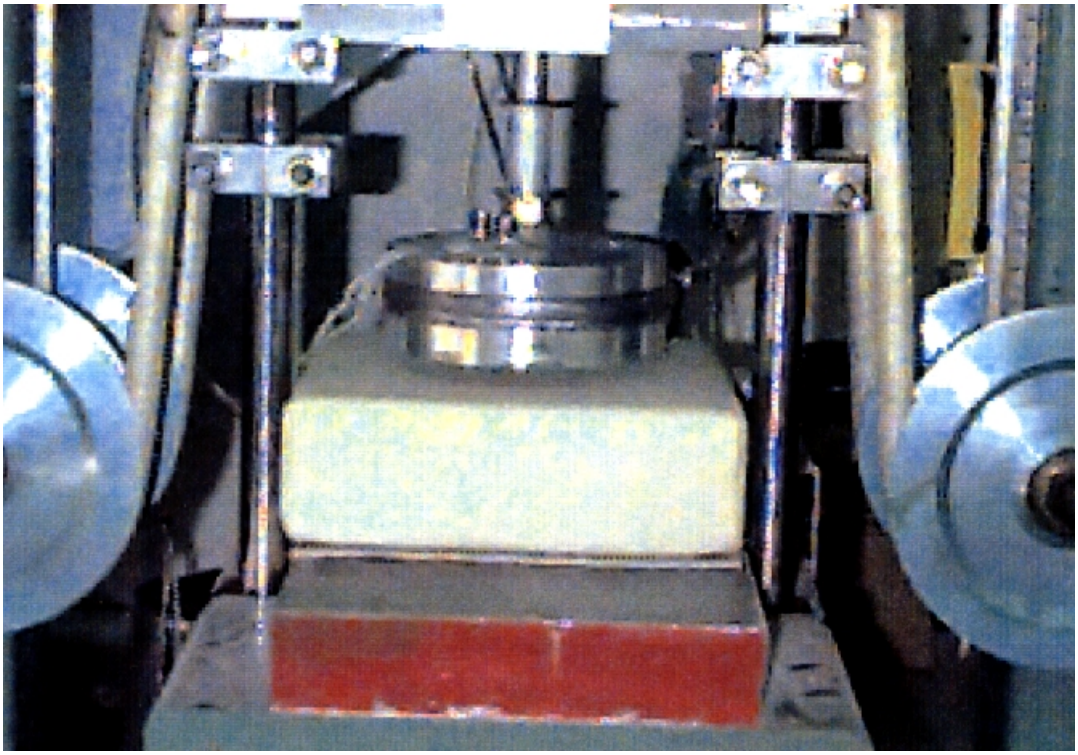


Figure 5-23.
A foam impact test.

THIS DOCUMENT PROVIDED BY THE ABBOTT AEROSPACE
TECHNICAL LIBRARY
ABBOTTAEROSPACE.COM

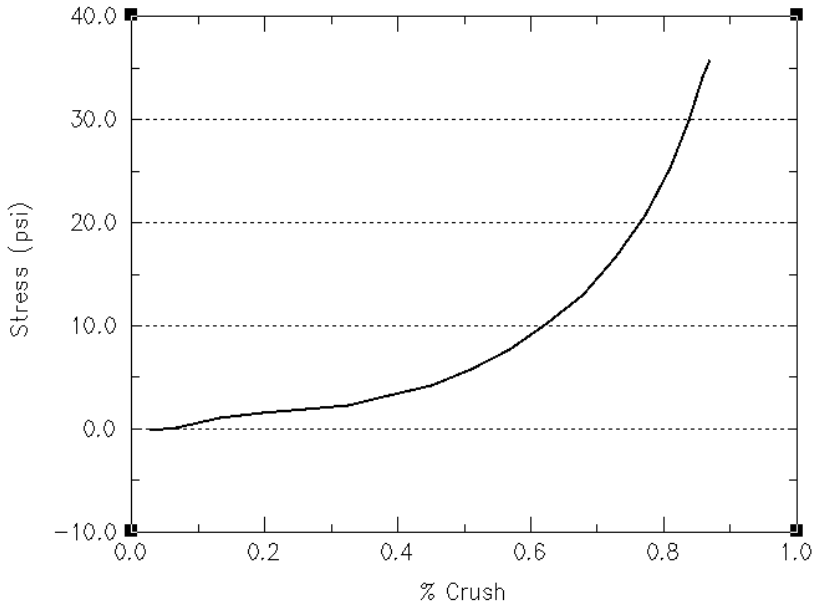


Figure 5-24.
An example of foam data showing stress as a function of the percent of crush.

```
$ -------- Material foam id =11 HR 10/30
FOAM1          11 3.33e-6           75.00       6    CRUSH                  +
+                           DYNA  1.6    0.1
$ dynamic test data HR10 with 12"x12" leather cover
TABLED1         6                                                           +
+,.0,.0,.067646,0.109,.132487,1.051,.187033,1.540,+
+,.261175,1.901,.324763,2.221,.387647,3.204,.449529,4.253,+
+,.510053,5.765,.568779,7.747,.625082,10.20,.678216,12.99,+
+,.727285,16.58,.771185,20.79,.808633,25.34,.838227,29.96,+
+,.858571,34.07,.868466,35.84,ENDT
```

Figure 5-25.
Example of a FOAM1 material model.

5.7 APPLYING BOUNDARY CONDITIONS

Multi-body and FE modeling requires the application of various boundary conditions. Boundary conditions are defined in the form of kinematic constraints and contact interactions.

5.7.1 Kinematic Constraints

Kinematic constraints consist of single- (SPC) or multi-point constraints (MPC). In theory, kinematic constraints constitute the release or removal of a particular degree of freedom. For MPC's, the motion of a dependent degree of freedom is expressed as a linear combination of one or more independent degrees of freedom. In practical terms, they are used to attach a structure to the ground, to apply symmetric boundary conditions, to remove degrees of freedom that are not used in structural analysis, or to attach structures together. The SPC's and MPC's used in dynamic analysis are applied in the same manner as in static FE analysis.

THIS DOCUMENT PROVIDED BY THE ABBOTT AEROSPACE
TECHNICAL LIBRARY
ABBOTTAEROSPACE.COM

A particularly effective constraint tool is the MSC/DYTRAN RCONN (equivalent to SPOT WELD in MADYMO) capability. The RCONN tool is used to connect different parts of the mesh together without having to coincident adjacent nodes. The desired effect is to simulate welded structures. An example application of RCONN is shown in Figure 5-26. In Figure 5-26a, the gusset and the seat frame FE mesh were modeled in separate groups and are tied together using the RCONN card to simulate a welded structure.

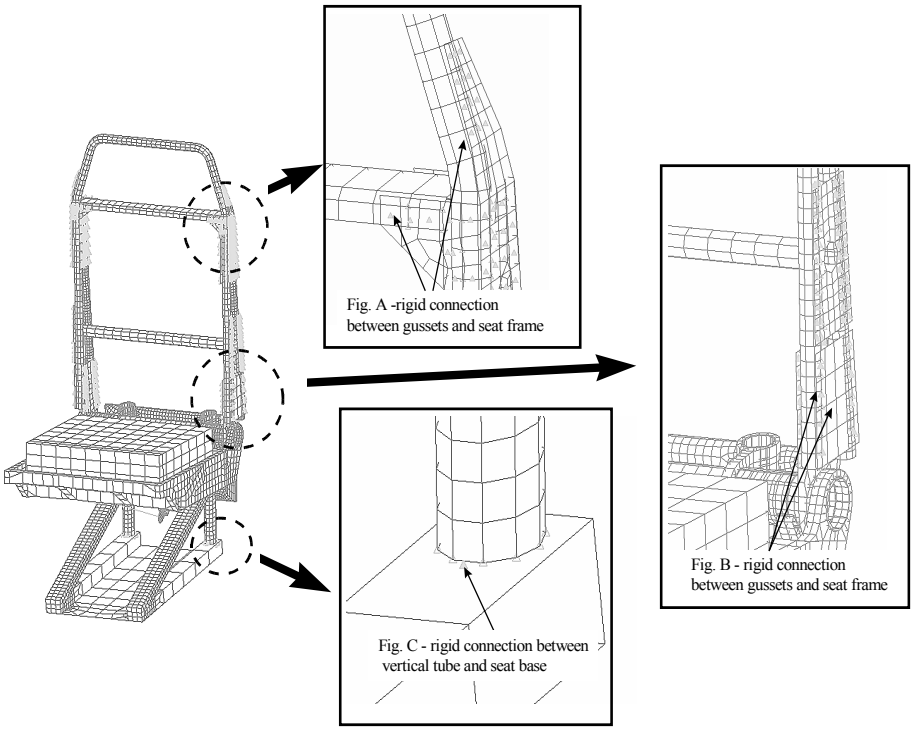


Figure 5-26.
Rigid connections in MSC/DYTRAN using the RCONN tool.

In MSC/DYTRAN, the RCONN input card structure is similar to the CONTACT card. The user specifies a set of slave nodes that will be tied to a master surface. The user also defines a monitoring distance such that nodes with distance larger than the specified range will not be included in the connection. An example input deck is shown in Figure 5-27. The slave nodes of the web (defined in the SET1 entry) are connected rigidly to the master surface of the tube structure (defined in the SURFACE entry). The monitoring distance was set at 0.020 in.

5.7.2 Contact Interactions

Contacts are defined to evaluate the interactions between the components of the structure in the model. To correctly define the contact interactions for the model, the user should understand the assumptions of the contact algorithms used in the analysis code. Detailed information regarding contact algorithms will not be included in this chapter. To learn more about the specific algorithms that are utilized by each software program, the user is referred to the user manuals and/or theory manuals for each type of software.

THIS DOCUMENT PROVIDED BY THE ABBOTT AEROSPACE
TECHNICAL LIBRARY
ABBOTTAEROSPACE.COM


```
$--------- web-tube weld
RCONN          26     GRID     SURF        1        2   NORMAL                  +A000073
+A000073                                                                        +A000074
+A000074       NODISTANCE     .020
$
$ Slave contact surface for web-tube
$
SET1           1     1402     1405     1411     1414     1420     1423
$
$ Master contact surface for web-tube
$
SURFACE        2              SEG        2
CFACE          1        2     772        1
CFACE          2        2     773        1
CFACE          3        2     774        1
```

Figure 5-27.
An example RCONN input deck.

Surface-to-Surface and Surface-to-Nodes are the two most commonly used contact algorithms. Surface-to-Surface contact definitions are used where shell elements are anticipated to contact each other. Surface-to-Nodes contact is defined where the elements form a T-joint between surfaces. Examples of contact applications are shown in Figure 5-28.

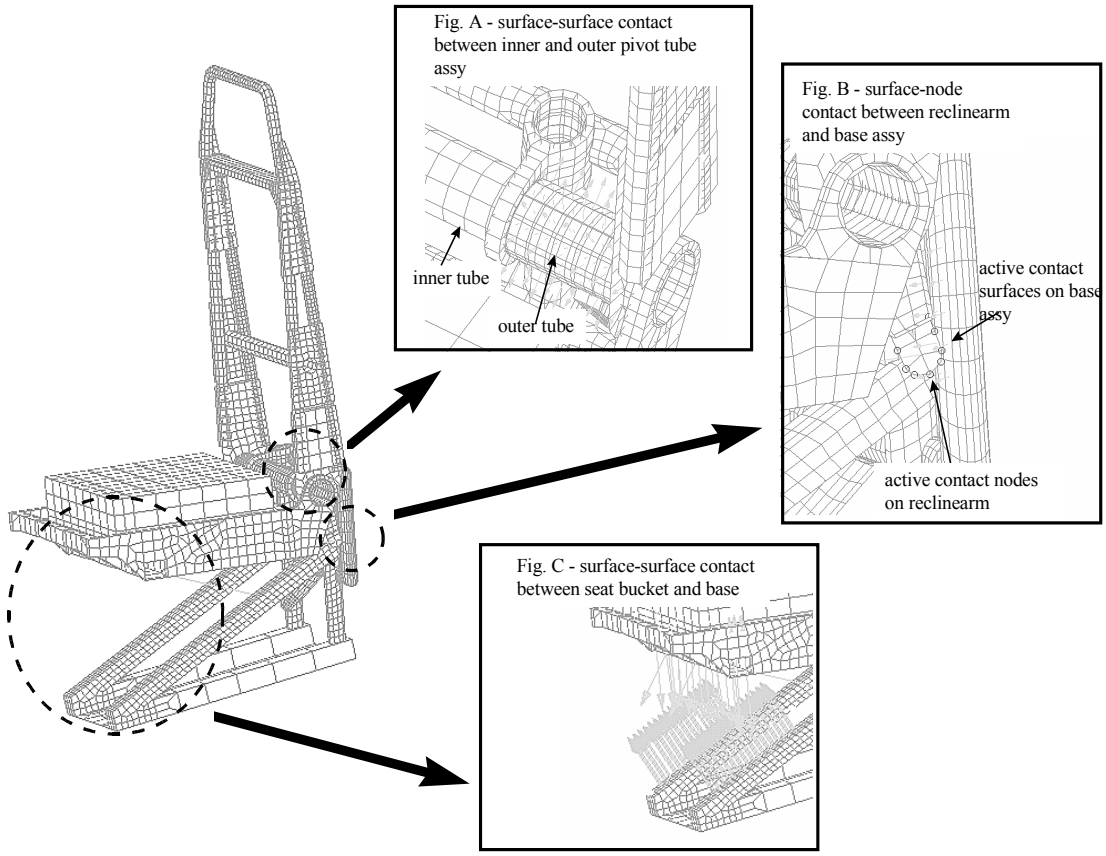


Figure 5-28.
Contact applications in a seat model.

THIS DOCUMENT PROVIDED BY THE ABBOTT AEROSPACE
TECHNICAL LIBRARY
ABBOTTAEROSPACE.COM

Contact interactions are usually formulated by defining master and slave contact entity sets (i.e., nodes, elements, and/or rigid bodies). The general rule of thumb is to define the coarse mesh as the master surface and the finer mesh as the slave surface. If the mesh densities are similar, the slave surface should be the surface with the softer underlying material. It is also recommended to use first-order elements for those parts of the model that will form a slave surface. Contact interactions are further defined by a variety of other parameters including static and dynamic friction, contact surface direction, search radius, damping parameters, contact stiffness, and contact start/stop time.

Initial penetration can be a problem in cases where FE membrane mesh is applied to a multi-body occupant. For example, in an occupant/belt model, it is common for the belt model to have a few nodes that lie just below the surface of the occupant "skin." This produces the initial penetration between the belt model and the occupant. Most contact algorithms calculate the contact force vector between the FE mesh and the multi-body occupant based on the restoration force required to move an intersecting slave node to the surface of the master entity. Without some method of compensation, the penetrated nodes will create enormous contact restoration forces, resulting in numerical instability. To correct this, some codes can detect penetration of master and slave contact entities at the start of the simulation by activating the penetration check option in the contact definition card. The code will adjust the violating node(s) or offset the initial contact forces to equilibrium.

Since the contact search process is computationally expensive, the user should attempt to minimize the entities included in the contact model. Predicting the kinematics of the simulation and estimating contact points can help to choose the appropriate contact entities. For example, consider simulating a pilot seat dynamic impact test. It is possible that the pilot's head may impact the instrument panel during the crash scenario. To define the occupant-instrument-panel contact interaction, the user should select only those areas of the instrument panel mesh that have the potential to come into contact with the occupant's head during the crash. After a simulation is run and the occupant-instrument-panel interactions have been observed, the contact interactions can be adjusted as necessary to achieve the proper response.

5.7.2.1 Defining Contacts within MSC/DYTRAN

An example MSC/DYTRAN surface-to-surface contact input deck is shown in Figure 5-29. The deck defines the contact interactions between the inner and outer pivot assembly shown in Figure 5-28a.

The contact specifies that the outer tube slave surface (defined by SURFACE 73) should be checked for contact with the inner tube master surface (defined by SURFACE 74). The outer tube is designated as the slave surface because it has a finer mesh in comparison to the inner tube. The value of the static and dynamic coefficient is 0.3. The contact employs a Version 4 algorithm (V4 input), which simultaneously tracks multiple contacts per slave node. By specifying BOTH in the contact card, slave nodes are checked for penetration on both sides of the master element, regardless of the direction of the normal vector on the master surface.

THIS DOCUMENT PROVIDED BY THE ABBOTT AEROSPACE
TECHNICAL LIBRARY
ABBOTTAEROSPACE.COM


```
$ -------- Contact : inner to outer pivot assembly
CONTACT      299     SURF     SURF       73       74       .3       .3       .1+A000644
+A000644      V4     BOTH                        1.0                          +A000645
+A000645                                                  0.1                 +A000646
+A000646                                 ON
$  Slave elements
SURFACE       73               SEG       73
CFACE       2163       73     5493         1
CFACE       2164       73     5494         1
.
.
CFACE       2171       73     9333         1
$ Master elements
SURFACE       74               SEG       74
CFACE       3252       74     5402         1
CFACE       3253       74     5403         1
.
.
CFACE       3271       74     5441         1
```

Figure 5-29.
MSC/DYTRAN surface contact definition.

5.7.2.2 Defining Contacts within MADYMO

Contact interactions in MADYMO can be defined between multi-body elements, as well as between FE meshes and multi-body elements. They are defined via the CONTACT INTERACTIONS card. An elastic contact algorithm is used for multi-body contacts where the contact characteristics are user-defined and the resultant contact force is a function of penetration depth. A kinematic contact algorithm is used for FE-to-multi-body contact scenarios. The contact force is calculated based on the relative velocity of the node and the contact surface. In most cases, contact characteristics are obtained from component tests and are specified in terms of force versus deflection.

Figures 5-30 and 5-31 illustrate an example of the contacts that are defined between a glareshield and an occupant's head. The occupant's head (system 1, body 6) and the glareshield (system 6, body 2) are modeled as ellipsoids. As shown in Figure 5-31, the ELLIPSOID-ELLIPSOID card is used, and the stiffness characteristic of the glareshield is defined in the FUNCTIONS card.

5.8 LOAD APPLICATION

There are two methods to simulate crash loads in a model.

Method One: Prescribe an initial velocity (or a velocity prior to impact) to the seat and the occupant and apply deceleration to the sled. This method simulates the physical impact event as experienced by the occupant.

Method Two: Apply the acceleration field to the occupant while maintaining the sled/seat as a stationary frame of reference. This method is an approximation of the impact event, because it assumes that the acceleration measured by the sled is the same that is experienced by the occupant. The crash loads are applied in reverse of the actual physical event by applying an acceleration pulse to the occupant, instead of a deceleration pulse to the seat. This allows the occupant to decelerate on his/her own. This method is acceptable only when the inertial effects

THIS DOCUMENT PROVIDED BY THE ABBOTT AEROSPACE
TECHNICAL LIBRARY
ABBOTTAEROSPACE.COM

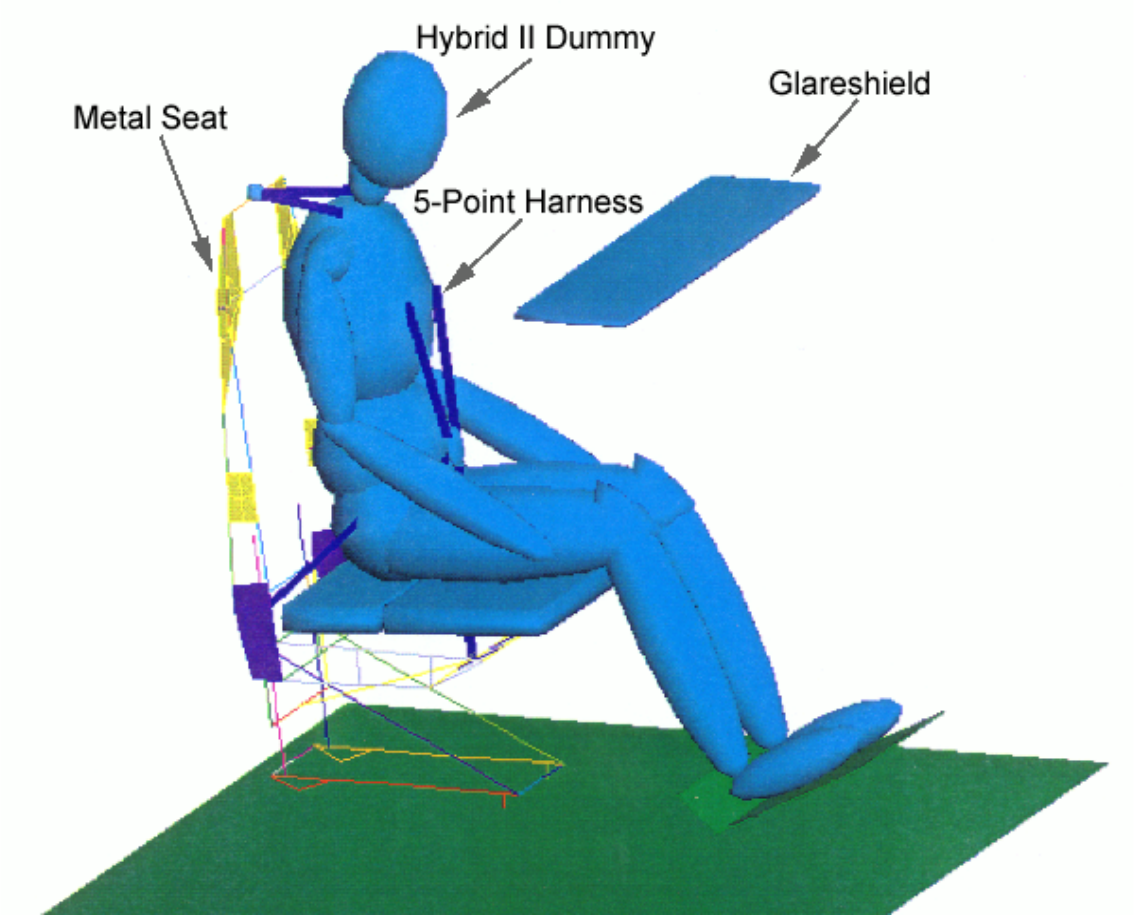


Figure 5-30.
MADYMO multi-body contact model.

```
CONTACT INTERACTIONS
ELLIPSOID-ELLIPSOID
! contact between glareshield and dummy's head
  6  2  1  6  4  -5  0  -1E+06  0.00000 0.00000  0.30000
END ELLIPSOID-ELLIPSOID
FUNCTIONS
! glareshield load-deflection curve
  27
  0.0000  0.0000
  0.0001  163.8842
  0.0030  326.5717
  .
.
  0.0267  1873.9352
END FUNCTIONS
END CONTACT INTERACTIONS
```

Figure 5-31.
Multi-body contact definition.

This Document Provided by the Abbott Aerospace
TECHNICAL LIBRARY
ABBOTTAEROSPACE.COM

of the seat are negligible in the direction of the applied load. The advantage of applying the acceleration field to the occupant is that it allows for the simulation of the 1 G pre-load, which is critical in predicting spine loads. Using this method, the impact acceleration can be offset by a certain amount of time to allow for the occupant to sink into the seat cushion. Example applications of each of these methods are provided in the following sections and are based on the certification of aircraft seats via FAR 23.562.

5.8.1 Load Application for 60-deg Pitch Test using MSC/DYTRAN

To accurately simulate the crash pulse for the FAR 23.562 60-deg pitch test, two sets of loads are required:

1. A 1-G gravity load in the -Z direction (down) applied to the seat and occupant.
2. The crash load simulating the 60-deg pitch condition.

Using Method 2, the crash-acceleration profile used in the simulation can be done in the form of an idealized triangular pulse per FAR 23.562, or from actual test data. As an example, Figures 5-32, 5-34, and 5-35 demonstrate the how to apply a crash pulse within a MSC/DYTRAN model. An acceleration field is applied to the occupant while maintaining the sled/seat as a stationary frame of reference. The 1-G gravity load is applied to the occupant via CARD A3 in the *ain data deck (Figure 5-32). The crash pulse is applied to the ATB occupant by means of the MSC/DYTRAN ATBACC and TLOAD card (Figure 5-33). The 60-deg vector is defined in the ATBACC card by using a load factor of (-0.5, 0.0, 0.866) in the (X,Y,Z) direction consistent with the direction of the occupant coordinate system. The crash pulse has an offset of 150 msec from time zero to allow for adequate 1-G cushion pre-loading (Figure 5-34).

```
SITTING HYBRID II DUMMY (50%) GENERATED WITH GEBOD                    CARD A1B
AGATE SLED TEST                                                       CARD A1
IN. LB.SEC.          0.0          0.0     -386.088      386.088       CARD A3
```

Figure 5-32.
ATB 1-G load application pitch test data.

```
$Crash Pulse
ATBACC,201,,386.04,-.5,0.0,-.866,,,+
+,LT,MT,UT,N,H,RUL,RLL,RF,+
+,LUL,LLL,LF,RUA,RLA,LUA,LLA
$
TLOAD1,13,201,,,1000
TABLED1,1000,,,,,,,,+
$ ACCELERATION WITH 0.15 SEC 1 G LOAD
+,0.0,0.0,0.150,0.0,0.16,4.92633,0.165,7.11431,+
+,0.17,10.4175,0.175,13.2985,0.18,14.6757,0.185,15.0433,+
+,0.19,16.9036,0.195,18.296,0.20,18.8951,0.205,19.0857,+
+,0.21,18.2143,0.215,17.4943,0.22,15.7737,0.225,15.8078,+
+,0.23,15.434,0.235,12.5829,0.24,5.92312,0.245,0.26516,+
+,0.25,-1.39478,0.255,0.0,0.35,0.0
$
```

Figure 5-33.
MSC/DYTRAN load application pitch test data.

THIS DOCUMENT PROVIDED BY THE ABBOTT AEROSPACE
TECHNICAL LIBRARY
ABBOTTAEROSPACE.COM

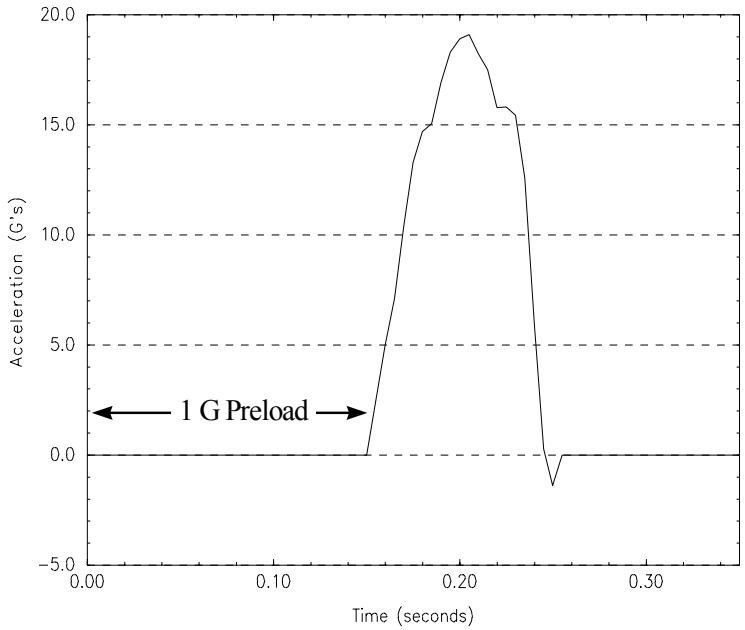


Figure 5-34.
Test 1 applied loads.

5.8.2 Load Application for 10-deg Yaw Test Using MSC/DYTRAN

To accurately simulate the crash pulse for the FAR 23.562 10-deg yaw test, two sets of loads are required:

1. A 1-G gravity load in the -Z direction (down) applied to the seat and occupant.
2. The crash load simulating the 10-deg yaw condition.

Using Method 1, the crash-acceleration profile used in the simulation can be done in the form of an idealized triangular pulse per FAR 23.562 or from actual test data. As an example, Figures 5-35 and 5-36 demonstrate how to apply a crash pulse within a MSC/DYTRAN model using Method 1. A 1-G gravity load is applied in the -Z direction. The 1-G load is applied to the seat via the MSC/DYTRAN TLOAD1 and GRAV card. The crash scenario is simulated by prescribing an initial velocity to all elements in the model prior to impact, and applying a deceleration field to the sled.

The ATB initial velocity is prescribed in the ATB input deck using the G2 card. All other MSC/DYTRAN elements receive the initial velocity definition through the TICGP card. Both ATB and MSC/DYTRAN initial velocities are defined at a vector of 10 deg from the horizontal plane to simulate the yaw condition. The sled is decelerated by prescribing a velocity profile (Figure 5-35) to all of the elements of the sled using the TLOAD1 and FORCE cards.

THIS DOCUMENT PROVIDED BY THE ABBOTT AEROSPACE
TECHNICAL LIBRARY
ABBOTTAEROSPACE.COM

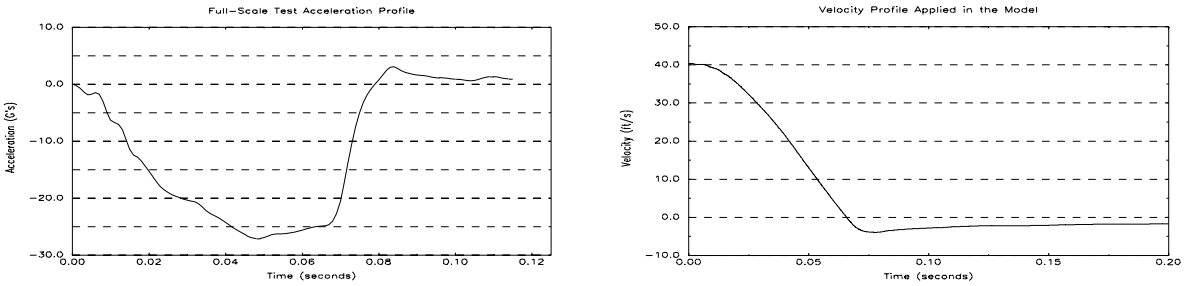


Figure 5-35.
Test 2 applied loads.

The data deck in Figure 5-36 shows the FE nodes (specified by SET1 and TICGP card) and ATB (the last three entries of the G2 card) have initial velocities of (-476.9,84.09,0.0) in./sec. This translates to a resultant impact velocity of 484.2 in./sec (40.35 ft/sec). The TLOAD1 card then prescribes a velocity change for the sled (elements 12020 through 44479 defined in the FORCE card), as specified in TABLE1 card profile.

```
$ATB Input Deck: Initial velocity definition
  -117.523      0.00  -27.9607    -476.9     84.07      0.00            CARD G2
$_____________________________________________________________________________
$MSC-DYTRAN Input Deck: Initial velocity & prescribed motion definition
$ ------- GRAVITATION -----
$1 G Load applied to the seat
TLOAD1         13     444               0
GRAV          444           32.17       0       0    -1.0
$ ------- Initial Velocity BC initial velocity entire model -----
TICGP          13     200    XVEL  -476.9    YVEL   84.09
$
SET1          200       1    THRU    2548    2550    THRU    4413    4421+A000652
+A000652    THRU    4509    4515    THRU    8026    8139    THRU    8538+A000653
+A000653    9000    THRU    9135   12020    THRU   13102   14500   14501+A000654
$ ========= PRESCRIBED SLED MOTION ==========
$ Apply prescribed velocity profile to rigid elements that respresents the sled
TLOAD1         13     294               2      90
FORCE         294   12020       0       1  -.9848   .1736       0
FORCE         294   12024       0       1  -.9848   .1736       0
.
.
FORCE         294   44479       0       1  -.9848   .1736       0
$ Pulse from crash test
$     ------- TABLE 90: velocity_table -------
TABLED1        90                                                    +A000658
+A000658        0   484.3    .004   483.3    .005   481.6    .007   480.8+A000659
+A000659     .009     480   .0094   478.7   .0098   477.1     .01   476.3+A000660
+A000660   .0105   474.5    .011     473   .0115   471.8   .0125   469.7+A000661
+A000661   .0135   467.7   .0145   464.4    .015   461.7     .02   435.5+A000662
+A000662     .03   363.7     .04   278.4     .05   177.3    .055   126.3+A000663
+A000663     .06    75.9    .065    27.3    .067     8.3   .0678     .76+A000664
+A000664     .15       0    ENDT
```

Figure 5-36.
MSC/DYTRAN load application yaw test data.

THIS DOCUMENT PROVIDED BY THE ABBOTT AEROSPACE
TECHNICAL LIBRARY
ABBOTTAEROSPACE.COM

5.9 FLOOR DEFORMATION

The specific method for simulating floor deformation is code-dependent. In MADYMO, floor deformation is produced by enforcing a prescribed displacement. In MSC/DYTRAN, floor deformation is simulated by prescribing a time-dependent velocity profile to the nodes corresponding to the location of the seat's feet attachment points. Integration of the velocity profile will yield the required displacement of the seat legs' nodes, which will then create a pre-stress on the seat. In either case, the enforced motion in the transient analysis can result in numerical instability if it is incorrectly executed.

5.9.1 Example Floor Deformation Simulation using MADYMO

In an occupant/seat model, floor deformation can be modeled by attaching a null system(s) to the seat leg fittings. The null system is used to model a system of a body with known motion relative to inertial space. Each null system, attached to the inboard or outboard seat leg, is prescribed the 10-deg pitch and 10-deg roll motions corresponding to actual test requirements. Typically, floor deformation simulation has to be performed for a minimum duration of 200 msec to avoid numerical instability. An example input deck illustrating floor deformation using null systems is shown in Figure 5-37.

```
NULL SYSTEM
INBOARD FWD LEG PITCH DOWN
MOTION
POSITION
0.0 0.05 -0.2286 -.05
0.01 0.055 -0.2286 -.10
0.35 0.055 -0.2286 -.10
END POSITION
END NULL SYSTEM
NULL SYSTEM
OUTBOARD FWD LEG ROLL OUT
MOTION
POSITION
0.0 0.05 -0.4445 -.05
0.01 0.05 -0.47 -.04
0.35 0.05 -0.47 -.04
END POSITION
END NULL SYSTEM
NULL SYSTEM
OUTBOARD AFT LEG ROLL OUT
MOTION
POSITION
0.0 0.05 -0.4445 -.05
0.01 0.05 -0.47 -.04
0.35 0.05 -0.47 -.04
END POSITION
END NULL SYSTEM
! constrain inboard fwd leg nodes to null system 1- pitch down
   NUMBER                6
   NULL SYSTEM           1
   DOF                   ALL
   SET                   82
! constrain outboard fwd and aft leg nodes to null system 2 roll out
   NUMBER                7
   NULL SYSTEM           3
   DOF                   ALL
   SET                   62
```

Figure 5-37.
Floor deformation data using MADYMO.

THIS DOCUMENT PROVIDED BY THE ABBOTT AEROSPACE
TECHNICAL LIBRARY
ABBOTTAEROSPACE.COM

5.9.2 Example of Floor Deformation Simulation Using MSC/DYTRAN

In MSC/DYTRAN, the floor deformation requirements can be simulated using a combination of the TLOAD1 and FORCE3 card. An example input deck is shown in Figure 5-38.

To define a rotation axis for each seat leg, a coordinate system is specified for each inboard and outboard seat rail via the COOR1C card. The TLOAD1 card then specifies the nodes, which are defined in the FORCE3 cards, to rotate in accordance with the COOR1C rotation definition and the velocity change function in the TABLE1 card. Figure 5-39 shows a seat with floor-deformation simulation using the technique described above.

```
$=========================================================================
$ ========= FLOOR DEFORMATION: 10 DEGREES PITCH & ROLL ==========
$=========================================================================
$
$  Inboard leg rotation coord system
CORD1C          1     368     346      54
$  Outboard leg rotation coord system
CORD1C          2     346      54      80
$
$ 10 deg. Pitch down on inboard seat leg
TLOAD1          1     995               2     995
FORCE3        995      80        1  5.8178              1.       0.
FORCE3        995     323        1  5.8178              1.       0.
FORCE3        995     366        1  5.8178              1.       0.
.
.
.
FORCE3        995     104        1  5.8178              1.       0.
TABLED1       995                                                    +
+             0.0     0.0    0.02     1.0    0.03     1.0    0.05     0.0+
+             1.0     0.0    ENDT
$
$ 10 deg. Outbd roll outboard seat leg
TLOAD1          1     996               2     996
FORCE3        996     332        2  5.8178             -1.
FORCE3        996     344        2  5.8178             -1.
.
.
FORCE3        996      78        2  5.8178             -1.
TABLED1       996                                                    +
+             0.0     0.0    0.02     1.0    0.03     1.0    0.05     0.0+
+             1.0     0.0    ENDT
```

Figure 5-38.
Floor deformation data using MSC/DYTRAN.

This Document Provided by the Abbott Aerospace
TECHNICAL LIBRARY
ABBOTTAEROSPACE.COM

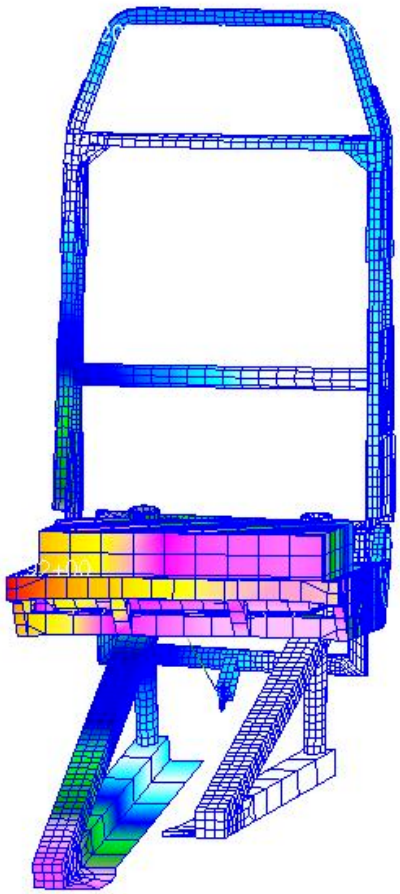


Figure 5-39.
Floor deformation data using MADYMO.

THIS DOCUMENT PROVIDED BY THE ABBOTT AEROSPACE
TECHNICAL LIBRARY
ABBOTTAEROSPACE.COM

References

5-1. Lim, T., “Methodology for Seat Design and Certification by Analysis,” Report No. C-GEN-341-1, prepared for NASA Langley Research Center, Cessna Aircraft Company, date for release - September 30, 2006.

5-2. MSC/DYTRAN User’s Manual Version 4.7, The MacNeal-Schwendler Corporation, 1999.

5-3. MADYMO User’s Manual 3D Version 5.4, TNO-MADYMO, 1999.

5-4. MADYMO Theory Manual 3D Version 5.4, TNO-MADYMO, 1999.

5-5. SAE J211, "Instrumentation for Impact Test", SAE Recommended Practice.

5-6. 49 CFR Part 572, Subpart B, ATD.

5-7. Articulated Total Body Version V.1 User’s Manual, U.S. Air Force Research Laboratory, 1998.

5-8. Cessna Aircraft Company, “Seat Certification Analytical Techniques,” AGATE Report No. C-GEN-3432-1, 1997.

5-9. Cessna Aircraft Company, “Evaluation and Correlation of Advanced Occupant-Seat Analysis to Dynamic Tests,” AGATE Report No. C-GEN-3433-1, 1998.

5-10. MADYMO Database Manual 3D Version 5.4, TNO-MADYMO, 1999.

5-11. Manning, J. E., and Happee, R., “Validation of the MADYMO Hybrid II and Hybrid III 50th-percentile Models in Vertical Impacts,” Presented at the Specialists’ Meeting: Models for Aircrew Safety Assessment: Uses, Limitations, and Requirements, Ohio, October 26-28, 1998.

5-12. Code of Federal Regulations, Title 14 Part 23 "Airworthiness Standards: Normal, Utility, and Acrobatic Category Airplanes".

5-13. Cessna Aircraft Company, “Foam Materials Study Test Results ,” AGATE Report No. C-GEN-3432A-2, 1997.

This Document Provided by the Abbott Aerospace
Technical Library
abbottaerospace.com

This Document Provided by the Abbott Aerospace
Technical Library
abbottaerospace.com

Chapter 6

Airframe Structural Crashworthiness

Lance C. Labun
Steven J. Hooper
Marilyn Henderson

This chapter addresses how the principles of crashworthiness influence structural design in the aircraft. The design of the aircraft's structure, in particular the design of the fuselage and appendages, is critical to achieving four of the five fundamentals of crashworthiness, specifically: 1) maintaining a survivable volume for the occupants, 2) restraining the occupants within that volume, 3) limiting the occupants' decelerations to tolerable levels, and 4) minimizing post-crash hazards. This chapter describes the crash resistance design requirements and recommendations, describes the crash environment in terms of the energy of the aircraft going into the impact, and discusses possible dissipation paths for that energy. This chapter also describes impact conditions, failure modes of aircraft structure in a crash impact, and resulting injury mechanisms. In addition, information is provided on the materials that are used in aircraft structure.

The majority of the information presented in Sections 6.1 through 6.7 has been drawn directly from Volume III of the U.S. Army Aircraft Crash Survival Design Guide (Reference 6-1). It should be noted that this area of General Aviation (GA) aircraft design is still a work in progress, and that future research efforts will continue to complement the content presented here. Section 6.8 presents a procedure that was used to estimate firewall loads for the AGATE ACG test airplane (Reference 6-2).

6.1 CRASH RESISTANCE REQUIREMENTS AND RECOMMENDATIONS

6.1.1 Static Requirements

The requirements for crash resistance in FAR Part 23 aircraft are specified under “Emergency Landing Conditions” in FAR Paragraphs 23.561 and 23.562 (References 6-3 and 6-4). The general requirements are stated in Paragraph 23.561, and the dynamic conditions are specified in Paragraph 23.562.

The requirements allow for the likelihood that the aircraft may be damaged in emergency landing conditions, but specify that the structure must be designed “…to give each occupant every reasonable chance of escaping serious injury...”. The requirement then goes on to describe specific conditions in terms of static loads. The structure must be sufficiently strong for all of the seats to remain attached during an event that subjects the occupants to the inertial loads described in Table 6-1. These loads are modified by a formula in Paragraph 23.562(d) for airplanes that exceed 61 kts V_{so} at maximum weight. For load purposes, the designer must assume that all occupants have used the provided restraints.

THIS DOCUMENT PROVIDED BY THE ABBOTT AEROSPACE
TECHNICAL LIBRARY
ABBOTTAEROSPACE.COM

Table 6-1. Static inertia load conditions - Structure bearing seat and restraint loads	
Acceleration Direction	**Structure Requirement (G)**
Upward (normal, utility, and commuter)[1] Upward (acrobatic)	3.0 4.5
Forward	9.0
Sideward	1.5
Downward	6.0
[1]With respect to turnover in the event of an emergency landing, separate requirements are given in Para 23.561(d).	

A further requirement is placed on items of mass within the cabin that could injure an occupant. The supporting structure and the means of attachment for these items must be designed to the static load requirements listed in Table 6-2.

Table 6-2. Static inertia load conditions - Structure supporting items of mass within the cabin	
Acceleration Direction	**Structure Requirement (G)**
Upward (normal, utility, and commuter)[1]	3.0
Forward	18.0
Sideward	4.5
Downward	-
[1]With respect to turnover in the event of an emergency landing, separate requirements are given in Para 23.561(d).	

6.1.1.1 Turnover in Emergency Landing

The designer is given two options regarding aircraft turnover. They can either demonstrate by analysis that the aircraft is unlikely to turnover, or they can demonstrate that the aircraft can sustain a structural load factor of 3.0 G in the upward direction and lateral loads with a friction coefficient of 0.5 to the ground.

6.1.2 Dynamic Requirements

The dynamic requirements called out in Paragraph 23.562 only apply to the seat/restraint system, and not to the structure supporting them or any items of mass in the cockpit. The regulations do not provide dynamic design requirements.

6.1.3 Recommendations

As described in Section 6.1.1, the requirements spelled out in the Airworthiness Standards address the second and fifth key elements of crashworthiness, i.e., restraining the occupants and minimizing post-crash hazards. However, they do not specifically require maintaining a survivable volume or limiting the occupant decelerations. Maintaining a survivable volume, also referred to as creating a high-strength “cage” around the occupant, is certainly the first step, if not the most critical step, in creating a crashworthy aircraft. The success of this "cage" strategy can be seen in the dramatic high-speed crashes that occur in NASCAR races with few attendant fatalities, due to the use of high-strength tubular steel to create a "cage" around the

THIS DOCUMENT PROVIDED BY THE ABBOTT AEROSPACE
TECHNICAL LIBRARY
ABBOTTAEROSPACE.COM

driver. In the aviation field, the success of this "cage" strategy is evident in agricultural aerial application aircraft, where the incident rate is relatively high, but few serious injuries or fatalities occur, partly due to the construction of a structrual "cage" around the pilot.

A reasonable minimum recommendation for dynamic design targets would be to apply the restraint static loads to the maintenance of survivable cabin volume. Thus, not only would the seats be required to stay attached in an emergency landing applying the specified static loads (Table 6-1), but the structural strength should be such that survivable volume is also maintained under those loads. Clearly, it makes little sense to successfully hold the occupant in place if the structure collapses into the occupied space. The most efficient crashworthy design will be a balanced one, in which all aspects of crashworthiness are designed to approximately the same set of impact criteria.

For the designer seeking a higher level of crashworthiness, the seat dynamic test conditions are a reasonable basis for recommending the structural design loads needed to maintain the occupied volume. Resolving the vectors in the two test conditions results in loads of 26 G forward, 16.5 G downward, and 4.5 G sideward. Table 6-3 presents the minimum and preferred recommendations for a structure's ability to maintain survivable volume.

Table 6-3.
Recommended structural load factors for maintaining survivable volume

Load Direction	Minimum Crush Strength (G)	Preferred Crush Strength (G)
Upward	3.0	4.5
Forward	9.0	26.0
Sideward	1.5	4.5
Downward	6.0	16.5

6.2 CRASH ENVIRONMENT (CRASH IMPACT CONDITIONS)

The energy content of the aircraft will give the designer an idea of the magnitude of energy that must be dealt with in a crash. This energy must either be absorbed by the aircraft or dissipated to the surroundings. Section 6.2.1 enumerates the energy dissipation paths, and Section 6.2.2 discusses crash kinematics.

6.2.1 Energy Content of Aircraft at Impact

The total energy that the complete aircraft system possesses immediately prior to impact is the sum of several energy terms. This energy includes the following:

- Translational kinetic energy, $(K.E.)_T$
- Rotational kinetic energy, $(K.E.)_R$
- Potential energy, P.E.
- Strain energy, S.E.

The total energy input during the crash sequence, T.E., is

$$T.E. = (K.E.)T + (K.E.)R + P.E. + S.E. \quad (6\text{-}1)$$

This is this total energy which must be absorbed or dissipated in the crash sequence.

THIS DOCUMENT PROVIDED BY THE ABBOTT AEROSPACE
TECHNICAL LIBRARY
ABBOTTAEROSPACE.COM

6.2.1.1 Translational Kinetic Energy, $(K.E.)_T$

The Translational Kinetic Energy, $(K.E.)_T$, component is a direct function of the aircraft mass and the velocity of the mass center at impact.

If: V = resultant velocity of the mass center
V_X = longitudinal component of velocity
V_Y = lateral component of velocity
V_Z = vertical component of velocity

Then:

$$(K.E.)T = 0.5* MV2 \quad (6\text{-}2)$$

$$(K.E.)T= 0.5* M(VX2 + VY2 + VZ2)$$

Thus, the total kinetic energy of the aircraft is the summation of the kinetic energy for all mass elements of the aircraft.

Generally, the translational kinetic energy, or $(K.E.)_T$, will be the predominant contribution to the total energy content of the aircraft.

6.2.1.2 Rotational Kinetic Energy $(K.E.)_R$

Rotational kinetic energy, $(K.E.)_R$, may be associated with the total aircraft and with aircraft elements such as the engine(s) and propeller(s). Selective assessment of rotational kinetic energy contributions to the crash energy balance must be made.

In general, rotational kinetic energy is calculated using the expression:

$$(K.E.)_R = 0.5*I_\theta\varpi_\theta^2 +0.5*I_\phi\varpi_\phi^2 +0.5*I_\psi\varpi_\psi^2 \quad (6\text{-}3)$$

Where: ϖ_θ = angular velocity component in the x-z plane (pitch)

ϖ_ϕ= angular velocity component in the y-z plane (roll)

ϖ_ψ = angular velocity component in the x-y plane (yaw).

and I_θ, I_ϕ, I_ψ, are the mass moments of inertia of the vehicle with respect to the pitch, roll, and yaw axes, respectively, at its mass center.

If the angular velocity about any of the axes is high enough to contribute a significant amount of kinetic energy, then the impact attitude of the aircraft will be difficult to predict. Such cases do not lend themselves to detailed analysis. Rotational kinetic energy of engines or propellers can most likely be neglected, unless that energy could be readily transferred to the entire airframe. For example, in a helicopter, if directional control is lost, the airframe may develop a very substantial angular velocity in reaction to the rotor blade or other applied torque. Depending on the orientation at impact, the angular rotation of the crew compartment may substantially increase the sideward loads upon the occupant when the cabin is brought to rest.

6.2.1.3 Potential Energy (P.E.)

For the crash sequence, the total potential energy (P.E.) input into the system equals the summation of the vertical displacement (ΔZ) contribution of each mass from the instant of first contact until the time of completion.

$$P.E. = \sum(mg\Delta Z) \quad (6\text{-}4)$$

This Document Provided by the Abbott Aerospace
TECHNICAL LIBRARY
ABBOTTAEROSPACE.COM

6.2.1.4 Strain Energy (S.E.)

Structural strain energy (S.E.) may exist due to in-flight loading. One example of strain energy is the upward bending of the aircraft's wings due to lift loading. This energy is released quickly upon contact with the ground and the resulting rapid loss of forward velocity. In addition, pressurized systems may have stored strain energy. However, stored strain energy due to pressurization is usually insignificant to the crash event.

6.2.2 Post-Impact Energy Dissipation

After the initial contact, there are several ways of absorbing energy to bring the vehicle to a stop while providing survivable conditions for the occupants. Keep in mind that one of the key elements of crashworthiness is limiting the deceleration of the occupants to tolerable limits. Absorbing the energy of the aircraft means doing work, and work is defined as force times distance. Thus, the design objective of limiting deceleration implies limiting the force factor of the work equation with a consequent increase in the distance factor. Also keep in mind that only forces or loads performing plastic deformation or created by friction are absorbing energy; forces performing elastic deformation are only storing energy to be released later in the crash event. Possible major contributors in the energy-absorption process are:

1. **Energy-Absorbing Landing Gear:** The landing gear may provide a portion of the energy absorption, depending on the design of the aircraft and the impact surface. Only the plastic deformation and friction of the landing gear displacement will absorb energy.
2. **Structural Deformation:** Structural deformation can provide a major means of energy absorption. Compression, tension, bending, torsion, and shear from low levels up to ultimate conditions all contribute to energy absorption. Vertical energy may be absorbed by the controlled deformation and crushing of the structure below the occupants. Controlled deformation implies crushing under forces which limit decelerations to those tolerable by the occupants and to decelerations which allow the frame and bulkhead members to still support large mass items. Longitudinal loads can likewise be limited by structural crushing.
3. **Breakaway of High-Mass Items:** The breakaway of high-mass items causes an instantaneous mass change and a corresponding reduction in kinetic and potential energies to be absorbed by the remaining structure. A major problem involved in using this strategy is designing the vehicle to ensure clean breakaway characteristics with adequate clearance between each free item and the occupied area. If potential hazards arise from breakaway items impacting occupied areas or generating fires, then a better design strategy is to retain the high-mass items.
4. **Ground Friction and Nose Plowing:** Longitudinal deceleration is generated by ground friction and/or nose plowing, depending on the type of impacted surface. Sliding and limited nose plowing are very desirable crash scenarios because the deceleration is spread over a long distance and, consequently, the forces on the occupants remain low. As indicated in Section 5.3.1.1, ground plowing must be carefully limited, otherwise sufficient earth can be pushed up in front of the aircraft to increase the deceleration to hazardous levels.
5. **Displacement of Soft Impact Surfaces During Vertical Impact:** Vertical deceleration may be limited by compacting and displacing soft earth (or loam, sand, mud, water, etc.). Forces are very high when a large flat portion of the fuselage contacts the earth all at once, and forces are more moderate for rounded corners of the fuselage

This Document Provided by the Abbott Aerospace
TECHNICAL LIBRARY
ABBOTTAEROSPACE.COM

penetrating soft soil or water. The aircraft's landing gear will provide virtually no energy absorption in water impacts. Water impacts can be surprisingly severe, depending upon the fuselage shape and angle of impact.

6. **Energy-Absorbing Seats:** The aircraft's seats are the final opportunity to absorb energy between the aircraft occupant and the ground. Because the human body has a relatively low tolerance to decelerations parallel to the spine, it is usually necessary that energy absorption be included in the seat design. Crash-resistant seat design is described in detail in Chapter 7.

6.3 STRUCTURAL BEHAVIOR UNDER CRASH IMPACT CONDITIONS

Impacts with a predominantly longitudinal velocity vector occur when an aircraft is flown into an inclined surface, such as a mountainside, a ground obstacle, or when ground impact occurs with the aircraft in an extreme nose-down diving attitude. When an impact occurs with an obstacle located near the ground, i.e., overhead wires, trees, or buildings, the subsequent rotational motions can result in ground impact occurring at almost any attitude. Fixed-wing aircraft can also impact with high vertical velocity if a stall occurs at low altitude, in high-sink-rate accidents, or in rollover accidents. Although the major impact generally produces the most severe hazard for occupants, additional hazards can be encountered during the remainder of the crash sequence. External objects such as trees and ground equipment may penetrate occupied aircraft sections. In addition, items such as engines and external stores may become detached from the aircraft and can also impact the occupied sections of the aircraft or cause the release of flammable fluids. In reality, there are an infinite number of crash scenarios that can occur, each with a relatively low probability. Thus, it is impractical, from a weight perspective, to try to design for all them.

6.3.1 Structural Damage that Frequently Results in Occupant Injury

Although airframe designs and accident scenarios may vary widely, there are certain types of structural damage that most often produce occupant injury. Usually, the structure that first contacts the impact surface is the first to deform. As deceleration forces increase, deformation spreads and more structure becomes involved. Eventually, buckling may occur throughout the aircraft. The protective shell is then compressed between the impact surface and masses aft or above the protective shell. If parts of the aircraft, such as the wings and tail sections, break free from the cabin section during the impact, this direct loss of kinetic energy may limit cabin deformation; however, the reduction in total mass may also produce a higher acceleration level within the cabin. The concept of mass shedding as a design strategy will be addressed in Section 6.4.5.

The following subsections describe frequently occurring impact conditions and injury-causing events. Generally, these events involve aircraft that are not designed to be crash-resistant, in accordance with this volume's guidelines.

6.3.1.1 Longitudinal (Crushing) of the Cockpit Structure

During a high-velocity, longitudinal impact into soft earth, the aircraft nose structure is sometimes deformed so that it scoops the earth as it slides along the ground. This building up of earth in front of the nose produces high forces that may collapse the forward cockpit structure and may cause entrapment of occupants and/or injury to their lower extremities. In addition, the high forces produce high aircraft decelerations, resulting in high loads on personnel and cargo restraint systems. A similar effect may be experienced on water.

This Document Provided by the Abbott Aerospace
TECHNICAL LIBRARY
ABBOTTAEROSPACE.COM

Another possible longitudinal crushing scenario is when a combination of nose structure crushing and friction between the structure and the terrain (particularly in “long-nose” aircraft) causes the forward structure to be pulled beneath the rest of the aircraft. This type of damage typically causes rupture of the cockpit floor and higher longitudinal acceleration than would be experienced if a smooth “skid” were maintained under the nose.

Longitudinal crushing also occurs if a high angle exists between the aircraft and the obstacle against which it crashes. A high impact angle can be created when a shallow-angle impact occurs into terrain features such as a hillock, or from a steep-flight angle impact with respect to relatively flat terrain, or from a “nose-on” impact into vertical walls, such as revetments or embankments. The resulting crushing may be sufficient to destroy occupied areas of the cockpit or cabin and significantly reduce the chances for occupant survival.

6.3.1.2 Vertical (Crushing) of the Fuselage Shell

Collapse of the protective shell due to vertical loading can occur in high-sink-rate accidents or rollover accidents. The collapse is often aggravated by large masses located above the fuselage structure, such as high wings or engines mounted on the aircraft. This damage results in loss of occupiable volume and reduces the chances for occupant survival.

If the underfloor structure collapses without absorbing sufficient energy, then the remaining deceleration will be taken in the seats and the occupants. If energy-absorbing seats are installed, then these seats may “bottom out”, and the high loads that are transmitted to the occupant may then cause spinal injury.

6.3.1.3 Lateral (Crushing) of the Fuselage Shell

If the sides of the fuselage are not designed for crash protection, severe injuries can result from relatively minor accidents. Occupants in GA aircraft are typically placed close to the sides of the fuselage, and often their restraint systems are inadequate to restrain them from moving laterally. On occasions, the aircraft’s doors are lost during the crash, which exposes the occupants to a variety of additional lateral hazards from outside of the aircraft.

6.3.1.4 Longitudinal Bending of the Fuselage Shell

Rupture or collapse of the protective shell around the occupants often occurs due to the high bending loads incurred during the rapid pitch change associated with longitudinal crashes at moderate-to-high impact angles. Rupture of the protective shell exposes occupants to injury through direct contact with the impact surface, contact with jagged metal, and loss of restraint. Detached items may also strike occupants after the breakup of the aircraft.

6.3.1.5 Deformation (Buckling) of Floor Structure

In most aircraft, occupant and cargo restraint depends heavily upon the integrity of the floor structure. When the floor structure fails, this restraint is lost. Often, floor failure is caused by the crushing and warping of the underfloor supporting structure. Localized damage is frequently caused when fuselage-mounted landing gear are driven into the floor structure.

6.3.1.6 Landing Gear Penetration of Fuselage Shell

Landing gear failures often result in personnel injuries, either directly (as mentioned above) or indirectly, through fire exposure caused by the rupture of flammable fluid lines and tanks by the landing gear being driven into the aircraft structure.

This Document Provided by the Abbott Aerospace
TECHNICAL LIBRARY
ABBOTTAEROSPACE.COM

6.3.1.7 Rollover

Aircraft most often roll over in the forward direction in a “nose over.” The cabin often has minimal vertical strength, particularly in low-wing aircraft. Injuries occur when the roof of the cabin collapses onto the occupants. Additionally, the doors are often jammed in a rollover scenario, hampering post-crash egress.

6.3.1.8 Rupture of Flammable Fluid Containers

The rupture of structure surrounding flammable fluid containers or fluid transfer lines is often an indirect cause of occupant injury as a result of post-crash fire.

6.4 GENERAL CRASHWORTHY DESIGN CONSIDERATIONS

An aircraft design requires a number of distinct features for crash survival. First, and most important, the structure surrounding the occupiable areas must remain reasonably intact, and must not reduce the occupied volume to the point of creating a hazard. If occupants are injured because the protective shell collapses onto them, then efforts to improve survivability through other methods are futile. An aircraft that does not provide a protective shell can never be considered crash-resistant. Second, the structure and the seats should be designed to attenuate occupant accelerations to survivable levels and to retain large mass items, interior equipment, seats, and cargo. In addition, the penetration of the cabin by external hazards should be minimized.

Survival is achieved by controlling the acceleration magnitudes and acceleration duration actually experienced by the occupants. Thus, the absolute velocity change is less important than the time and distance over which the velocity change occurs. Since deceleration loads are a function of the strength of the structure, a systems analysis should be performed to plan the distribution of energy-absorbing properties to the landing gear, fuselage, and seats. For new aircraft, these major elements can then be designed to provide the required properties. For older aircraft undergoing retrofit, certain elements cannot be changed. Thus, those elements that can be changed should be modified as much as possible within practical limits to provide some compensation for those items that cannot be changed.

The design of an aircraft's structure involves a series of compromises with respect to payload, performance, aerodynamics, strength, simplicity of fabrication, economics, etc. Applying the additional requirement for crash-resistant structure may cause further compromise and require more good judgment from the designer. As more attention is directed toward airframe crash resistance, methods and techniques of construction will improve so that adequate crash resistance can be achieved with acceptable weight, cost, and performance penalties.

Often, upgraded crash resistance will not result directly from increasing structural strength. An excessively strong airframe structure is no more acceptable for crash resistance than an under-strength structure. Not only will excessive strength impose an undesirable weight penalty, but excessive strength may cause high accelerations that actually reduce survivability. Structural deformations should be carefully considered and even planned to occur. The issue of high structural strength causing high accelerations is particularly a problem for underfloor structure, which must be designed not only to support normal flight and landing loads but also to absorb energy when subjected to vertical crash loads.

Fabrication techniques and structural configurations, especially for areas where severe damage is probable, should be selected after careful consideration of the overall effects of structural failure on occupant protection. The designer should ensure that several parallel load paths are available to keep the structure intact even though localized damage occurs. Wherever

This Document Provided by the Abbott Aerospace
TECHNICAL LIBRARY
ABBOTTAEROSPACE.COM

possible, multiple structural members should be used instead of single larger structural members, so that localized impact damage will not result in complete loss of structural integrity. Multiple load paths also aid in maintaining uniform force transmission characteristics throughout structural collapse.

The airframe structure should, of course, be designed for normal flight loads, ground handling loads, and fatigue life, while considering the parameters of the aircraft specification with respect to size, range, performance, space envelopes, etc. After the basic structural layout has been defined, the effects of crash loads must be considered to determine where structural modifications are needed to improve crash resistance. Concurrent with this process, space allocations must be made for critical systems, such as landing gear, seats, fuel tanks, and emergency exits, to ensure an integrated approach to crash resistance.

Once the preliminary aircraft design is established, computer simulations, such as those described in Chapter 5, may be used to model primary structure, large-mass items, systems, occupants, and cargo. Then, potential impact conditions may be simulated to investigate the aircraft's dynamic response, structural collapse, and acceleration.

An iterative process is used to optimize energy-absorption concepts, structural distributions, failure modes, mass retention concepts, landing gear locations, etc. This process is conducted concurrently with the design effort, stress analysis, and performance evaluation, to ensure design optimization. Further modifications are made throughout the process to control weight and weight distribution, producibility, maintainability, safety, and cost. Several iterations should be expected in the evolution of the optimum design that adequately satisfies the requirements of the basic aircraft specification.

When designing with composite materials in the primary fuselage structure, it is desirable to conduct representative sub-structure crush tests as part of the design process to evaluate the energy-absorbing properties of proposed structural concepts.

In designing for crashworthiness, the aircraft design should attempt to manage the failure modes of the structure. In order to manage the failure modes, the designer must consider both the structure's materials properties and joining concepts. The following sections look at various failure modes and then at the materials properties and joining techniques that affect failure modes.

6.4.1 Considering Failure Modes

In designing for crashworthiness, the designer should actively seek to control failure modes, rather than designing adequate structure and accepting whatever failure modes result. The following failure modes should be avoided:

- Penetration of the occupied area by failed structural elements
- Inward buckling of structures, such as sidewalls, bulkheads, and floors
- Failures of members such as frames that result in jagged, failed ends protruding into occupied space or fuel tanks
- Fastener failures that may produce structural discontinuities and projectiles
- Brittle fractures that suddenly unload, causing impulse effects in adjacent structures with the potential for progressive failures and the generation of projectiles
- Excessive distortion of emergency exit surrounds that precludes the opening or removal of doors or windows
- Penetration of flammable fluid containers.

THIS DOCUMENT PROVIDED BY THE ABBOTT AEROSPACE
TECHNICAL LIBRARY
ABBOTTAEROSPACE.COM

Pre-determined failure points can be introduced into a design to help control structural response under dynamic loading conditions. These points may be plastic hinges that allow plastic yielding earlier in the crash sequence and allow rotations in weaker sections. Alternately, joints may be designed to fail progressively to allow rotation of structural elements and thus subsequent load redistribution. In other words, a joint design that still effectively pins the members together even though they may have deformed with respect to their original positions is preferable to a joint that allows the ends of the structure to break free.

6.4.2 Selecting Materials

Until recently, most aircraft were constructed primarily of metallic materials. However, this situation is rapidly changing. Presently, a significant quantity of composite aircraft are being produced. Therefore, both metallic and composite materials will be considered for crash-resistant design. Subsequent sections provide guidance for using both metals and composites in crashworthy structural designs.

6.4.2.1 General Material Considerations

The deformation of aircraft structure is a key mechanism for absorbing the kinetic energy of an aircraft in a crash. Absorbing energy through structural deformation can be an effective tool for occupant protection, if the structural deformation is carefully planned to attenuate the forces transmitted to the occupant. The use of surrounding structure as a buffer can be accomplished more safely if the impact causes crushing without complete rupture of structural members. Material properties can greatly affect the degree to which crushing without rupture is actually achieved. Sufficient material ductility is required to ensure that crushing, twisting, and buckling can occur without rupture. In the case of composites, this ductility must often be designed into the failure mode of the component, because ductility is not inherent in all composite structures.

6.4.2.2 Material Strength and Elongation Characteristics

Material strength and elongation characteristics are described in applicable military handbooks. MIL-HDBK-17 (Reference 6-5) and MIL-HDBK-5 (Reference 6-6) contain basic design data for composite and metallic materials, respectively. When using these handbooks to obtain information on materials properties, the designer should bear in mind that for some materials, such as steel, the handbooks present only the guaranteed minimum strength and elongation data; but for other materials, such as aluminum, values are presented indicating both minimum guaranteed strength and the strength values which statistics show will be met or exceeded by 90 pct of the materials under consideration. The 90-pct probability values are normally somewhat higher than the guaranteed values. The selection of the strength value should be based upon the consequences of failure. For design of structural members, such as members supporting heavy overhead masses where failure could result in a severe loss of occupant protection, the use of minimum guaranteed values would be reasonable. For design of structures likely to be subjected to massive crushing, such as airplane nose structures, the use of statistical values would be justified.

6.4.2.3 Composite Materials

Composite materials offer certain advantages over metallic materials in some areas of aircraft structure; primarily the advantage of reduced weight for a given ultimate strength. Other advantages are ease of fabrication, ease of forming complex shapes, and the capability of tailoring the stress-strain properties to the local loading. However, when compared to a ductile metal such as aluminum, most composite materials, when used in aircraft structures, cannot

THIS DOCUMENT PROVIDED BY THE ABBOTT AEROSPACE
TECHNICAL LIBRARY
ABBOTTAEROSPACE.COM

tolerate large strains without fracture. Because of the low inherent ductility of most composite materials, crash energy absorption must come from innovative component design to enhance material stress-strain behavior.

At present, the energy-absorbing behavior of composites is not easily predicted. This difficulty in predicting energy absorption is compounded by the fact that composites are frequently very anisotropic in their properties. Thus, sub-structure testing will usually be required in order to verify that a proposed configuration will actually perform as intended.

Figure 6-1 compares typical stress-strain curves for an aluminum alloy and a graphite/epoxy composite in tension. The shaded areas indicate the potential energy absorption capabilities, and the difference between the two materials should be noted: i.e., the ratio $A_{7075}/A_{GE} = 12.3$.

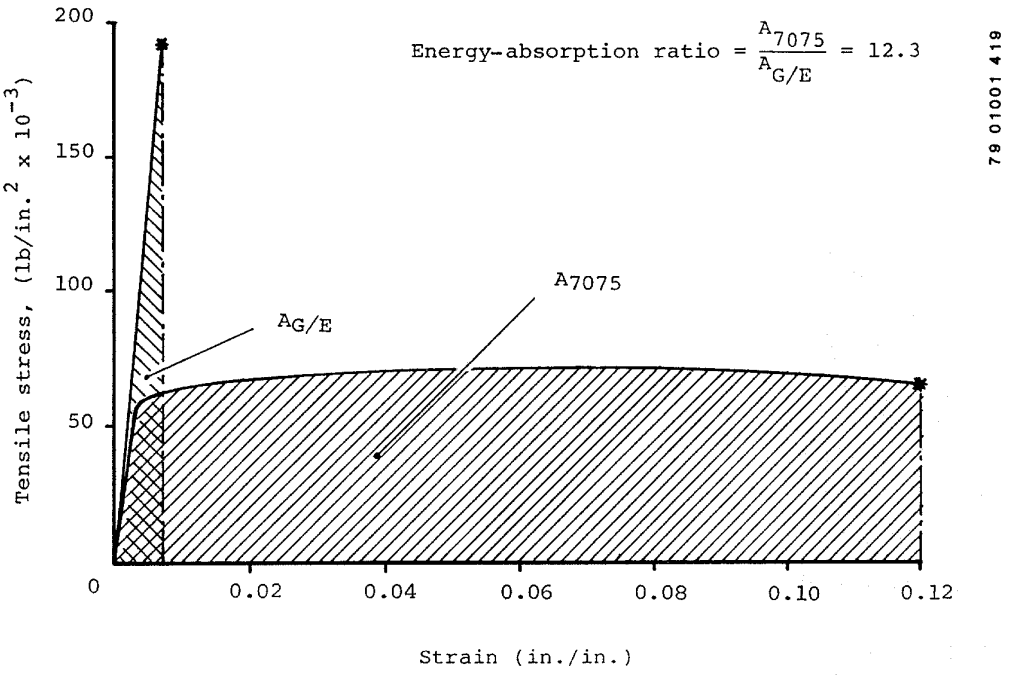


Figure 6-1.
Stress-strain relationship for aluminum alloy (7075) and 0-deg graphite/epoxy composite.

However, if composite components are designed to crush progressively, these components can exhibit high energy absorption. Figure 6-2 shows a composite tube having the largest Specific Energy Absorption (SEA) of nine alternate designs (Reference 6-7). Specific Energy Absorption is a parameter giving the amount of energy absorbed per unit weight. Beyond seeking a high SEA value, the designer should consider the failure mode of each composite material. Typically, a graphite/epoxy composite has poor post-crushing integrity and exhibits fracture and separation during crushing. On the other hand, a Kevlar® epoxy composite typically has good post-crushing integrity.

® Kevlar is a registered trademark of E. I. Du Pont de Nemours & Co., Inc.

THIS DOCUMENT PROVIDED BY THE ABBOTT AEROSPACE
TECHNICAL LIBRARY
ABBOTTAEROSPACE.COM

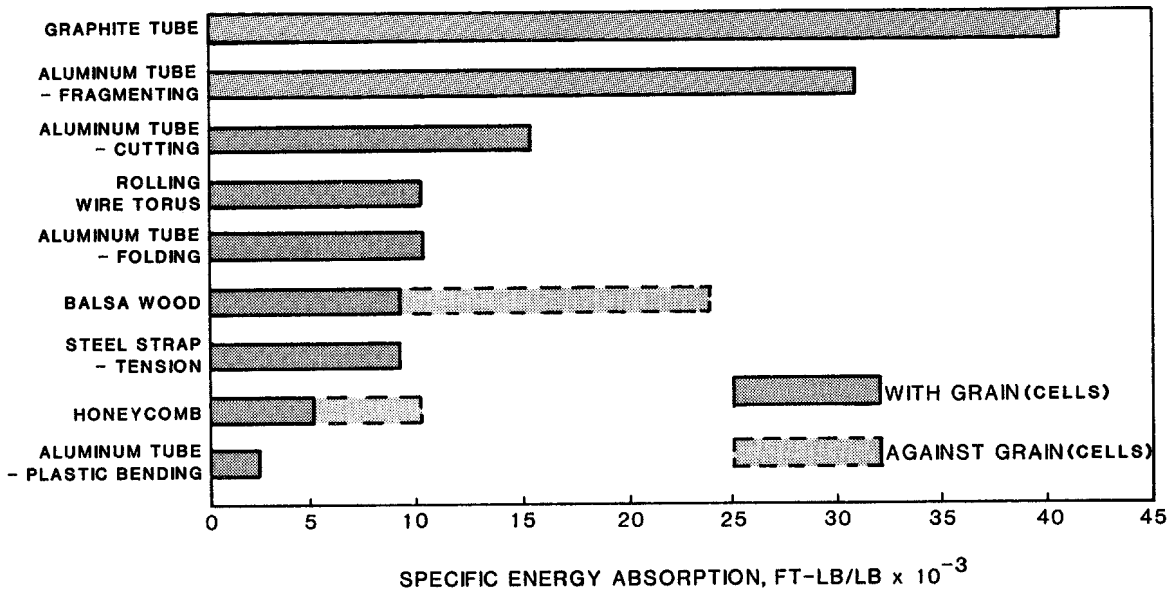


Figure 6-2.
Specific energy absorption comparisons (From Reference 6-7).

Much design and development test work has been conducted to find composite geometries that will serve the dual purpose of carrying normal flight and landing loads as well as providing energy absorption when subjected to crash loads. Detailed information on this subject may be obtained from References 6-8 through 6-26.

Additionally, much information concerning the inclusion of crash resistance in composite aircraft, using the techniques presented in Reference 6-8 through 6-26, is available from the U.S. Army-sponsored Advanced Composite Airframe Program (ACAP). Results from these programs are available in References 6-20 and 6-27 through 6-30. Two U.S. Army ACAP helicopter drop tests, reported in Reference 6-31 and 6-32, have demonstrated the feasibility of crash-resistant composite structures.

Another available method of energy absorption that may achieve adequate performance is an incorporation of filler materials, such as honeycomb materials and structural foams. For longitudinal and lateral impacts, it is feasible to incorporate energy-absorption features of this type; however, for the support of large mass items with high energy content, other techniques are more prudent.

Limitations on the use of energy-absorption techniques are dependent on the size and overall layout of the aircraft needed to satisfy the mission requirements. For a given aircraft, optimization studies may indicate that some major primary structural elements need to be manufactured from metallic materials, whereas composites may be used in other areas. If construction techniques are mixed, the effect of thermal stresses during manufacture and operation must be fully investigated. If curing of the bonding agent at elevated temperatures is required, warpage of the finished product may result. Table 6-2 gives values of thermal expansion coefficients for composite and metallic materials. Other useful design information can be found in Reference 6-28.

This Document Provided by the Abbott Aerospace
TECHNICAL LIBRARY
ABBOTTAEROSPACE.COM

Table 6-2. Thermal coefficients of expansion for composite and metallic materials (Reference 6-32)		
Composite Materials	**Coefficient of Thermal Expansion (10^{-6} in./in. °F)**	
	Longitudinal	**Transverse**
Boron filament	2.7	N/A
Epoxy matrix resin	2.7	27.0
Graphite fiber	-0.05	N/A
E-glass filament	2.8	N/A
Boron/epoxy [0]	2.3	10.7
Boron/epoxy [0_2/±45]	2.4	7.7
Graphite/epoxy [0]	0.3	14.4
Graphite/epoxy [0_2/±45/90]	1.9	1.9
E-glass/epoxy [0]	4.8	--
E-glass (181-style weave)/epoxy	5.5	6.7
PRD-49/epoxy [0]	-6.0	--
PRD-49 (181-style weave)/epoxy	0.0	--
Metallic Material	**Coefficient of Thermal Expansion (10^{-6} in./in. °F)**	
Aluminum	13.0	
Steel	6.0	
Titanium	5.6	

If the composite crash-resistant primary structure is not designed carefully, it may be less effective than anticipated. If a composite structure with an energy-absorption capability that is less than that of a metallic structure is used, a survivable deceleration environment must be created by the use of landing gear with greater energy-absorbing capacity, energy-absorbing seats, and possibly some form of floor load attenuation other than that obtained through primary structural deformation. This approach may introduce additional weight and require extra installation space to allow adequate stroking distances. Reference 6-31 presents a survey of crash impact characteristics of composite structures and suggests possible design concepts. (See also Reference 6-33 for the results of recent crashworthiness testing.)

6.4.3 Joint Concepts

The joints and attachment fittings of a crash-resistant airframe structure must be able to:

- Withstand large deformations without failure
- Connect items in a manner so that structural deformation or separation occurs before the joint fails.

Of the two considerations, the first imposes the greater constraint on a joint constructed of composite materials or, for that matter, on a metallic fitting manufactured from a casting or a forging. Joint concepts that cannot themselves meet the above criteria should have redundant or back-up load paths to satisfy the above considerations while relying on the airframe structure to absorb the energy and redistribute crash loads. Many composite joints contain some metal for this purpose and are considered hybrids.

This Document Provided by the Abbott Aerospace
TECHNICAL LIBRARY
ABBOTTAEROSPACE.COM

6.4.4 Margins of Safety

Safety margins of 0.0, based upon the crash load factors presented elsewhere in this volume, will generally be considered satisfactory. Safety factors may be increased as necessary to ensure performance in critical areas, particularly in load paths for occupant retention. Designs allowing the structure to remain more nearly intact through improved compliance or improved progressive, yet predictable, deformation are sometimes more effective than direct increases of strength. Plastic yielding can relieve stress concentrations before the ultimate strength of members are reached.

6.4.5 Mass Shedding

Designing aircraft structure for mass shedding is viewed as a controversial design strategy. If everything happens as planned, mass shedding can be a beneficial crashworthiness strategy in terms of reducing the kinetic energy of the occupant compartment. However, the benefits of mass shedding can be neutralized or worse by unplanned consequences. Because of the difficulty in designing for all scenarios, mass shedding is generally not recommended for light airplanes.

The main benefit of mass shedding is the reduction of vehicle kinetic energy. By shedding a large mass item(s) early in the event, the kinetic energy to be absorbed is reduced. For example, in a longitudinal impact into an embankment, if a rear-mounted engine can be made to break away cleanly and not impact the occupied space, then the amount of kinetic energy to be absorbed by the forward structure is reduced, and thus a weight reduction may also be achievable.

The key to successfully exploiting the benefits of mass shedding lies in controlling the breakaway of the masses and designing the crush zone based on the reduced mass. To be successful, the mass must break away precisely as designed, and it must move clear of the occupied volumes in the aircraft.

The drawbacks to mass shedding are the consequences of failure in the design. Clearly, the loose mass impacting the occupied volume is undesirable. If the crush zone is designed based on certain components breaking away, but these components do not break away in the crash, then the crush zone will be used up before the energy of the aircraft is dissipated (the crushing force will have been set too low, based upon the expectation of reduced mass). Conversely, in another impact scenario, where the mass is intended to remain attached, but breaks free, the occupants are subjected to higher-than-intended decelerations (the crushing force will have been set too high, based upon the expectation of the full mass being involved). Retaining mass can also be an advantage when the surface or object struck is deformable. In this case, the extra mass can help the vehicle “plow through” the obstacle, thereby increasing the stopping distance and reducing the accelerations.

The term mass shedding is sometimes also used to describe a load-limiting concept in which structures supporting high mass parts of the aircraft are allowed to deform and the masses contact the ground rather than be supported through the occupant compartment. An example of this is can be found for tilt-rotor aircraft (Reference 6-34). On tilt-rotor designs, the rotors and, sometimes, the engines are located near the wing tips, well away from the occupied areas. Allowing the wings to fail under high vertical accelerations in a controlled manner near the wing roots transfers most of the engine and rotor weight to the ground and reduces the loads on the occupant compartment. The wings are generally not designed to separate from the fuselage, so it is difficult to call this load-limiting concept mass shedding per se. Semantics aside, this concept may have usefulness in the design of high-wing airplanes.

This Document Provided by the ABBOTT Aerospace
TECHNICAL LIBRARY
ABBOTTAEROSPACE.COM

6.5 SUBSYSTEM DESIGN

This section offers specific suggestions for achieving the greatest crash resistance from the fuselage, landing gear, and other subsystems. However, it must be emphasized that systems integration is essential for optimizing aircraft crash performance. The specification for the performance of each subsystem is presumably created from an aircraft systems model that considers the interaction between subsystems. Conversely, the systems model requires input about achievable subsystems capabilities. Therefore, development of optimum crash-resistance performance for the aircraft will require an iterative approach.

6.5.1 Fuselage

An aircraft's fuselage is expected to perform many important functions during a crash, such as:

- Maintaining a livable volume around the occupants
- Shielding occupants from contact with outside hazards, such as trees, rocks, flying debris, etc.
- Providing hard points for attaching seats, cargo, etc.
- Reacting and distributing point loads from the landing gear
- Avoiding rupture of subsystems containing flammable fluids
- Preserving structural integrity around emergency egress openings, in order to facilitate post-crash egress.

Effective crash resistance begins with a well-planned fuselage design, since the fuselage provides the protective shell for the occupants and can appreciably control the accelerations applied to the seats/occupants. In this section, principles and methods for improving fuselage structure are presented.

A graphic example of cabin collapse is depicted in the sequence of photographs in Figure 6-3 (Reference 6-35). These photographs, taken during a NASA fuselage drop test, illustrate how an occupied volume can be briefly reduced to the point where human survival is unlikely even though the post-crash deformations may be small. Note in Frame 1 that there are four windows visible, in Frames 4 and 5, the forward window completely disappears and the second window is heavily deformed, and in Frame 6, all four windows are visible again.

Fuselage crash performance can be improved through the following design techniques:

- Altering the structure that makes initial contact with the ground to reduce gouging and scooping of soil, thus limiting accelerations.
- Reinforcing the cockpit and cabin structure to prevent collapse and to provide adequate tiedowns for occupants and cargo.
- Modifying the fuselage structure to provide energy absorption through controlled deformation.
- Selectively reinforcing the structure to resist fuselage penetration.
- Modifying components such as the wing struts, external accessories, and the landing gear to ensure that if these parts fail, they fail safely.
- Providing for component breakaway to effect a reduction in the mass of the aircraft and reduce the fuselage strength requirements.

Potential benefits from each method depend upon the structural characteristics of the particular aircraft design and its mission constraints.

This Document Provided by the Abbott Aerospace
Technical Library
abbottaerospace.com

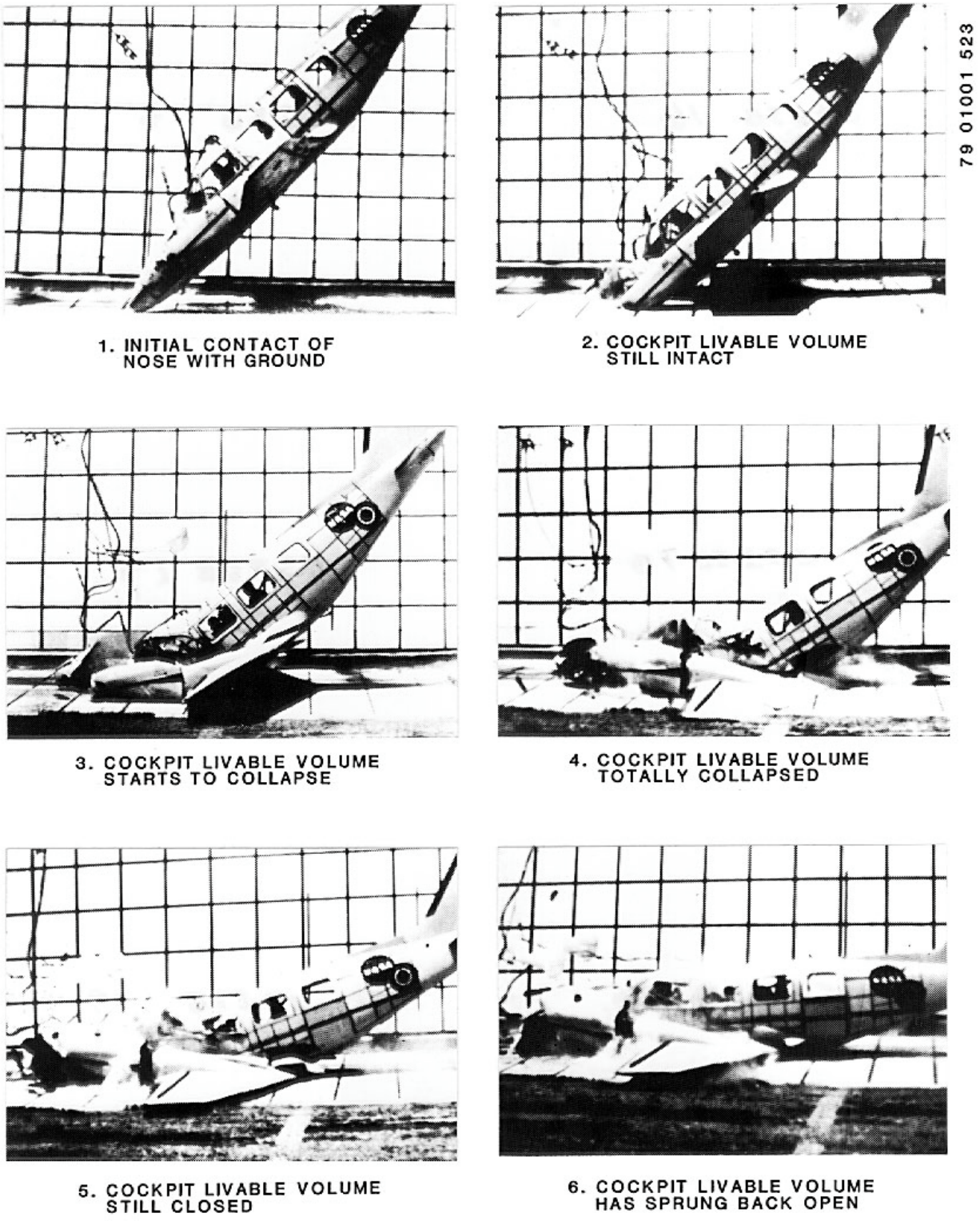


Figure 6-3.
NASA drop test of civil light twin-engine aircraft (Reference 6-35).

THIS DOCUMENT PROVIDED BY THE ABBOTT AEROSPACE
TECHNICAL LIBRARY
ABBOTTAEROSPACE.COM

The sections that follow discuss the design of crash-resistant fuselages. Load-limiting strategies are discussed first. These are used to reduce the forces on the occupants and to reduce loads within the fuselage, thus preserving the protective shell with minimum weight. The next section describes the methods that may be used to avoid unnecessary failures of the protective fuselage shell or blockage of emergency escape routes by crash-induced fuselage deformation. Last, attention is directed to structural interfaces with other subsystems: engines, transmissions, fuel tanks, seats, cargo, and ancillary equipment. Although landing gear, wings, empennage, external engine pylons, and external stores are also mounted to the fuselage, these major external subsystems and their structural interfaces are described in other sections.

6.5.1.1 Crash Characteristics

Most crashes have a combination of vertical and longitudinal characteristics. Helicopters often experience pure vertical crashes (aircraft level but velocity vertical), whereas GA aircraft crashes are often predominantly longitudinal in character. Longitudinal crashes can be divided into two types. In longitudinal slide-out impacts on relatively flat surfaces (high velocity, low angle), a high percentage of the aircraft's kinetic energy is dissipated by the displacement of earth and in friction between the aircraft and the earth. Consequently, in this type of crash, a relatively low percentage of the kinetic energy is absorbed by structural deformation. The other type of longitudinal crash is a horizontal crash into a barrier or a combined longitudinal and vertical crash with the nose pitched sharply downward. In this second type of longitudinal crash involving primarily a vertical impact, much more of the kinetic energy must be absorbed by the aircraft's structure. Thus, the structure must include concepts for improving crash resistance in at least two separate directions - forward and downward.

6.5.1.2 General Fuselage Design Considerations

The design of floor structures and the floor support structure has a considerable effect upon the protection offered by the cabin structure as a protective shell. The floor structure should be strong enough to carry the loads that will be applied to it by passenger and cargo restraint systems (see Chapter 8) without the need for supports which carry through to the lower fuselage skin and its stiffeners. Such supports transfer crash loads applied at the outer fuselage surface directly into the floor. Buckling of the floor produced by such a load transfer can reduce the bending strength of the fuselage and also reduce the effectiveness of restraint systems that depend upon floor integrity. Evacuation of the aircraft may also be impeded by disruptions to the floor surface.

The shape of the fuselage has an inherent influence on survivability. Rectangular cross-sections provide more usable interior volume, but must be more carefully designed to provide the same crash-resistant characteristics as spherically, cylindrically, or elliptically shaped fuselages. Rectangular-shaped fuselages can also provide resistance to rollover after landing gear failure and provide added energy-absorbing structure in an impact with a roll attitude.

Most aircraft crashes occurring at impact angles up to 30 deg involve a rapid change in pitch attitude to quickly align the aircraft fuselage with the impact surface. The resulting angular acceleration produces a fuselage bending moment that usually causes a compression of the upper members of the forward fuselage. This compression is combined with compression of the fuselage due to the longitudinal forces of impact. The result may be a compressive buckling failure of the structure.

This Document Provided by the Abbott Aerospace
TECHNICAL LIBRARY
ABBOTTAEROSPACE.COM

It is sometimes possible to provide sufficient strength to prevent a fuselage-bending failure. If this is not practical, it is desirable to determine the probable failure points and to position passengers away from those locations. Cargo tiedown attachments should be designed to prevent loss of cargo restraint, should a fuselage-bending failure occur.

6.5.1.3 Design for Longitudinal Crashes into a Barrier and Nose-down Crashes

In a longitudinal impact, the main considerations are to ensure the integrity of the structural shell, to minimize earth scooping or plowing of the lower fuselage, and to provide some energy-absorbing material forward of the occupied area to limit forces due to impact with obstacles such as earth berms. Crushable space should be provided in front of the occupants. This space should be designed to crush at a force that will limit the deceleration of the occupants to tolerable levels. The crushing space needed depends on the maximum impact velocity for which the aircraft is being designed. The peak acceleration is established by human tolerance in the forward direction (Section 4.3.3), and the crushing force is determined by the mass of the aircraft. In the longitudinal direction, the structure around the occupied space must be stronger than the design forces for the crushable space.

6.5.1.4 Design for Longitudinal Crashes that Involve Earth Plowing

Longitudinal impacts with slide-out are very desirable because the change in velocity is spread over a long distance and a long time; thus, acceleration levels are low. An initial slide may be followed by a higher acceleration pulse with fuselage crush due to earth plowing followed either by more slide-out (desirable) or a sudden deceleration (undesirable). The designer's objective should be to avoid earth plowing, so that the slide-out can continue.

Reference 6-1 has a detailed analysis of earth plowing. The analysis shows that the deceleration of the aircraft is caused by the acceleration of an increasing mass of earth pushed ahead of the aircraft. The severity of the deceleration in these events is greater with higher initial impact velocity. The deceleration severity is also greater, depending on the density of the soil. Specifically, the more dense (mass/unit volume) the soil, the more severe the deceleration. For the designer who wishes to estimate the effects of earth plowing, the following expression is useful:

$$a_A = (\rho_s A_p v_o^2)/(m_A+\rho_s A_p v_o \Delta t)$$

where:

a_A = the average acceleration of the aircraft
ρ_s = the density of the soil (mass/unit volume)
A_p = the area of the aircraft pushing or plowing earth
v_o = the initial impact velocity
m_A = the mass of the aircraft
Δt = the increment of time from initial impact.

Earth plowing is dangerous for two reasons: 1) accelerations can be very high, and 2) the force tends to be concentrated on a relatively small area, causing this area to deform severely with possible negative consequences for the occupied volume of the aircraft.

Reduction of earth scooping can be accomplished by using a structural design that eliminates those surfaces that can gouge or dig into terrain. The structural design should provide a large, relatively flat surface so that the aircraft skids along on top of the terrain. Design techniques include reinforcement of underfloor structure and the canting of major structural components, as illustrated in Figure 6-4. If this reinforcement is to be effective, the lower skin should be a ductile, tough material with enough thickness to resist tearing. The skin should remain

THIS DOCUMENT PROVIDED BY THE ABBOTT AEROSPACE
TECHNICAL LIBRARY
ABBOTTAEROSPACE.COM

continuous to provide a skidding surface. Additionally, the underbelly skins, made from thick sheet material, should be shingled in an aftward direction to preclude their picking up soil at the front edge. It is recommended that the forward fuselage belly skins on aircraft weighing up to 3,000 lb be capable of sustaining loads of 1,500 lb/in.; over 3,000 lb but under 6,000 lb, 2,400 lb/in.; and over 6,000 lb, 3,000 lb/in. The above running loads are to be applied over the forward 20 pct of the basic fuselage length.

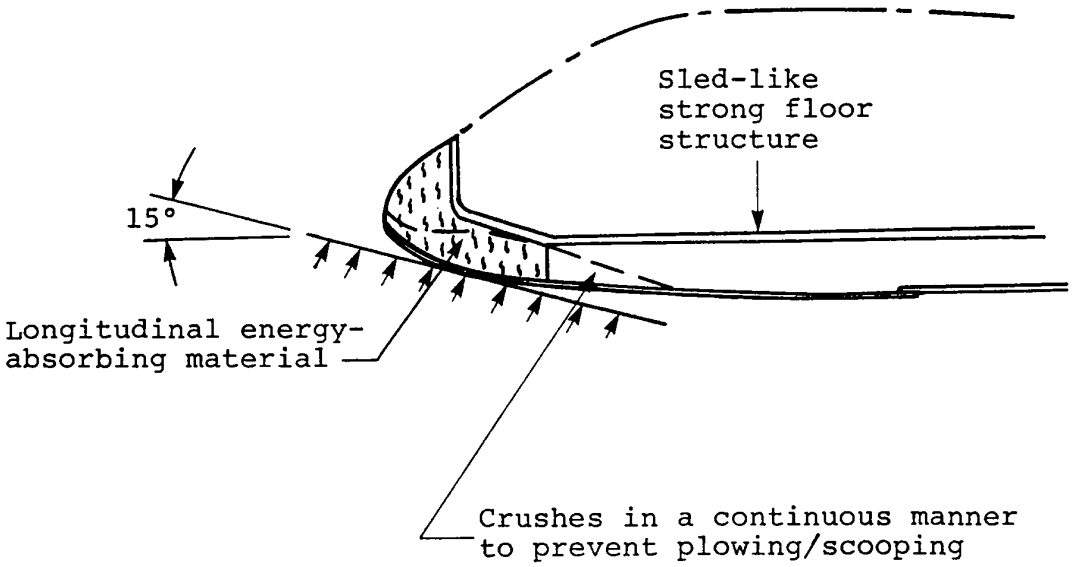


Figure 6-4.
A method of designing aircraft nose structure to reduce earth scooping.

This method for reducing earth scooping increases the deformation strength of the underfloor structure, thus increasing the deceleration levels at the floor level due to vertical velocity components. Therefore, the reinforcement should not be continued back any further than necessary under the occupied sections of the fuselage.

Strong structural crossmembers can present abrupt contour changes during deformation, thus forming the "lip" on the scoop that tends to trap earth. Forward underfloor frame members may be canted aftward at the bottom to provide an upward load component on the aircraft that tends to prevent, or limit, the digging in of the structure. The longitudinal strength of the nose section can be increased by the use of strong continuous structural members running fore and aft in the underfloor section of the aircraft. These beams can be used to support the crossmembers and act as skids to further reduce scooping or digging-in tendencies.

The results of full-scale crash tests indicate that longitudinal aircraft accelerations produced by earth scooping can be significantly reduced by the application of the methods discussed above.

In multi-engine aircraft, the engine nacelles may present as much of an earth scooping mechanism as the nose of the fuselage, and since the engines are often attached to the strong, rigid wing center section, the forces produced by engine earth scooping are transmitted to the fuselage cabin.

THIS DOCUMENT PROVIDED BY THE ABBOTT AEROSPACE
TECHNICAL LIBRARY
ABBOTTAEROSPACE.COM

A caveat to designing for crashworthiness in longitudinal impacts is the phenomenon of "tail slap". Tail slap often occurs in high-angle slide out crashes. In these types of impacts, high vertical loads are experienced in the rear of the aircraft. These loads can be as high as or even higher than the loads experienced in the front of the aircraft during the initial impact.

6.5.1.5 Energy-Absorbing Capacity of Forward Fuselage

In consideration of the conservation of energy, the initial kinetic energy of an impacting aircraft must be accounted for in energy dissipated during the deformation of both soil and structure. The designer will realize that energy not absorbed by the ground will be absorbed by the aircraft's crush zone, other areas of the aircraft structure, or in the cabin (occupied space). The goal is to avoid absorbing energy in the cabin (U_c in the following equation) and dissipate it or absorb it all in the crush zone and other parts of the fuselage. As a simplified model, the energy absorbed by the cabin can be expressed as:

$$U_C = \left[\frac{m_A (v_o^2 - v_f^2)}{2} - U_G\right] - (P_{av}S + U_S') \qquad (6\text{-}15)$$

where:

U_C = energy to be absorbed in cabin deformation.
M_A = mass of the aircraft
v_o & v_f = initial and final velocity of the aircraft
U_G = energy absorbed in ground friction and earth plowing
P_{av} = average force developed in the collapse of crush zone ahead of the cabin
S = linear deformation (reduction in length) of the crush zone
U'_S = deformation energy in structure other than in the cabin or the crush zone.

This equation for cabin deformation energy is valid if conditions reach or exceed the point of onset of cabin deformation.

Assuming a fixed mass and velocity, and ignoring control over energy dissipated outside the aircraft, the factors that are controllable in Equation 6-15 are P_{av}, S, and U'_S. Consequently, U_C, the energy that must be absorbed by the collapse of the cabin or the collapse of the protective shell, may be reduced by:

- Increasing the P_{av}, which is the average crushing force acting during the collapse of structure forward of the cabin. The P_{av} may be increased by providing a forward structure which will maintain a force as nearly uniform as possible. In addition, the P_{av} may be further increased by increasing the maximum force. However, the upper limit for the P_{av} is the forward acceleration tolerance of the occupants. The force required to crush the cabin in the forward direction should be well above either the P_{av} or the human tolerance.
- Increasing the available deformation distance, S, by maximizing the length of the nose on the aircraft.
- Increasing the deformation energy absorbed by aircraft structure other than the forward structure or the cabin structure.

Application of any of these principles to the airframe design, with a given cabin structural configuration, will make it possible for the aircraft to withstand impact at the design velocity without collapse of the protective shell.

THIS DOCUMENT PROVIDED BY THE ABBOTT AEROSPACE
TECHNICAL LIBRARY
ABBOTTAEROSPACE.COM

6.5.1.6 Design for Vertical Crashes

For a non-crashworthy aircraft in a vertical impact against a rigid surface, no possibility exists for a low-force (and therefore, a low-acceleration-level) event. The velocity change in the vertical direction must be accomplished in a short distance. Thus, when the vertical velocity component is high, these crashes are generally characterized by large structural deformation and high floor accelerations. Crashworthiness in the system design extends the deceleration by using a long-stroke landing gear, crushable underfloor structure, and stroking seats.

Figure 6-5 illustrates an approach to maintaining a protective shell and absorbing vertical crash energy. This protection can be accomplished by providing rollover strength in the form of stiffened ring frames on the top and sides of the fuselage. The crushable webs of the subfloor beams contribute strength and stiffness to satisfy the normal airworthiness criteria, and they also function as energy absorbers to attenuate the vertical crash impact forces.

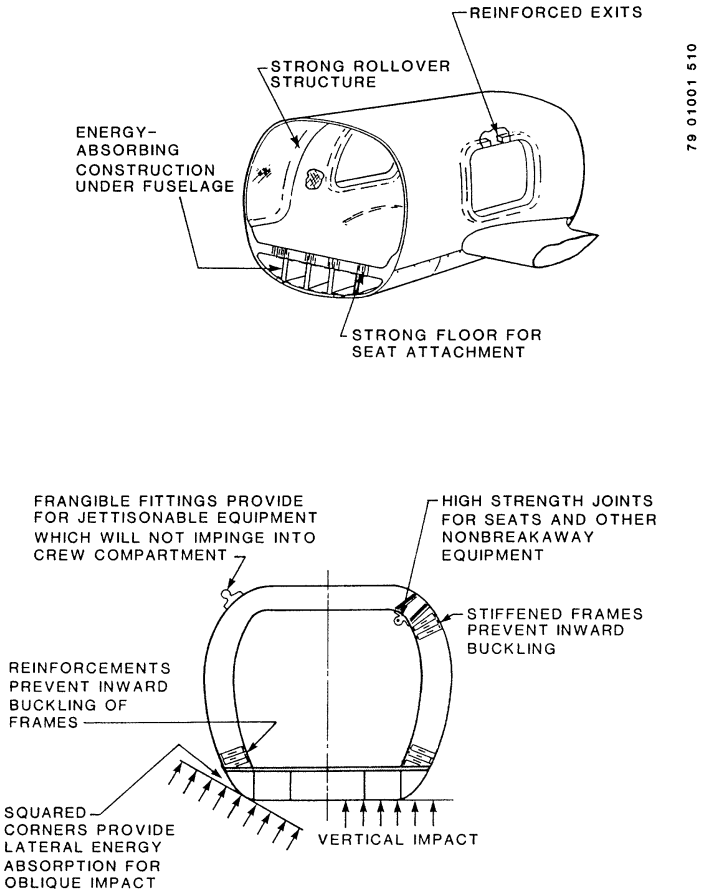


Figure 6-5.
Overall fuselage concepts (From Reference 6-36).

Figure 6-6 summarizes a design consideration for proper vertical energy absorption design. The landing gear, the crushable subfloor, the energy-absorbing seats, and the cabin must be designed to work together. The landing gear should be designed to produce deceleration loads less than the level required to stroke the seat or damage the structure. The load-deformation curve for the subfloor should exhibit a relatively uniform crushing load to provide efficient energy absorption. The crushable structure should not have a high peak load at the initiation of

THIS DOCUMENT PROVIDED BY THE ABBOTT AEROSPACE
TECHNICAL LIBRARY
ABBOTTAEROSPACE.COM

stroking. The cabin structure must be strong enough to prevent collapse of the cabin or elastic downward movement of the cabin roof during either the landing gear stroke or the subfloor crushing. The floor should stroke at a load slightly less than or equal to the stroking loads for the seat. The seat stroking load is determined by the human tolerance level in the vertical direction. Finally, the seats should provide enough stroke so that, when combined with the landing gear and the subfloor, the occupant is decelerated through a velocity change equal to the upper-limit crash design velocity. Also, the underfloor design should possess enough post-crush structural integrity to retain the seats through subsequent crash motions such as roll-over or slide-out.

The optimum energy-absorption capability of subfloor structure is a direct function of the available stroking distance between the cockpit/cabin floor and underside of the aircraft. This distance varies for different aircraft types. The stroke-to-length ratio of the involved structure should be such that the useful stroke is sufficient to provide the necessary energy absorption. This results in differing landing-gear-to-structure-to-seat energy-absorption distributions. Thus, for a given maximum crash velocity, sufficient stroke must be provided in the landing gear, subfloor, and seat. If design considerations limit the stroke available in one of these three subsystems, then either more stroke must be designed into the other two subsystems or the maximum survivable crash velocity for the design must be adjusted downward. This trade-off emphasizes the benefits provided by a crash-resistant seat that has been designed as an integral part of the aircraft.

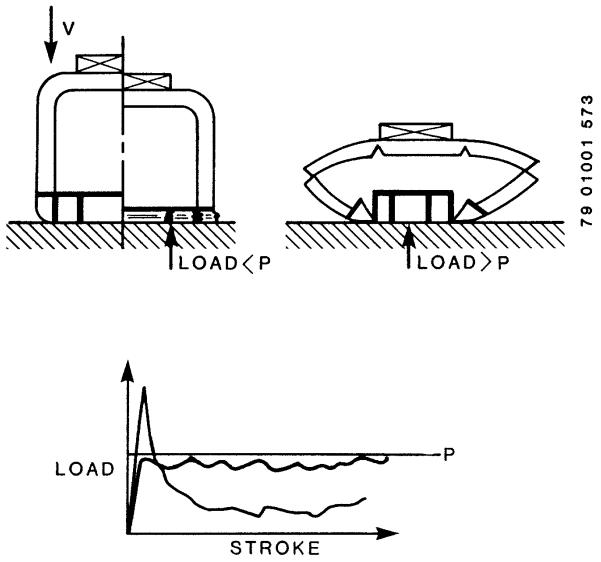


Figure 6-6.
Vertical impact crushing loads.

The vertical impacts in Figure 6-7 shows the result of a successful execution of this strategy. The heavy line shows the deceleration measured at the floor, and the dashed line shows the deceleration transmitted to the occupant by the seat pan. There is a constant low-level acceleration for an extended period of time as the gear strokes. This phase is followed by fuselage impact, which occurs at a much higher G level for a shorter time. (The gear may still be stroking and contributing to the load during this time). Seat stroke coincides with fuselage

THIS DOCUMENT PROVIDED BY THE ABBOTT AEROSPACE
TECHNICAL LIBRARY
ABBOTTAEROSPACE.COM

crush and continues afterward until the seat and occupant's energy is expended. The corresponding velocity and displacement are also shown to clarify the dynamics of the system interactions.

Design guidance for seats and restraints is provided in Chapter 7. Design guidance for the landing gear is provided in Section 6.5.3.

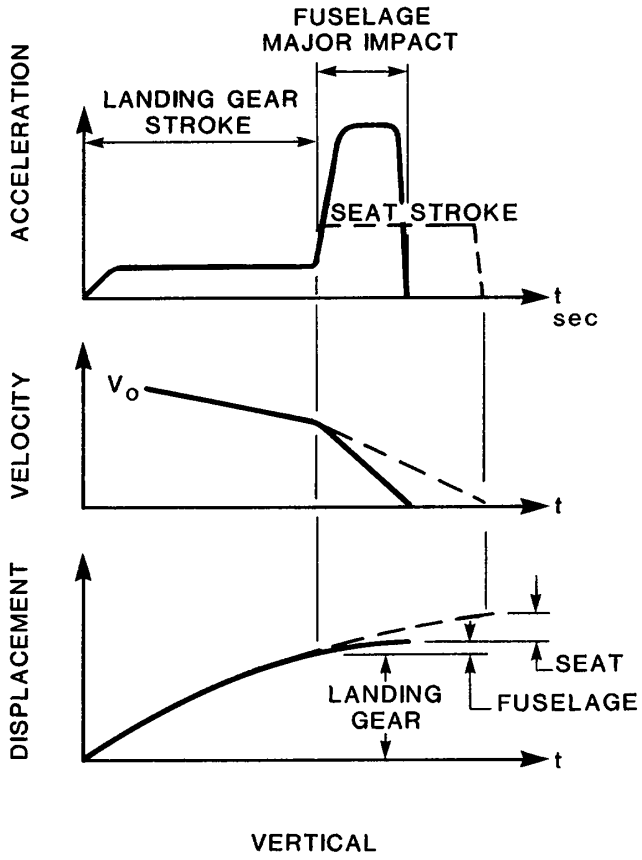


Figure 6-7.
Response of a successful crashworthy design to a vertical impact (solid line is floor, dashed line is seat pan).

6.5.1.7 Designing Load-limiting Subfloors

The fuselage underfloor structure can help protect occupants from high decelerations by absorbing energy during the crushing process that occurs during vertical impacts. This structure should demonstrate large plastic deformation during the crash. Metal structures generally accomplish this through the process of instability failures, followed by large plastic deformations. Some components are also capable of absorbing energy following compressive collapse. References 6-37 through 6-45 provide additional information concerning the mechanics of large-deformation structural energy absorption.

THIS DOCUMENT PROVIDED BY THE ABBOTT AEROSPACE
TECHNICAL LIBRARY
ABBOTTAEROSPACE.COM

Considerable work has been done to investigate various underfloor structural geometries capable of sustaining normal flight loads and landing loads while providing significant energy absorption during a crash with vertical velocity. Examples of such structures are shown in Figures 6-8 and 6-9. Other concepts are presented in References 6-46 through 6-48. These concepts, when used underneath a strong floor structure, result in the desired combination of a continuous strong floor and an energy-absorbing understructure.

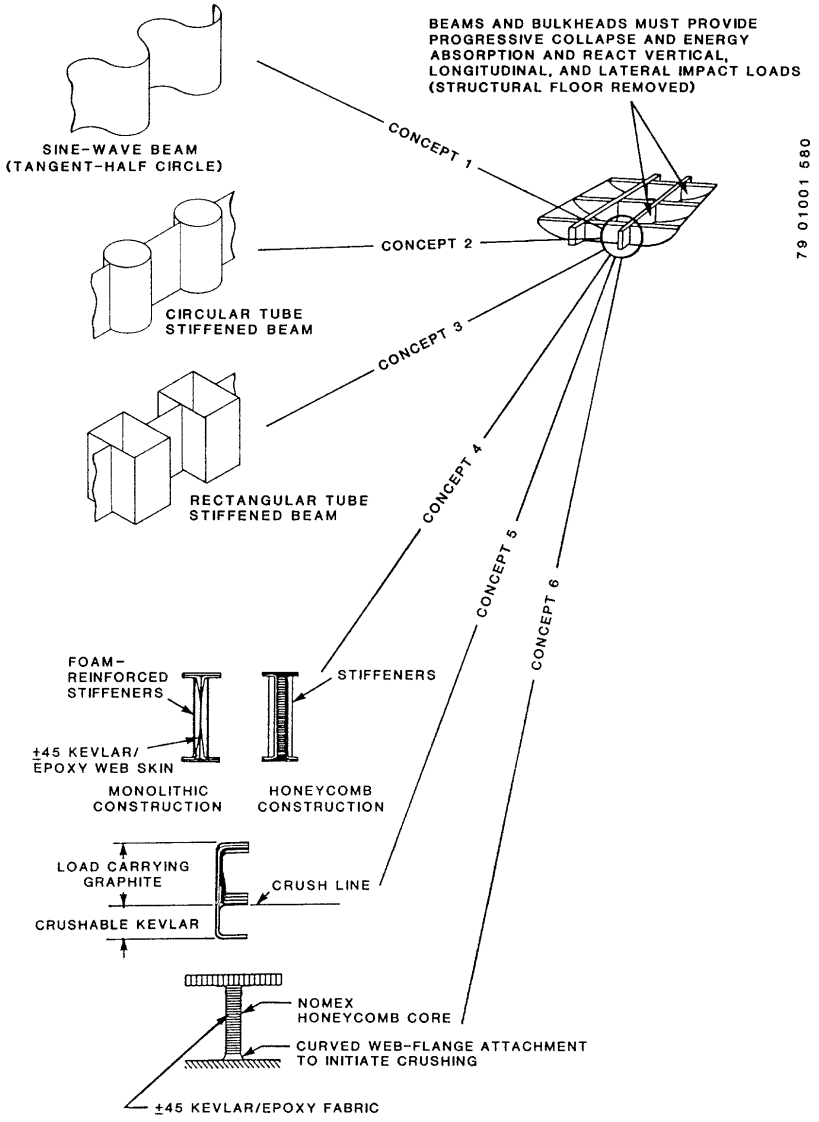


Figure 6-8.
Energy absorption concepts - beams and bulkhead (vertical impact).

The beam and bulkhead concepts shown in Figure 6-8 are designed to react to the vertical, longitudinal, and lateral impact loads; however, the most efficient direction for providing a progressive collapse is vertically. In each of the concepts shown, it is assumed that the floor structure would also be designed to react the crash impact forces without failure.

THIS DOCUMENT PROVIDED BY THE ABBOTT AEROSPACE
TECHNICAL LIBRARY
ABBOTTAEROSPACE.COM

Figure 6-8, Concepts 1, 2, and 3, are web designs for floor beams made of composite materials. These webs may be designed so that crushing is initiated at the desired load and the beam absorbs energy through progressive crushing of the web. The sine, circular, and square tube features of the web designs provide enhanced specific energy absorption. Performance can be analyzed based on a single cell or a section of the web, and extensive performance characterization studies have been made for various materials, lay-ups, and dimensions. Further information on the performance of these crushable beam webs is contained in Reference 6-15.

Figure 6-8, Concept 4, shows rib-stiffened floor beams constructed in a manner very similar to metal beams. However, their webs are designed to crush and absorb energy when they are subjected to high vertical loads. The stiffeners provide the buckling resistance necessary to ensure that the webs will crush rather then bend laterally under load. Component test results for this configuration are given in Reference 6-11.

Figure 6-8, Concept 5, is a solid laminate approach that utilizes the high strength of graphite fibers to provide the strong load-carrying portion of the floor structure. The crushable portion of the floor takes advantage of the favorable crushing mode of failure of Kevlar to provide its energy-absorbing capability. Test data and details are presented in Reference 6-28.

Figure 6-8, Concept 6, illustrates schematically a sandwich underfloor construction that consists of Kevlar/epoxy face sheets and a honeycomb core that crushes and provides energy absorption when the beam is subjected to crash loads. Further test data and details are presented in Reference 6-15.

The energy-absorbing concepts shown in Figure 6-9 are of aluminum construction. Details of these and other metallic concepts may be found in References 6-40 and 6-45.

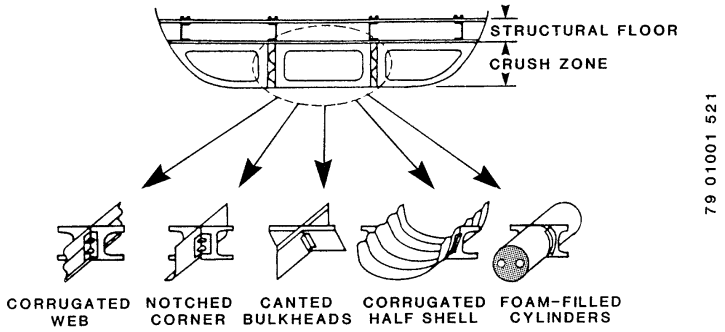


Figure 6-9.
Underfloor beams designed with potential energy-absorbing capability (Reference 6-46).

A fuselage concept using a crushable composite sandwich underfloor structure to absorb the crash impact kinetic energy is shown in Figure 6-10. The lightweight crushable underfloor structure is integral to the airframe and serves a dual purpose by providing the structural strength to withstand flight, landing, ditching, and floor loads, as well as the energy-absorption capacity to dissipate crash-impact kinetic energy and decelerate the aircraft until it is at rest.

THIS DOCUMENT PROVIDED BY THE ABBOTT AEROSPACE
TECHNICAL LIBRARY
ABBOTTAEROSPACE.COM

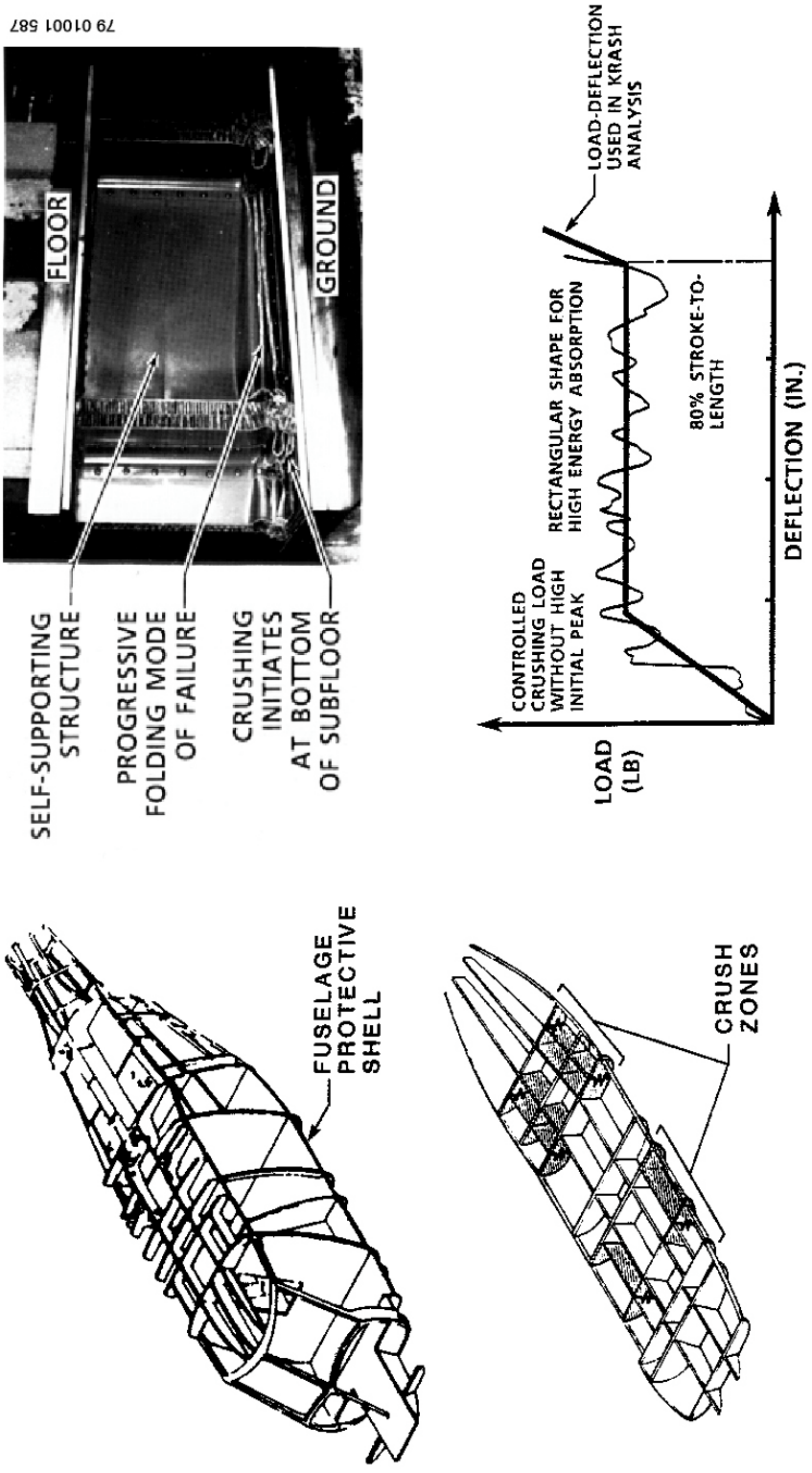


Figure 6-10.
Energy-absorbing underfloor structure.

THIS DOCUMENT PROVIDED BY THE ABBOTT AEROSPACE
TECHNICAL LIBRARY
ABBOTTAEROSPACE.COM

As shown in Figure 6-11, the composite energy-absorbing underfloor was developed in a systematic manner proceeding from design support testing, to full-scale cabin testing, to the incorporation of the underfloor into the design of the ACAP aircraft (Reference 6-49). Details of the cabin test configuration are shown in Figure 6-12. A mix of frangible and crushable structure was used to control crash loads under various impact conditions.

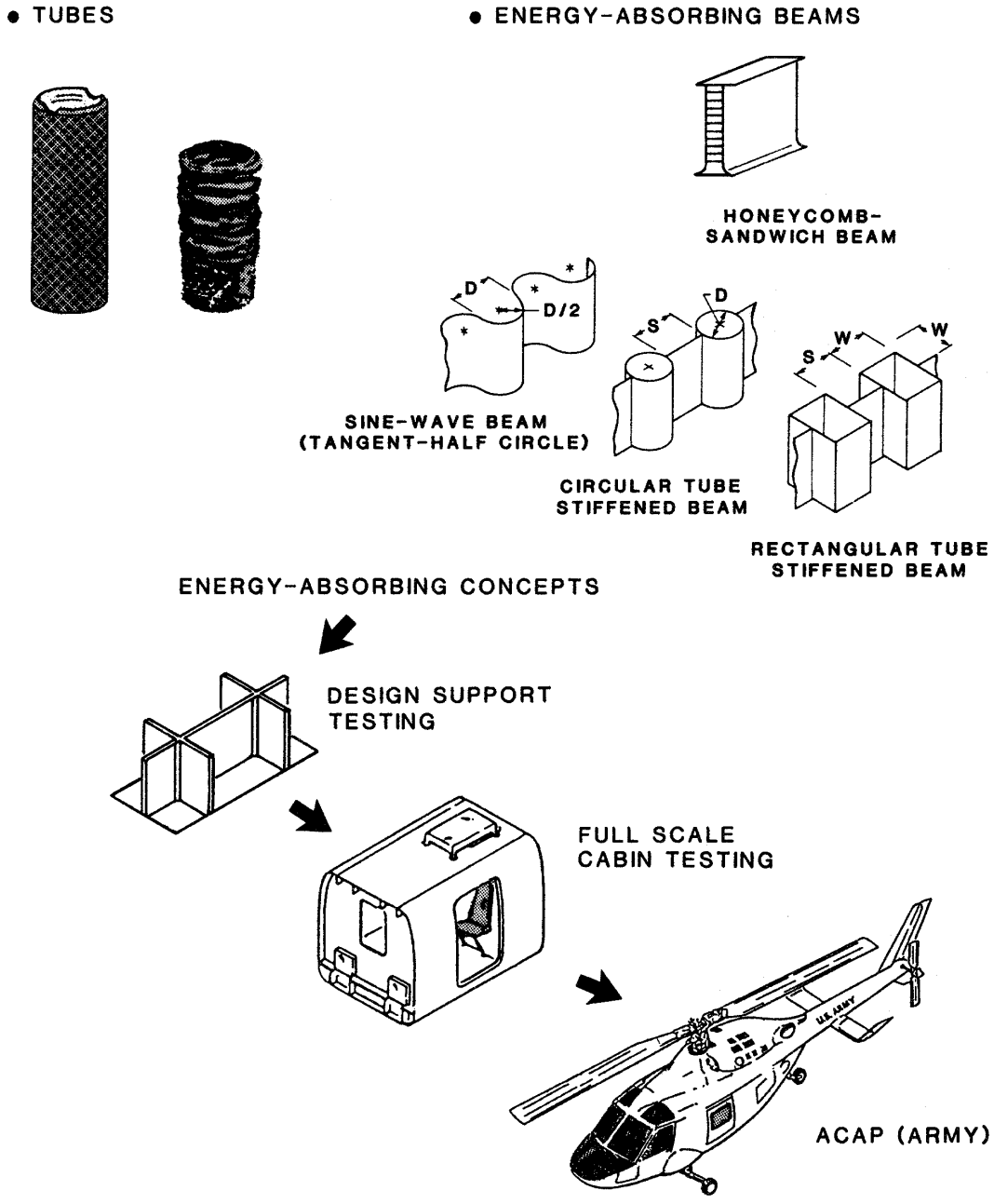


Figure 6-11.
Development of composite energy-absorbing underfloor structure (From Reference 6-49).

THIS DOCUMENT PROVIDED BY THE ABBOTT AEROSPACE
TECHNICAL LIBRARY
ABBOTTAEROSPACE.COM

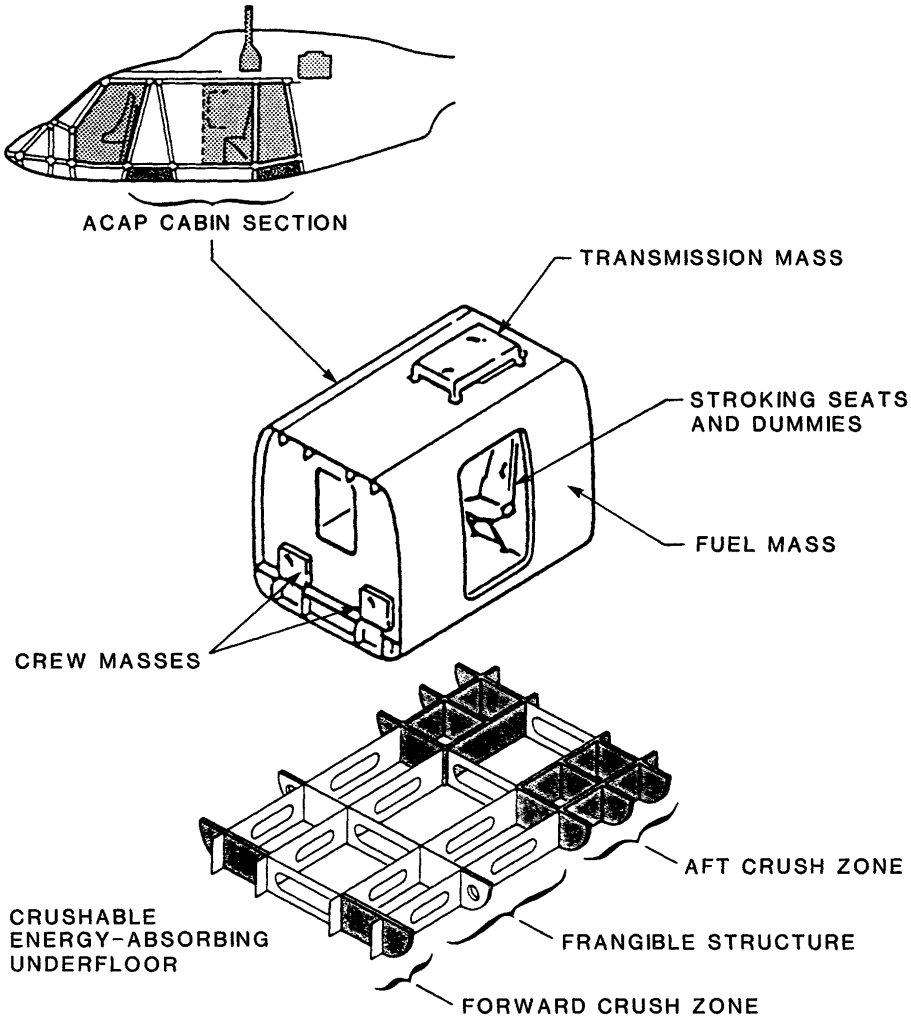


Figure 6-12.
Composite cabin test section.

Details of a low-cost castable polyurethane foam underfloor energy absorber design are described in Reference 6-47. A composite fuselage section was modified by filling the gap between the wing spars and lower skin with the foam, as shown in Figure 6-13. Dynamic drop tests were conducted with a baseline and a modified fuselage section. With just over 2 in. of stroking space available, the seat vertical accelerations dropped by 25 pct and the occupant lumbar load was reduced by 36 pct.

Another approach to absorbing energy in the subfloor is to use crushable materials. However, honeycombs, expanded foams, or similar materials share the major disadvantage of occupying much of the subfloor volume. Such space usage can result in system installation compromises, enlarged aircraft profiles, and increased primary structure weight to accommodate such energy-attenuation methods. Foams, in particular, usually have low stroke-to-height ratios. They do, however, still provide an energy-absorbing method warranting consideration.

THIS DOCUMENT PROVIDED BY THE ABBOTT AEROSPACE
TECHNICAL LIBRARY
ABBOTTAEROSPACE.COM

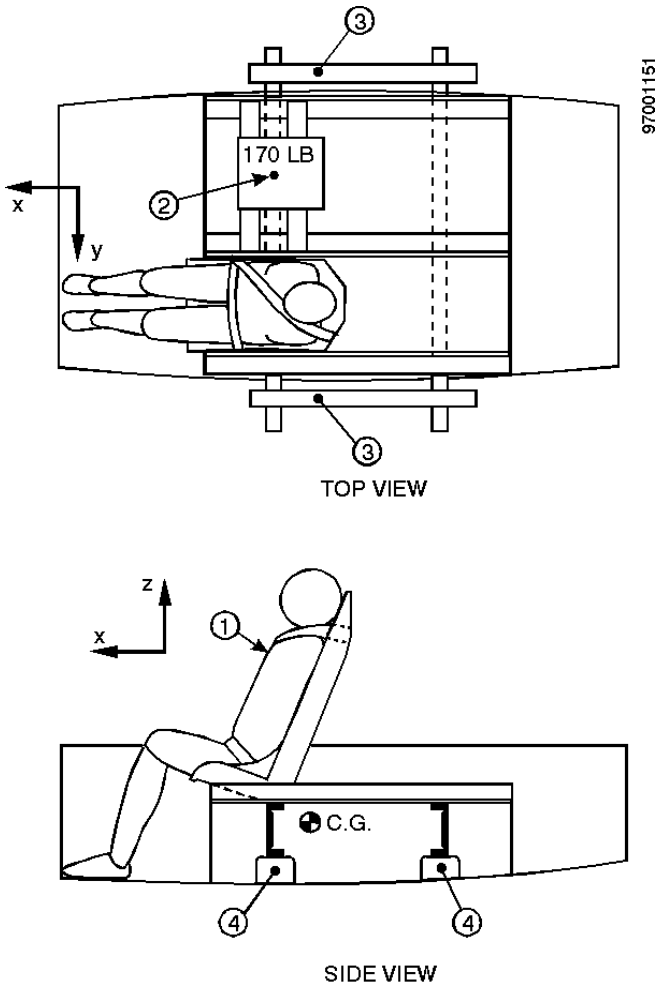


Figure 6-13.
Composite fuselage test section with polyurethane energy-absorbing elements (Reference 6-50).

6.5.1.8 Emergency Exit.
The structural framing of the emergency exits should be rigid enough to prevent deformation so that they remain operable following a crash. Ideally, the emergency exit closure will be expelled or released by the structure when structural damage does occur in a crash.

Exits should be placed in locations that are favorable for rapid egress. If components near exit locations are likely to be damaged to the extent that the exit will be blocked, allowances should be made to offset the partial blockage. An example is the location of an emergency exit near a landing gear attachment. Upon vertical impact, the landing gear could be driven upward into

This Document Provided by the Abbott Aerospace
TECHNICAL LIBRARY
ABBOTTAEROSPACE.COM

the floor structure, causing severe distortion of the floor structure and subsequent deformation of the emergency exit. Therefore, the floor should be reinforced near the exit or the relative locations of the landing gear and emergency exit should be changed.

6.5.2 Engine Mounts

The design of the engine mount is an important consideration in the “systems approach” design of a crashworthy GA aircraft (Reference 6-33). In a recent research investigation conducted by Terry, et al. (Reference 6-33), full-scale drop tower testing methods were used to evaluate the feasibility of integrating crashworthiness into individual components of an aircraft. One of the components selected was the engine mount. The objective of the engine mount work was to develop a dynamic analysis method for evaluating the engine mount during an impact and to verify the analysis method with quasi-static half-scale model tests onto a hard surface and soft soil. Analysis of the test data indicated that absorption of energy via the engine mount, as opposed to the cabin structure, increased accelerations at the rear seat for hard surface impacts by moving the ground reactions farther from the center of gravity (c.g.). This led to a second impact as the airplane rotated its tail down ("tail slap") with the severity of the second impact increasing as the measuring position moved aft. As a result, the rear seat loading was higher than the front seat loading for this class of airplane during the secondary impact.

These issues, among others, need to be addressed in the design of an engine mount. Engine mounts should be designed to keep the engines attached to the basic structural members supporting the mounts (nose section, wing, aft fuselage section, etc.) under the crash conditions cited in Section 6.1, even though considerable distortion of the engine mounts and/or support structure may occur. In GA aircraft, the engine represents a substantial portion of the total mass, so the engine mounts and surrounding structure should be carefully designed to retain the engine even if substantial deformation occurs. The breaking free of an engine can have devastating consequences if the loose engine contacts occupied space or fuel tanks.

6.5.3 Landing Gear

Landing gear, normally the aircraft’s first energy-absorbing subsystem to contact the ground, can contribute significantly to the avoidance of damage to the fuselage and mission equipment in hard landings and to the survival of the crew and passengers in severe survivable crashes. The performance of the landing gear depends heavily on the impacted terrain, as well as on the aircraft’s velocity and attitude. Ground that is firm, smooth, and level is conducive to the proper performance of the landing gear. In general, the closer the aircraft is to its nominal landing attitude, the more benefit the landing gear will provide. Likewise, the more the aircraft diverges from its nominal landing attitude, the less benefit the landing gear will provide.

The energy-absorbing capability of the landing gear is important primarily in the vertical impact, because maximum occupant protection can be obtained only if every inch of available vertical stopping distance is used to provide a controlled deceleration of the fuselage section. Since aircraft may sometimes impact with vertical velocities of 30 ft/sec or more, the landing gear should provide maximum energy absorption to reduce the velocity of the fuselage cabin before ground contact.

THIS DOCUMENT PROVIDED BY THE ABBOTT AEROSPACE
TECHNICAL LIBRARY
ABBOTTAEROSPACE.COM

The formula for calculating landing gear stroke is:

$$S = v^2/(2\eta gG)$$

where: S = The landing gear stroke
v = The vertical velocity of the aircraft
η = The energy absorbing efficiency of the landing gear
g = The gravitational constant
G = The uniform deceleration rate of the landing gear expressed in G's.

For example, a 10-G load-limited landing gear (at 100-pct EA efficiency) with a stroke of 6 in. would decelerate the aircraft completely from an impact with a vertical velocity of 18 ft/sec.

The benefits that could be gained from effective vertical energy-absorbing landing gear design extend even further. In the example, the fuselage would be protected from impacts until much of the vertical energy is dissipated for initial velocities up to 18 ft/sec. With the vertical energy absorption in the seats remaining the same, the limits of survivability could be extended. Also, less kinetic energy would be available for deformation of the fuselage structure. Less fuselage deformation means that the floor structure would remain more continuous, emergency exits would be more likely to operate, and flammable fluids could be contained in their tanks more easily. Thus, provision of effective energy-absorbing landing gear for high sink rates yields improvement of all survivability factors.

Longitudinal impacts present a different situation. In severe longitudinal impacts, kinetic energy levels are so great that effective use of landing gear as an energy absorber does not appear to be practical. Also, in these crashes, sufficient stopping distance is available (except perhaps in some very steep impacts) to keep accelerations to relatively low levels. In these crashes, landing gear failure occurs due to the gear's striking an abrupt obstacle, such as the lip of a runway. Experimental full-scale crash tests show that under these conditions, the energy absorbed in landing gear failure during impacts at velocities from 100 to 240 ft/sec is less than 1 pct of the total impact kinetic energy (Reference 6-51).

The problem to be faced in the design of landing gear for longitudinal impact, then, is not to provide energy absorption capable of protecting the occupiable portion of the aircraft, but to design landing gear systems so that failure of the gear does not produce increased danger for the occupants. The hazards involved include the rupture of flammable fluid tanks and lines and local penetration of the fuselage shell, particularly in the occupiable areas, by the landing gear components. NOTE: The damage caused by local penetration of the landing gear and the hazards it presents also occur in vertical impacts that cause gear failure. The use of proper energy-absorbing landing gear, however, can work to minimize this problem in vertical crashes.

Prevention of the hazards caused by the failure of the structure supporting the landing gear could be accomplished by locating the landing gear away from flammable fluid systems and occupiable areas. However, if isolation of the landing gear is impractical, then the landing gear components should be designed so that the gear is carried away on impact, with the points of failure located so that minimum damage to critical areas will occur. The particular problems associated with a specific aircraft will dictate the method to be used.

Certain operations will always be required in which impact might occur with a combined longitudinal velocity and vertical velocity. Provisions must be made to allow the landing gear to be driven upward and rearward into supporting structure without increasing the impact hazards. One method of accomplishing this would be to leave an open bay behind and above landing gear locations to permit "displacement" space.

This Document Provided by the ABBOTT AEROSPACE
TECHNICAL LIBRARY
ABBOTTAEROSPACE.COM

6.6 WINGS AND EMPENNAGE

Wing impacts usually occur in one of two ways. Either a tree, pole, or similar object is hit, producing highly concentrated loading, or the wing strikes a barrier, such as an earthen mound or a dike, which produces loading that is more evenly distributed along the wing's leading edge. Crushing and shear strength, for typical wings, will allow trees/poles to cut into the wing as the aircraft moves forward, until the wing is cut off or until the pole breaks. The fore-and-aft loads under these conditions are low in terms of their effect on fuselage accelerations. In fact, even the more evenly distributed loads can produce fuselage accelerations of perhaps only 5 G.

Wing failures in fixed-wing aircraft typically account for only 5 pct or less of the total kinetic energy that may be present in a crash of moderate velocity (Reference 6-52). Therefore, the use of the wing structure as an effective energy absorber does not appear to be promising. Increasing this energy-absorption capability would involve adding material to structural members that can already withstand normal loading. In all likelihood, most of the added material could not be used effectively for any particular crash.

The wings could be designed to break free from the fuselage structure under high longitudinal impact forces. Shedding the wings could reduce the mass considerably, especially if the wings contain fuel. As discussed earlier, this reduction could effectively reduce the energy absorption requirements for the cabin structure. Wing removal may also provide the possibility of removing flammable fluids away from the fuselage and occupants. However, the drawbacks of mass shedding that were discussed in Section 6.4.5 should be considered before settling on this strategy, as there may be additional issues that must be addressed. For instance, wings designed to be shed would require self-sealing breakaway fittings in the fuel transfer system to reduce the possibility of post-crash fire.

Empennage structure or, for that matter, any structure aft of the occupiable cabin, seldom provides beneficial energy-absorbing effects during a longitudinal crash. Instead, the mass tends to increase the loads that must be supported by the cockpit/cabin structure. Therefore, if empennage structures can be designed to collapse at a pre-determined load during a longitudinal impact, the requirements for cockpit/cabin structural strength and energy-absorption capability are reduced. This reduction is achieved because the force applied forward by the empennage mass deceleration is limited to the design crush load.

6.7 AIRFRAME AND COMPONENT DESIGN TESTING

In designing crash-resistant structures, testing is needed to support many phases of the work. In the design process, component tests are essential to the proper sizing and configuration of crash-resistant structures. Qualification tests verify that an airframe or components of an airframe will satisfy the crash-resistance performance requirements.

Tests may be either static or dynamic. A static test is usually performed by applying force(s) to a structural test component anchored to a rigid fixture, but can also be performed on a centrifuge. Static testing is suitable for many component design tests. Dynamic tests utilize high-rate deformation typical of a crash. They are usually conducted by impacting the test specimen into a mechanism or material that will deform in a controlled manner to simulate the dynamic response of the appropriate structural interface. For example, in seat tests, the fixture is decelerated in a manner that simulates the response of the aircraft's underfloor structure in a crash.

THIS DOCUMENT PROVIDED BY THE ABBOTT AEROSPACE
TECHNICAL LIBRARY
ABBOTTAEROSPACE.COM

Tests may be conducted with the full-scale structure, or with a scale model of the structure. A complete structure may be tested, or just a component of the structure. The type of test must be matched to the specific need for information. Typical possibilities are shown in Table 6-3. Scale-model testing is mostly useful for supporting analytical development efforts.

Table 6-3.
Types of test possibilities

	Static				Dynamic			
	Full Scale		Scale Model		Full Scale		Scale Model	
Application	Complete Structure	Compo-nent	Complete Structure	Compo-nent	Complete Structure	Compo-nent	Complete Structure	Compo-nent
Analysis - Component								
Characterization		X		X				
Analysis - Validation			X				X	
Design Support		X				X		
Qualification					X			

Full-scale component tests are primarily useful for design support, including analytical component characterization. Full-scale complete structure tests are appropriate for system qualification.

6.7.1 Structural Static Testing

Compatibility is important at the structural interfaces between the airframe and all attached components. The design of the fuselage structure, including the hard points and load distribution structure around the hard points, must be coordinated with the design of the attaching components. Structural properties for all loading conditions and design features, such as structural releases, must be coordinated to achieve the desired compatibility.

A comprehensive system design approach requires that such compatibility be demonstrated. Ideally, static tests of components attached to the fuselage structure by their normal attachment provisions should be performed to demonstrate compatibility. Components that should be tested include such items as seats, engines, transmission mounts, landing gear, and attachments for any ancillary or heavy equipment located in an area that could create a hazard for the occupants if freed during a crash. The ultimate design crash loads should be applied in all hazardous loading directions to demonstrate that the attachment points, as well as the load-bearing sections of the fuselage, are capable of maintaining structural integrity during a crash.

At a minimum, all components and their attachment hardware should be tested on suitable fixtures and hardpoints for their mounting, and the fuselage should be verified by a combination of analysis and complete aircraft system qualification testing.

6.7.2 Full-Scale Testing

Instrumented, full-scale crash test(s) may be conducted to: 1) verify the analyses performed, 2) substantiate the capability of the aircraft system to meet crash-resistance specifications, and 3) gather further engineering data on the impact response of aircraft structures.

This Document Provided by the Abbott Aerospace
TECHNICAL LIBRARY
ABBOTTAEROSPACE.COM

The present state of the art in the analysis of structural behavior under crash impact conditions is such that predictions of location and modes of collapse and failure, as well as predictions of impact forces, accelerations, and deformations, have only limited accuracy. For this reason, full-scale dynamic crash testing to complement and substantiate the analytical simulation of airframe behavior is highly recommended. Such crash tests should be conducted under conditions representative of a severe survivable crash, and testing should demonstrate that the required design specifications are met.

Full-scale tests of the complete aircraft can demonstrate proof of compliance for fuselage and related structures such as landing gear, engines, transmissions, seat tiedown provisions, and fuel cells and systems. Full-scale testing will validate that the entire energy-absorption system of landing gear, fuselage structure, and seats operate satisfactorily.

When full-scale crash tests are conducted, test results should also be carefully studied to provide information for design improvements to that specific aircraft design, as well as to provide background information to improve future aircraft designs.

Controlled testing has been done in the past on a variety of aircraft to demonstrate the capabilities of structure, landing gear, fuel systems, etc., in typical crash impact conditions (See, for example, References 6-53 through 6-58). Initially, such tests were often performed using powered aircraft that were remotely controlled or pre-aligned for impacts into selected terrain conditions. Useful data were obtained from many of these tests, although some resulted in significant post-impact fires and subsequent information loss.

A more recent approach for full-scale testing has been to drop test specimens from a fixed site or from a moving carrier. Structural assemblies, small aircraft, and helicopters have been tested in this manner. Representative impact conditions and velocities can be achieved by adjusting the vertical drop height and/or the longitudinal velocity of the carrier, as well as the roll and yaw attitudes of the aircraft.

The largest facility used for full-scale crash testing of light aircraft and helicopters is the Impact Dynamics Research Facility (IDRF) at the NASA Langley Research Center (Reference 6-59), shown in Figure 6-14. At this facility, aircraft are allowed to swing on cables that are pre-set to determine the overall impact attitude. Velocity components are controlled by varying the drop height, cable length, and cable anchor points. Immediately prior to impact, the aircraft is released from the cables by pyrotechnic means. The ground impact and subsequent motions are then completely unrestrained. A schematic of the NASA Langley facility is shown in Figure 6-15, and the test setup is that is shown is for the full-scale drop test of the YAH-63 helicopter.

The primary advantage of testing full-scale aircraft is that there is no need to interpret the data or attempt to extrapolate the results to other structural formats. All data such as velocities, attitudes, accelerations, and structural strains are measured directly as functions of time from impact. In addition, high-speed cameras can record displacement from various locations inside and outside the aircraft in order to provide visual time-histories of structural and occupant responses during the crash sequence. Instrumented anthropomorphic test devices (ATDs) positioned and restrained in seats with actual restraint systems aid in the evaluation of the occupant's potential for impacting the aircraft interior and for occupant survival. Post-crash review of damage also provides a direct indication of the aircraft's performance with respect to occupied volume penetration, seat and landing gear performance, large-mass item retention, and flammable fluid containment.

This Document Provided by the Abbott Aerospace
Technical Library
abbottaerospace.com

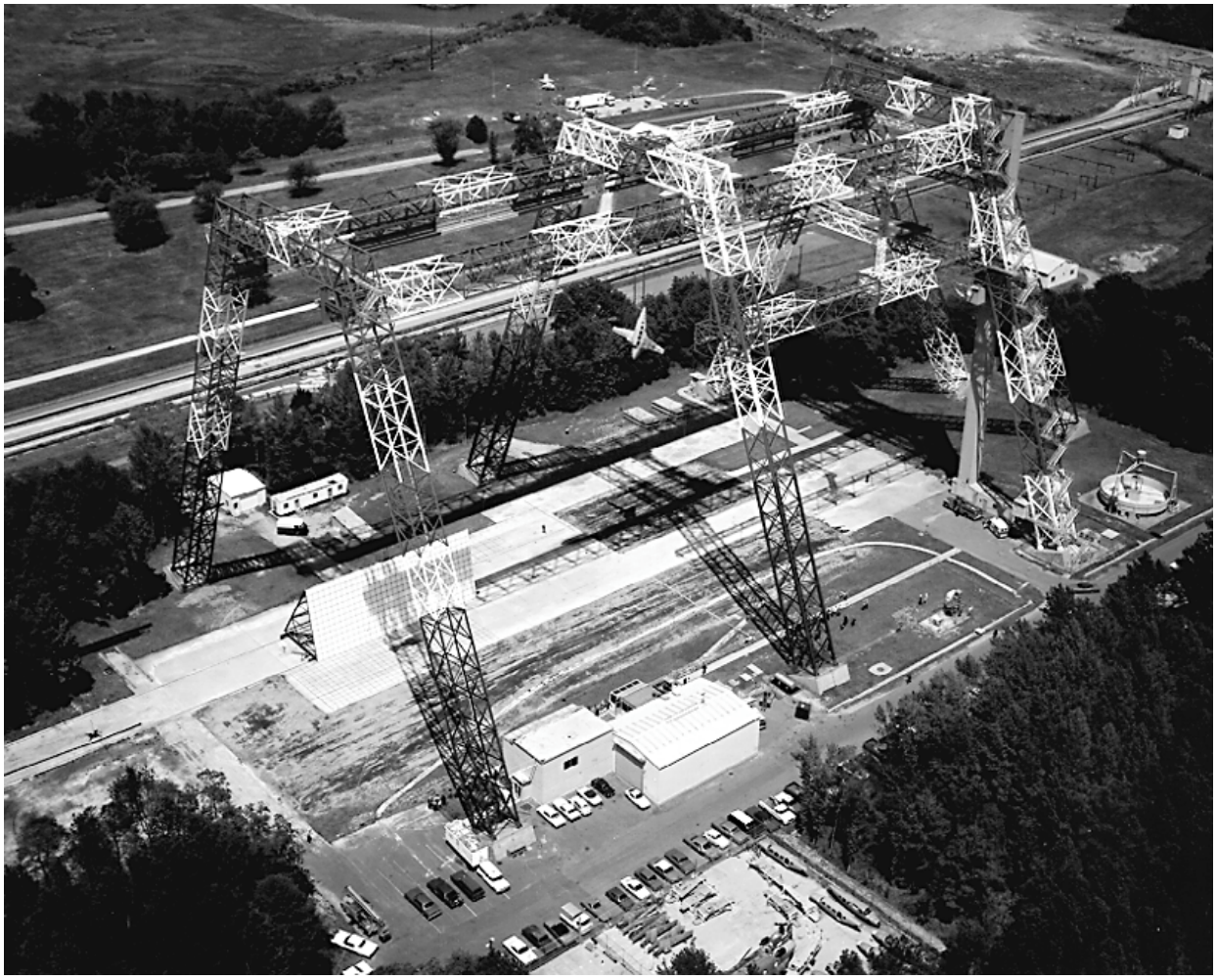


Figure 6-14.
The NASA Langley dynamic impact facility.

THIS DOCUMENT PROVIDED BY THE ABBOTT AEROSPACE
TECHNICAL LIBRARY
ABBOTTAEROSPACE.COM

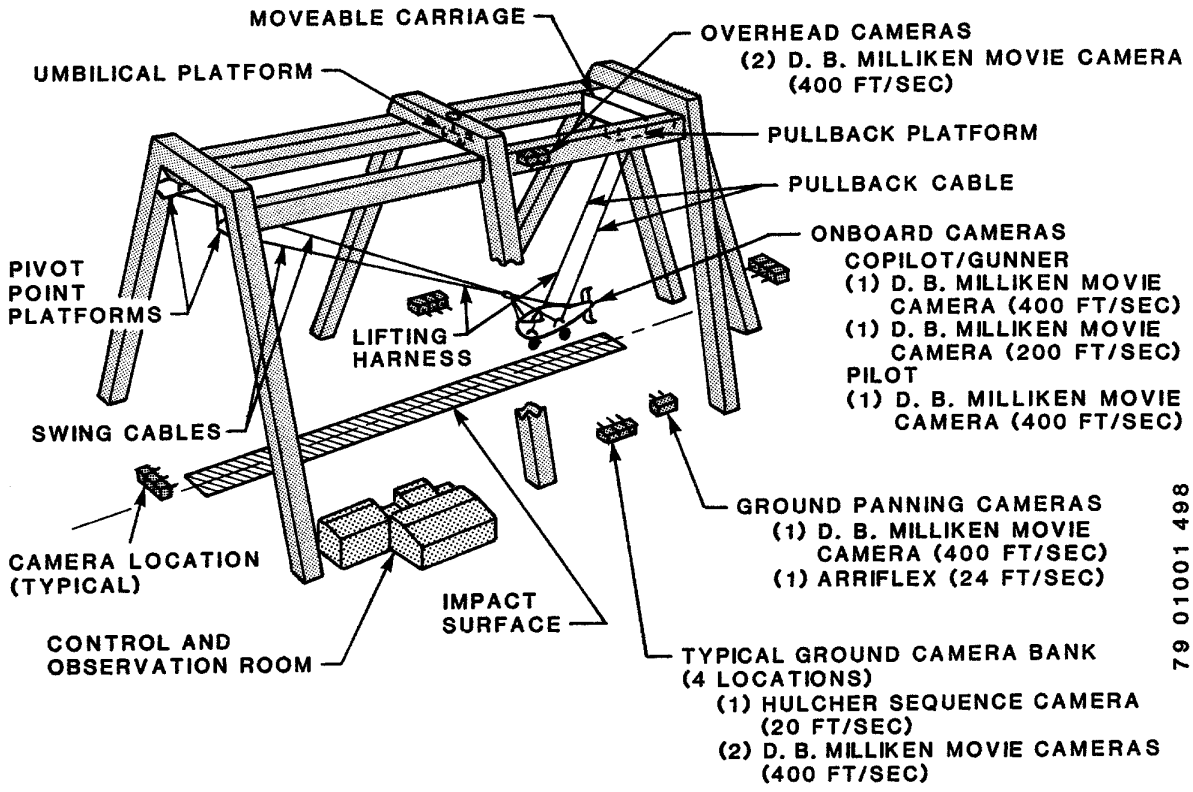


Figure 6-15.
NASA Langley crash facility layout and fixed camera positioning (from Reference 6-55).

For very small aircraft, full-scale testing may be the only way to obtain an assessment of the system's crash performance. The above description of full-scale testing may imply that this is the only technique worth using to attain realistic crash simulation. However, such tests are expensive to run, and aircraft, especially new design prototypes, are difficult to obtain. In addition, such tests require careful planning with a redundancy of recording equipment because of the probability that data may not be obtained from all instrumentation channels.

6.7.3 Scale-Model Testing

Scale-model testing has been used extensively when investigating the aerodynamic characteristics of aircraft, bridges, buildings, etc. Scale-model testing for structural strength and deflection verification also has been used where material sizes allow. For evaluating crash resistance, however, scale-model testing becomes a very difficult problem, especially when severe plastic deformation and element rupture occur.

Scale modeling of major structural members may provide data that can be used for crash-resistance studies; however, when semi-monocoque construction is considered, stringers and skin are often made from relatively thin sheet material, measuring from approximately 0.015 to 0.06 in. Depending on the structure being modeled, certain non-dimensional parameters must be satisfied for both the model and the aircraft. Examples of these are:

THIS DOCUMENT PROVIDED BY THE ABBOTT AEROSPACE
TECHNICAL LIBRARY
ABBOTTAEROSPACE.COM

$$\frac{X_i}{L}, \varepsilon, \frac{\sigma}{E}, \dot{\varepsilon}t, \frac{vt}{L} \tag{6-16}$$

where X_i = spatial coordinate
L = characteristic length
ε = strain
σ = stress
E = Young's Modulus
$\dot{\varepsilon}$ = strain rate
t = time
v = velocity

Some of these parameters involve the thickness of the material, and, for example, scaling 0.016-in.-thick sheet metal for a one-tenth scale model poses major problems in the manufacture, handling, and tolerance effects when using 0.0016-in. shim material.

Reference 6-58 presents a discussion of scale-modeling techniques applied to structural crash resistance. Practical considerations in geometric scaling are discussed and illustrated using barrier tests of two different automobile front-end structures and an impulsively loaded section of semi-monocoque cylinder similar to an aircraft fuselage.

6.8 FIREWALL LOAD ESTIMATION

The information presented in this section was provided courtesy of Steve Hooper and Marilyn Henderson of the National Institute for Aviation Research at Wichita State University.

6.8.1 Background

The crash dynamics of GA aircraft vary depending on the characteristics of the impact surface. Several full-scale crash tests of GA aircraft have been conducted at the NASA Langley IDRF (References 6-33, 6-56, 6-60 though 6-65). Test articles are often observed to rebound into the air twice during severe (high-velocity, nose-down) hard-surface tests of composite airframes before sliding out on the impact surface. A tail slap-down response has frequently been observed for nose-down tests, but this response seems to be more pronounced in tests of composite airframes at the higher impact velocities.

Soft-soil tests produce a very different response. An aircraft displaces a large mass of soil during a soft-soil impact. In these tests, the ejected soil was projected a considerable distance downrange from the impact point. The momentum transfer associated with the soil ejection imposes significant forces on the lower forward fuselage.

Many pre-1990 GA aircraft designs tested at the NASA Langley IDRF did not perform very well in soft-soil crash tests (References 6-60 and 6-63). Many of these airframes exhibited very high longitudinal decelerations that were either associated with forward fuselage loads of such a magnitude that they compromised the survivable volume or they defeated the occupant protection systems (seats and restraints). In many cases, the source of these high loads is the momentum transfer produced as the aircraft displaces soil during the impact event. Terry reported that approximately 560 lb of soil was ejected from the crater in his first soft-soil test and 390 lb of soil in his second soft-soil test (Reference 6-33). This ejected material was distributed up to 300 ft downrange from the impact point.

THIS DOCUMENT PROVIDED BY THE ABBOTT AEROSPACE
TECHNICAL LIBRARY
ABBOTTAEROSPACE.COM

Terry studied the behavior of a GA aircraft impacting a soft-soil surface and concluded that a crashworthy GA aircraft must be designed to "ride up" on the soil much like a ski glides over snow. He also identified the engine mount and lower cowl structure as the two important components in a crashworthy system that must be designed to produce the desired, low-acceleration, response. Finally, he restated the necessity of designing the lower firewall in a manner that does not scoop soil. This feature was clearly described in the U.S Army Crash Survival Design Guide (Reference 6-1), but was generally not reflected in many of the pre-1990 GA aircraft designs.

The importance of a non-scooping design is easily explained in terms of fundamental impulse-momentum theory. The familiar impulse-momentum equation is written as

$$\int_{t_1}^{t_2} F(t)\,dt = mV_2 - mV_1 \qquad (6\text{-}17)$$

When applying this equation, it is important to recognize that the velocity change $V_2 - V_1$ is a function of the crash conditions, not the airplane design. Also recall that it is necessary to attenuate the forces $F(t)$ to levels tolerable to the occupants. Clearly, this becomes more likely as the stopping time t_2 - t_1 increases, and it is this increasing of the stopping time that is precisely the function of the engine mount / cowl / lower firewall system. It is of fundamental importance to recognize that the occupant protection is significantly enhanced by designing the vehicle to maximize the vehicle's stopping time. In many good designs, this is achieved without employing any energy-absorbing structures.

The engine mount/cowl /lower firewall system is also critical in managing the vertical component of the momentum change since it is this structure that makes first contact with the ground. Thus, it is this same structure that must appropriately resist the contact forces and produce the pitching moments that rotate the aircraft's velocity vector to a direction parallel to the ground. The deformation characteristics of the engine mount are very important in producing the desired airframe response and may, as in the case of the Terry designs, involve non-conservative energy-absorbing mechanisms.

While it is not possible to directly measure impact forces during full-scale drop tests, it is relatively easy to measure accelerations at various locations in the test articles. This section describes an analysis procedure that can be used to develop airframe design loads from these acceleration data. This analysis presumes the AGATE impact condition, which has been defined as 30-deg nose-down impact at V_{so}. The aircraft kinematics following the impact are illustrated in Figure 6-16 below. The symbols defined for the analysis are listed in Table 6-4.

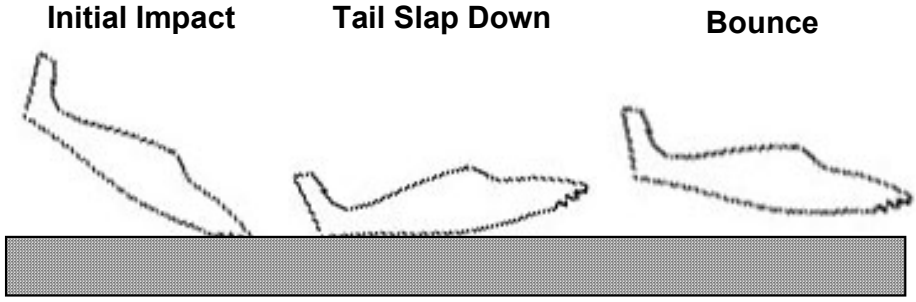


Figure 6-16.
Aircraft kinematics following impact.

THIS DOCUMENT PROVIDED BY THE ABBOTT AEROSPACE
TECHNICAL LIBRARY
ABBOTTAEROSPACE.COM

Table 6-4. Symbols	
Variable	**Description**
a	Distance
b	Distance
C_x, C_z	Contact force
d	Distance
F_{LX}, F_{LZ}	Lower engine mount forces
F_{UZ}, F_{UZ}	Upper engine mount forces
h	Distance
I_{YY}	Aircraft moment of inertia about the pitch axis
I_{YYe}	Engine moment of inertia about the pitch axis
m	Aircraft mass
m_e	Engine mass
n_x, n_z	Load factor
V_{fp}	Velocity
Wt	Weight
Wt_e	Engine weight
x	Aircraft longitudinal axis
$\bar{x}_e$	Distance between the aircraft and engine centers of gravity (defined in Figure 6-19)
$\ddot{x}$	Longitudinal acceleration
z	Aircraft vertical axis
$\ddot{z}$	Vertical acceleration
γ	Flight path angle of the aircraft
θ	Pitch angle of the aircraft
$\ddot{\theta}$	Pitch acceleration
Subscripts	
x	x direction
y	y direction
z	z direction

6.8.2 Analysis

An engineer needs two kinds of information to address crashworthiness issues in aircraft design. The first is a definition of the loads that the aircraft cabin structure must be designed to resist, and the second is the accelerations to which the occupants will be exposed. This presumes that the aircraft design includes a crashworthy engine mount and that the vehicle response is known at the start of this analysis. The nose-down impact condition is illustrated in Figure 6-17.

THIS DOCUMENT PROVIDED BY THE ABBOTT AEROSPACE
TECHNICAL LIBRARY
ABBOTTAEROSPACE.COM

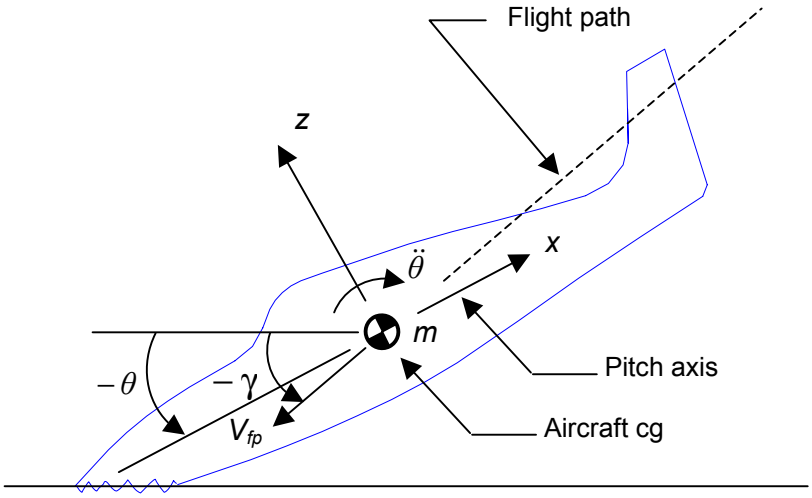


Figure 6-17.
Nose-down impact condition.

The aircraft response is predicted using classical rigid-body dynamics analysis based on the free-body diagram shown in Figure 6-18.

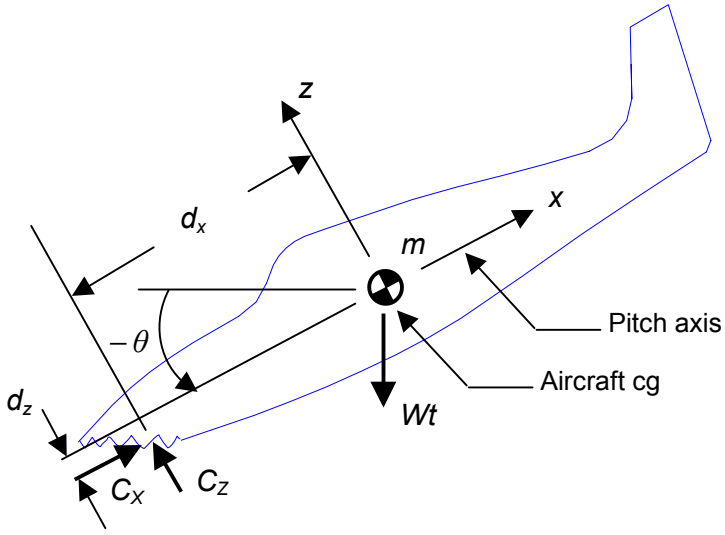


Figure 6-18.
Contact forces.

THIS DOCUMENT PROVIDED BY THE ABBOTT AEROSPACE
TECHNICAL LIBRARY
ABBOTTAEROSPACE.COM

The governing equations are summarized as

$$\sum F_x = m\,\ddot{x} = C_X + Wt\sin\theta \tag{6-18}$$

$$\sum F_z = m\,\ddot{z} = C_Z - Wt\cos\theta \tag{6-19}$$

$$\sum M_{cg} = I_{yy}\,\ddot{\theta} = d_x C_Z - d_z C_X \tag{6-20}$$

Note that nose-up pitch rotations θ are defined as positive. Hence, negative values for this variable should be substituted into Equations 6-18 through 6-20 when they are evaluated for aircraft orientations such as that shown in Figure 6-18. The distances d_x and d_z locate the contact forces as illustrated in Figure 6-18. The magnitudes of the contact forces are evaluated by substituting the acceleration of the c.g. into Equations 6-18 and 6-19. These data are generally acquired at points along the fuselage of the drop test articles. A least-squares analysis of these data produces the following relationship for the vertical acceleration as a function of fuselage station *x* shown in Equation 6-21 below. The angular acceleration $\ddot{\theta}$ is the negative of the slope of the line produced by the linear regression.

$$\ddot{z} = \ddot{z}_{CG} - \ddot{\theta}\,x \tag{6-21}$$

The location of the contact force, defined by the distances d_x and d_z cannot be determined from the remaining governing equation without assuming a value for one of these variables. In this analysis, d_z is assumed; in other cases it may be possible to estimate this moment arm from video data of the crash test. Note that these equations can only be solved for the location of non-zero-contact forces. An attempt to evaluate the equation for the position of a zero-contact force will produce a trivial singular solution.

The impact loads on the cabin are analyzed using a free-body diagram of the engine mount and nacelle, shown in Figure 6-19.

The equilibrium equations for this free body diagram are presented below. Note that Equation 6-21 relates the engine acceleration to the aircraft acceleration. Specifically,

$$\ddot{z}_e = \ddot{z}_{CG} - \ddot{\theta}\,\bar{x}_e \tag{6-22}$$

where $\bar{x}_e$ is the difference in fuselage stations between the aircraft c.g. and the engine c.g. and $\ddot{\theta}$ is the pitch acceleration. Summation of forces yields Equations 6-23 and 6-24, where, as above, the reader is reminded that the pitch angle is defined as a negative quantity.

$$\sum F_X = m_e\,\ddot{x} = C_X + F_{UX} + F_{LX} + Wt_e\sin\theta \tag{6-23}$$

$$\sum F_Z = m_e\,\ddot{z}_e = C_Z + F_{UZ} + F_{LZ} - Wt_e\cos\theta \tag{6-24}$$

Assuming that the vertical shear force is equally shared between the upper and lower engine mounts results in the following equation for the average vertical force acting on the firewall

$$F_{UZ} = F_{LZ} = \left(m_e\,\ddot{z}_e + Wt_e\cos\theta - C_Z\right)/2 \tag{6-25}$$

The same result would be obtained if these forces were calculated using a rigid-body analysis. Summing moments about the lower engine mount attach point yields the following:

$$\sum M_L = I_{YYe}\,\ddot{\theta} \tag{6-26}$$

$$I_{YYe}\,\ddot{\theta} = d\,C_Z - x_e\left(Wt_e\cos\theta + m_e\,\ddot{z}_e\right) - h\left(m_e\,\ddot{x}_e - Wt_e\sin\theta\right) + b\,F_{UX} - a\,F_{UZ} \tag{6-27}$$

THIS DOCUMENT PROVIDED BY THE ABBOTT AEROSPACE
TECHNICAL LIBRARY
ABBOTTAEROSPACE.COM

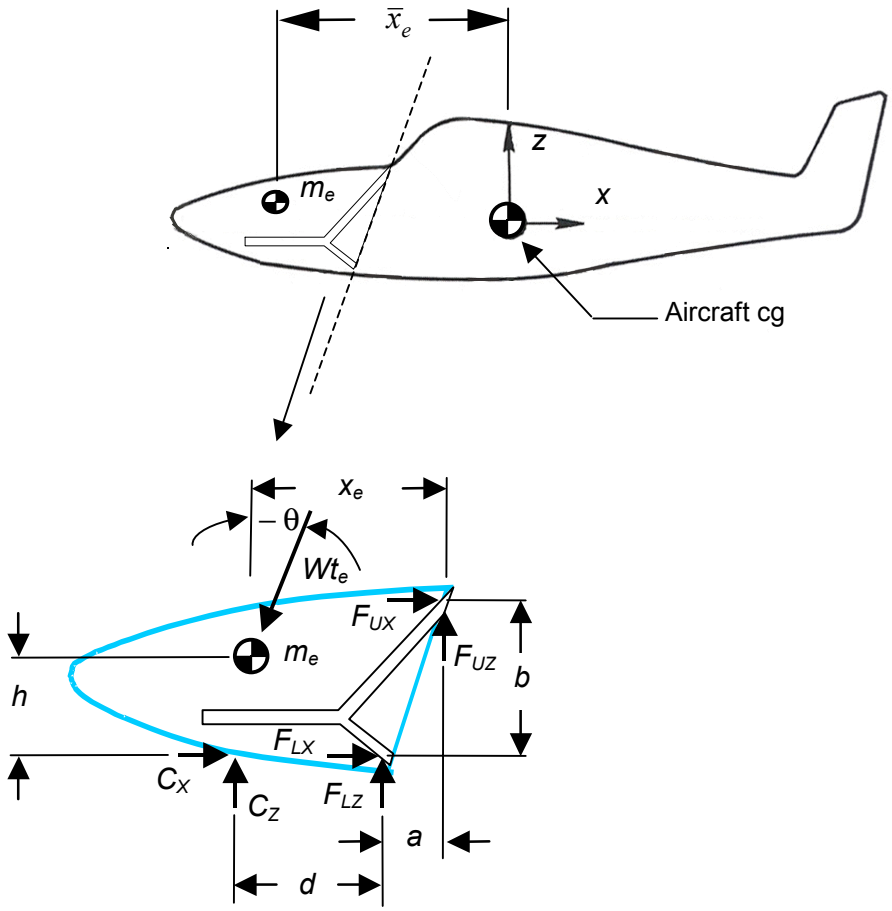


Figure 6-19.
Firewall free body diagram.

that can be solved for F_{UX}. Note that this equation neglects the contribution of the longitudinal acceleration of the engine, since the engine c.g. and the aircraft c.g. are considered to be at nearly the same waterlines.

$$F_{UX} = \left(I_{YYe}\,\ddot{\theta} + x_e\left(Wt_e\cos\theta + m_e\,\ddot{z}_e\right) + h\left(m_e\,\ddot{x}_e - Wt_e\sin\theta\right) + a\,F_{UZ} - d\,C_Z\right)/b \qquad (6\text{-}28)$$

F_{LX} is now determined from Equation 6-23, as

$$F_{LX} = m_e\,\ddot{x} - C_X - F_{UX} - Wt_e\sin\theta \qquad (6\text{-}29)$$

Note that the quantities calculated using Equations 6-25 through 6-29 represent the forces acting on both sides of the aircraft; thus, they are twice the magnitude of the engine mount forces acting on the left and right sides of the fuselage.

THIS DOCUMENT PROVIDED BY THE ABBOTT AEROSPACE
TECHNICAL LIBRARY
ABBOTTAEROSPACE.COM

Crashworthiness load factors for the aircraft cabin are now easily defined using these results and the standard definitions:

$$n_x = -(F_{UX} + F_{LX}) / Wt \tag{6-30}$$

$$n_z = -(F_{UZ} + F_{LZ}) / Wt \tag{6-31}$$

where Wt represents the weight of the test article.

Terry's "Full-Scale Test 3, Soft-Soil" (Test 3) data will be now be used to illustrate this analysis technique (Reference 6-33). Using drop-test data from accelerometers located at the lower engine mount attachments, the pilot and co-pilot seat floors, and a rear floor location, time-histories for the longitudinal forces at the aircraft c.g., the vertical forces at the aircraft c.g., and the angular accelerations of the aircraft were calculated.

The longitudinal forces were calculated using the accelerations measured at the lower engine mounts. These data were used based on completeness of test data and the assumption of rigid-body behavior. The longitudinal acceleration data is presented in Figure 6-20, and the longitudinal force data is presented in Figure 6-21.

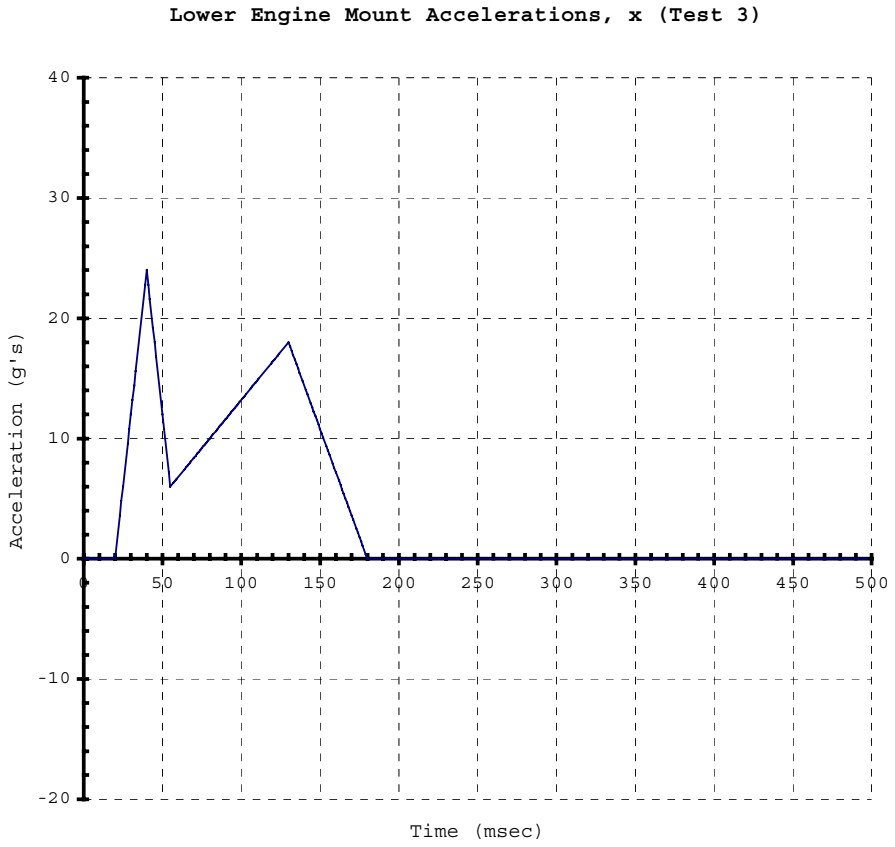


Figure 6-20.
Longitudinal lower engine mount accelerations, $\ddot{x}$ (Reference 6-33).

THIS DOCUMENT PROVIDED BY THE ABBOTT AEROSPACE
TECHNICAL LIBRARY
ABBOTTAEROSPACE.COM

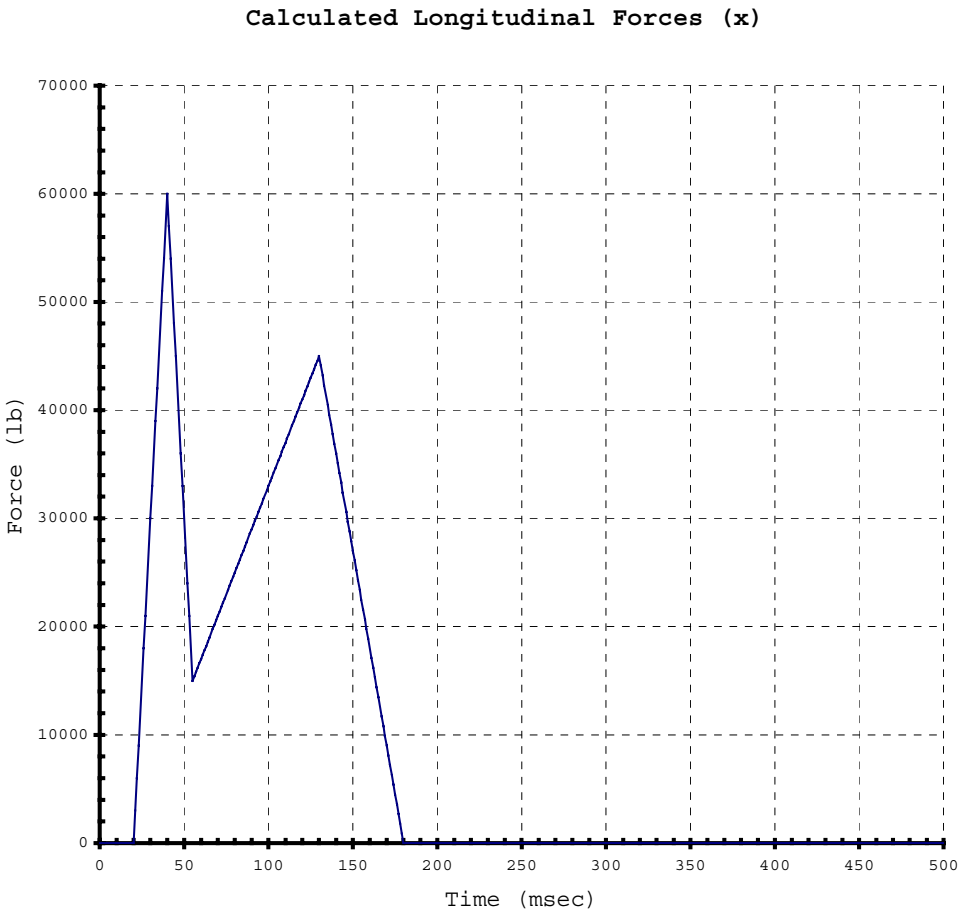


Figure 6-21.
Longitudinal force time-history (Reference 6-33)

The vertical forces were calculated using the accelerations measured at all three accelerometer locations. It was assumed that the pilot/co-pilot seat floor accelerometer positions represent the longitudinal location of the aircraft c.g. The vertical acceleration data from the three accelerometers were analyzed by the method of least squares, fitting a straight line through the three acceleration values, and then extracting an acceleration value from the line at the assumed c.g. location. These resulting vertical acceleration data at the c.g. are shown in Figure 6-22. The corresponding vertical force data is presented in Figure 6-23.

The pitching acceleration of the airplane, $\ddot{\theta}$, was simply calculated as the slope of the resulting straight line of the least-squares representation of $\ddot{z}(x)$ described above. These results are shown in Figure 6-24.

These data were then used along with the free-body diagram in Figure 6-19 and Equations 6-22 through 6-29 to calculate the longitudinal and vertical loads at the engine mount attachment locations. The time-histories for F_{UX}, F_{LX}, and $F_{UZ} = F_{LZ}$ are presented in Figures 6-25, 6-26, and 6-27.

THIS DOCUMENT PROVIDED BY THE ABBOTT AEROSPACE
TECHNICAL LIBRARY
ABBOTTAEROSPACE.COM

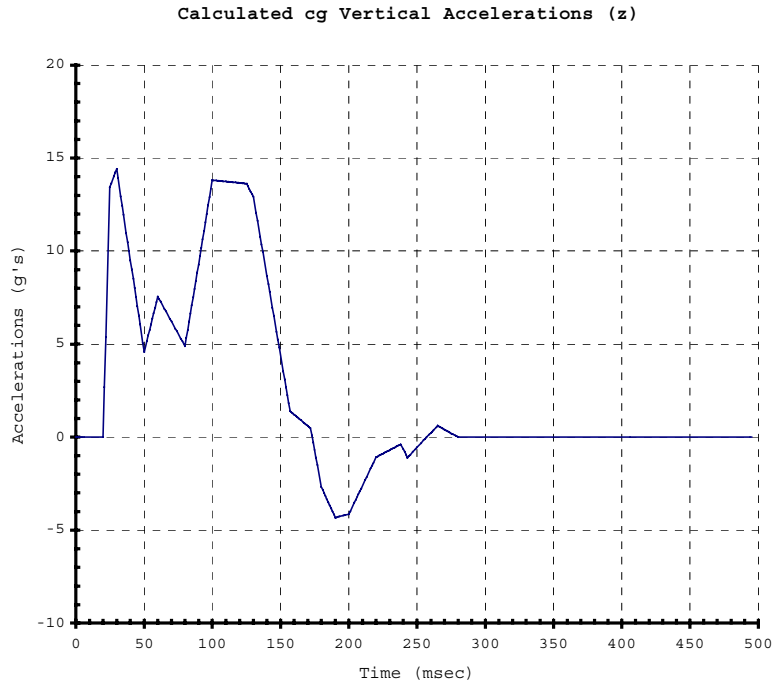


Figure 6-22.
Vertical accelerations at airplane center of gravity, $\ddot{z}$ (Reference 6-33).

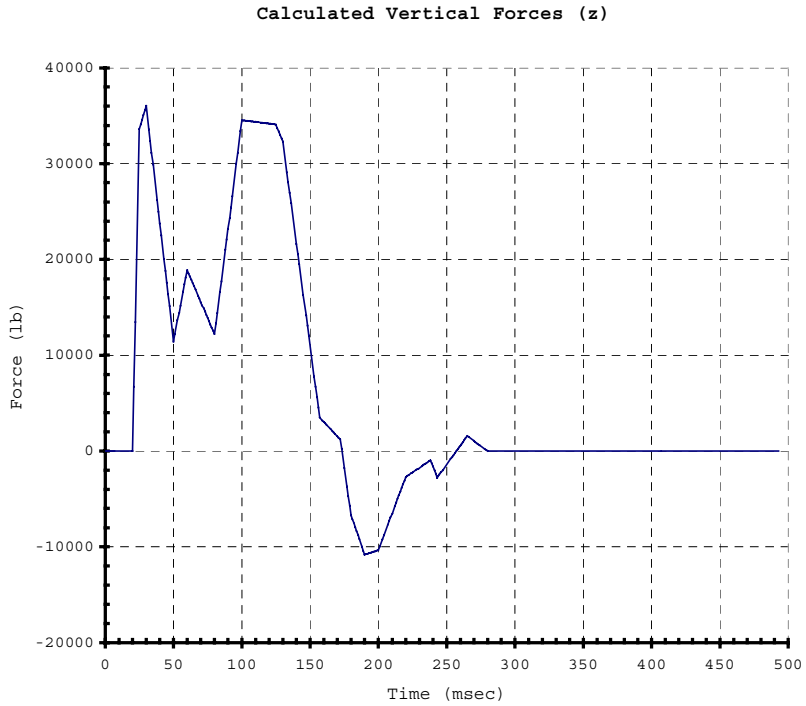


Figure 6-23.
Vertical force time-history (Reference 6-33).

THIS DOCUMENT PROVIDED BY THE ABBOTT AEROSPACE
TECHNICAL LIBRARY
ABBOTTAEROSPACE.COM

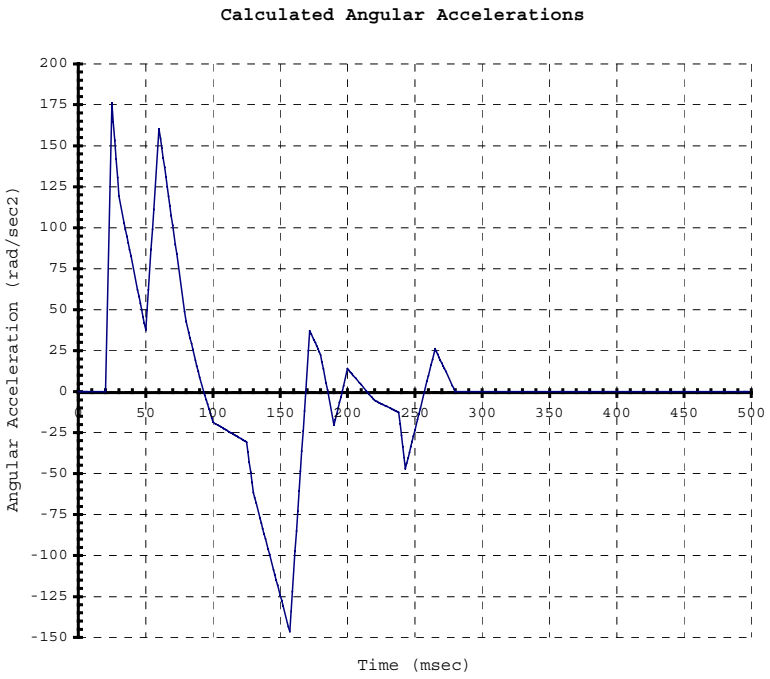


Figure 6-24.
Aircraft pitch accelerations, $\ddot{\theta}$ (Reference 6-33).

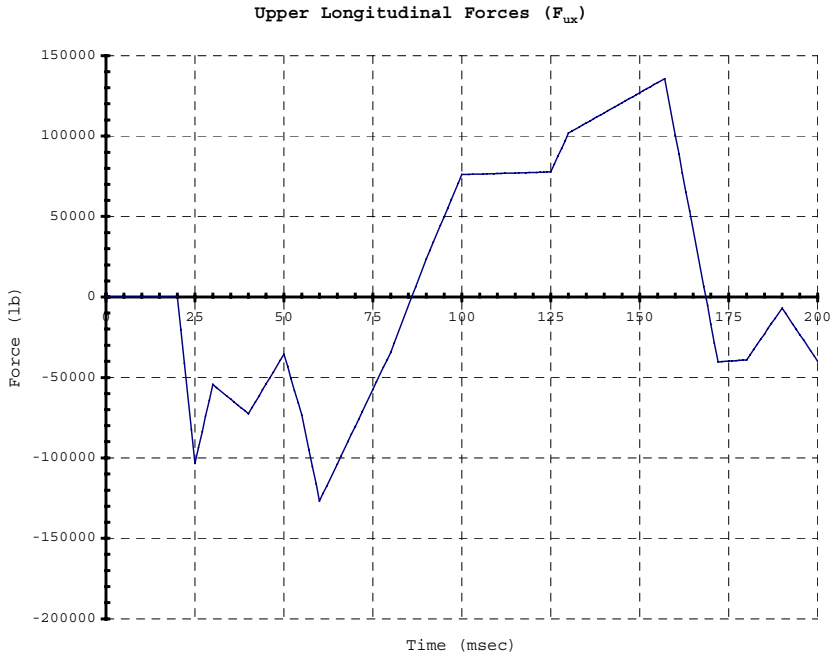


Figure 6-25.
Longitudinal loads at upper engine mount attachment points, F_{UX} (Reference 6-33).

THIS DOCUMENT PROVIDED BY THE ABBOTT AEROSPACE
TECHNICAL LIBRARY
ABBOTTAEROSPACE.COM

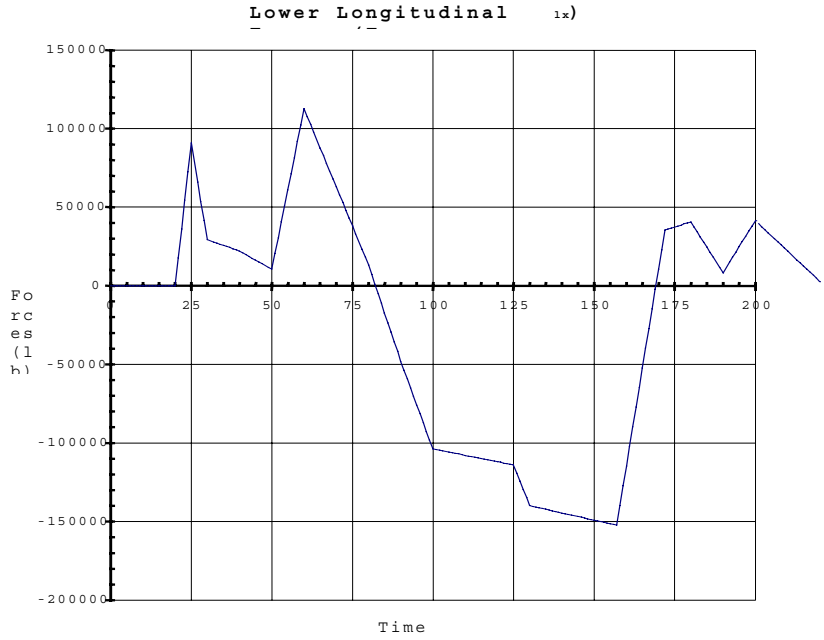


Figure 6-26.
Longitudinal loads at lower engine mount attachment points, F_{LX} (Reference 6-33).

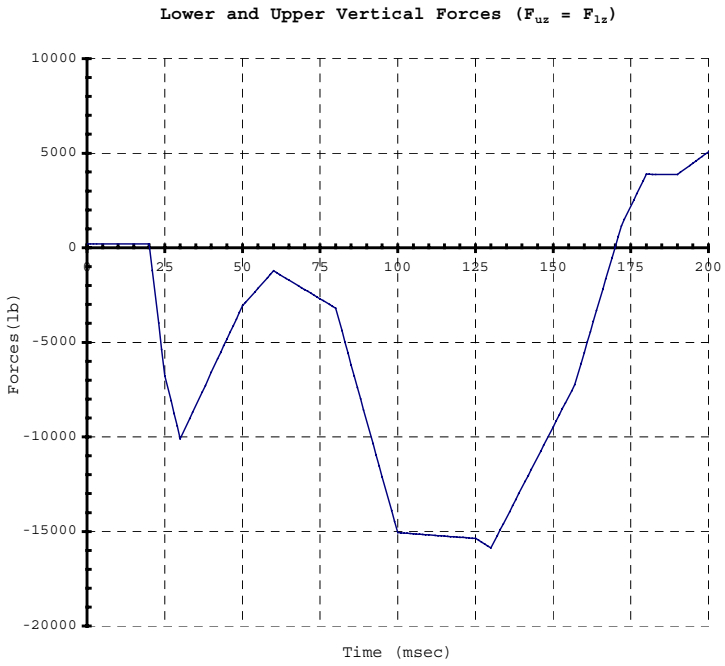


Figure 6-27.
Vertical loads at lower and upper engine mount attachment points, $F_{UZ} = F_{LZ}$ (Reference 6-33).

THIS DOCUMENT PROVIDED BY THE ABBOTT AEROSPACE
TECHNICAL LIBRARY
ABBOTTAEROSPACE.COM

Looking at the resultant of the longitudinal forces at the aircraft c.g. and the vertical forces at the aircraft c.g., the initial maximum resultant load occurs at *t* = 40 msec. At this time, then, the loads on the aircraft cabin are as follows:

Longitudinal load factor

$$n_x = \frac{-(F_{UX} + F_{LX})}{Wt} = \frac{50{,}400\ lb.}{2{,}500\ lb.} = 20.16 \tag{6-32}$$

Vertical load factor

$$n_z = 1 + \frac{-(F_{UZ} + F_{LZ})}{Wt} = 1 + \frac{13{,}200\ lb.}{2{,}500\ lb.} = 6.28 \tag{6-33}$$

It is interesting to compare the load factors for Test 3 to those prescribed for occupants in 14 CFR Part 23.561(b)(2), which specifies a vertical load factor of 3.0 G and a forward load factor of 9.0 G. The definitions differ in that the engine load factors n_x and n_z are applied simultaneously, whereas the load factors specified in 14 CFR Part 23.561 are applied one at a time.

THIS DOCUMENT PROVIDED BY THE ABBOTT AEROSPACE
TECHNICAL LIBRARY
ABBOTTAEROSPACE.COM

References

6-1. Simula, Inc., Aircraft Crash Survival Design Guide Volume III - Aircraft Structural Crash Resistance, Phoenix, Arizona, December 1989.

6-2. Hooper, S. J., Henderson, M. J., Seneviratne, W. P., “Design and Construction of a Crashworthy Composite Airframe,” National Institute for Aviation Research - Wichita State University, Wichita, Kansas, August 9, 2001.

6-3. Federal Aviation Regulation Part 23, Airworthiness Standards: Normal, Utility, Acrobatic, and Commuter Category Airplanes, Section 23.561, “General,” Washington, D.C., October 22, 2001.

6-4. Federal Aviation Regulation Part 23, Airworthiness Standards: Normal, Utility, Acrobatic, and Commuter Category Airplanes, Section 23.562, “Emergency Landing Dynamic Conditions,” Washington, D.C., October 22, 2001.

6-5. Military Handbook, MIL-HDBK-17, "Plastics for Aerospace Vehicles, Part I, Reinforced Plastics", Department of Defense, Washington, D.C.

6-6. Military Handbook, MIL-HDBK-5, "Metallic Materials and Elements for Aerospace Vehicle Structures", Department of Defense, Washington, D.C.

6-7. Ezra, A. A., Fay, R. J., "An Assessment of Energy-Absorbing Devices for Prospective Use in Aircraft Impact Situations", Dynamic Response of Structures, Pergamon Press, New York, New York, 1972, pp. 226-246.

6-8. Kirsh, P. A., Jahnle, H. A., "Energy Absorption of Glass Polyester Structures", SAE Technical Paper Series No. 810233, The Budd Company Technical Center, SAE International Congress and Exposition, Bobo Hall, Detroit, Michigan, February 23-27, 1981.

6-9. Gustafson, A. J., Shek, N. G., Singley, G. T, Impact Behavior of Fibrous Composites and Metal Substructures, Report No. USAAVRADCOM TR-82-D-31, Applied Technology Laboratory, U.S. Army Research and Technology Laboratories (AVRADCOM), Fort Eustis, Virginia, October 1982.

6-10. Cronkhite, J. D., Hass, T. J., Winter, R., Siongley, G. T., III, Investigation of the Crash Impact Characteristics of Composite Airframe Structures, Bell Helicopter Textron, Inc., Fort Worth, Texas, Grumman Aerospace Corporation, Bethpage, New York, and Applied Technology Laboratory, U.S. Army Research and Technology Laboratories (AVRADCOM), Fort Eustis, Virginia, paper presented at the 34th National Forum of the American Helicopter Society, Washington, D.C., May 1987.

6-11. Sen, J. K., Votaw, M. W., "A Skin-Stringer Design for a Crashworthy Composite Fuselage for the Hughes 500E Helicopter", Hughes Helicopter, Inc., paper presented at the 41st Annual Forum of the American Helicopter Society, Fort Worth, Texas, May 16-17, 1985.

6-12. Carden, H. D., "Impact Dynamics Research on Composite Transport Structures", NASA Technical Memorandum 86391, National Aeronautics and Space Administration, Langley Research Center, Hampton, Virginia, March 1985.

6-13. Farley, G. L., "Energy Absorption of Composite Material and Structure", Aerostructures Directorate, U.S. Army Aviation Research and Technology Activity (AVSCOM), Hampton, Virginia, paper presented at the American Helicopter Society 43rd Annual Forum and Technology Display, St. Louis, Missouri, May 18-20, 1987.

This Document Provided by the ABBOTT Aerospace
TECHNICAL LIBRARY
ABBOTTAEROSPACE.COM

6-14. Farley, G. L., "Effect of Fiber and Matrix Strain on the Energy Absorption of Composite Materials", NASA Langley Research Center, Hampton, Virginia, paper presented at the 41st Annual Forum of the American Helicopter Society, May 16-17, 1985.

6-15. Cronkhite, J. D., "Impact of MIL-STD-1290 Crashworthiness Requirements on the Design of Helicopter Composite Structures", Bell Helicopter Textron, Inc., Fort Worth, Texas, Paper No. 1567, presented at the 42nd Annual Conference of Society of Weight Engineers, Inc., Anaheim, California, May 23-25, 1983.

6-16. McComb, H. G., Jr., Safe Structures for Future Aircraft, NASA Langley Research Center, Astronautics and Aeronautics, September 1983.

6-17. Gibbs, H. H., "K-Polymer Composite Materials - A New Approach to Damage-Tolerant Aerospace Structures", E. I. Du Pont de Nemours and Co., Inc., Wilmington, Delaware, SAE Technical Paper Series 841518, paper presented at the Aerospace Congress and Exposition, Long Beach, California, October 16-18, 1984.

6-18. Alexander, J. V., Messinger, R. H., Advanced Concepts for Composite Structure Joints and Attachment Fittings - Volume I; Design and Evaluation, Hughes Helicopter Division of Summa Corp., Culver City, California, Report No. USAAVRADCOM TR-81-D-21A, Applied Technology Laboratory, U.S. Army Research and Technology Laboratories (AVRADCOM), Fort Eustis, Virginia, November 1981, AD A110212.

6-19. Cronkhite, J. D., Berry, V. L., Winter, R., Investigation of the Crash Impact Characteristics of Helicopter Composite Structures, Bell Helicopter Textron, Inc., and Grumman Aerospace Corporation, Report No. USAAVRADCOM TR-82-D-14, Applied Technology Laboratory, U.S. Army Research and Technology Laboratories (AVADCOM), Fort Eustis, Virginia, February 1983, AD B071763L.

6-20. Foye, R. L., Hodges, W. T., "Some Results from a Crash Energy Absorption Test for Evaluating Composite Fuselage Construction", U.S. Army Research and Technology Laboratories (AVRADCOM), Applied Technology laboratory, Fort Eustis, Virginia, and Structures Laboratory, NASA Langley Research Center, Hampton, Virginia, paper presented at the 37th Annual Forum of the American Helicopter Society, New Orleans, Louisiana, May 1981.

6-21. Sen, J. K., "Designing for a Crashworthy All-Composite Helicopter Fuselage", Hughes Helicopters, Inc., Culver City, California, paper presented at the 40th Annual Forum of the American Helicopter Society, Arlington, Virginia, May 16-18, 1984.

6-22. Rich, M. J., "Design, Fabrication, and Test of a Complex Helicopter Airframe Section", Sikorsky Aircraft Division of United Technologies Corporation, Stratford, Connecticut, Paper No. 801213, Society of Automotive Engineers, Inc., Warrendale, Pennsylvania, 1980.

6-23. Minecci, J. J., Hess, T. E., "Composite Fuselage Development for Naval Aircraft", Naval Air Development Center, Warminster, Pennsylvania, paper presented at the 25th National SAMPE Symposium and Exhibition, May 6-8, 1980.

6-24. Kindervator, C. M., "Crash Impact Behavior and Energy Absorbing Capability of Composite Structural Elements", DFVLR, Stuttgart, FRG, Visiting Scientist at the Air Force Materials Laboratory/MLBM, Wright-Patterson Air Force Base, Ohio, paper presented at the 30th National SAMPE Symposium, March 19-21, 1985.

THIS DOCUMENT PROVIDED BY THE ABBOTT AEROSPACE
TECHNICAL LIBRARY
ABBOTTAEROSPACE.COM

6-25. Thornton, P. M., Harwood, J. J., Beardmore, P., "Fiber-Reinforced Plastic Composites for Energy Absorption Purposes", Ford Motor Company, Dearborn, Michigan, paper presented at the International Symposium on Composites: Materials and Engineering, University of Delaware, Newark, Delaware, September 24-28, 1984, published in Composite Science and Technology 24 (1985), 276-298, by Elsevier Applied Science Publishers, Ltd. (England).

6-26. Torres, M., "Development of Composite Material Helicopter Structures", Helicopter Division, Aerospatiale, paper presented at the 37th Annual Forum of the American Helicopter Society, New Orleans, Louisiana, May 1981.

6-27. Kay, B. F., "ACAP Structural Design", Sikorsky Aircraft Division, United Technologies Corporation, Stratford, Connecticut, paper presented at the 39th Annual Forum of the American Helicopter Society, May 19-11, 1983.

6-28. Goldberg, J., Camaratta, F. A., "Crashworthiness of the ACAP Design", Sikorsky Aircraft Division, United Technologies Corporation, Stratford, Connecticut, paper presented at the 39th Annual Forum of the American Helicopter Society, May 9-11, 1983.

6-29. Mazza, L. T., Foye, R. L., "Advanced Composite Airframe Program Preliminary Design Phase", U.S. Army Research and Technology Laboratories (AVRADCOM), Fort Eustis, Virginia, and Moffett Field, California, paper presented at the 36th Annual Forum of the American Helicopter Society, Washington, D.C., May 1980.

6-30. Alsmiller, G. R., Jr., Anderson, W. P., Advanced Composites Airframe Program - Preliminary Design, Volume I - Basic Report (Part I), Bell Helicopter Textron, Inc., Fort Worth, Texas, Report No. USAAVRADCOM TR-80-D-37A, Applied Technology Laboratory, U.S. Army Research and Technology Laboratories (AVRADCOM), Fort Eustis, Virginia, February 1982, AD B063687L.

6-31. Cronkhite, J. D., Mazza, L. T., "Bell ACAP Full-scale Aircraft Crash Test and KRASH Correlation", Bell Helicopter Textron, Inc., Fort Worth, Texas, and Aviation Applied Technology Directorate, U.S. Army Aviation Research and Technology Activity (AVSCOM), Fort Eustis, Virginia, paper presented at the 44th Annual Forum and Technology Display of the American Helicopter Society, Washington, D.C., June 16-18, 1988.

6-32. Clarke, C. W., "Evolution of the ACAP Crash Energy Management System, Engineering Structural Technologies - Loads and Criteria", United Technologies - Sikorsky Aircraft, Stratford, Connecticut, paper presented at the 44th Annual Forum and Technology Display of the American Helicopter Society, Washington, D.C., June 16-18, 1988.

6-33. Terry, J. E., Hooper, S. J., Nicholson, M., Design and Test of an Improved Crashworthiness Small Composite Airframe - Phase II Report, NASA SBIR Contract NAS1-20427, Terry Engineering, Andover, Kansas, October 1997.

6-34. Cronkhite, J. D., Tanner, A. E., “Tilt Rotor Crashworthiness,” Bell Helicopter Textron, Inc., Fort Worth, Texas, and Boeing Vertol Company, Philadelphia, Pennsylvania, presented at the 41st Annual Forum of the American Helicopter Society, Forth Worth, Texas, May 15-17, 1985.

6-35. Castle, C. B., Alfaro-Bou, E., "Light Airplane Crash Tests at Three Flight-Path Angles", NASA Technical Paper 1210, NASA Langley Research Center, June 1978.

This Document Provided by the Abbott Aerospace
TECHNICAL LIBRARY
ABBOTTAEROSPACE.COM

6-36. Cronkhite, J. D., et al., Investigation of the Crash-Impact Characteristics of Advanced Airframe Structures, Bell Helicopter Textron, Inc., USARLT Technical Report 79-11, U.S. Army Research and Technology Laboratories (AVRADCOM), Fort Eustis, Virginia, April 1979, AD A0751063.

6-37. Jones, N., Wfierzbicki, T., Eds, Structural Crashworthiness, a book of 15 lectures presented at the First International Symposium on Structural Crashworthiness, Department of Mechanical Engineering at the University of Liverpool, September 14-16, 1983, published by Butterworths, London, England.

6-38. Sharman, P. W., "Energy Absorption of Channel Beams During Gross Deformation", Department of Transport Technology, Loughborough University of Technology, Vehicle Structural Mechanics, Fourth International Conference Proceedings, Code 811303, SAE 1981 Proceedings.

6-39. Gannon, B. T., Maris, J. L., Waldrop, P. S., Crew Survivable Helicopter Undercarriage, LTV Vought Corporation, Report No. AMMRC TR 84-1, Army Materials and Mechanics Research Center, Watertown, Massachusetts, January 1984.

6-40. Cronkhite, J. D., Berry V. L., Crashworthy Airframe Design Concepts - Fabrication and Testing, NASA Contractor Report No. 3603, September 1982.

6-41. Mahmood, H. F., Paluszny, A., "Design of Thin Walled Columns for Crash Energy Management - Their Strength and Mode of Collapse", Ford Motor Company, Vehicles Structural Mechanics, Fourth International Conference Proceedings, Code 811302, SAE 1981 Proceedings.

6-42. Sen, J. K., Dremann, C. C., "Design Development Tests for Composite Crashworthy Helicopter Fuselage", Hughes Helicopters, Inc., Culver City, California, SAMPE Quarterly, Volume 17, No. 1, October 1985, pp. 29-39.

6-43. Farley, G. L., Energy Absorption of Composite Materials, NASA Technical Memorandum 84638, AVRADCOM Technical Report TR-83-B-2, Structures Laboratory, U.S. Army Research and Technical Laboratories (AVRADCOM), Langley Research Center, Hampton, Virginia, March 1983.

6-44. Hanagud, S., Chen, H. P., Sriram, P., "A Study of the Static Post Buckling Behavior of Composite Sandwich Plates", School of Aerospace Engineering, Georgia Institute of Technology, Atlanta, Georgia, paper presented at the International Conference on Rotorcraft Basic Research, Research Triangle Park, North Carolina, February 19-21, 1985.

6-45. Reddy, A. D., Rehfield, L. W., "Post Buckling and Cripple Behavior of Graphite/Epoxy Thin-walled Airframe Members", Center for Rotary Wing Aircraft Technology, School of Aerospace Engineering, Georgia Institute of Technology, Atlanta, Georgia, Paper No. A-86-41-8000, paper presented at the 41st Annual Forum of the American Helicopter Society, May 16-17, 1985.

6-46. Cronkhite, J. D., "Helicopter Structural Crashworthiness", Bell Helicopter Textron, Inc., paper presented at the ASME Winter Meeting, Anaheim, California, December 7-12, 1986.

6-47. Cronkhite, J. D., Crashworthy Design Concepts for Airframe Structures of Light Aircraft, Bell Helicopter Textron, Inc., Fort Worth, Texas, SAE Technical Paper Series 810613, Business Aircraft Meeting and Exposition, Wichita, Kansas, April 7-10, 1981.

THIS DOCUMENT PROVIDED BY THE ABBOTT AEROSPACE
TECHNICAL LIBRARY
ABBOTTAEROSPACE.COM

6-48. Carden, H. D., Hayduk, R. J., Aircraft Subfloor Response to Crash Loadings, NASA Langley Research Center, Hampton, Virginia, SAE Technical Paper Series No. 810614, Business Aircraft Meeting and Exposition, Wichita, Kansas, April 7-10, 1981.

6-49. Bark, L. W., Burrows, L. T., Cronkhite, J. D., et al., “Crash Testing of Advanced Composite Energy-Absorbing Repairable Cabin Subfloor Structures,” paper presented at the American Helicopter Society National Technical Specialists’ Meeting on Advanced Rotorcraft Structures, Williamsburg, Virginia, October 26-27, 1988.

6-50. Richards, M. K., Hurley, T. R., Low-cost Energy-absorbing Subfloor for a Composite General Aviation Aircraft, TR-96183, Simula Government Products, Inc., Phoenix, Arizona, May 1997.

6-51. Reed, W. H., Avery, J. P., Principles for Improving Structural Crashworthiness for STOL and CTOL Aircraft, USAAVLABS Technical Report 66-39, U.S. Army Aviation Materiel Laboratories, Fort Eustis, Virginia, June 1966.

6-52. Greer, D. L., Crashworthy Design Principles, Convair Division of General Dynamics Corporation, San Diego, California, September 1964.

6-53. Shefrin, J., Demonstration of Advanced Cargo Restraint Hardware for COD Aircraft, Boeing Vertol Company; NADC Technical Report 77154-60, Naval Air Development Center, Warminster, Pennsylvania, December 1978.

6-54. Sechler, E. E., Dunn, L. G., Airplane Structural Analysis and Design, Dover, New York, 1963.

6-55. Smith, K. F., Full-scale Crash Test (T-41) of the YAH-63 Attack Helicopter, Report No. USAAVSCOM TR-86-D-2, Aviation Applied Technology Directorate, U.S. Army Aviation Research and Technology Activity (AVSCOM), Fort Eustis, Virginia, April 1986, AD A167813.

6-56. Alfaro-Bou, E., Vaughan, V. L., Jr., Light Airplane Crash Test at Impact Velocities of 13 and 27 m/sec, NASA Technical Paper 1042, NASA Langley Research Center, National Aeronautics and Space Administration, Washington, D.C., November 1977.

6-57. Castle, C. B., Alfaro-Bou, E., Light Airplane Crash Tests at Three Roll Angles, NASA Technical Paper 1477, National Aeronautics and Space Administration, Washington, D.C., October 1979.

6-58. Haley, J. C., Turnbow, J. W., Walhout, G. J., Floor Accelerations and Passenger Injuries in Transport Aircraft Accidents, Aviation Safety Engineering and Research (AVSER), Division of Flight Safety Foundation, Inc.; USAAVLABS Technical Report 67-16, U.S. Army Aviation Materiel Laboratories, Fort Eustis, Virginia, May 1967, AD 815877L.

6-59. Vaughan, V. L., Alfaro-Bou, E., "Impact Dynamics Research Facility for Full-scale Aircraft Crash Testing", NASA Technical Note D-8179, National Aeronautics and Space Administration, Washington, D.C., April 1976.

6-60. Alfaro-Bou, E. Castle, C. B., "Crash Tests of Three Identical Low-Wing Single-Engine Airplanes," NASA TP 2190, Washington, D.C., September, 1983.

6-61. Castle, C. B, et. al., "Light Airplane Crash Tests at Three Roll Angles, " NASA TP 1477, 1979.

6-62. Vaughan, V. L., et. al., "Crash Tests of Four Identical High-Wing Single-Engine Airplanes," NASA TP 1699, 1980.

THIS DOCUMENT PROVIDED BY THE ABBOTT AEROSPACE
TECHNICAL LIBRARY
ABBOTTAEROSPACE.COM

6-63. Vaughan, V. L., et. al., "Light Airplane Crash Tests at Three Pitch Angles," NASA TP 1481, 1979.

6-64. Williams, S. M., et. al., "Crash Tests of Four Low-Wing Twin-Engine Airplanes With Truss-Reinforced Fuselage Structures," NASA TP 2070, September 1982.

6-65. Carden, H. D., "Correlation and Assessment of Structural Airplane Crash Data With Flight Parameters at Impact," NASA TP 2083, 1982.

This Document Provided by the Abbott Aerospace
Technical Library
abbottaerospace.com

Chapter 7

Seats

Marvin K. Richards
Jill M. Vandenburg

Seats are an integral part of the occupant restraint system and play a major role in occupant crash protection, as well as providing comfort and proper occupant position. Seats must accommodate a range of occupant sizes, both male and female, be designed to withstand crash loads, provide comfort, and be lightweight. Most GA seats are single-place, particularly crewseats. However, many passenger seats accommodate two or more occupants.

Certain design criteria should be followed to provide a seat that will minimize weight and maximize comfort and crashworthiness. Regulations pertaining to seat performance and design for light airplanes are found in 14 CFR Part 23 (Reference 7-1), specifically in paragraphs 23.785, 23.562, and 23.561. Guidance on seat design can also be found in the FAA Advisory Circular AC 23.562-1 (Reference 7-2) and in SAE Aerospace Standard AS 8049 (Reference 7-3). Section 7 repeats some of this guidance, but also provides additional information from the U.S. Army Aircraft Crash Survival Design Guide (Reference 7-4), as well as from various other sources.

7.1 SEAT GEOMETRY

The geometry of the seat affects both its crashworthiness, as well as normal aircraft operation. For crewmembers (pilot/co-pilot), the seat should be adjustable so that the occupant can safely operate the aircraft controls, and have a clear view of the aircraft instruments and the aircraft's flight path. Figure 7-1 illustrates the aspects of seat geometry that will be discussed in the following paragraphs.

7.1.1 Seat Back Angle

The seat back angle is the angle relative to aircraft vertical (during level flight) of a straight line passing tangent to the curvatures of the occupant's back when leaning back and naturally compressing the seat cushion. Increasing the seat back angle will generally increase occupant comfort, and can also increase occupant tolerance to pure vertical crash loads (it reduces spinal compression load). However, an excessive recline angle can promote occupant submarining during crashes with high longitudinal accelerations unless the seat pan angle is also increased. For optimum comfort, the seat back angle should be between 13 and 30 deg.

THIS DOCUMENT PROVIDED BY THE ABBOTT AEROSPACE
TECHNICAL LIBRARY
ABBOTTAEROSPACE.COM

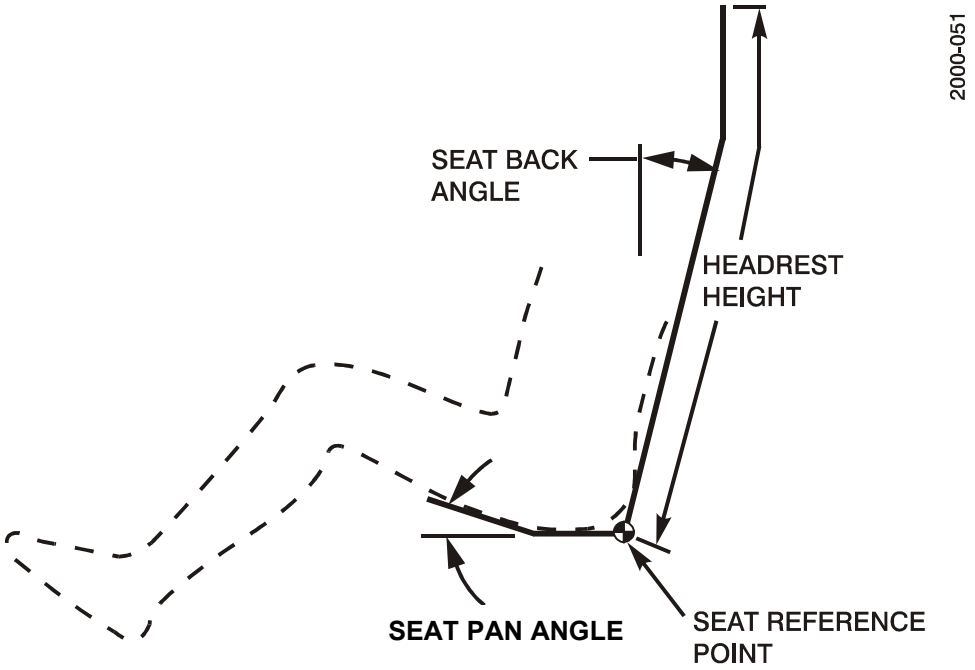


Figure 7-1.
Seating geometry.

7.1.2 Seat Reference Point (SRP)

The seat reference point (SRP) is a point on the vertical mid-plane of the seat where the back tangent line and a horizontal line that is tangent to the lowermost position of the occupant seated in the cushion intersect. This point is referenced in other critical seat dimensions, such as headrest height, and for locating the restraint system.

7.1.3 Headrest Height

The headrest height is the distance measured from the SRP, along the seat back tangent line and a line parallel to the head rest, to the top of the head rest. The headrest must provide proper head restraint (prevent neck hyperextension) during the rebound phase of a crash event. The height needs to be set for the tallest (stature) expected occupant. To accommodate a 95th-percentile male occupant, the headrest height should be a minimum of 32 in., as measured from the SRP, parallel with the backrest reference plane (Reference 7-5).

7.1.4 Seat Pan Angle

The seat pan angle is the angle, with respect to aircraft horizontal (during level flight), of a line passing tangent to the occupant's thigh when naturally compressing the seat pan cushion. For the most part, this angle is defined by the occupant's anthropometry and feet position. To enhance crashworthiness, the seat pan structure should be designed to be parallel to the occupant's thigh tangent angle, which will minimize cushion compression during crash loading. Having the seat pan angle upward toward the front of the seat can provide lower-body retention during high-longitudinal-acceleration crashes, and help reduce the likelihood of occupant

THIS DOCUMENT PROVIDED BY THE ABBOTT AEROSPACE
TECHNICAL LIBRARY
ABBOTTAEROSPACE.COM

submarining. Higher seat pan angles and thinner cushions will enhance occupant lower body restraint. However, thin cushions are less accommodating to a large range of occupant thigh angles, which is often required by crewmembers to allow operation of the rudder pedals.

It is recommended that the seat pan angle be no less than 5 deg. In addition, the seat pan angle should be between 10 and 25 deg less than the seat back angle. For example, a seat with 25-deg back angle should have a seat pan angle of 5 to 15 deg.

7.1.5 Design Eye Point

The design eye point is a reference datum point based on the desired location of the occupant's eye. Positioning at the design eye point enables the specified vision envelope desired for the aircraft design. For crewmembers, the seat would ideally provide sufficient adjustment so that each operator can achieve the desired design eye point (Reference 7-6).

7.2 SEAT POSITION ADJUSTMENT

Seat position adjustment is necessary in order for the occupant to be positioned at the proper design eye point in the crew station, to enable the operation of the aircraft controls (i.e., rudder pedals), and to maximize comfort. For passenger seats, adjustment is typically not necessary, and many aircraft do not offer passenger seat adjustment.

The seat adjustment mechanisms must have sufficient strength to meet the seat crash loading requirements and preferably will allow adjustment of the seat while occupied. Activation of adjustment mechanisms is typically accomplished by pulling, lifting, or rotating a small handle(s). The adjustment handle(s) need to be located in a convenient location for occupant access while seated, but should not be located where they might injure the occupant in a crash event. The handle(s) must be also designed so that they will not be inadvertently activated during normal flight or during a crash event.

7.2.1 Fore-Aft Adjustment

Fore-aft adjustment is typically accomplished via a pair of floor tracks. If a seat base is used, the seat adjuster can be located between the seat bucket and the seat base to minimize moments applied to the adjustment mechanism (this may also reduce weight).

The adjustment locks should be designed to lock positively in small pitch increments, typically 0.5 in. The adjustment system should provide positive feedback to the seat occupant indicating that the lock(s) are engaged. This feedback can be provided by the adjustment handle (i.e., a pulled handle will not return to its original position until all locking pins are engaged). Typically two locks are utilized, one for each track, so the design needs to ensure that both locks are engaged before the positive feedback is provided.

The locking mechanism must be metal-to-metal (i.e., a metal locking pin inserted into a metal track). Mechanical stops must be included at both ends of the adjustment range to prevent the seat from falling off of the adjustment tracks during seat adjustment.

If the adjustment is required to provide rudder pedal reach for 5th-percentile female through 95th-percentile male crewmembers, then an adjustment range of approximately 10 in. will be required (Reference 7-5). This measurement is based on anthropomorphic data gathered for from both military and civilian sources, and may need to be adjusted for the specific demographics for each application (Reference 7-5). Most seat hardware and airplane installations do not allow this much adjustment. A typical real-world adjustment range is actually 6 to 8 in. Refer to Section 4.3 for additional information on occupant anthropometry.

This Document Provided by the Abbott Aerospace
Technical Library
abbottaerospace.com

7.2.2 Vertical Adjustment

Vertical adjustment is normally desired to maintain the design eye point height, but these adjustment mechanisms typically add weight and complexity to the seat. For some crashworthy seat designs that have guided vertical stroke, it may be possible to combine the vertical adjustment with the guided-stroke mechanism. This can reduce complexity and weight.

Vertical adjusters need assist springs to provide an upward seat load when the adjustment mechanism is moved with a seated occupant. A net upward load (the load after compensating for the seat's weight) of 30 to 50 lb may be required over the adjustment range, depending on whether the adjuster is a continuous-engagement type (i.e., a jackscrew) or a release-and-lock type. For stroking seats, the assist spring should be mounted so that the spring load does not contribute to the stroking load (springs should not stretch as the seat strokes). Damping of the spring is highly desirable for release-and-lock systems to prevent an unoccupied seat from banging into the upper stop if the release lever is pulled. Damped vertical adjusters are also beneficial, as it makes selecting a particular height easier. Gas springs, similar to those used on airplane and automobile doors, can combine the spring and damping functions.

All design features of the fore-aft adjustment (Section 7.2.1) apply to the vertical adjustment with the exception of the adjustment range. If the adjustment is required to provide optimum design eye point height for 5th-percentile female through 95th-percentile male crewmembers, then an adjustment range of approximately 9 in., as measured from the eye to the floor, will be required (Reference 7-5). The adjustment range may need to be adapted for the specific demographics for each application. Again, due to real-world limitations, this range is typically selected to be 2 to 6 in. Refer to Section 4.3 for additional occupant anthropometry information.

7.2.3 Combined Horizontal and Vertical Seat Adjustment

Adjustment mechanisms that combine horizontal and vertical adjustment are common in aircraft and automobiles. Typically, the horizontal adjuster or seat track is placed on an incline that moves the seat up as it moves forward. The angle of the incline could be set to a ratio based on anthropomorphic data. This would, however, make for a very steep incline that would make adjustment difficult. Real-world applications usually use 5 to 10 deg angles, since the reach distance to the controls is usually more critical than the design eye position. Unfortunately, occupants who have short legs and a tall torso (or long legs and a short torso) may not be able to achieve the optimum seat adjustment. If combined seat adjustment is utilized, all design features of the horizontal and vertical adjustment apply (Sections 7.2.1 and 7.2.2).

7.2.4 Back Angle adjustment

An adjustable back angle further accommodates occupant preferences and anthropomorphic ranges. This is often a ground-adjustable feature in small airplanes. Mechanisms that allow in-flight adjustment should be carefully considered as abrupt motion of the seat can cause unintended inputs into the controls of the aircraft. Constant-mesh (Taumel style) or other backrest adjuster mechanisms that do not allow the backrest to move abruptly are preferred over mechanisms that release the backrest and then allow free movement (pawl and sector style). If the adjuster design allows for free movement, then an assist spring is highly recommended to help push the backrest and occupant upright during adjustment, and stops must be placed at the adjustment extremes (i.e., at 10- and 30-deg back angles). All other design features of the horizontal adjustment apply to the back angle adjustment (Section 7.2.1).

This Document Provided by the ABBOTT AEROSPACE
TECHNICAL LIBRARY
ABBOTTAEROSPACE.COM

7.3 SEAT ORIENTATION

Seat orientation can vary from forward-facing to aft-facing, oblique, and side-facing, based on the aircraft's configuration and mission needs. Crewseats and passenger seats are typically oriented in a forward-facing direction in small airplanes. This orientation is well accepted by occupants, as they are facing the direction of motion. Standard forward-facing crewseats and restraint systems are designed to withstand large accelerations in the longitudinal direction, which is in the primary direction of flight and crash loading. Injury tolerances for the forward direction are also well understood, due to the large amount of research and accident data that has been generated by the aviation and automotive industries. A properly designed seat and restraint system can protect occupants in a relatively severe crash, provided that the seat remains attached to the airframe and there is enough survivable space around the occupant.

Passenger seats can also be arranged in other orientations, such as aft-facing and side-facing. Aft-facing seats are capable of the highest level of occupant protection because they provide the most support to the occupant and because injury tolerances are highest for this direction of loading. However, aft-facing seats are not as well accepted by passengers as forward-facing seats, and often impose higher loads to the aircraft interface than forward-facing seats. Aft-facing seats also increase occupant exposure to loose objects that may fly forward during the crash event.

Oblique orientations can also be utilized. However, the angle from the airplane centerline needs to be limited to minimize the problems of lateral occupant restraint stated in the next paragraph. Transport-category airplane regulations (Reference 7-7) specify additional protection requirements for seating that exceeds a maximum oblique angle of 18 deg from forward (14 CFR 25.785(d)). Small-airplane regulations (Reference 7-1) do not specify at what angle additional protection is required, but do state that seat orientations other than forward-facing or aft-facing must provide an equivalent level of safety (14 CFR 23.785(b)). Given the lack of specific guidance for small airplanes, limiting oblique-facing seats in small airplanes to $\pm$18 deg from forward, as is specified in the transport airplane regulations, seems reasonable.

From a crashworthiness standpoint, side-facing seats are the most difficult to design. This is because it is difficult to provide effective occupant restraint in the aircraft's longitudinal direction (lateral with respect to the occupant) and because lateral injury mechanisms and tolerances are not well as understood as are forward-facing mechanisms and tolerances. Some research and development of an industry standard for side-facing seats is being conducted, but, as of this writing, no conclusions have been reached. Areas of concern include the lateral injury mechanisms due to occupant-to-restraint, occupant-to-occupant, and occupant-to-structure interactions. For example, a three-point restraint can produce high neck moments and localized neck loads if the occupant's head is not otherwise restrained. Inflatable belt restraints (See Section 8.2.13) have shown great promise regarding occupant protection in side-facing seats, but these are still in the development stage.

7.4 SEAT STRUCTURAL DESIGN

Common to all seat types are the seat bottom and the seat back (the occupant interface). The seat bottom and seat back can take many forms, such as a formed bucket, a “rag-and-tube” suspension system, or sheet-metal-covered tubing. These components can have a simple contour incorporated that provides lumbar support and buttock support. A contoured seat bottom that distributes the occupant load evenly over as much area as possible is desirable.

THIS DOCUMENT PROVIDED BY THE ABBOTT AEROSPACE
TECHNICAL LIBRARY
ABBOTTAEROSPACE.COM

A seat frame is generally used to transfer the loads from the occupant seating surface to the aircraft mounting hard points. The seat frame also commonly provides the seat's energy absorption (load-limiting). The seat structure can take several forms in order to balance the requirements of low weight, low cost, operational requirements, energy absorption, etc. Several common seat designs and methods of attaining vertical energy absorption are described in the following sections.

7.4.1 Methods of Providing Vertical Energy Absorption

In order to prevent excessive occupant spinal loading during impacts with high vertical accelerations, seat load-limiting, or energy absorption, in the vertical direction may be necessary. The following sections show some of the most common design concepts for providing seat vertical energy absorption.

7.4.1.1 Guided-Stroke Seat

Figure 7-2 shows a schematic representation of a guided-stroking seat. The guided stroke is often provided through a set of linear bearings attached to the seat bucket, and a pair of guide tubes attached to the aircraft structure (or to a frame that is attached to aircraft structure).

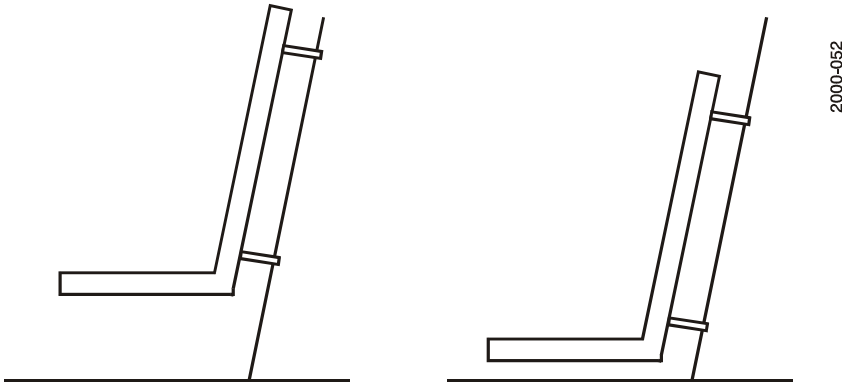


Figure 7-2.
Schematic for a guided-stroke energy-absorber design.

One advantageous crashworthy feature of this particular design that is the restraint can be anchored directly onto the seat bucket, thereby maintaining optimum restraint geometry during full seat stroke. In addition, since the seat stroke is guided, the occupant's forward motion can be well controlled, even during high stroking distances or high longitudinal loads. The guided-stroke design concept is often used for military helicopter seats, where the stroking distance can exceed 12 in.

The linear bearings and slides can take many forms, but need to be designed to move freely (i.e. not bind) during compound loading, guide deflection, or frame warp. The linear guides can also be utilized for seat vertical height adjustment to reduce system weight and complexity.

THIS DOCUMENT PROVIDED BY THE ABBOTT AEROSPACE
TECHNICAL LIBRARY
ABBOTTAEROSPACE.COM

Other methods of guided seat stroke can be utilized, such as a four-bar pivot-arm linkage. However, pivoting-arm designs should ensure that the seat motion does not significantly amplify the occupant's exposure to acceleration. For example, a pivot arm that moves the occupant forward and then backward as the seat strokes downward can amplify the forward load on the occupant during a common downward/forward crash acceleration.

7.4.1.2 Deformable Seat Structure

For this concept, a carefully designed deformable seat structure is typically located under the seat pan, as shown in Figure 7-3. This concept utilizes plastic structural deformation to limit the vertical load. This particular seat concept is commonly referred to as the "S"-leg seat, named after the shape of the deformable structure. However, the deformable structure can be formed in various shapes to provide the best combination of vertical load attenuation and longitudinal retention.



a) normal position **b) after stroke**

Figure 7-3.
Schematic for a deformable seat structure EA design.

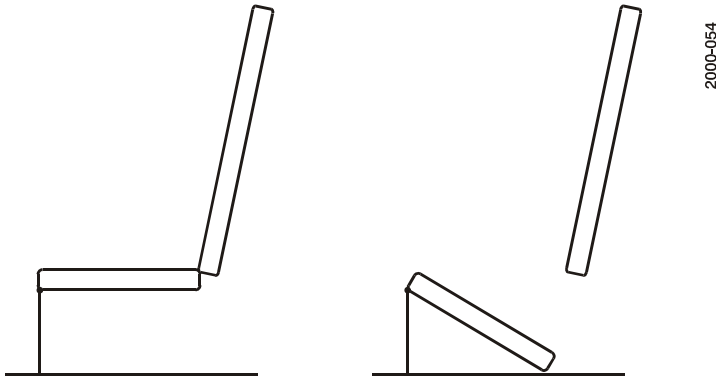
Several versions of this simple and economical design have been developed, and have shown the capability to pass the current regulatory seat dynamic tests.

One of the challenges of this design is to provide a structure that deforms vertically at a relatively low and constant load, but still provides tightly limited longitudinal deformation. Anchoring the shoulder belt to the seat back is usually not practical, as the seat would pivot forward during a high longitudinal acceleration crash, allowing excessive occupant motion. Anchoring the shoulder strap to aircraft structure is recommended for this design concept. The lap belt anchors should be attached to the seat structure to ensure proper lower-restraint geometry during the unpredictable seat motion of a crash event.

7.4.1.3 Pivoting Seat Pan

For this concept, a hinge point is located near the front of the seat pan, and the back of the pan deforms downward, as shown in Figure 7-4. The seat back is normally attached to a bulkhead. This type of design has been incorporated into some commercial helicopter seats.

THIS DOCUMENT PROVIDED BY THE ABBOTT AEROSPACE
TECHNICAL LIBRARY
ABBOTTAEROSPACE.COM



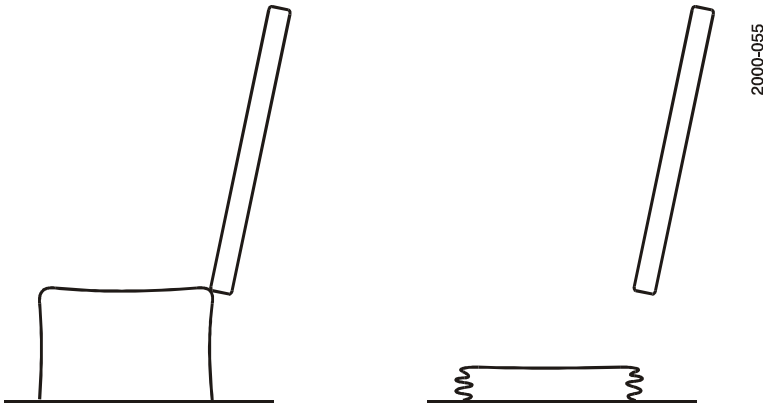
a) normal position **b) after stroke**

Figure 7-4.
Schematic for a pivoting seat pan EA design.

The main challenge of this design is to maintain proper restraint geometry as the seat pan pivots. The commercial helicopter that utilizes this design utilizes “Y” lap belt configuration with one anchor point mounted on the stroking seat pan, and the other anchor point fixed to the bulkhead. The shoulder straps are anchored to the bulkhead, which will cause a tensioning effect as the seat strokes. This tensioning could affect seat stroke, and may produce higher-than-desired shoulder belt loads.

7.4.1.4 Crushing Seat Pan

This design concept is shown in Figure 7-5, and is also referred to as an energy-absorbing seat-pan cushion.



a) normal position **b) after stroke**

Figure 7-5.
Schematic for a crushing-seat-pan EA design.

THIS DOCUMENT PROVIDED BY THE ABBOTT AEROSPACE
TECHNICAL LIBRARY
ABBOTTAEROSPACE.COM

This design concept uses a crushing material located directly under the seat pan surface. The seat pan needs to be designed to distribute the load to the EA crushable material, and to prevent damage to the EA material under normal use (i.e., stepping on the cushion with hard heels). Since most crushing materials will not hold high shear loads after crushing, the restraint will most likely need to be anchored to aircraft structure. Thus, it is difficult to maintain the optimal lap belt restraint geometry as the seat pan strokes. For this reason, this design concept should only be utilized when minimal vertical stroke is required. One advantage of this design is there is minimal stroking mass, so dynamic overshoot will be minimized.

7.4.1.5 Amount of Vertical Seat Stroke Required and Selecting EA loads

The seat should be designed to provide the maximum amount of vertical stroke within the confines of the aircraft structure. At a minimum, the seat needs to stroke far enough to pass the dynamic testing requirements shown in Section 7.5.4. Increasing the seat stroke generally expands the crash envelope and/or can provide occupant spinal protection over a broader occupant weight range.

The amount of seat stroke and the optimum EA load required to limit occupant spinal loading is based on several factors, including, but not limited to:

- Type of crash pulse (onset rate, magnitude, and duration)
- Total velocity change
- Load-stroke profile of the energy absorber
- Direction of seat stroke relative to the impact acceleration
- Angle of seat stroke relative to the occupant back angle
- Stroking mass of the seat
- Occupant stroking mass
- Seat pan cushion design
- Occupant feet location/support
- Restraint geometry.

Calculating the amount of seat stroke and defining the energy-absorber load can be difficult, due to the variability of the above factors. Even the most advanced computer simulations require expertise by the person building the model as well as similar dynamic test results to validate the model in order to obtain useful information (Chapter 5). Generally, multiple developmental seat dynamic tests are required to optimize the energy-absorber load and seat-stroking distance for peak performance.

As a general guideline, dynamic tests and models have shown that the minimum vertical seat stroke necessary to pass the regulatory test requirements of 14 CFR 23.562(b)(1) (see also Section 7.6.4) is about 2 in. Energy absorbers which stroke at a fixed, constant load of up to approximately 12 G parallel to the occupant's seat back angle have also been used without exceeding the 14 CFR 23.562(c) spinal load tolerance for the 50th-percentile male ATD. The regulations do not require dynamic testing or design for smaller or larger occupants. A fixed-load seat optimized for the 50th-percentile male ATD, however, will likely produce a spinal load that exceeds the tolerance level for the 5th-percentile female ATD, indicating an increased probability of injury in the smaller occupant. Likewise, a stroking distance optimized for the 50th-percentile male ATD may not be sufficient for the 95th-percentile male ATD, allowing the occupant to "bottom-out" the energy absorber, thus increasing the likelihood of spinal injury for larger occupants.

This Document Provided by the Abbott Aerospace
TECHNICAL LIBRARY
ABBOTTAEROSPACE.COM

Ideally, with a fixed-load energy absorber, the energy-absorber load should be sized for the smallest expected occupant, and the stroke length sized for the largest. In practice, however, it is very difficult to accommodate the stroking load and distance needed for all sizes of occupant in the space available in small airplanes without a variable-load energy-absorber mechanism. A variable-load energy absorber allows the stroking load to be adjusted based on the weight of the occupant. Adjusting the load to the occupant also makes the most the effective use of the available stroking distance for all occupant sizes. However, variable-load energy absorbers increase the cost, weight, and complexity of the seat system. Crashworthy seats that use variable-load energy absorbers have been fielded in some military rotorcraft, but the most common energy absorbers seen in civil and military aircraft are still fixed-load devices.

As a recommended practice, fixed-load seat systems for light airplanes should be designed to produce a spinal load in the 50th-percentile male ATD that is 200-300 lb less than the 1,500-lb regulatory limit (that is, a maximum load between 1,200 and 1,300 lb). This lower load will help reduce the chance of spinal injury in smaller occupants. The seat stroke should also be 4-6 in. to better protect the larger-than-average occupant (that is, 2 to 3 times the 2-in. minimum stroking distance mentioned above). These recommendations will also provide extended protection in crashes that exceed the test pulse in 14 CFR 23.563(b)(1).

7.4.2 Seat-to-Aircraft Mounting Location

The attachment location of the seat in the aircraft is of vital importance in ensuring that the seat remains intact under crash loads. Using a systems design approach, the aircraft structure can be designed to efficiently transfer seat loads without significantly increasing the aircraft weight. The seats can be attached to the airframe in many ways, depending on the specific application. In general, there are six types of seat mounting attachment methods, which are listed below.

1. Floor-mounted
2. Bulkhead-mounted
3. Sidewall-mounted
4. Ceiling-mounted
5. Combinations
6. Integral to the airframe.

Each of these mounting methods can incorporate energy absorbers for improving crashworthiness and occupant safety. For seats with energy absorbers, seat stroke should be considered when selecting seat locations in the aircraft. The seat should be able to stroke without interfering or "bottoming out" on other objects or aircraft structure. In addition, the occupant flail envelope should be considered when locating seats in the aircraft.

Airframe distortions as a result of an aircraft crash can cause failure of the seat structure or tiedown connections. Aircraft distortion can take the form of a bulge or dish in the floor, or an outboard bow in the aircraft sidewall during impact. The amount and type of deformation is primarily dependent on the mounting location.

7.4.2.1 Floor-Mounted

Floor-mounted seats should be designed to withstand floor distortion due to the aircraft impacting irregular terrain such as tree stumps and rocks. These objects can locally distort the floor and cause the seat to detach from the aircraft.

This Document Provided by the ABBOTT Aerospace
TECHNICAL LIBRARY
ABBOTTAEROSPACE.COM

For basically rigid seat structures that are distorted in a crash, the critical design parameter appears to be the torsional rigidity of the seat pan, bucket, and/or structural members. If the torsional rigidity is low, only small forces are introduced. However, for stiff seat members, the warpage forces may produce a structural failure or impose a pre-load that, when coupled with crash inertial loads, results in failure.

The recommended floor-warp deflection requirement for floor-mounted seats is a 10-deg pitch rotation of one seat track and a 10-deg roll angle of the other seat track (References 7-2, 7-3, and 7-7; see also the seat test conditions in Section 7.6.4). To accommodate local deformation, each attachment should be released to allow +/- 10 deg of rotation in any direction.

7.4.2.2 Bulkhead-Mounted

The same general principles that apply to floor-mounted seats also apply to bulkhead-mounted seats, except that the deflections and the degree of warping of the bulkhead appear to be less than that of the floor. This is probably due to the bulkhead being less vulnerable to local planar distortion caused by objects such as rocks and tree stumps impacted by the under-floor structure. The recommended angular deflection requirement for bulkhead-mounted seats is a 5-deg rotation of the bulkhead in the plane of the bulkhead. To accommodate local deformation, each attachment should be released to allow +/- 10 degrees of rotation in any direction. One technique for accomplishing this is through the use of spherical bearings.

7.4.2.3 Sidewall-Mounted

Sidewall-mounted seats require the same consideration as bulkhead-mounted seats, except the sidewalls of aircraft tend to bow outboard during impacts with high vertical loading. Therefore, it is advisable that these seats be designed to accept relatively large distortions without failure. Although the angles are not known, it is expected that they may reach 25 deg. Seats that are mounted totally on the sidewall should not create a problem, as they will simply move with the sidewall. Extremely flexible seats also should be inherently immune from these problems. However, rigid seats mounted to both the floor and the sidewall will require special design considerations.

7.4.2.4 Ceiling-Mounted

Ceiling-mounted seats are not susceptible to local floor deformation that can cause seats to detach during crash loads. However, these seats must be able to transfer lateral loads to the aircraft and be able to resist upward accelerations due to the aircraft's encountering air pockets. Occupant loads can be transmitted to the aircraft structure by using straps, cables, or rigid structural members as long as the attachments are released as described in the floor-mounting section.

7.4.2.5 Combinations

Several methods of seat attachment can be combined to provide a seat that meets the applicable requirements for the particular aircraft. The design should utilize the methods for attachment, as described in the proceeding sections. Designing flexible connections can eliminate stress concentrations and allow a lightweight design to withstand crash-loading conditions.

This Document Provided by the Abbott Aerospace
TECHNICAL LIBRARY
ABBOTTAEROSPACE.COM

7.4.2.6 Integral-to-Airframe

Seats that are designed directly into the airframe rely on surrounding structure to support the weight of the occupant without adding excessive weight. In many cases, these seats are the lightest and strongest type that can be used. However, the seat position is often fixed, based on the location of the aircraft structure such as the main spar and bulkheads. Seats that are integrated into the aircraft structure should be designed so that there is sufficient crush space below the seat. This space will allow occupant loads to be less severe. Seats that are located directly over the wing spar, for example, can transmit the crash loads directly through the spar into the seat pan and then to the occupant. Any rigid structure under the seat should be avoided. Seats that rest directly on the outer skin of the airplane are also not recommended.

A fixed seat can compromise visibility and the use of flight controls for smaller- and larger-than-average occupants. The base of the seat can be integral to the airframe with a seat adjuster attached for fore-aft positioning of the seat. The seat back angle can sometimes be ground adjustable by using simple tools to adjust bolt stops to set the seat back angle. Additional foam padding or wedges can also be installed to accommodate different occupant sizes. Seats that are integrated into the airframe should be designed with crush zones directly below them, or the seat bottom should incorporate some energy absorption.

7.4.3 Energy-Absorbing Devices

Many different devices for absorbing energy and limiting loads have been proposed, developed, and tested. As shown in Section 2.3, applying a force over a distance can absorb the kinetic energy of a moving mass; this is the primary mechanism for absorbing crash energy. For the same energy, the larger the distance through which the force acts, the lower the average load

will be on the mass. Energy-absorbing mechanisms in aircraft that transmit crash forces directly to the occupant should limit the loads to those that are tolerable to humans, and should provide stroke distances consistent with those loads and with the energy to be absorbed.

Past experience has shown that plastic deformation of material, primarily metal, results in a reasonably efficient energy-absorbing process. Consequently, most load-limiting or energy-absorbing devices use that principle. Desirable features of EAs are as follows:

- The device should stroke at a constant, predictable force.
- The rapid loading rate expected in crashes should not cause higher force-versus-deformation characteristic of the device than are measured in low-speed tests.
- The device(s) should decelerate the occupant in the most efficient manner possible, while maintaining the loading environment within the limits of human tolerance.
- The device should resist loads in the direction opposite to the stroking (rebound) or be capable of the same load-deformation performance in either direction. (Anti-rebound may be provided by the energy absorber or by the basic structure itself).
- The device should be as light and as small as possible.
- The device should be economical.
- The device should be capable of being relied upon to perform satisfactorily throughout the life of the aircraft (a minimum of 10 years or 8,000 flight hours) without requiring maintenance.
- The device should not be affected by vibration, dust, dirt, heat, cold, or other environmental factors, and should be protected from corrosion.

THIS DOCUMENT PROVIDED BY THE ABBOTT AEROSPACE
TECHNICAL LIBRARY
ABBOTTAEROSPACE.COM

The discussion that follows refers to load-limiters as separate devices; however, this treatment does not imply that load-limiters must be separate devices, nor does it exclude integral design concepts wherein the structure itself is designed to deform in a controlled and predictable fashion. Rather, the discussion is presented in this way to simplify the portrayal of different methods of absorbing energy and limiting loads.

Research on simple, compact, load-limiting devices has been conducted by Government and by private industry. These data are recorded in References 7-8 through 7-20, and are also summarized in Reference 7-4. A discussion of the more common energy absorbers actually used in production seats is presented in the following section.

7.4.3.1 Wirebenders

Wirebenders are a type of energy-absorbing device that uses the force required to bend a metal wire or strap around a die or roller(s). They can be as simple as a steel wire threaded through a perforated plate or a wire wound around rollers, as shown in Figure 7-6. One characteristic of wire benders (as with all devices affected by or utilizing friction from metal-to-metal contact) is that they can have a higher initial load than the nominal-stroking load. This higher initial load can be reduced or eliminated by providing some initial slack in the wire when passing it over the rollers. Wires, by themselves, do not have the ability to sustain compressive loads. However, by anchoring both ends of the wire and attaching the seat (or seat frame) to the rollers, the stroking force can be approximately equal in both directions.

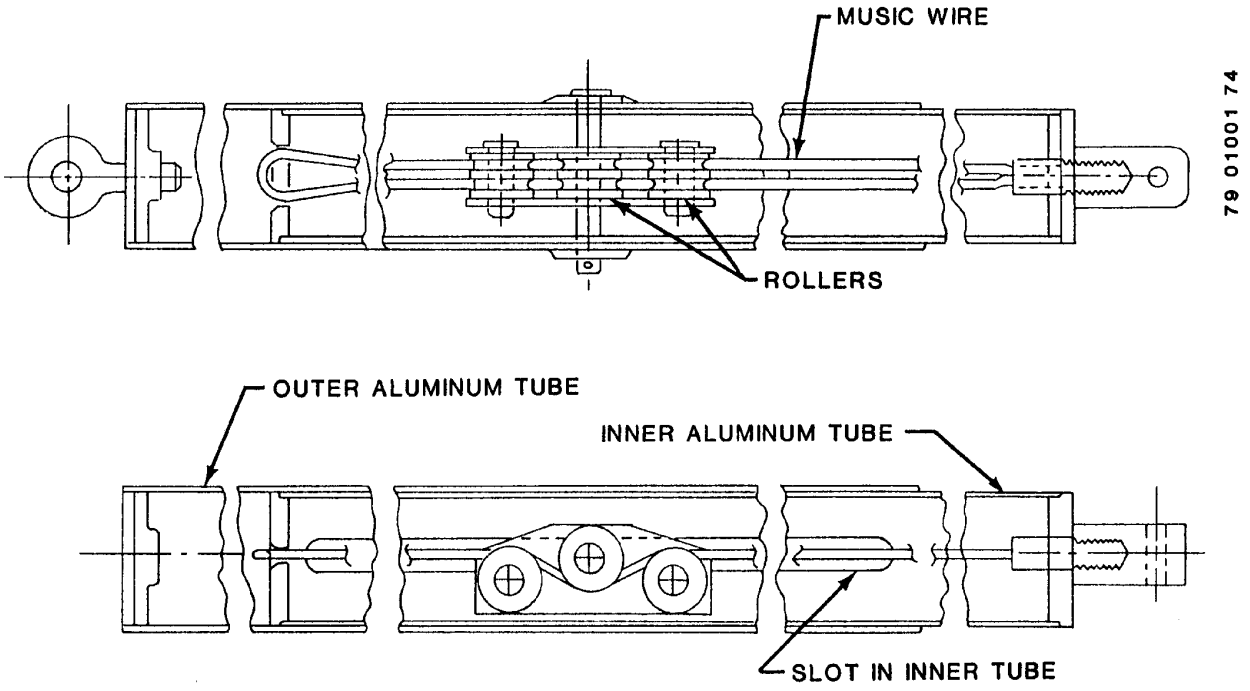


Figure 7-6.
Typical wirebender energy absorber.

THIS DOCUMENT PROVIDED BY THE ABBOTT AEROSPACE
TECHNICAL LIBRARY
ABBOTTAEROSPACE.COM

7.4.3.2 Inversion-Tube

An inversion-tube EA uses the force required to invert (i.e., to turn inside-out or outside-in) a length of metal tubing (Figure 7-7). An American automobile manufacturing company initially developed the concept for incorporation into steering columns to produce controlled collapse loads in accidents (Reference 7-10).

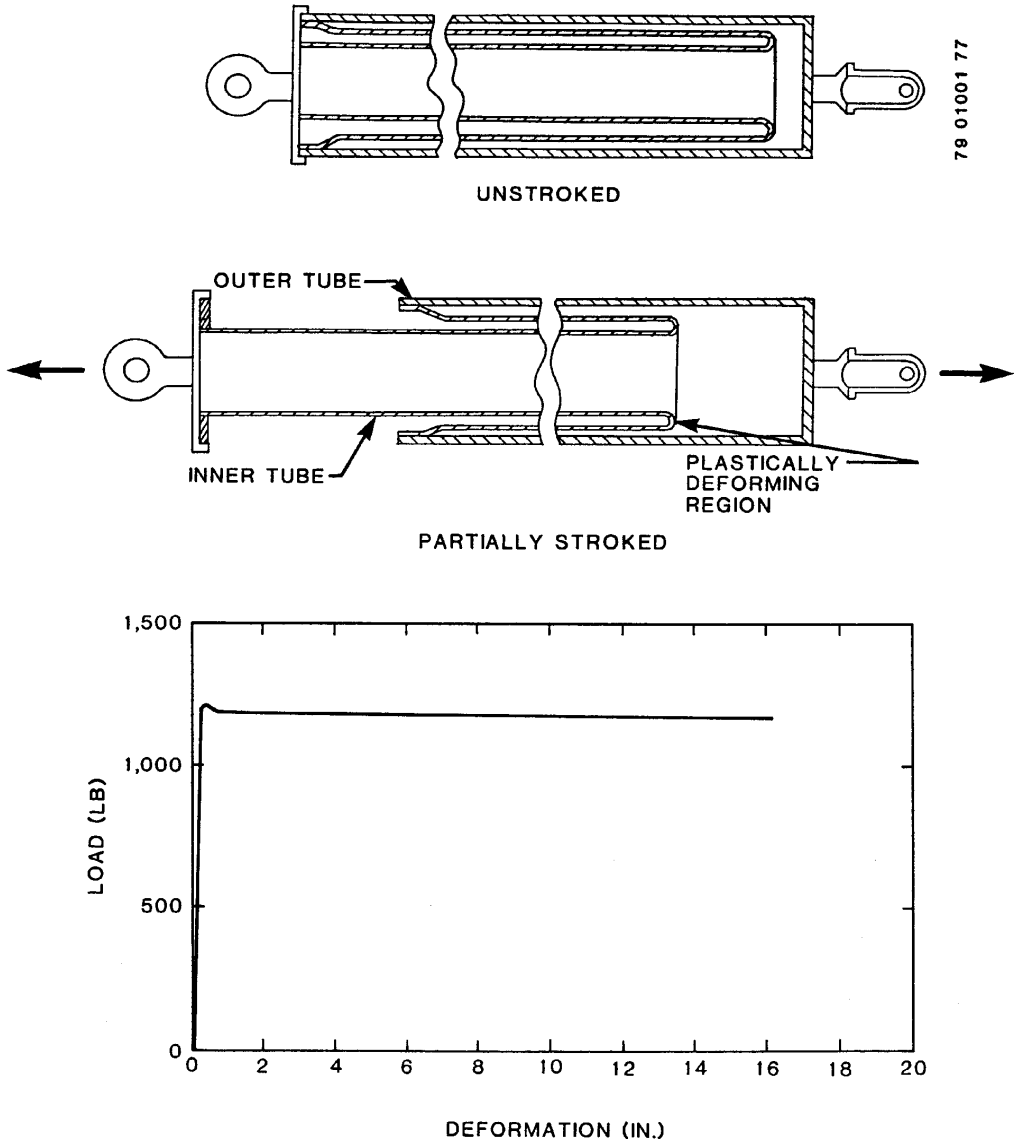


Figure 7-7.
Inversion-tube energy absorber (tensile design) and its load-deflection curve (Reference 7-22).

The materials most commonly used in inversion tubes have been 3003-H14 aluminum and mild steel, as described in References 7-10 through 7-12. It is possible that an annealed, higher-strength alloy steel, such as 4130 or stainless steel, could be also be used.

THIS DOCUMENT PROVIDED BY THE ABBOTT AEROSPACE
TECHNICAL LIBRARY
ABBOTTAEROSPACE.COM

Figure 7-7 illustrates a specific design concept for an inversion-tube EA (Reference 7-22). The load curve is essentially flat for the entire stroke distance after a brief initial peak. Seats using this type of EA are used in U.S. Army, Navy, and Air Force helicopters. No real disadvantages have been noted in experimental tests to date except with those EA's loaded in compression (Referring to Figure 7-7, the EA would begin fully extended and the tube would be stroked into itself). In dynamic tests of troop seats (Reference 7-21) using these devices in compression, there was a tendency for the outer and inner tubes to misalign, which resulted in failure and crippling of the inner tube. However, using an internal guide to keep the initial eccentricity from developing can solve this problem.

7.4.3.3 Crushing-Material

The crushing-material type of EA uses the force required to crush or deform a column of low-density material. In order to provide sufficient column stability and transverse load resistance, most applications require a telescoping cover to give additional support to the material. Typically, this device will not provide rebound load capability. Rebound load capacity can be added by the incorporation of a suitable mechanism that allows movement in only one direction.

This device is also used as a load-limiter in the main landing gears of some helicopters. In these applications, the crushable material is installed above the oleo piston, as outlined in Reference 7-13. The energy-absorption ability of these devices has been responsible for preventing major structural damage to numerous aircraft in severe accidents.

One of the most common types of crushable material for use in this type of device is corrugated aluminum foil backed by flat foil and cemented at the nodal points. Figure 7-8 shows a typical aluminum honeycomb column force-deflection curve. Further research information on the development of crushable aluminum columns may be found in Reference 7-14.

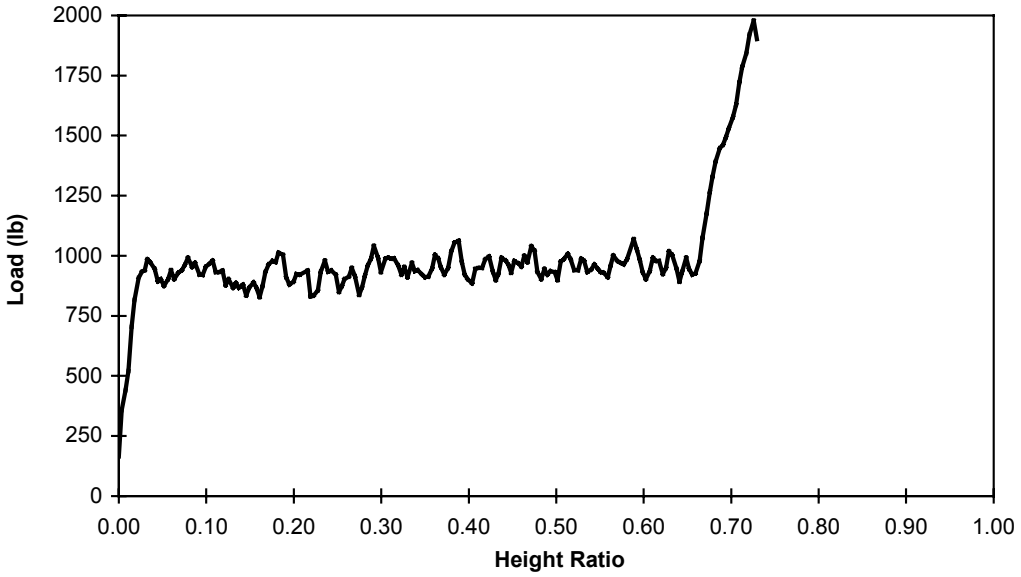


Figure 7-8.
Typical aluminum honeycomb column crush characteristics

THIS DOCUMENT PROVIDED BY THE ABBOTT AEROSPACE
TECHNICAL LIBRARY
ABBOTTAEROSPACE.COM

Rigid foams can be used in a manner similar to honeycomb energy absorbers. Various materials can be used, including polyvinyl chloride (PVC), urethane, and polyimide (Reference 7-23). Carbon foams are also being developed that show promise for use as an energy absorber if the manufacturing costs can be reduced. Carbon foams are attractive alternates, as they have improved flame resistance and toxicity compared to conventional rigid foams. Figure 7-9 shows typical load-displacement curves for some rigid foams tested.

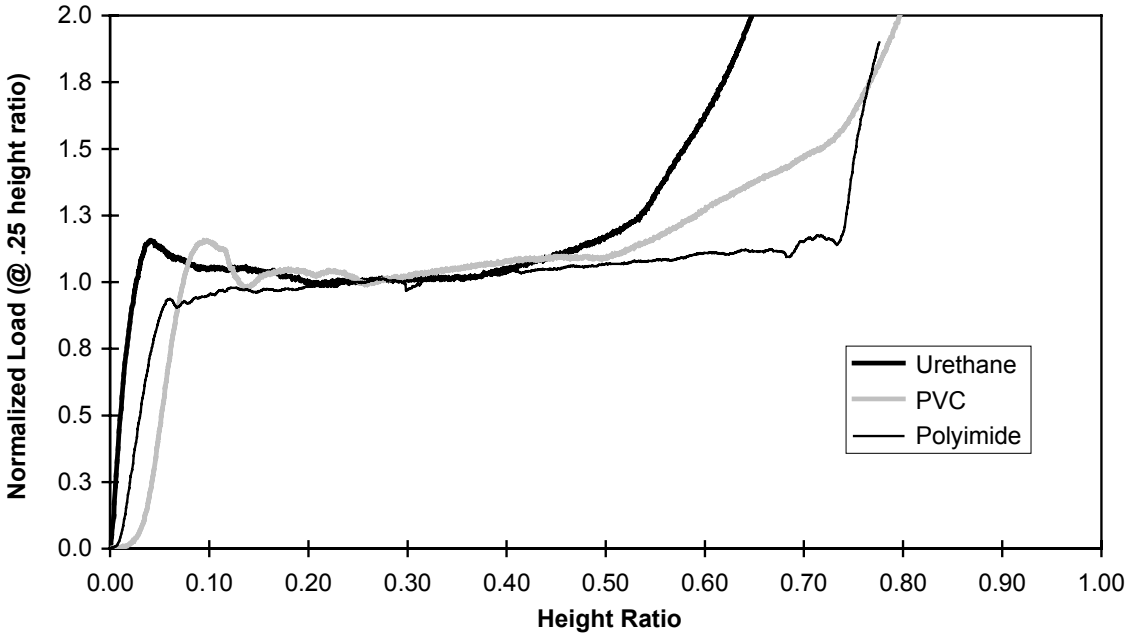


Figure 7-9.
Typical rigid foam crush characteristics (Reference 7-23).

7.4.3.4 Extension of Basic Metal Rod or Cable

This concept uses the inherent plasticity of certain ductile metals that elongate under a relatively constant force. The primary problem with this device is strain concentration at the end connections. Research performed to date indicates that annealed stainless steel in the AISI 300 series is least susceptible to strain concentrations because of its excellent ductility (45 to 50 pct). Typical load elongation characteristics of a 0.02-in. wall by 0.50-in.-diameter stainless steel tube, based on 2 static and 12 dynamic tests, are illustrated in Figure 7-10. Note that the load is not very constant, so more stroking distance would be required to absorb a given amount of energy.

THIS DOCUMENT PROVIDED BY THE ABBOTT AEROSPACE
TECHNICAL LIBRARY
ABBOTTAEROSPACE.COM

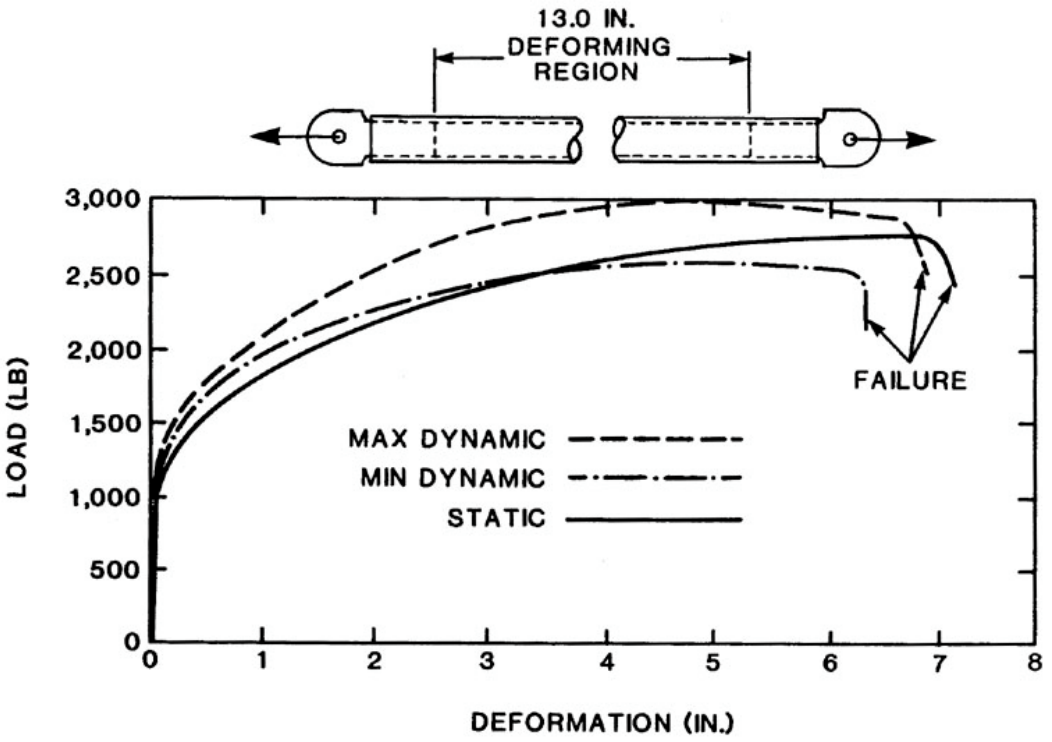


Figure 7-10.
Elongation of a metal tube to absorb energy (Reference 7-4).

7.4.3.5 Tube and Die, Rod and Die, Tube and Mandrel

These devices use the force required to compress a rod or tube as it is drawn through a die, or to expand the diameter of a tube as an oversized rod, tube, or mandrel is drawn through it. The force required to overcome friction also contributes to the energy absorbed by this device, and, unless this friction is carefully controlled, the load may be unpredictable. The frictional resistance of the device tested in Reference 7-12 (a compression tube device with a rigid outer cylinder) was reduced by lubrication, but the device exhibited an initial peak load, as indicated by Point A in Figure 7-11. A version of this device is now being used in helicopter seats.

7.4.3.6 Bending Metal

This type of device uses the plastic bending of machined or pre-formed metal to absorb crash energy. Typically, the member is “S”- or “V”-shaped and is connected to the seat structure through pin joints at each end. These devices are typically loaded in bending through the pin joints and can resist tensile loads in rebound.

Link-bender energy absorbers have found successful applications in an aftermarket seat for GA aircraft and in an emergency medical service (EMS) attendant seat for helicopters.

Another example of bending metal to limit vertical loading is through the use of a piece of sheet metal that has been bent so its cross-section has the shape of the Greek letter sigma (Σ). While this device has yet to be used in aviation, it has been successfully applied to a load-limiting seat in a kit developed for mine blast protection for a U.S. Army land vehicle.

THIS DOCUMENT PROVIDED BY THE ABBOTT AEROSPACE
TECHNICAL LIBRARY
ABBOTTAEROSPACE.COM

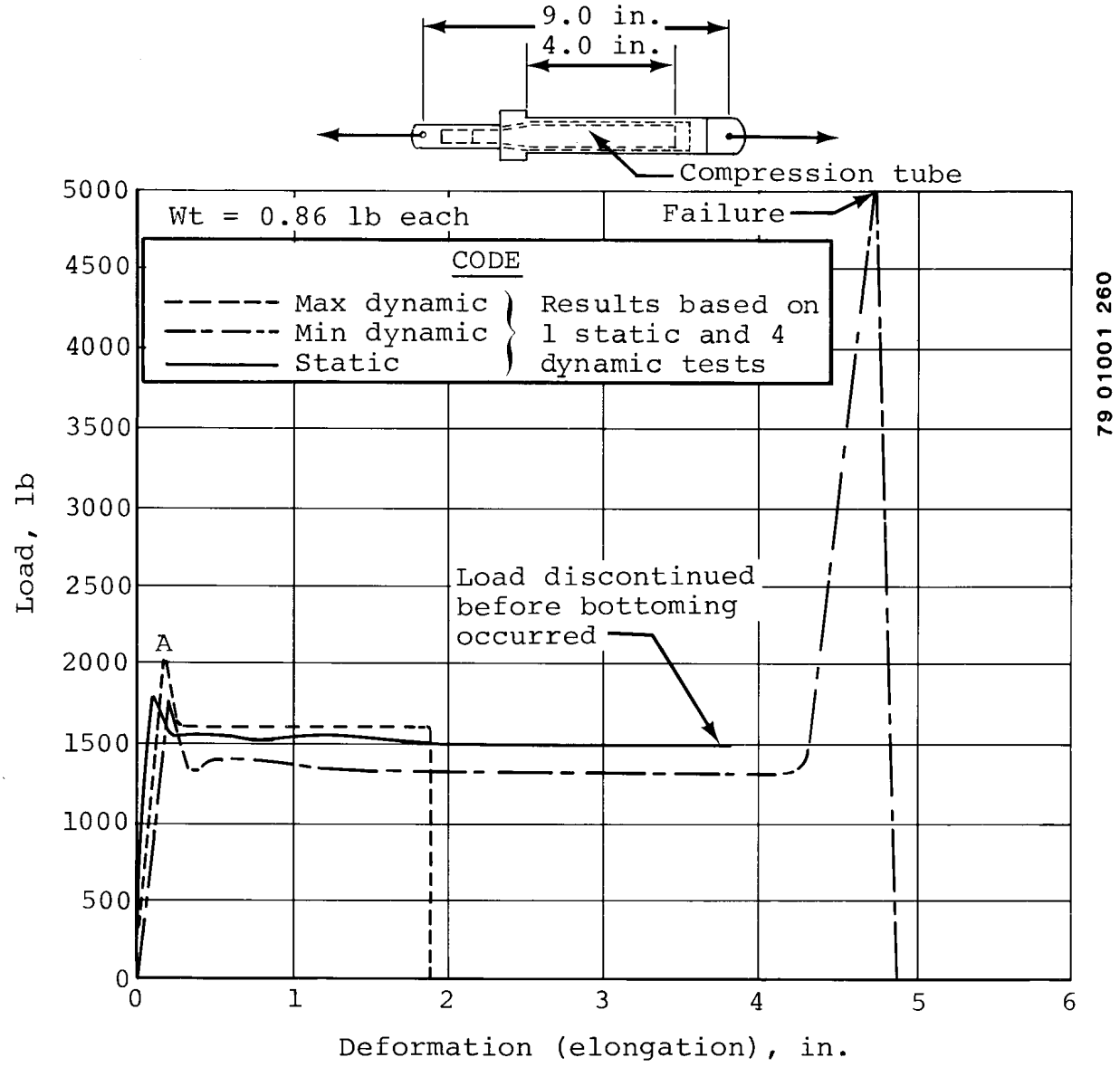


Figure 7-11.
Typical rod and die energy absorber and force deflection curve

7.4.4 Materials of Construction

Seats are generally constructed from the same materials as the aircraft. This includes, but is not limited to, metal tubing, cloth, sheet metal, and composites. Designers should construct the seats from materials that will provide a high strength-to-weight ratio while still providing sufficient ductility to prevent brittle failures. The standard method of selecting materials using elastic analysis is adequate for most conditions in the working life of the seat. For crashworthiness, however, only one application of the maximum load is expected, and the behavior of the material beyond its yield point generally is important.

This Document Provided by the Abbott Aerospace
TECHNICAL LIBRARY
ABBOTTAEROSPACE.COM

Ductile materials must be used to allow plastic deformation of the seat structure during a crash event. As a general rule, a value of 10-pct elongation is recommended as a minimum for use on all critical structural members. In some applications, a minimum elongation of 5 pct can be used for critical members, provided the load members are in a load-limited path.

7.4.5 Cushions

The seat bottom and seat back with which the occupant is in constant contact should be designed for comfort and durability. Well-designed cushions should provide comfort for the occupant, as well as complement the crashworthiness of the seat.

7.4.5.1 Seat Bottom Cushions

The seat bottom cushion can have a significant effect on the comfort and crashworthiness of the seat. The problem is one of developing a compromise design that will provide both comfort and safety. In general, comfort is provided by providing relatively thick and soft foam cushions, which distribute the load and decrease localized point loading. However, an excessively thick/soft cushion can promote dynamic overshoot during a high vertical acceleration crash, thus increasing the occupant's spinal load. In addition, a thick/soft cushion may not assist in providing the occupant lower torso with longitudinal restraint.

A design approach that has been successfully employed is a contoured cushion, which approximates the shape of the occupant's buttocks. Thus, the cushion thickness can be reduced with minimal effect on comfort. The contour can be provided by the seat pan structure (recommended) or by an insert between the seat pan and the soft cushion material. To minimize dynamic overshoot, the compressed cushion thickness under the buttocks (specifically, the ischial tuberosities) should be no more than 0.75 in. thick. Thicker cushioning can be provided in the occupant thigh region to accommodate various thigh angles, especially for crewmembers who operate the rudder pedals of the aircraft.

Use of rate-sensitive foams has also demonstrated increased crashworthiness and comfort. In general, rate-sensitive foams will deform slowly to accommodate comfort, but "stiffen" during high compression rates. This rate-sensitive stiffening helps to couple the occupant to the seat energy-absorbing system and reduces dynamic overshoot. However, rate-sensitive foams are generally more dense and less durable than conventional polyurethane foams.

The seat bottom cushion can also be designed as a floatation device. This is normally accomplished by providing a layer of semi-rigid closed-cell foam under the comfort cushion. This layer can double as the contoured interface between the seat pan and the occupant's buttock contour.

7.4.5.2 Energy-Absorbing Seat Bottom Cushions

As previously mentioned in Section 7.4.1.4, the seat pan cushion can be used to attenuate the spinal load. This approach has been successfully used in a few light GA aircraft certified to the dynamic requirements of 14 CFR 23.562. These seats use crushable material (Section 7.4.3.3) to absorb energy; typically a rigid, friable polyurethane foam or aluminum honeycomb. The energy-absorbing cushion must be designed to distribute the load to the crushable material. Otherwise, severe soft tissue injury can occur during a crash. The load distributor also prevents damage to the crushable material under normal use (i.e., from stepping on the cushion with hard heels).

Since most crushing materials will not hold high shear loads after crushing, the restraint will most likely need to be anchored to the aircraft structure. Thus, it is difficult to maintain the optimal lap belt restraint geometry as the seat pan strokes. For this reason, an energy-

This Document Provided by the Abbott Aerospace
Technical Library
abbottaerospace.com

absorbing cushion should only be utilized when minimal vertical stroke is required. One advantage of this design is that there is minimal stroking mass, so dynamic overshoot is minimized.

Cushions fabricated from rate-sensitive foams have demonstrated the capability of just meeting the 14 CFR 23.562(c) spinal load requirements during dynamic tests when used on extremely stiff, non-stroking seats. Rate-sensitive foam cushions did not meet the spinal load requirement when tested on more-compliant (real-world) non-stroking seat structures (Reference 7-24). The dynamic performance of rate-sensitive foams currently in use is also extremely temperature sensitive. Using rate-sensitive foam as the only means of limiting the spinal load is not recommended, unless the foam's performance can be verified through testing over the entire operational temperature range of the aircraft using a production seat structure.

7.4.5.3 Backrest Cushions

In most cases, the backrest cushion has a minimal effect on crashworthiness, but it will influence comfort, and can influence the injury tolerance of the occupant's spine. A relatively firm lumbar support can help keep the lumbar spine curvature forward, which generally increases the occupant's tolerance to compressive loading.

In addition to a firm lumbar support, side bolsters are also recommended, as they increase comfort and can also provide some level of occupant lateral support. For acrobatic aircraft, the seat back and cushion must be designed to accommodate an occupant wearing a parachute.

7.4.5.4 Head Rest Cushions

The head rest cushion should be designed to cushion head impact and help prevent whiplash injury due to backward extension of the neck. The cushion is generally not designed for comfort. If possible, the cushion thickness should be at least 1.5 in. thick. Use of rate-sensitive foams is recommended.

7.4.6 Environmental Design Conditions

All primary seat structure should be protected to prevent deterioration from environmental factors. The design should address loss of strength caused by vibration, humidity, dissimilar metals, fluid spillage, dust/dirt, exposure to cleaning solutions, in-service wear and tear, etc. Special considerations should be given to aircraft that are expected to operate in harsh environments. For example, the corrosive environment for a floatplane will be harsher than for land-based aircraft.

7.4.7 Seat Strength and Deformation

Seat strength requirements are defined in 14 CFR 23.395, 23.397, 23.561, 23.562, and 23.785. Based on the requirements specified in these regulations, an aircraft seat designer must be concerned with three different loading conditions: the maximum expected flight and ground load factors, the reaction of pilot forces on the primary flight controls, and the emergency landing dynamic conditions (Reference 7-1). The maximum load factors and the reaction of pilot forces are treated as static conditions, whereas 14 CFR 23.562 is purely a dynamic test. Regulations require that seat strength be substantiated for both the static and dynamic conditions.

This Document Provided by the Abbott Aerospace
TECHNICAL LIBRARY
ABBOTTAEROSPACE.COM

7.4.7.1 Static Strength and Deformation Requirements

The static load conditions are selected from the worst-case load factors (flight, ground, or reaction) for each principle direction: fore, aft, up, down, and lateral. The lateral loads are assumed to be symmetric. Each aircraft must be analyzed for their individual worst-case loads, as they can differ from aircraft to aircraft. Typically, these worst-case scenario loads can be represented by the loads defined in 14 CFR 23.395, 23.397, and 23.561 (Reference 7-1). The 14 CFR 23.395 and 23.397 regulations provide the rudder pedal reaction loads, while 14 CFR 23.561 provides the fore and lateral emergency landing loads, as well as the up and down gust and/or ground loads.

All static load calculations are determined using a 215-lb occupant plus the seat weight. A safety factor of 1.33 is also incorporated into the calculations. For example, a 9.0-G forward load with a 30-lb seat would require a load rating of 2,933 lb (9.0 X 1.33 X (215 + 30)).

The 14 CFR 23.785 regulation states that compliance with the static strength requirements may be demonstrated by either analysis and/or static testing (Reference 7-1). In practice, however, static tests to ultimate loads are generally conducted even if the structure can be shown to comply by analysis. These tests are often conducted as a proof of seat and restraint strength before performing the more severe and costly dynamic tests. Usually, a seat/restraint that fails the static tests will also fail the structural requirements of the dynamic tests. Passing the static load tests, however, does not guarantee the seat/restraint system will pass the dynamic tests.

The 14 CFR 23.305 regulation outlines some the deformation requirements for GA seats. This regulation requires that the seat cannot deform to the point where the occupants cannot egress the aircraft. Specifically, the regulation states that:

> "(a) The structure must be able to support limit loads without detrimental, permanent deformation. At any load up to limit loads, the deformation may not interfere with safe operation.
>
> (b) The structure must be able to support ultimate loads without failure for at least three seconds, except local failures or structural instabilities between limit and ultimate load are acceptable only if the structure can sustain the required ultimate load for at least three seconds. However when proof of strength is shown by dynamic tests simulating actual load conditions, the three-second limit does not apply" (Reference 7-1).

Additional seat deformation requirements are defined in 14 CFR 23.785(k). This regulation requires that "each seat/restraint system may use design features, such as crushing or separation of certain components, to reduce occupant loads when showing compliance with the requirements of 23.562 of this part; otherwise, the system must remain intact" (Reference 7-1).

7.4.7.2 Dynamic Strength and Deformation Requirements

Seat strength and deformation is also substantiated by the dynamic test requirements of 14 CFR 23.562. The structural requirements for the dynamic tests are found in 14 CFR 23.562(c)(1) and (c)(2). Subsection (1) of Section (c) in 14 CFR 23.562 requires that even in the presence of seat "deformation, elongation, displacement, or crushing intended as part of the design," the seat and restraint system must restrain the ATD (Reference 7-1). Subsection (2) requires that even in the presence of seat deformation the "attachment between the seat/restraint system and the test fixture must remain intact" (Reference 7-1).

To comply with this regulation, the seat is subjected to two different dynamic impact tests. The testing requirements for both dynamic tests are displayed in Table 7-1. The testing requirements for 14 CFR 25, 27, and 29 are also provided as a basis for comparison. Table 7-2 provides a description of the injury criteria defined in 14 CFR 23.

THIS DOCUMENT PROVIDED BY THE ABBOTT AEROSPACE
TECHNICAL LIBRARY
ABBOTTAEROSPACE.COM

Table 7-1. Dynamic Test Requirements for 14 CFR 23, 25, 27, and 29 (References 7-1, 7-7 – 7-26)				
TEST 1	**FAR 23**	**FAR 25**	**FAR 27**	**FAR 29**
Min velocity (ft/sec)	31	35	30	30
Max time to peak (sec)	0.05/0.06	0.08	0.031	0.031
Min G	19/15	14	30	30
Seat pitch angle (deg)	30	30	30	30
Seat yaw angle (deg)	N/A	N/A	N/A	N/A
Roll (deg)	0	0	10	10
Pitch (deg)	0	0	10	10
TEST 2	**FAR 23**	**FAR 25**	**FAR 27**	**FAR 29**
Min velocity (ft/sec)	42	44	42	42
Max time to peak (sec)	0.05/0.06	0.09	0.071	0.071
Min G	26/21	16	18.4	18.4
Seat pitch angle (deg)	N/A	N/A	N/A	N/A
Seat yaw angle (deg)	10	10	10	10
Roll (deg)	10	10	10	10
Pitch (deg)	10	10	10	10

Table 7-2. Occupant Injury Criteria Specified in 14 CFR 23.562 (Reference 7-1)		
Description	**Injury Criteria**	**Instrumentation**
HIC (Head Injury Criterion)	1,000	Triaxial linear accelerometer installed at the c.g. of the ATD's head
Shoulder harness strap loads	1,750 lb for single straps; 2,000 lb for dual straps	Load cell(s) attached directly to the shoulder harness straps
Lumbar compression load	1,500 lb	Load cell installed between the lumbar spine and pelvis
Abdominal lap belt loading	Lap belt must remain on ATD's pelvis	None required

Test 1, referred to as the "down test", determines the protection provided when the crash environment is such that the crash impact load component is directed along the spinal column of the seat occupant, in combination with a forward component. The test sled fixture used to conduct Test 1 is illustrated in Figure 7-12. By changing the direction of the velocity vector, this test can also be conducted on a drop tower, as shown in Figure 7-13.

Test 2, referred to as the "sled test," determines the protection provided when the crash environment is such that the crash impact load is in the longitudinal direction, with a lateral component. The sled test fixture used to conduct Test 2 is illustrated in Figure 7-14.

THIS DOCUMENT PROVIDED BY THE ABBOTT AEROSPACE
TECHNICAL LIBRARY
ABBOTTAEROSPACE.COM

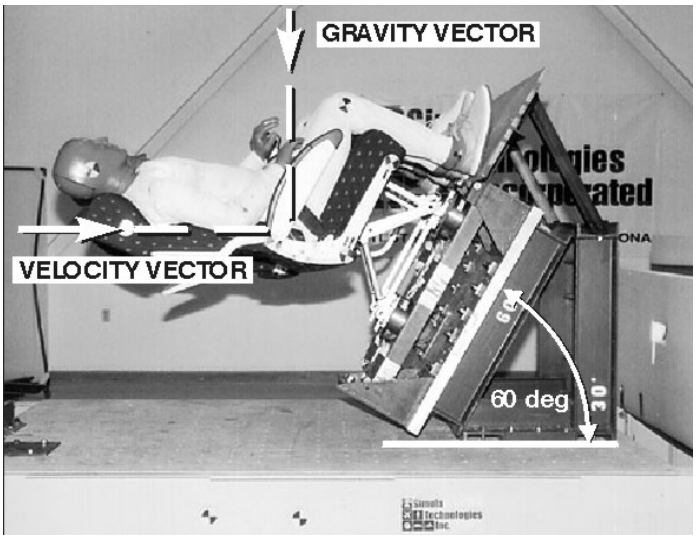


Figure 7-12.
Dynamic Impact Test 1: As conducted on a horizontal sled, with the seat positioned 60-deg above horizontal.



Figure 7-13.
Dynamic Impact Test 1: As conducted on a drop tower with the seat tilted 30-deg nose-down.

THIS DOCUMENT PROVIDED BY THE ABBOTT AEROSPACE
TECHNICAL LIBRARY
ABBOTTAEROSPACE.COM



Figure 7-14.
Dynamic Impact Test 2: Longitudinal sled test.

7.4.7.3 Recommended Strength and Deformation

The aircraft designer must remember that the seat strength and deformation requirements in 14 CFR Part 23 are minimum standards, and that occupants and real-world accident conditions vary considerably from those described in the regulations. On the other hand, a seat designed for all potential occupant sizes and accident conditions would be impractical from both a cost and weight standpoint.

The strength of the seat/restraint system should be consistent with the strength of the structure to which it is attached, and should be consistent with strength or limit-loads of the occupant protection system.

Paragraph 4.1.1 in AS8049 recommends a flight-control reaction load of 1,000 lb applied aft at 8 in. above the seat reference point (Reference 7-3). This is slightly higher than that required in 14 CFR 23.395 and 23.397, but seems reasonable. The other static factor directions in AS8049 are very similar to those in 14 CFR 23.561, but with slight differences.

7.4.7.4 Recommended Occupant Weights for Seat Design

It is recommended that the upper and lower limits of occupant weights to be considered in seat design be based on the 95th-percentile male and 5th-percentile female. Typical male and female aviator weights are presented in Table 7-3 (Reference 7-27). Other anthropomorphic populations may be more appropriate, depending on the expected user demographics. Ideally, for a fixed-load energy absorber, the limit-load should be sized for the smallest occupant, while the stroking distance should be determined for the largest occupant. That way, the load would be tolerable, and the stroke length would be adequate for all occupants in the design range. In most situations, however, sufficient stroke distance is not available in the aircraft to use the ideal approach; therefore, compromises must be made.

THIS DOCUMENT PROVIDED BY THE ABBOTT AEROSPACE
TECHNICAL LIBRARY
ABBOTTAEROSPACE.COM

Table 7-3. Typical Aviator Weights (Reference 7-27)						
Item	95th-Percentile Weight (lb)		50th-Percentile Weight (lb)		5th-Percentile Weight (lb)	
	Male	Female	Male	Female	Male	Female
Aviator	211.7	164.3	170.5	131.4	133.4	102.8
Clothing	3.1		3.1		3.1	
Shoes	2.0		2.0		2.0	
Total Weight	216.8	169.4	175.6	136.5	138.5	107.9
Effective Vertical Weight	171.8	133.9	138.9	107.6	109.2	84.7

The effective weight in the vertical direction of a seated occupant is approximately 80 pct of the occupant's total weight, because the lower extremities are partially supported by the floor. The effective weight is determined by summing:

- 80 pct of the occupant's body weight (without clothing)
- 80 pct of the weight of the occupant's clothing, not including the weight of the shoes
- 100 pct of the weight of any equipment carried on the body above the knee level.

The effective vertical weights listed in Table 7-3 assume a nominal clothing weight of 3.1 lb and no additional body-carried weight such as headsets or parachutes. The effective vertical weight is used in the design of the downward seat strength and limit-load, whereas the total weight is used in the design of seat strength (and limit-load, if applicable) in all the other loading directions.

7.5 AIRCRAFT SEAT TESTING

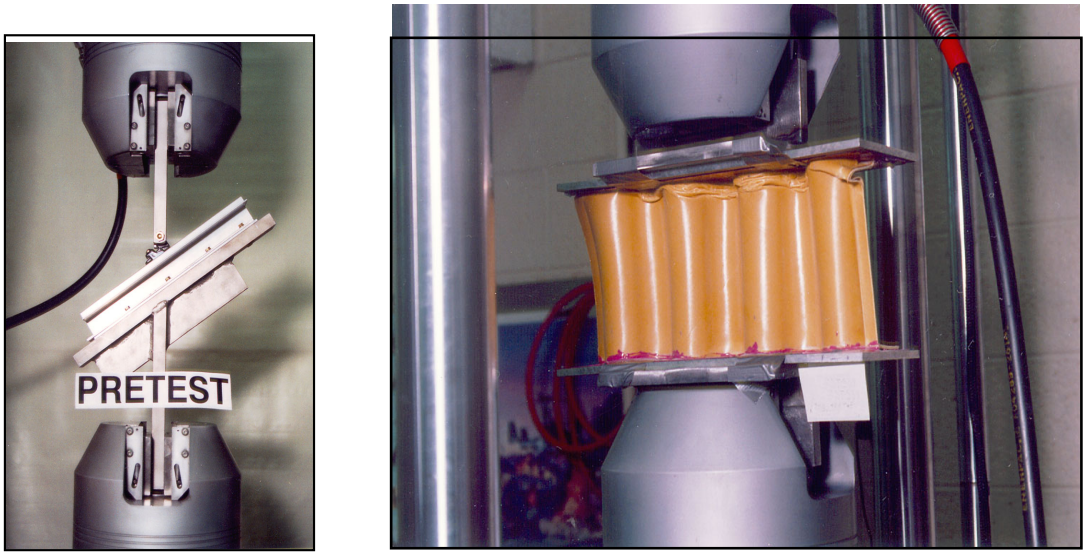
Design validation and certification of aircraft seats is accomplished by evaluating seating structures on both a component and system level. Evaluation can be conducted via component, flammability, static, and dynamic testing. The following sections will describe the difference among these testing methods. These sections will also provide guidance on how to:

1. Choose a proper testing facility
2. Generate and document an organized Test Plan
3. Document test results.

7.5.1 Component Testing

Component testing of the floor/wall attachments and fittings, laminated structures, restraint hardware, sewn components, and energy-absorbing systems is used to validate the strength of the seat. Figure 7-15 displays Instron load testing of floor fittings and energy-absorbing material.

THIS DOCUMENT PROVIDED BY THE ABBOTT AEROSPACE
TECHNICAL LIBRARY
ABBOTTAEROSPACE.COM



(a) (b)

Figure 7-15.
Instron load testing of (a) transport seat floor fittings and (b) an energy-absorbing subfloor element.

7.5.2 Flammability Testing

Flammability testing of laminated structures, cushions/covers, and soft good/webbing materials is required to certify an aircraft seat design. The AC 23-2, Flammability Tests, provides guidance for complying with the flammability requirements specified in 14 CFR 23.853 (References 7-1 and 7-28). Figure 7-16 is a photograph of an FAA flammability chamber that is used for 14 CFR 23.853 testing.

7.5.3 Static Testing

Static testing of aircraft seats is conducted to assess a structure's capability to withstand static design loads and to understand the deformation behavior of a structure with respect to the level of loading. Figure 7-17 displays the static test set-up for an aircraft seat. As the name implies, loads are applied slowly, at a specific rate, to achieve a quasi-static loading condition. Generally, static testing is less expensive than dynamic testing. Therefore, static tests are usually among the earliest tests conducted during design validation. Static loading can be applied in along a single axis or along multiple axes simultaneously. Section 7.4.7.1 describes the static test requirements for GA aircraft seats.

This Document Provided by the Abbott Aerospace
Technical Library
abbottaerospace.com

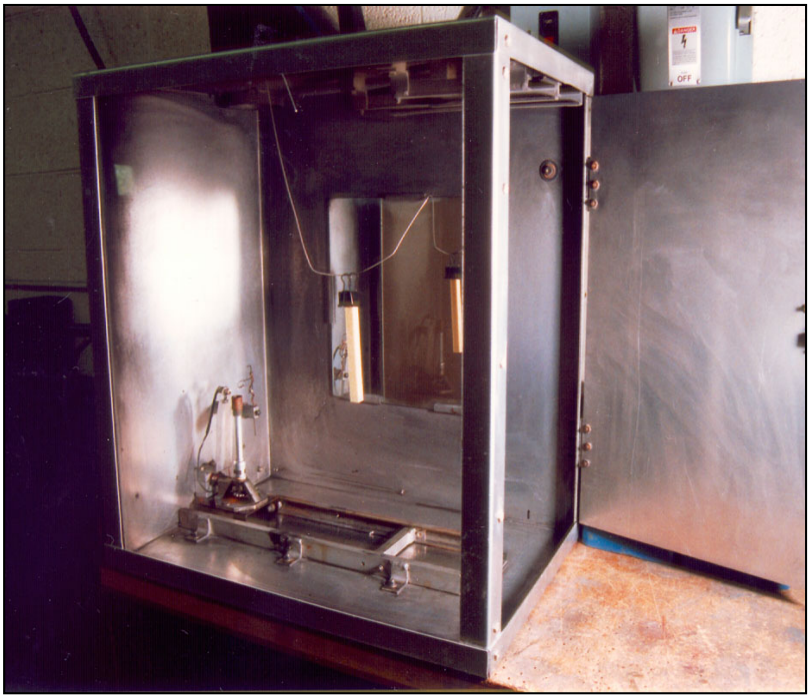


Figure 7-16.
FAA flammability test chamber.

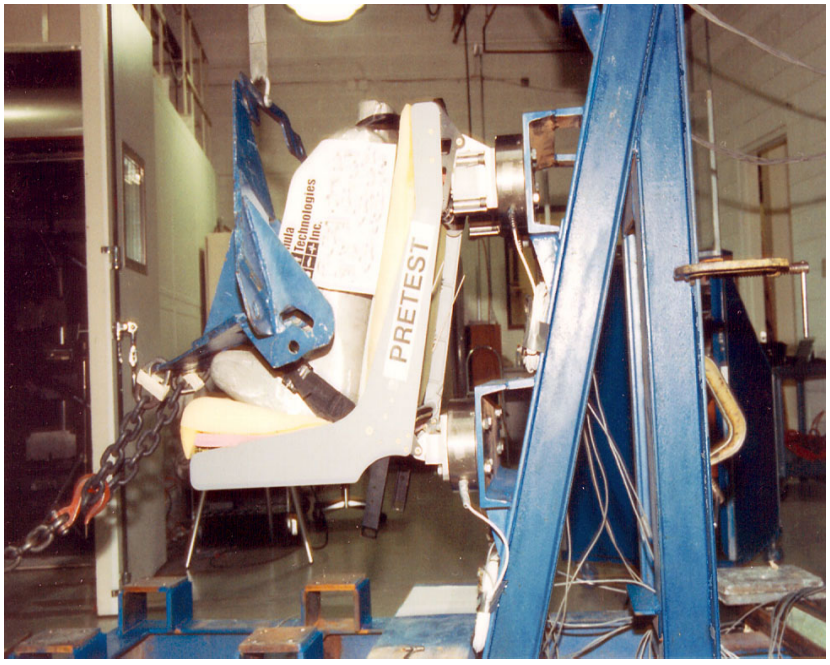


Figure 7-17.
Structural static test set-up of an aircraft seat.

THIS DOCUMENT PROVIDED BY THE ABBOTT AEROSPACE
TECHNICAL LIBRARY
ABBOTTAEROSPACE.COM

7.5.4 Dynamic Testing

Dynamic testing is conducted to provide a controlled, realistic, and repeatable simulation of a crash event. It is used to assess the capabilities of crash-protective hardware. Dynamic testing is also used to simulate other non-crash, transient dynamic events such as the effect of mine blasts on vehicles. Figure 7-18 shows the progression of a dynamic sled test conducted to assess the structural capabilities of row-to-row transport category aircraft seats. Section 7.4.7.2 describes the dynamic test requirements for GA aircraft seats.

There are four major types of dynamic testing facilities: deceleration-sled, acceleration-sled, impact-with-rebound, and drop-tower. The following sections describe the advantages and disadvantages of each facility.

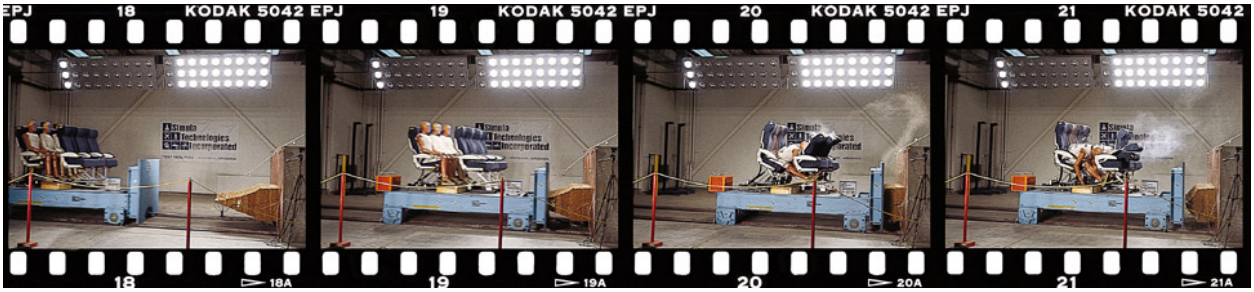


Figure 7-18.
Dynamic impact test of 14 CFR 25 transport category aircraft seats.

7.5.4.1 Deceleration Sleds

A deceleration-sled dynamic testing system accelerates a sled and test specimen into a deceleration mechanism (wirebender, steel bar bender, or crushable honeycomb stack) that generates the required crash simulation pulse. Figures 7-19 and 7-20 illustrate a small airplane fuselage fixed to a deceleration sled. The sled is poised to impact a crushable paper honeycomb stack to generate the desired crash pulse. The velocity before impact must be equal to or be very close to the desired test crash velocity. Some deceleration mechanisms generate rebound, which is included into the crash velocity, thus reducing the initial velocity required.

The advantages of the deceleration sled are:

- Simple
- Easy to understand.

The disadvantages of the deceleration sled are:

- Requires a long acceleration distance
- Requires a high impact velocity
- The sled is not well suited for aft-facing seat testing in the Test No. 1 “down test” configuration.

The following organizations have deceleration sled facilities:

- FAA’s Civil Aeromedical Institute (CAMI), Oklahoma City, Oklahoma
- Simula Technologies, Inc., Phoenix, Arizona
- Wichita State University, Wichita, Kansas.

This Document Provided by the Abbott Aerospace
Technical Library
abbottaerospace.com

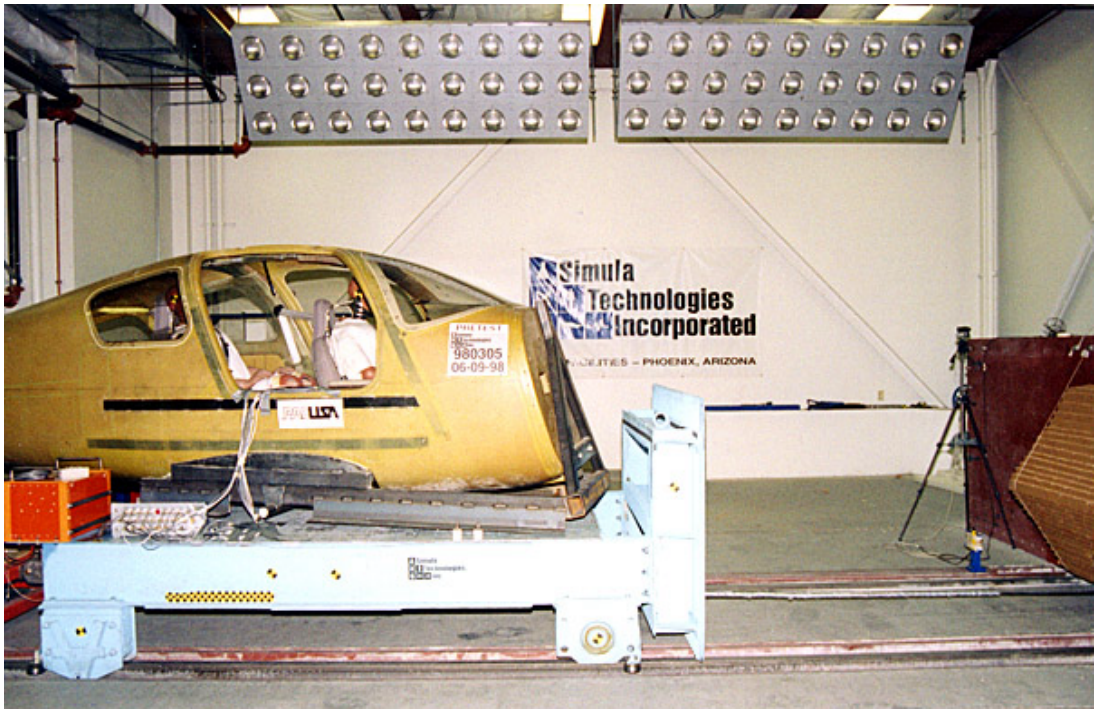


Figure 7-19.
Small airplane fuselage fixed to a deceleration sled. The sled is preparing to impact the crushable honeycomb stack to generate the desired crash pulse.



Figure 7-20.
Crushable honeycomb stack attached to a rigid barrier.

This Document Provided by the Abbott Aerospace
TECHNICAL LIBRARY
ABBOTTAEROSPACE.COM

7.5.4.2 Acceleration Sleds

This type of system is typically described as a hydraulically controlled gas-energy (HYGE) accelerator (Figure 7-21). The test specimen begins at rest and is then subjected to the simulated crash pulse. The desired input velocity and acceleration profiles are produced by an actuator with an internal metering pin that controls the actuator stroke. At the end of the simulated crash pulse, the sled is moving at the impact velocity in the reverse direction. It must be decelerated over a long distance at a relatively low G level.

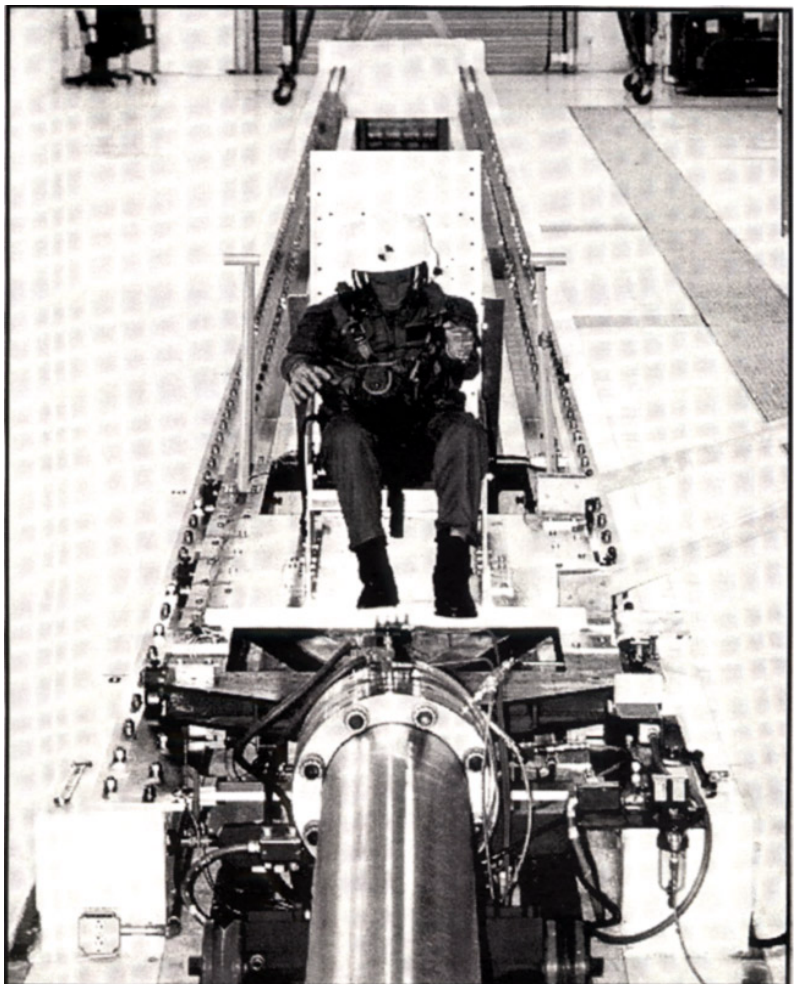


Figure 7-21.
Hydraulically controlled gas-energy (HYGE) sled (Reference 7-29).

The advantages of the acceleration sled are:

- Can test large specimens at high energies
- The acceleration pulse is extremely reproducible.

THIS DOCUMENT PROVIDED BY THE ABBOTT AEROSPACE
TECHNICAL LIBRARY
ABBOTTAEROSPACE.COM

The disadvantages of the acceleration sled are:

- Changing the metering pins for each pulse requirement is expensive (machining costs), time-consuming, and somewhat difficult (requiring disassembly and assembly of the actuator)
- The system consumes large quantities of high-pressure air or nitrogen
- The sled is not well suited for testing aft-facing seats in the Test No. 1 “down test” configuration.

The following organizations have acceleration sled facilities:

- MGA Research Corporation, Burlington, Wisconsin
- Transportation Research Center, East Liberty, Ohio
- Veridian Engineering (Calspan), Buffalo, New York.

7.5.4.3 Impact-with-Rebound Sleds

When using this type of system, the deceleration mechanism can be mounted on the sled or the reaction mass. The crash pulse simulator mechanism is designed to act like a resilient spring (Figure 7-22). The impact takes place as the moving sled contacts the mechanism, which stores the energy of the impact and then returns the stored energy to the sled, accelerating it back to its initial starting position. The acceleration of the sled is in the same direction during both the acceleration and rebound portions of the pulse (Figure 7-23).

The advantages of the impact-with-rebound sled are:

- Only 50 pct of the required input velocity is required (assuming 100-pct efficiency), thus requiring a much shorter track.

The disadvantages of the impact-with-rebound sled are:

- The sled is not well-suited for testing the aft-facing seat in the Test No 1 “down test” configuration
- It is difficult to obtain the acceleration just before or after the impact.

The following organizations have impact-with-rebound sled facilities:

- Simula Technologies, Inc., Phoenix, Arizona (acceleration sled with ~ 20 pct rebound-generating crash velocity).

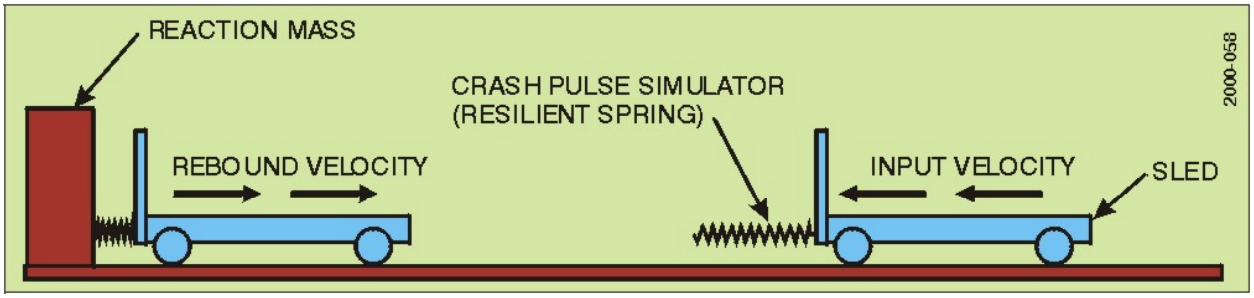


Figure 7-22.
Impact-with-rebound sled.

THIS DOCUMENT PROVIDED BY THE ABBOTT AEROSPACE
TECHNICAL LIBRARY
ABBOTTAEROSPACE.COM

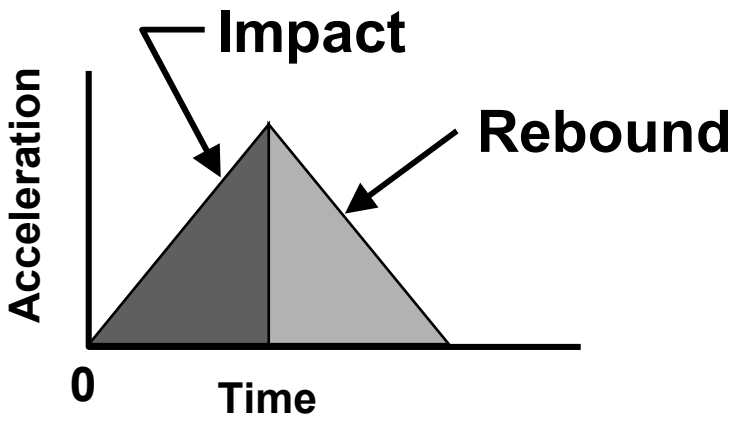


Figure 7-23.
Impact and rebound acceleration pulse for an impact-with-rebound sled.

7.5.4.4 Drop Tower

Deceleration drop towers are easy to build and operate. Since the pull of the Earth's gravity is used to accelerate the drop carriage to impact velocity, there is no need for a complex accelerating system (Figure 7-24).

The advantages of the drop tower are:

- This system is well-suited for performing testing of the aft-facing seat in the Test No.1 "drop test" configuration
- It is better suited than the sled systems for all Test No. 1 drop tests

The disadvantages of the drop tower are:

- This system is not well-suited for performing the Test No. 2 "sled test", as the ATD's tend to fall from the carriage due to gravity
- Gravity will also oppose the final rebound of the ATD into the seat back, which minimizes the ability to test the seat back strength

The following organizations have drop tower facilities:

- Simula Technologies, Inc., Phoenix, Arizona (indoor and outdoor drop towers)

7.5.5 Compliance of Facilities and Documentation

All test facilities used for FAA certification testing should have the following:

- A Test Facilities Document
  This document is a Process Control Manual that defines in detail all the processes and methods used to meet the requirements of the Federal Aviation Regulation (FAR)
- A document from the FAA stating that:
  -The FAA has reviewed its Facilities Document
  -The FAA has reviewed / audited the test facility on-site and found its test practices and methods to be acceptable.

THIS DOCUMENT PROVIDED BY THE ABBOTT AEROSPACE
TECHNICAL LIBRARY
ABBOTTAEROSPACE.COM



(a) (b)

Figure 7-24.
Drop tower facilities: (a) outdoor drop tower configured for a forward test and (b) indoor drop tower configured for a downward test.

7.5.6 Test Scheduling

It is important to allow sufficient time to schedule and conduct the tests. This section provides a list of recommendations for creating an effective test schedule.

1. Provide as much information to the test facility as early in the process as possible.
2. Communicate early and often with the test facility.
3. Details typically required by the test facility.
   - Expected number of seat configurations
   - Fixturing requirements
     - Simulation of cockpit / aircraft structure and who will provide it
4. Schedule a DER (Designated Engineering Representative)
5. Allow at least 30 - 40 days for the DER and the FAA to review and approve the Test Plan
6. Provide a minimum of two seats for each dynamic test condition
7. Define the desired data types and formats

Note: Due to scheduling constraints, many test facilities will require a deposit to hold dates.

THIS DOCUMENT PROVIDED BY THE ABBOTT AEROSPACE
TECHNICAL LIBRARY
ABBOTTAEROSPACE.COM

7.5.7 Reporting Documentation

Following the testing process, the test facility should provide all of the necessary documentation needed to generate a Final Test Report. The documentation should include:

- Certifications of the instrumentation / equipment used
- Original photographs for the FAA / customer
- Hardcopy plots and summary sheets of all reported data
- An electronic copy of all reported data
- Film or high-speed video of each test.

THIS DOCUMENT PROVIDED BY THE ABBOTT AEROSPACE
TECHNICAL LIBRARY
ABBOTTAEROSPACE.COM

References

7-1. "Federal Aviation Regulations, Part 23, Airworthiness Standards: Normal, Utility, Acrobatic, and Commuter Category Airplanes," 14 CFR 23, Federal Aviation Administration, Washington, D.C.

7-2. "Dynamic Testing of Part 23 Airplane Seat/Restraint Systems and Occupant Protection," FAA Advisory Circular AC23.562-1, Federal Aviation Administration, Washington, D.C., June 1989.

7-3. "Performance Standards for Seats in Civil Rotorcraft, Transport Aircraft, and General Aviation Aircraft," SAE Aerospace Standard AS8049, Rev. A, Society of Automotive Engineers, Warrendale, Pennsylvania, September 1997.

7-4. Desjardins, S. P., et al., Aircraft Crash Survival Design Guide, Volume IV – Aircraft Seats, Restraints, Litters, and Cockpit/Cabin Delethalization, Simula, Inc., Phoenix, Arizona; USAAVSCOM TR 89-D-22D, Aviation Applied Technology Directorate, U.S. Army Aviation Research and Technology Activity (AVSCOM), Fort Eustis, Virginia, December 1989.

7-5. Diffrient, N., Tilley, A. R., and Bardagjy, J. C., Humanscale 1/2/3, MIT Press, Cambridge, Massachusetts, 1974.

7-6. Military Standard, MIL-STD-1333A, Aircrew Station Geometry for Military Aircraft, Department of Defense, Washington, D.C., 20301, November 21, 1977.

7-7. "Federal Aviation Regulations, Part 25, Airworthiness Standards: Transport Category Airplanes," 14 CFR 25, Federal Aviation Administration, Washington, D.C.

7-8. Ezra, A., and Fay, R. J., An "Assessment of Energy Absorbing Devices for Prospective Use in Aircraft Impact Situations", in Dynamic Response of Structures, G. Herrmann and N. Perrone, eds., Pergammon Press, Elmsford, New York, 1972, pp. 225-246.

7-9. Reilly, M. J., Crashworthy Troop Seat Investigation, The Boeing Vertol Company; USAAMRDL Technical Report 74-93, Eustis Directorate, U.S. Army Air Mobility Research and Development Laboratory, Fort Eustis, Virginia, December 1974, AD/A-007090.

7-10. Kroell, C. K., "A Simple, Efficient, One Shot Energy Absorber", Reprint from Bulletin No. 30, Shock, Vibration, and Associated Environments, Part III, General Motors Research Laboratory, Warren, Michigan, February 1962.

7-11. Guist, L. R., and Marble, D. P., Prediction of the Inversion Load of a Circular Tube, NASA Technical Note D-3622, Ames Research Center, Moffett Field, California, June 16, 1966.

7-12. Haley, J. L., Klemme, R. E., and Turnbow, J. W., Test and Evaluation of 1000-4000 Pound Load-limiting Devices, Dynamic Science, AvSer Facility Report M69-2, for U.S. Army Aviation Material Laboratories, Fort Eustis, Virginia, February 1969.

7-13. Rich, M. J., Vulnerability and Crashworthiness in the Design of Rotary-Wing Vehicle Structures, Paper No. 680673, presented at the Aeronautic and Space Engineering and Manufacturing Meeting at Los Angeles, California, Society of Automotive Engineers, Inc., New York, New York, October 1968.

7-14. Bendix Products Aerospace Division, Energy Absorbing Characteristics of Crushable Aluminum Structures in a Space Environment, Report No. SPP-65-107 (NASA-Cr-65096), prepared for NASA Manned Spacecraft Center, Houston, Texas, July 1965.

THIS DOCUMENT PROVIDED BY THE ABBOTT AEROSPACE
TECHNICAL LIBRARY
ABBOTTAEROSPACE.COM

7-15. McGehee, J. R., A Preliminary Experimental Investigation of an Energy-Absorption Process Employing Frangible Metal Tubing, NASA Technical Note D-1477, National Aeronautics and Space Administration, Washington, D.C., October 1962.

7-16. Schwartz, M., Dynamic Testing of Energy-Attenuating Devices, NADC Report No. AC-6905, Naval Air Development Center, Warminster, Pennsylvania, October 1969.

7-17. Energy Absorbers for Helicopter Crashworthy Seats, NC 632, Alkan U.S.A. Inc., 235 Loop 820 N.E., Hurst, Texas 76053, February 1980.

7-18. Energy Absorbers for Alkan S10, S12 and S20 Crashworthy Seats, Technical Note No. 78-037, Alkan U.S.A. Inc., 235 Loop 820 N.E., Hurst, Texas 76053.

7-19. Farley, G. L., Energy Absorption of Composite Materials, NASA Technical Memorandum 84638, AVRADCOM Technical Report TR-83-B-2, Structures Laboratory, U.S. Army Research and Technology Laboratories (AVRADCOM), Langley Research Center, Hampton, Virginia, 23665, March 1983.

7-20. Jones, N., and Wiergbicki, T., eds, Structural Crashworthiness, Butterwork and Co., Ltd., London, England, 1983.

7-21. Singley, G. T., III, Full Scale Crash Testing of a CH-47C Helicopter, paper presented at the 32nd Annual National V/STOL Forum, American Helicopter Society, Washington, D.C., May 1976.

7-22. Desjardins, S. P., et al., Crashworthy Armored Crewseat for the UH-60A Black Hawk, paper presented at the 35th Annual National Forum, American Helicopter Society, Washington, D.C., May 1979.

7-23. Richards, M. A., and Hurley, T. R., "Low-Cost Energy-Absorbing Subfloor for a Composite General Aviation Aircraft," TR-96183, Simula Technologies, Inc., Phoenix, Arizona, May 20, 1997.

7-24. "Correlation of Component Foam Test Method to Full-Scale Dynamic Test," Cessna/AGATE report C-GEN-3433B-1, Cessna Aircraft Company, Wichita, Kansas, March 1997.

7-25. "Federal Aviation Regulations, Part 27, Airworthiness Standards: Normal Category Rotorcraft, 14 CFR 27, Federal Aviation Administration, Washington, D.C.

7-26. "Federal Aviation Regulations, Part 29, Airworthiness Standards: Transport Category Rotorcraft, 14 CFR 29, Federal Aviation Administration, Washington, D.C.

7-27. Simula, Inc., Aircraft Crash Survival Design Guide, Volume I – Design Criteria and Checklists, USARTL-TR-79-22B, Simula, Inc., Tempe, Arizona, January 1980.

7-28. "Flammability Tests," FAA Advisory Circular AC23-2, Federal Aviation Administration, Washington, D.C., August 20, 1984.

7-29. Aircrew Systems Facilities, Naval Aviation Systems Team, Patuxent River, Maryland.

This Document Provided by the Abbott Aerospace
TECHNICAL LIBRARY
ABBOTTAEROSPACE.COM

Chapter 8

Restraint Systems

Gregory B. Grace
Todd R. Hurley
Jill M. Vandenburg
Robert F. Gansman
Bill Bihlman

The purpose of the personnel restraint system is to restrain the occupant within the aircraft seat during aircraft maneuvers and turbulence, as well as during a crash event. To minimize injury during a crash event, the restraint must limit occupant motion within the protective shell so that the occupant's secondary impact with the interior is prevented or minimized. The restraint system must also limit loads to those tolerable by humans. In general, the restraint should minimize occupant motion as much as possible, which will minimize the secondary impact hazards, as well as limit dynamic overshoot.

Two types of restraint systems are discussed in this section: conventional belts or harnesses, and inflatables (including air bags and inflatable belt systems). Additionally, child restraint systems and issues regarding their installation in light airplanes are discussed. There is another form of restraint, which is referred to as occupant compartmentalization (knee bolsters, bulkheads, consoles, and sidewalls), but this type of passive restraint is not discussed here.

The restraint system can also be categorized as active or passive. An active system utilizes input from a crash sensor and some type of stored energy to activate and/or alter the restraint system during the crash event. Examples of active systems include air bags, inflatable belts, and belt pre-tensioners. A passive system is not activated by the crash event. Examples of passive restraints include conventional belts and knee bolsters. Aircraft designers should be aware that the terms “active” and “passive” restraints are used differently in the automotive industry: the automotive industry defines an active restraint as a device which requires occupant action (such as the buckling a seat belt), whereas a passive system provides restraint regardless of occupant action (such as an air bag or knee bolster).

At a minimum, all aircraft must have a belt or harness-type restraint for each occupant that includes a lower torso (lap belt) and upper torso (shoulder belt) restraint. Each occupant belt or harness restraint system must be used by a single occupant only. Other types of supplemental restraints (inflatable restraints and compartmentalization) are used to augment the belt or harness restraint performance for specific applications. A single supplemental restraint can be designed for multiple occupant use, if desired.

8.1 BELT OR HARNESS RESTRAINTS

This section provides general criteria and guidelines for the design of personnel restraint systems to reduce injury or debilitation in a crash situation.

This Document Provided by the Abbott Aerospace
TECHNICAL LIBRARY
ABBOTTAEROSPACE.COM

Restraint harnesses for aircraft occupants should provide the restraint necessary to prevent injuries in crash conditions approaching the upper limits of survivability. New aircraft designs undergoing certification should be equipped with restraint harnesses certified to TSO-C114 (Reference 8-1). Older type-certified aircraft are permitted to utilize restraints certified to TSO-C22 (Reference 8-2). However, the use of TSO-C22-certified restraints is not allowed in new designs and, as a result, they are not covered by this design guide. Appropriate strength analysis and tests as described in TSO-C114 and SAE AS8043 (Reference 8-3) are conducted by the restraint manufacturer to ensure that a restraint system is acceptable.

Numerous methods of restraining the human body have been proposed, investigated, and used. Some of these have proven to be exceptionally effective and some have left much to be desired. However, there are certain qualities that a harness should possess if it is to be used routinely for aircraft. These desirable qualities are listed below (Reference 8-4):

- The restraint harness should be comfortable and light in weight
- The restraint harness should be easy for the occupant to put on and take off, even in the dark
- The restraint harness should use a single-point release system that is easy to operate with one (either) hand, since an injured person might have difficulty in releasing more than one buckle with a specific hand. Also, the release system should be protected from inadvertent release. In other words, the buckle should not release if struck by the control stick, nor should it release due to inertial loading during a crash
- The restraint harness should allow occupants enough freedom of movement to operate the aircraft controls. This requirement may necessitate the use of an inertia reel in conjunction with the shoulder harness
- Each restraint harness system should provide sufficient restraint in all directions to prevent injury due to decelerative forces in a survivable crash
- The restraint harness webbing should provide a maximum area, consistent with weight and comfort, for force distribution in the upper torso and pelvic regions and should be woven with low-elongation (high-modulus) fiber to minimize dynamic overshoot under loads.

8.1.1 Restraint Regulations

General aviation (GA) belt and harness restraints are currently regulated by:

- TSO-C114, Torso Restraint Systems (Reference 8-1)
- FAR Part 23.562 and 23.785 (References 8-5 and 8-6).

Other related documents which describe the design, performance, and installation of belt and harness restraint systems include AC 21-34 “Shoulder Harness-Safety Belt Installations” (Reference 8-7), AC 23.562-1 “Dynamic Testing of Part 23 Airplane Seat/Restraint Systems and Occupant Protection” (Reference 8-8), and SAE AS8043 “Torso Restraint Systems” (Reference 8-3).

Restraint dynamic performance requirements are largely based on human tolerance to injury (covered in Section 4.3) and are found in 14 CFR 23.562(c). Some are based on observation, such as the requirements that the shoulder belt stay on the shoulder and the lap belt stay on the pelvis during the crash impact. Others are based on measurements of the shoulder strap load or measurements taken by an anthropomorphic test device (ATD). While belt restraints have a relatively simple appearance, there are design and installation subtleties that can have a profound influence on the occupant injury measurements.

THIS DOCUMENT PROVIDED BY THE ABBOTT AEROSPACE
TECHNICAL LIBRARY
ABBOTTAEROSPACE.COM

8.1.2 Types of Belt and Harness Restraint Systems

Belt restraints are typically described by the number of anchor points (or load paths) that they use. Three-point and five-point restraint types are the only fully developed systems currently recommended by this design guide for use in GA aircraft.

8.1.2.1 Three-Point System

The three-point belt configuration (using a single diagonal shoulder harness) is shown in Figure 8-1. This configuration is widely used in GA and is similar to the belt restraints found in most automobiles. The diagonal shoulder belt and the lap belt should attach to a single release buckle near the occupant's hip. Systems in which the buckle and shoulder belt attach near the center of the lap belt should not be used, as this can promote occupant submarining and can also allow upper torso rotation out of the belt due to the unfavorable position of the occupant's torso center of gravity (c.g.) (Section 8.1.3.2.1). The shoulder belt should ideally pass over the occupant's outboard shoulder**,** since the belt will only provide significant lateral support in one direction.

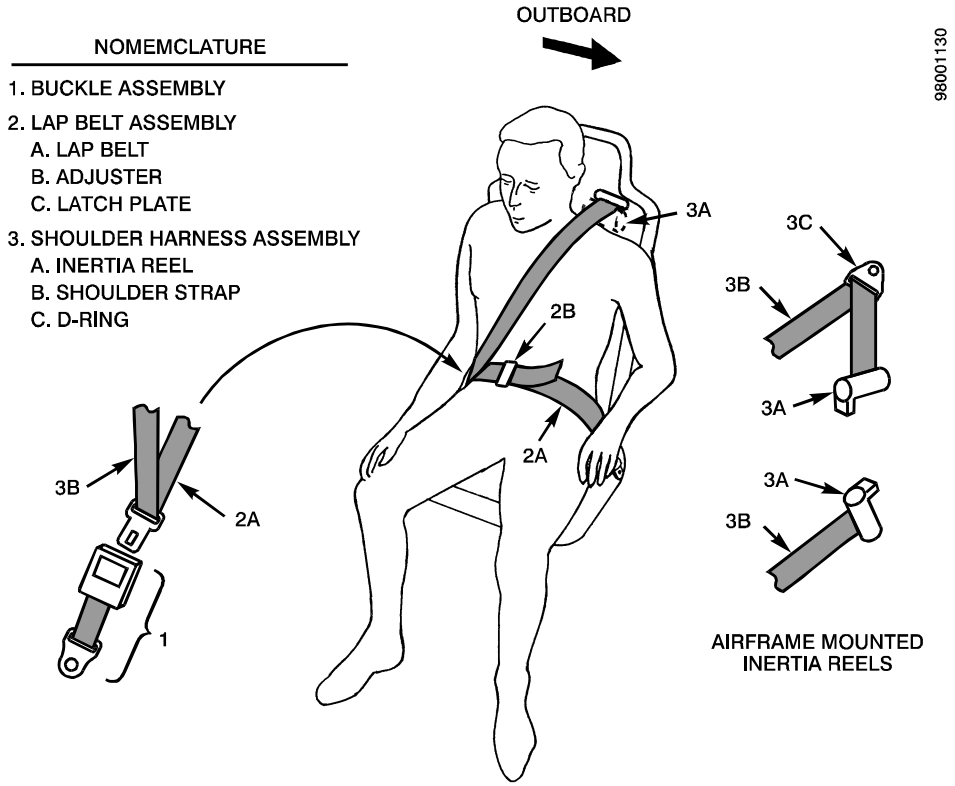


Figure 8-1.
Basic three-point occupant restraint system.

The upper torso restraint must allow each crewmember (pilot and/or copilot) to reach all required aircraft controls without removing and/or loosening the shoulder belt. A shoulder belt inertia reel is recommended to allow crewmembers to lean forward during flight. Inertia reels can also be provided to the other occupants for comfort and convenience, if desired. The

THIS DOCUMENT PROVIDED BY THE ABBOTT AEROSPACE
TECHNICAL LIBRARY
ABBOTTAEROSPACE.COM

shoulder belt must have an independent manual adjuster if an inertia reel is not used. A snap stud or other fitting which allows independent removal of the shoulder harness during flight—such as those seen on some older GA aircraft—should not be installed because of the potential for misuse.

The lap belt should be manually adjustable, since the lap belt provides most of the restraint during turbulence and maneuvering loads. A system with a single strap of retractable webbing and a sliding latch plate (as seen in most late-model automotive designs) should not be used, as the lap belt can loosen and allow occupant motion; especially during negative-G loading.

For the dynamic test requirement of 14 CFR 23.562, single diagonal shoulder belts are allowed a maximum load of 1,750 lb. In practice, the 1,750-lb maximum load can be difficult to meet for the front seat Test No. 2 condition (26-G horizontal test) depending on the installation. Small alterations in the shoulder belt's anchor point location or in the webbing's elongation capability are sometimes enough to bring the load below the maximum. In other cases, load-limiting (Section 8.1.7), pre-tensioning (Section 8.1.8) or inflatable restraints (Section 8.3) may be needed to reduce the belt load.

8.1.2.2 Five-Point System

The five-point harness configuration, which uses a center tie-down strap (See Figure 8-2), is the accepted standard crew harness for use by military pilots and other high-performance/ aerobatic aircraft. This system is generally considered to offer the best crash safety performance (for a webbing-only system) and occupant retention during high-G maneuvers.

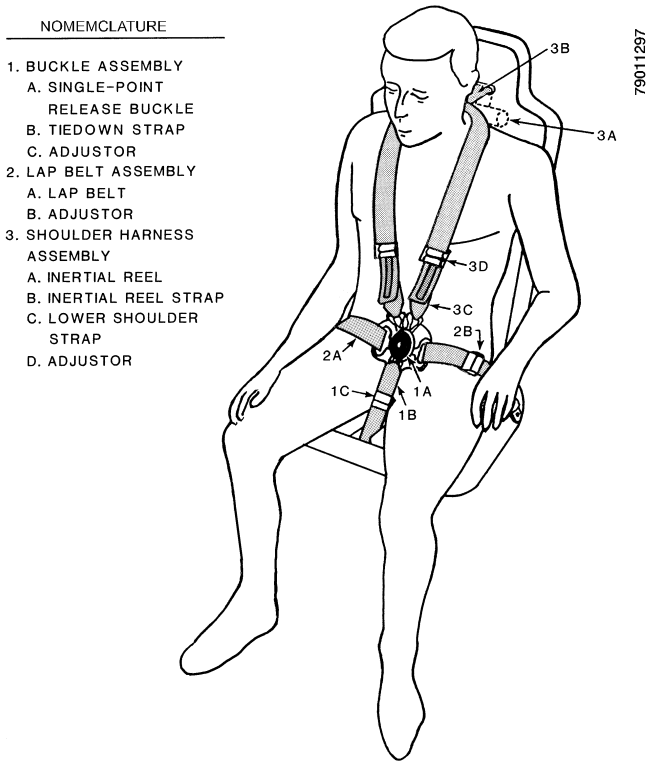


Figure 8-2.
Basic five-point restraint system (Reference 8-9).

This Document Provided by the Abbott Aerospace
TECHNICAL LIBRARY
ABBOTTAEROSPACE.COM

The lap belt tie-down strap of a five-point restraint resists the upward pull of the shoulder straps and prevents lap belt displacement into the abdomen during a crash. The tie-down strap should be narrow enough, within the limits of acceptable strength, to minimize leg rubbing encountered by the wearer during rudder pedal operation. The tie-down strap can be a fixed length, or can be manually adjustable (this is highly recommended). Each lap belt half needs to have an adjuster so the occupant can center the buckle. Like the three-point restraint, the shoulder straps on a five-point restraint must allow each crewmember (pilot and/or copilot) to reach all required aircraft controls without removing and/or loosening the upper torso restraint. A shoulder strap inertia reel is recommended to allow the occupant to lean forward. Manual adjusters are often used on the shoulder straps in conjunction with an inertia reel on five-point restraints; most commonly on "Y"-yoke shoulder strap, single-reel systems. Manual adjusters are required if an inertia reel is not used.

The centrally located buckle provides a single-point release for the five-point restraint system. The buckle is permanently attached to either the center tie-down strap or one of the lap belt straps. Permanent attachment of the buckle to the center tie-down strap is preferred, to ensure that the tie-down strap is utilized. However, some systems use buckles which are permanently attached to the lap belt with provisions for the center tie-down strap release (without removing the lap or shoulder belts) allowing the occupants the ability to relieve themselves during long flights. While this is a distinct convenience, the downside is that some occupants may be tempted to regularly use the restraint without the tie-down strap. NOTE: A five-point restraint should not be used in a four-point configuration. There are two reasons for this statement, both of which are concerned with the tendency of the occupant to "submarine" under the lap belt during a crash. The four-point configuration with the shoulder belt attached to the center of the lap belt has a greater tendency to lift the lap belt up onto the abdomen (increasing the tendency for submarining) than other designs. Second, the lap belt anchor points of the five-point system are placed in a different location than other restraint systems precisely because of the addition of the tie-down strap (Section 8.1.2.2). The five-point lap belt anchor points are located further back than other systems. While this location improves the frontal-impact performance of the lap belt, it also increases the tendency for the occupant to submarine if the tie-down strap is not used. In other words, an occupant using a five-point restraint without the tie-down strap has a greater likelihood of submarining (and consequently a higher probability of abdominal or lumbar spine injury) during an accident. Ultimately, the aircraft designer must weigh the convenience of the detachable tie-down strap design against the possibility that some occupants will misuse the restraint.

Dual shoulder belt systems have a maximum allowable combined strap load of 2,000 lb to meet the dynamic test requirements of 14 CFR 562. This combined total load is generally not difficult to meet in practice. If the maximum is exceeded during testing, load-limiting (Section 8.1.7), pre-tensioning (Section 8.1.8) or inflatable restraints (Section 8.3) can be used to reduce the load.

8.1.2.3 Other Belt Restraint Types

Other restraint types that have been used in small aircraft, but are not recommended by this design guide, include lap-belt-only (a two-point restraint) and four-point restraints.

The lap-belt-only configuration is predominately used for passenger seats in commuter and transport-category aircraft, and is also seen in some older GA aircraft. Lap-belt-only configurations are no longer allowed in newly manufactured GA aircraft per FAR 23.785(b) and Amendment 23-32 (References 8-6 and 8-10). The lap-belt-only restraint allows too much occupant head and torso motion, which significantly increases secondary impacts within the small airplane interior.

This Document Provided by the Abbott Aerospace
TECHNICAL LIBRARY
ABBOTTAEROSPACE.COM

Four-point systems with shoulder belts attached at the center of the lap belt have been utilized in GA aircraft and for crewseats of commuter and transport-category aircraft. This restraint type is allowed per FAR 23.785(b), but is not recommended for GA aircraft by this design guide. The reason this restraint type is not recommended is because the loading of the shoulder strap tends to raise the lap belt and promote occupant submarining. Also, the potential for misuse, especially by those unfamiliar with this type of restraint, is high. Some occupants who are mostly familiar with automotive restraints and expect automatic lap belt tightening may not tighten a manually adjusted lap belt enough. This places the lap belt and buckle even higher on the abdomen for four-point systems. Three- and five-point system performance will also suffer due to a loosely adjusted lap belt, but, because the shoulder strap doesn't pull on the center of the lap belt, the chance of submarining is less. Four-point restraints do provide more lateral support than single-diagonal (three-point) restraint systems. If two shoulder straps are desired to provide upper torso lateral restraint, then the five-point system is preferred. If a four-point system is installed, then the lap belt anchor locations specified for the three-point restraint in Section 8.1.2.1 should be used to minimize the potential for submarining.

An alternative four-point restraint geometry anchors the shoulder belts near the hips (the so-called "flight-attendant-type" restraint). This design solves the lap belt lift problem, and can also provide improved lateral restraint compared to the three-point system. However, this design lacks the required single-point release and also typically requires occupant side-to-side motion and twisting to don and/or remove. Thus, occupant egress could be compromised.

8.1.3 Restraint System Anchors

Restraints are generally anchored directly to the seat or to the basic aircraft structure. For optimum crash protection, the anchors should be mounted on the seat or mounted as near to the seat as possible to minimize the webbing length in order to reduce elongation, and also to enhance lateral support.

Seat-mounted anchors are preferred, as this allows optimum restraint geometry regardless of seat adjustment, seat stroking, and/or airframe deformation during a severe crash. However, seat-mounted restraint anchors require that the seat structure and the seat interface with the airframe carry all the restraint loads. Therefore, seat-mounted anchors typically increase the overall aircraft system weight. Systems in which all belts attach to the seat are also called "All Belts to Seat" or ABTS restraint systems.

Restraint anchors mounted to the aircraft structure provide a direct load path between the occupant and the mounting hardpoints. This minimizes the seat loading, which allows for a lighter seat structure and lighter seat mounting interface. However, mounting to the aircraft structure will increase the webbing length, and may induce restraint geometry problems during seat adjustment, seat stroke, and/or aircraft structural deformation. Routing the webbing through strap guides on the seat can minimize the geometry problem. However, if this approach is used, the strap guides must be able to withstand loads equal to the restraint system's strength. In addition, the webbing routing path must be free of sharp edges/corners that may reduce the webbing strength or induce fraying, and the path must be free of protrusions on which the webbing may hang-up, thus altering the webbing load path. The seat guides must also be sized/oriented so that the webbing does not tend to fold or twist, but remains properly oriented for optimum occupant comfort and crash protection. Systems in which all belts attach to airplane structure are also called "All Belts to Airframe" or ABTA restraint systems.

This Document Provided by the ABBOTT Aerospace
TECHNICAL LIBRARY
ABBOTTAEROSPACE.COM

A good compromise between the crash safety benefits of seat-mounted anchors and the lighter weight of aircraft-mounted anchors is to use seat-mounted lap belts combined with airframe-mounted shoulder belts. This approach provides a minimal weight penalty, since the high overturning moment on the seat frame is eliminated. Another three-point configuration, seen frequently in newer automobiles, attaches the buckle to the seat, and the shoulder belt and the free end of the lap belt to the vehicle structure. This configuration is typically done so that the stowed restraint lies flat against the B-pillar of the car, while still giving some of the convenience and performance advantages of a seat-mounted lap belt. This configuration also improves access and egress to the rear seat. Systems that combine seat- and airframe-mounted anchors are known as “Hybrid” restraint systems.

Each occupant should have separate restraint system load paths to primary aircraft structure. Common load paths in which multiple occupants could be released due to a single anchor point's failure must be avoided.

The anchor locations described in the following sections generally ensure adequate restraint performance during the dynamic seat tests. Some installations, however, may require slight deviations from these recommended locations in order to tune the seat/restraint system to meet the test and occupant injury tolerance requirements.

8.1.3.1 Lap Belt Anchor Points

The anchor points for the lap belt may be located either on the seat or on the basic aircraft structure. If the anchor points are located on the basic aircraft structure, then the movement of the seat under the action of load-limiting devices and seat adjustment must be taken into consideration to ensure that the lap belt restraint remains effective regardless of seat position.

The lap belt should be anchored to provide optimum restraint for the lower torso when subjected to "eyeballs-out” ($-G_X$) forces. One of the variables which has a great influence on restraint system performance is the location of the lap belt anchorage. A farther-aft location provides an efficient path for supporting longitudinal loads, while a farther-forward location provides an efficient system for supporting vertical loads. However, if the lap belt anchor is too far aft, the belt can tend to slip over the iliac crests of the pelvic bone, allowing the pelvis to rotate under the belt. The inertial load of the hips and thighs tends to pull, or submarine, the pelvis under the belt, possibly causing visceral injury. This submarining movement is illustrated in Figure 8-3.

The width between the lap belt anchor points also affects the restraint's performance. The optimum width for forward restraint would be the same as the occupant’s hips, aligning the strap tension in the same plane as the loading vector. Widths that are too narrow will cause unwanted pelvis compression. Widths wider than the occupant’s hips will increase the belt tension required to react the longitudinal loads. Excessive widths also increase the likelihood of occupant submarining, as reported in Reference 8-11.

Restraint performance is enhanced if the belts are worn tight on the occupant, as shown in studies reported in Reference 8-12. Thus, care should be taken to instruct occupants to tighten the lap belt to the maximum tension consistent with comfort, and to not loosen the belt anytime during a flight.

THIS DOCUMENT PROVIDED BY THE ABBOTT AEROSPACE
TECHNICAL LIBRARY
ABBOTTAEROSPACE.COM

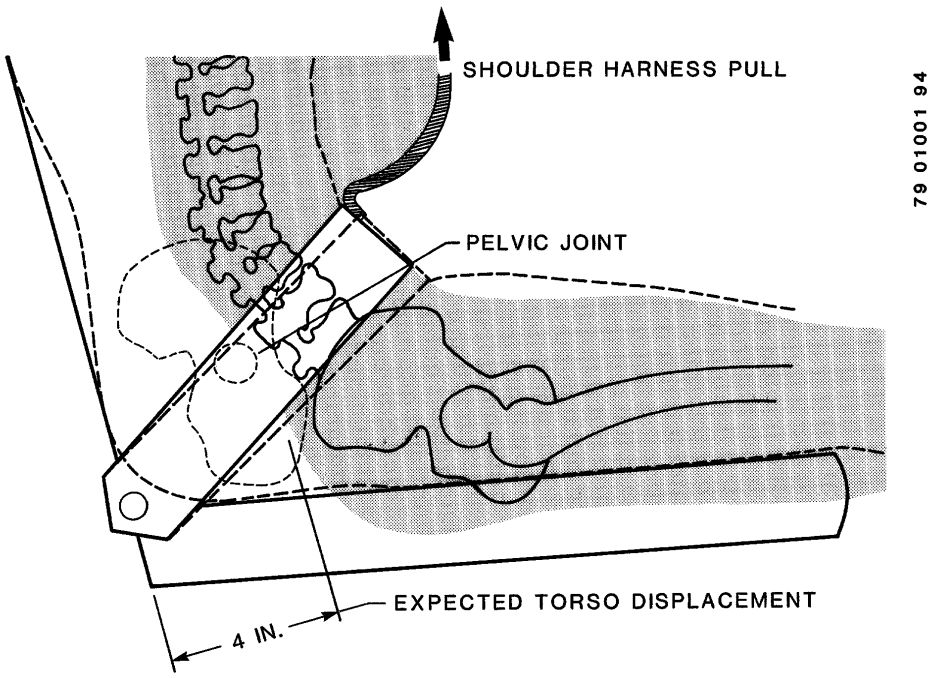


Figure 8-3.
Pelvic rotation and submarining caused by high longitudinal forces.

8.1.3.1.1 Lap Belt Anchor Points for Three-Point Restraints

The optimum lap belt anchorage point is within the area defined by Figures 8-4 and 8-5. The anchor point should be on or just below the buttock reference line for optimum comfort and performance. A low mounting point will also allow the lap belt to be adjusted taut for the restraint of some child safety seats. If the anchor point must be located above the buttock reference line, the anchor point should be located on a 45-deg line intersecting the buttock reference line 1.5 to 2.0 in. forward of the seat reference point (SRP), and no higher than 2 in. above the buttock reference line.

The buckle assembly should be mounted on the side opposite of the shoulder belt anchor point and close to the occupant's hip point. To facilitate this, the buckle assembly should be below the hip point, if practicable.

8.1.3.1.2 Lap Belt Anchor Points for Five-Point Restraints

The addition of the tie-down strap allows the anchor point to be moved farther aft, enhancing occupant forward retention. The tie-down strap limits the tendency of the lap belt to rotate upward so that occupant submarining is minimized. The optimum lap belt anchorage point is within the area defined in Figures 8-5 and 8-6. The anchor point should be at or below the SRP for optimum comfort and performance. If the anchor point must be located above the SRP, the anchor point should be located on a 45-deg line intersecting the SRP and no higher than 2 in. above the buttock reference line.

THIS DOCUMENT PROVIDED BY THE ABBOTT AEROSPACE
TECHNICAL LIBRARY
ABBOTTAEROSPACE.COM

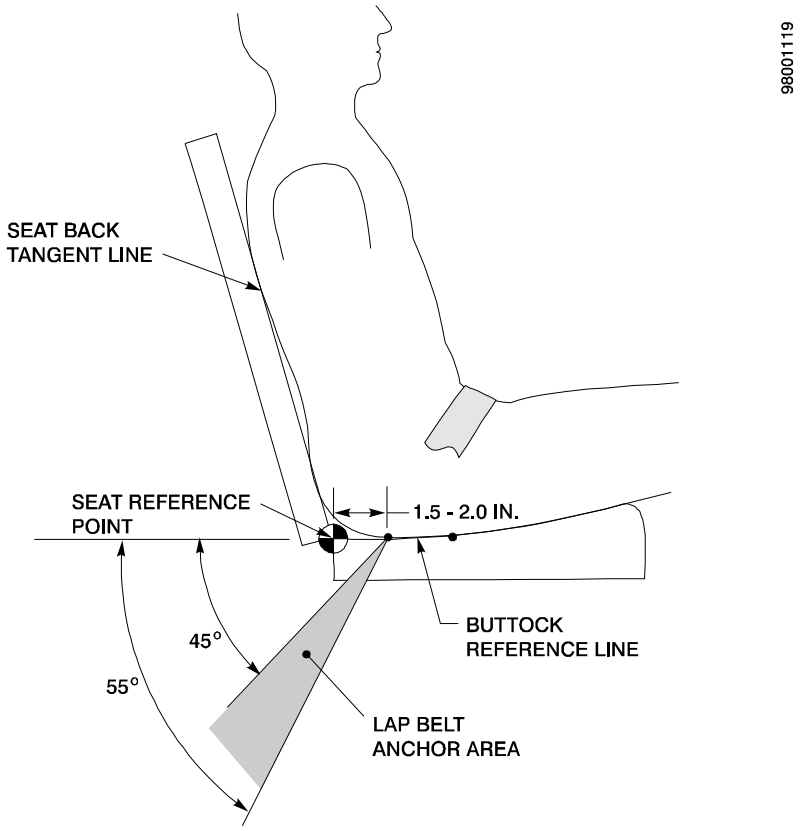


Figure 8-4.
Lap belt anchorage location for three-point restraints.

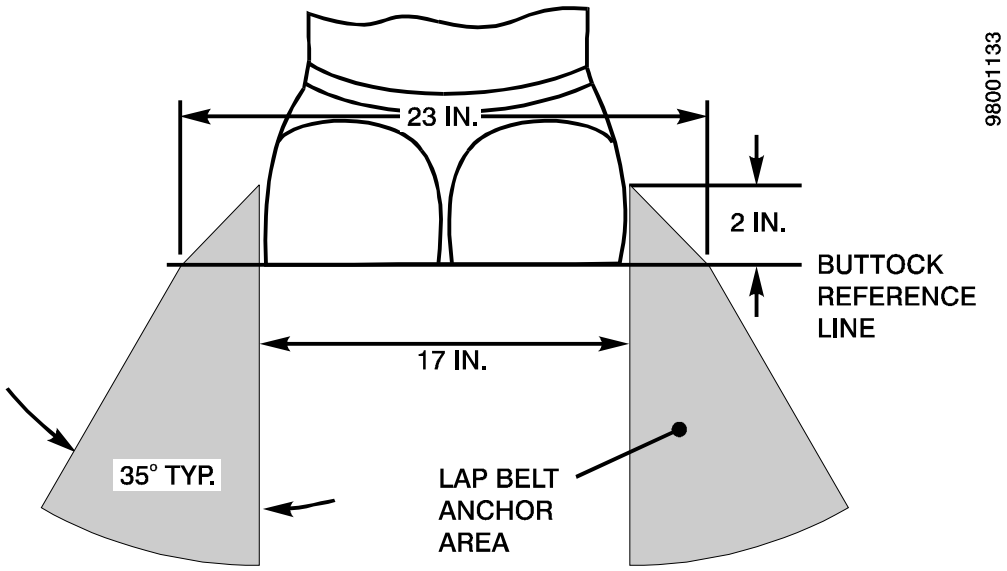


Figure 8-5.
Lap belt anchorage location (width) for three-point and five-point restraints; viewed parallel to the buttock reference plane.

THIS DOCUMENT PROVIDED BY THE ABBOTT AEROSPACE
TECHNICAL LIBRARY
ABBOTTAEROSPACE.COM

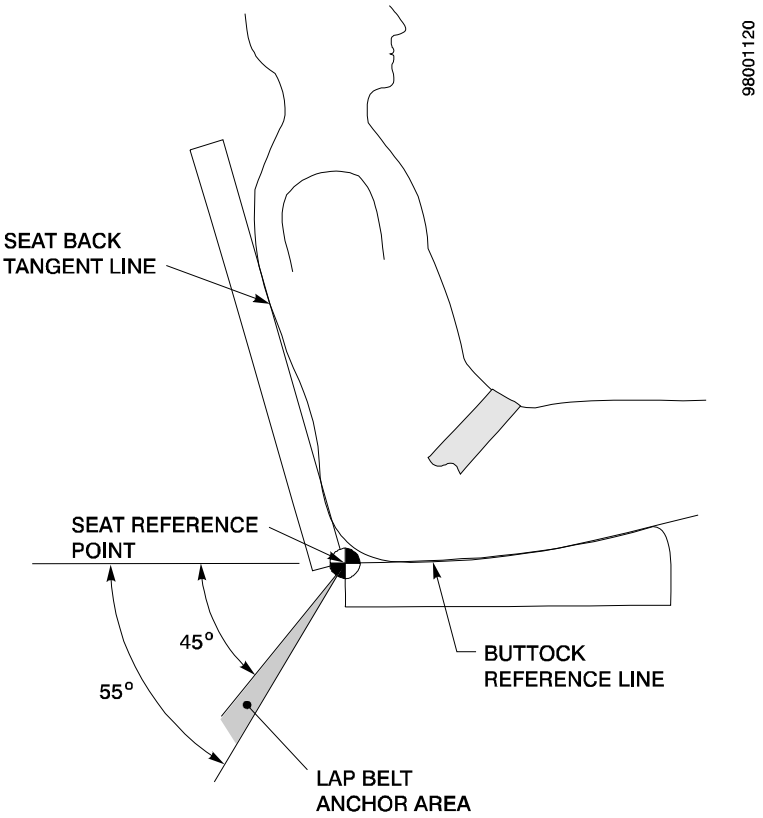


Figure 8-6.
Lap belt anchorage location for five-point restraints.

8.1.3.2 Shoulder Harness Anchor Point

The shoulder harness or inertia reel anchor point can be located either on the seat structure or on the basic aircraft structure. When selecting the placement of the inertia reel, strap routing and possible reel interference with structure during seat adjustment or energy-absorbing stroke of the seat must be considered. Location of the anchor point on the basic aircraft structure will relieve a large portion of the overturning moment applied to the seat in longitudinal loading; however, due consideration must be given to the effect of seat bucket movement in load-limited seats. Vertical movement of the seat can be accommodated by placing the inertia reel a sufficient distance aft of the seat back shoulder strap guide so that seat vertical movement will change the horizontal position and the angle of the straps very little. However, increasing this distance will also increase elongation and reduce lateral support. Therefore, a seat-mounted shoulder harness is preferred from a crashworthiness standpoint.

Shoulder straps should pass over the shoulders in a horizontal plane or at any upward (from shoulders to pull-off point) angle not to exceed 30 deg. Any installation that causes the straps to pass over the shoulders at an angle below the horizontal adds additional compressive force to the occupant's spine. Installations in which the shoulder belt passes at an angle higher than 30 deg tend to amplify the belt load, which can put unneeded stress on the webbing, belt anchors, and buckles.

This Document Provided by the Abbott Aerospace
TECHNICAL LIBRARY
ABBOTTAEROSPACE.COM

For systems with strap guides or inertia reels/anchors on the seat, the optimum shoulder harness pull-off point is 26.5 in. above the buttock reference line measured along the back tangent line. This dimension should not be increased, because then the harness would not provide adequate restraint for shorter occupants.

The shoulder harness anchor point or the strap guide at the top of the seat back should permit no more than 0.5 in. of lateral movement (with the slot no more than 0.5 in. wider than the strap) to ensure that the seat occupant is properly restrained laterally. The guide should provide smooth transitions to the slot. The transition contour should be of a radius no less than 0.25 in., and should extend completely around the periphery of the slot to minimize edge wear on the strap and reduce the possibility of webbing failure due to contact with sharp edges under high loading. Also, the guide that the strap actually loads should be sufficiently stiff to limit its deflection under load. Excessive deflection can produce edge loading and cause premature failure of the webbing.

For dual-shoulder-belt installations, the lateral location of the strap guide, inertia reel, and/or anchor should be placed on, or as close as possible to, the occupant's centerline. Shoulder belt performance for single-diagonal (three-point) systems is more sensitive to the lateral location of the anchor and to strap routing, and is covered in more detail in the next section.

8.1.3.2.1 Special Considerations for Three-Point Shoulder Harness Anchor Points

For the following discussion, the location of the shoulder belt anchor can refer to either the location of the inertia reel for systems with direct shoulder strap routing, or to the location of the strap guide for systems in which the shoulder strap route changes direction from the inertia reel to the occupant. Strap guides that are mounted to the sidewall of the aircraft (and those mounted to the window pillars in automobiles) are often called “D-rings.”

The shoulder belt anchor point needs to be located laterally to minimize contact between the belt and the occupant’s neck and to also provide optimum forward restraint. Tests conducted in Reference 8-13 show that optimum forward restraint is provided when the shoulder harness crosses in front of the upper torso’s c.g., as shown in Figure 8-7. If the shoulder harness crosses too far below the torso’s c.g., the occupant can rotate out of the shoulder harness. If the harness passes too far above the torso’s c.g., the upper torso can slip under the belts and cause neck injury. A mounting location placed too high can also cause occupant discomfort by strap interference with the neck. The optimum location to compromise between acceptable comfort and crash safety for the configuration studied in Reference 8-13 was found to be 4.0 in. from the occupant’s centerline.

Figure 8-7 also shows how routing the webbing directly over a large occupant’s c.g. can cause neck interference for the smaller occupant’s neck. Note that this illustration is for a 5th-percentile male occupant. A small female occupant or child will have even more neck interference. Perhaps the best shoulder harness mount would allow adjustment of the attachment point or strap guide to the optimum location. However, an adjuster can increase the likelihood of misuse and improper location. Shoulder belt height adjusters are beginning to be implemented in the automotive market. The effect of these height adjusters on automotive crash safety is not known, but the benefits of supplemental restraints (air bags) may mask the effects of a mis-adjusted shoulder belt.

Systems in which the shoulder belt attaches near the center of the lap belt should not be used, as this can promote occupant submarining, and can also allow upper torso rotation out of the belt due to the unfavorable position of the occupant’s torso c.g. (see Figure 8-7).

THIS DOCUMENT PROVIDED BY THE ABBOTT AEROSPACE
TECHNICAL LIBRARY
ABBOTTAEROSPACE.COM

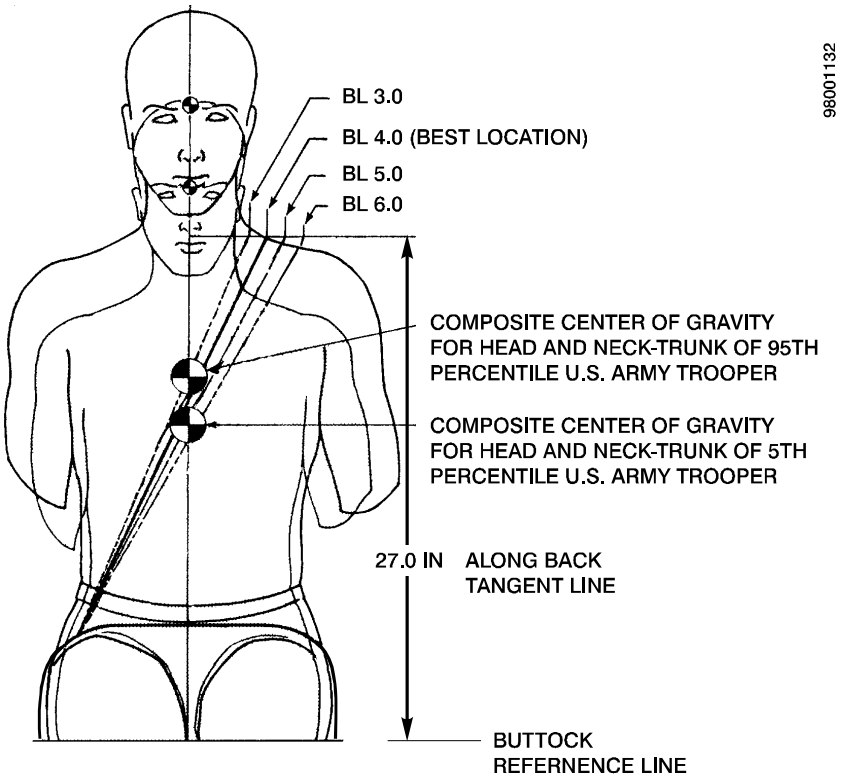


Figure 8-7.
Shoulder harness anchor point geometry (Reference 8-13).

The neck interference problem can also be compounded by the short strap on a seat-mounted inertia reel or strap guide, as this restricts the lateral motion of the belt. Thus, an airframe-mounted shoulder belt anchor can provide improved comfort for smaller occupants.

Three-point restraints only provide lateral support in the direction of the shoulder belt mount. For side-by-side seating, the shoulder belt should normally go over the occupant's outboard shoulder to minimize outward motion during lateral loading. However, in some aircraft, it may be desirable to place the belt over the inboard shoulder due to availability of structural mount hardpoints and/or to facilitate egress. For tandem seating or in a single-place aircraft, the shoulder belt anchor can be placed on the side opposite of the primary emergency egress route to minimize the occupant's snagging the belt during egress.

8.1.3.3 Lap Belt Tie-down Strap Anchorage

When the upper body is thrown forward against the shoulder straps, an upward pull is exerted on the lap belt in four-and five-point systems. Without a lap belt tie-down strap, the tendency is for the belt to be pulled up over the iliac crests and onto the abdomen, with the likelihood of injury to the abdominal viscera, as previously shown in Figure 8-3. A tie-down strap attached to the buckle in the center of the lap belt prevents this upward belt movement. It is recommended that the tie-down strap anchor point be located on the seat pan centerline at a point 14 to 15 in. forward of the occupant back tangent line. For shorter seat pans, the anchor point must be placed as far forward as possible.

THIS DOCUMENT PROVIDED BY THE ABBOTT AEROSPACE
TECHNICAL LIBRARY
ABBOTTAEROSPACE.COM

8.1.4 Restraint Hardware

This section outlines specific restraint hardware component-level requirements that are typically the responsibility of the restraint manufacturer. Restraints certified to TSO-C114 will meet these requirements (Reference 8-1). This design data is provided here primarily for informational purposes.

8.1.4.1 Release Hardware

A shoulder harness/lap belt combination should have a single point of release that can be operated by either hand so that debilitated occupants can quickly free themselves from their restraint to avoid the dangers of post-crash fire or sinking in water. However, vibration, decelerative loading, or contact with the occupant or aircraft controls should not inadvertently open the buckle. It should be emphasized that, if contact between the control stick and the buckle is possible in an operational mode, a considerable overlap can exist during crash loading when the restraint system may be deformed forward several inches.

The intentional release of the restraint harness, using only one finger, should require at least 5 lb (22 N) of force. An excessive force could hinder rapid emergency release, while a light force could cause inadvertent release. Further, release should be possible even with the occupant is hanging inverted in the restraint system after experiencing a severe survivable crash. The force required to release the system with a 170-lb (77-kg) occupant inverted in a crash should not exceed 30 lb (134 N).

The release buckle should either have the capability to withstand the bending moments associated with deflections and motions during loading, or it should contain features that allow the fittings to align themselves with the loads, thereby reducing or eliminating the moments. If the belt loading direction is such as to cause the strap to bunch up in the end of a slot, failure can occur through initiation of edge tear. As a result of an investigation of restraint system design criteria reported in Reference 8-14, the fitting angles illustrated in Figure 8-8 are recommended for five-point systems.

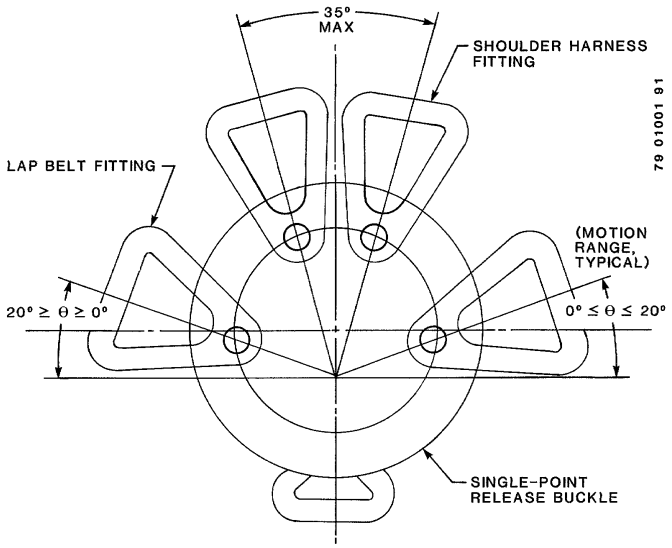


Figure 8-8.
Buckle fitting attachment and motion angles for five-point restraint.

This Document Provided by the Abbott Aerospace
TECHNICAL LIBRARY
ABBOTTAEROSPACE.COM

8.1.4.2 Adjustment Hardware

Adjusters should carry the full design load of their restraint system subassembly without slipping, crushing, or cutting the webbing. In extremely highly loaded applications, this may require that the strap be double-reeved in a manner that allows the adjuster to carry only half of the strap assembly load. The force required to adjust the length of webbing should not exceed 11 lb, in accordance with TSO-C114. Insofar as possible, all adjustments should be easily made with one (either) hand. Adjustment motions should be toward the single-point release buckle to tighten the belts and away from the single-point release buckle to slacken the belts.

An adjuster in the lap belt tie-down strap is desirable to accommodate variations in occupant size. However, high loads in this strap usually result in adjuster slippage, and thus some compromise in the function of the tie-down strap.

8.1.4.3 Location of Adjustment and Release Hardware

Adjusters should not be located directly over hard points of the skeletal structure, such as the iliac crests of the pelvis or the collarbones. The lap belt adjusters should be located either at the center of the belt or at the side of the hips below the iliac crests, preferably the latter. The shoulder strap adjusters, if used, should be located as low on the chest as possible.

8.1.4.4 Hardware Materials

All materials used for the attachment of webbing (release buckles, belt anchors, and length adjusters) should be ductile enough to deform locally, particularly at stress concentration points. A minimum elongation value of 10 pct (as determined by standard tensile test specimens) is recommended for all metal harness fitting materials. There are obviously some components that, for operational purposes, rely on hardness. These components should be designed to perform their necessary function but be made from materials that are as immune as possible to brittle failures.

8.1.4.5 Adjustment Range

Restraint adjusters must be capable of fitting the full range of occupants from children to large adults over the complete seat adjustment range. For the minimum length, it is recommended that the adjusters be capable of removing all slack out of the restraint with the seat unoccupied.

In order to fit a large adult, the lap belt should accommodate a seated hip circumference of up to 50 in. This will require an adjustment range of approximately 24 in. for the adjuster to remove all of the slack available. The shoulder belt strap(s) require an adjustment range of approximately 12 in. to accommodate the anticipated range of occupant sizes. These dimensions may need to be adjusted, depending on the anticipated range of occupant sizes.

All adjusters need provisions to prevent inadvertent webbing removal when extended. This is normally accomplished by sewing a stop or a fold of webbing at the end of the strap.

8.1.5 Webbing

This section outlines specific requirements for webbing which are typically the responsibility of the webbing and restraint manufacturers. Restraints certified to TSO-C114 will meet these requirements (Reference 8-1). This design data is provided here primarily for informational purposes.

Aviation restraint webbing was initially manufactured from polyamid, or nylon, whereas the automotive industry originally used polyester. Today, almost all new vehicle restraints are

THIS DOCUMENT PROVIDED BY THE ABBOTT AEROSPACE
TECHNICAL LIBRARY
ABBOTTAEROSPACE.COM

composed of polyester. Low-elongation polyester will reduce head travel and HIC, but can increase the restraint belt loads. If webbing stretch is not a critical issue, nylon webbing may be used to reduce belt loads. Reference 8-15 reports that nylon can decrease peak loads in the straps by up to 10 pct.

Unless specially processed, the old, standard nylon will no longer satisfy the new TSO-C114 requirements of 20 pct maximum elongation with a 2,500-lb load. Nylon elongation rates range from 18 to 28 pct, whereas polyester webbing is available with elongation as low as 6 pct (Reference 8-15). Figure 8-9 compares the typical elongation characteristics of nylon and polyester webbing. Dynamic testing of polyester webbing has demonstrated the dynamic elongation to be approximately 60 to 75 pct of the static elongation under the same load, as illustrated in Figure 8-10 (References 8-16 and 8-17).

The dyeing and processing of fabric may significantly influence the amount of fabric required for an economical production run. Webbing mills currently require a minimum production run of 5,000 yards for polyester (Reference 8-15). Custom dyes can be prohibitively expensive unless quantities can support the minimum production requirements.

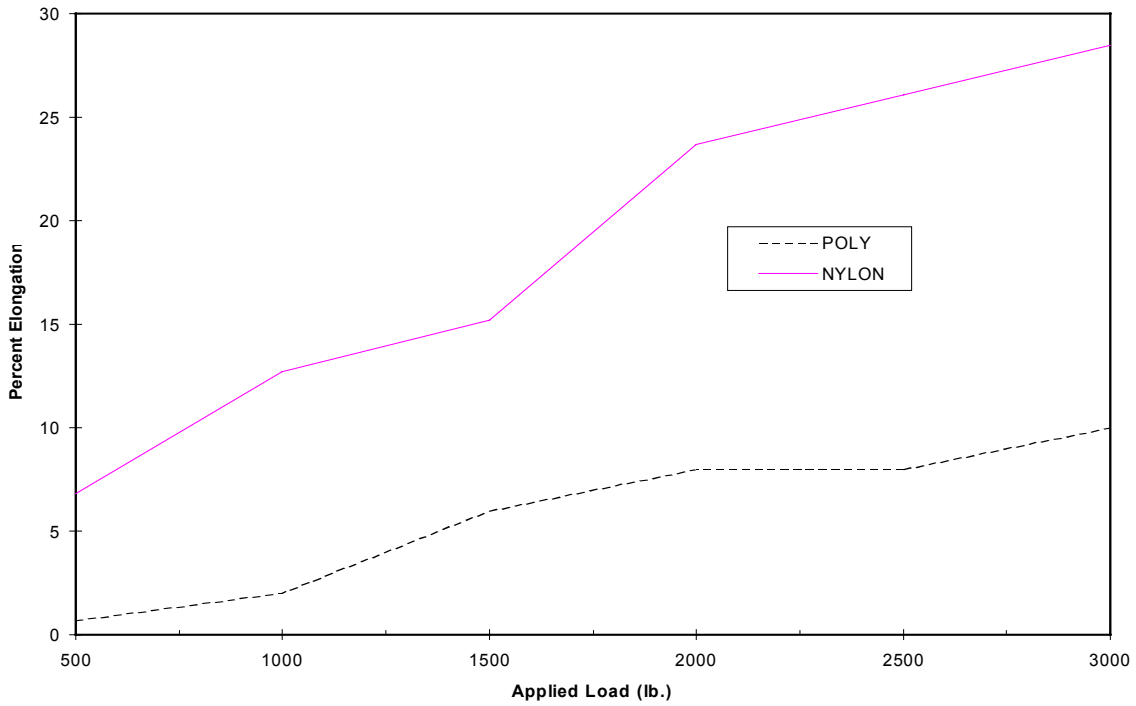


Figure 8-9.
Webbing elongation test results, polyester versus nylon (Reference 8-15).

THIS DOCUMENT PROVIDED BY THE ABBOTT AEROSPACE
TECHNICAL LIBRARY
ABBOTTAEROSPACE.COM

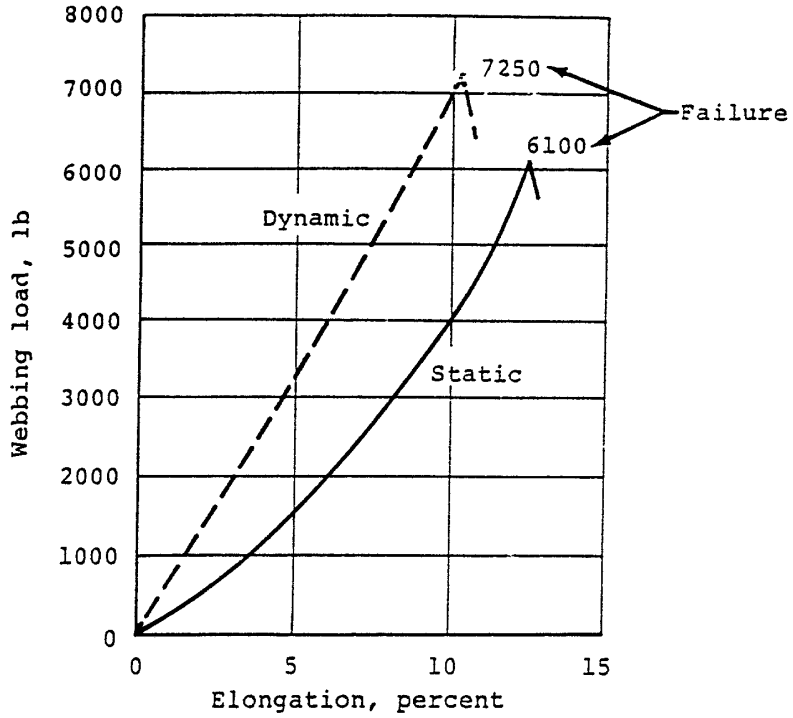


Figure 8-10.
Load elongation characteristics for MIL-W-25361 (Type II) polyester webbing for static and rapid loading rates.

8.1.5.1 Webbing Requirements

Webbing width affects both restraint comfort and performance. Wider widths increase the contact area and lower the contact pressure, but narrower widths are preferred for comfort and weight savings. In addition, all webbing used for restraint harnesses must be thick enough to ensure that the webbing does not fold or crease to form a “rope” or present a thin sharp edge under high loading that will cause damage to soft tissue. Such damage is more likely to occur in the neck region during lateral loading or in the pelvic region during forward loading. Although requirements based on early investigations using nylon webbing specified a minimum thickness of 0.090 in., it has since been determined that state-of-the-art webbing materials must be thinner in order to achieve the desired low elongation. No significant problem of injuries caused by the thin webbing has been observed with this low-elongation webbing, which has seen extensive automotive use. Therefore, based on currently available materials, a minimum thickness of 0.045 in. is considered acceptable. Shoulder harness webbing used on inertia reels is generally thinner than lap belt webbing. This provides the maximum webbing storage capacity on the inertial reel. Table 8-1 summarizes the webbing and restraint system requirements per TSO-C114.

THIS DOCUMENT PROVIDED BY THE ABBOTT AEROSPACE
TECHNICAL LIBRARY
ABBOTTAEROSPACE.COM

Table 8-1.
TSO-C114 Occupant Restraint Harness Requirements (Reference 8-1)

	Harness Webbing			Harness Assembly	
Component	Required Width (in.)	Min Tensile Breaking Strength (lb)	Maximum Elongation	Minimum Ultimate Strength (lb)	Maximum Elongation
Shoulder Harness	1.8 min	4,000	20% @ 2,500 lb	2,500 (1)	(3)
Lap Belt	1.8 min	5,000	20% @ 2,500 lb	3,000	12 in. @ 3,000 lb and 48-50 in. length
Lap Belt Tie-down (2)	2.0 max	4,000	20% @ 2,500 lb	2,500	(3)

NOTES:
(1) If webbing retractors or inertia reels are used, assembly test loads must be met with 12 in. of webbing wound on the spool.
(2) Lap belt tie-down requirements are not specified in TSO-C114.
(3) Not specified in TSO-C114

8.1.5.2 Stitched Joints and Hardware Attachment

The strength and reliability of stitched seams must be ensured by using the best-known thread sizes and stitch patterns for a specified webbing type. The stitch patterns and thread sizes used in existing high-strength webbing appear to provide good performance. The basic stitch pattern used in these harnesses is typically a "W-W" configuration for single-lapped joints, as shown in Figure 8-11.

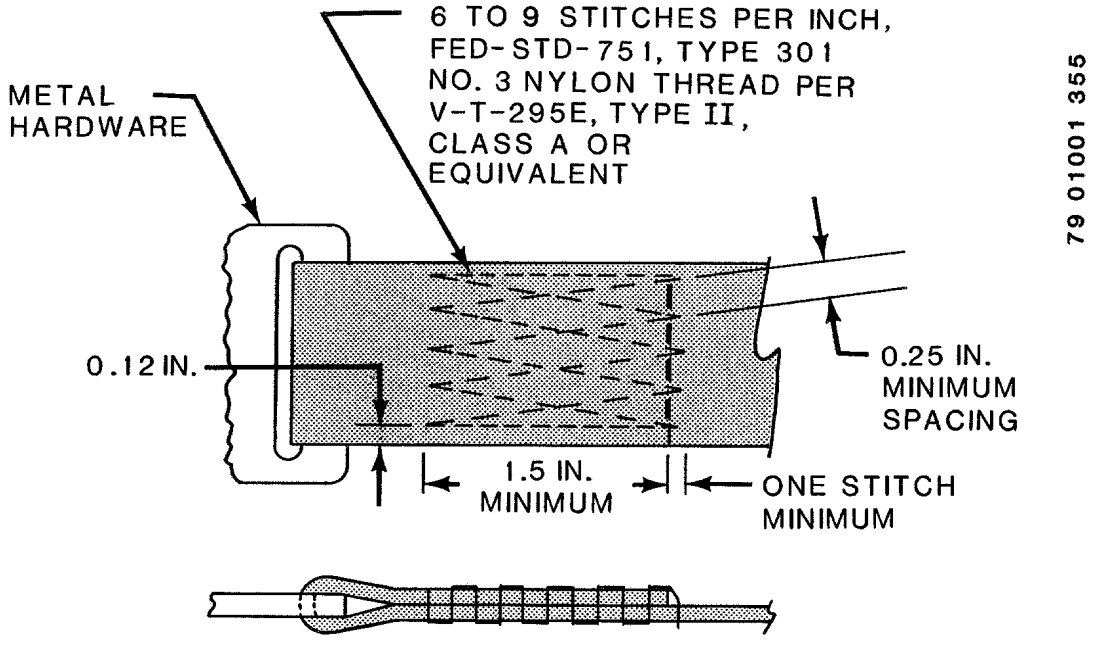


Figure 8-11.
Stitch pattern and cord size. (Reference 8-4).

THIS DOCUMENT PROVIDED BY THE ABBOTT AEROSPACE
TECHNICAL LIBRARY
ABBOTTAEROSPACE.COM

The strength of stitched joints can be expected to decrease with age because of normal weather exposure and because of the normal collection of dust and grit between the webbing surfaces. The dust and grit can gradually abrade the stitching over a period of time. Covering the stitched joints to provide wear protection is recommended. Additional information concerning webbing stitch patterns and calculation of strengths can be found in Reference 8-4.

8.1.5.3 Webbing Wrap Radius

The webbing wrap radius is the radius of the fitting over which the webbing is wrapped at buckles, anchor points, and adjusters, as illustrated in Figure 8-12. Detailed information on just how small this radius can be before the strength of the webbing is affected is not available; however, the 0.062-in. minimum radius shown is based upon the geometry of existing high-strength restraint harnesses. This radius should be carried around the ends of the slot, as shown in Figure 8-12, to preclude edge cutting of the webbing if the webbing becomes loaded against the slot end.

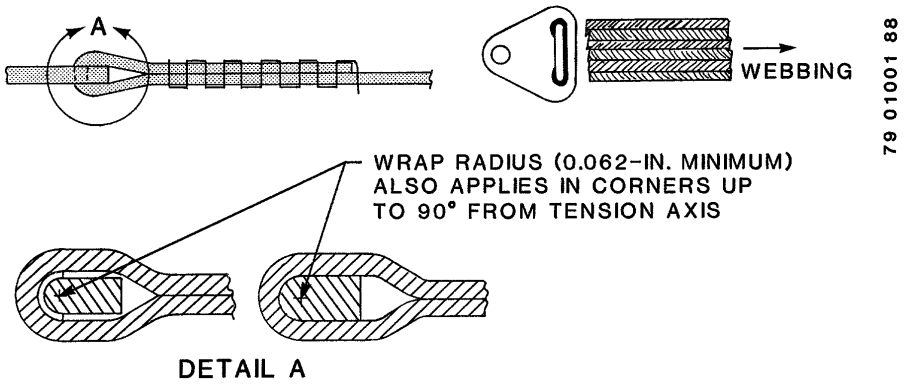


Figure 8-12.
Wrap radius for webbing joints.

8.1.5.4 Hardware-to-Webbing Folds

One method of reducing fitting width at anchor points, buckles, or adjuster fittings is to fold the webbing, as shown in Figure 8-13. This reduces the weight and size of attachment fittings; however, it can also cause premature webbing failure because of the compressive force applied by the top layer of webbing to the lower layer against the fitting slot edge. If this technique is to be used, tests to demonstrate webbing integrity are recommended. Also, for configurations that require that the webbing be freely drawn through the fitting (such as a slip joint or adjuster), the webbing must be looped through a full-width slot (not folded).

8.1.5.5 Surface Roughness of Fittings

A surface roughness of no more than RMS-32 is recommended for any fittings to prevent the fraying of the webbing due to the frequency of movement over the metal.

THIS DOCUMENT PROVIDED BY THE ABBOTT AEROSPACE
TECHNICAL LIBRARY
ABBOTTAEROSPACE.COM

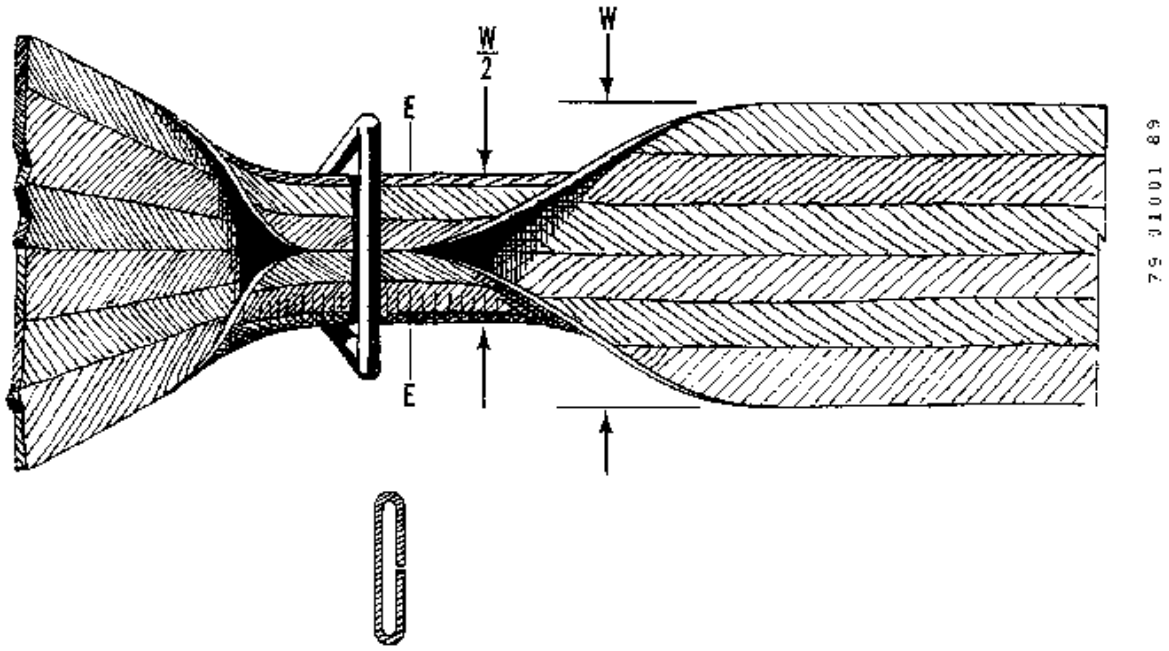


Figure 8-13.
Webbing fold at metal hardware attachment.

8.1.6 Inertia Reels and Webbing Retractors

The basic function of an inertia reel is to give the crewmember full freedom of movement during normal operating conditions, while automatically locking the shoulder harness during an abrupt deceleration. Webbing retractors are used in lap belt assemblies to stow the belt when not in use, but, for the reasons described below, are not recommended for light aircraft use.

8.1.6.1 Inertia Reels

Emergency locking retractors, or inertia reels, make the shoulder harness easier to use, more comfortable, and practically ensure proper adjustment. In aviation, inertia reels are only allowed on shoulder straps. These reels allow the shoulder strap(s) to extend freely during normal operations, but lock in a crash to help restrain the occupant.

The freedom of movement is obtained by spring-loading the webbing reel to which the shoulder straps are attached. This allows the shoulder harness to be extended without apparent restraint of the shoulders (only 6 lb tension at maximum extension). The spring-loaded reel constantly takes up any slack in the harness.

There are three basic types of inertia reels that are categorized by their locking mode. The first is a rate-of-extension type reel, whereby locking is activated when the strap's linear acceleration (pay-out) exceeds a set threshold. The second basic type is the impact-sensitive reel, which requires a deceleration on the inertia reel housing itself to activate the lock. The third basic type of reel is a combination of the first two types called the dual-mode inertia reel that locks under either strap acceleration or inertia reel housing acceleration.

This Document Provided by the Abbott Aerospace
Technical Library
abbottaerospace.com

Rate-of-extension inertia reels are the most commonly used in GA. The mechanism is cued by the linear acceleration of webbing pay-out. The automatic operation of this reel can be checked at any time by a quick jerk on the shoulder straps. This inertia reel, after being locked, will unlock and spool freely in either direction when tension in the shoulder strap is removed.

Impact-sensitive reels (also called vehicle-, or "G"-sensing reels) usually employ a spring-loaded pendulum or ball which moves in response to airframe acceleration to engage the locking mechanism. Multi-axis sensing is possible and desirable with this type of reel. From an impact dynamics standpoint, vehicle-sensitive reels are preferred, because they minimize the amount of webbing extracted during an impact condition: i.e., they do not require strap movement. Unlike the rate-of-extension inertia reels, the locking mechanism will normally not be engaged by a quick jerk on the shoulder straps. These reels also automatically unlock after locking when the shoulder strap tension is released. Because of the design of the sensing mechanism, impact-sensitive inertia reels must be mounted in the orientation recommended by the manufacturer. Failure to mount the reel in the correct orientation can cause the reel to remain locked or can adversely change the locking threshold in one or more axes.

Dual-mode inertia reels combine both locking methods (rate-of-extension and G-sensing) which should increase the probability of the mechanism locking in an accident. This type of inertia reel is preferred from a crashworthiness standpoint.

Some pilots believe that impact-sensitive inertia reels can be a nuisance or possibly a hazard during normal operation (Reference 8-15). Depending on the sensitivity and the natural frequency of the G-sensing mechanism, the inertia reel may lock during moderate turbulence or extreme flight maneuvers. The TSO-C114 standard requires a 1.0-G nominal deceleration with a maximum allowed 1.5-G deceleration to lock the reel. Problems with inadvertent lock-up may be circumvented by setting a higher threshold for the vehicle sensing reels. As reported in Reference 8-12, one restraint manufacturer sets the locking sensitivity between 0.75 to 3.0 G.

A special category of inertia reels have a control lever that is usually mounted under the seat pan, on the seat side, or at some other convenient location. These inertia reels are generally called manual locking reels. The control lever is connected to the inertia reel with a push-pull cable and has two positions, manual and automatic. The manual position permits the occupant to lock the reel, if desired, during extreme maneuvers and turbulence. In the automatic position, the reel acts just like a standard inertia reel and will only lock up when the webbing and/or G-sensor is activated. The control lever is normally placed in the automatic position to allow the wearer to lean forward easily and reach all controls without first having to release the control lever. One significant advantage of the manual-locking control lever inertia reels is that the reel stays locked after sensor activation, even if the webbing tension is released. The inertia reel is unlocked by cycling the control lever through the "manual" position back to "automatic" position. Films of full-scale, small aircraft testing have shown that standard inertia reels (those without control levers) sometimes pay out webbing after the initial impact, even if the reel locked properly during the first impact. This pay-out has often resulted in the ATD striking the interior of the airplane during subsequent impacts. The fact that the manual-locking inertia reel remains locked after the initial impact can greatly reduce the chance of injury during the relatively long duration, and often multiple impacts, of airplane accidents. Manually locking inertia reels are most commonly found on crewseats of military aircraft and on special restraints called "gunner's belts" used on military and medical evacuation helicopters.

THIS DOCUMENT PROVIDED BY THE ABBOTT AEROSPACE
TECHNICAL LIBRARY
ABBOTTAEROSPACE.COM

8.1.6.2 Film-Spool Effect

The "film-spool effect" refers to webbing slack that is almost instantaneously removed from the inertia reel spool during crash loading. In general, the film-spool effect is not desired, as this increases occupant motion and can increase the possibility of a secondary strike with interior structure. However, the film-spool effect can be used in a positive way to reduce the shoulder belt strap load in cases where the occupant strike hazard is minimal.

Significant webbing length can be extracted from the reel after lock-up, depending on several factors including: spool diameter, webbing type, retractor tension load, length of webbing stored, total applied load, and, rate of load and duration. Inertia reel design factors that are utilized to minimize the film-spool effect for a given length and type of webbing include increasing the spool diameter and increasing the retractor tension load. A larger spool diameter decreases the number of webbing wraps (layers) required to store a given length of webbing. Thus, the total webbing packing thickness and the compressive loading of the inner wraps are reduced. A sufficiently strong return spring can also reduce the film-spool effect by tightly winding the webbing about the spool, but too much spring tension can be uncomfortable for the occupant. The return spring should rewind webbing at a smooth and steady rate, maintaining a taut shoulder harness. This will help ensure the webbing is tightly wrapped and stowed with a minimum amount of slack.

Results of an inertia reel static pull test are presented in Figure 8-14 (Reference 8-15). This figure compares the film-spool effect for 0, 6, 12, and 17 in. of polyester webbing stowed on the inertia reel spool.

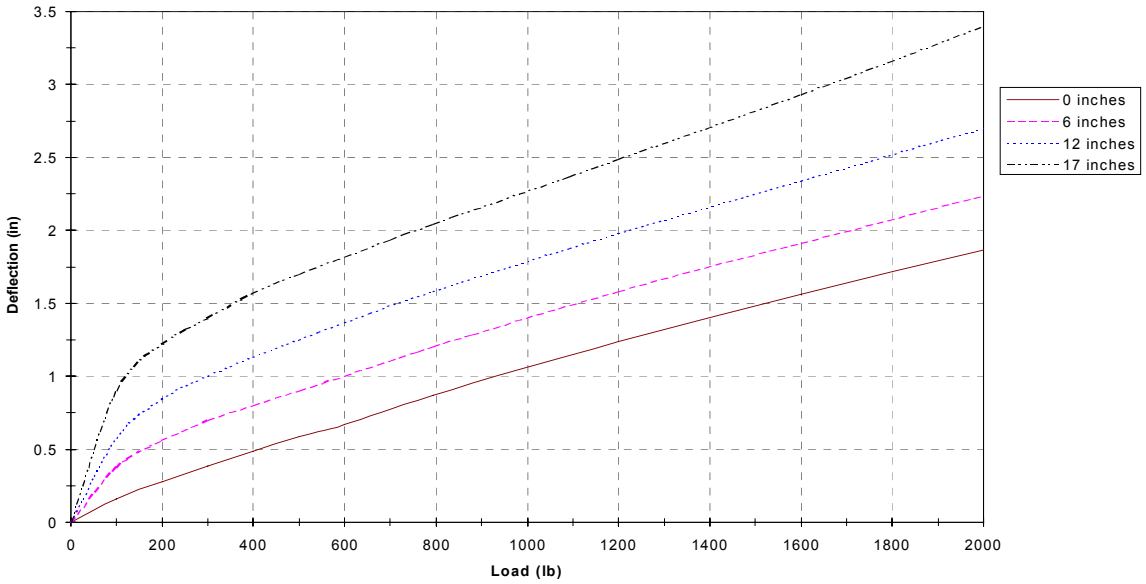


Figure 8-14.
Inertia reel film-spool effect for various lengths of stored webbing (Reference 8-15).

As shown in the figure, webbing pay-out increases non-linearly until approximately 400 lb for each of the three cases. The webbing pay-out is relatively linear beyond that point. By 200 lb, there is a four-fold increase in the pay-out when comparing 0 in. versus 17 in. of webbing stored.

This Document Provided by the Abbott Aerospace
TECHNICAL LIBRARY
ABBOTTAEROSPACE.COM

8.1.6.3 Webbing Retractors

The automatically locking seat belt was the first type of automatic locking retractor for restraint systems. This mechanism was used in automobiles during the 1960's and 1970's to conveniently stow lap belt webbing. The lap belt can be easily pulled out from the spring-loaded stowage reel; but, once the webbing returns, the mechanism locks and ratchets to prevent further webbing extension. The belt must be fully retracted before it can be extended a second time.

Auto-lock webbing retractors are not recommended for light aircraft, as they typically do not apply enough tension to remove belt slack. The retractor can also allow excessive elongation due to the film spool effect. In addition, the retractor can also "ratchet down" when encountering turbulence, which can cause uncomfortably high belt tension. The only way to lessen the tension is to fully remove the restraint and fully retract the belt, which should not be done during flight—especially during turbulence.

8.1.7 Load-Limiting Restraints

Traditional occupant restraint philosophy could be summed-up with the idea that the less the occupant moved relative to the airframe, the better. In practice, restraints were designed with low-elongation (or stiff) webbing and with features that would minimize restraint slack. This philosophy is based on sound logic: the less the occupant flails, the lower the probability of the occupant striking the interior; in addition, the more closely coupled the occupant is to the airframe, the less the chance of developing dynamic overshoot. However, in higher-severity crashes, stiff restraint systems can transmit injurious loads to the occupant. Load-limiting the restraint is one way to reduce the loads to the occupant.

Load-limiting a restraint works in a similar fashion to the seat load-limiters discussed in Chapter 7: some property of the restraint limits the strap load to a pre-determined value. When that limit-load is reached, the restraint strokes, which absorbs energy. In practice, the strap load is typically limited to just under a human tolerance value. For instance, a single diagonal shoulder strap might be designed to have a limit-load of 1,500 lb, thereby protecting the occupant from experiencing the maximum strap load of 1,750 lb (per 14 CFR 23.562(c)). The limit-load can also be selected based on the strength of the restraint's anchor structure.

As mentioned, load-limited restraint systems stroke; this, in turn, will allow more occupant excursion than a standard, non-load-limited restraint. The designed stroke should not exceed more than a few inches to minimize additional occupant flail. Load-limiting can be an effective way to manage energy only if there is sufficient space in the cabin to accommodate the additional flail.

Load-limiting should not be confused with controlled pay-out. Controlled pay-out is similar to load-limiting, except that the limit load is relatively low—typically just above abuse loads (300 to 600 lb). Controlled pay-out is often implemented in restraints with progressive ripping of stitched bar tacks (rip-stitches) on a loop of webbing. The automotive industry uses controlled pay out to improve interaction with the supplemental inflatable restraint (airbag). These rip-stitch devices are often found in the lap belts of cars where they allow the occupant's pelvis to move forward early in the crash event to delay the rotation of the upper torso and head. This delay allows more time to deploy the airbag, and positions the occupant so the interaction with the air bag is less hazardous.

Controlled pay-out has also been used in the shoulder harness of dual-strap systems (four-and five-point) to minimize submarining (for example, in the Schroth Safety Products ASM device). This system produces a small amount of slack in one or both of the shoulder belts during the

This Document Provided by the Abbott Aerospace
TECHNICAL LIBRARY
ABBOTTAEROSPACE.COM

impact which allows the torso to rotate forward relatively early in the event. This torso rotation, in turn, positions the pelvis so the lap belt hooks up with the pelvis better and reduces the chance for submarining.

8.1.7.1 Load-Limiting Webbing

Three webbing load-limiting concepts are presented below for informational purposes. Only one of the three concepts is currently available commercially.

Non-plastic Fibers

Carbon-fiber thread reinforcements can be used for limiting restraint loads, as explained in Reference 8-15. By integrating these fibers into the weave of the webbing, manufacturers can enhance the force-verses-deflection characteristics of the webbing. This technology incorporates low-elongation carbon fibers that fail at a pre-determined load. Controlled elongation prevents significant load increases in the belt, and increases the energy-converting capability of the fabric. Fiberglass fiber is another possibility for this type of reinforcement.

Pre-shrunk Fibers

A similar concept includes pre-shrinking the webbing fibers. As described in Reference 8-17, polyester filaments, for example, can be initially heat-shrunk to provide a plastic-like energy-absorbing capability during loading in a crash pulse. However, the authors of Reference 8-4 cautioned that this technique does not optimize the stroking distance, due to a linear force-deflection curve.

Engineered Polymer Fibers

Recently, the Performance Polymers and Chemical Division of Honeywell began marketing a fiber specifically designed for restraint webbing call Securus®. This fiber is a block co-polymer of two plastics that allows the chemist to control the fiber properties. Webbing made from this fiber is relatively stiff at the beginning of its load-deflection curve, becomes less stiff (flattens out) for an energy-absorption phase, and then stiffens again. Honeywell reports that several automotive restraint manufacturers are currently testing belt restraints made with the Securus fiber. Webbing made of this fiber may also soon be available for aviation restraints.

8.1.7.2 Webbing Rip-Stitching

Rip-stitch devices consist of a loop, or bight, of webbing that has been stitched down by a series of bar tacks. Tension on the free ends of the webbing stresses the stitching in the first bar tack. When the limit-load, which is pre-determined by the strength of the thread and number of stitches, is reached, the first bar tack “rips,” or fails, thus absorbing energy and transferring the load to the next bar tack. The process then repeats until all the bar tacks are torn. These devices have a relatively jagged, but well controlled, load-deflection curve.

Careful consideration must be made regarding the placement and failure load of the bar tacks. A bar tack too close to the webbing edge and too strong can initiate an edge tear, thus failing the webbing. In practice, rip-stitch load-limiters make good controlled-pay-out devices, but should not be used in applications that require higher limit-loads that could cause webbing failure.

8.1.7.3 Load-Limiting Anchors/Inertia Reels

A mechanical load-limiter can be attached between the aircraft mount and the webbing anchor point to provide a more controlled load-deflection curve. Any number of load-limiters could be implemented, similar to the seat load-limiters shown in Section 7.1.8.

®Securus is a trademark of Honeywell

THIS DOCUMENT PROVIDED BY THE ABBOTT AEROSPACE
TECHNICAL LIBRARY
ABBOTTAEROSPACE.COM

An inertia reel that utilized a torsion bar was tested in Reference 8-18. As shown in Figure 8-15, this design allowed the plastic twisting of a torsion bar to limit the shoulder strap loading. Dynamic sled tests with a 50th-percentile ATD and peak decelerations of 28.5 G showed that peak strap loads were reduced by 50 pct. However, the shoulder peak forward displacement increased by 5.1 in., thus increasing the occupant strike envelope.

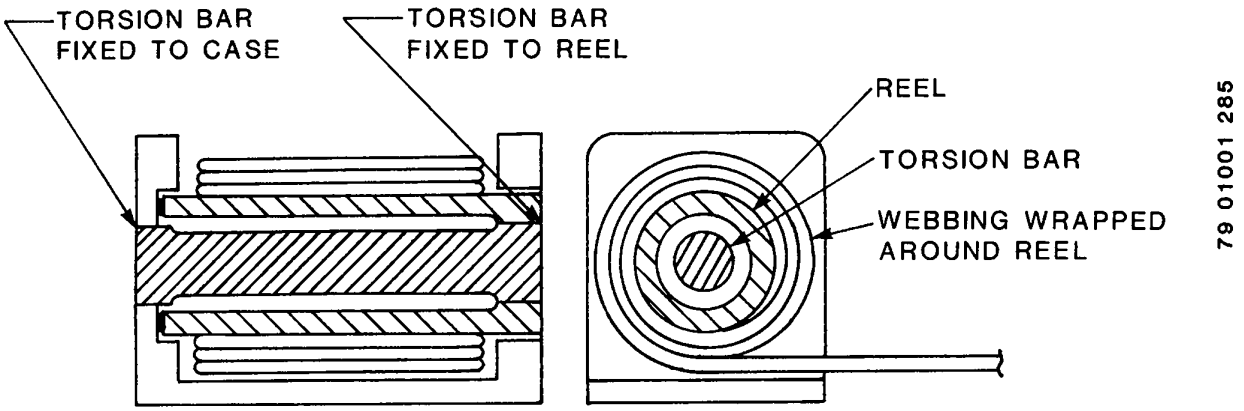


Figure 8-15.
Schematic of a load limiting inertia reel (Reference 8-18).

8.1.8 Pre-tensioners

Pre-tensioners in automobiles have proven to effectively mitigate dynamic overshoot by minimizing the slack in the restraint. Restraint slack induces a time-lag between vehicle and occupant deceleration. This critical time-lag imparts higher deceleration and biomechanical stresses upon the occupant; specifically, the longer the time-lag, the greater the dynamic overshoot. In essence, a pre-tensioner allows the occupant to load the restraint earlier in the crash event, thereby reducing the peak restraint load.

There are two basic methods of pre-loading the restraint system: pre-winding the inertia reel, and displacing the belt anchor. Both devices were investigated and compared to a baseline three-point restraint and an inflatable belt in a series of sled tests (see Section 4.2 for results and discussion). The shoulder belt inertia reel pre-tensioner and the buckle pre-tensioner were both effective in removing slack in the restraint (References 8-19 and 8-20). Reductions in occupant motion, loads, and accelerations were realized for most of the ATD measurements when compared to the baseline restraint. By eliminating restraint slack, head and chest deceleration and strap loads were reduced. It should be noted that commercial pre-tensioning systems for light aircraft have not yet been developed.

The pre-tensioner must be activated by a crash sensor early in the crash event to be effective. Automotive belt anchor pre-tensioning systems typically fire within 7 msec after the initial impact and pre-load the restraint systems within 5 to 8 msec. A conventional automotive restraint (with normal slack) is typically not loaded until 40 msec after initial impact. The belt, therefore, is loaded 2 to 3 times faster than a restraint system without a pre-tensioner.

This Document Provided by the Abbott Aerospace
Technical Library
abbottaerospace.com

Pre-tensioners can also be strategically used with load-limiters to provide more energy conversion. The belt slack removed by pre-loading can be used for additional elongation by the load-limiter, thereby increasing the time and distance for the occupant to ride down the crash. The combination of pre-tensioners and load-limiters is used in several European cars.

Pre-tensioners should not be confused with power haul-backs. Power haul-backs are more aggressive mechanisms, designed for military ejection seats to pull the pilot back into an upright and more injury-tolerant position before ejection from an aircraft. Power haul-back devices typically produce much higher tension in the belt—often just below human tolerance. Since pre-tensioners are used only to remove belt slack, they are much less aggressive and typically use a pre-loading force of less than a few hundred pounds.

8.1.8.1 Inertia-Reel Pretensioners

Inertia-reel pre-tensioners are currently in production and are primarily used in automobiles. Inertia-reel pre-tensioners remove the slack in the shoulder harness by pre-winding or pre-spinning the inertia reel spool. The pre-winding can be accomplished mechanically with a large clock spring, or pyrotechnically (typically by a cable wound around the ratchet mechanism that is pulled by a pyrotechnically-driven piston). These devices typically remove 3 to 6 in. of slack from the shoulder belt and typically produce a belt pre-load between 75 to 150 lb (Reference 8-19). In addition to removing slack, the device tightly winds the webbing, thereby reducing the film-spool effect.

8.1.8.2 Belt Anchor and Buckle Pretensioners

Belt anchor and buckle pre-tensioners are also currently in production and are also primarily used in automobiles. Belt anchor and buckle pre-tensioner devices differ mainly by which end of the belt attaches to the pre-tensioner. These devices are typically placed in the load path between the lap belt or buckle and the vehicle anchor. Automotive three-point harness applications typically utilize a continuous webbing loop for the lap and shoulder belt, so that a lap belt anchor pre-tensioner operating on the lap belt also pre-tensions the shoulder belt somewhat. Anchor pre-tensioners may not work as well on aviation restraints, due to the manually adjusted lap belt. Buckle pre-tensioners on three-point restraints pull on the latch plate which pre-loads both the lap belt and the shoulder belt. Displacement (slack removal) of

the buckle averages 2 to 3 in., and typically pre-loads both belts between 50 and 100 lb (Reference 8-20). The net result is a potential reduction in head displacement of 3 to 4 in., and a decrease in head and chest deceleration up to 20 pct (Reference 8-14).

8.1.9 Belt Restraint-Induced Injury

In a study (Reference 8-36) conducted of 810 automobile accidents in Switzerland and France in which the occupants used three-point restraints, particular attention was given as to whether the belt itself could have been the cause of neck injuries during lateral collisions. In 98 of the 810 accidents, there were near-side lateral impacts. In 10 of these accidents, neck injuries were registered, but only 2 of them could be attributed to contact with the shoulder belt webbing. The corresponding incidence of neck injuries, 111 in the 712 cases of frontal, far-side, and rollover impacts, was not considered significantly different. The conclusion from the study was that the number of hazardous effects of three-point restraints to the occupant's neck region is insignificant.

THIS DOCUMENT PROVIDED BY THE ABBOTT AEROSPACE
TECHNICAL LIBRARY
ABBOTTAEROSPACE.COM

High-velocity impacts can cause severe injury to the occupant's body, especially if the restraint permits lateral and forward movement of the mid-section of the torso (Reference 8-37). Depending upon the acceleration-profile variables, the internal organs and tissues can be distorted, with varying degrees of resulting injury. To prevent this, the torso could be confined in a flexible full-area restraint system, which minimizes the distortion and, in essence, allows the organs and bones to "float." Experimental verification was obtained using guinea pigs and monkeys at a 40-ft/sec velocity change. This work indicates the desirability of restraining as large an area of the occupant's torso as practicable, in order to decrease the severity of internal injury during crash impacts.

8.2 CHILD RESTRAINTS

The protection of child occupants through the use of a child restraint system (CRS) is an important consideration in the design of passenger seats for GA aircraft. The effective installation of a CRS in a passenger seat will be especially important for the design of light planes that are designed primarily for cross-country travel by families. Therefore, the recommendations provided within this section are intended for the design of four-place or larger GA aircraft, and are not for the design of two-place sport aircraft.

The overall function of a CRS is similar to that of an adult restraint system (Reference 8-21). The restraint system should be able to operate effectively during dynamic events such as in-flight turbulence or crash landing, allowing the child to "ride down" the event, along with the aircraft. Effective "ride down" is accomplished by tightly coupling the child to the aircraft frame through the use of the aircraft seat's built-in restraint system. The CRS should provide an effective means for distributing the applied loads from the impact over the most stable areas of the child's body and should employ the use of specialized padding or structural deformation to promote energy absorption.

In addition to these performance requirements, a CRS must also account for the differences in biomechanical structure that exist between children and adults. For example, infants and young children tend to possess a much larger head mass relative to their body size. The child's large head mass is accompanied by an immature musculoskeletal neck structure. Therefore, adequate protection of a child's head and neck complex is crucial to avoid serious injury. In addition, the skeletal structure of a child is primarily cartilaginous in composition, and that creates an elastic-type structure. This difference in skeletal structure indicates that the internal organs and soft tissues within a child's body do not receive the same degree of protection as an adult's (Reference 8-22). Overall, the restraint system must be able to redistribute high, localized crash forces over large, stable areas of the child's body, while providing proper protection for the child's head and neck.

The primary concern for the GA aircraft designer involves the compatibility of the CRS with the aircraft. To address the issue of compatibility, the following section will discuss several different topics, including:

- Current regulations that control the certification of a CRS
- The performance of a CRS in the aviation environment
- Aircraft design considerations employed to enhance the compatibility between the CRS and the aircraft seat
- Any present and future CRS research activities.

This Document Provided by the Abbott Aerospace
TECHNICAL LIBRARY
ABBOTTAEROSPACE.COM

8.2.1 Current Regulations

Currently, a CRS is approved for use in automobiles and airplanes by its adhering to all of the requirements specified in FMVSS 213 (References 8-23 and 8-24). However, it is important to remember that the crash environments for airplanes and automobiles can be very different and that these differences may affect the overall performance of a CRS during a crash. For example, automotive impacts primarily occur within a two-dimensional, planar surface, since roll-over or vertical landing scenarios are not as common in automobiles as they are in airplanes. This allows the principal direction of force in an automotive crash to be described as a two-component vector. On the other hand, aircraft impacts occur in three-dimensional space, where a third (vertical) component is added. This allows the principal direction of force in aircraft crashes to be described as a three-component vector. This indicates that a CRS used in an aircraft must be able to withstand crash forces from potentially three different directions.

8.2.2 Dynamic Test Conditions

In GA, FAR 23.562 specifies the dynamic test conditions used to evaluate the performance of aircraft seats and restraint systems during emergency dynamic landing scenarios (Reference 8-5). As shown in Table 8-2, these test conditions differ from those specified in FMVSS 213 (Reference 8-24). In FMVSS 213, the horizontal test requires a change in velocity of 44 ft/sec and a minimum peak deceleration of 24 G occurring not more than 0.02 sec after impact. In FAR 23.562, the horizontal test requirements vary depending on the location of the seat (Reference 8-5). For first-row seats, FAR 23.562 requires a change in velocity of 42 ft/sec and a minimum peak deceleration of 26 G occurring not more than 0.05 sec after impact. For all other seats, the change in velocity remains the same and the minimum peak deceleration decreases to 21 G within 0.06 sec after impact. The FAR 23.562 horizontal test is conducted with a 10-deg adverse yaw relative to the impact direction that results in the greatest load on the shoulder harness (Reference 8-5).

In addition, FAR 23.562 requires a vertical dynamic test with a change in velocity of 31 ft/sec and a minimum peak deceleration of 19 G in 0.05 sec for first-row seats and 15 G in 0.06 sec for all other seats. This test is conducted with a 30-deg nose-down pitch relative to the impact direction with no yaw.

Comparison of the horizontal test pulses for FMVSS 213 and FAR 23.562 indicates that the impact severity of the two tests is quite similar. Therefore, a CRS that has been approved by the FMVSS 213 certification tests may also perform well in a light airplane subject to the conditions required in the FAR 23.562 horizontal test.

Table 8-2.
Test pulse comparison between FMVSS 213 and FAR 23.562 (References 8-5 and 8-24).

Federal Standard	Seat Orientation	Change in Velocity (ft/sec)	Minimum Peak Deceleration (G)	Rise Time (sec)
FMVSS 213	horizontal	44	24	0.02
FAR 23.562	horizontal (10 deg adverse yaw)	42	26 (first row) 21 (other row)	0.05 (first row) 0.06 (other row)
FAR 23.562	vertical (30 deg nose down)	31	19 (first row) 15 (other row)	0.05 (first row) 0.06 (other row)

This Document Provided by the Abbott Aerospace
TECHNICAL LIBRARY
ABBOTTAEROSPACE.COM

8.2.3 Certification of Child Restraint Systems

In the certification of a CRS, FMVSS 213 includes only one requirement that is truly representative of the aviation environment (Reference 8-24). For this requirement, a rollover test indicates whether the restraint system will contain the child occupant in an inverted aircraft. The CRS is installed in a representative aircraft passenger seat with an FAA-approved aircraft seat belt. The rollover test is conducted twice by rotating the aircraft passenger seat with the installed CRS in two different planes as follows:

1. The seat is "…rotated forward around a horizontal axis which is contained in the median transverse vertical plane of the seating surface portion of the aircraft seat..." (Reference 8-24)
2. The seat is"…rotated sideways around a horizontal axis which is contained in the median longitudinal vertical plane of the seating surface portion of the aircraft seat..." (Reference 8-24)

In each of these tests, the aircraft seat is rotated "…at a speed of 35 to 45 degrees per second to an angle of 180 degrees" (Reference 8-24). In this orientation, the rotation ceases and the aircraft seat is held in position for 3 sec. During the 3-sec period, the CRS must not fall out of the seat belt on the aircraft passenger seat and the ATD must not fall out of the CRS.

Other than this particular test, the remainder of the test methods described in this standard are more representative of the automotive environment. Specifically, the test fixture and components that are used better represent an automobile seat rather than a standard airplane passenger seat (Reference 8-23). For example:

- The lap belts on the test fixture attach at geometrically different locations than on an airplane passenger seat
- The seat back on the test fixture does not necessarily behave in a manner similar to an aircraft seat back during impact testing
- The type of restraint system is not specified
- The release mechanism for the seat belt buckle is different
- The location of the belt buckle may be different (center of lap belt versus at occupant's hip)
- The arm rests on airplane seats limit the available lateral space for the CRS.

Nonetheless, a CRS must pass all of the requirements in the standard, in addition to the inversion test, in order to be certified for use in aircraft. After a CRS is certified, FMVSS 213, FAR 91.107, and FAR 121.311 specify that the manufacturers of approved CRS's are required to clearly label these restraints with a statement that reads "This restraint is certified for use in motor vehicles and aircraft" (References 8-24, 8-25, 8-26). The FAA has also provided several other recommendations for the use of a CRS in airplanes. For more information on these additional limitations, refer to FAA Advisory Circular AC91-62 (Reference 8-27).

8.2.4 Performance of Child Restraint Systems in the Aviation Environment

Since the initial development of the CRS in the early 1960's, several different types of restraint systems have been available to consumers (References 8-21,8-28). These systems have been designed to accommodate infants and young children of varying ages, sizes, and weights. In recent years, increasing interest within the aviation community has encouraged researchers to evaluate the performance of different styles of CRS on transport-category aircraft passenger seats. In the early 1990's, a study conducted by Van Gowdy and Richard DeWeese of the FAA's Civil Aeromedical Institute (CAMI), investigated the dynamic performance of six different types of CRS: rear-facing infant restraints, convertible restraints, booster seats, a torso

This Document Provided by the Abbott Aerospace
TECHNICAL LIBRARY
ABBOTTAEROSPACE.COM

harness, a lap-held child restraint (belly belt), and passenger-seat lap belts (Reference 8-23). During the time of the study, all six of these CRS types were certified for use in transport-category aircraft.

In the study, Gowdy and DeWeese conducted both horizontal and vertical impact tests using economy-class cabin triple-position passenger seats from transport-category aircraft. During the horizontal sled tests, the seats were either arranged in single-row or double-row configurations. During the vertical drop tests, the seats were arranged in a single-row configuration. To accurately represent the seat placement in an economy-class cabin, the tests using the double-row configuration maintained a 32-in. seat pitch between the rows of seats.

The dynamic test conditions for the impact tests were defined by using the conditions specified for transport-category aircraft in FAR 25.562 (Reference 8-5). The horizontal test required a change in velocity of 44 ft/sec and a minimum peak deceleration of 16 G occurring not more than 0.09 sec after impact. This test was conducted with a 10-deg adverse yaw relative to the impact direction that results in movement of the upper torso restraint off of the occupant's shoulder. The vertical drop test required a change in velocity of 35 ft/sec and a minimum peak deceleration of 14 G occurring not more than 0.08 sec after impact. This test was conducted with a 60-deg nose-down pitch relative to the impact direction.

The results of the CAMI study indicated that only two of these six devices provided adequate protection for child ATDs during horizontal and vertical impact tests: the rear-facing infant restraint and the convertible restraint. The following sections will describe the characteristics of all six types of CRS tested, as well as the advantages and disadvantages of using these restraint systems in aircraft seats. In addition, a seventh type of CRS that was not included in the CAMI study, referred to as a car-bed infant restraint, will also be discussed.

It is important for the GA aircraft designer to be aware of the compatibility issues that exist between transport-category aircraft seats and a CRS. Although there can be significant differences between the styles of seats and restraint systems used in GA aircraft versus transport-category aircraft, some of the same basic issues will arise when installing a CRS in a seat. Therefore, the general knowledge acquired from these studies can also be applied to the GA environment.

8.2.4.1 Rear-facing Infant Restraints

Rear-facing infant restraints can be used in both automobiles and airplanes. As illustrated in Figure 8-16, the restraint system consists of a semi-upright seat that is anchored to the vehicle or airplane seat using a seat belt (Reference 8-21). This type of CRS must be installed facing rearward with the back surface oriented at an angle approximately 45 deg to the vertical. The harness straps that are used to secure the infant within the restraint system must cross directly over the infant's shoulders and must be tightened to fit snugly around the infant. In a crash situation, the restraint system is used to transfer the applied loads from the impact to the most stable surfaces of the occupant's body. For infants, this involves the transfer of the applied loads to the posterior surface, or back, of the infant. The infant will outgrow this type of restraint once the top of his or her head has extended beyond the top of the back of the restraint or when the infant has exceeded the weight limitations specified by the manufacturer of the CRS. For most rear-facing infant restraint manufacturers, the weight requirement is approximately 20 lb. At that point, the infant will need to be transferred into a convertible restraint system.

During the study conducted by Gowdy and DeWeese, it was discovered that the restraint performed well during both horizontal and vertical impact tests (Reference 8-23). For example, during the horizontal impact tests, forward dynamic excursions of the child ATD were minimal.

THIS DOCUMENT PROVIDED BY THE ABBOTT AEROSPACE
TECHNICAL LIBRARY
ABBOTTAEROSPACE.COM

During the vertical impact tests, forward displacement and rotation of the various types of CRS were also minimal. In addition, the study revealed that installation of the rear-facing infant restraints was the simplest of all the types of CRS tested. These restraints were able to fit between the armrests of the seat and could be secured tightly using the aircraft seat's lap belt.

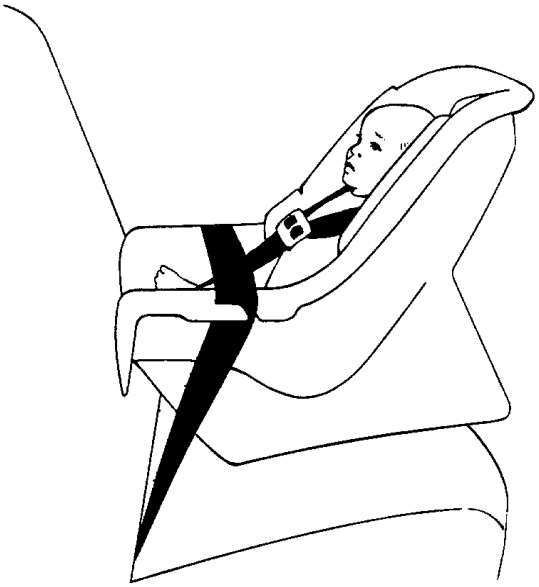


Figure 8-16.
Rear-facing infant restraint installed in the back seat of an automobile (Reference 8-21).

A disadvantage to this particular restraint was that it hung over the airplane seat cushion, reducing the already-limited passage space between seat rows. The overhang of the CRS may also hinder the recline of the seat back immediately in front of the CRS. In GA aircraft, these disadvantages may or may not be issues, depending on the size of the aircraft, the number of seat rows, and the seat pitch. In order to avoid the overhang problems that arise when using a rear-facing infant restraint on transport-category aircraft seats, it will be necessary to allow the seat pitch in GA aircraft to be greater than 32 in., or to place the restraint in a seat where it will not interfere with the movement and/or egress of the other passengers.

8.2.4.2 Convertible Restraints

Convertible restraints can be used to protect both infants and young children (Reference 8-21). As illustrated in Figure 8-17, this type of restraint can be oriented rearward for infants or forward for children over 1 yr old. One advantage to using convertible restraint systems is that the back of the restraint has a much higher support surface. This permits young children who have just surpassed the weight requirement for traditional rear-facing infant restraint systems to continue to sit facing rearward for a longer period of time. In the United States, regulators in the automotive industry have recommended that the convertible restraint should be transferred to a forward-facing position once the child reaches the age of 1 yr or when the child's head reaches the top of the restraint shell. Unfortunately, it is often difficult to keep the child facing rearward past 6 mo of age, when they weigh approximately 17 lb.

THIS DOCUMENT PROVIDED BY THE ABBOTT AEROSPACE
TECHNICAL LIBRARY
ABBOTTAEROSPACE.COM

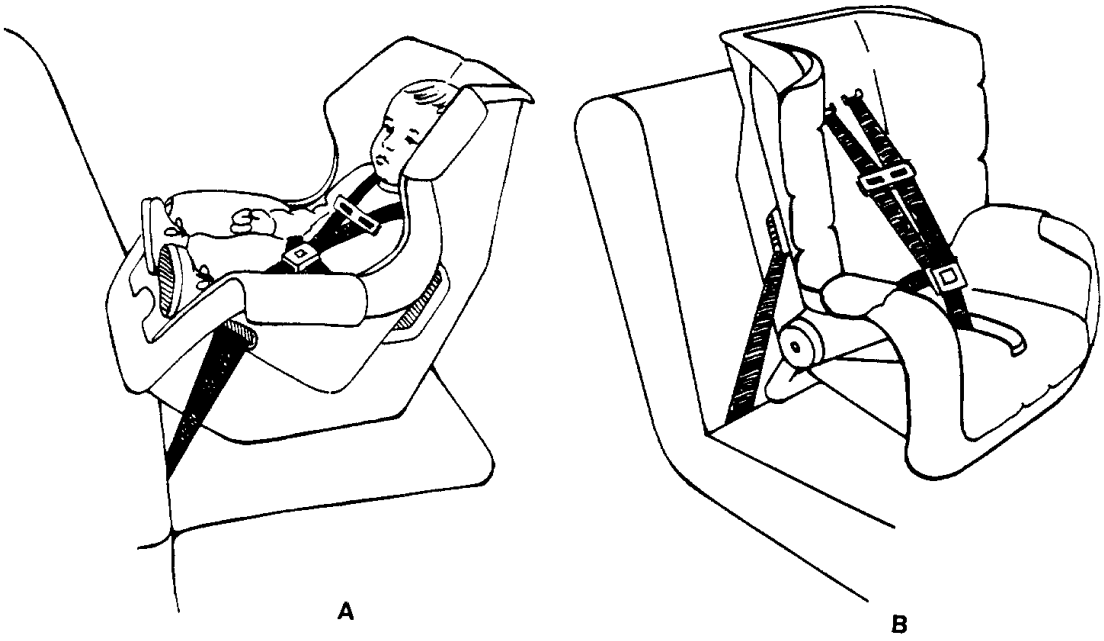


Figure 8-17.
Convertible child restraint in (A) rear- and (B) forward-facing use (Reference 8-21).

Also available on the market are forward-facing-only restraints that are designed to be used after the child has reached the age of 1 yr or when the child's head reaches the top of the restraint shell. Although these particular restraints where not tested during the CAMI study, the performance of this type of restraint would most likely be similar to a convertible restraint positioned in the forward-facing orientation and subject to the same test conditions.

The results of the CAMI study concluded that the forward-facing convertible restraints were the most difficult type of restraint to install and adjust in a transport-category aircraft seat (Reference 8-23). The limited space between the seat rows made it extremely difficult for the installer to properly route the lap belt through the CRS. In addition, the forward-facing convertible restraints were usually too wide and did not fit within the space provided between the seat armrests. This became a significant problem in those cases where the aircraft seat possessed non-stowable arm rests. Aircraft seat designers should recognize that these installation issues might also exist for GA aircraft seats, depending on the style, size, and structure of the seat and restraint system.

The installers also had difficulty tightly securing the CRS into the aircraft seat. As illustrated in Figure 8-18, this problem resulted from the large vertical angle of the airplane lap belt that varied from 85 to 93 deg above the horizontal when routed around the CRS. Under these conditions, in order for the belt tension forces to properly restrain the CRS during a horizontal impact, the seat must translate forward until the belt angle is less than 90 deg. During the testing, this forward excursion caused the ATD's head to contact the forward row's seat back.

As illustrated in Figure 8-19, this problem was reduced by moving the lap belt anchor points for the aircraft seat aft and up to the seat back recline pivot bolt. The modification reduced the belt angle on three of the models of CRS tested to 30, 50, and 65 deg. A second series of tests using the modified seat belt demonstrated a reduction in the forward excursion of the CRS, an

This Document Provided by the Abbott Aerospace
TECHNICAL LIBRARY
ABBOTTAEROSPACE.COM

elimination of head contact with the forward row's seat back, and an improvement in the installation process for the CRS. Section 8.2.6 will further discuss the importance of an appropriate lap belt angle for restraint systems used in GA aircraft.



Figure 8-18.
Double-row seat test with forward-facing convertible restraints (Reference 8-23).



Figure 8-19.
Forward-facing convertible restraint installed with the modified anchor attachments (Reference 8-23).

This Document Provided by the Abbott Aerospace
TECHNICAL LIBRARY
ABBOTTAEROSPACE.COM

8.2.4.3 Child Booster Seats

In automobiles, child booster seats are used to help bridge the transition between convertible restraints and vehicle seat belts (Reference 8-21). The booster seat helps to elevate the child to a height that allows for the correct positioning of the vehicle seat belt across the child's torso and lap. The booster also provides better visibility for the child within the back seat of the vehicle. There are two different types of child boosters currently available on the market: shield boosters and belt-positioning boosters. Shield boosters are designed to be used in the rear seat of vehicles that possess only a lap belt, whereas belt-positioning boosters are used in seats with both a lap and shoulder belt.

The CAMI study evaluated the performance of shield boosters in transport-category aircraft seats and demonstrated that they do not provide adequate protection to the child occupant during air travel (Reference 8-23). As a result, the FAA has banned the use of shield boosters on aircraft and requires the manufacturers of shield boosters to label these devices as "not certified" for use in aircraft.

During the study, there was a significant concern regarding the effects of seat back breakover and occupant impact with the aft row. Seat back breakover can force the child occupant against the booster shield, while the absence of a back shell on the booster allows forces to be transferred from the aircraft seat back directly to the child occupant. For GA aircraft seats, seat back breakover may only be a concern for those seats that are similar in style, size, and structure to transport-category aircraft seats.

The CAMI study also concluded that the molded webbing path provided by the front shield of the booster is not compatible with the airplane passenger seat's belt buckle. This incompatibility is capable of altering the seat belt webbing path and buckle position, which demonstrates that the booster is not properly installed according to the guidelines provided by the booster manufacturer.

In addition to the conclusions provided from the CAMI study, the authors of this design guide have speculated that shield boosters may not provide adequate vertical restraint for the child occupant during air travel. It is possible that this lack of vertical restraint could induce bending of the occupant's femur. Overall, the shield boosters should not be used to restrain child occupants in aircraft seats. In terms of the second type of child booster seat, the belt-positioning booster, no research has been conducted to evaluate its performance in passenger aircraft seats.

8.2.4.4 Other Types of Child Restraint Systems

There are several other types of CRS currently available on the market, including torso harnesses, lap-held child restraints (belly belts), passenger-seat lap belts, and car-bed infant restraints (Reference 8-21, 8-23). A torso harness is a forward-facing restraint that is constructed from webbing and created for children weighing approximately 25 to 40 lb. Gowdy and DeWeese discovered that this type of restraint could not be properly installed on a passenger airplane seat. A significant amount of slack was left in the lap belt, which prevented the torso harness from tightly coupling the child to the airplane seat.

The lap-held child restraint, or belly belt, is a belt that attaches to an adult passenger's lap belt that secures a child under the age of two directly onto an adult's lap. In the United States, this type of restraint is not certified for use by any automotive or aviation standards. In fact, it is illegal to use this restraint in automobiles driven within the United States. Tests conducted at CAMI revealed that it is impossible to properly restrain a child during impact using the belly belt restraint. Despite these findings, many countries still permit the use of belly belts in airplanes.

This Document Provided by the Abbott Aerospace
TECHNICAL LIBRARY
ABBOTTAEROSPACE.COM

A passenger-seat lap belt can also serve as a child restraint. However, the results from the tests conducted at CAMI demonstrated that the standard passenger seat lap belt does not fit snugly on the lap of a small child. Slack that was present in the lap belt promoted greater head excursion, as well as occupant contact, with a forward-row seat. Therefore, the passenger seat lap belt should be reserved for use only by those children that have outgrown the approved types of CRS (children weighing over 40 lb).

A car-bed infant restraint, or carry-cot, is a type of CRS that is used to protect infants who are not permitted to ride in a semi-reclined position (Reference 8-21). This restriction usually arises from certain temporary medical conditions that occur as a result of a premature birth or a low infant birth weight. In automobiles, the restraint is positioned on the back seat of the vehicle with the long side of the restraint oriented perpendicular to the direction of travel. The infant lies flat in the restraint, facing either up or down, with his or her head placed on the end that is closest to the center of the vehicle seat. There is only one car-bed infant restraint model available in the United States market and, presently, no evaluation of the performance of this restraint in aircraft seats has been conducted (Reference 8-29).

The CAMI study evaluated the performance of the torso harnesses, lap-held child restraints (belly belts), and passenger-seat lap belts (Reference 8-23). All three restraint systems performed very poorly, and they were not able to adequately restrain the motion of the small child ATD during impact. These results have encouraged the FAA to ban the torso harnesses and belly belts from use in aircraft and to recommend that the passenger seat lap belt only be used by children weighing over 40 lb. These requirements are defined in FMVSS 213, FAR 91.107, and FAR 121.311 (References 8-24, 8-25, and 8-26).

Overall, the results of the CAMI study have led Gowdy and DeWeese to conclude that consumers should not expect the exact same level of protection for their children in aircraft passenger seats as they do in automobile seats with the types of CRS available on the market today (Reference 8-23). In light of this discovery, the FAA has developed the following list of recommendations to help provide the best protection to child occupants using the available types of CRS:

- Children that weigh less than 20 lb should be restrained in an approved rear-facing CRS
- Children weighing between 20 to 40 lb should be restrained in an approved forward-facing CRS (either a forward-facing-only child restraint or a convertible restraint positioned in the forward-facing orientation)
- Children weighting over 40 lb should use the aircraft seat safety belt.

Presently, these are the guidelines that parents should follow in order to increase the level of protection provided for their child during travel on a transport-category aircraft. To date, no regulations have been developed specifically for the design and use of a CRS in GA aircraft.

8.2.5 Design Considerations for General Aviation Aircraft

Integration of a CRS into the GA environment will require designers to evaluate different aspects of the overall aircraft design, including:

- The interface between the CRS and the aircraft seat/restraint system
- The appropriate location for the CRS within the aircraft.

The following sections will provide a thorough discussion of these issues. It is important to note that the majority of the recommendations have been developed by evaluating the research data provided for transport-category aircraft seats and applying it to GA aircraft seats. Since there

THIS DOCUMENT PROVIDED BY THE ABBOTT AEROSPACE
TECHNICAL LIBRARY
ABBOTTAEROSPACE.COM

are numerous differences between the design characteristics of transport-category and GA aircraft seats, designers should consider variations in seat style, dimensions, pitch, seat back height, attachment to airframe, and restraint system while reviewing the following sections.

8.2.6 Interface Between the CRS and the Aircraft Seat/Restraint System

In the design of "family-oriented" aircraft, designers should develop aircraft seats and restraint systems that can accommodate conventional types of CRS. These CRS-compatible aircraft seats should have the ability to enhance the level of safety for the child occupant while not compromising the safety of other passengers on the aircraft. They should provide protection during a variety of potentially dangerous dynamic events ranging from in-flight turbulence to crash landings.

To achieve optimal performance of the CRS within the aircraft seat, designers will need to investigate the following issues:

- The type of aircraft seat and seat cushion
- The orientation of the aircraft seat
- The restraint system selection and belt angle geometry
- The design and placement of surrounding features (armrests, consoles, etc.).

The performance of the CRS is dependent on the behavior of the CRS-compatible aircraft seat under dynamic loading conditions (Reference 8-25). Therefore, aircraft designers must carefully evaluate all of the components of the aircraft seat and their potential relationship with the CRS. One essential component of an aircraft seat is the seat cushion. The cushion's elasticity, energy-absorbing capabilities, contour, and thickness will be important properties to examine during the design of the aircraft seats. For example, seat cushions that are too soft may create large deflections that can eject the child from the restraint, whereas seat cushions that are more rigid do not tend to demonstrate this problem. In the automotive industry, SAE Surface Vehicle Recommended Practice J1819 suggests that when a load of 155 N ±5 N (35 lb_f ±1 lb_f) is applied horizontally to the top-central portion of the CRS seat back, the stiffness of the vehicle seat cushion shall not permit an angular deflection of the CRS of greater than 12 deg (Reference 8-30).

In terms of the seat cushion contour, designers may want to consider a curvature that increases the snugness of the fit of the CRS within the aircraft seat. The current recommendation suggests that the shape of the seat cushion should allow 85 pct or greater of the bottom surface area of the CRS to contact the surface of the seat cushion (Reference 8-31). In addition, the perimeter dimensions of the seat cushion must be large enough to properly support a CRS. The passenger seat cushion should be able to accommodate a CRS that is at least 15 in. wide and 16 in. deep (Reference 8-31).

Another important seat component is the airplane seat back. Transport-category airplane seat backs are not designed to remain upright during an impact. This feature allows for inertial loads to be transferred from the seat back to the seat cushion via the restraint system, potentially causing injuries to the child. Therefore, for those GA aircraft seats that are similar to transport-category seats in style, size, and structure, designers should evaluate the following:

- The weight of the seat back
- The deformation of the seat pan and back pan
- The location of the mass center and mass moment of inertia of the seat back relative to the point of rotation of the seat.

This Document Provided by the Abbott Aerospace
TECHNICAL LIBRARY
ABBOTTAEROSPACE.COM

The orientation of the CRS-compatible aircraft seat is also an important design parameter. In GA airplanes, the seats can be arranged in a forward-facing, rear-facing, or side-facing orientation. However, current certification standards only certify the use of a CRS in seats that are positioned in the forward-facing orientation. Since this design guide recommends that any CRS be used in the manner originally intended by the restraint system designer and manufacturer, the CRS should be installed in a forward-facing aircraft seat, following the exact instructions provided by the CRS manufacturer. The manufacturer of the aircraft may want to include this recommendation within the owner's manual for the aircraft. They may also want to inform parents that no type of CRS is certified for use in rear-facing and side-facing aircraft seats.

The type of restraint system selected for the aircraft seats will directly influence the functions of the CRS. As previously mentioned, this design guide recommends, at a minimum, the implementation of a three-point restraint system on all newly designed passenger seats in non-acrobatic aircraft. For CRS-compatible passenger seats, the buckle and shoulder belt of the three-point restraint system should attach near the occupant's hip and not near the center of the lap belt. This type of buckling configuration is similar to a current automotive restraint system's configuration and is more compatible with most types of CRS.

This design guide also recommends the use of five-point restraint systems in GA aircraft. However, no research has been conducted to evaluate the performance and compatibility of a CRS with five-point restraints. Therefore, the authors of this design guide recommend that a CRS should be installed in a seat that possesses a three-point restraint system, as described above.

According to FMVSS 210, "…all CRS's are designed to be secured in vehicle seats by lap belts or the lap belt portion of a lap-shoulder belt" (Reference 8-32). This indicates that the design of the lap belt portion of the vehicle or aircraft restraint system is integral to the effective performance of the CRS. In the design of a CRS-compatible aircraft seat, one issue to consider is the overall length of the lap belt. The lap belt should be long enough to be routed around or through a CRS that has a minimum width of 15 in. and depth of 16 in.

Another issue to address is the belt angle that is formed by the placement of the belt anchorage points and the routing of the belt through the designated pathway on the CRS (Reference 8-33). In both the automotive and aviation industries, the lap belt anchorage can be located either directly on the seat structure or on the frame of the vehicle or aircraft. This design guide stresses the benefits of placing the lap belt anchorage directly on the seat, while the torso harness anchorage is attached to the aircraft frame (see Section 8.1.2).

In terms of the appropriate belt angle to use, it has been noted that adult occupants require different belt angles than does a CRS (Reference 8-33). In general, a CRS will benefit from belt angles that are as horizontal as possible with the belt anchors placed farther back, whereas adult passengers typically benefit from belt angles that are more vertical and are placed farther forward. For GA aircraft seats with three-point restraint systems, the proper belt angles for adult occupants are described in Section 8.1.2.1. In order to accommodate a CRS, a low mounting point for the belt anchor should be selected. This should allow the passenger seat lap belt to be adjusted taut to improve the degree of restraint available for certain types of CRS.

Finally, the aircraft designer should evaluate the design and placement of specialized features, such as fixed armrests and consoles, which attach to or surround the seats of the aircraft. These features may interfere with the proper installation and operation of a CRS or may pose as a potential strike hazard for the child occupant.

This Document Provided by the Abbott Aerospace
TECHNICAL LIBRARY
ABBOTTAEROSPACE.COM

8.2.7 Location of the CRS

Aircraft designers should consider where the CRS-compatible aircraft seats will be located within the GA aircraft. The following design issues should be addressed:

- The number and arrangement of seats within the aircraft
- The potential for airbag/inflatable restraint interaction with the CRS
- The potential for interaction between the CRS and the primary flight controls
- The interaction with restraint system load-limiting features
- The potential for interference with passenger egress.

Based on the precautions listed in Advisory Circular AC91-62, this design guide recommends that the CRS-compatible seats be located farthest from the most likely impact site, specifically, farthest from the front of the aircraft (Reference 8-27). Therefore, rear passenger seats are the preferred location for a CRS. This will also help to eliminate any potential interaction of the CRS with front-seat airbags (if installed) and the primary flight controls.

In terms of the built-in passenger seat restraint systems, if the designer is intending to install belt pre-tensioners or load-limiting features, special considerations will need to be evaluated for any seats that might need to accommodate a CRS. Research has been conducted within the automotive community to study the effects of belt pre-tensioners on the performance of a CRS (Reference 8-34). However, the results have not been very conclusive, and created more issues to be investigated. Regarding the use of load-limiting features, the effects of these systems on the performance of a CRS in an aircraft seat is unknown (Reference 8-29). However, the combined weight of the child occupant and the CRS would most likely be less than the average weight of the adult occupant for whom the load-limiter was designed. This indicates that the presence of the child and CRS within the seat may not even be capable of activating the load-limiting features. However, until more research can be conducted on the use of belt pre-tensioners and load-limiting systems, the authors of this design guide recommend that the aircraft owner should avoid installing a CRS in a passenger seat that possesses these features unless no other appropriate seating options are available.

Finally, the CRS-compatible seats should be located farthest from any aisles or passageways within the aircraft and not in a location that is near to or blocks a passenger exit. This will help to avoid inhibiting the egress of other passengers. Adherence to these general guidelines will enhance the level of safety of all passengers on board the aircraft.

8.2.8 Current Advancements in Child Restraint Systems

Increasing the level of protection provided to child occupants is an important priority for both the automotive and aviation industries. Current research studies are striving to improve the overall compatibility among all types of CRS, seats, and seating restraint systems. In 1999, the newest innovation in CRS design, the Universal Child Safety Seat System (UCSSS), was approved by the United States Department of Transportation (DOT) (Reference 8-35). The UCSSS is a uniform anchorage system that will be incorporated into all new motor vehicles and types of CRS by September 1, 2002. The UCSSS was designed to: 1) Provide greater protection for a child during an automobile accident and 2) simplify the child safety seat installation process.

Once the new systems are incorporated into all vehicles and child safety seats, the National Highway Transportation Safety Administration (NHTSA) expects the UCSSS to save approximately 50 lives and to prevent 3,000 injuries annually.

THIS DOCUMENT PROVIDED BY THE ABBOTT AEROSPACE
TECHNICAL LIBRARY
ABBOTTAEROSPACE.COM

As illustrated in Figure 8-20, two lower anchorage points and one upper anchorage point will be installed in at least two of the automobile's rear seating positions. The rigid bar or rod-like lower anchorages will be located at the juncture of the vehicle seat cushion and the vehicle seat back. The CRS will snap onto the two lower anchorage points via special connectors. The ring-like upper anchorage point will be permanently attached to the top of the vehicle's rear seat. A tether strap fixed to the CRS will secure it to the upper anchorage point. In an effort to continue to protect children during air travel, the DOT has required the UCSSS to be compatible with both aircraft and automobile seats. This will enable families to continue to use an airplane seat lap belt to properly secure the CRS.

Within the GA community, further research is needed to better understand the performance of all types of CRS, including the new UCSSS, in airplane seats. Future research studies should develop tests that utilize realistic aircraft seats in the simulation of dynamic events that occur during air travel. Some of these dynamic events may include:

- Roll-over, or inversion, types of scenarios (as seen in FMVSS 213)
- In-flight turbulence
- Crash-landing scenarios at varying attitudes.

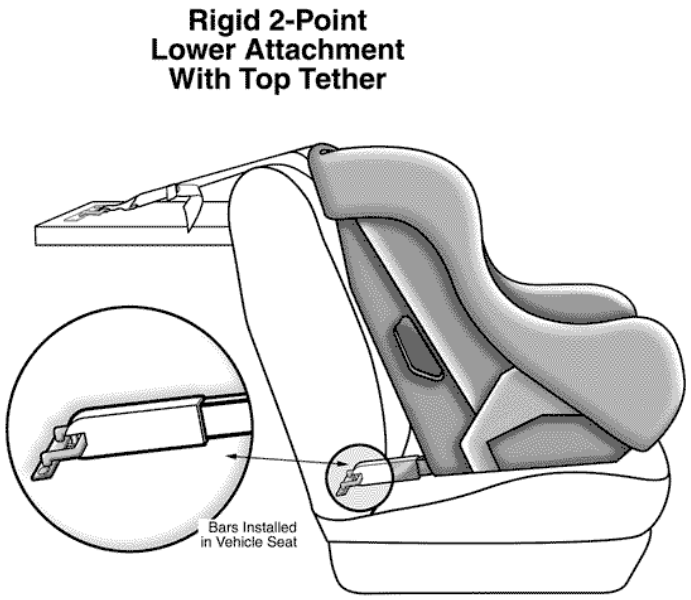


Figure 8-20.
Automobile attachment configuration for the Universal Child Safety Seat System (UCSSS) (Reference 8-35).

Until more research can be conducted, the authors of this design guide recommend that the manufacturer of the aircraft may want to comment on the use of a CRS in the owner's manual for the aircraft. Comments can encourage parents to:

- Carefully read and follow the manufacturer's instructions that accompany the CRS
- Consider the overall weight of the CRS; making sure that the CRS does not affect the weight and balance of the aircraft (Reference 8-27)

THIS DOCUMENT PROVIDED BY THE ABBOTT AEROSPACE
TECHNICAL LIBRARY
ABBOTTAEROSPACE.COM

- Remember to limit the child's movement in the CRS by ensuring that the restraint harness is snugged down for a tight fit
- Route the aircraft seat belt around the CRS according to the guidelines specified in the CRS manufacturer's manual.

Overall, it is important to stress the importance of restraining an infant or child during air travel, and how the proper use of a CRS can greatly contribute to the protection of a child occupant. The manufacturer should also indicate which passenger seats within the aircraft are capable of effectively supporting a CRS, according to the recommendations provided in this design guide.

Finally, the aircraft owner's manual might also include a discussion regarding the appropriate care of a child during air travel. It is important to remind parents that the conveniences they have while driving an automobile, such as being able to pull over to the side of the road to attend to a child, are not available to them while flying an aircraft. This realization should encourage parents to consider how demanding their child is and to determine what options they will have if a problematic situation arises. A useful recommendation may be to ensure that a second adult, who is not responsible for the flight operations of the aircraft, is available to attend to the child.

8.3 INFLATABLE RESTRAINTS

Inflatable restraints are devices that inflate and limit the motion of an occupant during a crash. Air bags and inflatable belt systems are two types of inflatable restraints. Air bags systems have become commonplace in automobiles and have been effective in saving thousands of lives. Air bag technology has advanced significantly in recent years, allowing air bags to become a reliable safety device. An inflatable belt system is a device that is stowed in the seat belt itself and inflates during a crash. The inflatable belt distributes the loads to a larger area of the occupant's torso, and limits occupant movement in a manner similar to an air bag. The inflatable belt is an enhancement of a standard belt restraint system and is only effective when worn by the occupant. Inflatable crash safety systems are being developed and introduced into commercial and military aircraft, and will likely be integrated into GA aircraft in the near future.

The concept of inflatable restraints in aircraft was conceived decades ago, but it has taken years to develop workable systems. Now that viable systems are available, the aircraft designer must give special consideration to when, where, and how these devices are used. An efficient standard belt restraint is the least costly approach to minimizing occupant injury and should be considered first. Any interior strike hazards should be removed, relocated, or padded to minimize the risk of occupant injury. However, in situations where the use of standard belt restraints, combined with moving or installing padding on strike hazards, will not provide enough protection, then inflatable restraints may be the most practical means of providing occupant protection. Once a crash is detected, the inflatable restraint deploys to prevent the occupant from striking interior components or structure of the aircraft and from receiving injuries ranging from minor to fatal. An inflatable restraint can provide greater protection than practical padding schemes. However, adding inflatable restraints to aircraft can increase the cost, weight, and complexity of the aircraft.

8.3.1 System Components

A typical inflatable restraint system consists of a crash sensor, an air bag module(s) or inflatable belt(s), a diagnostics module, and a system control unit along with wiring, a power supply, and any required mounting hardware. Often, the crash sensor, diagnostics module, and system control unit are combined into one unit. Figure 8-21 shows an example of an air

THIS DOCUMENT PROVIDED BY THE ABBOTT AEROSPACE
TECHNICAL LIBRARY
ABBOTTAEROSPACE.COM

bag restraint system for a small commuter aircraft. It is important to consider the range of the occupants' weight, stature, and injury tolerance when designing the inflatable restraint system so that protection can be provided for all the intended users.

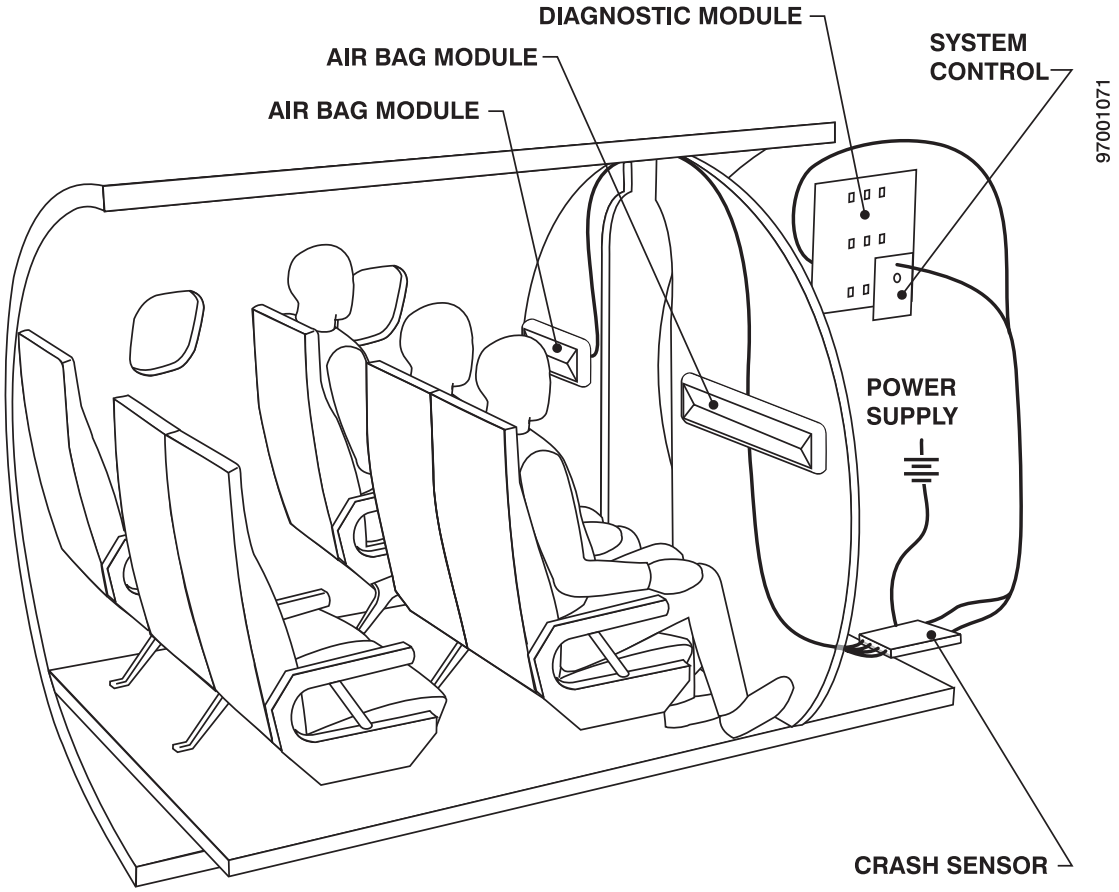


Figure 8-21.
Commuter aircraft air bag restraint system.

This section provides general information on inflatable restraint systems and is for use by light aircraft designers as an aid to select or specify inflatable restraints. This also provides general information on the aircraft interface requirements (structural, positioning, electrical, etc.) for installing inflatable restraint system components. Much of the information contained in this section originally came from Reference 8-38.

8.3.1.1 Crash Sensor

All active crash safety systems, such as inflatable restraints, need some means to determine that a crash is occurring. Crash sensors developed for automobiles are accurate and reliable because the designers fully understand the normal operating and crash environments for that particular class of vehicles. However, the operating environment of an airplane is much different from that of a car. The operating environment of an aircraft imposes unique design requirements for the crash sensor. For aircraft crash sensors to work reliably and effectively,

This Document Provided by the Abbott Aerospace
TECHNICAL LIBRARY
ABBOTTAEROSPACE.COM

their designers must consider complex three-dimensional crash kinematics, powerplant and propeller vibrations, motion caused by maneuver and gust loads, temperature extremes, and electromagnetic fields. Both hardware and crash discrimination software must work effectively throughout the entire range of conditions. Characterization and understanding of these environments, and the requirements they impose, is critical to fielding a successful design.

8.3.1.1.1 Sensing Elements

Several types of sensing elements are used to detect crash events (Reference 8-39).

All-Mechanical An all-mechanical crash sensor is directly attached to the inflator and generally initiate inflation through a mechanical linkage and firing pin. As such, all-mechanical systems require no electrical power. The actual sensing element can be a mass whose motion is affected by the crash acceleration, or a mechanical link that detects some sort of structural deformation of the vehicle. All-mechanical systems have been used in the past to fire automotive side-impact airbags (early Volvo seat-mounted side airbags, for example). Another all-mechanical system was developed by Breed Technologies for retrofit installations in older cars (Reference 8-40). No all-mechanical systems have been proposed for aircraft, due to concerns over their reliability and because they may be difficult to tune for the crash response of a particular airframe. Multi-axis sensing, if desired, could also be a problem. However, the absence of electrical power requirements could possibly simplify some aspects of installation and certification.

Electromechanical An electromechanical sensor typically uses a mass and some sort of mechanical resistance to establish the acceleration and velocity change required to close a switch. A spring, magnet, friction, or viscous fluid can provide the mechanical resistance. Like the all-mechanical sensor, electromechanical sensors can be difficult to tune for the crash response of a particular vehicle. Electromechanical sensors are commonly used in automotive multi-point systems where several sensor-switches are distributed in key vehicle locations to detect the crash. The sensor-switches in a multi-point system can be oriented to provide multi-axis sensing, if desired. Multi-point systems can also be configured so that more than one sensor-switch must be closed before the airbag fires (Reference 8-40). Electromechanical crash sensors require electrical power that can be designed to be drawn from aircraft power or from a self-contained battery.

Accelerometers The third, and quickly becoming the most common, sensing element is the accelerometer. Accelerometer-based systems require some sort of analog or digital processing of the acceleration signal to determine the appropriate time to fire the airbags. Microprocessor systems have an advantage in that a software-based crash discrimination program determines when the airbags fire, rather than the physical properties of the sensing element. This feature allows much easier tuning of the system for a particular vehicle and allows the same model of crash sensor to be used on multiple vehicles by customizing the program for each vehicle (Reference 8-40). Microprocessor systems have sometimes incorporated data logging to record the actual crash accelerations for post-accident analysis (References 8-40 and 8-41). Many of the newer automotive accelerometer-based systems use micromachined silicon accelerometers that can be integrated into the same chip as the microprocessor. Accelerometer-based crash sensor systems are often configured in a single-point system where all the sensing occurs in one location in the vehicle. A single-point system may still use more than one accelerometer for redundancy or for multi-axis sensing, but the sensing elements are all located close together inside the sensor. This eliminates some of the additional wiring needed for the distributed multiple sensing elements typically used in multi-point electromechanical systems. Microprocessor systems can also control different combinations of

This Document Provided by the Abbott Aerospace
TECHNICAL LIBRARY
ABBOTTAEROSPACE.COM

airbag deployments (for instance, frontal airbag only, lateral only, or both), each with different triggering thresholds, to give the best combination of occupant protection for a given situation. Like electromechanical crash sensors, accelerometer-based systems also require electrical power - either from the aircraft electrical systems or from a self-contained battery.

8.3.1.1.2 Crash Discrimination

Crash discrimination is one of the main performance considerations for a crash sensor. Software-based crash discrimination algorithms in accelerometer-based systems process sensor output to decide whether a crash is occurring. Mechanical and electromechanical systems must also be designed to discriminate a crash event from normal operation.

The automotive industry has evolved the design of crash sensing systems so it is almost routine for cars. The process consists of selecting sensors and their mounting locations, then conducting road tests and crash tests with those locations instrumented. The road tests provide data to ensure that the sensors and algorithms will not cause air bag deployment during normal use. The crash tests ensure that the algorithm will deploy the air bags for serious impacts in time to protect the vehicle occupants, and that the air bags will not deploy in minor, low-speed crashes where they are not needed. Crash testing may include low- and high-speed barrier crashes, offset and angled crashes, lateral crashes, and pole and curb impacts. Tests may be repeated, as necessary, to gather a statistically significant sample.

Given this wealth of data, automotive industry researchers have been able to investigate many sophisticated algorithms. While the algorithm details are often proprietary, the basic approaches include neural networks, frequency domain analysis, and different combinations of acceleration-derived quantities, such as position, velocity, acceleration squared, jerk (acceleration rate), energy (velocity squared), power (energy rate), and power rate. Based on the excellent injury-reduction performance and safety record of automotive air bag systems, it can be inferred that many different discrimination schemes have been successfully implemented.

Developing successful discrimination algorithms for aircraft is more difficult. A flying vehicle can sustain significant crash forces in all directions, whereas a ground vehicle's operation is primarily restricted to two dimensions (forward and lateral). A flying vehicle can crash on loose or hard soil, through vegetation, or in water, each of which has a very different dynamic response. The need to define a larger range of crash conditions requires more testing than automobiles. But crash testing of aircraft is expensive and, consequently, only a handful of full-scale crash tests are conducted each year. Qualitative data is available from accident records, but post-crash investigations provide only crude estimates of the peak accelerations and total velocity change - far short of the detail needed.

The limited amount of airplane crash data virtually prohibits the use of complicated algorithms that must be trained, tuned, or calibrated with real data. For example, a frequency-based algorithm would require data defining the frequency content of most types of crashes. Otherwise, the algorithm may fail to recognize a crash or activate the restraints too late to protect the occupants. Algorithm optimization would also need to be started anew for each different airframe, because each one will have a different frequency response.

Given the lack of crash data, effective aircraft crash discrimination must be based on the fundamental physics of vehicle kinematics. For example, it is known, without having any data, that non-crash events like in-flight maneuvers have relatively low accelerations with high velocity changes, and that shocks, such as landing, have higher accelerations with relatively low velocity changes. Only crashes cause both high accelerations and high velocity changes.

This Document Provided by the Abbott Aerospace
Technical Library
abbottaerospace.com

It is also known that a more severe crash will have a higher velocity change, and thus a velocity-change-threshold-based algorithm can be made to fire sooner in a more severe crash - a desired trend. Such a physically based algorithm will always behave in a predictable manner, and can be extrapolated with confidence beyond the range of conditions tested. Predictable extrapolation allows the use of simple safety factors when setting deployment thresholds based on non-crash sensor data. This kind of physical intuition is absent with regard to quantities like frequency response.

The other aspect of algorithm development, tailoring an algorithm to not deploy during normal vehicle use, is no more difficult on airplanes than for ground vehicles. It simply requires that flight and ground tests be conducted to gather sensor data in all possible aircraft operating modes. These might include taxiing, take-off, landing, extreme flight maneuvers, turbulence, and hard landings where air bag deployment is not needed.

8.3.1.1.3 Location and Mounting

The location of sensing elements is also an important design decision. Generally, crash sensors should be mounted on relatively rigid aircraft structure to ensure accurate transmission of crash accelerations through the structure with no dynamic amplification or damping effects. The sensor should be placed in an area that will offer it protection during normal operations and crash conditions. Protection of the inflatable restraint's power supply and wire harnesses, and, in the case of multi-point systems, the sensor wire harness from normal wear and tear and from crash-induced deformations should also be considered when determining the sensor location. Areas that experience high vibration levels, areas exposed to high-intensity radio frequencies, and other areas of potential interference should be avoided when selecting a mounting location. The crash sensor should be located in an area so that the sensor and/or sensing elements experience a discriminating crash acceleration before the acceleration results in the relative motion of the occupants. One crash sensor location which has proven effective in small airplane crash tests is on the floor between the pilot and co-pilot's footwell near the firewall (see Figure 8-22 and Reference 8-42).

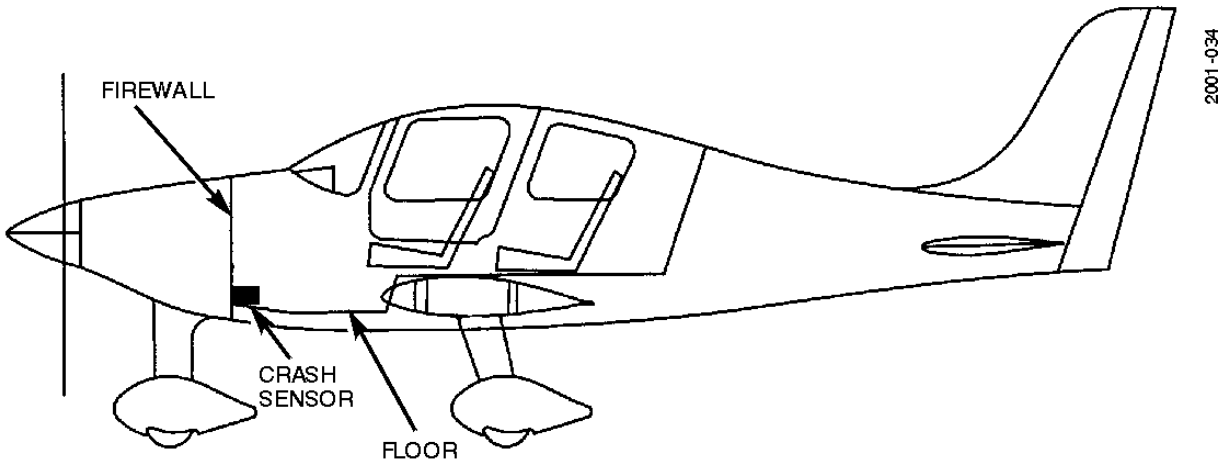


Figure 8-22.
Air bag sensor location.

This Document Provided by the Abbott Aerospace
TECHNICAL LIBRARY
ABBOTTAEROSPACE.COM

8.3.1.1.4 Power Supply

The inflatable restraint system should be designed to be compatible with an available vehicle power supply, or it should have a self-contained power source. Terminals and/or wire routing may be required at the location of the crash sensor to provide a source of power. Batteries can be used to meet the system's power requirement. However, batteries can cause maintenance headaches, and no existing battery can meet the reliability needed under extreme temperatures. The temperature-versus-power sensitivity of electrochemical batteries can be mitigated somewhat by locating them inside the climate-controlled spaces of the occupant compartment.

8.3.1.1.5 Wiring

The inflatable system's wiring shall meet the same minimum requirements as all of the other electrical devices in the vehicle. Shielding, wire gage, and connectors shall be selected to match the electrical requirements of the inflatable restraint system and to minimize the probability of an inadvertent deployment due to interference or wire degradation.

8.3.1.1.6 Backup Power

Sensing systems cannot entirely depend on the aircraft's electrical power system. Initial aircraft damage during a crash can occur several seconds before the primary impact, potentially cutting power to the crash sensing system. Some emergencies can even be caused by or result in a loss of aircraft power. In addition, some emergency procedures, like the response to an electrical fire, require pilots to shut down power. Sensing units must therefore store energy internally to provide their own backup power for a significant amount of time and to activate air bag deployment. The amount of time the sensor system is required to operate on backup power must be determined for each aircraft and must consider the aircraft's mission, the aircraft's performance, and the most common accident scenarios. For example, the backup time required for a loss of propulsion during take-off (potential for low-altitude stall-spin) is much different than that required for the loss of propulsion during while cruising at altitude.

Batteries can be used to meet this backup power requirement. However, batteries can cause maintenance headaches, and no existing battery can meet the reliability needed under extreme temperatures. The temperature-versus-power sensitivity of electrochemical batteries can be mitigated somewhat by locating them inside the climate-controlled spaces of the occupant compartment. Backup power has also been effectively supplied by capacitor systems in some aviation crash sensors (Reference 8-41). Whatever method is used for a backup power source must fit within the size and weight constraints of the aircraft.

8.3.1.2 Diagnostics Module

The diagnostics module monitors the status of the inflatable restraint system and is often integrated into the crash sensor. This module includes a visual and/or audible signal that indicates the condition of the power supply, inflatable restraint, and crash sensor. The diagnostics module monitors the bridgewire circuit resistance or continuity of the gas generator initiator for each air bag module. In the case of a hybrid or compressed gas generator, the generator’s pressure, weight, or some other indicator would also be monitored to detect leaks, in addition to monitoring the bridgewire resistance. The module also checks the condition of the aircraft power supplied to the system, and searches for faults in the crash sensor circuitry. Short or open circuits in the wiring, pressure leaks, poor power supply conditions, and crash sensor faults would be detected by the diagnostics module and displayed in some fashion. This display could be as simple as LED’s on the crash sensor diagnostics module itself or on the

THIS DOCUMENT PROVIDED BY THE ABBOTT AEROSPACE
TECHNICAL LIBRARY
ABBOTTAEROSPACE.COM

instrument panel, or the faults could be integrated into the aircraft's annunciator system (Master Caution/Master Warning) or electronic flight instrument system (EFIS), if available. The display should also indicate when the system is functioning properly.

Activation of the diagnostic system is most often done once before the flight rather than continuously. This activation could be done manually (press-to-test) during pre-flight, or could be done automatically by the system after the aircraft is powered up. System readiness or faults should be clearly displayed at that time. If activated manually, the faults display and test switch should be located in an accessible area, along with other aircraft systems that are monitored.

8.3.1.3 System Control

The system control enables or disables the inflatable restraint system. Although the inflatable restraint could be enabled for the entire flight from aircraft power-up to shut-down, there are times when the system is not needed and could be disabled, if desired. For example, the system could be disabled during cruise flight or other phases of flight which historically show low accident probability. The system could be enabled and disabled manually, or it could occur automatically as a result of other flight operations. The main reason for disabling the system during certain phases of flight is to reduce the likelihood of inadvertent deployments. However, the experience of automotive air bag industry has demonstrated a very low probability (0.999999 at a 95-pct confidence level) of inadvertent deployments; this low probability level should be achievable for aircraft as well. The disadvantage of disabling the inflatable restraint system is the possibility that the system would not be active for occupant protection.

A manual system control must be provided to disable the system during maintenance procedures. The system could be disabled for maintenance by a dedicated switch or by pulling the system circuit breaker. The maintenance manual for the aircraft must also include warnings to disable the inflatable restraint system for any procedure in which inadvertent deployment would be hazardous to the aircraft mechanic. Shunting the bridgewire circuit of the gas generator may also be necessary during certain maintenance procedures such as installation and removal of the inflatable restraint system.

8.3.1.4 Air Bags

The air bags are the inflatable portion of the system that are stored out of the way until needed. The air bags inflate in less than a tenth of a second and cushion the occupant from potentially lethal strikes with objects inside the aircraft. The reason for using air bags is to provide additional protection to a belted occupant. Air bags supplement the seat belt restraint system by carrying some of the occupant load during a crash. Airbags help reduce belt loads, chest deflection, and upper torso and head movement compared to the seat belt restraint by itself. Properly designed air bags dissipate the kinetic energy of the occupant in a controlled manner to minimize occupant deceleration and injury.

8.3.1.4.1 Air Bag Module Construction

The air bag module typically consists of a cover, an air bag, a retainer, a mounting plate, and a gas generator, as shown in Figure 8-23. In some designs, a gas generator housing is used in addition to the other components. The air bag module is most often integrated directly into the aircraft interior in order for it to be as tamper-resistant and as unobtrusive as possible. The air bag module should meet all flame-resistance and other environmental specifications.

THIS DOCUMENT PROVIDED BY THE ABBOTT AEROSPACE
TECHNICAL LIBRARY
ABBOTTAEROSPACE.COM

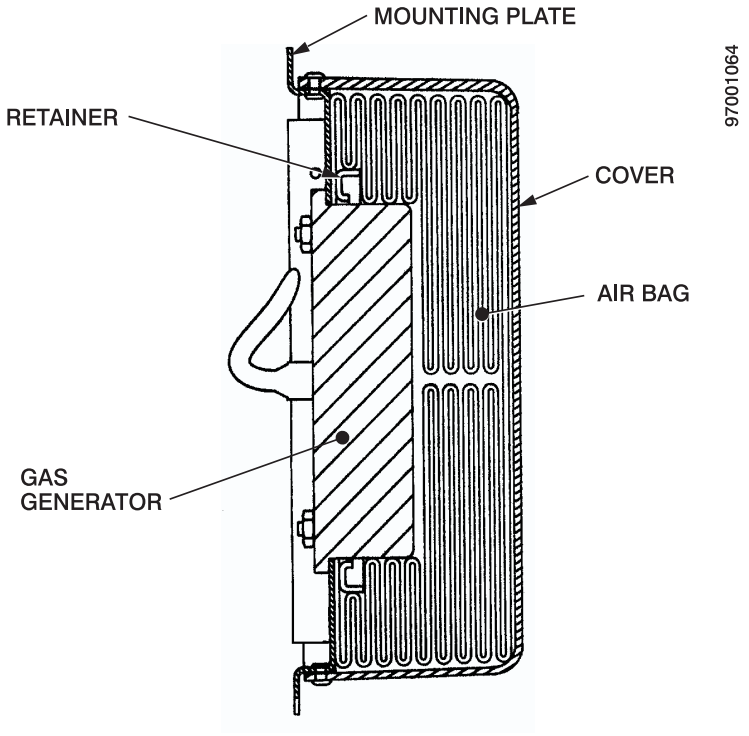


Figure 8-23.
Air bag module cross-section.

In order for the air bag module to be effective, the occupant loads must be transferred to the air bag and the loads are then transferred to the aircraft structure, as shown in Figure 8-24. In other words, the bag requires a reaction surface in order to transfer the occupant loads to the airframe. The air bag module's location and corresponding reaction surfaces are important to the success of the air bag system for providing occupant protection.

The air bag module should be positioned so that the air bag can deploy into the space between the occupant and the strike hazard. Egress and other operations should not be hindered due to the air bag's deployment, its opened cover, or the deflated air bag. The module should be located so that the likelihood of cover damage and tampering is minimized. Access should be available so that the module can be removed and replaced if necessary. The module should be firmly mounted to an aircraft structure that can support the deployment loads and occupant loads. These loads need to be quantified by analysis and/or testing in order to provide sufficient structure to support the inflatable restraint system. Objects, instruments, and structure with sharp edges should be relocated or redesigned to minimize air bag damage and the potential for occupant injury.

THIS DOCUMENT PROVIDED BY THE ABBOTT AEROSPACE
TECHNICAL LIBRARY
ABBOTTAEROSPACE.COM

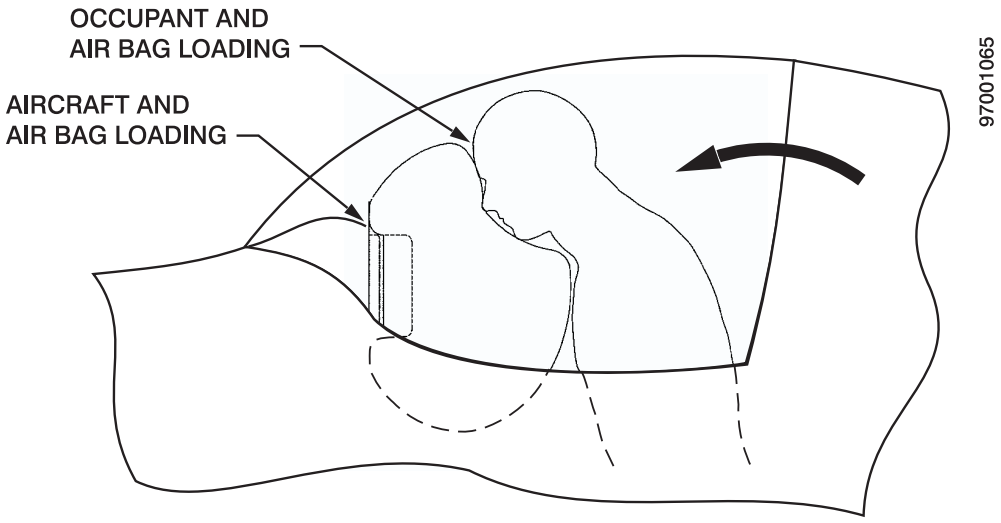


Figure 8-24.
Occupant, air bag, and aircraft loading.

8.3.1.4.2 Air Bag Module Cover

The air bag module's cover serves several functions. It is a decorative cover that protects the air bag from day-to-day abuse. The cover holds the air bag in its folded position until it is deployed. During the deployment phase, the cover should hinge open and remain attached to the module. The cover's opening characteristics should have little variation over a wide operating range of temperatures in order to ensure proper air bag performance.

Cover Materials The cover material should be lightweight, durable, flexible, and retain its shape at extreme temperatures. The material cannot become brittle at cold temperatures, because deployment could cause the cover to fragment. On the other hand, the cover cannot become so flexible at elevated temperatures that the fasteners pull through the cover material upon deployment. The cover material should be selected based on the temperature range requirements, the system's specified life, the material's stability, and other performance requirements such as those listed in FAR 23.853 (Flammability). Typical cover materials are thermoplastic elastomers and thermoplastic olefins. Covers can also be made from a combination of materials, such as an external layer of vinyl over a thermoplastic olefin.

Cover Module Tear Seam Typical cover designs incorporate an area of the cover that is designed to separate and allow the air bag to deploy. This area is known as a tear seam. Tear seams can be located across the center, at the bottom, or at the top of the cover. Tear seams are usually constructed by thinning or slotting the cover material along a specific cover profile, as shown in Figure 8-25. This thin region or remaining web of material in the cover requires less force to tear than the surrounding material, ensuring consistent cover opening. Tear seam thickness should be minimized, thereby requiring only a small amount of the gas generator's energy to open the cover, but should be strong enough to provide protection for the air bag. The tear seam's strength should vary as little as possible across the operating temperature range.

THIS DOCUMENT PROVIDED BY THE ABBOTT AEROSPACE
TECHNICAL LIBRARY
ABBOTTAEROSPACE.COM

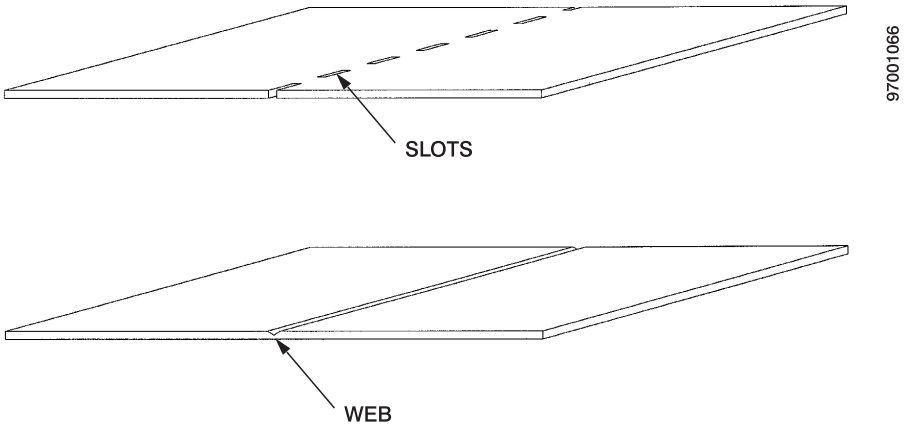


Figure 8-25.
Tear seam construction.

Cover Attachment Reinforcements During deployment, the cover tears along the seams and opens to allow the air bag to inflate. Typically, the cover will hinge open from at least one attachment area. The cover opening forces are high during the deployment. Often, the cover needs to be reinforced so that it will remain attached to the mounting plate during deployment. The cover can be reinforced at the attachments in many ways. This can be accomplished by increasing the thickness of the cover at the attachments or by designing a lip of material in the cover to transfer the loads to the mounting plate, as shown in Figure 8-26. From a hardware standpoint, the number of fasteners can be increased, the rivet strength and rivet head size can be increased, or a rivet strip can be used to distribute the loads and prevent the fasteners from pulling though the cover. A rivet strip is a piece of metal with a series of holes to which the rivets are attached, effectively increasing the rivet head area, as shown in Figure 8-27.

8.3.1.4.3 Air Bag Module Mounting Plate

The air bag module mounting plate is typically a stamped piece of metal to which the air bag components attach. The mounting plate must be rigid enough to minimize gas leakage around the gas generator and air bag mounting area. The mounting plate also provides protection to the air bag during shipping and handling (especially prior to module installation). The loads due to air bag deployment and occupant loading are transferred through the mounting plate to the aircraft structure. Inflatable restraint loads can exceed 1,000 lb in some cases. These loads can be caused by the dynamic effects of the cover's opening, the air bag's filling, and the occupant's loading the air bag. Specific module deployment loads should be determined by analysis and/or testing to determine the design strength of the mounting plate, and to design the mounting attachment on the aircraft structure.

THIS DOCUMENT PROVIDED BY THE ABBOTT AEROSPACE
TECHNICAL LIBRARY
ABBOTTAEROSPACE.COM

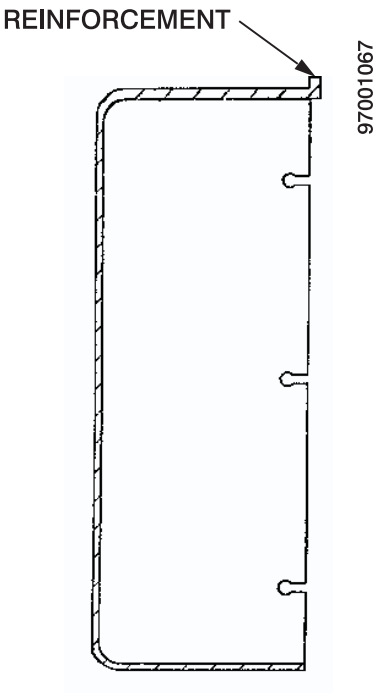


Figure 8-26.
Module cover reinforcement cross section.

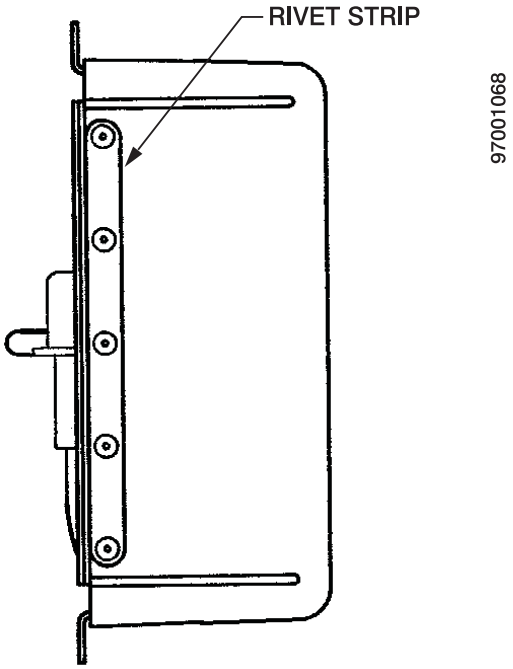


Figure 8-27.
Module cover rivet strip assembly.

THIS DOCUMENT PROVIDED BY THE ABBOTT AEROSPACE
TECHNICAL LIBRARY
ABBOTTAEROSPACE.COM

8.3.1.4.4 Air Bag

The air bag itself is typically constructed from multiple flat fabric panels that are sewn together to create the desired air bag shape. The air bag is then folded and stowed under the cover of the air bag module until it is deployed. The air bag is attached to the mounting plate with a retainer and common fasteners such as rivets or bolts, as shown in Figure 8-28.

The air bag is designed to deploy during a crash and decelerate an occupant at a rate that will not cause injury. The air bag is also designed to prevent the occupant from striking hazardous objects in the interior of the aircraft during a crash. The air bag design process is one of iteration, compromise, and optimization. For instance, if the air bag pressure is too high, the occupant could decelerate too rapidly, causing occupant injury. Excessive occupant rebound could also occur due to a high-pressure air bag. On the other hand, if the air bag pressure is too low, the occupant could "bottom out" on the strike hazard, causing occupant injury. If the air bag is too large, excessive interaction between the air bag and the occupant could occur during deployment, causing occupant injury. If the air bag is too small, the occupant deceleration could be too great or the occupant could again "bottom out" on the strike hazard. Many factors must be considered when designing an air bag in order to obtain a robust inflatable restraint system.

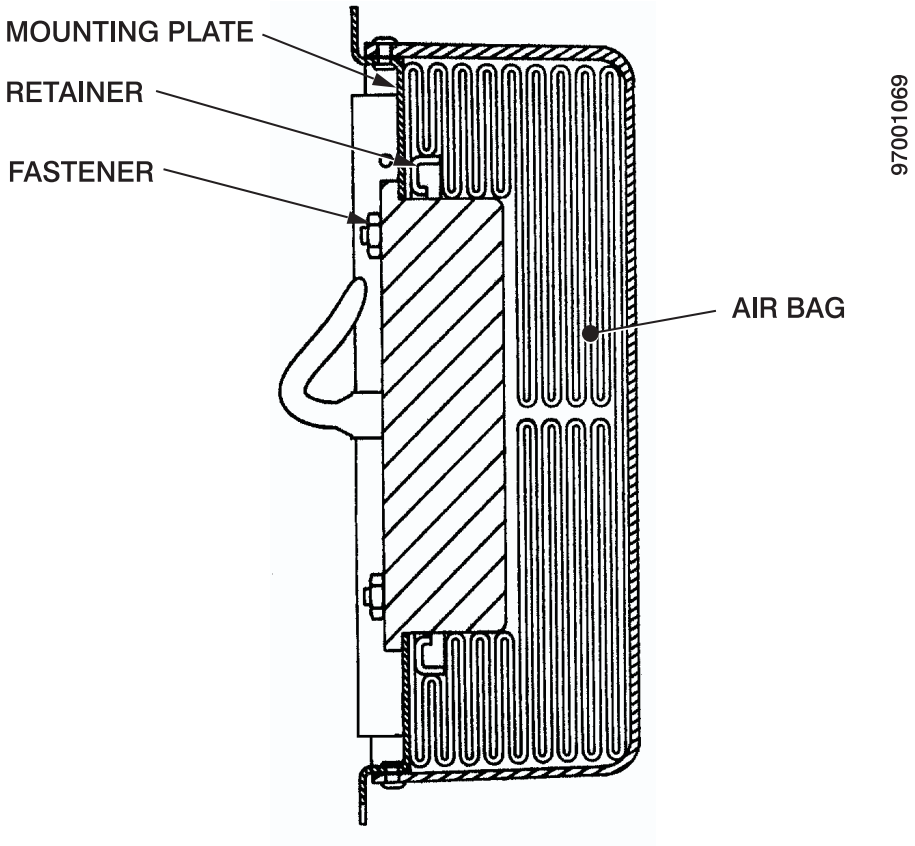


Figure 8-28.
Air bag module attachment.

THIS DOCUMENT PROVIDED BY THE ABBOTT AEROSPACE
TECHNICAL LIBRARY
ABBOTTAEROSPACE.COM

Air Bag Materials Current automotive air bags are usually made from woven nylon fabric. Other fabric materials to be considered are polyester fabrics and films such as Mylar. Knowing the expected life of the system, the strength requirements, and the environment to which it will be exposed will enable the designer to select the proper material. There are many fabrics to choose from, depending on the particular application. A typical air bag fabric would be a high-tenacity nylon 6-6 with 640-denier yarns. This fabric, in an uncoated state, would exhibit a gas permeability of greater than 6 CFM/ft^2. It is common to have the fabric coated in order to reduce its permeability to less than 1 CFM/ft^2 and to protect the fabric from the hot gases from the gas generator, if necessary. (See Section 8.3.1.4.4.6 on air bag vents to help in the selection of air bag materials). Some of the coatings typically used are silicone, urethane, and neoprene. Each coating has specific properties that make its selection appropriate to the application. Silicone coating thickness typically is between 0.5 and 1.0 oz per yd, for example. The flammability of these fabrics must also be considered. The materials need to meet FAR 23.853. Selection of the proper coating, thickness, and fire retardant will ensure that the flammability requirements are met.

An important part in the selection of air bag fabrics is the material's suppleness. Since the material is folded, the suppleness of the fabric will affect the packed volume of the air bag and, consequently, the size of the air bag module.

Air Bag Seams/Stitches The air bag is typically made from two or more panels of fabric that are cut to shape and sewn together. There are many types of stitches to choose from to create the seams. Common stitches include, but are not limited to, the LSq (FED-STD-751A), SSa (FED-STD-751A), LSa, double-lap-joint, LSc, and SSw, as shown in Figures 8-29 through 8-34. Each stitch has its advantages and should be matched to the particular application. Table 8-3 compares the six stitches listed above for each of the three threads mentioned in the following section. In the case of a sealed air bag, which requires a coated fabric, the seams are sealed by the application of film or seam tape over the stitched seam. These films or tapes may be chemically bonded or heat sealed to the fabric coating to create an airtight seam. Seams can be chemically bonded or heat sealed with or without stitching. If chemical bonding or heat sealing is desired, it is imperative that the adhesion between the base fabric and coating be adequate.

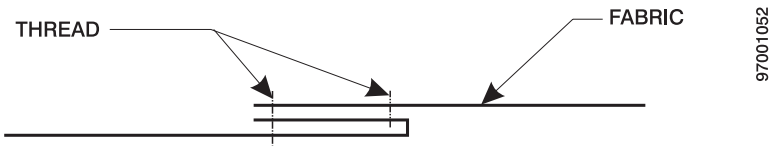


Figure 8-29.
The LSq (FED-STD-751A) stitch.

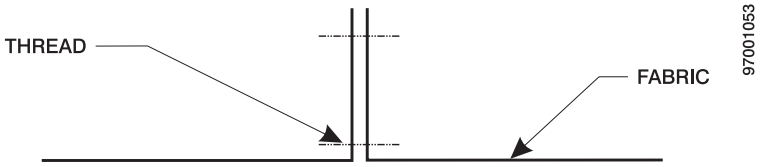


Figure 8-30.
The SSa (FED-STD-751A) stitch.

THIS DOCUMENT PROVIDED BY THE ABBOTT AEROSPACE
TECHNICAL LIBRARY
ABBOTTAEROSPACE.COM

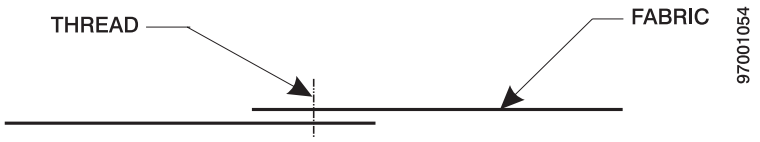


Figure 8-31.
The LSa single-lap-joint stitch.

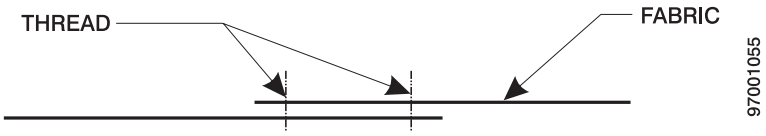


Figure 8-32.
The double-lap-joint stitch.

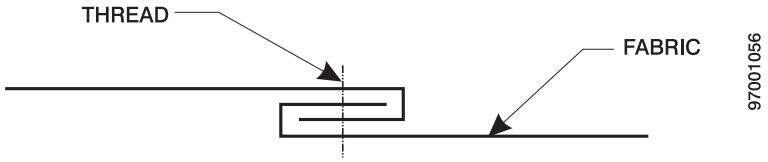


Figure 8-33.
The LSc single-interlock-joint stitch.

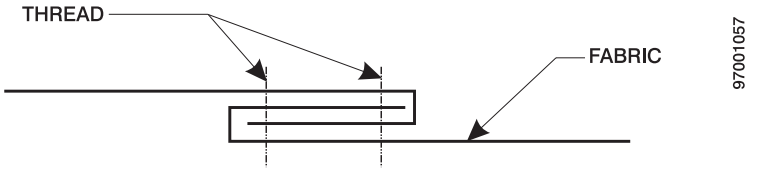


Figure 8-34.
The SSw double-interlock-joint stitch.

Table 8-3.
Seam construction comparison

Seam Type	Thread Type*		
	Nylon	Nomex	Kevlar
LSq	81	57	90
SSa	43	40	73
LSa	40	40	40
Double Lap	33	40	67
LSc	30	27	20
SSw	73	70	63

*The numerical ranking is based on a 0-100 scale, with 100 as the best choice

This Document Provided by the Abbott Aerospace
TECHNICAL LIBRARY
ABBOTTAEROSPACE.COM

Air Bag Threads Nylon is a thread that is commonly used in air bag fabrication. This thread is a multi-core spun filament that is twisted and bonded. Nylon thread has good elongation and tensile strength.

Nomex® thread is a twisted and bonded spun-filament single-core material. This thread has above-average tensile strength, excellent heat resistance (700 °F), and is resistant to chemical fluids.

Kevlar® thread is a twisted and bonded single-core spun-filament material with outstanding heat resistance (900 °F). This thread has excellent tensile strength and is resistant to shrinkage in hot air and water. The Kevlar thread is typically stronger in tension than the air bag fabric.

All three of these threads were tested with different seam construction methods as described above. The results can be found in Table 8-3. Other threads are available, such as polyester, but these are not commonly used in air bag construction. Therefore, they are not included in this design guide.

Air Bag Doublers and Heat Shields Doublers (reinforcement patches) are commonly used in air bag construction as reinforcements for high-stress areas. The mouth of the air bag, the tether attachments, and the vent holes are typically strengthened with doublers. The doublers are generally made from the same material as the air bag, usually the remnants of material once the air bag shape is cut from the fabric. In some cases, a different air bag material is used if additional strength or coating thickness is required. The doubler can also act as a heat shield. Heat shields are usually additional layers of material added to the air bag in areas where the hot gases from the gas generator would impinge directly on the air bag. The heat shield material is selected based on the severity of the gases. The effectiveness of the heat shield is dependent on its coating type and thickness. Neoprene, silicone, and urethane coatings are commonly used as coatings for heat shields. In some cases, additional protection is achieved by coating the fabric on both sides. However, it should be noted that doublers, heat shields, coating types, and coating thicknesses all affect the size and weight of the air bag module.

Air Bag Tethers Internal tethers are used in some air bag designs to restrain the motion and shape of the air bag. For example, if a round air bag protrudes too far into the occupant area, tethers can be used on the inside of the air bag between the panels to limit air bag protrusion. The resulting air bag shape will be oval in cross-section. However, tethers add complexity, cost, higher inertia mass, and local regions of higher stress. Despite these factors, in many cases, the benefits of the tethers justify their use.

Air Bag Vents Venting the air bag is desirable in many cases as a means of reducing occupant rebound. As the occupant loads or compresses the air bag, the gases in the air bag are allowed to escape through the vent holes, and this dissipates energy. The vents act as dampers by controlling the rate of gas flow from the air bag. Vents are placed in regions of the air bag that will minimize the risk of occupant injury from the expelled hot gases. Typically, vents are placed on the rear panel of the air bag facing away from the occupant.

Some vented air bags are constructed from uncoated porous fabrics. The fabric permeability is typically controlled, since the entire permeable fabric acts as the vent. Gas also vents through needle perforations from the sewing process. These perforations must be considered when

---

®Nomex is a registered trademark of E. I. Du Pont de Nemours & Co., Inc.
®Kevlar is a registered trademark of E. I. Du Pont de Nemours & Co., Inc.

This Document Provided by the Abbott Aerospace
TECHNICAL LIBRARY
ABBOTTAEROSPACE.COM

determining the amount of venting required. Since the cost for uncoated fabric is less than coated fabric, and since vent holes, vent hole doublers, and the attachment of the vent hole doublers are eliminated, there can be a significant cost benefit to using uncoated air bags, provided that the performance objectives are met.

A hybrid air bag is made from a combination of uncoated porous fabric and coated fabric. The rear panel is made from the porous fabric that allows the gases to escape at a controlled rate. The coated fabric, which is used for the front panel, prevents hot gases from contacting the occupant.

A non-vented or sealed air bag is desirable if occupant rebound is minimal and there is an emphasis on providing secondary impact protection. Sealed air bags are generally desired for aircraft systems because of the relatively long duration (on the order of several seconds) of aviation accidents. For comparison, the duration for automobile accidents is on the order of 100 msec. One scenario where extending the air bag inflation time is highly desirable would be when an aircraft strikes the ground, slides, and then impacts a berm or an object on the ground. The air bag would deploy due to the first impact if the sensor threshold was exceeded. The air bag would provide occupant protection for the first impact and remain inflated, providing a level of occupant protection for the second impact. Occupant egress would not necessarily be impeded, because the air bag can be designed to deflate in a few seconds by selecting the temperature and amount of inflation gases. The deflated air bag could then be moved out of the way during egress.

Air Bag Fabric Anti-Blocking Agents Coated fabrics are sometimes treated with an anti-blocking agent so that the layers do not stick (block) to each other when in intimate contact. There are several types of anti-blocking agents commercially available that include, but are not limited to, zinc stearate, magnesium silicate (talc), and cornstarch. The release agent is applied to the coated side of the air bag prior to folding to prevent the air bag from blocking. There are several degrees of blocking, and a rating system has been developed to identify them. Blocking tests would be conducted as follows: A specimen is conditioned coated-side to coated-side at 5 lb/in.^{2} minimum for at least 7 days at 100 ^{o}C. A 50-gram weight is then attached to the tabs of the specimen. The specimens should separate within 30 sec of attaching the weight. Table 8-4 describes the levels of blocking.

Table 8-4.
Blocking levels

Blocking Severity	Description of Blocking Level
I S	Immediate separation of the specimens
1-30	Time, in seconds, it takes for the specimens to separate
D N S	The specimens do not separate

Air Bag Size, Shape, Strength The size and shape of the air bag is a function of numerous parameters and design constraints that are dictated by the specific vehicle application. Once the strike hazards are identified, the air bag's size and shape can be estimated. The air bag should be positioned between the occupant and the strike hazards close enough so that the occupant loads the air bag early in the crash event, thereby minimizing the occupant's velocity relative to the aircraft. The size and shape of the air bag must also be designed to minimize the injury potential of the air bag itself for the anticipated range of occupants. The air bag design

This Document Provided by the Abbott Aerospace
TECHNICAL LIBRARY
ABBOTTAEROSPACE.COM

should prevent any interaction with the primary flight controls in the unlikely event of an inadvertent deployment. The shape of the air bag should be of a smooth contour to minimize stress risers. Air bag volume typically can range from 12 - 25 L for lateral air bags and 40 - 60 L for forward air bags. In general, the size of the air bag can be reduced as the level of occupant restraint by other means is increased.

Air bags are typically designed to fail in the base fabric at pressures that are well above the operating pressure. To achieve a 1.5 margin of safety for air bag strength, the Maximum Expected Operating Pressure (MEOP) must be determined. The MEOP usually occurs at the hottest temperature during occupant loading. Occupant loading and the deployment environment must be considered when determining the MEOP, because air bag pressure increases when the occupant loads the air bag and when the air bag volume is restricted by an object such as a control stick. Once the MEOP is determined, the minimum burst strength required is a minimum of 1.5 times the MEOP. For example, the peak air bag pressure for a hot static deployment is 2 lb/in.^{2}. An additional 8 lb/in.^{2} occurs due to occupant loading. Therefore, the MEOP would be 10 lb/in.^{2}, and the corresponding minimum burst strength requirement would be 1.5 times the MEOP, or 15 lb/in.^{2}. Peak air bag pressures due to cover opening are usually not considered to be the MEOP, because the air bag is usually supported by the cover during these pressure spikes, and this does not result in air bag degradation or rupture.

Air Bag Folding Patterns The air bag is stowed in a folded condition until it is deployed. Air bag module size, shape, and position, along with air bag shape, size, and material thickness are factors in determining the air bag folding patterns. Flight controls, yokes, glareshields, and other equipment may interact with the air bag's deployment. The folding patterns can affect the trajectory of the air bag. Some folding patterns are designed to minimize opening pressures and prevent occupant injuries during inflation. The air bag folding pattern can help the air bag to clear objects, such as flight controls, during deployment. The folding patterns should not cause unnecessary binding of the air bag, because the air bag pressure and the energy required to unfold the air bag could become unnecessarily high. The additional energy required to unfold the air bag could result in under-inflation and a reduction in occupant protection. The increased pressure due to binding can also cause the air bag to rupture, resulting in a loss of occupant protection.

Air Bag Inflation The air bag begins to pressurize in the folded and stowed position at the onset of gas generation. The pressure increases rapidly, because the air bag is constrained by the cover. Once the cover tear seams and inertial forces are overcome, the air bag begins to unfold. The cover opening pressure is usually short in duration (5 msec) and can range from 10 to 40 lb/in.^{2}, depending on the particular air bag module configuration. Module cover and air bag velocities can reach 200 mph, in some cases. Once the air bag begins to unfold, the volume increases and, consequently, the pressure decreases. The magnitude of the decrease in pressure depends on air bag volume, inertia, and gas generator flow rate. Once the air bag is unfolded, the pressure begins to increase. Peak pressure occurs between 35 - 60 msec for a typical front air bag. Side air bags reach peak pressure in 15 - 25 msec. These times and pressures depend on the particular air bag module. After peak pressure is achieved, the air bag pressure decreases due to gas venting and cooling. Figure 8-35 represents a typical air bag pressure-versus-time plot for a front air bag module.

THIS DOCUMENT PROVIDED BY THE ABBOTT AEROSPACE
TECHNICAL LIBRARY
ABBOTTAEROSPACE.COM

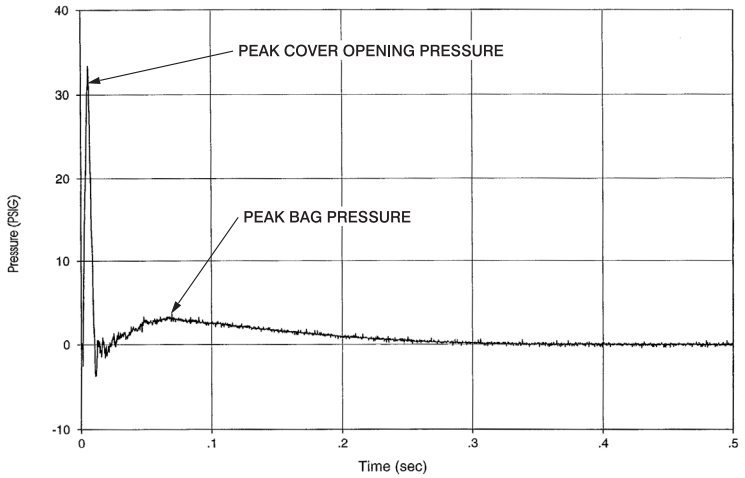


Figure 8-35.
Typical air bag pressure-versus-time plot.

Air Bag Position A large number of aircraft fatalities and serious injuries are due to the occupant's head striking objects in the cabin interior during the crash. Air bags can be used to prevent the head from striking the cabin interior. However, in order for an air bag to be most effective, it is important that occupant and air bag interaction include the torso as well as the head to minimize neck injuries. The air bag should be positioned so that the occupant's head and torso are decelerated with a minimal amount of neck rotation. In addition, air bag mounting and reaction surfaces can control the air bag position. In general, the air bag should be mounted so that the deployment is normal to the reaction surface and occupant loading. Sharp objects and edges should be avoided in order to minimize the potential for air bag damage and occupant injury. The methods for controlling air bag trajectory, described previously, should be followed. Some of these methods include internal tethers, external tethers, limiting the cover's opening to provide a deployable reaction surface, and deploying the air bag against windshields. The air bag mounting surface (the retainer and mounting plate interface) is important for providing air bag stability and positioning, and should be considered when designing the air bag module.

In the unlikely event of an inadvertent deployment, the deploying air bag(s) must be designed to avoid any interaction with flight controls. Deployment forces should be directed away from controls such as yokes or control sticks. For example, a yoke-mounted air bag module would at first appear to be a good location because of the similar air bag position used in automotive steering wheels. But a yoke-mounted air bag would generate significant deployment forces potentially causing loss of control of the aircraft. Air bags that deploy in the direction of control sticks should be designed to avoid stick contact. An air bag can be designed to deploy over a control stick and inflate between the occupant and the control stick. Inadvertent deployment air bag tests have been conducted with pilots flying nap-of-the-earth in an AH-64 flight simulator (Reference 8-43) and during actual flight in a UH-60 (Reference 8-44). In both cases, the air bags were deployed during flight with no loss of control of the aircraft.

Air Bag Deflation After the crash event is over, some air bag designs remain inflated. In the case of a sealed air bag, the air bag can remain at full volume for more than 6 sec. Occupant egress may be a concern if the inflated air bag cannot be pushed out of the way. A deployed

THIS DOCUMENT PROVIDED BY THE ABBOTT AEROSPACE
TECHNICAL LIBRARY
ABBOTTAEROSPACE.COM

air bag could potentially hinder post-crash occupant movement. The benefits of an extended-inflation air bag system have to be weighed against potential egress issues. An air bag that remains inflated for only 6 sec probably will not be of concern, since some time is required for the occupants to react to the crash situation. If needed, a mechanical vent could be physically opened, or timed venting could be incorporated into the design. Understanding and specifying the gas generator requirements will help provide an inflatable restraint system that meets extended inflation times without adversely affecting occupant egress and movement.

8.3.1.4.5 Air Bag Retainer

The air bag retainer is a component that is placed inside the mouth of the air bag that prevents the air bag from detaching from the mounting plate. The air bag is sandwiched between the mounting plate and the retainer. Bolts, studs, pins, or rivets are used to complete the assembly. The retainer can be contoured to improve stiffness. For example, a retainer can be formed into a "C" or "J" shape cross-section from a thin piece of metal, as shown in Figure 8-36. The added lip provides the additional stiffness needed to retain the bag and minimize leakage due to retainer deflection. Loads that are transmitted through the retainer can be around 1,000 lb, depending on the particular air bag configuration, so the number and type of retainer fasteners needs to be selected accordingly.

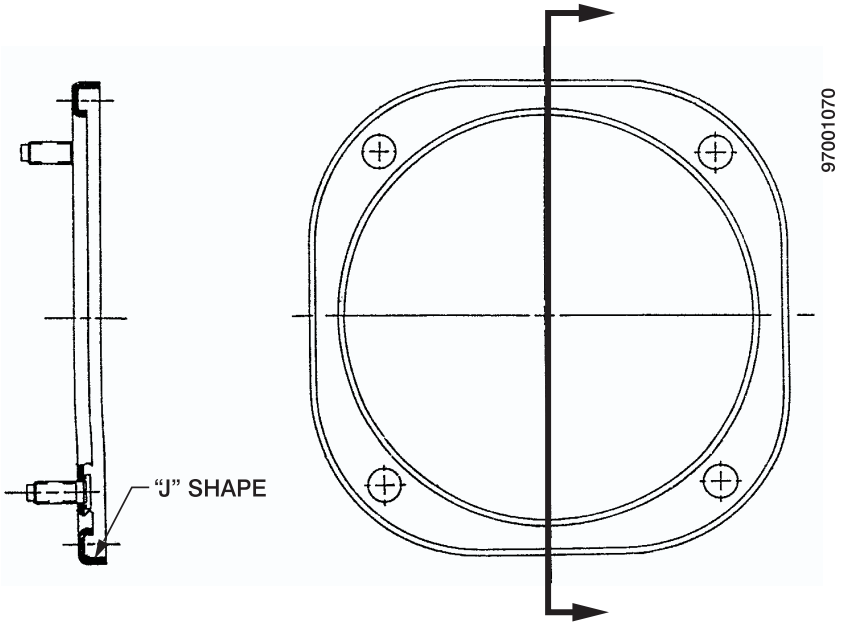


Figure 8-36.
Air bag retainer.

8.3.1.5 Gas Generator

The gas generator or inflator is the component that produces the gas required to fill the inflatable restraint. Once the gas generator receives the electrical signal from the crash sensor, the electrical energy is used to heat a bridgewire and ignite pyrotechnic material, which then releases the gas. Available space, weight, gas output, gas temperature, amount of particles, expected life, reliability, and cost are some of the factors to consider when selecting a type of

This Document Provided by the Abbott Aerospace
TECHNICAL LIBRARY
ABBOTTAEROSPACE.COM

gas generator. It is very important to determine the type of gas required, because there is not just one type of gas generator that is appropriate for all applications. Three common types of gas generators are described in the following paragraphs. Each type has its advantages and disadvantages. They all can provide safe and reliable gas generation. Gas generators must be designed to meet the rigors of the vehicle environment. These tests include, but are not limited to, impact (drop), thermal cycling, heat aging, and bonfire testing. In the event of a cabin fire or a fire during the transport of the inflatable restraint, most gas generators are designed to auto-ignite before their structure is significantly weakened, preventing an additional hazard due to the fragmentation of the case.

8.3.1.5.1 Pyrotechnic Gas Generators

A pyrotechnic gas generator, the smallest and lightest type of gas generator, utilizes stored chemical energy in the form of a propellant that burns and produces hot gases. Solid propellants, pressed into tablets or disks, are widely used in gas generators. However, some liquid propellants are being used with equal success. In either case, the gases produced are the by-products of combustion and typically consist of nitrogen, carbon dioxide, oxygen, carbon monoxide, water vapor, and other compounds in trace amounts. The gas is typically filtered to remove particles and to cool the gases slightly. The propellant is formulated in such a way as to provide the desired gas output. The gas output is very repeatable, with little change occurring across the required temperature range. Several propellant formulations are very stable and have been shown to have a useful life of 15 years and more. These generators produce the hottest gasses, which cool more rapidly.

In general, the propellant combustion should occur entirely within the gas generator. However, some pyrotechnic gas generators produce unburned gases or particles that burn outside of the gas generator. This is called afterburning or flaming. This poses no immediate risk or injury to the occupant, provided that vents are properly located and the inflatable restraint system's integrity is not compromised. The occupant may experience a sensation of heat on exposed areas of the skin due to radiant heat transmitted through the inflatable restraint.

8.3.1.5.2 Compressed Gas Generators

A compressed gas generator, the largest and heaviest type of gas generator, utilizes a sealed pressure vessel filled with inert gasses under pressure. The vessel is opened when an igniter ruptures a burst disk. The pressure is then released in a controlled fashion to provide the desired gas output. The gas output is repeatable, with some change in output occurring across the temperature range. The life of this type of gas generator is dependent on the leak rate of the pressure vessel. This requires that the gas generator must be monitored for leakage, which means there is an additional cost associated with it. However, this type of gas generator requires no filtration, and produces the coolest and largest amount of gas.

8.3.1.5.3 Hybrid Gas Generators

A hybrid gas generator combines a pyrotechnic charge and compressed gas. The pyrotechnic charge can be inside or outside of the compressed gas chamber. In either case, the hybrid system bridges the gap between the pyrotechnic gas generator and the compressed gas generator in many ways. The life of this gas generator is again dependent on the leak rate of the pressure vessel, and so, like the compressed gas generator, the hybrid must be monitored for leakage with some cost associated with it. The gas output is very repeatable, with some change in output occurring across the temperature range. The gas output is not as hot, requires less filtration, and cools less rapidly than the pyrotechnic gas generator.

This Document Provided by the Abbott Aerospace
TECHNICAL LIBRARY
ABBOTTAEROSPACE.COM

8.3.1.5.4 Gas Output

The composition of the gases in current gas generators is typically considered to be non-toxic. The major component of the gas output is generally an inert gas such as Nitrogen or Argon. The greatest concern is the displacement of oxygen within the vehicle upon the release of the inert gases. However, the amount of gas and the duration which an occupant would be exposed to it are very small. The other gases that are produced are generally in small concentrations. Looking at the gas levels and the durations or exposed times show that, according to OSHA limits, the gases are non-toxic. However, there have been reported cases where people with respiratory problems have been affected by the inflation of gases or anti-blocking agents from some air bag deployments.

Gas temperature should be such that the air bag is not damaged due to its inflation by the gases. Also the temperature of the gas that comes into direct contact with the occupant should not cause harm. In order to achieve extended inflation, high-temperature gas should be avoided, since the cooling effects are greater. Increasing the amount of gas would improve extended inflation, however.

8.3.1.5.5 Solids Output

Unconsumed particles of propellant, especially hot particles, can be very damaging to inflatable restraint fabrics. Even though the total mass of the particles is typically small (< 1 gm), they can cause damage because they exit the gas generator at high velocities. Particles should be kept to a minimum when possible. Even particles that do not contain metal can be abrasive to the fabric coating. Airborne solids can also affect occupant breathing and visibility that could affect occupant egress.

8.3.1.5.6 Noise

The noise from an air bag deployment is typically in the range of 120 to 140 dB (above the established pain threshold). However, the duration at these levels is quite short. Often times, the noise level of the crash itself exceeds the noise level produced by the air bag.

8.3.1.5.7 Surface Temperature

The surface temperatures of some pyrotechnic gas generators can reach levels high enough to melt or ignite the materials with which they are in contact. Typically, it takes several seconds after deployment to reach the maximum surface temperature. If this type of gas generator is used, insulation or an air gap between the gas generator and aircraft components can prevent the melting or ignition of materials.

8.3.1.5.8 Gas Generator Housing

Some gas generator designs require the use of a housing as a means of directing gases and retaining the gas generator. A housing is typically used when the gas generator output is radial and the generator axis is oriented parallel to the reaction surface, as shown in Figure 8-37. Flow restrictions, preferential flow, and energy losses should be taken into consideration when a housing is used.

THIS DOCUMENT PROVIDED BY THE ABBOTT AEROSPACE
TECHNICAL LIBRARY
ABBOTTAEROSPACE.COM

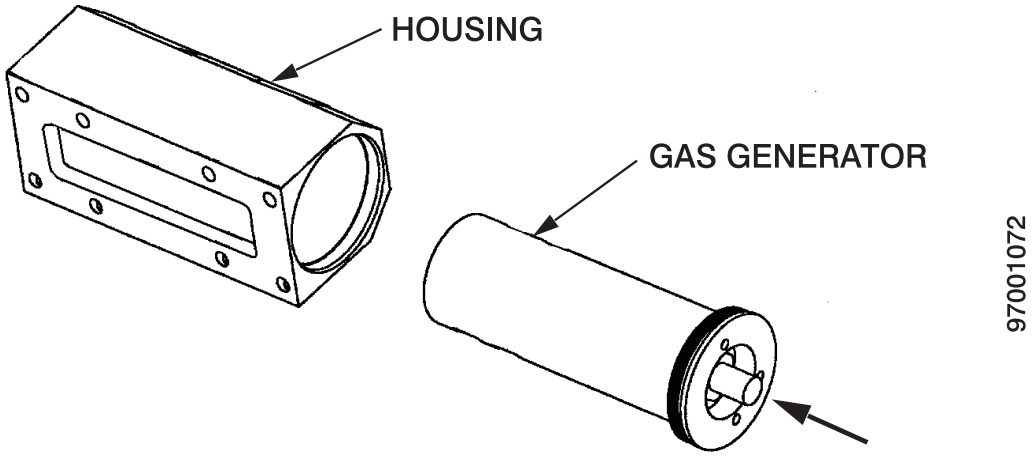


Figure 8-37.
Gas generator housing.

8.3.2 Multiple Air Bag Systems

The air bag module should be placed near the strike hazard so that the inflated air bag can prevent the occupant from reaching the hazard. Since aircraft can impact objects at any attitude, the hazards can be all around the occupant. Knowledge of the primary hazards will aid in determining the placement and the number of air bag modules to be used.

Multiple air bag systems can provide occupant protection for a variety of crash scenarios. A three-airbag system, for example, that has one frontal air bag and two side airbags can provide protection to the occupant by surrounding the occupant and reducing the occupant's motion and velocity within the cabin. Air bag size and over-pressurization of the cabin must be considered, especially with multiple air bag systems. The amount of gases and the effluent levels produced by the inflatable restraint system must not cause harm to the occupants.

The cost, space requirements, and weight penalties of multiple air bag systems can be significantly higher than a conventional seat belt restraint system. However, the lifesaving benefits may justify the use of a multiple air bag system.

8.3.3 Inflatable Belt Systems

The concept of an inflatable belt system has been around for many years. These types of occupant restraint systems are being included in this section because of recent development efforts in the industry. Although these systems are not yet commercially available, they are considered viable and have been shown to be effective in a trade study (Reference 8-45) and testing (References 8-46, 8-19, and 8-20) conducted during the AGATE program. The gas generator for an inflatable belt system is similar to the gas generators used in air bag systems as described in Section 8.3.1.5. The performance of the gas generator would be matched with the inflatable belt system to optimize occupant protection.

There are two inflatable belt approaches. One approach is to inflate an air bag between the occupant and the belt. This approach provides more area of contact on the occupant to react the loads and minimizes occupant's torso movement by taking out the slack in the restraint.

THIS DOCUMENT PROVIDED BY THE ABBOTT AEROSPACE
TECHNICAL LIBRARY
ABBOTTAEROSPACE.COM

Early three-point restraint systems with this approach found it difficult, if not impossible, to prevent the air bag from slipping out from under the belt, thereby eliminating the effectiveness of the air bag.

The Inflatable Body and Head Restraint System (IBAHRS) is a inflatable restraint system that successfully achieves the goals. The IBAHRS utilizes a four- or five-point restraint system and has eliminated slipping of the air bag from under the belts. Details of the IBAHRS are described in Section 8.3.3.1.

The other approach is to carry the loads by the inflatable itself. In one system, generically known as an *air belt*, the upper portion of the shoulder belt is replaced with a tube-shaped (or other configuration) air bag. Some of the slack is reduced because the centerline of the inflated tube effectively moves away from the occupant without increasing the belt length. The net result is some reduction in the slack and an increase in the contact area provided by the inflated tube. The actual effectiveness of this type of air belt restraint has shown only marginal improvement over a standard three-point restraint, and this comes at a significant cost penalty (Reference 8-45). In contrast, Inflatable Tubular Structure (ITS®) technology has been applied to a three-point restraint system known as the Inflatable Tubular Torso Restraint (ITTR™) and has shown remarkable improvements in limiting occupant motion (see Section 8.3.3.2). Other inflatable belt systems are in development that appear similar to the air belt concept, but the performance of these new systems is unknown, as test results had not been published at the time this guide was written.

8.3.3.1 Inflatable Body and Head Restraint Systems (IBAHRS)

An inflatable body and head restraint system (IBAHRS) for helicopter crewmen has been jointly developed and tested by the U.S. Naval Air Development Center and the Aviation Applied Technology Directorate. As illustrated in Figure 8-38, this system provides increased crash protection because it provides automatic restraint pre-tensioning that forces the occupant back into the seat, thereby reducing dynamic overshoot and reducing strap loading on the wearer when the inflated restraint is compressed during the crash (Reference 8-47). The concentration of strap loads on the body is reduced because of the increased bearing surface provided when the restraint is inflated; thus both head rotation and the possibility of whiplash-induced trauma are also reduced. Although more complex and costly than conventional restraint systems, the use of such a system may be justified because of its potential for improved occupant protection.

8.3.3.2 Inflatable Tubular Torso Restraint (ITTR)

An inflatable three-point seat belt restraint, as shown in Figure 8-39, is under development and is not yet commercially available. However, the potential restraint capabilities of the device are worth discussing. The ITTR has the ability to reduce occupant motion by inflating and thus shortening the restraint in length around the occupant during a crash. The inflatable portion provides head and neck protection and distributes the crash forces over a larger area of the occupant's torso. When the ITTR inflates, the seat belt webbing also tightens across the occupant's lap, thereby reducing the likelihood of submarining. Results from testing of the ITTR versus a standard three-point restraint (Reference 8-46) indicate that forward head motion was reduced by 67 pct and head rotation was reduced by 69 pct. The ITTR technology can also be applied to four- and five-point restraint systems. Occupant restraint in a four- or five-point restraint system is expected to improve with the use of the ITTR technology.

®ITS is a registered trademark of Simula Inc.
™ITTR is a trademark of Simula Inc.

This Document Provided by the Abbott Aerospace
Technical Library
abbottaerospace.com



Figure 8-38.
Inflatable body and head restraint system (IBAHRS) designed for the AH-1 Cobra attack helicopter.



Figure 8-39.
Inflatable Tubular Torso Restraint (ITTR) stowed and deployed.

This Document Provided by the Abbott Aerospace
Technical Library
abbottaerospace.com

A trade study was conducted to determine the efficacy of the ITTR in reducing occupant motion and injury potential compared to a baseline three-point restraint (Reference 8-45). Included in the study were the results of similar tests with the five-point IBAHRS. According to the test results reported for frontal impact tests, the IBAHRS reduced forward head motion by 51 pct and the ITTR reduced forward head motion by 67 pct over a standard three-point seat belt restraint system. For more information on the testing of the ITTR, refer to Reference 8-46.

Another study, performed under the AGATE program, conducted comparison sled tests of a standard three-point restraint, a three-point restraint with an automotive shoulder belt pre-tensioner, a three-point restraint with an automotive buckle pre-tensioner, and a three-point restraint with an ITTR (Reference 8-19 and 8-20). The flail results of this study are shown in Section 4.2 in Figures 4.12 and 4.13. The belt-load-versus-time plots are shown in Figures 8-40 and 8-41. The ITTR provided the greatest improvement in occupant protection in this study, as compared to the baseline three-point restraint and the pre-tensioners. The motion of the occupant's head, neck, and torso was significantly reduced by the ITTR. The head motion was reduced by 38 pct as compared to the baseline three-point restraint. Restraint loads were reduced by 63 pct.

8.3.4 Inadvertent Deployment

As previously mentioned, an air bag system can be designed to minimize inadvertent deployments (Section 8.3.1.3). However, the air bags should be positioned to direct deployment forces away from the flight controls if an inadvertent deployment does occur, and the air bag should also be designed to minimize the potential of the bag to cause injury (Section 8.3.1.4.4.8). One other concern regarding inadvertent deployment is that the pilot must maintain control of the aircraft if the air bag deploys during flight - especially during phases of flight with high workload. Several studies have been conducted to determine if the so-called "startle response" could cause a pilot to lose control of the aircraft during an unexpected, in-flight air bag deployment. In one study, cockpit air bags were deployed while pilots flew nap-of-the-earth missions in an AH-64 flight simulator (Reference 8-43). In another study, pilots flew an actual UH-60 equipped with cockpit air bags, and the air bags were deployed in various phases of flight, including hover (Reference 8-44). In both studies, pilots maintained control of the aircraft during and after the air bag deployment. In fact, many of the pilots described the deployment as a "non-event". These studies demonstrated that a properly designed air bag system will not cause the pilot to lose control of the aircraft even if the air bag deploys during high workload phases of flight.

THIS DOCUMENT PROVIDED BY THE ABBOTT AEROSPACE
TECHNICAL LIBRARY
ABBOTTAEROSPACE.COM

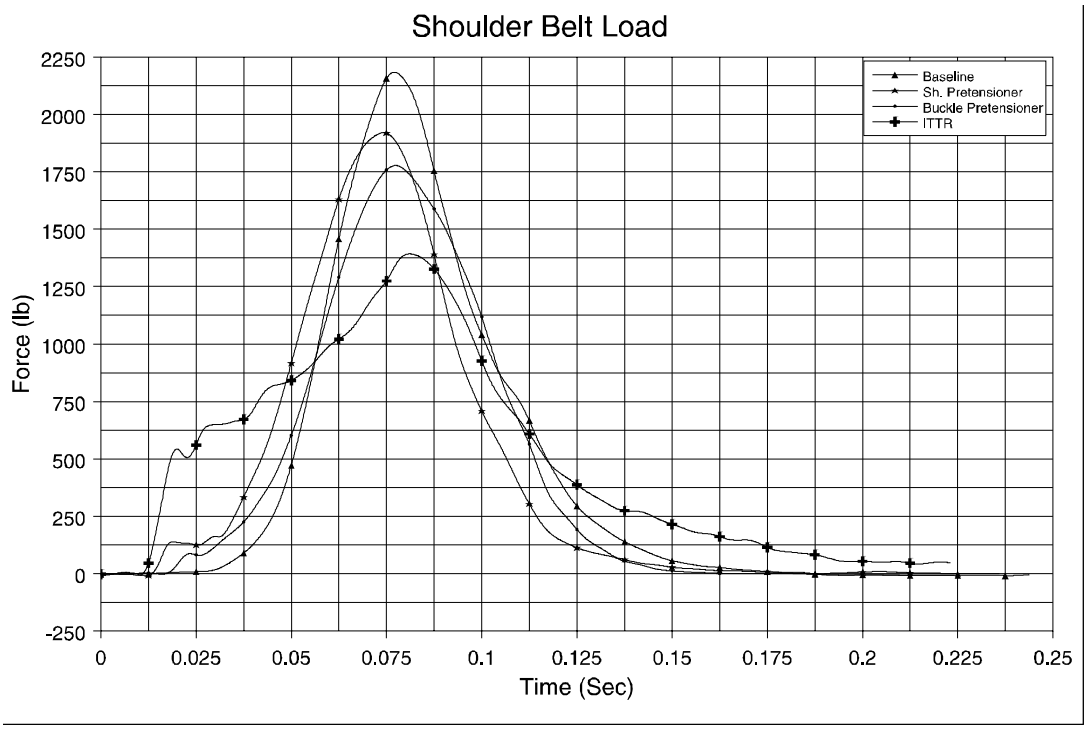


Figure 8-40.
Shoulder Belt Load (Reference 8-20).

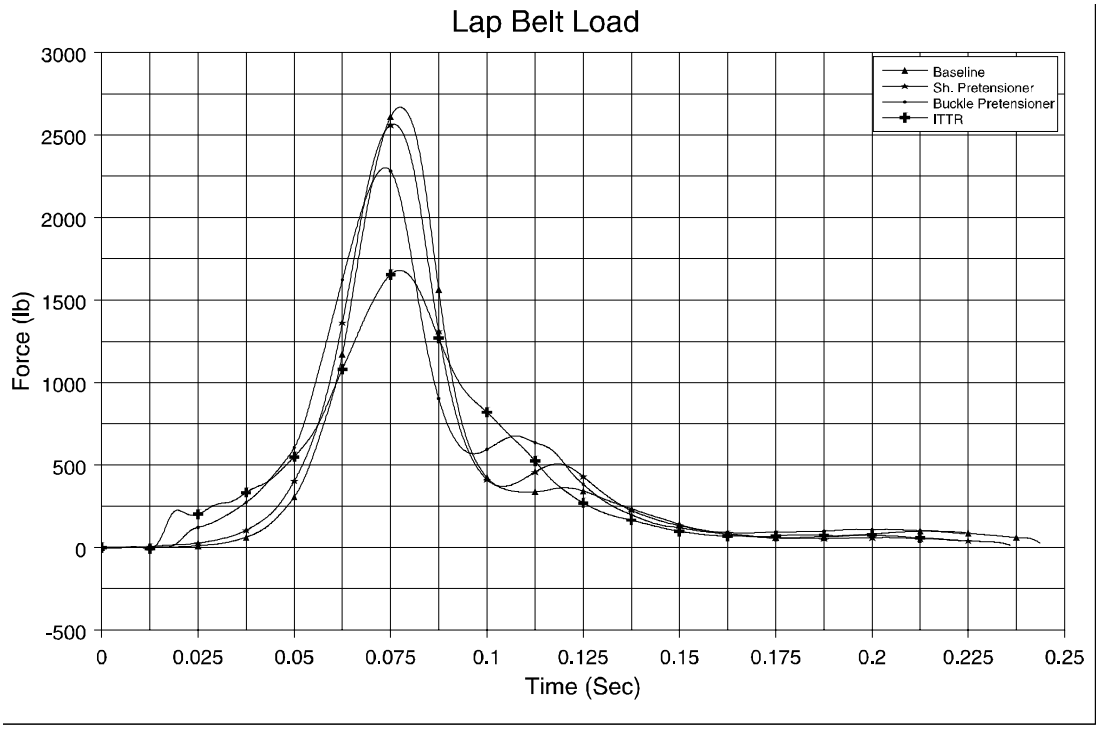


Figure 8-41.
Lap Belt Load (Reference 8-20).

THIS DOCUMENT PROVIDED BY THE ABBOTT AEROSPACE
TECHNICAL LIBRARY
ABBOTTAEROSPACE.COM

References

8-1. Technical Standard Order C114 (TSO-C114), Torso Restraint Systems, Federal Aviation Administration, March 27, 1987.

8-2. Technical Standard Order (TSO-C22), Safety Belts, Federal Aviation Administration, March 5, 1993.

8-3. "Torso Restraint Systems," SAE Aerospace Standard AS8043, Society of Automotive Engineers, Warrendale, Pennsylvania, March 1986.

8-4. Desjardins, S. P., Zimmerman, R. E., Bolukbasi, A. O., and Merritt, N. A., Aircraft Crash Survival Design Guide, Volume IV: Aircraft Seats, Restraints, Litters, and Cockpit/Cabin Delethalization, USAAVSCOM TR 89-D-22D, December 1989.

8-5. Federal Aviation Administration, 14 CFR Part 23 Subpart 562, Emergency Landing Dynamic Conditions, Washington, D.C., March 26, 1998.

8-6. Federal Aviation Administration, 14 CFR Part 23 Subpart 785, Seats, Berths, Litters, Safety Belts, and Shoulder Harnesses, March 26, 1998.

8-7. "Shoulder Harness - Safety Belt Installations," FAA Advisory Circular AC21-34, Federal Aviation Administration, Washington, D.C., June 1993.

8-8. Federal Aviation Administration, Advisory Circular AC23.562-1, Dynamic Testing of Part 23 Airplane Seat/Restraint Systems and Occupant Protection, Washington, D.C., June 22, 1989.

8-9. Military Specification, MIL-S-58095A (AV), SEAT SYSTEM: CRASH-RESISTANT, NON-EJECTION, AIRCREW, GENERAL SPECIFICATION FOR, Department of Defense, Washington, D.C., January 31, 1986.

8-10. Federal Aviation Regulations 14 CFR Part 23, Amendment 23-32 Shoulder Harnesses in Normal, Utility, and Acrobatic Category Airplanes, December 12, 1985.

8-11. Leung, Y. C., et al., Submarining Injuries of 3 Point Belted Occupants in Frontal Collisions - Description, Mechanisms, and Protection, Proceedings of the 26th Stapp Car Crash Conference, Ann Arbor, Michigan, 20-21 October 1982.

8-12. Roberts, V. L., and Robbins, D. H., Multidimensional Mathematical Modeling of Occupant Dynamics Under Crash Conditions, Paper No. 690248, Society of Automotive Engineers, New York, New York, January 1969.

8-13. Carr, R. W., Helicopter Troop/Passenger Restraint Systems Design Criteria Evaluation, Dynamic Science, A Division of Ultrasystems, Inc., USAAMRDL Technical Report 75-10, Eustis Directorate, U. S. Army Air Mobility Research and Development Laboratory, Fort Eustis, Virginia, June 1975.

8-14. Carr, R. W., and Desjardins, S. P., Aircrew Restraint System - Design Criteria Evaluation, Dynamic Science, A Division of Ultrasystems, Inc., USAAMRDL Technical Report 75-2, Eustis Directorate, AD A009059, U.S. Army Air Mobility Research and Development Laboratory, Fort Eustis, Virginia, February 1975.

This Document Provided by the Abbott Aerospace
TECHNICAL LIBRARY
ABBOTTAEROSPACE.COM

8-15. Bihlman, B., Summary of Current Restraint System Technology For Light Aircraft, report for AGATE Integrated Design and Manufacturing, Raytheon Aircraft Company, Wichita, Kansas, April 8, 1997.

8-16. Reilly, M. J., Crashworthy Troop Seat Investigation, The Boeing Vertol Company; USAAMRDL Technical Report 74-93, Eustis Directorate, AD/A-007090, U.S. Army Air Mobility Research and Development Laboratory, Fort Eustis, Virginia, December 1974.

8-17. Kourouklis, G., Glancy, J. L., and Desjardins, S. P., The Design Development, and Testing of an Aircraft Restraint System for Army Aircraft, Dynamic Science, Division of Ultrasystems, Inc., USAAMRDL Technical Report 72-26, Eustis Directorate, AD 746631, U.S. Army Air Mobility Research and Development Laboratory, Fort Eustis, Virginia, June 1972.

8-18. Sarrailhe, S. R., and Hearn, N. D., The Performance of Conventional and Energy Absorbing Restraints in Simulated Crash Tests, Structures Report 359, Aeronautical Research Laboratories, Australian Defense Scientific Service, Department of Defense, Melbourne, Victoria, September 1975.

8-19. Manning, J., and Grace, G., "AGATE Alternative Restraint Dynamic Sled Test Report – Evaluation of a Shoulder Belt Pre-tensioner," TR-98109, Simula Technologies, Inc., Phoenix, Arizona, December 31, 1998.

8-20. Grace, G., and Manning, J., "AGATE Alternative Restraint Dynamic Sled Test Report - Evaluation of Inflatable Tubular Torso Restraint (ITTR) and Buckle Pre-tensioner," TR-98110, Simula Technologies, Inc., Phoenix, Arizona, March 19, 1999.

8-21. Weber, K., "Child Passenger Protection," Accidental Injury: Biomechanics and Prevention, Springer-Verlag, New York, New York, 1993.

8-22. Chandler, R. F., Trout, E. M., Child Restraint Systems for Civil Aircraft, Civil Aeromedical Institute, Federal Aviation Administration, Oklahoma City, Oklahoma, March 1978.

8-23. Gowdy, V., DeWeese, R., The Performance of Child Restraint Devices in Transport Airplane Passenger Seats, Civil Aeromedical Institute, Federal Aviation Administration, Oklahoma City, Oklahoma, September 1994.

8-24. Code of Federal Regulations, Title 49, Federal Motor Vehicle Safety Standard 571.213, Child Restraint Systems, October 1997.

8-25. Federal Aviation Regulation 91.107, Use of Safety Belts, Shoulder Harnesses, and Child Restraint Systems, April 29, 1998.

8-26. Federal Aviation Regulation 121.311, Seats, Safety Belts, and Shoulder Harnesses, April 29, 1998.

8-27. Federal Aviation Regulation Advisory Circular AC91-62, Use of Child/Infant Seats in Aircraft, February 26, 1985.

8-28. Isaksson-Hellman, I., et al., "Trends and Effects of Child Restraint Systems Based on Volvo's Swedish Accident Database", Child Occupant Protection 2nd Symposium Proceedings, SAE 973299, November 1997.

8-29. SafetyBeltSafe U.S.A. Internet Site, Technical Encyclopedia of Child Passenger Safety, http://www.carseat.org, accessed 12 January 1999.

8-30. Society of Automotive Engineers Surface Vehicle Recommended Practice J1819, Securing Child Restraint Systems in Motor Vehicles, 1994.

This Document Provided by the ABBOTT AEROSPACE
TECHNICAL LIBRARY
ABBOTTAEROSPACE.COM

8-31. Society of Automotive Engineers Aerospace Recommended Practice 4466, Dimensional Compatibility of Child Restraint Systems and Passenger Seat Systems in Civil Transport Airplanes, 1997.

8-32. Code of Federal Regulations, Title 49, Federal Motor Vehicle Safety Standard 210, Seat Belt Assembly Anchorages, October 1997.

8-33. Weber, K., Radovich, V. G., Performance Evaluation of Child Restraints Relative to Vehicle Lap-Belt Anchorage Location, SAE 870324, 1987.

8-34. Czernakowski, W., Bell, R., "The Effects of Belt Pretensioners on Various Child Restraint Designs in Frontal Impacts," Child Occupant Protection 2nd Symposium Proceedings, SAE 973314, November 1997.

8-35. Department of Transportation, National Highway Traffic Safety Administration, 49 CFR Parts 571 and 596, Federal Motor Vehicle Safety Standards, Child Restraint Systems; Child Restraint Anchorage Systems, Final Rule, Docket No. 98-3390, Notice 2, RIN 2127-AG50, March 5, 1999.

8-36. Walz, F. H., Niederer, P. F., Thomas, C., and Hartemann, F., Frequency and Significance of Seat Belt Induced Neck Injuries in Lateral Collisions, Paper 811031, Society of Automotive Engineers, Inc., 1982.

8-37. Lombard, C. F., and Advani, S. H., Impact Protection by Isovolumetric Containment of the Torso, Space Laboratories, Northrop Corporation, Paper 660796, Society of Automotive Engineers, 1967.

8-38. Grace, G. B., and Hurley, T. R., "Inflatable Restraint Performance and Design Guidelines," TR-97018, Simula Technologies, Inc., Phoenix, Arizona, May 15, 1997.

8-39. Chan, Ching-Yao, Fundamentals of Crash Sensing in Automotive Air Bag Systems, Society of Automotive Engineers, Warrendale, Pennsylvania, 2000.

8-40. Yaklin, P., and Brinkman, G., "Aircraft Airbag Sensor Study," Impact Dynamics Incorporated, Wichita, Kansas, January 1997.

8-41. Gansman, R. F., "Design Considerations for Aircraft Crash Sensing," Proceedings of the Technical Cooperative Program Workshop: Inflatable Restraints in Aviation, U.S. Army Aeromedical Research Laboratory, Report No. 2000-21, 2000.

8-42. Terry, J. E., Hooper, S. J., and Nicholson, M., "Design and Test of an Improved Crashworthiness Small Composite Airframe," SBIR Phase II Final Report, Terry Engineering, Andover, Kansas; NASA SBIR Contract NAS1-20427, NASA Langley Research Center, Hampton, Virginia, October 1997.

8-43. Bark, L. W., Zimmerman, R. E., and Smith, K. F., "Inadvertent Helicopter Air Bag Deployment - Evaluation of the Effects in a Flight Simulator," American Helicopter Society 49th Annual Forum, 1993.

8-44. Woodhouse, J., "In-flight Inadvertent Deployment Test," Proceedings of the Technical Cooperative Program Workshop: Inflatable Restraints in Aviation, U.S. Army Aeromedical Research Laboratory, Report No. 2000-21, 2000.

8-45. Richards, M. K., et al., "Evaluation of Alternative Approaches to General Aviation Crash Safety," TR-97026, Simula Technologies, Inc., Phoenix, Arizona, August 25, 1999.

THIS DOCUMENT PROVIDED BY THE ABBOTT AEROSPACE
TECHNICAL LIBRARY
ABBOTTAEROSPACE.COM

8-46. Grace, G., and Yaniv, G., Dynamic Test Report on the National Highway Traffic Safety Administration Air Belt and the Simula Inflatable Tubular Torso Restraint, TR-96190, Simula Government Products, Inc., Phoenix, Arizona, June 1996.

8-47. Domzalski, L., Inflatable Body and Head Restraint System (IBAHRS): YAH-63 Crash Test, Aircraft And Crew Systems Technology Directorate, Naval Air Development Center, Warminster, Pennsylvania, Report No. NADC-84141-60, June 1984.

This Document Provided by the Abbott Aerospace
Technical Library
abbottaerospace.com

Chapter 9

Delethalizing Aircraft Interiors

Marvin K. Richards

The motion of an aircraft occupant's body during a crash event can be quite violent. Even with a lap belt and shoulder harness that are drawn up tightly, multi-directional flailing of the occupant's head, arms, and legs can be extensive. This flailing action poses relatively little injury risk if the designer can provide adequate open space within the occupant's immediate environment. However, by necessity, most aircraft cockpits are very compact. The instrument panel and flight controls must be close enough to be reached comfortably and seen easily by the pilot and co-pilot. These interior components can pose significant injury risk to the occupants during an accident and thus need to be designed to reduce the threat of occupant injury.

Other hazards are created when the surrounding aircraft structure or interior components move or deform due to impact forces or inertia. This movement can decrease the amount of space around the occupant, thus increasing the potential for secondary impact. Movement of interior components can also increase the potential to trap the occupant's limbs, which can prevent or delay egress. For example, an instrument panel that is not sufficiently supported can break free or deform downward during a crash. This can trap the pilot/co-pilot's legs. Even if the instrument panel motion is not enough to cause entrapment, it may move into the leg flail space enough to become a strike hazard and increase the chance of leg injury or fracture.

Four objectives should be addressed when delethalizing aircraft interiors:

1. When possible, relocate strike hazards outside of the occupant flail envelope. Opening up this space will help prevent injury to the head, neck, and upper torso.
2. Design objects that must remain within the flail envelope to be non-injurious by providing impact-compliant surfaces and components. Use large surface radii, select deformable or breakaway components, and/or pad the impact surface.
3. Securely tie down all items of mass. Items of mass include any equipment or objects inside the aircraft that could come loose during a crash, potentially injuring the occupants.
4. Prevent occupant entrapment. Instrument panels, rudder pedals, consoles, seats, and other cabin furnishings must be designed to prevent trapping the occupant's extremities.

This chapter provides information on delethalization of interior components. The pertinent FAA light airplane regulations for the crashworthy design and evaluation of interiors are found in 14 CFR Part 23 (Reference 9-1), specifically in Paragraphs 23.785, 23.562, and 23.561. Other related regulations that address the strength of the primary flight controls and other control levers (23.305, 23.307, 23.395, 23.397, 23.399, and 23.405) and the location of controls and instruments (23.777, 23.1141, and 23.1321) should be considered while designing the interior. These related regulatory paragraphs do not address the crashworthiness of the interior, but will constrain potential design solutions.

This Document Provided by the Abbott Aerospace
TECHNICAL LIBRARY
ABBOTTAEROSPACE.COM

9.1 DELETHALIZATION OF COMPONENTS WITHIN THE FLAIL ENVELOPE

Much of the aircraft interior will be within the flail envelope of the occupant's head, neck, and extremities. This section describes several delethalization techniques for common aircraft components within the occupant flail envelope (refer to Section 4.2 for detailed information on occupant flail envelopes). Flail envelopes should be used as the starting point for the cockpit and interior layout to identify potential hazards. Flail envelopes depend on the seat and restraint system design, occupant size, and the severity of the acceleration pulse. The designer should consider the available adjustment positions of the seat and any potential motion during a crash due to energy-absorbing devices (seat stroke) when considering flail envelopes. Currently, flail envelopes are rarely available from seat and restraint manufacturers, but can be obtained from prior seat dynamic performance research, seat developmental testing, or computer simulations.

9.1.1 Flight Controls

The aircraft flight controls are often located in front of the occupant and can present a serious hazard to the occupant's head, neck, or chest during a crash. When evaluating if a flight control is within the occupant flail envelope, the full operational-motion region of the control needs to be considered. Care should be taken when placing the flight controls or control rods near crush zones so that collapse of the crush zone does not cause potentially injurious control motion or loading toward the occupant. The preferred design would move the flight control out of harm's way during an impact condition.

In general, it is recommended that flight controls be located as far away from the head, neck and upper torso flail envelope as possible. One location that works well from a crashworthiness perspective is the side-stick or side-yoke control. This location does not completely remove the hazard from the entire flail envelope, but it does locate the hazard away from the direction of flail in a primarily longitudinal impact. In other words, a side-stick or side-yoke is located in region of the flail envelope that has a lower probability of impact than the region located directly in front of the occupant. Side-located controls can also provide other operational benefits, such as an unobstructed view of the instrument panel and a more ergonomic interface.

An example of a flight control that is a strike hazard is the centrally located control stick. Control sticks must be designed as relatively strong structural compression members in order to withstand the high bending loads that can be exerted by the pilot during emergency flight control. However, this high column strength, coupled with a small projected top surface area, results in a blunt "spear" which could impale the occupant during a crash event. This control location is in a high strike probability region of the flail envelope (the direction of occupant response to longitudinal loading). This probability is further increased during combined vertical and horizontal loading as seat stroke can move the occupant closer to the control.

Control yokes or wheels located in front of the pilot can pose similar risks for head and chest strikes. The yoke itself can help spread impact loads over a wider area of the body, but often the yoke is made from brittle plastic or Bakelite that can break and expose the control shaft. Yoke pedestals or control arms can be designed such that the shaft-to-yoke attachment mechanism does not protrude from the pedestal body. This makes the design safer by removing the "spear," but still does not completely remove the strike hazard. Control yoke designs that have horizontal shafts that pass through instrument panel and into the aircraft crush zone should be avoided. Full-scale tests have shown that these horizontal shafts can be thrust into the occupant with great force during the impact.

THIS DOCUMENT PROVIDED BY THE ABBOTT AEROSPACE
TECHNICAL LIBRARY
ABBOTTAEROSPACE.COM

References 9-2 through 9-4 describe development work that has been conducted to delethalize rotorcraft control sticks. Two common themes for delethalizing the control stick include (1) the addition of energy-absorbing padding and/or (2) creating a breakaway control stick. Figure 9-1 illustrates a concept for adding padding to the control stick handle. If needed, thumb buttons on top of the handle can be bridged over, leaving enough space for operation.

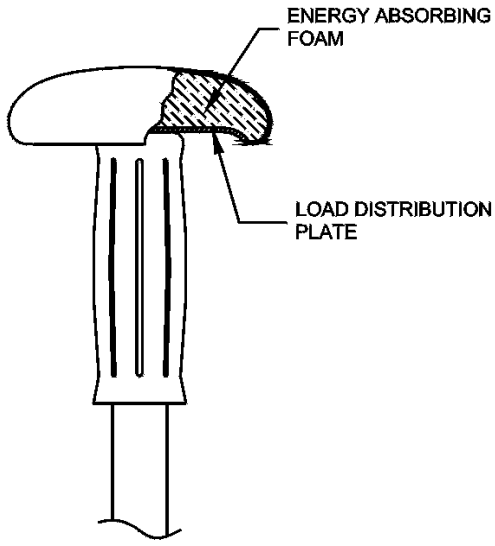


Figure 9-1.
Delethalization of a control stick using energy absorbing padding.

Figure 9-2 illustrates the delethalization of the control stick via the use of a load-limiting or breakaway joint. If this concept is utilized, there needs to be an open path for the separated control stick to travel through. An alternate load-limiting control stick design could use a telescoping section with a simple shear pin, as shown in Figure 9-3. The telescopic joint should have a one-way stop so that the stick will not extend into two separate pieces after the shear pin failure. The advantage of this design, compared to the breakaway concept, is that inadvertent shear pin failure does not result in loss of aircraft control. However, the stroking distance is limited to less than one-half the length of the control stick below the handle, unless additional telescoping sections are added in series.

All flight controls should be fabricated from ductile materials that will bend and not fracture during impact loading. Fractured controls can leave a torn, jagged edge that can inflict serious injury if impacted by the occupant.

9.1.2 Miscellaneous Controls

Other aircraft controls, such as engine throttle, fuel mixture, propeller speed, flaps, landing gear, etc., also need to be delethalized and located outside of the occupant's flail envelope. Preferably, many of the engine controls can be eliminated altogether by utilizing a single-lever power control system.

This Document Provided by the Abbott Aerospace
Technical Library
abbottaerospace.com

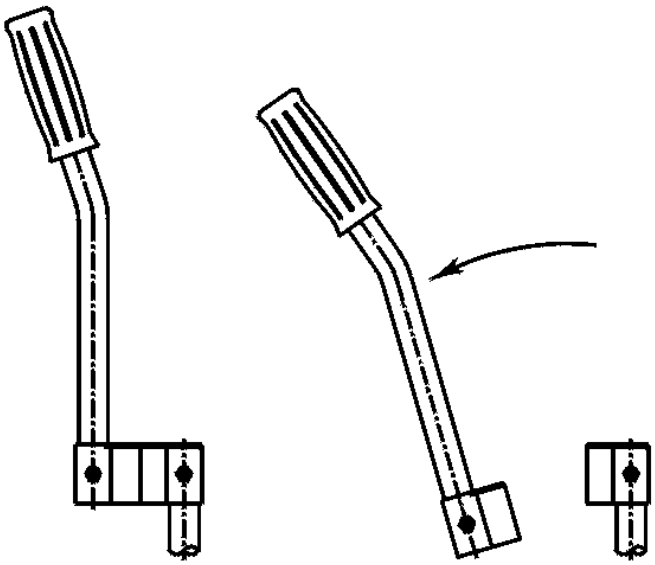


Figure 9-2.
Control stick with a breakaway joint

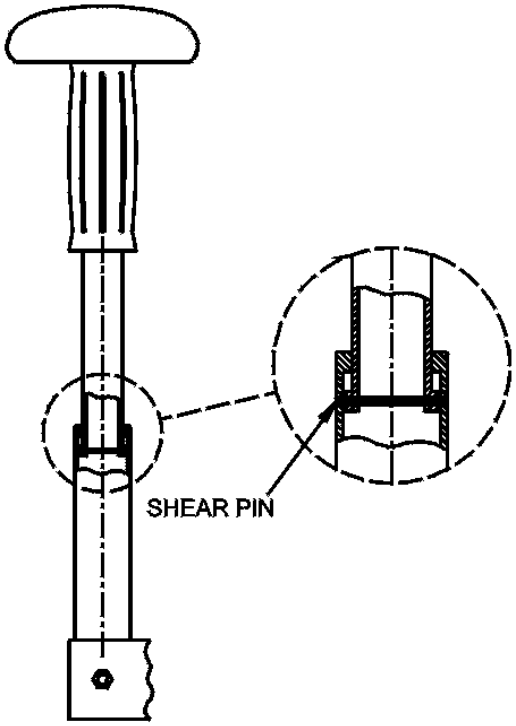


Figure 9-3.
Control stick with a telescopic joint

THIS DOCUMENT PROVIDED BY THE ABBOTT AEROSPACE
TECHNICAL LIBRARY
ABBOTTAEROSPACE.COM

Knobs on the ends of control arms/shafts often break off during impact, thus exposing the arm/shaft end and increasing the potential for injury. Therefore, any control arm/shaft should be designed to minimize potential hazards that may be present if the knob is broken off. In some cases, the control arm can be designed with a kink or joggle to initiate deformation when impacted. Figure 9-4 shows one concept to reduce the compressive load capability of a control arm by adding a kink to initiate buckling.

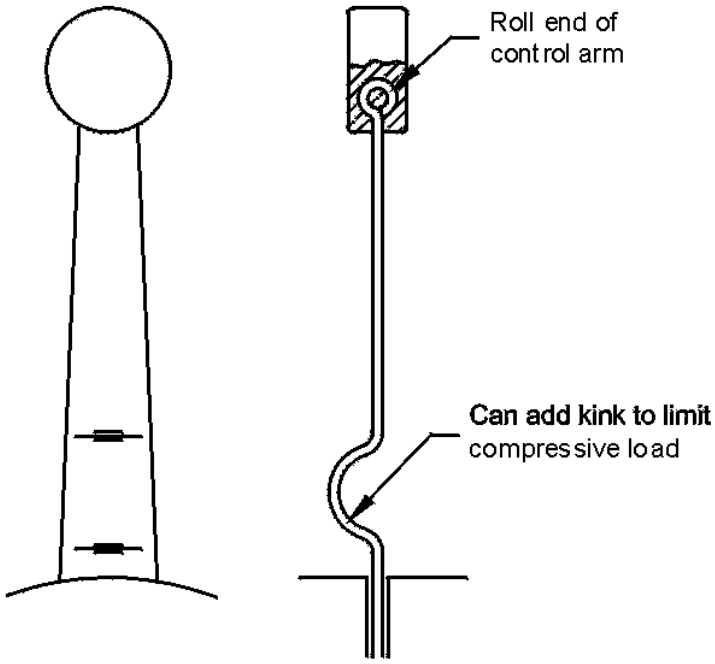


Figure 9-4.
Load-limiting control arm and delethalized knob mount.

9.1.3 Instrument Panel

Occupant safety should be considered when selecting and placing instrumentation, switches, and other controls in the cabin. The controls should be as blunt as possible without compromising function. Rocker switches, for example, could be used instead of protruding mandrel-type toggle switches. Instrument dials should be flush-mounted in the panel so that a more uniform impact area is provided.

Figure 9-5 shows examples of occupant strike hazards at the instrument panel location. This panel has sharp corners, toggle switches, and protruding instrument adjustment knobs and propeller/engine controls. Note that the ignition switch becomes a significant strike hazard after the keys are installed.

THIS DOCUMENT PROVIDED BY THE ABBOTT AEROSPACE
TECHNICAL LIBRARY
ABBOTTAEROSPACE.COM

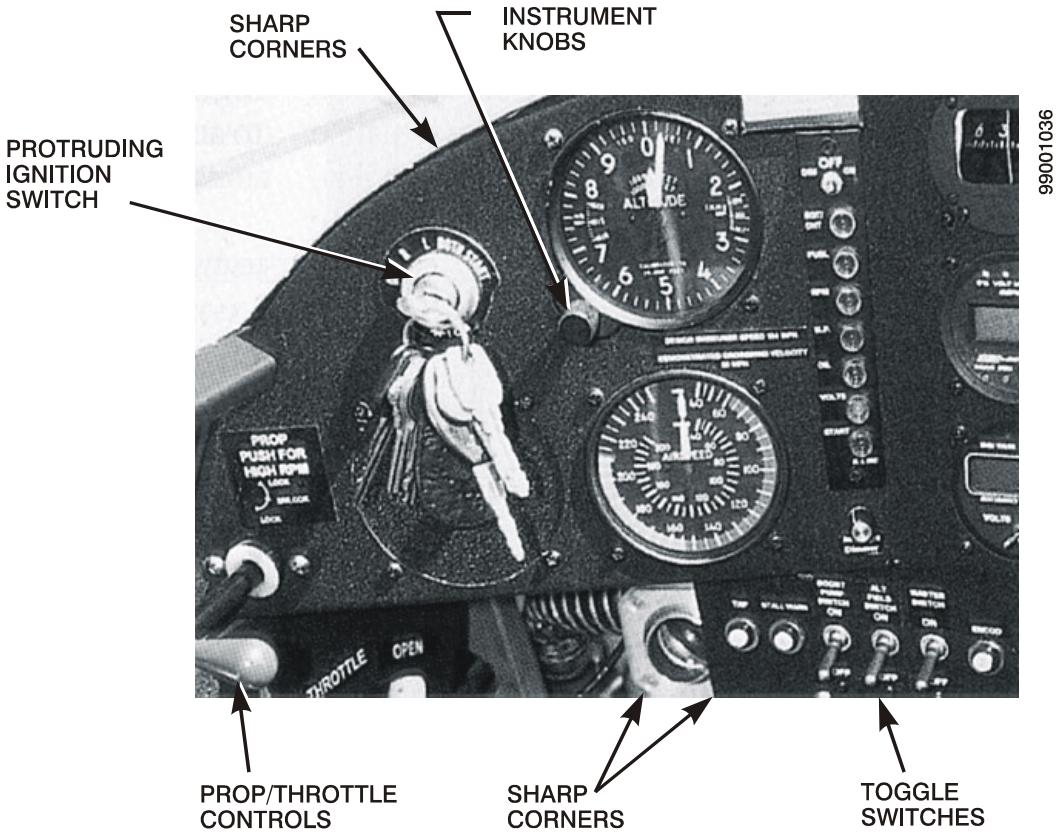


Figure 9-5.
Examples of occupant strike hazards on an instrument panel.

Figure 9-6 shows examples of some techniques that can be used to delethalize the instrument panel area. The ignition switch and cabin air vent have been recessed into a padded panel with generous radii. The rounded edges and padding on the lower edge of the panel will minimize injuries to the knees/legs should the lower extremities flail upward. Rocker switches are also used in place of the more lethal toggle-type switch. This aircraft also uses the preferred side-control yoke.

Most instrument panels will have some level of strike hazard due to the design of currently available instrumentation. Instruments are often made from rigid materials and cannot be padded due to operational considerations. As an example, certain types of instrumentation, such as altimeters, often have an adjustment knob that could be a strike hazard. To reduce the injury potential, these typically hard plastic knobs could be replaced with a more compliant material, such as rubber.

In cases where the instrument panel is placed within the occupant's head flail envelope, the rigidity of the panel itself could cause head injury. To combat this issue, the panel could be designed to break away or deform during impact. For example, "S"-shaped deformable mounting brackets could be utilized to attach the instrument panel to the airframe. However, the inertial mass of the panel alone may be sufficient to cause head injury if the impact velocity is relatively high. In this case, an energy-absorbing head-impact barrier could be used to help mitigate occupant injury.

THIS DOCUMENT PROVIDED BY THE ABBOTT AEROSPACE
TECHNICAL LIBRARY
ABBOTTAEROSPACE.COM

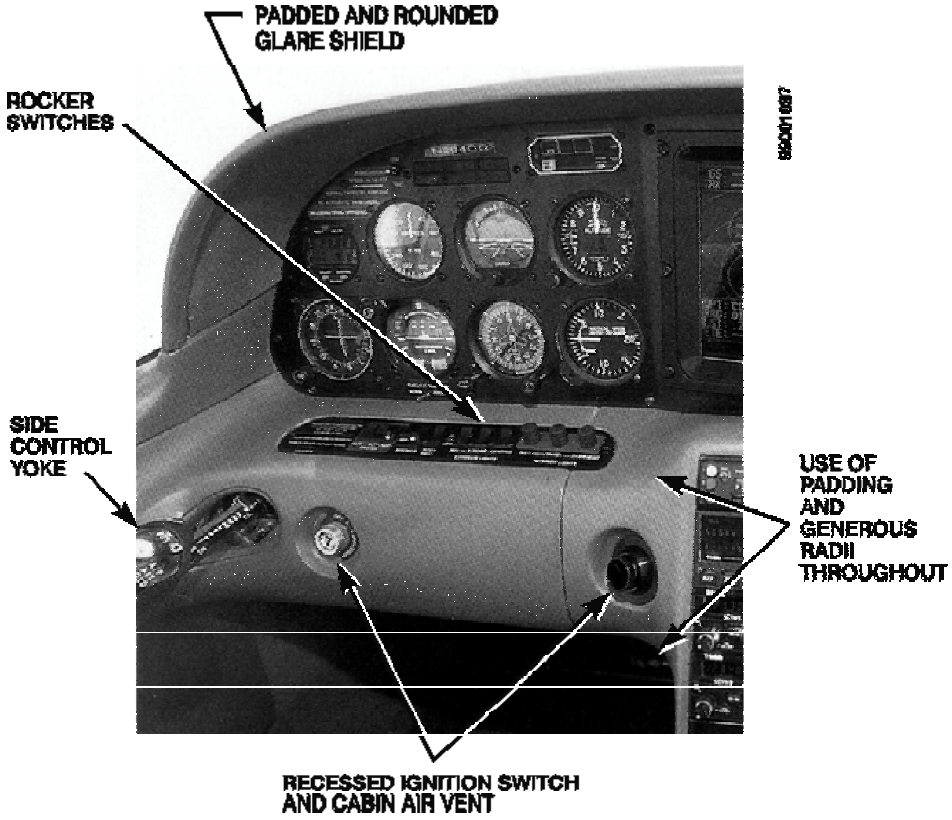
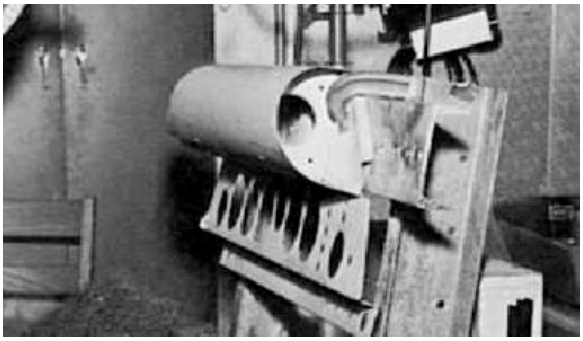
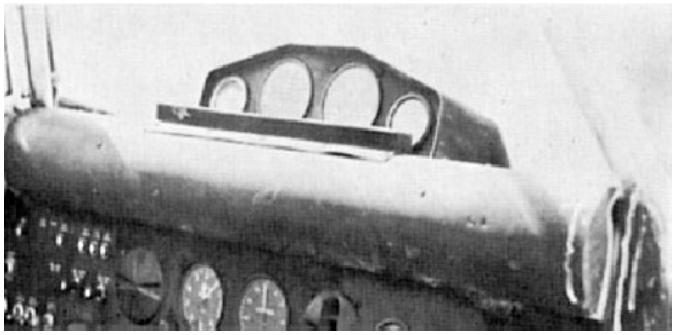


Figure 9-6.
Design techniques used to delethalize an instrument panel.

Figure 9-7 shows an energy-absorbing semicircular aluminum barrier designed to minimize head injury during impact. Laboratory tests and investigation of accidents of agricultural aircraft out in the field with the barrier in place have shown that this design is capable of reducing occupant head injuries (References 9-5 and 9-6).





a) Barrier installed on test fixture. **b) Barrier installed in aircraft.**

Figure 9-7.
Semicircular energy-absorbing head-impact barrier utilized in agricultural aircraft.

THIS DOCUMENT PROVIDED BY THE ABBOTT AEROSPACE
TECHNICAL LIBRARY
ABBOTTAEROSPACE.COM

9.1.4 Glare Shield

Glare shields are often fabricated from relatively thin materials and provide only minimal strength when loaded at an angle perpendicular to the shield's surface. However, the shield can be relatively stiff when loaded parallel (edgewise) to the surface, which is also the minimum projected area. To compound problems, the glare shield is usually aligned with the occupant's line-of-sight, thereby creating a potential strike hazard for the occupant.

The first design consideration of the glare shield, as for all interior components, is to locate the shield out of the occupant's head flail envelope. However, even if the glare shield is positioned out of the head flail envelope, the leading surface still needs to be rounded and padded using a minimum radius of 0.25 in. Padding the sharp edge of the glare shield without rounding out the edge will not be effective, since the edge will easily slice though the padding when impacted.

The glare shield should be fabricated from a material that will not fail in a brittle fashion and cause multiple shards. If a brittle material such as carbon/epoxy is utilized, the shield should be fully encapsulated so that sharp edges are not exposed to the occupant if the shield is impacted.

Glare shields typically extend far enough aft of the instrument panel to prevent direct sunlight from reflecting off of the instrumentation. This typically positions a portion of the glare shield within the flail envelope. To resolve this issue, one approach, similar to automotive instrument panels, would be to add a curved transparency in front of the instrument panel, as shown in Figure 9-8. The curvature is designed so reflections off the transparency are from darker, shadowed areas of the interior. This design can significantly reduce the length of the glare shield. This design approach has been utilized in the automotive market for many years with success.

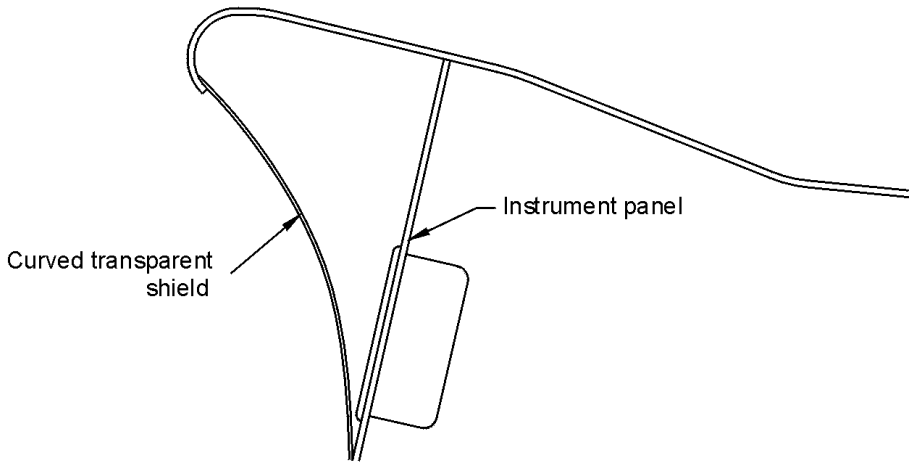


Figure 9-8.
Alternate method of reducing instrumentation glare.

THIS DOCUMENT PROVIDED BY THE ABBOTT AEROSPACE
TECHNICAL LIBRARY
ABBOTTAEROSPACE.COM

9.1.5 Leg Well and Rudder Pedals

The design and positioning of the instrument panel, supporting structure, and rudder pedals are critical for the mitigation of lower extremity injuries in aircraft crashes. In most aircraft, the instrument panel and supporting structure are placed directly above the occupant's lower legs. During a crash, the occupant's lower extremities can impact with these structures, potentially causing injury. For the instrument panel and supporting structure, designers should consider using suitable energy-absorbing padding materials, frangible breakaway panels, or ductile panel materials.

Rudder pedals can contribute to occupant foot and ankle injury via blunt loading and/or foot entrapment. Pedals should be designed to support the ball of the foot and the heel. The surrounding supporting structure should be designed with sufficient strength to prevent crushing and trapping of the foot during a crash. The geometry required by MIL-STD-1290 to prevent entrapment of an occupant's feet (Reference 9-7) is illustrated in Figure 9-9.

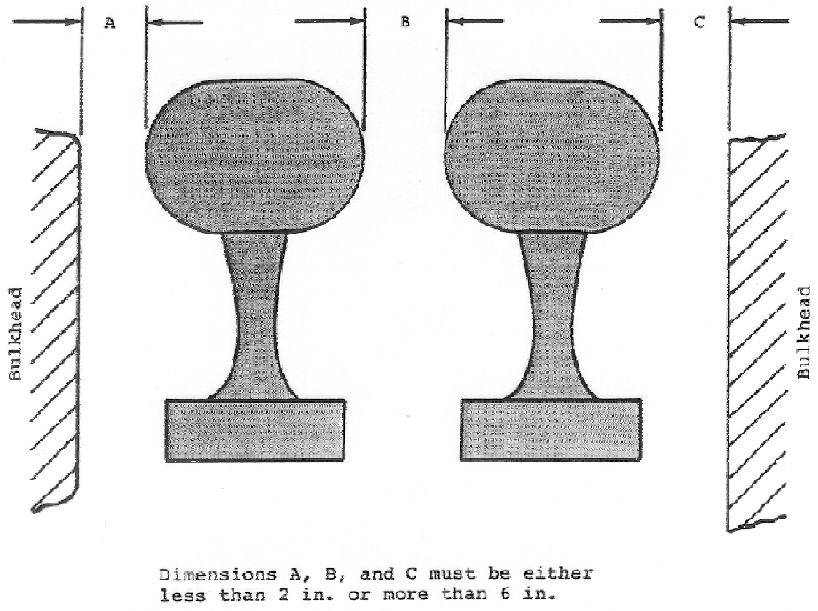


Figure 9-9.
Rudder pedal geometry per MIL-STD-1290 to prevent entrapment of feet.

9.1.6 Aircraft Interior Structure

Strike hazards commonly found in aircraft cabin areas include windows, door frames, seats, instrument panels, and the fuselage structure. Each of these components has a primary function that is critical to the overall function of the aircraft. While many of these components require strength and rigidity, the surface should still be designed to reduce the likelihood of injury during a crash.

Each of these components is made from a variety of materials. Aluminum, steel, wood, and composites are traditional materials found in aircraft interiors. Occupant interaction with these materials produces different effects on the occupant, depending on the material's properties. Rigid or semi-rigid materials allow for little deformation during occupant impact. Brittle materials

This Document Provided by the Abbott Aerospace
Technical Library
abbottaerospace.com

can produce sharp, jagged edges when fractured that can be lethal if struck by an occupant. Ductile materials do not produce the sharp, jagged edges as the brittle materials do; however, they often don't meet the strength requirements specified for the given components.

Assuming that the function of the aircraft component is not compromised, the geometry of the strike hazard should minimize the likelihood of occupant injury during a crash. Door frames and instrument panels should be of smooth contour. Transitions from one surface to another should be gradual so that impact loads can be distributed to both surfaces. External radii in the cabin area should be made as large as possible, preferably with radii of 0.5 in. or more.

Interior decorative panels can also be used to reduce occupant injury. Although decorative panels may increase the cost and weight of the aircraft, their use is justified in that they help to increase the level of occupant protection, reduce interior noise levels, and improve the appearance of the cabin.

9.2 ENERGY-ABSORBING PADDING

Energy-absorbing padding is one of the most practical tools used to reduce the likelihood of occupant injury during a crash. Padded surfaces can distribute the impact loads over a larger area of contact and reduce peak impact acceleration to the occupant. The padding material, thickness, placement, and attachment method, as well as the added cost and weight, must be considered in order to design for maximum occupant safety.

The preferred padding material is one that provides a near-constant crushing load and limits rebound. This type of material will provide the maximum energy absorption within the limited thickness available. Semi-rigid crushable foams or rate-sensitive foams are preferred to elastic foams.

A padding material should not only reduce the decelerative force exerted on an impacting body segment, but should distribute the load in order to produce a more uniform pressure of safe magnitude. It is suggested that areas within the occupant head flail envelope having radii of 2 in. or less be padded, and that such padding has a minimum thickness of 0.75 in.

Caution must be exercised in padding sharp edges and corners. Padding installed in a manner that allows it to be broken away from the corner or cut through by sharp edges offers minimal protection. It is recommended that any edges and corners to be padded have a minimum radius of 0.5 in. prior to padding.

Padding that is placed on window frames, the instrument panel, and the glare shield could potentially reduce the pilot's field of view both inside and outside of the cockpit. The pilot's line of sight must not be impaired by the addition of padding. For certain components, the padding can be beveled in such a way to provide protection with minimal effects on the line of sight.

In cases where the use of padding material is impractical, or the padding thickness allowed is inadequate to provide the necessary protection, ductile energy-absorbing materials or frangible, breakaway components should be used where possible.

9.3 AIRBAGS

Airbags can also be used to delethalize the interior as well as provide occupant restraint (See Section 8.3). They should be considered for delethalization when injury tolerances (particularly HIC) are exceeded and the strike hazard can't be moved or delethalized by other means.

This Document Provided by the Abbott Aerospace
Technical Library
abbottaerospace.com

9.4 HELMETS

Helmets are a very effective delethalization device. They provide protection from point loading and have a self-contained energy-absorption system. Helmets are used by the aircrew in U.S. military and Coast Guard rotorcraft, police helicopters, medical evacuation helicopters, and sometimes by agricultural application (crop-duster) pilots. However, it will take a major change in public acceptance before helmets become common in light airplanes.

9.5 EQUIPMENT RETENTION

During a crash, injury can be caused by unrestrained or dislodged objects striking the occupants. Therefore, proper retention of all ancillary equipment (fire extinguishers, baggage, etc.) is needed to avoid additional occupant injury during a crash. All ancillary equipment frequently carried aboard the aircraft should be provided with integrated restraint devices or anchors. Stowage space for non-restrained items that are not regularly carried aboard the aircraft should also be provided. This storage space should either be strong enough to contain the stowed items or be located where the stored items will not become hazardous to the occupants in a crash. Retention strength should exceed the load required to deform the occupiable space by 20-25 pct in each primary loading direction.

It is a relatively simple task to restrain small items of equipment to withstand the static loads specified above. For larger items, however, significant weight penalties may be incurred, or the available supporting structure may not be capable of withstanding the loads. For these reasons, load-limiting devices are recommended for the restraint of heavier equipment. However, the load-limiter's stroking must not allow any equipment to enter an occupant's strike envelope.

9.6 EVALUATION OF POTENTIAL STRIKE HAZARDS

Evaluation of potential strike hazards can be done through dynamic testing and/or computer simulation. Certification of aircraft components to meet the Head Injury Criteria (HIC) must currently be determined by dynamic test.

9.6.1 Component Testing

Aircraft interior components that are within the occupant's head flail envelope must be shown by dynamic test to provide a HIC of 1,000 or less (See Reference 9-1, specifically Paragraph 23.562(c)). However, passing the HIC value does not necessarily mean the head strike zone has been properly delethalized. The HIC is calculated from the duration and magnitude of the ATD's measured head acceleration, without regard to concentrated point loading or potential penetration of sharp objects. The formulation and use of HIC as an injury tolerance parameters is described in Section 4.3.4.2.

In addition to using an ATD to assess HIC, the automotive industry also uses a device called a Free Motion Headform (Reference 9-8). This device is essentially a modified Hybrid III ATD headform that is propelled by an actuator that is used to aim the headform at specific parts of the vehicle interior. The headform is actually launched over a short distance prior to impact during which time it is only attached to data acquisition cables. The Free Motion Headform allows component-level testing at a cost generally less than expensive full-scale sled testing, but it hasn't been used much in the aviation industry. The FAA currently does not require testing using the Free Motion Headform. The device cannot be used for certification, but it does provide the designer with another evaluation tool.

This Document Provided by the Abbott Aerospace
Technical Library
abbottaerospace.com

9.6.2 Computer Simulation

Computer simulation (See Chapter 5) of the occupant's behavior in the aircraft cabin environment can be used to support the design and testing of components with delethalization as the goal. Simulation should be used early in the aircraft design phase to improve integration. Two simulation approaches can be used to gain an understanding of occupant motion and interfaces: rigid structure analysis or deformable structure analysis.

Rigid structure analysis can be performed for locations where the aircraft cabin and components do not deform significantly due to crash loads. It can be valid for cases where the cabin structure is not expected to deform significantly, i.e., the crash pulse is low relative to the aircraft's structural strength; or where a less-complex analysis is desired to identify potential impact areas for the occupant's head, torso, and limbs.

Deformable structure analysis can be performed for locations where the aircraft structure is allowed to deform during a crash. This type of analysis can identify occupant interactions that may not have been considered within the original flail envelope. This type of analysis is more complex and, as a result, is generally more costly to perform.

Overall, these types of computer models can provide load and acceleration impact data between the occupant and the object(s) the occupant strikes. The aircraft components can be modeled and analysis performed to aid in their selection and placement within the cabin.

THIS DOCUMENT PROVIDED BY THE ABBOTT AEROSPACE
TECHNICAL LIBRARY
ABBOTTAEROSPACE.COM

References

9-1. "Federal Aviation Regulations, Part 23, Airworthiness Standards: Normal, Utility, Acrobatic, and Commuter Category Airplanes," 14 CFR 23, Federal Aviation Administration, Washington, D.C.

9-2. Eisentraut, D. K., and Zimmerman, R. E., Crashworthy Cyclic Control Stick, Simula, Inc., Report No. USAAVRADCOM-TR-83-D-23, Applied Technology Laboratory, U.S. Army Research and Technology Laboratories (AVRADCOM), Fort Eustis, Virginia, AD 628678, November 1983.

9-3. Whitaker, C. N., and Zimmermann, R. E., Delethalized Cyclic Control Stick, Simula, Inc., Report No. USAAVSCOM TR-86-D-5, Aviation Applied Technology Directorate, U.S. Army Aviation Research and Technology Activity (AVSCOM), Fort Eustis, Virginia, AD A173931, July 1986.

9-4. Zimmerman, R. E., and Smith, K. F., Delethalized Cyclic Control Stick, Simula, Inc., and U.S. Army Aviation Applied Technology Directorate (AVSCOM), paper presented at the 24th Annual Symposium of SAFE Association, San Antonio, Texas, December 11-13, 1986.

9-5. Swearingen, J. J., Injury Potentials of Light-Aircraft Instrument Panels, Federal Aviation Agency, Civil Aeromedical Institute, Oklahoma City, Oklahoma, April 1966, AM 66-12.

9-6. Swearingen, J. J., et al, Crash Survival Analysis of 16 Agricultural Aircraft Accidents, Federal Aviation Agency, Civil Aeromedical Institute, Oklahoma City, Oklahoma, April 1972, FAA-AM-72-15.

9-7. Military Standard, MIL-STD-1290A(AV), Light Fixed- and Rotary-Wing Aircraft Crash Resistance, Department of Defense, Washington, D.C., 26 September 1988.

9-8. "Occupant Protection in Interior Impact," 49 CFR Part 571.201, Federal Motor Vehicle Safety Standards, Standard No. 201, National Highway Traffic and Safety Administration, Department of Transportation, Washington, D.C.

This Document Provided by the Abbott Aerospace
Technical Library
abbottaerospace.com

This Document Provided by the Abbott Aerospace
TECHNICAL LIBRARY
ABBOTTAEROSPACE.COM

Chapter 10
Post-Crash Factors

Jill M. Vandenburg

Occupant survivability in aircraft accidents is dependent on the passenger's ability to survive the impact and then safely egress the aircraft. This chapter provides information regarding aircraft post-crash conditions and the design strategies that can be implemented to eliminate injuries and fatalities in survivable impacts. It discusses various factors related to post-crash fire, crashworthy fuel system design, and occupant egress and survival.

10.1 POST-CRASH FIRE ENVIRONMENT

Post-crash fire most commonly occurs when flammable fluids on board the aircraft are released and ignited (Reference 10-1). A fire can be produced by a variety of means, including engine displacement, fuselage crush, wing and wing root damage, ruptured fuel and oil tanks, and damaged fuel and oil pumps, filters, and/or drains. The magnitude and threat of the post-crash fire are influenced by (Reference 10-2):

- The amount of fuel available to spill
- The number of structural openings (designed-in or crash-produced) that meter the in-flowing air available for an internal fire
- The location of the fluid spillage within the aircraft
- The distribution of the fuel
- The type of terrain onto which the flammable fluid has spilled
- The relative wind speed.

Fire prevention can be achieved by eliminating the spillage of flammable fluids and by controlling hazardous ignition sources (Reference 10-1).

In 1998, a safety analysis of 68 GA aircraft accidents revealed that 22 pct of the crashes involved post-crash fire (Reference 10-3). Forty-eight pct of the occupants in these accidents were fatally injured. The crash scenarios evaluated in the study were selected to approximate the limits of survivability, and the statistics obtained from their analysis suggest that although there are not a large number of GA aircraft crashes involving post-crash fire, the accidents that do involve fire are extremely life-threatening for the occupants. Human survival in a post-crash fire is dictated by the heat, toxic gases, and smoke existing in or near the occupiable area. The total fire threat to the occupant depends upon the magnitude of these hazards, combined with the human tolerance limits to each hazard. The following sections describe post-crash fire conditions and discuss human tolerance to heat, toxic gases, and other hazards that greatly affect human survival in a post-crash fire.

10.1.1 Heat

A fire is initiated and sustained via hydrodynamic, thermodynamic, chemical, and mass-transfer processes, which heat, decompose, and ignite the molecular structure of flammable fuels and exposed structures of the aircraft (Reference 10-4). The effects of heat from the fire are observed in the burn-through of the aircraft structure and interior components, as well as the heat-related skin and respiratory injury to the occupants.

THIS DOCUMENT PROVIDED BY THE ABBOTT AEROSPACE
TECHNICAL LIBRARY
ABBOTTAEROSPACE.COM

10.1.1.1 Heat Damage to Aircraft Structure

The aircraft's skin burn-through time is a function of fire severity, skin thickness, insulation, and temperature. Full-scale fire tests on standard aluminum aircraft skin panels have revealed that skin burn-through may occur in as little as 10 sec for a fuel fire of maximum severity and with minimum skin thickness (Reference 10-5). Larger aircraft, which possess thicker skin panels, have burned through in as little as 30 to 40 sec. These relationships are better quantified in Figure 10-1, which illustrates the minimum skin melting times as a function of aircraft gross weight. As illustrated in the figure, skin melting time increases as aircraft gross weight increases.

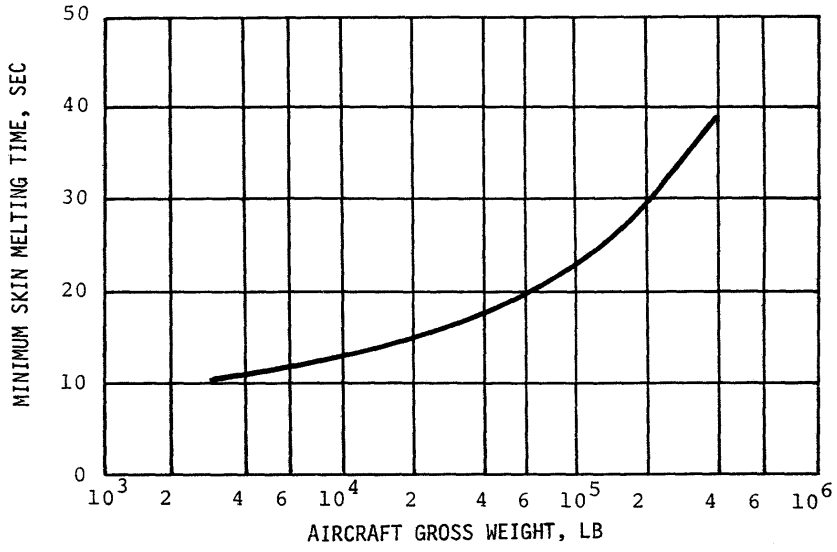


Figure 10-1.
Aircraft skin melting time based on aircraft gross weight (Reference 10-5).

Another factor that can influence skin burn-through time is insulation. When aircraft skin is heated externally by a fire, the metal skin attempts to radiate the heat internally. When this heat radiation is prevented by insulation, skin burn-through occurs more rapidly. Several studies have documented skin burn-through time as a function of skin thickness, insulation characteristics, and the temperature of the heat source (Reference 10-6 – 10-9). For an aluminum fuselage, the insulation can be exposed and distorted due to the melting of the aircraft skin, as well as the high turbulence generated within the liquid fuel fire (Reference 10-5).

The temperature of the fire also influences skin burn-through time. A typical ambient and radiant temperature curve for large cargo/passenger-carrying aircraft tested by the National Advisory Committee for Aeronautics (NACA) is presented in Figure 10-2 (Reference 10-5). As shown, the temperature doesn't increase until approximately 80 sec following impact. In this particular test series, the protective shield provided by the fuselage helped to delay the temperature increase. Skin burn-through averaged approximately 80 sec, although some burn-through times occurred before 40 sec. The figure also displays the estimated escape time, based on human tolerance to heat. Escape times varied from 53 to 220 sec, with the average escape time equal to 135 sec.

THIS DOCUMENT PROVIDED BY THE ABBOTT AEROSPACE
TECHNICAL LIBRARY
ABBOTTAEROSPACE.COM

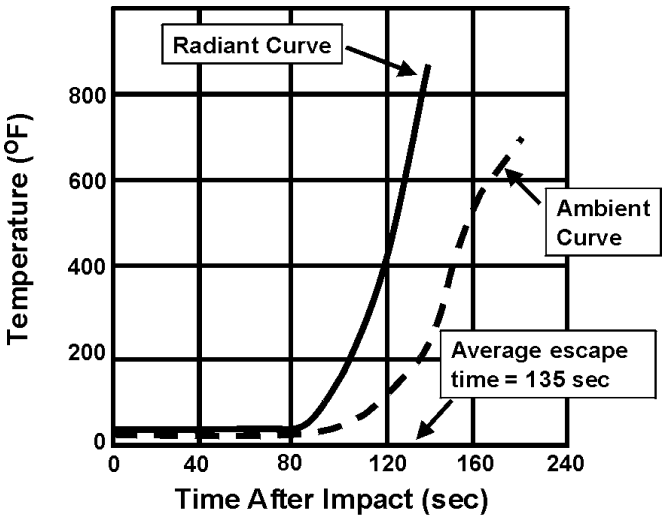


Figure 10-2.
Average recorded ambient and radiant temperatures in large, crashed, burning, passenger/cargo-carrying, fixed-wing aircraft (Reference 10-5).

The scenario is much different for small aircraft, where the occupants are seated within close proximity to the fuel and the skin-burn through of the aircraft structure occurs at a much faster rate than in large aircraft. As illustrated in Figure 10-3, the average escape time is 17 sec. Since the occupants are in such close proximity to the fuel, they must rely on built-in, protective measures that will slow down the skin burn-through time in order to increase the amount of time available for egress. Additional information regarding the effect of heat on escape time is provided in Section 10.1.2.2.

10.1.2 Smoke and Toxic Gases

Aircraft crash fires generate a large amount of dense smoke consisting of unburned carbon particles, ash, and gaseous combustion products that are typically toxic to humans (Reference 10-4). The smoke originates from the following materials (Reference 10-4):

1. Burning of aircraft fuel.
2. Ignition of polymeric materials used in interior design structures (i.e., the synthetic fabrics of seats, carpets, drapes, and insulation, as well as the polymeric materials used in interior walls, bulkheads, counter tops, and serving trays).
3. Secondary ignition of fabrics, materials, and structures made from vegetable or organic fibers (i.e., paper, fiberboard, cotton, wool, and wood).

The predominant toxic gas generated during an aircraft fire is carbon monoxide (CO) (Reference 10-4). Carbon monoxide is generated by incomplete combustion and is produced in larger amounts than any other toxic gas. Other gases that can be generated during an aircraft fire include: hydrogen chloride (HCl), cyanide (CN), hydrogen cyanide (HCN), hydrogen fluoride (HF), carbon dioxide (CO_2), phosgene (CCl_2O), and sulfuric acid (H_2SO_4) (References 10-10 – 10-12). Early concentrations of toxic gases may contribute to occupant impairment, thus hindering the occupant's egress abilities. As a result, designers are cautioned against using materials that give off these types of toxic gases during a fire.

THIS DOCUMENT PROVIDED BY THE ABBOTT AEROSPACE
TECHNICAL LIBRARY
ABBOTTAEROSPACE.COM

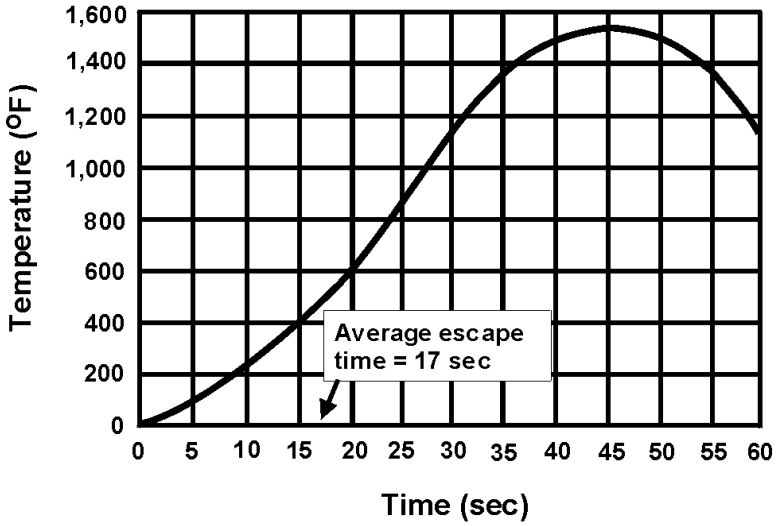


Figure 10-3.
Average recorded ambient and radiant temperatures in small, crashed, burning, passenger/cargo-carrying, fixed-wing aircraft (Reference 10-5).

As illustrated in Figure 10-4, the phenomenon of flashover plays a role in the production of toxic gases during an aircraft fire (Reference 10-13). Flashover is the transition from a small controllable fire to a widespread blaze within the aircraft's cabin when all combustible surfaces become involved in flames (Reference 10-5). It typically occurs in situations where there are no openings or breaks in the fuselage. The air within the fuselage is not permitted to vent, and as a result, the temperature and smoke levels increase significantly while the oxygen level in the cabin decreases. Flashover can be followed by the sudden production of flames from unburned gases and vapor collected under the ceiling in un-vented fuselages. When a flashover occurs, the conditions within the cabin become non-survivable within a matter of seconds.

The data in Figure 10-4 indicates that the acid gases, HF and HCl, accumulate in the cabin at least 1 min before any of the remaining hazards (Reference 10-13). These acid gases are generated by the burning of composite honeycomb panels from the ceiling, storage bins, and hat racks. Elevated temperature, smoke, and HCN were the remaining hazards detected before the onset of flashover. After flashover had occurred, small increases in CO_2, HF, and HCN were observed, while large increases in HCl and CO were observed.

10.1.2.1 Airflow of Smoke and Toxic Gases Through the Aircraft

Studies of transport category aircraft (References 10-6 and 10-7), GA aircraft, and helicopters have been conducted to address the problem of smoke and toxic gas formation and dispersion inside a fuselage during a post-crash fire. Findings suggest that smoke and toxic gases enter the cabin through openings in the fuselage that are near the fire. The amount of smoke and toxic gases that enter the cabin are related to the location and orientation of the openings and the relative wind speed traveling through the openings. If there is a second opening in the fuselage where there is no fire, the airflow inside the fuselage can travel from the fire area to the smoke-free opening, filling the fuselage with smoke. If the air travels in the opposite direction (smoke-free opening to fire opening), smoke-free air is carried throughout the fuselage providing clean air for the occupants to breathe.

THIS DOCUMENT PROVIDED BY THE ABBOTT AEROSPACE
TECHNICAL LIBRARY
ABBOTTAEROSPACE.COM

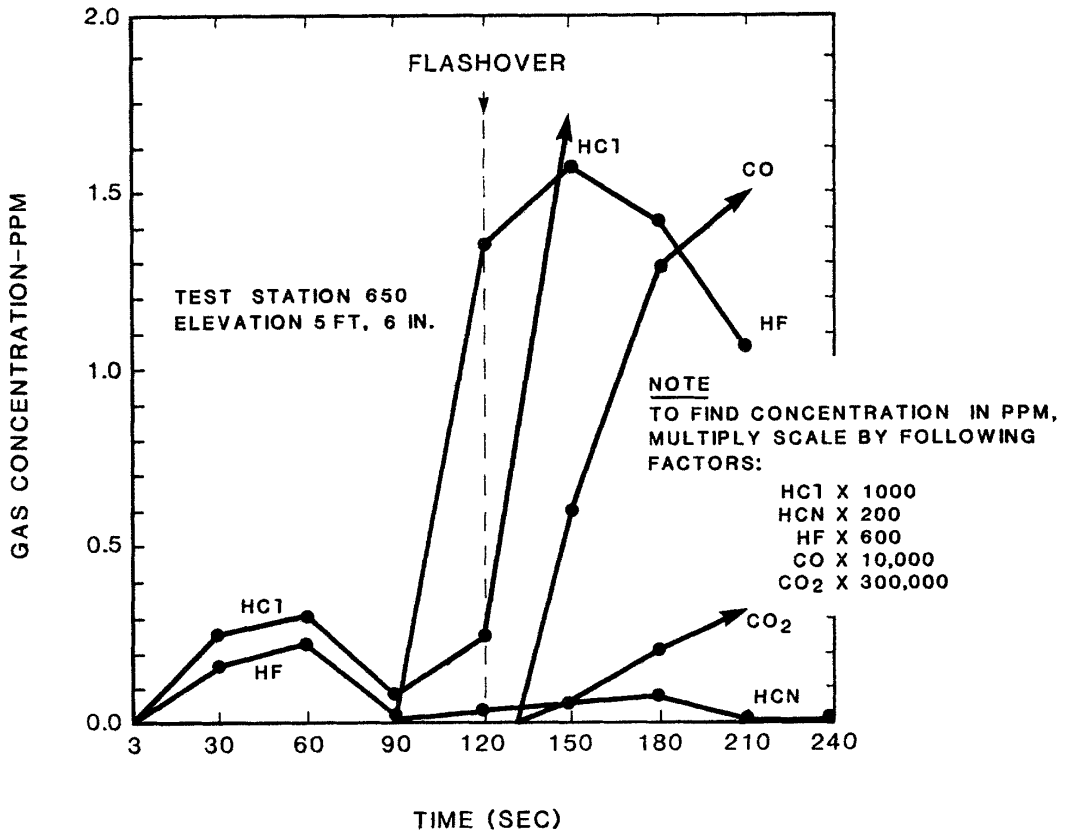


Figure 10-4.
Concentrations of toxic gases during a full-scale fuel fire test (Reference 10-13).

Fires that exist at two or more openings in the fuselage may create a “chimney” effect (Reference 10-5). The fuselage structure must have multiple openings separated by a considerable distance in order for the "chimney" effect to occur. In this scenario, smoke-filled air from one of the fires will flow toward another opening that has lower relative air pressure. The speed of the airflow through the fuselage during the "chimney" effect has been measured in experiments using dual-opening GA aircraft, large aircraft, and cargo helicopter fuselages. The "chimney" effect can create high-speed airflow in excess of 35 mph. In addition to the rapid airflow, the problem is exacerbated by the seats and occupants contained within the fuselage, which create a turbulent, vortex-generating effect of the airflow. This increases the speed in which the smoke from the fire and the smoke-free air mix.

10.1.3 Materials

Many GA aircraft structures are currently being manufactured with composite materials instead of traditional metallic alloys. Composite materials, such as graphite and fiberglass, possess some structural advantages over traditional metallic alloys including (1) a superior strength-to-weight ratio, and (2) resistance to fatigue crack propagation (Reference 10-4). However, composite materials do not currently provide an equivalent level of crashworthiness protection as do metallic structures. Regarding the potential for post-crash fire in a composite fuselage structure, it is important to note that composites are bound with polymeric resins, which will burn even though the composite material itself will not burn (Reference 10-4). In addition,

THIS DOCUMENT PROVIDED BY THE ABBOTT AEROSPACE
TECHNICAL LIBRARY
ABBOTTAEROSPACE.COM

composites are electrically conductive materials with fibers that have the potential to short-circuit electrical and electronic equipment, thus becoming a potential ignition source. However, the average expected risk of this event occurring is low, and no specialized design criteria have been defined to account for the substitution of composites for metallic alloys in aircraft structures (Reference 10-14).

10.1.4 Human Tolerance to Injury

10.1.4.1 Thermal Injury

Thermal injuries occurring in aircraft crash fires can be divided into two categories: skin injury and respiratory injury. The information provided in this section pertains to short-term exposures (≤15 min) rather than heat prostration-type injuries that require a considerably longer exposure time.

Skin Injury - When exposed to heat, two factors govern an occupant's survivability: tolerance to pain and the thermal level at which the exposed skin will experience second-degree burning. Generally, the pain threshold is exceeded when the human skin is heated to a temperature between 108 and 113 ^{o}F, with the average occupant experiencing unbearable pain at skin temperatures of greater than or equal to 124 ^{o}F (Reference 10-15 and 10-16). At skin temperatures greater than 111 ^{o}F, the rate of cellular destruction is faster than cellular repair and the extent of the injury is dependent on the heat transferred during the exposure time.

Figure 10-5 displays a collection of the experimental work conducted to date on human tolerance to heated ambient air (Reference 10-17). As illustrated in the figure, decreases in ambient air temperature increase the tolerance time to the heated air. Tolerance time directly correlates to escape time for the occupant. Based on the data presented in Figure 10-5, the available tolerance/escape time at 400 ^{o}F would be approximately 20 sec.



Figure 10-5.
Human tolerance versus ambient air temperatures measured at 30-pct humidity (Reference 10-17).

THIS DOCUMENT PROVIDED BY THE ABBOTT AEROSPACE
TECHNICAL LIBRARY
ABBOTTAEROSPACE.COM

Respiratory Injury - Occupants who inhale hot gases during a post-crash aircraft fire have the potential to sustain thermal injuries to the respiratory system. The threshold value for thermal respiratory system injury is 390 ^{o}F (Reference 10-18). This value is highest-known temperature to which a human respiratory system has been exposed without damage. The threshold value was defined by the NACA in an effort to permit a gross comparison of the relative hazards between respiratory and skin injuries. The respiratory threshold value is comparable to the 400 ^{o}F tolerance value discussed in the previous paragraph.

Toxic Gases - The hazards of toxic gases may be both physical (blocked vision) and physiological (increased breathing rate, faintness, irritation of the eyes, throat, and respiratory tract). Table 10-1 displays the estimated human tolerance limits in parts per million (PPM) to the most common toxic gases produced during an aircraft fire (Reference 10-11). As expected, the human tolerance to toxic gases decreases over time.

Table 10-1.
Tolerance to selected combustion gases (Reference 10-11)

Combustion Gas	Hazardous Levels (PPM) for Times Indicated			
	Minutes	**0.5 hr**	**1-2 hr**	**8 hr**
Carbon dioxide (CO_2)	50,000	40,000	35,000	32,000
Carbon monoxide (CO)	3,000	1,600	800	100
Sulfur dioxide (SO_2)	400	150	50	8
Nitrogen dioxide (NO_2)	240	100	50	30
Hydrogen chloride (HCl)	1,000	1,000	40	7
Hydrogen cyanide (HCN)	200	100	50	2

The uptake of CO into the body is of great concern for aircraft occupants. As CO is inhaled into the body, the toxic gas rapidly displaces the oxygen being carried in the blood. For large aircraft, Figure 10-6 illustrates the relationship between CO level, COHb level, and time, where COHb represents the percentage of CO saturation in the blood. As shown, the data reveals that CO concentrations remained below the 0.8-pct level for approximately 250 sec and then rapidly increased to 4 pct. The human tolerance limit of CO saturation in the blood is defined as 35 pct. Based on the data presented in Figure 10-6, 35-pct saturation would be reached in approximately 6 min. At this incapacitating COHb level, the occupant's judgement becomes severely impaired and the egress capability is hindered (Reference 10-10). As shown in Figure 10-7, lethal levels of COHb are reached at 60-pct saturation (Reference 10-12).

The threat of incapacitation from CO uptake during post-crash fire is much lower for small aircraft (Reference 10-12). During a GA aircraft crash, breaks in the fuselage structure often occur early during the crash sequence, thus preventing toxic gases from collecting within the fuselage. As shown in Figure 10-8, the concentration of COHb plateaus around 13 pct, which is 22 pct below the human tolerance limit for CO saturation in the blood. As a result, the COHb level will rarely be high enough to incapacitate small aircraft passengers during egress.

THIS DOCUMENT PROVIDED BY THE ABBOTT AEROSPACE
TECHNICAL LIBRARY
ABBOTTAEROSPACE.COM

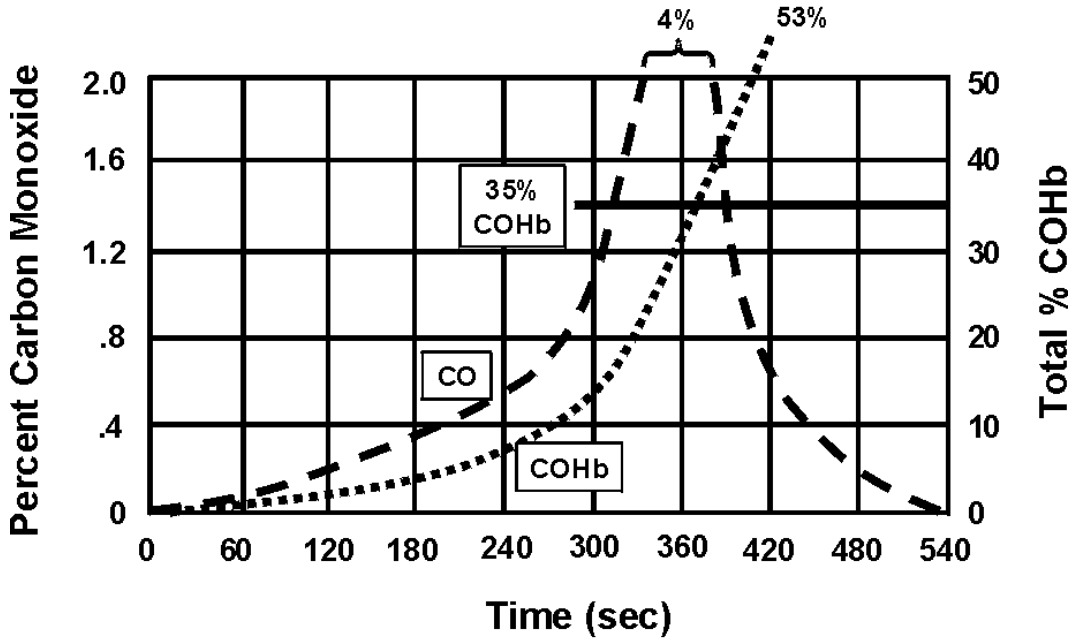


Figure 10-6.
Average recorded CO concentrations and calculated COHb levels in post-crash, burning, large fixed-wing aircraft (Reference 10-10).

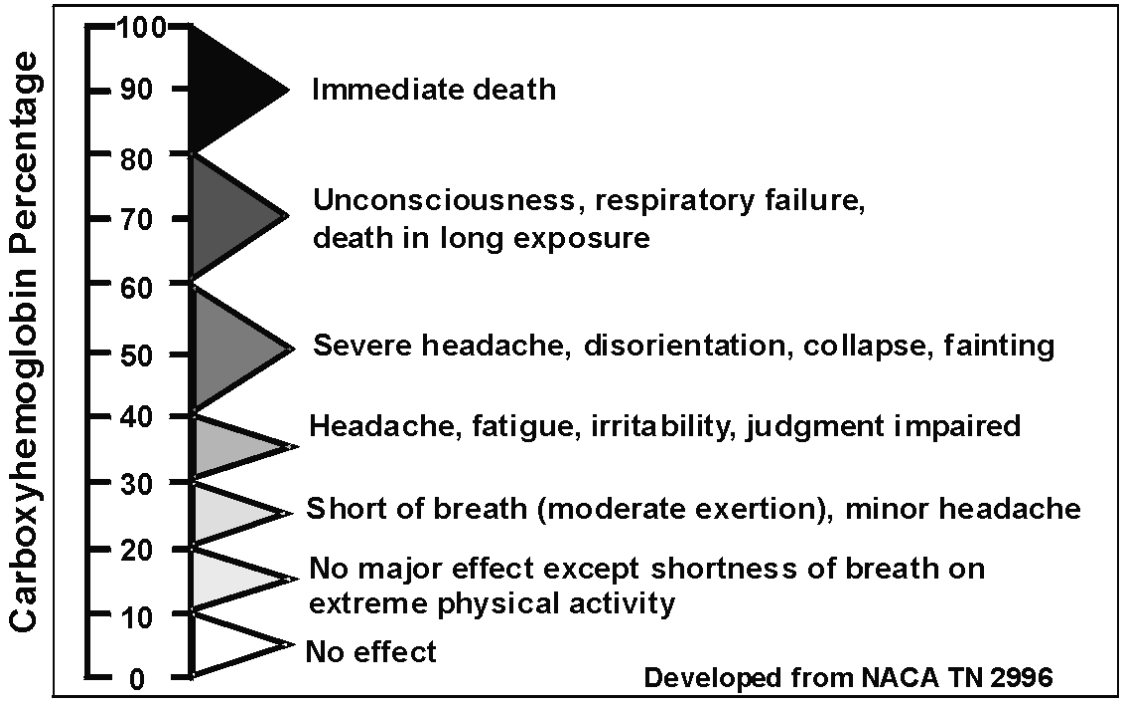


Figure 10-7.
Physiological effects of various COHb percentages (Reference 10-12).

THIS DOCUMENT PROVIDED BY THE ABBOTT AEROSPACE
TECHNICAL LIBRARY
ABBOTTAEROSPACE.COM

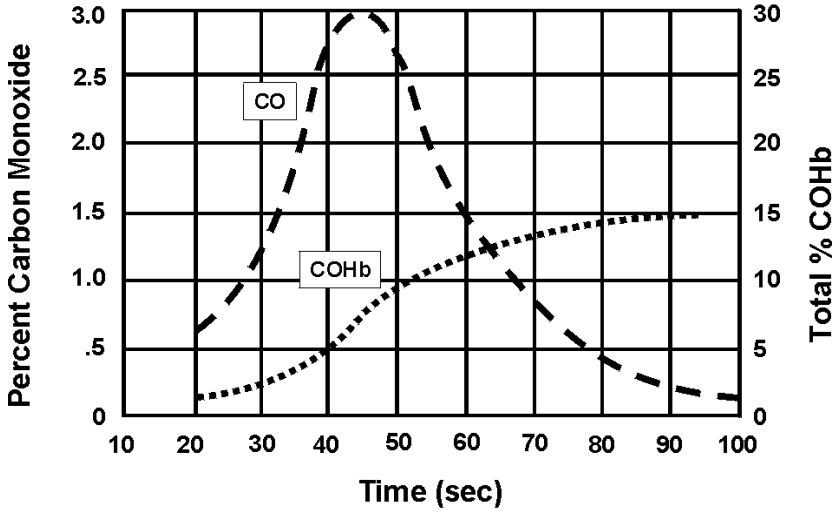


Figure 10-8.
Average recorded CO concentrations and calculated COHb levels in post-crash, burning small fixed-wing aircraft (Reference 10-12).

10.2 CRASHWORTHY FUEL SYSTEMS

Post-crash fire in GA aircraft presents a significant threat based on the close proximity of the occupants to the fuel systems and the reduced time available for egress from the aircraft. However, the prevention of post-crash fires can be achieved through the addition of a well-designed crashworthy fuel system (Reference 10-5). Accident investigations and post-crash fire research involving crashworthy fuel systems have demonstrated that: (1) a reduction of fuel spillage and ignition sources during and following a crash will reduce the probability of a post-crash fire (Reference 10-5), (2) a greater emphasis on "built-in" post-crash fire protection during the aircraft design phase will improve overall post-crash fire resistance (Reference 10-5), and (3) there isn't a single set of design rules that can be applied across-the-board for all aircraft structures. This section outlines basic design guidelines for the creation of crashworthy fuel systems for GA aircraft. Additional information on crashworthy fuel system design and evaluation can be found in Appendices C and D.

10.2.1 Design Guidelines

As previously mentioned, prevention of post-crash fire can be achieved by eliminating the spillage of flammable fluids and by controlling hazardous ignition sources (Reference 10-1). The ideal fuel system is one that completely contains its flammable fluid both during and after the accident, and has components that resist rupture regardless of the degree of failure of the surrounding structure.

General design guidelines for controlling spillage and ignition include (Reference 10-19):

- Tank displacement should not cause the tank to rupture or tear; this minimizes spillage
- The filler cap should either remain attached to the tank or should separate from the tank without spilling fuel
- Fuel lines should either remain attached to the tank or should separate from the tank without spilling fuel
- Fuel lines and components should displace safely or remain stationary safely

THIS DOCUMENT PROVIDED BY THE ABBOTT AEROSPACE
TECHNICAL LIBRARY
ABBOTTAEROSPACE.COM

- Wing separation or movement should not allow the spillage of fuel
- Fuselage or wing crush should not damage the fuel tanks or lines
- Engine displacement should not permit spillage from fuel / oil lines, filters, reservoirs, etc.

To adhere to these design guidelines, a variety of system components can be added including crashworthy bladders, self-sealing breakaway valves, and frangible fasteners for wires, tanks, and fuel lines. In addition to these general guidelines, Sections 9.2.1.1 and 9.2.1.2 provide descriptions of supplemental techniques that can be implemented to control spillage and ignition (Reference 10-19). A crashworthy fuel system design checklist is also available in Appendix D.

10.2.1.1 Spillage Control

Fuel Storage Location and Containment

Location - Design the location of the fuel tank taking into account the anticipated impact area, occupiable area, any large weight masses, and the primary ignition sources in the vicinity. The placement of wing tanks forward of the main spar should be avoided due to the possibility of rupture upon tree or pole impacts.

Vulnerability due to structural deformation - The vulnerability of a fuel tank should be accounted for with respect to possible tank ruptures caused by various aircraft structural failures, such as landing gear failure and wing deflection or separation. Fuel tank failures associated with structural displacement, such as ruptures around the filler neck, the fuel line entry and exit area, the quantity indicators, and the tank tiedown devices, should also be considered.

Construction technique - The fuel tank's geometry should be composed of smooth contoured shapes; avoid interconnected multi-cell tanks and irregular cell shapes. Crash-resistant bladders are preferred fuel tank materials; avoid using metal cells and tanks that are integral with the wing structure (“wet wing”).

Oil Containment

The location of the oil tank should be designed from the standpoint of rupture resistance as well as its proximity to the anticipated impact area, the occupiable area, large weight masses, and primary ignition sources. An integral sump, especially if made from ductile materials, gives good rupture resistance in a vulnerable area. An oil tank that is separate from the engine should be designed to withstand rupture during deformation in the engine area.

Flammable Fluid Lines

Construction of fuel lines - The construction of fuel lines should be designed based on the hose material and hose couplings. Experience has shown that rigid lines fail before flexible lines; thus, flexible fuel lines with a steel braided outer sheath are desirable. The fewer the couplings in the line, the better. Ninety-degree couplings are less desirable than the straight type. The use of any fuel line coupling is less desirable than the use of an uncut hose. In addition, aluminum fittings usually fail before steel fittings.

Routing of the fuel lines - The fuel lines should not pass through areas where they can become trapped, cut, or pulled. Extra hose length (20-30 pct in areas of anticipated structural deformation) should be provided. Holes through which the fuel lines pass should be considerably larger than the outer diameter of the hose.

This Document Provided by the Abbott Aerospace
TECHNICAL LIBRARY
ABBOTTAEROSPACE.COM

Breakaway fittings - Breakaway fittings should be installed on each fuel line that enters and exits the fuel tank. It is also advisable to have them installed at strategic locations throughout the fuel system.

Firewall

In the design of the firewall, the objective is to separate the fire sources from occupied areas with an adequate barrier to provide sufficient time for egress.

Fuel Boost Pump

Fuel boost pump location and type - The fuel boost pump should be designed to prevent fuel spillage due to fuel cell rupture or fuel line failure. The designer should consider the location of the pump in an area away from anticipated impact, and should consider the method of its attachment to the fuel cell, including the use of breakaway fittings.

Fuel boost system - The fuel boost system should be designed with respect to its function as an ignition source. The designer should consider its location and the method of its attachment to the fuel cell, as well as the pump type (an air-pressure system is the best, a hydraulic system is the next best, and an electrical system is the least desirable).

Fuel-Flow Interrupters

Fuel-flow interrupters are devices that block or divert the flow of spilled flammable fluids. There are many different methods to perform this function, including baffles, drain holes, drip fences, and curtains. Ideally, these devices should be designed to divert spilled flammable liquids away from potential ignition sources, likely sites of fire, and occupied areas.

10.2.1.2 Ignition Control

Air Induction and Exhaust Locations

Air induction and exhaust locations are most important in turbine engines where the turbine might still be operating after a crash. It is important to monitor the location of expelled exhaust with respect to the locations of possible spilled flammable liquids.

Location of Hot Metals and Shielding

The engine, exhaust system, and heater should be designed to shield hot items (temperatures above 400 °F) and protect them from fuel spillage.

Engine Location and Tiedown Strength

When deciding on the engine location and strength the engine tiedowns, it is important to consider the consequences of engine separation in relation to post-crash fire hazards. Where will the engine go in a crash, and how will its movement affect the fuel cells, exhaust system, electrical wiring, fuel lines, and oil lines? Will the engine come into contact with spilled flammable fluids?

Battery Location and Tiedown Strength

The battery should be located as far as possible from fuel and oil tanks, as well as away from potential areas of flammable fluid spillage such as fuel lines. Consider the vulnerability of the battery and its attached wiring to damage during a crash, and design the tiedown strength to safely secure the battery to the aircraft structure.

This Document Provided by the Abbott Aerospace
TECHNICAL LIBRARY
ABBOTTAEROSPACE.COM

Electrical Wire Routing

Electrical wire routing should be designed with excess length (about 20-30 pct) to account for structural airframe deformation during the crash; otherwise, the wiring should be attached with frangible fittings.

Locations of Lights

The filaments of lights and/or the wiring leading to the attachment points of beacon, search, landing, and navigation lights should be located away from areas of potential flammable fluid spillage.

Antenna Location

Avoid installing antennas and antenna wiring in areas that are at risk for possible flammable fluid spillage.

10.2.2 Design Aids

During the design process, it is helpful to utilize hazard-reduction analyses to optimize the design of the crashworthy fuel system. A standard hazard-reduction analysis can be performed to assess the following characteristics of the system (Reference 10-19):

- Failure of a component, thus causing fuel spillage
- Likelihood of spillage catching fire
- Likelihood of the fire starting other fires
- Estimated passenger and crew escape times.

Appendix D presents a specific hazard level rating system, developed by Robertson and Turnbow, that can be used to determine what design considerations and hardware are needed to obtain a desired reduction in the fire hazard level of a given fuel system.

10.3 EGRESS AND SURVIVAL

As previously mentioned, occupant survivability in aircraft accidents is dependent on the passenger's ability to survive the impact and safely egress the aircraft. An occupant's ability to initiate and perform an escape is a function of numerous mechanical (properly functioning emergency lighting, exit doors, emergency slides, etc.), environmental (obstructed escape routes/aisles, collapsed airframe structure, thick smoke which hinders vision), and human factors (panic, pain caused by injury, shock, etc.), which dictate what the occupant feels (temperature, panic, pain, etc.), breathes (smoke and toxic gases), and sees (smoke, emergency lighting, exits, escape routes, etc.) following the accident (Reference 10-5). There are several guidelines that an aircraft designer should follow in order to improve the opportunity for occupant survival (Reference 10-19).

1. Ease and reliability of exit operation
   - Simplicity of operation
   - Capability of being opened from inside and outside
   - Single-motion, single-hand levers and handles on doors
   - Avoid designs that may potentially jam due to fuselage distortion during a crash
2. Availability and access to exits
   - Consider the ratio of usable exits to the number of passengers; there should be a minimum of two exits for up to nine passengers and three exits for 10-19 passengers
   - Each occupant should have a unimpeded access to one exit and a relatively easy access to a second exit

THIS DOCUMENT PROVIDED BY THE ABBOTT AEROSPACE
TECHNICAL LIBRARY
ABBOTTAEROSPACE.COM

- Consider all equipment that may hinder egress
- Consider the ability of an injured occupant to egress

3. Identification of exits
   - Clearly marked and readily identifiable in a crash
   - Identifying letters should be a minimum of 0.75 in. in height and must be lighted by the emergency lighting system
   - Operation instructions should be readily readable and a minimum of 0.33 in. in height
   - The color of the operation instructions text should be offset from the background (i.e., red on white or vice versa)
   - Identify which exit each passenger should attempt to use for his/her particular seating position (i.e., using markings on the wall or on a seat back ahead of the passenger)
4. Availability of exits in rolled and/or deformed aircraft
   - Consider crash scenarios where exit doors are blocked and/or jammed
   - Exits should be easily accessible and operable to the occupant when the aircraft is in a pitched, rolled, or inverted position

In addition to these standard design guidelines, it is also important for design engineers to play a role in developing emergency egress training for aircraft crew and passengers. Training should include formal emergency egress and leadership training sessions for crew members as well as egress information cards and detailed pre-flight emergency briefings for passengers (Reference 10-19).

THIS DOCUMENT PROVIDED BY THE ABBOTT AEROSPACE
TECHNICAL LIBRARY
ABBOTTAEROSPACE.COM

References

10-1. Robertson, H. S., Improvements in Fuel Containment Crashworthiness for Aircraft Operated by the Mission Aviation Community, Phase I Report, Robertson Aviation, Inc., Tempe, Arizona, September 15, 1980.

10-2. Johnson, N. B., et al., An Appraisal of the Postcrash Fire Environment, Dynamic Science (The AvSER Facility); USANLABS Technical Report 70-22-CE, U.S. Army Natick Laboratories, September 1969.

10-3. Grace, G. B., Hurley, T., and Labun, L., General Aviation Crash Safety Analysis and Crash Test Conditions: A Study of Accident Data from 1988 to 1995, Simula Technologies, Inc., Phoenix, Arizona, February 15, 1998.

10-4. AGARD Lecture Series Number 123, Aircraft Fire Safety, AGARD-LS-123, May 1982, Advisory Group for Aerospace Research and Development (AGARD).

10-5. Simula, Inc., U.S. Army Aircraft Crash Survival Design Guide, Volumes I-V, USAAVSCOM TR 89-0-22A, December 1989.

10-6. Miniszewski, K. R., and Waterman, T. E., Fire Management/Suppression/Systems/ Concepts Relating to Aircraft Cabin Fire Safety, DOT/FAA/CT-82/134, Federal Aviation Administration, October 1983.

10-7. Quintiere, J. G., and Tanaka, T., An Assessment of Correlations Between Laboratory and Full-Scale Experiments for the FAA Aircraft Fire Safety Program, Part Five: Some Analysis of the Post Crash, NBSIR 82-2537, Federal Aviation Administration, July 1982.

10-8. Bankson, C.P., Back, L.H., Cho, Y.I., and Shakkottai, P., “Pool Figures in a Simulated Aircraft Cabin Interior with Ventilation,” Journal of Aircraft, Volume 24, Number 7, July 1987.

10-9. Middleton, V.E., A Computer Simulation of Aircraft Evacuation with Fire, Contract NAS2-11184, Ames Research Center, Moffett Field, California, April 1983.

10-10. Forbes, W. H., Sargent, F., and Roughton, F. J. W., “The Rate of Carbon Monoxide Uptake by Normal Man,” American Journal of Physiology, Vol. 143, April 1945.

10-11. Fire Safety Aspects of Polymeric Materials, Volume 6 - Aircraft: Civil and Military, Publication NMAB 3186, National Materials Advisory Board, National Academy of Sciences, Washington, D.C., 1977.

10-12. Simula, Inc., International Center for Safety Education Basic Course 00-1 Notebook, Simula, Inc., Phoenix, AZ, 2000.

10-13. Hill, R. G., et al., Aircraft Seat Fire Blocking Layers; Effectiveness, and Benefits Under Various Fire Scenarios, Federal Aviation Administration, DOT/FAA/CT-83/29, U.S. Department of Transportation, June 1983.

10-14. Shiltz, Jr., R. J., Investigation of the Structural Degradation and Personnel Hazards Resulting From Helicopter Composite Structures Exposed to Fires and/or Explosions, Bell Helicopter Textron, USAAVRADCOM-TR-81-D-16, Applied Technology Laboratory, U.S. Army Research and Technology Laboratories, August 1981.

10-15. Buettner, K., “Effects of Extreme Heat on Man,” Journal of the American Medical Association, Volume 144, October 1950, pp.732-740.

10-16. Mortiz, A. R. et al., “An Exploration of the Casualty Producing Attributes of Conflagrations: Local and Systemic Effects of General Cutaneous Exposure to

THIS DOCUMENT PROVIDED BY THE ABBOTT AEROSPACE
TECHNICAL LIBRARY
ABBOTTAEROSPACE.COM

Excessive Heat of Varying Duration and Intensity," Archives of Pathology, Volume 43, 1947, pp.466-502.

10-17. Pryer, A. J., and Yuill, C. H., Mass Fire Life Hazard, Southwest Research Institute, San Antonio, Texas, September 1966.

10-18. Pesman, G. J., Appraisal of Hazards to Human Survival in Airplane Crash Fires, NACA Technical Note 2996, Lewis Flight Propulsion Laboratory, National Advisory Committee for Aeronautics, Cleveland, Ohio, September 1953.

10-19. Simula Technologies, Inc., and AGATE, Small Airplane Crashworthiness Design Seminar Notebook, Phoenix, Arizona, October 11-13, 2000.

Additional Reading Materials:

Demaree, J., Examination of Aircraft Interior Emergency Lighting in a Postcrash Fire Environment, Federal Aviation Administration, DOT/FAA/CT-82/55, Department of Transportation, June 1982.

Geyer, G. B., and Urban, C. H., Evaluation of an Improved Flame Resistant Aircraft Window System, Federal Aviation Administration, DOT/FAA/CT-8310, U.S. Department of Transportation, May 1984.

Heine, D., and Brenneman, J., "The Fire Test Results", The Airplane Pilot, Vol. 35, No. 10, October 1966, pp. 8-11, 18-19.

Knapp, S. C., Allemond, P., and Karney, D. H., Helicopter Crashworthy Fuel Systems and Their Effectiveness in Preventing Thermal Injury, U.S. Army Aeromedical Research Laboratory, ADA102198, Fort Rucker, Alabama, July 1981.

Marcy, J. F., A Study of Air Transport Passenger Cabin Fires and Materials, National Aviation Agency, National Aviation Facilities Experimental Center, Atlanta City, New Jersey, December 1965.

Mohler, S. R., "Air Crash Survival: Injuries and Evacuation - Toxic Hazards", Aviation, Space and Environment Medicine, January 1975, pp. 86-88.

This Document Provided by the ABBOTT AEROSPACE
TECHNICAL LIBRARY
ABBOTTAEROSPACE.COM

THIS DOCUMENT PROVIDED BY THE ABBOTT AEROSPACE
TECHNICAL LIBRARY
ABBOTTAEROSPACE.COM

Appendix A
Definitions

A.1 AIRCRAFT COORDINATE SYSTEMS AND ATTITUDE PARAMETERS

Aircraft Coordinates: Positive directions for velocity, accelerations, and force components and for pitch, roll, and yaw are illustrated in Figure A-1. When referring to an aircraft in any flight attitude, it is standard practice to use a basic set of orthogonal axes as shown in Figure A-1, with x, y, and z referring to the longitudinal, lateral, and vertical directions, respectively. Aircraft axes are not right-handed due to tradition.

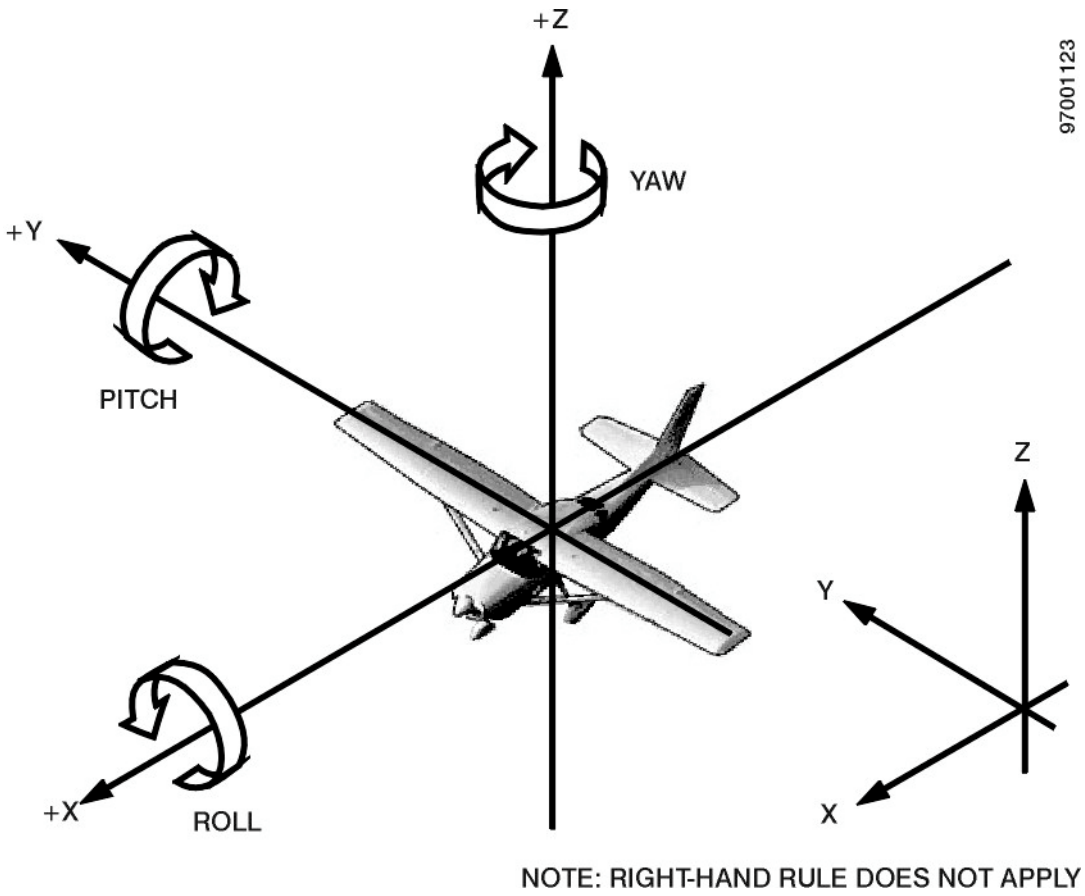


Figure A-1.
Aircraft coordinates and attitude directions.

THIS DOCUMENT PROVIDED BY THE ABBOTT AEROSPACE
TECHNICAL LIBRARY
ABBOTTAEROSPACE.COM

However, care must be exercised when analyzing ground impact cases where structural failure occurs, aircraft geometry changes, and reaction loading at the ground surface takes place. In the simulation of such impacts, it is often necessary to use more than one set of reference axes, including the earth-fixed system shown in Figure A-1 as X, Y, Z.

Attitude at Impact: The aircraft attitude, with respect to the aircraft coordinate system, at the moment of initial impact. The attitude at impact is stated in degrees of pitch, yaw, and roll (See Figure A-1). Positive and negative directions for yaw and pitch are indicated in Figure A-1.

Aircraft pitch is the angle between the aircraft's longitudinal axis and a horizontal plane. Pitch is considered positive when the nose of the aircraft points above the horizon and negative when it points below the horizon. Yaw is measured between the aircraft's longitudinal axis and the flight path. Roll is the angle between the aircraft lateral axis and the horizontal, measured in a plane normal to the aircraft's longitudinal axis.

Flight Path Angle: The angle between the aircraft's flight path and the local horizontal at the moment of impact (See Figure A-2).

Terrain Angle: The angle between the impact surface and the local horizontal, measured in a vertical plane (See Figure A-2).

Impact Angle: The angle between the flight path and the terrain, measured in a vertical plane. The impact angle is the algebraic sum of the flight path angle plus the terrain angle (See Figure A-2).

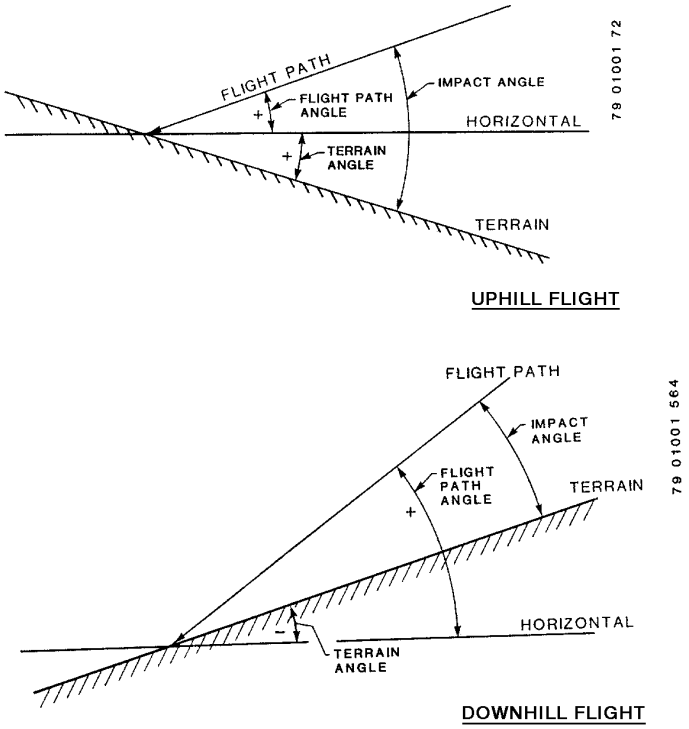


Figure A-2.
Impact angle calculation.

THIS DOCUMENT PROVIDED BY THE ABBOTT AEROSPACE
TECHNICAL LIBRARY
ABBOTTAEROSPACE.COM

A.2 ACCELERATION-RELATED TERMS

Acceleration: The rate of change of velocity. An acceleration is required to produce any velocity change, whether in magnitude or in direction. Acceleration may produce either an increase or a decrease in velocity. There are two basic types of acceleration: linear, which changes transitional velocity, and angular (or rotational), which changes angular (or rotational) velocity. With respect to crash impact conditions, unless otherwise specified, all acceleration values are those at a point approximately at the center of the floor of the fuselage or at the center of gravity of the aircraft.

Deceleration: Acceleration in a direction to cause a decrease in velocity.

Abrupt Acceleration: Accelerations of short duration primarily associated with crash impacts, ejection seat shocks, capsule impacts, etc. Abrupt accelerations are defined as having a total duration of less than 0.200 sec. In abrupt accelerations, the effects on the human body are limited to mechanical overloading (skeletal and soft tissue stresses).

The Term "G": The ratio of a particular acceleration (a) to the acceleration (g) due to gravitational attraction of the earth at sea level (32.2 ft/sec^2); G = a/g. This report will be consistent with common practice, and express acceleration G's. To illustrate, it is customarily understood that 5 G represents an acceleration of 5 x 32.2, or 161 ft/sec^2.

Rate of Onset: The rate of application of G's, expressed in G's per sec (the rate of change of acceleration). Sometimes referred to as the rise time of the crash pulse.

$$\text{Rate of onset} = \frac{\Delta G}{\Delta t} \quad \text{(G's per sec)}$$

A.3 VELOCITY-RELATED TERMS

Velocity Change in Major Impact (Δv): The decrease in velocity of the airframe during the major impact, expressed in feet per second (ft/sec). The major impact is the one in which the highest forces occur, and is not necessarily the initial impact. For the acceleration pulse shown in Figure A-3, the major impact should be considered ended at time t_2. Elastic recovery in the structure will tend to reverse the direction of the aircraft velocity prior to t_2. Should the velocity actually reverse, its direction must be considered in computing the velocity change. For example, an aircraft impacting downward with a vertical velocity component of 30 ft/sec and rebounding with an upward component of 5 ft/sec should be considered to experience a velocity change of

$$\Delta v = 30 - (-5) = 35 \text{ ft/sec}$$

during the major impact.

THIS DOCUMENT PROVIDED BY THE ABBOTT AEROSPACE
TECHNICAL LIBRARY
ABBOTTAEROSPACE.COM

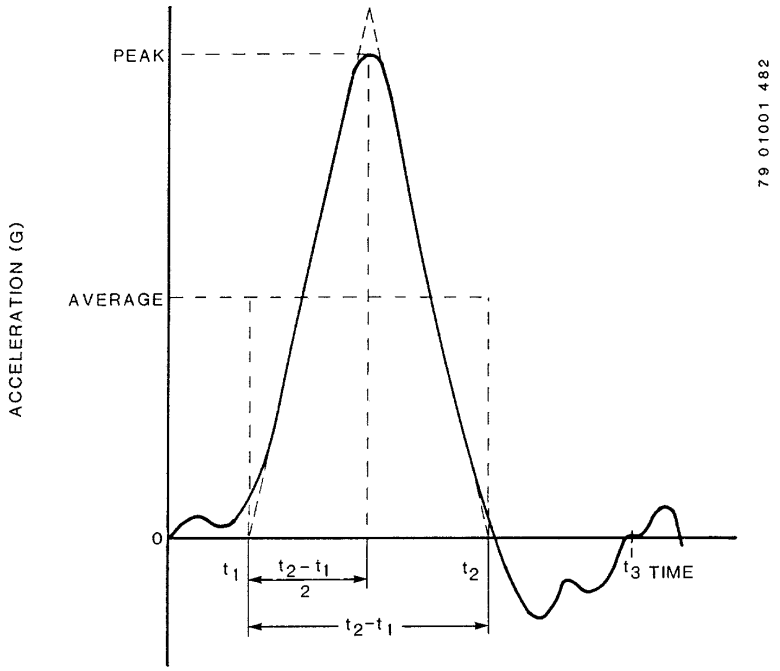


Figure A-3.
Typical aircraft floor acceleration pulse.

Longitudinal Velocity Change: The decrease in velocity during the major impact along the longitudinal (roll) axis of the aircraft. The velocity may or may not reach zero during the major impact. For example, an aircraft impacting the ground at a forward velocity of 100 ft/sec and slowing to 35 ft/sec would experience a longitudinal velocity change of 65 ft/sec during this impact.

Vertical Velocity Change: The decrease in velocity during the major impact measured along the vertical (yaw) axis of an aircraft. The vertical velocity generally reaches zero during the major impact and may reverse if rebound occurs.

Lateral Velocity Change: The decrease in velocity during the major impact measured along the lateral (pitch) axis of the aircraft.

A.4 FORCE TERMS

Load Factor: A crash force can be expressed as a multiple of the weight of an object being accelerated. A crash load factor, when multiplied by a weight, produces a force which can be used to establish ultimate static strength (see Static Strength). The load factor is expressed in G's.

Forward Load: Loading in a direction toward the nose of the aircraft, parallel to the longitudinal (roll) axis of the aircraft.

Aftward Load: Loading in a direction toward the tail of the aircraft, parallel to the longitudinal (roll) axis of the aircraft.

Downward Load: Loading in a downward direction parallel to the vertical (yaw) axis of the aircraft.

THIS DOCUMENT PROVIDED BY THE ABBOTT AEROSPACE
TECHNICAL LIBRARY
ABBOTTAEROSPACE.COM

Upward Load: Loading in an upward direction parallel to the vertical (yaw) axis of the aircraft.

Lateral Load: Loading in a direction parallel to the lateral (pitch) axis of the aircraft.

Combined Load: Loading consisting of components in more than one of the directions described in Section A.1.

Crash Force Resultant: Assuming there are no lateral forces acting on the plane, it is the geometric sum of the horizontal and vertical crash forces: horizontal and vertical velocity components at impact, and horizontal and vertical stopping distances. The crash force resultant is fully defined by the determination of both its magnitude and its direction. The algebraic sign of the resultant crash force angle is positive when the line of action of the resultant is above the horizontal, and negative if the line of action is below the horizontal. (See Figure A-4.)

Crash Force Angle: The angle between the resultant crash force and the longitudinal axis of the aircraft. For impacts with little lateral component of force, the crash force angle is the algebraic sum of the crash force resultant angle plus the aircraft pitch angle. (See Figure A-4.)

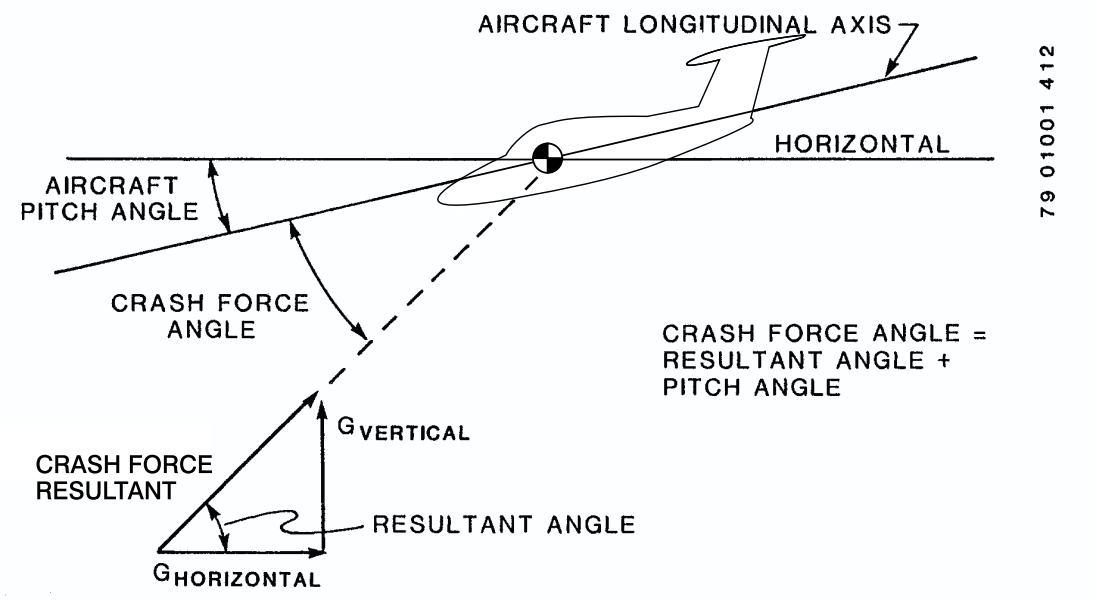


Figure A-4.
Crash force angle calculation.

A.5 DYNAMICS TERMS

Primary Impact: The impact experienced by the vehicle. Generally, in airplanes, the impact between the airplane and the ground. Can also mean the part of the crash with the largest vehicle acclerations.

Secondary Impact: An impact between an occupant and the interior of the vehicle.

THIS DOCUMENT PROVIDED BY THE ABBOTT AEROSPACE
TECHNICAL LIBRARY
ABBOTTAEROSPACE.COM

Tertiary Impact: Impacts that occur inside an occupant, typically between an organ such as the brain and bony structure like the skull.

Rebound: A rapid return toward the original position upon release or rapid reduction of the deforming load, usually associated with elastic deformation.

Dynamic Overshoot: The amplification of decelerative force on cargo or personnel above the floor input decelerative force (the ratio of output to input). This amplification is a result of the dynamic response of the system.

Transmissibility: The amplification of a steady-state vibrational input amplitude (the ratio of output to input). Transmissibilities maximize at resonant frequencies and may increase acceleration amplitude similar to dynamic overshoot.

A.6 CRASH SURVIVABILITY TERMS

Survivable Accident: An accident in which the forces transmitted to the occupant through the seat and restraint system do not exceed the limits of human tolerance to abrupt accelerations. In addition, the structure in the occupant's immediate environment remains substantially intact to the extent that a livable volume is provided for the occupants throughout the crash sequence. Traditionally, whether or not an accident was survivable was based on an accident investigator's *opinion* regarding if the occupants should have survived. Design for crashworthiness places the responsibility on the designer to choose the level of survivability.

Survivable Envelope: The range of impact conditions, including magnitude and direction of crash pulses and duration of forces occurring in an aircraft accident, wherein the occupiable area of the aircraft remains substantially intact, both during and following the impact, and the forces transmitted to the occupants do not exceed the limits of human tolerance when current state-of-the-art restraint systems are used.

It should be noted that, where the occupiable volume is altered appreciably through elastic deformation during the impact phase, survivable conditions may not have existed in an accident that, from post-crash inspection, outwardly appeared to be survivable.

Flail Envelope: The extent of space surrounding a restrained occupant defined by the flailing of extended body parts during a crash impact of the aircraft. Parts of the body may strike objects located within this envelope. Some regions of the flail envelope, like that in front of the occupant within ±10 degrees of yaw relative to the ariplane, have a higher probability of flail due to the the direction of travel in small airplanes.

A.7 OCCUPANT-RELATED TERMS

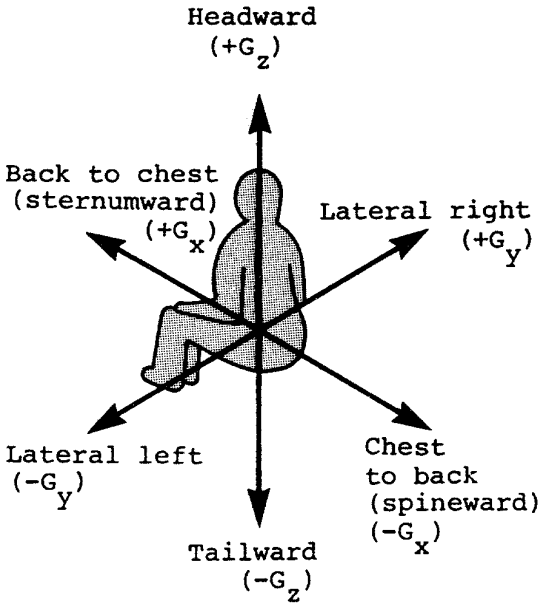
Human Body Coordinates: In order to minimize the confusion sometimes created by the terminology used to describe the directions of forces applied to the body, a group of NATO scientists compiled the accelerative terminology table of equivalents shown in Figure A-5 (Reference A-1). The terminology used throughout this guide is compatible with the NATO terms as illustrated.

Anthropomorphic Test Dummy (ATD): A device designed and fabricated to represent not only the appearance of humans but also the mass distribution, joint locations, motions, geometrical similarities such as flesh thickness and load/deflection properties, and relevant skeletal configurations such as iliac crests, ischial tuberosities, the rib cage, etc. Attempts are

THIS DOCUMENT PROVIDED BY THE ABBOTT AEROSPACE
TECHNICAL LIBRARY
ABBOTTAEROSPACE.COM

also made to simulate human dynamic response of major structural assemblages such as thorax, spinal column, neck, etc. The ATD is strapped into seats or litters and used to simulate a human dynamic occupant in dynamic tests.

Headform: A device used to ensure protection of the occupant in interior impact. The headform is the head of a Hybrid III test dummy which has had the skullcap removed for the installation of a propulsion shaft. The headform can be thrust into interior surfaces to measure loads and reactions.



Direction of accelerative force

Vertical

Headward - Eyeballs-down
Tailward - Eyeballs-up

Transverse

Lateral right	- Eyeballs-left
Lateral left	- Eyeballs-right
Back to chest	- Eyeballs-in
Chest to back	- Eyeballs-out

Note:

The accelerative force on the body acts in the same direction as the arrows.

Figure A-5.
Terminology for directions of forces on the body.

Injury Criteria: Injury criteria are the loading conditions for which a serious injury is likely for a given population. Injury criteria may be for the whole body or specific to a single body segment. Injury criteria may be single-point “go/no go” values in which a load magnitude and direction are specified, or they may be time-dependent and include time duration or load onset rate in addition to load magnitude and direction.

Whereas human tolerance is defined for an individual or for a particular type of injury, injury criteria are often used as an assessment of injury potential for a population. Injury criteria are often used to determine the potential for injury when a human surrogate is used in testing. In these cases, injury criteria may be the ATD loads which correspond to serious injury in the human.

Impact Tolerance: Impact tolerance is the human tolerance for an impact to a specific body segment.

Injury Scale: An injury scale is a quantitative or qualitative rating system for the severity of injury. Injury scales may assess the severity of a particular type of injury, the whole body injury severity, or the chance of survival.

THIS DOCUMENT PROVIDED BY THE ABBOTT AEROSPACE
TECHNICAL LIBRARY
ABBOTTAEROSPACE.COM

Head Injury Criterion: The numeric value used to determine the severity of injury to the head. The value is based on the resultant linear acceleration of the center of gravity of the head, during a specified time interval. Mathematically, HIC is defined as

$$HIC = \max_{T0 \le t_1 \le t_2 \le TE} \left[\frac{1}{t_2 - t_1} \int_{t_1}^{t_2} R(t)dt \right] (t_2 - t_1)$$

Where: **T0** is the beginning of the head impact,
TE is the end of the head impact,
R(t) is the head acceleration,
$\mathbf{t_1}$ and $\mathbf{t_2}$ are the initial and final times of the calculation (in sec), such that the HIC is a maximum value.

The maximum time interval (TO to TE) used in avation testing is often 50 ms which is defined in the rotorcraft regulations (14 CFR Parts 27 & 29). The maximum time interval used in the automotive industry for airbag testing is 36 ms or less.

Human Tolerance: For the purposes of this document, human tolerance is defined as the load on an individual at which it is believed that serious injury is likely. As used in this volume, designing for the limits of human tolerance refers to designing features that will maintain conditions at or below tolerable levels, enabling the occupant to survive the given impact.

The tolerance of the human body to impact is a function of many variables, including the unique characteristics of the individual person, as well as the loading variables. Human tolerance values are, therefore, often specific to an individual and to a loading scenario. Loading parameters include magnitude, direction, duration, rate of onset, location, and distribution of loading. The loads applied to the body include decelerative loads imposed by seats and restraint systems, as well as localized forces due to impact with surrounding structure.

Submarining: The rotation of the hips under and about the lap belt as a result of a forward inertial load exerted by deceleration of the thighs and lower legs, accompanied by lap belt slippage up and over the iliac crests. Lap belt slippage up and over the iliac crests can be a direct result of the upward pull of the shoulder harness straps at the middle of the lap belt.

Effective Weight: The portion of occupant weight supported by the seat with the occupant seated in a normal flight position. Since the weight of the feet, lower legs, and part of the thighs is carried directly by the floor through the feet, this is considered to be 80 percent of the occupant weight plus the weight of the headset/helmet and any equipment worn on the torso. Clothing, except for shoes, is included in the occupant weight.

Iliac Crest Bone: The upper, anterior portion of the pelvic (hip) bone. These ”inverted saddle” bones are spaced laterally about 1 ft apart. The lower abdomen rests between these crest bones.

THIS DOCUMENT PROVIDED BY THE ABBOTT AEROSPACE
TECHNICAL LIBRARY
ABBOTTAEROSPACE.COM

Anterior-Superior Iliac Spine: A bony prominence on the forward, upper portion of each iliac crest. Also known as the "ASIS." These projections help keep the lap belt on an adult occupant's pelvis, but are not present in children, thus making child restraint more difficult. The ASIS develops with the onset of puberty.

Ischial Tuberosities: Two bony prominences located in the lower, rearward region of the pelvis. These prominences support the pelvis and torso when the subject is in a seated position. Referred to by some as "perch bones" or "sit bones."

Cerebral Concussion: A brain injury that can range from mild (confusion, disorientation, no loss of consciousness), to severe (loss of consciousness, amnesia, possible contusions and fractures).

Lap Belt Tiedown Strap (also Negative-G Strap, Crotch Strap): A strap used to prevent the tensile force in shoulder straps from pulling the lap belt up when the restrained subject is exposed to the $-G_X$ (eyeballs-out) acceleration.

A.8 SEATING GEOMETRY

(NOTE: All definitions in Section A.8 may be seen in Figure A-6.)

Pilot Compartment View: The arrangement of interior components, free of glare and reflections, such that the pilot can safely taxi, takeoff, approach, land, and perform any maneuvers within the capabilities of the aircraft. (Reference A-2)

Horizontal Vision Line: A reference line passing through the Design Eye Position parallel to the true horizontal in the normal cruise position.

Line of Sight: A reference line from the Design Eye Position to the top of the glare shield.

Back Tangent Line: A straight line in the mid-plane of the seat passing tangent to the curvatures of a seat occupant's back when leaning back and naturally compressing the back cushion.

Buttock Reference Line: A line in the mid-plane of the seat parallel to the Horizontal Vision Line and tangent to the lowermost natural protrusion of a selected size of occupant sitting on the seat cushion.

Neutral Seat Reference Point (NSRP): The intersection of the Back Tangent Line and the Buttock Reference Line. The seat geometry and location are based on the NSRP. The NSRP is set with the seat in the nominal mid-position of the seat adjustment range. This seat position will place the 50th-percentile (seated height) man with his eye in the Design Eye Position.

Buttock Reference Point: A point 5.75 in. forward of the Seat Reference Point on the Buttock Reference Line. This point defines the vertical and longitudinal position of the approximate bottoms of the ischial tuberosities, thus, representing the lowest points on the pelvic structure and the points that will support the most load during downward vertical loading.

Heel Rest Line: The reference line parallel to the Horizontal Vision Line passing under the tangent to the lowest point on the heel in the normal operational position, not necessarily coincidental with the floor line.

THIS DOCUMENT PROVIDED BY THE ABBOTT AEROSPACE
TECHNICAL LIBRARY
ABBOTTAEROSPACE.COM

DISTANCE FROM DESIGN EYE POSITION TO VERTICAL PLANE OF NEUTRAL SEAT REFERENCE POINT FOR VARIOUS SEAT BACK ANGLES

SEAT BACK ANGLE (DEGREES)	"X" (INCHES)
10	7.7
10½	7.4
11	7.1
11½	6.9
12	6.6
12½	6.3
13	6.1
13½	5.8
14	5.5
14½	5.3
15	5.0

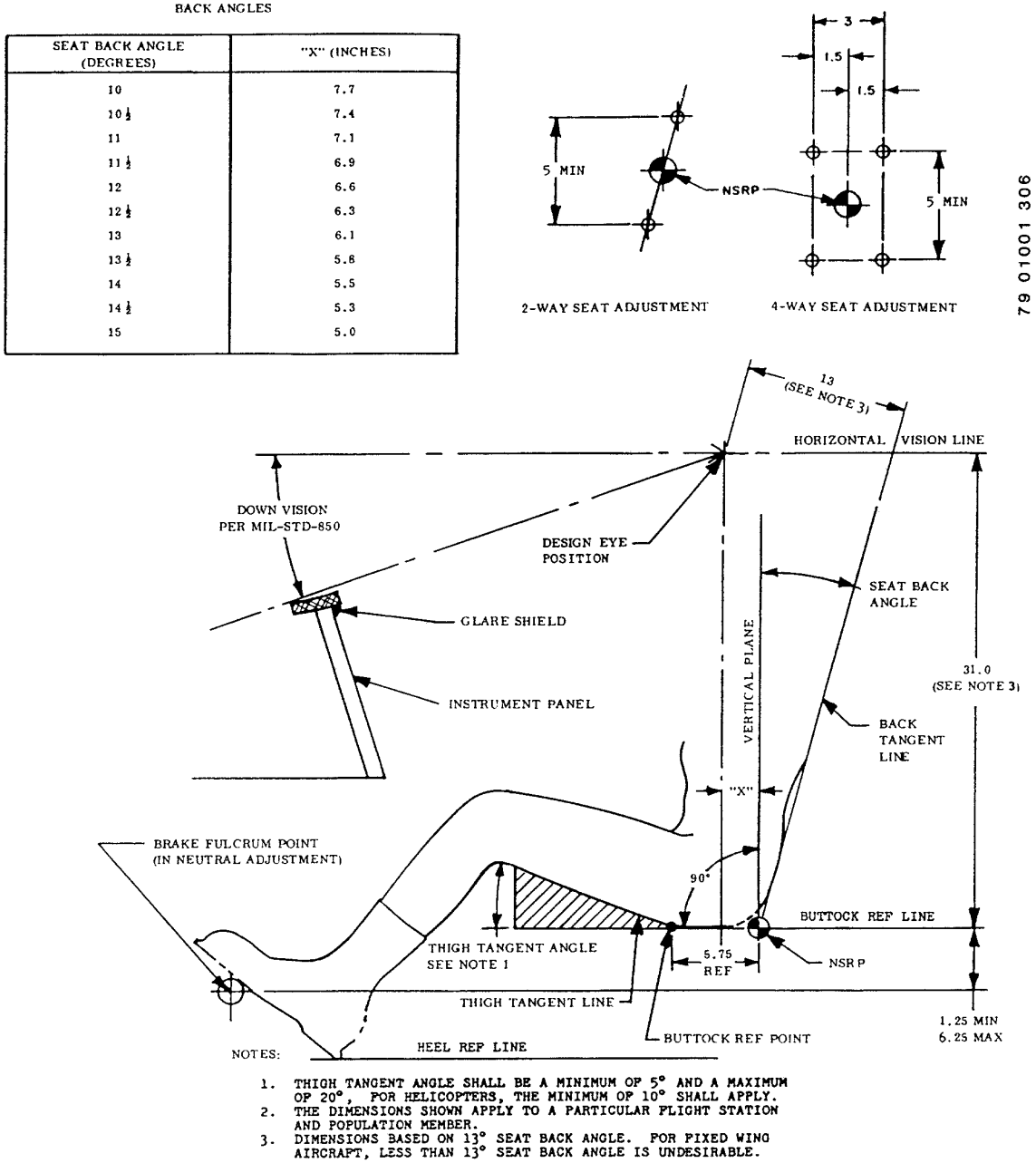


Figure A-6.
Seating Geometry. (Reference A-3).

A.9 STRUCTURAL TERMS

Airframe Structural Crash Resistance: The ability of an airframe structure to maintain a protective shell around the occupants during a crash and to minimize accelerations applied to the occupiable portion of the aircraft during crash impacts.

This Document Provided by the Abbott Aerospace
TECHNICAL LIBRARY
ABBOTTAEROSPACE.COM

Structural Integrity: The ability of a structure to sustain crash loads without collapse, failure, or deformation of sufficient magnitude to: (1) cause injury to personnel or (2) prevent the structure from performing as intended.

Static Strength: The maximum static load which can be sustained by a structure, often expressed as a load factor in terms of G (see Load Factor, Section 2.4). Also known as ultimate static load.

Strain: The ratio of change in length to the original length of a loaded component.

Collapse: Deformation or fracture of structure to the point of loss of useful load-carrying ability or useful volume.

Failure: Loss of load-carrying capability, usually referring to structural linkage rupture or collapse.

Fatigue: Weakness in a metal that is caused by prolonged stress.

Limit Load: In a structure, limit load refers to the load the structure will carry before yielding. Similarly, in an energy-absorbing device, it represents the load at which the device deforms in performing its function.

Load Limiter, Load-Limiting Device, or Energy Absorber: These are interchangeable names of devices used to limit the load in a structure to a pre-selected value. These devices absorb energy by providing a resistive force applied over a deformation distance without significant elastic rebound.

Specific Energy Absorbed (SEA): The energy absorbed by an energy-absorbing device or structure divided by its weight.

Bottoming: The exhaustion of available stroking distance accompanied by an increase in force, e.g., a seat stroking in the vertical direction exhausts the available distance and impacts the floor. With respect to energy-absorbing structure, bottoming is a condition in which the deforming structure or material becomes compacted and the load increases rapidly with very little increased deformation. Bottoming usually results in an acceleration spike.

Bulkhead: A structural partition extending upward from the floor and dividing the aircraft into separate compartments. Seats can be mounted to bulkheads instead of the floor.

A.10 FUEL, OIL, AND HYDRAULIC SYSTEM TERMS

Crash-Resistant Fuel Tank: A fuel tank which, when filled to normal capacity with water, can be dropped from a height of 65 ft, impact a non-deforming surface, and not leak (Reference A-4).

Crash-Resistant Fuel System: A fuel system that is designed and built using proper Crash-Resistant Fuel Tank, Fuel Valves, and Self-Sealing Breakaway Valves.

Frangible Attachment: An attachment possessing a part that is designed to fail at a pre-determined location and/or load.

Bladder Tank: A flexible fuel tank, usually contained or supported by other more rigid structures.

Fuel Pump: A pump installed in the fuel system to move fuel. Usually located at one or more of the following places: the tank, the engine, or the interconnecting plumbing.

THIS DOCUMENT PROVIDED BY THE ABBOTT AEROSPACE
TECHNICAL LIBRARY
ABBOTTAEROSPACE.COM

Fuel Valve: Any valve, other than a self-sealing breakaway valve, contained in the fuel supply system, such as fuel shutoff valves, check valves, etc.

Self-Sealing Breakaway Valve: A valve, for installation in fluid-carrying lines or hoses, that will separate at a predetermined load and seal at one or both halves to prevent dangerous flammable fluid spillage.

A.11 IGNITION SOURCE CONTROL TERMS

Fire Curtain: A baffle made of fire-resistant material that is used to prevent spilled flammable fluids and/or flames from reaching ignition sources or occupiable areas.

Fire-Resistant Material: Material able to resist flame penetration for 5 min when subjected to a 2,000-^{o}F flame and still be able to meet its intended function. (Reference A-5)

Firewall: A partition capable of withstanding a 2,000-^{o}F flame over an area of 5 in.^{2} for a period of 15 min without flame penetration. (Reference A-5)

Flammable Fluid: Any fluid that ignites readily in air, such as hydrocarbon fuels and lubricants.

Flow Diverter: A physical barrier that interrupts or diverts the flow of a liquid.

Ignition Temperatures: The lowest temperature at which a flammable mixture will ignite when introduced into a specific set of circumstances.

Inerting: The rendering of an aircraft system or the atmosphere surrounding the system incapable of supporting combustion.

A.12 INTERIOR MATERIALS SELECTION TERMS

Auto-Ignition Temperature: The lowest temperature at which a flammable substance will ignite without the application of an outside ignition source, such as flames or sparks.

Flame-Resistant Material: Material that is self-extinguishing after removal of a flame. (Reference A-6)

Flashover: The sudden spread of flame throughout an area due to ignition of combustible vapors that are heated to their flash point.

Flash Point: The lowest temperature at which vapors above a combustible substance will ignite in air when exposed to flame.

Intumescent Paint: A paint that swells and chars when exposed to flames, thus providing additional insulation to the underlying structure.

Optical Density (DS): The optical density is defined by the relationship where T is the

$$D_S = \log \frac{100}{T}$$

percent of light transmission through a medium (e.g., air , smoke, etc.).

THIS DOCUMENT PROVIDED BY THE ABBOTT AEROSPACE
TECHNICAL LIBRARY
ABBOTTAEROSPACE.COM

A.13 DITCHING AND EMERGENCY ESCAPE TERMS

Brightness: The luminous flux emitted per unit of emissive area as projected on a plane normal to the line of sight. Measured in foot-lamberts.

Candela (cd): A unit of luminous intensity equal to 1/60 of the luminous intensity of one square centimeter of a blackbody surface at the solidification temperatures of platinum. Also called candle or new candle.

Class A Exit: A door, hatch, canopy, or other exit closure intended primarily for normal entry and exit.

Class B Exit: A door, hatch, or other exit closure intended primarily for service or logistic purposes (e.g., cargo hatches and rear loading ramps or clamshell doors).

Class C Exit: A window, door, hatch, or other exit closure intended primarily for emergency evacuation.

Cockpit Enclosure: That portion of the airframe that encloses the pilot, copilot, or other flight crew members. An aircraft may have multiple cockpits, or the cockpit may be physically integrated with the troop/passenger section.

Ditching: The landing of an aircraft on water with the intention of abandoning it.

Emergency Lighting: Illumination required for emergency evacuation and rescue when normal illumination is not available.

Exit Closure: A window, door, hatch, canopy, or other device used to close, fill, or occupy an exit opening.

Exit Opening: An opening provided in aircraft structure to facilitate either normal or emergency exit and entry.

Exit Release Handle: The primary handle, lever, or latch used to open or jettison the exit closure from the fuselage to permit emergency evacuation.

Foot-candle (fc): A unit of illuminance on a surface that is everywhere one foot from a uniform point source of light of one candela.

Foot-lambert (fl): A unit of photometric brightness or luminous intensity per unit emissive area of a surface in a given direction. One foot-lambert is equal to $1/\pi$ candela per square foot.

Illumination: The luminous flux per unit area on an intercepting surface at any given point. Measured in foot-candles.

THIS DOCUMENT PROVIDED BY THE ABBOTT AEROSPACE
TECHNICAL LIBRARY
ABBOTTAEROSPACE.COM

References

A-1. Gell, C. F., Table of Equivalents for Acceleration Terminology, Aerospace Medicine, Volume 32, No. 12, December 1961, pp. 1109-1111.

A-2. Federal Aviation Regulations Part 23.773 “Pilot Compartment View,” Federal Aviation Administration, Washington, D.C., October 1, 2001.

A-3. Military Standard, MIL-STD-1333B, Aircrew Station Geometry for Military Aircraft, Department of Defense, Washington, D.C., January 9, 1987.

A-4. Military Standard MIL-T-27422b, Tank, Fuel, Crash-resistant, Aircraft, Department of Defense, Washington, D.C., April 13, 1971.

A-5. “Flammability Tests,” FAA Advisory Circular AC23-2, Federal Aviation Administration, Washington, D.C., August 20, 1984.

A-6. Federal Aviation Regulations Part 23.853 “Passenger and Crew Compartment Interiors,” Federal Aviation Administration, Washington, D.C., October 1, 2001.

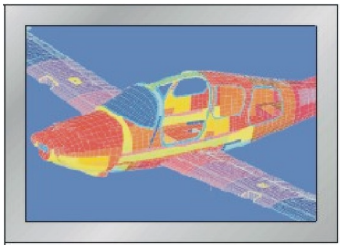
THIS DOCUMENT PROVIDED BY THE ABBOTT AEROSPACE
TECHNICAL LIBRARY
ABBOTTAEROSPACE.COM

Appendix B
General Aviation
Crashworthiness Design Evaluation

The General Aviation Crashworthiness Design Evaluation was originally presented at the AGATE Small Airplane Crashworthiness Design Seminar held in Phoenix, Arizona, during October of 2000. This evaluation is based on the Aircraft Crash Survivability Evaluation found in Appendix 1 of ADS-11B, “Survivability Program, Rotary-Wing” (U.S. Army Aviation Systems Command, St. Louis, Missouri, May, 1987, pp. 15-24), but was extensively modified to be applicable to modern light airplanes.

THIS DOCUMENT PROVIDED BY THE ABBOTT AEROSPACE
TECHNICAL LIBRARY
ABBOTTAEROSPACE.COM

This Document Provided by the Abbott Aerospace
TECHNICAL LIBRARY
ABBOTTAEROSPACE.COM



General Aviation Crashworthiness Design Evaluation

GENERAL AVIATION CRASHWORTHINESS DESIGN EVALUATION

When evaluating an aircraft from a crash-survival point of view, there are six basic factors that should be considered. These are:

1. Basic Airframe Crashworthiness
2. Crew Seats and Restraints
3. Passenger Seats and Restraints
4. Interior Crashworthiness
5. Post-Crash Fire Potential
6. Evacuation

In order to develop a reasonable Crashworthiness Design Evaluation, weighted values have been assigned to the various factors. The percentage of weight assigned to each is based on their relative hazard potential. The six factors, along with their hazard potential, are as follows:

Factors	Hazard Potential (%)	Optimum Number	Actual Value
1. Basic Airframe Crashworthiness	28	200	
2. Crew Seats and Restraints	21	150	
3. Passenger Seats and Restraints*	15	110	
4. Interior Crashworthiness*	8	60	
5. Post-Crash Fire Potential	21	155	
6. Evacuation	7	50	
Totals	100	725	

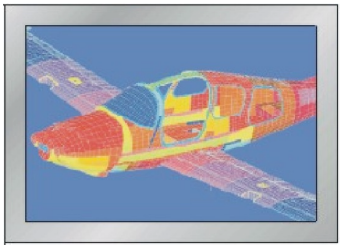
To make the job of rating easier, the hazard potential percentage has been converted to an optimum numerical value, where a perfect score on all six factors would equal 725. For the existing general aviation fleet, inadequate occupant compartment strength and inadequate restraints and seats have been identified as the two most frequent causes of injury and fatalities in accidents. Approximately 10 pct of general aviation accidents result in post-crash fire. In these accidents, the number of occupants fatally injured is disproportionately high. A poor score on any of these important items could indicate a critical situation from a crash-survival point of view, depending on such variables as the number of personnel carried, the operating terrain, and the available rescue facilities.

Each of the six main factors is, in turn, broken down into sub-factors against which a hazard potential percentage has been assigned and converted to an optimum numerical value. The person conducting the evaluation simply selects that portion of the optimum numerical value that each sub-factor is worth and lists it opposite the optimum value in the space provided under “Actual Value”.

*NOTE: For an aircraft without a passenger-carrying capability, the rating for Passenger Seats and Restraints is deleted and the rating for Interior Crashworthiness is reduced by 15 points. The optimum score for this type of aircraft is 600 points.

10016 South 51st Street,
Phoenix, AZ, USA 85044
Phone: 480.753.2000
Fax: 480.893.8643

This Document Provided by the Abbott Aerospace
TECHNICAL LIBRARY
ABBOTTAEROSPACE.COM



General Aviation Crashworthiness Design Evaluation

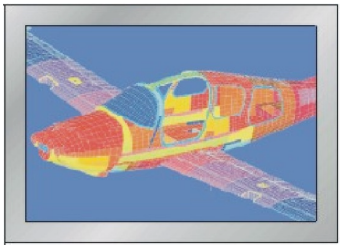
1. BASIC AIRFRAME CRASHWORTHINESS RATING		
	Optimum Number	**Actual Value**
Basic Airframe Configuration	25	
Airframe Energy Absorption	60	
Occupant Container Structural Integrity	50	
Anti-Plowing Structures	30	
Deformation and Failure Consequences	35	
Total Points	**200**	

2. CREW SEATS AND RESTRAINTS RATING				
	Optimum Value			**Actual Value**
	ABTS[1]	**ABTA[2]**	**Hybrid[3]**	
Vertical Energy Absorption Capacity of Seat	16	16	16	
Seat Vertical Strength	8	8	8	
Seat Longitudinal Strength	20	12	16	
Seat Lateral Strength	12	8	12	
Use of Ductile and/or Failure-Tolerant Materials in Stressed Areas	12	8	8	
Seat Adjuster Strength	8	8	8	
Accommodation of Airframe Distortion	12	4	12	
Belt Restraint Strength	16	16	16	
Belt Anchor Strength	8	16	8	
Lap Belt Geometry and Effectiveness	16	24	16	
Shoulder Belt Geometry and Effectiveness	16	24	24	
Inertia Reel Type	6	6	6	
Bonus Points	TBD	TBD	TBD	
Total Points	**150**	**150**	**150**	

[1]All Belts to Seat
[2]All Belts to Airframe
[3]Hybrid - Lap Belts to Seat / Shoulder Belts to Airframe

10016 South 51st Street,
Phoenix, AZ, USA 85044
Phone: 480.753.2000
Fax: 480.893.8643

THIS DOCUMENT PROVIDED BY THE ABBOTT AEROSPACE
TECHNICAL LIBRARY
ABBOTTAEROSPACE.COM



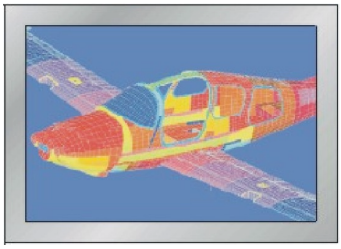
General Aviation Crashworthiness Design Evaluation

3. PASSENGER SEATS AND RESTRAINTS RATING		
	Optimum Number	**Actual Value**
Vertical Energy-Absorption Capacity of the Seat	18	
Vertical Strength	5	
Longitudinal Strength	10	
Lateral Strength	5	
Use of Ductile and/or Failure-Tolerant Materials in Stressed Areas	5	
Accommodation of Airframe Distortion	5	
Belt Restraint Strength	18	
Belt Anchor Strength	10	
Lap Belt Geometry	15	
Shoulder Belt Geometry	15	
Inertia Reel Type	4	
Bonus Points	TBD	
Total Points	**110**	

4. INTERIOR CRASHWORTHINESS RATING		
	Optimum Number	**Actual Value**
Crew Environment	25	
Passenger Environment	15	
Retention of Interior Equipment	10	
Delethalization	10	
Bonus Points	TBD	
Total Points	**60**	

10016 South 51st Street,
Phoenix, AZ, USA 85044
Phone: 480.753.2000
Fax: 480.893.8643

THIS DOCUMENT PROVIDED BY THE ABBOTT AEROSPACE
TECHNICAL LIBRARY
ABBOTTAEROSPACE.COM



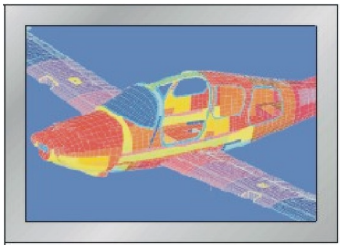
General Aviation Crashworthiness Design Evaluation

5. POST-CRASH FIRE POTENTIAL RATING		
Spillage Control	**Optimum Number**	**Actual Value**
Fuel Storage Location and Containment	35	
Oil Containment	5	
Flammable Fluid Lines	20	
Firewall	20	
Fuel Boost Pump Location and Type	10	
Fuel-Flow Interrupters	5	
Ignition Control		
Air Induction and Exhaust Location	15	
Location of Hot Metals and Shielding	10	
Engine Location and Tiedown Strength	15	
Battery Location and Tiedown Strength	5	
Electrical Wire Routing	5	
Locations of Lights	5	
Locations of Antennas	5	
Total Points	**155**	

6. EVACUATION RATING		
	Optimum Number	**Actual Value**
Ease and Reliability of Exit Operation	20	
Availability and Access to Exits	15	
Identification of Exits	5	
Availability of Exits in Rolled and/or Deformed Aircraft	10	
Total Points	**50**	

10016 South 51st Street,
Phoenix, AZ, USA 85044
Phone: 480.753.2000
Fax: 480.893.8643

THIS DOCUMENT PROVIDED BY THE ABBOTT AEROSPACE
TECHNICAL LIBRARY
ABBOTTAEROSPACE.COM



General Aviation Crashworthiness Design Evaluation

EVALUATION CRITERIA

GENERAL

Each of the subfactors listed previously is discussed briefly on the following pages. In rating an aircraft, the subfactors should be given a point value proportional to the desirable qualities outlined in the discussion.

1. BASIC AIRFRAME CRASHWORTHINESS

Basic Airframe Configuration **Optimum = 25**

The choice of the general layout of the aircraft can have a profound influence on its crash performance. In general, low-wing aircraft perform better in a crash than high-wing aircraft. Additional features are required of high-wing aircraft to get optimum points:

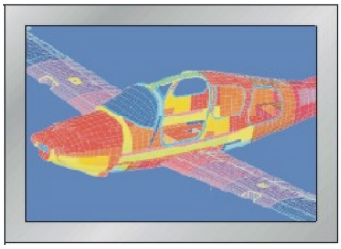
- Load transfer of wing mass to ground early in the crash event
  - By load-limiting in the wing root (like the Bell 609)
  - Through the landing gear mounted to the wing
  - Through the fuselage structure
- Maintaining occupant volume
  - Accommodate shear loads in the fuselage – high-mass, low ground reaction forces

For either configuration, the positioning of landing gear and their likely displacement in a crash can alter the crashworthy performance of the fuselage.

Suggested scoring for basic airframe configuration is shown in the following table.

Landing Gear Configuration	Low-wing	High-wing	Biplane	Canard
Tricycle	25	15	20	18
Taildragger	15	10	15	N/A

THIS DOCUMENT PROVIDED BY THE ABBOTT AEROSPACE
TECHNICAL LIBRARY
ABBOTTAEROSPACE.COM



General Aviation Crashworthiness Design Evaluation

Airframe Energy Absorption **Optimum = 60 points**

Nose/Engine Mount Energy Absorption

a) Frontal Impact (15 of the 60 total)

This item will obviously affect the crashworthiness of any aircraft as long as the crash force acts generally along the longitudinal axis. Thus, some method is needed to grossly evaluate the advantage of increased crushable structure forward of the seats. For most general-aviation-type aircraft, the cockpit and cabin must be considered as one unit.

The amount of crushable structure ahead of the passengers should logically be related to the airport approach speed of the aircraft, since most survivable accidents will occur at or less than this velocity. Thus, for an aircraft with a very slow stall/approach speed, the crushable structure needed can be less than for an aircraft with a very high approach/stall speed.

The optimum length of crushable structure or deforming distance can be calculated for various velocity changes by using the formula

$$d = \frac{V_1^2 - V_2^2}{64G}$$

Where:
$d =$ total deforming distance
$V_1 =$ aircraft impact velocity - ft/sec
$V2 =$ aircraft velocity after major impact - ft/sec
$G =$ fuselage crushing strength

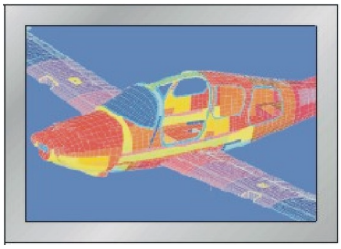
Experimental test results indicated that a 20-G fuselage crushing strength is a reasonable value. It is assumed that about 75 pct of fuselage structure is compressible longitudinally, while the remaining 25 pct is "incompressible". For purposes of this gross calculation, it seems reasonable to further assume that the terrain deformation offsets the "incompressible" portion of the fuselage. Thus, the calculated deforming distance (*d*) is assumed to be the length of the aircraft from its nose to the foot location of the front-seat occupants. The most severe crash is a complete stop from approach speed in a single pulse; for this situation, the term V_2 is 0 and the desired distance (*d*) can be computed for various approach (impact) velocities.

Scoring: Assume that the aircraft comes to rest during the major impact ($V_2 = 0$) measure distance d; reduce the value of d if more than 25 pct of the structure is "incompressible". Use a fuselage crushing strength of 20 G unless an alternative value of crushing strength is known. Calculate V_1 according to the above equation and score as follows:

$V_1 \geq$ aircraft stall speed (V_{so}) in ft/sec - 15 points
$V_1 \cong 0.8\ V_{so}$ - 10 points
$V_1 \cong 0.6\ V_{so}$ - 6 points
$V_1 < 0.5\ V_{so}$ - 0 points

10016 South 51st Street,
Phoenix, AZ, USA 85044
Phone: 480.753.2000
Fax: 480.893.8643

This Document Provided by the Abbott Aerospace
Technical Library
abbottaerospace.com



General Aviation Crashworthiness Design Evaluation

b. Vertical Impact (20 of the 60 total)

In the vertical direction, energy absorption is highly desirable due to the lower limit of human tolerance in the vertical direction. The best designs will incorporate a structural floor with crushable material between the structural floor and the skin of the aircraft (a "crushable subfloor"). Landing gear on general aviation aircraft provide relatively little energy absorption in a typical crash, because of their low "stroke load" and/or due to the landing gear's prevalence to fail on impact. The crushing material in the fuselage should be designed to crush at approximately 25 G over the full crush distance. Greater crushing strength places high loads on structure and high-mass items. Lower crushing strength requires long crush distances, and aircraft structure may be easily damaged in a "plowing" situation, thus contributing to shorter stopping distances.

Score the vertical energy absorption as follows:

Rigid floor with 9-in. crushable subfloor	20 points
Rigid floor with 6-in. crushable subfloor	15 points
Rigid floor with 3-in. crushable subfloor	10 points
Deformable fuselage/floor structure of 3-in. depth	5 points
Fuselage honeycomb panel or stiffened skin less than 1 in. in thickness	0 points

c. Nose-down Impact (25 of the 60 total)

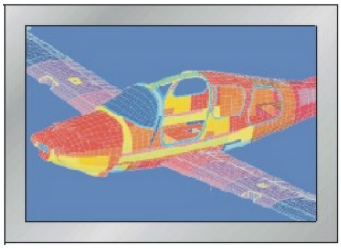
One of the most common crash scenarios for general aviation aircraft is a pitched-down impact in which the nose contacts the ground first. During this principal impact, the fuselage has to sustain the contact loads, while the aircraft rights itself so it can "slide out" the crash. The contact forces during the principal impact tend to crush the undersurface of the fuselage on the forward portion of the aircraft and drive that forward portion of the aircraft upward and backward toward the occupied area.

Energy absorption in the nose area is intended to manage the impact loads of the aircraft. For aircraft designs with the engine located in this area, energy absorption can take the form of a compressive, load-limited strut that allows the engine mount and engine to deform upward under a controlled load without failing (and thus being driven back into the occupied area). A design of this type can also help reduce failure of high-mass items located elsewhere in the fuselage structure and minimize the "slap down" of the rear fuselage.

In scoring this parameter, consider the effect of a crash with a -30-deg impact angle with the aircraft aligned with the impact vector. Optimum scoring would be given to an aircraft design with inherent energy-absorbing devices or structures that can manage the impact forces from the -30-deg condition.

Energy-absorbing engine mount and/or structure aligned with the –30-deg impact vector	25 points
Continuous keel beams or structures extending forward to the front of the structure	15 points
Sled-type engine mount with struts extending to the upper area of the firewall. Struts should be capable of sustaining dynamic compressive loads without failure.	7 points
Engine mount attached to firewall with aerodynamic cowling on underside of engine	0 points

This Document Provided by the Abbott Aerospace
Technical Library
abbottaerospace.com



General Aviation Crashworthiness Design Evaluation

Occupant Container Structural Integrity **Optimum = 50 points**

General:

This section evaluates the structural integrity of the fuselage in resisting crash loads that are induced throughout the structure during the impact. The type and magnitude of the crash loads depends upon the direction of the crash, the impact velocity, and the structural design concept. Four different types of impact-induced loading conditions are evaluated below.

a. Resistance to Longitudinal Impact Loads (15 of the 50 total) **Optimum = 15 points**

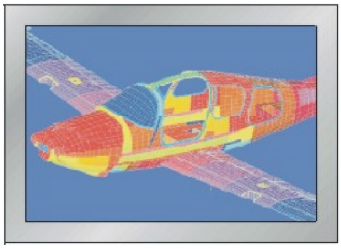
The evaluator should think of the fuselage as a tubular structure with masses concentrated at various locations. This tube should be able to sustain an impact on the end parallel to the fuselage axis without release of the massive items (engines, wings, seats, baggage, etc.). The optimum structure would resist these loads without diminishing the occupied volume or deforming in a way that releases attached items (such as seats). A monocoque structure that maintains a round or oval shape is ideal. This is because the longitudinal loading (primarily compressive) can be shared through the entire structure. However, the evaluator should examine the fuselage "splices" that are likely to fail during compression of the fuselage. This is especially important for longer-body general aviation aircraft. An alternative design, consisting of continuous beams running from the nose of the aircraft under the floor for the entire length of the occupied section, is good, but somewhat less desirable, since the longitudinal loads are carried by a relatively small portion of the structure.

b. Resistance to Vertical Impact Loads (15 of the 50 total) **Optimum = 15 points**

Resistance to vertical impact loads is usually very good in low-wing designs since no heavy components are located above the seated occupants. High-wing aircraft, however, can be more hazardous, because the entire weight of the wing structure, fuel, and engines (two-thirds of the aircraft weight) is pressing downward at one point on the fuselage that is not designed for such a loading. High-wing aircraft with fuselage-mounted landing gears (which have fuselage reinforcement to sustain normal landing loads) are generally more resistant to vertical crash forces than high-wing aircraft with wing-mounted landing gears.

The structure must be evaluated in terms of its resistance to vertical impact loads. If the engine and transmission are located over the cabin or just aft of the cabin, it is recommended that the design tiedown strength be not less than 20 G in the longitudinal and vertical directions in order to prevent cabin penetration. Regardless of tiedown strength, the fuselage shell should contain peripheral frames at a spacing not to exceed 20 in. in order that a maximum amount of energy is absorbed before a mass will penetrate the structure.

THIS DOCUMENT PROVIDED BY THE ABBOTT AEROSPACE
TECHNICAL LIBRARY
ABBOTTAEROSPACE.COM



General Aviation Crashworthiness Design Evaluation

c. Resistance to Lateral and Rollover Impact Loads (10 of the 50 total) **Optimum = 10 points**

Typical general aviation aircraft are not designed to resist primary impact forces on the top or sides of the fuselage. There is very little energy absorption capability in these areas other than the crushing of the fuselage into the occupied areas. Thus, it is not necessary to evaluate the capability of the structure to withstand primary impact loads on the top or sides. There are, however, a sizeable percentage of accidents that cartwheel, flip end-over-end, or roll (typically after wing separation). The fuselage should be capable of sustaining up to 4 G distributed static loading on the sides or top of the aircraft without a reduction of the occupied volume by more than 15 pct. Better designs will allow the load to be distributed over a substantial surface area to give redundancy in case of structural deformation from the primary impact. Fewer points are awarded for designs in which the load is applied to a small surface (point loading).

Scoring for this category should be done as follows:

Minimum 4-G Load-Bearing Capability	10 points
Minimum 3-G Load-Bearing Capability	5 points
2-G Load-Bearing Capability	2 points

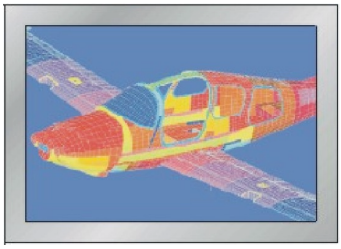
d. Resistance to Airframe Bending Loads (10 of the 50 total) **Optimum = 10 points**

A relatively frequent crash scenario for general aviation aircraft is a nose-down (0 to -30 deg) impact at, or just below the aircraft stalling speed. Under these impact conditions, the fuselage structure is placed in bending and occupant compartment intrusion can occur due to roof or sidewall buckling. Plastic hinges in the structure can also occur, typically just forward of the cabin doors. The buckling and plastic hinges are transient and can be difficult to detect in the crash wreckage.

The best airframe designs resist these bending loads and potential occupant compartment intrusion through several paths, notably the sidewalls (in bending), the floor (in tension), and the roof structure (in compression). These load paths can be compromised in many aircraft by the placement of the door openings, which reduce the contribution of the sidewall structure, or by thin windshield surround or roof structure, which doesn't allow as much load to be carried above. Bending loads can be carried solely by the floor structure, but these designs usually carry a weight penalty. Optimum points should be awarded for designs that resist bending through the roof, floor, and sidewalls. Fewer points are given for designs that compromise these paths.

10016 South 51st Street,
Phoenix, AZ, USA 85044
Phone: 480.753.2000
Fax: 480.893.8643

This Document Provided by the Abbott Aerospace
Technical Library
abbottaerospace.com



General Aviation Crashworthiness Design Evaluation

Anti-Plowing Structures **Optimum = 30 points**

General:

The purpose of anti-plowing structures is two-fold:

- To prevent large decelerations caused by aircraft structure digging into and accelerating a mass of soil.
- To change the direction of the airplane's velocity to reduce the interaction with the ground and to increase the stopping distance.

The designer should address the following areas:

a. Aircraft Skin on the Lower Cowl and Belly (10 of the 30 total) **Optimum = 10 points**

The bottom of the aircraft should be smooth and be tough enough to resist punctures from objects on the ground and from structure in the airplane. Panel junctions should also overlap like shingles for several inches to prevent a leading edge from snagging the dirt. Ductile aluminum or steel sheet of sufficient thickness does well in this area. Kevlar, Kevlar-blended composites, and fiberglass composites also work well.

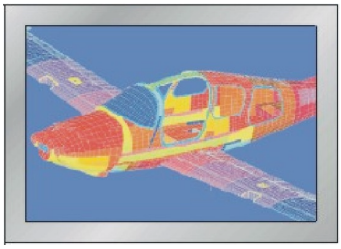
b. Crush Zone (10 of the 30 total) **Optimum = 10 points**

The region for crushing should be evaluated for possible soil scooping or digging after the region has deformed. The landing gear - especially the nose gear on fixed-gear airplanes - and engine mounts should be included in the crush zone analysis. Optimum points are given for designs that are anticipated to maintain a smooth, non-snagging surface.

c. Shape of the Aircraft Bottom (10 of the 30 total) **Optimum = 10 points**

Aircraft with a pronounced rocker (curvature from nose to tail) tend to dig into soil less than aircraft with flat bottoms. Optimum points are given to aircraft with a "ski-tip" type nose and curvature that continues to aft of the occupant compartment. Low or no points are given to aircraft with downward-pointing noses and flat bottoms.

This Document Provided by the Abbott Aerospace
Technical Library
abbottaerospace.com



General Aviation Crashworthiness Design Evaluation

Deformation and Failure Consequences **Optimum = 35 points**

General:

Certain modes of structural failure that are typical in general aviation aircraft can influence the occupant's chance for survival. In this section, three of these failure modes are evaluated.

a. Landing Gear Location (5 of the 35 total) **Optimum = 5 points**

Evaluate the damage that will be caused by this item as it is displaced during a crash. For example, if the gear is located directly under the cabin floor, the probability of its being driven upward into the occupiable area must be evaluated. No consideration need be given to the proximity of ignition sources or fuel storage to the landing gear, since these items are evaluated under Post-Crash Fire Potential.

b. Effect of Wing Separation on Cabin Occupants (15 of the 35 total) **Optimum = 15 points**

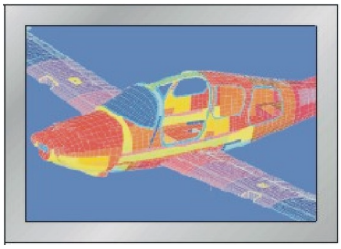
Evaluate as to whether the tearing away of the wing will be hazardous to the cabin occupants. The complete separation of the wing structure without effect on the seat occupants illustrates acceptable performance in this respect. Ideally, failure of the wing structure would not intrude on the occupied areas or tear the fuselage structure. The failure of the wing should not disrupt energy-absorbing features in the subfloor or seats, as can happen with a main spar that runs through the occupied areas.

c. Engine Retention / Location (15 of the 35 total) **Optimum = 15 points**

Retention of the engine is most critical when it can enter the occupied areas of the aircraft. This can occur for engine locations above the occupied areas, above and behind the occupied areas, or behind the occupied areas. The engine mounts and fuselage structure need to resist the inertial loads generated by the engine during the crash. Engines located in front of the occupied areas can also be driven backwards by crash forces. For front-mounted engines, the structure (firewall) should resist intrusion into the occupied areas. Optimum score would be given for designs that minimize intrusion of the engine into the occupied areas in the –30-deg angle condition.

10016 South 51st Street,
Phoenix, AZ, USA 85044
Phone: 480.753.2000
Fax: 480.893.8643

THIS DOCUMENT PROVIDED BY THE ABBOTT AEROSPACE
TECHNICAL LIBRARY
ABBOTTAEROSPACE.COM



General Aviation Crashworthiness Design Evaluation

2. CREW SEATS AND RESTRAINTS RATING

General:

In these sections, the seating position terms "crew" and "passengers" refer to a conventional two- to six-place light aircraft in which there are two seats per row. The front-row occupants are in the crew positions, and any occupants aft of the front row are considered to be in the passenger positions.

For dual-control tandem seating, evaluate both positions using the crew section. For single-control tandem seating, evaluate the pilot position as crew and the other position as passenger regardless of which position is forward.

All belt restraint systems used in new designs must meet the requirements of TSO-C114 and AS8049. Belt restraints meeting these standards do not necessarily guarantee that the seat/restraint system will pass the dynamic requirements of 14 CFR 23.562. Developmental tests or modeling may be needed to demonstrate performance prior to certification.

The following abbreviations will be used to describe the belt restraint load path.

- **ABTS** - All Belts to Seat - The lap belt, shoulder belt, and tie-down strap all anchor to the seat structure. Belt restraint loads are carried by the seat structure into the airframe.
- **ABTA** - All Belts to Airframe - The lap belt and shoulder belt all anchor directly to the airframe.
- **Hybrid** - In this system, the lap belt (and tie-down strap) anchor to the seat structure, and the shoulder belt anchors to the airframe.

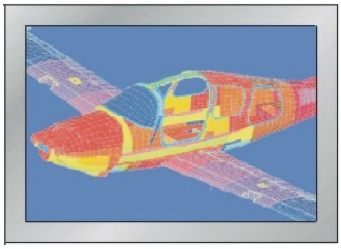
Vertical Energy Absorption Capacity — **Optimum = 16 points** (For all seat types)

Some method should be provided in the seat structure to attenuate vertical impact forces to a value of less than 1,500 lb as a measured in the pelvic/lumbar load cell of the anthropomorphic test device (ATD, a.k.a. test dummy). This decelerative loading must be maintained through a minimum stroke of 3 in. in order to offer protection in the majority of fixed-wing aircraft accidents. However, a stroke of 4 to 6 in. is highly desirable. The evaluator should consider whether possible structural deformation, storage of items beneath the seat, or occupant foot placement could impede the seat stroke.

The seat vertical energy-absorption capacity can be rated as follows:

	Points
A. A seat with a discrete energy-absorber having a minimum of 5 in. of stroke	16
B. An energy-absorbing seat meeting FAR Part 562 and having 3 in. of total stroke	12
C. A crushable, expanded-foam cushion or other energy-absorbing device meeting FAR Part 562 minimum requirements	8
D. A slow-rebound foam (Confor foam, “Ensolite”, or “Ethafoam”) of 4-in. thickness	4
E. Elastic foam rubber cushion or no attenuating material	0

This Document Provided by the Abbott Aerospace
TECHNICAL LIBRARY
ABBOTTAEROSPACE.COM



General Aviation Crashworthiness Design Evaluation

Seat Vertical Strength — **Optimum = 8 points** (For all seat types)

The seat should have sufficient vertical strength to allow it to stroke, i.e., attenuate vertical impact forces, in the presence of longitudinal and lateral crash forces. At the completion of the seat stroke, the seat should be able to support the occupant with vertical crash forces up to 25 G.

Seat Longitudinal Strength — **Optimum = ABTS - 20 points**
ABTA - 12 points
Hybrid - 16 points

The seat structure should be designed to withstand FAR Part 562 dynamic testing. Excessive forward deformation (elastic and/or plastic) that would increase the occupant strike hazard should be minimized. Give a maximum score for 1.5 in. or less of maximum forward deflection during the dynamic test. Deduct one-third of the score for each additional inch of maximum deflection, up to 4.5 in.

Seat Lateral Strength — **Optimum = ABTS - 12 points**
ABTA - 8 points
Hybrid - 12 points

In the lateral direction, the seat structure should withstand an applied static load of 4.5 G (i.e., 4.5 times the weight of the seat and occupant) with minimum deflection. Full points would be given for 2.0 in. of deflection or less. Deduct one-third of the score for each additional inch of maximum deflection up to 5.0 in. Aircraft with side bolsters or structure that limits seat lateral deflection may be evaluated as installed and not as a stand-alone seat.

Use of Ductile and/or Failure-Tolerant Materials in Stressed Areas — **Optimum = ABTS - 12 points**
ABTA - 8 points
Hybrid - 8 points

Seat structures should be designed with materials that can sustain deformation of fuselage and/or deflection due to occupant loads. The maximum score would be given for structures using materials with elongations greater than 10 pct, or for structures with built-in features to accommodate deformation. Castings are noted for their poor ductility. If castings are used in critically stressed areas, the rating should be 0, unless it is known that the casting material has been treated to ensure ductility.

Seat Adjuster Strength — **Optimum = 8 points** (For all seat types)

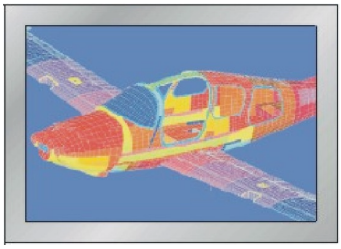
The seat fore-aft and vertical adjusters should be designed to withstand seat design loads without failure and without allowing seat motion. The adjuster should be designed to hold even when the seat has been deformed due to fuselage deformations.

Accommodation of Airframe Distortion — **Optimum = ABTS - 12 points**
ABTA - 4 points
Hybrid - 12 points

The seat should be designed to withstand ± 10 deg pitch / ± 10 deg roll per 23.562 (b)(3). A seat that can sustain this gets two-thirds of the total score. Full score should be given for seats that can withstand ± 15 deg pitch / ± 15 deg roll.

10016 South 51st Street,
Phoenix, AZ, USA 85044
Phone: 480.753.2000
Fax: 480.893.8643

THIS DOCUMENT PROVIDED BY THE ABBOTT AEROSPACE
TECHNICAL LIBRARY
ABBOTTAEROSPACE.COM



General Aviation Crashworthiness Design Evaluation

Belt Restraint Strength **Optimum = 16 points**
(For all seat types)

The webbing used in the restraint system must meet TSO-C114 and AS8043 requirements. The strength and width of the lap belt, shoulder strap, and tie-down strap are listed below:

Item	Width (in.)	Webbing Strength (lb)
Lap Belt	1.8	5,000
Shoulder Strap(s)	1.8	4,000
Belt Tie-down Strap	1.25	2,000

Each of the above factors on restraint-webbing can be rated as a percent of the total points as follows:

Item	Percent
Strength and width of lap belt	50
Strength and width of shoulder straps	50

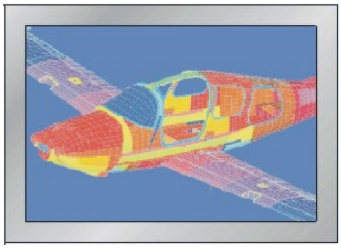
The strength is more important than the width of the webbing; therefore, the number of points allowed should be proportional to the strength values.

Belt Anchor Strength **Optimum = ABTS - 8 points**
ABTA - 16 points
Hybrid - 8 points

The shoulder harness and lap belt anchors should be designed to withstand 1.5 times the maximum load of the webbing attached to it, within a 30-deg angle in any direction from the normal position of the belt for a 50th-percentile male occupant. The strength requirement at angular deviations up to 30 deg may be relieved if the belt has a guide between the attachment and the occupant. In such cases, the guide should meet the strength and angular requirement.

10016 South 51st Street,
Phoenix, AZ, USA 85044
Phone: 480.753.2000
Fax: 480.893.8643

THIS DOCUMENT PROVIDED BY THE ABBOTT AEROSPACE
TECHNICAL LIBRARY
ABBOTTAEROSPACE.COM

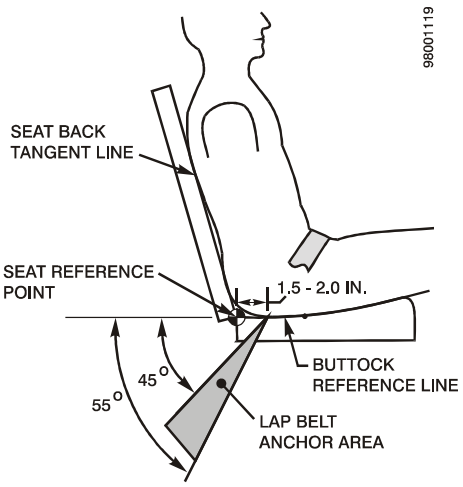


General Aviation Crashworthiness Design Evaluation

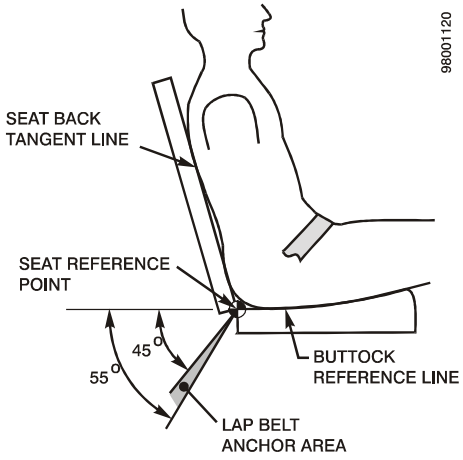
Lap Belt Geometry and Effectiveness

Optimum = ABTS - 16 points
ABTA - 24 points
Hybrid - 16 points

The lap belt should be designed to sit firmly on the bony portions of the pelvis without showing a tendency to ride up. The lap belt anchor location should comply with the optimum location shown below for belts with (five-point restraints) and without (three- and four-point restraints) tie-down straps. Any strap guides should be designed to minimize the crimping of the webbing during a crash.



Optimum three- or four-point geometry

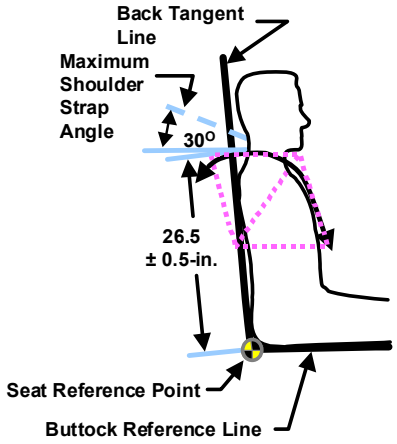


Optimum five-point geometry

Shoulder Belt Geometry and Effectiveness

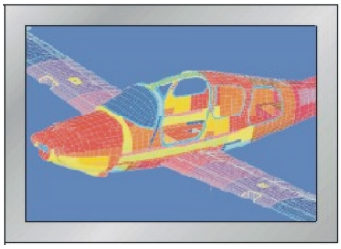
Optimum = ABTS - 16 points
ABTA - 24 points
Hybrid - 24 points

The shoulder belt strap guide should be located a minimum of 26 in. above the deflected seat cushion. If the shoulder harness is connected to structure aft of the seat back, the angle of the strap, with respect to the seat cushion, should be between 0 and 30 deg upward as illustrated. The width of the guide at the top of the seat back should not be more than 3.0 in.



10016 South 51st Street,
Phoenix, AZ, USA 85044
Phone: 480.753.2000
Fax: 480.893.8643

This Document Provided by the Abbott Aerospace
Technical Library
abbottaerospace.com



General Aviation Crashworthiness Design Evaluation

Inertia Reel Type **Optimum = 6 points**
(For all seat types)

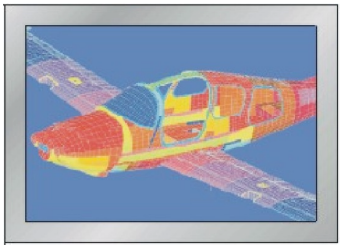
Inertia reels are convenience devices that allow the occupant more reach and comfort than fixed (manually adjusted) shoulder belts. Inertia reels, however, allow some belt movement during a crash. The inertia reel should be designed to minimize belt extension at the time of a crash. Full score would be given to rate-of-extension reels that lock between 0.5 and 1.5 G and vehicle-inertia-sensing reels that lock between 2.0 and 3.0 G. For positions without inertia reels, give 0 points if the pilot will have difficulty reaching instruments or controls, since he or she is then more likely to fly without the restraint or with the shoulder belt loosely adjusted.

Extra Credit

Five extra points may be given for dual-mode inertia reels (rate-of-extension and vehicle-inertia-sensing).

10016 South 51st Street,
Phoenix, AZ, USA 85044
Phone: 480.753.2000
Fax: 480.893.8643

This Document Provided by the Abbott Aerospace
TECHNICAL LIBRARY
ABBOTTAEROSPACE.COM



General Aviation Crashworthiness Design Evaluation

3. PASSENGER SEATS AND RESTRAINTS RATING

Vertical Energy-Absorption Capacity **Optimum = 18 points**

The same criteria used to evaluate the crew seats' vertical attenuation is also used here.

For the passenger seat, the vertical energy-absorption capacity can be rated as follows:

	Points
A. A seat with a discrete energy-absorber having a minimum of 5-in. of stroke	18
B. An energy-absorbing seat meeting FAR Part 562 and having 3 in. of total stroke	14
C. A crushable, expanded-foam cushion or other energy-absorbing device meeting FAR Part 562 minimum requirements	10
D. A slow-rebound foam (Confor foam, “Ensolite”, or “Ethafoam”) of 4-in. thickness	4
E. Elastic foam rubber cushion or no attenuating material	0

Seat Vertical Strength **Optimum = 5 points**

The seat should have sufficient vertical strength to allow it to stroke, i.e., attenuate vertical impact forces, in the presence of longitudinal and lateral crash forces. At the completion of the seat stroke, the seat should be able to support the occupant with vertical crash forces up to 25 G.

Seat Longitudinal Strength **Optimum = 10 points**

The seat structure should be designed to withstand FAR Part 562 dynamic testing. Optimum points are awarded for passenger seats designed and tested to the more stringent Part 562 crew seat test. Excessive forward deformation (elastic and/or plastic) that would increase the occupant strike hazard should be minimized. Give a maximum score for 1.5 in. or less of maximum forward deflection during the dynamic test. Deduct one-third of the score for each additional inch of maximum deflection, up to 4.5 in.

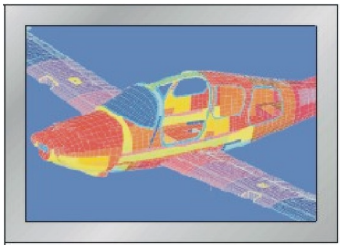
Seat Lateral Strength **Optimum = 5 points**

In the lateral direction, the seat structure should withstand an applied static load of 4.5 G (i.e., 4.5 times the weight of the seat and occupant) with minimum deflection. Full points would be given for 2.0 in. of deflection or less. Deduct one-third of the score for each additional inch of maximum deflection up to 5.0 in. Aircraft with side bolsters or structure that limits seat lateral deflection may be evaluated as installed and not as a stand-alone seat.

Use of Ductile and/or Failure-Tolerant Materials in Stressed Areas **Optimum = 5 points**

Seat structures should be designed with materials that can sustain deformation of fuselage and/or deflection due to occupant loads. The maximum score would be given for structures using materials with elongations greater than 10 pct or for structures with built-in features to accommodate deformation. Castings are noted for poor ductility. If castings are used in critically stressed areas, the rating should be 0, unless it is known that the casting material has been treated to ensure ductility.

THIS DOCUMENT PROVIDED BY THE ABBOTT AEROSPACE
TECHNICAL LIBRARY
ABBOTTAEROSPACE.COM



General Aviation Crashworthiness Design Evaluation

Accommodation of Airframe Distortion **Optimum = 5 points**

The seat should be designed to withstand ± 10 deg pitch / ± 10 deg roll per 23.562 (b)(3). A seat that can sustain this gets two-thirds of the total score. Full score should be given for seats that can withstand ± 15 deg pitch / ± 15 deg roll.

Belt Restraint Strength **Optimum = 18 points**
(For all seat types)

The webbing used in the restraint system must meet TSO-C114 and AS8043 requirements. The strength and width of the lap belt, shoulder strap, and tie-down strap are listed below:

Item	Width (in.)	Webbing Strength (lb)
Lap Belt	1.8	5,000
Shoulder Strap(s)	1.8	4,000
Belt Tie-down Strap	1.25	2,000

Each of the above factors on restraint-webbing can be rated as a percent of the total points as follows:

Item	%
Strength and width of lap belt	50
Strength and width of shoulder straps	50

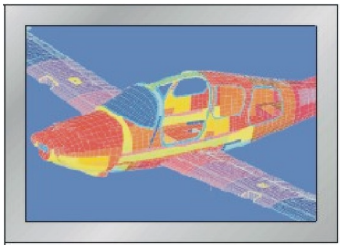
The strength is more important than the width of the webbing; therefore, the number of points allowed should be proportional to the strength values.

Belt Anchor Strength **Optimum = 10 points**

The shoulder harness and lap belt anchors should be designed to withstand 1.5 times the maximum load of the webbing attached to it, within a 30-deg angle in any direction from the normal position of the belt for a 50th-percentile male occupant. The strength requirement at angular deviations up to 30 deg may be relieved if the belt has a guide between the attachment and the occupant. In such cases, the guide should meet the strength and angular requirement.

10016 South 51st Street,
Phoenix, AZ, USA 85044
Phone: 480.753.2000
Fax: 480.893.8643

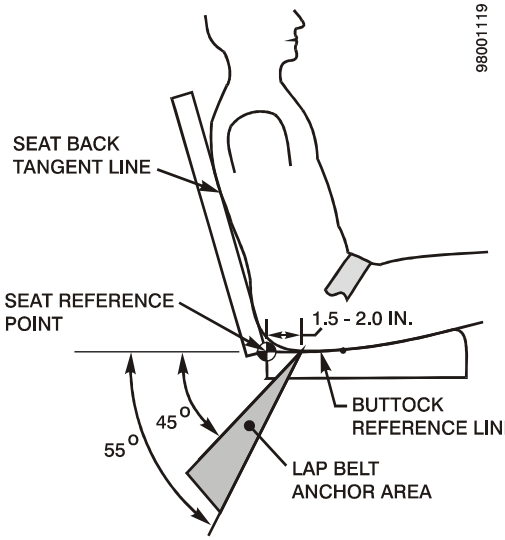
THIS DOCUMENT PROVIDED BY THE ABBOTT AEROSPACE
TECHNICAL LIBRARY
ABBOTTAEROSPACE.COM



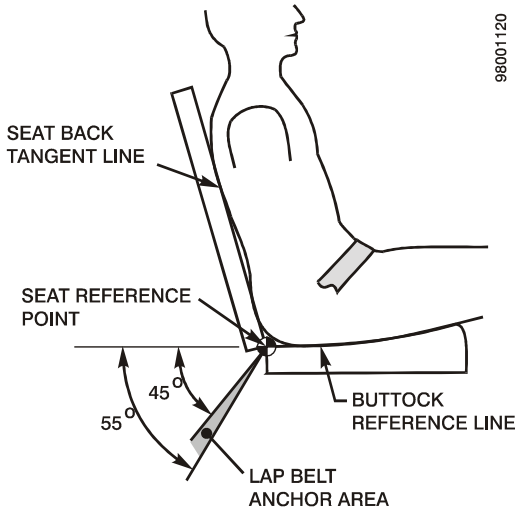
General Aviation Crashworthiness Design Evaluation

Lap Belt Geometry and Effectiveness **Optimum = 15 points**

The lap belt should be designed to sit firmly on the bony portions of the pelvis without showing a tendency to ride up. The lap belt anchor location should comply with the optimum location shown below for belts with (five-point restraints) and without (three- and four-point restraints) tie-down straps. Any strap guides should be designed to minimize the crimping of the webbing during a crash.



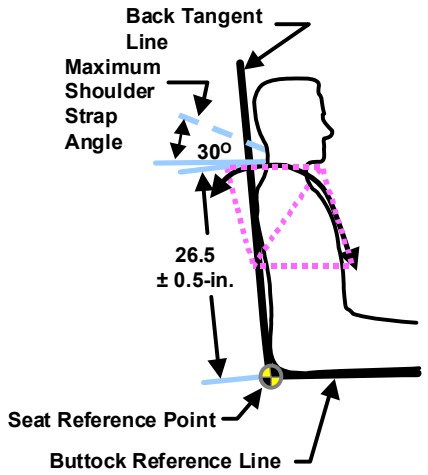
Optimum three- or four-point geometry



Optimum 5-point geometry

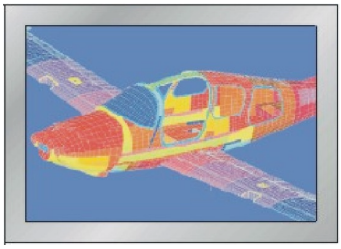
Shoulder Belt Geometry and Effectiveness **Optimum = 15 points**

The shoulder belt strap guide should be located a minimum of 26 in. above the deflected seat cushion. If the shoulder harness is connected to structure aft of the seat back, the angle of the strap, with respect to the seat cushion, should be between 0 and 30 deg upward as illustrated. The width of the guide at the top of the seat back should not be more than 3.0 in.



10016 South 51st Street,
Phoenix, AZ, USA 85044
Phone: 480.753.2000
Fax: 480.893.8643

This Document Provided by the Abbott Aerospace
Technical Library
abbottaerospace.com



General Aviation Crashworthiness Design Evaluation

Inertia Reel Type **Optimum = 4 points**
(For all seat types)

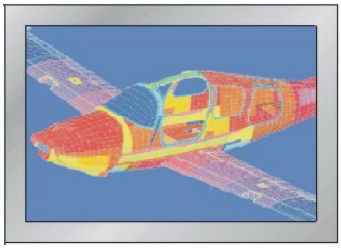
Inertia reels are convenience devices that allow the occupant more reach and comfort than fixed (manually adjusted) shoulder belts. Inertia reels, however, allow some belt movement during a crash. The inertia reel should be designed to minimize belt extension at the time of a crash. Full score would be given to rate-of -extension reels that lock between 0.5 and 1.5 G and vehicle-inertia-sensing reels that lock between 2.0 and 3.0 G. Seating positions without inertia reels receive full credit.

Extra Credit

Five extra points may be given for dual-mode inertia reels (rate-of-extension and vehicle-inertia-sensing).

10016 South 51st Street,
Phoenix, AZ, USA 85044
Phone: 480.753.2000
Fax: 480.893.8643

THIS DOCUMENT PROVIDED BY THE ABBOTT AEROSPACE
TECHNICAL LIBRARY
ABBOTTAEROSPACE.COM



General Aviation Crashworthiness Design Evaluation

4. INTERIOR CRASHWORTHINESS AND DELETHALIZATION

Crew Environment **Optimum = 25 points**

Evaluate the potential for injury to the front-seat occupants from secondary impact hazards and entrapment hazards for the feet.

a. Flail Envelope Evaluation - 15 points (15 of the 25 total)
- For a given restraint system and a 50th-percentile male, check the location of flight controls, instrument panel, and other structure (door frames, overhead consoles, windshield frames, etc.) relative to head and chest.
- Maximum points are given if no objects are within the occupant's flail envelope.
- Delethalization is handled in another section.
- Evaluate throughout the entire seat adjustment range.

b. Rudder/Brake Pedal and Footwell Evaluation - 10 points (10 of the 25 total)
- Evaluate the possibility of trapping the feet between the rudder/brake pedals and adjacent structure. Check if the area may collapse easily onto the feet during a crash. Rudder pedals should support both the ball of the foot and the heel. A simple bar-type pedal is unsatisfactory. Consideration should also be given to possible entrapment of the legs due to structural support collapse of the instrument panel.

Passenger Environment **Optimum = 15 points**

Evaluate the potential for injury to the passenger(s) from secondary impact hazards and entrapment hazards for the feet.

NOTE: For aircraft without a passenger-carrying capability, the rating for the Passenger Environment is deleted. The rating for Interior Crashworthiness and Delethalization is reduced to an optimum score of 45 points.

a. Flail Envelope Evaluation - 10 points (10 of the 15 total)
- For a given restraint system and a 50th-percentile male, check the location of seat backs, bulkheads, and other structure relative to head and chest.
- Maximum points are given if no objects are within the occupant's flail envelope.

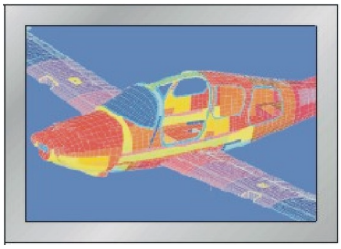
b. Footwell Evaluation - 5 points (5 of the 15 total)
- Similar to the crew environment evaluation, but is mainly concerned with the footspaces under other seats and the possibility of foot entrapment by collapse of the seat or due to seat energy-absorber motion.

Retention of Interior Equipment **Optimum = 10 points**

Check the tiedown design strength of equipment such as baggage, fire extinguishing bottles, tool boxes, etc., and evaluate it against an optimum of 26 G in the longitudinal direction, or higher if the aircraft is designed to withstand higher G values.

10016 South 51st Street,
Phoenix, AZ, USA 85044
Phone: 480.753.2000
Fax: 480.893.8643

THIS DOCUMENT PROVIDED BY THE ABBOTT AEROSPACE
TECHNICAL LIBRARY
ABBOTTAEROSPACE.COM



General Aviation Crashworthiness Design Evaluation

Delethalization **Optimum = 10 points**

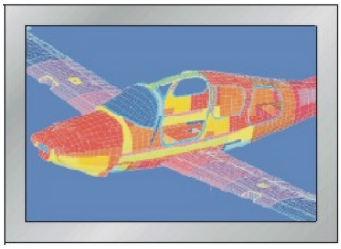
- All objects and surfaces inside the aircraft should be designed without sharp corners, edges, protrusions, etc.
- Objects and surfaces near the occupant(s) (flail envelope plus 6 in.) should receive special attention.
- Objects and surfaces inside the flail envelope should be delethalized by design - padding; energy absorption; broad, large-radius surfaces
- If airbags are used, they must be designed so no interference with the primary flight controls will occur when the airbag is deployed.

Bonus Points

- Add 10 points if the interior was designed and evaluated using the 95th-percentile male flail envelopes.
- Add 15 points if an airbag system is used for delethalization (not for airbelts or pre-tensioners - these are accounted for by reduced flail).

10016 South 51st Street,
Phoenix, AZ, USA 85044
Phone: 480.753.2000
Fax: 480.893.8643

THIS DOCUMENT PROVIDED BY THE ABBOTT AEROSPACE
TECHNICAL LIBRARY
ABBOTTAEROSPACE.COM



General Aviation Crashworthiness Design Evaluation

5. POST-CRASH FIRE POTENTIAL

SPILLAGE CONTROL

Fuel Storage Location and Containment **Optimum = 35 points**

Location (23 pct of the total value) - 8

The location of the fuel tank should be evaluated with respect to the anticipated impact area, the occupiable area, any large weight masses, and the primary ignition sources. Wing tanks forward of the main spar should be avoided due to the possibility of rupture upon tree or pole impacts.

Vulnerability Due to Structural Deformation (43 pct of the total value) - 15

The vulnerability of a fuel tank should be evaluated with respect to possible tank ruptures caused by various aircraft structural failures, such as landing gear failure and wing deflection or separation. Tank failures associated with structural displacement, such as ruptures around the filler neck, the fuel-line entry and exit area, the quantity indicators, and the tie-down devices should also be considered.

Construction Technique (34 pct of the total value) - 12

The construction technique is evaluated for two primary considerations. One consideration is tank geometry and the other is tank construction materials.

a. Fuel Tank Geometry - 4 (4 of the 12 total)

Smooth contoured shapes are given the highest number of points, whereas irregular shapes and interconnected multicell fuel tanks are given the lowest number of points.

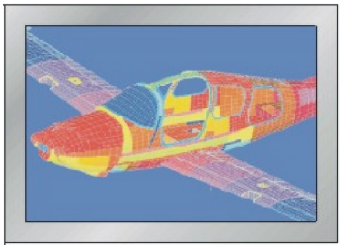
b. Fuel Tank Construction Material - 8 (8 of the 12 total)

The fuel tank is given a certain number of points, depending upon its construction.

Crash-Resistant Bladder	8
Elastomeric Bladder	6
Metal Container	3
Integral with structure ("wet wing")	0

10016 South 51st Street,
Phoenix, AZ, USA 85044
Phone: 480.753.2000
Fax: 480.893.8643

This Document Provided by the Abbott Aerospace
TECHNICAL LIBRARY
ABBOTTAEROSPACE.COM



General Aviation Crashworthiness Design Evaluation

Oil Containment **Optimum = 5 points**

The location of the oil tank should be evaluated from the standpoint of its proximity to the anticipated impact area, the occupiable area, any large weight masses, and the primary ignition sources. Evaluate it from the standpoint of rupture resistance.

An integral sump, especially if made from ductile materials, gives good rupture resistance in a vulnerable area. A separate oil tank should be evaluated for its likelihood of rupture during deformation in the engine area.

Flammable Fluid Lines **Optimum = 20 points**

Construction (35 pct of total value) - 7

The construction of fuel lines should be judged in accordance with the hose material and couplings. Experience has shown that rigid lines fail before the flexible type; thus, flexible lines with a steel braided outer sheath are given the most points. Also included in this phase of the evaluation are the couplings. The fewer the couplings the better. Ninety-degree couplings are less desirable than the straight type. Any coupling is less desirable than an uncut hose. Aluminum fittings usually fail before steel ones.

Routing (35 pct of total value) - 7

The routing of the fuel lines is an important consideration. The lines must not pass through areas where they can get trapped, cut, or pulled. Extra hose length (20-30 pct in areas of anticipated structural deformation) should be provided. Holes through which the fuel lines pass should be considerably larger than the O.D. of the hose.

Breakaway Fittings (30 pct of total value) - 6

Breakaway fittings should be installed on each fuel line that enters and exits the fuel tank. It is also advisable to have them installed at strategic locations throughout the system.

Firewall **Optimum = 20 points**

Evaluate the firewall from the standpoint of separating fire sources from occupied areas for sufficient time to permit egress. Consider the likely damage to the firewall during a crash.

Fuel Boost Pump Location and Type **Optimum = 10 points**

The fuel boost pump should be evaluated according to its potential for causing fuel spillage due to fuel cell rupture or fuel line failure. This includes its location and its method of attachment to the fuel cell.

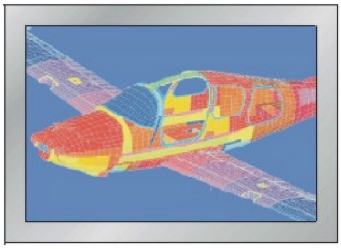
The fuel boost system should also be evaluated with respect to its function as an ignition source. The following items should be considered:

- Location and method of fuel cell attachment (if applicable)
- Power Supply - (An air-pressure system is best, a hydraulic system is next best, and an electrical system is least desirable).
- Pump Location - (A suction system with the pump located on the engine is best. A pump located outside the tank is next best, and an internally mounted pump in the tank is least desirable.)

Fuel-Flow Interrupters **Optimum = 5 points**

Fuel-flow interrupters are devices that block or divert the flow of spilled flammable fluids. There are many different methods to perform this function; including baffles, drain holes, drip fences and curtains. Ideally, these devices divert spilled flammable liquids away from ignition sources, likely sites of fire, and occupied areas.

THIS DOCUMENT PROVIDED BY THE ABBOTT AEROSPACE
TECHNICAL LIBRARY
ABBOTTAEROSPACE.COM



General Aviation Crashworthiness Design Evaluation

IGNITION CONTROL

Air Induction and Exhaust Location **Optimum = 15 points**

Evaluate from the standpoint of:

- Location of expelled exhaust in relation to the location of possible spilled flammable liquids
- Fuel Ingestion.

Note: Air induction and exhaust locations are most important in turbine engines where the turbine might still be operating after a crash. It is less important for piston-powered aircraft where the engine will likely stop during the crash.

Location of Hot Metals and Shielding **Optimum = 10 points**

Evaluate from the standpoint of how well the hot (temperatures above 400 °F) metal items are shielded or protected from fuel spillage. Components included are:

- Engine (external and internal)
- Exhaust System
- Heater.

Engine Location and Tiedown Strength **Optimum = 15 points**

Consider consequences of engine separation from the standpoint of post-crash fire hazards. Where will the engine go and how will it effect the fuel cell, exhaust system, electrical wiring, and fuel and oil lines? Will the engine come into contact with spilled flammable fluids?

Battery Location and Tiedown Strength **Optimum = 5 points**

Evaluate from the standpoint of tie-down strength and of the vulnerability of the battery and attached wiring to damage during a crash. The location should also be as far as possible from fuel and oil tanks and potential areas of flammable fluid spillage.

Electrical Wire Routing **Optimum = 5 points**

Evaluate from the standpoint of the crashworthiness of the wires' routing and its vulnerability to damage during a crash. Some excess length (20-30 pct) should be provided to allow for airframe deformation during a crash.

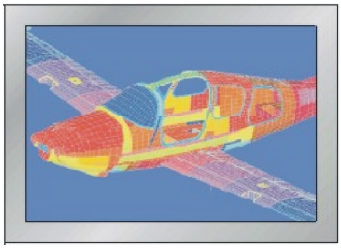
Locations of Lights (Beacon, Search and Navigation) **Optimum = 5 points**

Are the light filaments and/or the wires immediately surrounding the light attachments located in an area of possible flammable fluid spillage?

Locations of Antennas **Optimum = 5 points**

Evaluate the antenna systems and their respective wiring from the standpoint of vulnerability to damage and their location in areas of possible flammable fluid spillage.

10016 South 51st Street,
Phoenix, AZ, USA 85044
Phone: 480.753.2000
Fax: 480.893.8643



General Aviation Crashworthiness Design Evaluation

6. EVACUATION

Ease and Reliability of Exit Operation **Optimum = 20 points**

Evaluate the aircraft exits from a standpoint of simplicity of operation. Include the regular entrance doors. Look for a “single-motion” jettison feature on all doors and their capability of being opened from the outside. Check for one-handed operation and cross-handed operation. Check for the possibility of jamming during a crash due to fuselage distortion, etc. Evaluate the likelihood that secondary exits such as baggage doors could be accessible in a crash

Availability and Access to Exits **Optimum = 15 points**

There should be a minimum of two exits for aircraft with up to nine passengers. There should be 3 exits for aircraft with 10 – 19 passengers. Each occupant should have clear, unimpeded access to one exit and relatively easy access to a second exit. Consideration should be given to equipment, such as seat backs, that could impede egress. Also, consider the ability of an injured occupant to egress the aircraft.

Identification of Exits **Optimum = 5 points**

Emergency exits should be clearly marked and readily identifiable as such. The identifying letters should be a minimum of 0.75 in. high, and they must be lighted by the emergency lighting system. Operation instructions should be readily readable; should be a minimum of 0.33 in. in height; and their color should be offset, for example, red on white or vice versa. Do not give an optimum score unless a method is used whereby the passenger is instructed as to the exit he should use for his particular seating position. This may be accomplished by suitable markings on the wall or seat back ahead; this method is considered necessary to alleviate panic and confusion in case of any emergency.

Availability of Exits in Rolled and/or Deformed Aircraft **Optimum = 10 points**

Take into consideration that the aircraft has rolled on either side, possibly blocking a certain exit(s), or that structural deformation of the airframe has jammed or blocked a certain exit(s). The egress paths to the alternative exits should be readily accessible and operable by an occupant in a pitched, rolled, or inverted position.

GENERAL AVIATION AIRCRAFT CRASH SURVIVABILITY RATING

Date of Evaluation: _____

Aircraft Evaluated: _____

Location: _____

Evaluators: _____

_____

POINTS

Basic Airframe Crashworthiness _____

Crew Seats and Restraints _____

Passenger Seats and Restraints _____

Interior Crashworthiness _____

Post-Crash Fire Potential _____

Evacuation _____

TOTAL POINTS _____

10016 South 51st Street,
Phoenix, AZ, USA 85044
Phone: 480.753.2000
Fax: 480.893.8643

10016 South 51st Street,
Phoenix, AZ, USA 85044
Phone: 480.753.2000
Fax: 480.893.8643

This Document Provided by the Abbott Aerospace
Technical Library
abbottaerospace.com

Appendix C
Fuel System Design Checklist

As mentioned In Chapter 10, the prevention of post-crash fire can be achieved by eliminating the spillage of flammable fluids and by controlling hazardous ignition sources. The ideal crashworthy fuel system is one that completely contains its flammable fluid both during and after the accident and has components that resist rupture regardless of the degree of failure of the surrounding structure. The following fuel system design checklist, reprinted from Section 6.9 of Chapter 6 of Volume I of the U.S. Army Aircraft Crash Survival Design Guide, provides guidelines to aid aircraft designers in the design and evaluation of crashworthy fuel systems.

This Document Provided by the Abbott Aerospace
Technical Library
abbottaerospace.com

THIS DOCUMENT PROVIDED BY THE ABBOTT AEROSPACE
TECHNICAL LIBRARY
ABBOTTAEROSPACE.COM

FUEL SYSTEM DESIGN CHECKLIST

Fuel Tanks

1. Are the fuel tanks located as far as possible from anticipated impact areas, occupiable areas, large weight masses, and primary ignition sources?

2. Are the fuel tanks located as high up in the structure as possible?

3. Are the fuel tanks located where there is not danger of puncture by a collapsing landing gear?

4. Are the fuel tanks located so that transmissions, engines, and similar massive components will not crush the tanks during a crash?

5. Are the fuel tanks relatively safe from penetrative damage by structural stringers and stiffeners?

6. Can each fuel tank displace in the airframe structure without tearing or inducing leaks around the filler area, the fuel line entry and exit, the quantity indicator, and the tank-to-structure attachment points?

7. Do the fuel tanks have smooth, regular shapes, with the sump gradually contoured into the tank bottom?

8. Do all fuel tank concave corners have a minimum radius of 3 in., and all convex corners a minimum radius of 1 in.?

9. Do all fuel tanks meet or exceed the requirements of MIL-T-27422B?

10. Do all fuel tank fittings meet or exceed the tank pullout strength specified in MIL-T-27422B?

Fuel Lines

11. Are all fuel lines made from flexible hose with a steel-braided outer sheath?

12. Do all hose assemblies meet the strength requirements listed in Table 17, Section 6.2.3.1 of the Crash Survival Design Guide (last page of this checklist)?

13. Can all hoses elongate 20% without the hose assemblies spilling fuel?

14. Do fuel lines exit the fuel tank in one protected location?

15. Has the number of fuel lines in the engine compartment been kept to a minimum?

16. Are fuel lines routed along heavier structural members wherever possible?

17. Is as much of the fuel line as possible routed through the fuel tanks?

THIS DOCUMENT PROVIDED BY THE ABBOTT AEROSPACE
TECHNICAL LIBRARY
ABBOTTAEROSPACE.COM

18. Are fuel lines routed as far as possible from occupiable areas and electrical compartments?

19. Are fuel lines routed as far as possible from all electrical equipment and wires?

20. Are fuel lines routed away from areas where large structural damage is likely during a crash?

21. Are fuel lines routed away from the exhaust system and high-temperature heating ducts?

22. Are the fuel system lines designed with as few fittings as possible?

23. Are the fuel system lines designed so that uncut hoses are run through bulkheads rather than attached to the bulkheads with fittings?

24. Are self-sealing breakaway valves used wherever a fuel line goes through a firewall or bulkhead or is attached to the bulkhead?

25. Are lines entering and exiting in-line boost pumps made of flexible hose that is approximately 20% longer than necessary?

26. If fuel lines are not longer than necessary for in-line boost pumps, are self-sealing breakaway valves used in the lines near the boost pump?

27. Are self-sealing breakaway valves used at all points in the fuel lines where aircraft structural deformation could lead to line failure?

28. Are fuel line supports frangible to ensure release of the line from the structure during crash impact?

29. Will the frangible supports meet all operational and service loads of the aircraft?

30. Are all continuous lines running through bulkheads stabilized by frangible panels?

Frangible Attachments

31. Are frangible attachments used at all attachment points between the fuel tanks and aircraft structure?

32. Do the specified frangible tank attachment separation loads exceed all operational and service loads by a satisfactory margin?

33. Are the specified frangible attachment separation loads between 25% and 50% of the loads required to fail the attached system or components?

34. Will the frangible attachments separate whenever the required loads are applied in all possible modes likely to occur during crash impacts?

This Document Provided by the Abbott Aerospace
TECHNICAL LIBRARY
ABBOTTAEROSPACE.COM

Self-Sealing Breakaway Valves

35. Are breakaway valves installed in all fuel-tank-to-fuel-line connections, tank-to-tank interconnects, and at other points in the fuel system where aircraft structural deformation could lead to system failure?

36. Are the shapes of the breakaway valves remaining in the fuel tank basically smooth?

37. Are the breakaway valves recessed into the tank wall so that the tank half does not protrude outside the tank wall more than 0.5 in. after valve separation?

38. Do the specified breakaway valve separation loads exceed all operational and service loads of the aircraft?

39. Are the specified breakaway valve separation loads between 25% and 50% of the loads required to fail the attached components or lines?

40. Are the breakaway valves required to separate whenever the required loads are applied in the modes most likely to occur during crash impacts?

Fuel Drains

41. Are all fuel line drain valves stabilized where necessary with frangible attachments?

42. Are all structural attachments of fuel tank drains made with frangible attachments?

43. Are all fuel tank drains recessed into the tank so that no part of the drain protrudes outside the tank wall?

Filler Units

44. Are filler units attached to the aircraft structure with frangible attachments?

45. Are filler caps recessed into the fuel tank wall?

46. Are long filler necks avoided?

47. If filler necks are used, are they made from frangible materials and designed so that the filler cap stays with the tank after filler neck separation?

Boost Pumps

48. Can an engine-mounted, engine-driven boost pump be used in the aircraft?

49. If an engine-mounted suction system cannot be used, can an air-driven boost pump be used?

50. Do in-line boost pumps have a structural attachment capable of withstanding a 30-G load applied in any direction?

51. Are tank-mounted boost pumps fastened to the structure with frangible attachments?

This Document Provided by the Abbott Aerospace
TECHNICAL LIBRARY
ABBOTTAEROSPACE.COM

Fuel Filters and Strainers

52. Are fuel filters and strainers mounted outside the engine compartment wherever possible?

53. Do all strainers and filters have a structural attachment capable of withstanding a 30-G load applied in any direction?

54. Do all strainers and filters retain as small a quantity of fuel as possible?

Fuel Valves

55. Has the number of fuel valves been kept to the minimum required for operation?

56. Are self-sealing breakaway valves used at all valve-to-fuel-line connections where crash-induced line failure is likely?

57. Are all small in-line valves fastened to the structure with frangible attachments?

58. Do large valves have a structural attachment capable of withstanding 30-G loads in any direction?

59. Are fuel shut-off valves located outside the engine compartment, either on the outside face of the firewall or at the fuel tank outlets?

Fuel Quantity Indicators

60. Can float-type quantity indicators be used in this fuel system?

61. If probe-type indicators are used, are they fabricated from material that either is frangible or possesses as low a flexural rigidity as possible?

62. Is a slightly rounded shoe incorporated at the probe bottom end of all probe-type indicators, or is the probe mounted at an angle toward the rear of the aircraft?

63. Are frangible attachments used where it is necessary to stabilize the indicator by fastening it to the structure?

Vent Systems

64. Are high-strength fittings used between the metal insert in the tank and the vent line?

65. If vent outlets must be supported, are they supported by frangible attachments to the structure?

66. Is the vent line made of wire-covered flexible hose?

67. Is the vent line routed so that it cannot be snagged in displacing structure during a crash?

This Document Provided by the Abbott Aerospace
TECHNICAL LIBRARY
ABBOTTAEROSPACE.COM

68. Is a self-sealing breakaway valve used at the tank-to-line attachment if there is danger of the tank being torn free of the supporting structure?

69. Are vent lines routed inside the fuel tank in such a manner that spillage cannot continue after a rollover accident?

70. If an antispillage vent valve is used inside the tank in lieu of the above items, will the valve remain fully open during all normal flight conditions?

71. Will the vent valve close in the extreme attitudes that will occur during a rollover?

72. Will the vent valve possess adequate venting cap ability under critical icing conditions in flight?

73. If the fuel system is to be pressure refueled, is a bypass system provided in case of tank overpressurization?

74. Is any spillage due to tank overpressurization released away from aircraft occupants and ignition sources?

OIL AND HYDRAULIC SYSTEM DESIGN CHECKLIST

Oil Tanks and Hydraulic Reservoirs

1. Are the tanks and reservoirs located as far as possible from anticipated impact areas, occupiable areas, large weight masses, and primary ignition sources?

2. Are the tanks and reservoirs located as high up in the structure as possible?

3. Are the tanks and reservoirs located where there is no danger of puncture from a collapsing landing gear?

4. Are the tanks and reservoirs located where transmissions, engines, and similar massive components will not crush them during a crash?

5 Are the tanks and reservoirs relatively safe from penetrative damage by structural stringers and stiffeners?

6. Can the oil tanks displace in the airframe structure and still not leak around the filler area, the fluid line entry and exit, the quantity indicator, and the tank-to-structure attachment points?

7. Are the hydraulic reservoirs constructed and mounted to withstand 30-G forces applied in any direction?

Oil and Hydraulic Lines

8. Are all oil and hydraulic lines made from flexible hose with a steel-braided outer sheath wherever possible?

This Document Provided by the Abbott Aerospace
TECHNICAL LIBRARY
ABBOTTAEROSPACE.COM

9. Do all hose assemblies meet the strength requirements listed in Table 17, Section 6.2.3.1 of the Crash Survival Design Guide (last page of this checklist)?

10. Can all hoses elongate 20% without the hose assemblies spilling fluid?

11. Is coiled metal tubing used in areas where flexible hose cannot be used, but large structural deformations are expected?

12. Has the number of fluid lines in the engine compartment been held to a minimum?

13. Are fluid lines routed along heavier structural members wherever possible?

14. Are fluid lines routed as far as possible from occupiable areas and electrical compartments?

15. Are fluid lines routed as far as possible from all electrical equipment and wires?

16. Are fluid lines routed away from areas where large structural damage is likely during a crash?

17 Are fluid lines routed away from the exhaust system and high-temperature heating ducts?

18. Are the fluid system lines designed with as few fittings as possible?

19. Are the fluid system lines designed so that continuous hoses are run through bulkheads rather than attached to the bulkheads with fittings?

20. Are self-sealing breakaway valves used wherever a fluid line goes through a firewall or a bulkhead or is attached to the bulkhead?

21. Are self-sealing breakaway valves used at all points in the fluid lines where aircraft structural deformation could lead to line failure?

22. Are fluid line supports frangible to ensure release of the line during crash impact?

23. Are uncut lines running through bulkheads stabilized by frangible panels?

Oil and Hydraulic System Components

24. Are all oil and hydraulic system components located as far as possible from anticipated impact areas, occupiable areas, and electrical compartments?

25. Are the components located in the engine compartment restricted to those absolutely necessary for engine operation?

26. Can the construction and mounting of all system components withstand 30-G forces applied in any direction without leakage?

This Document Provided by the Abbott Aerospace
TECHNICAL LIBRARY
ABBOTTAEROSPACE.COM

Oil Coolers

27. Is the oil cooler located outside of the engine compartment?

28. Is the oil cooler located as far as possible from anticipated impact areas, occupiable areas, and other potentially injurious components?

29. Can the oil cooler and connecting lines experience considerable deformation without leaking?

30. Can the oil cooler mounting withstand 30-G forces applied in any direction?

IGNITION SOURCE CONTROL CHECKLIST

Electrical Systems

1. Are wires routed as high up in the structure as possible?

2. Are wires routed away from areas of anticipated structural damage, i.e., landing gear failure, nose crush-in, etc.?

3. Are wires routed above or away from flammable fluid lines?

4. Are all wires routed through the structure so that extensive structural collapse or displacement can take place without breaking wiring?

5. Are wire bundles supported at frequent intervals by frangible attachments to the aircraft structure?

6. Are wires shielded by felt or similar protective covers in areas where crushing is likely?

7. Are wires to electrically operated boost pumps 20% to 30% longer than necessary?

8. Is all electrical wiring going through the fuel tank compartments shrouded?

9. Is wiring in the fuel tank compartment routed as high as possible in the compartment?

10. Are electrical wires in the fuel tank compartment 20% to 30% longer than necessary?

11. Are batteries, generators, and inverters located in areas relatively free from structural collapse?

12. Are batteries, generators, and inverters located as far as possible from flammable fluids?

13. Are batteries and generators (unless engine-mounted) housed in compartments built into the airframe?

14. Are battery, inverter, and generator mountings capable of withstanding a 30-G force applied in any direction?

THIS DOCUMENT PROVIDED BY THE ABBOTT AEROSPACE
TECHNICAL LIBRARY
ABBOTTAEROSPACE.COM

15. Are the wires connecting the generator, battery, and inverter into the system located in relatively crush-free areas?

16. Are light bulbs and attaching wires on lower airframe surfaces designed to readily displace, rather than remain stationary and be broken?

17. Are all electrical compartments lined with a tough, non-conductive paneling?

Shielding

18. Are fuel tanks isolated from the occupants by a minimum of two spillage barriers?

19. Are firewalls designed to withstand all survivable crash impacts without losing their structural integrity or sealing ability?

20. Are drainage holes located in all flammable fluid tank compartments?

21. Is the hot metal of the engine shielded from flammable fluid spillages?

INTERIOR MATERIALS SELECTION CHECKLIST

1. Do all interior materials meet the flammability requirements specified in the current Federal Air Regulation?

2. Do all interior materials produce the lowest possible amount of smoke and toxic gases as specified in the current Federal Air Regulations?

This Document Provided by the Abbott Aerospace
Technical Library
abbottaerospace.com

Appendix D

Fire Hazard Level Rating System

This Appendix presents a hazard level rating system that can be used to determine what design considerations and hardware are needed to obtain a desired reduction in the fire hazard level of a given fuel system. This document has been reprinted with permission from Harry Robertson, President of Robertson Aviation in Tempe, Arizona.

This Document Provided by the Abbott Aerospace
Technical Library
abbottaerospace.com

This Document Provided by the Abbott Aerospace
TECHNICAL LIBRARY
ABBOTTAEROSPACE.COM

HAZARD LEVEL RATING SYSTEM

S. Harry Robertson, P.E.
And
James W. Turnbow, Ph.D.

SUMMARY

A complete crashworthy fuel system (CRFS) involves many design considerations as well as an abundant use of specialized hardware. By necessity, design trade-offs are involved in the evaluation of each fuel system design.

Presently, there is no single fuel system that is universally adaptable to all aircraft. Consequently, each fuel system designer is confronted the problem of deciding how much CRFS hardware should be incorporated into the fuel system design to achieve the desired safety level.

This paper discusses a rating method that a CRFS designer can use to help determine the amount of hardware and special design considerations needed to obtain a desired reduction in the fuel system "Fire Hazard Level." It uses, as its basis, man's tolerance to the thermal environment, and deals particularly with changes in the escape times available to the aircraft occupants.

INTRODUCTION

When an aircraft crashes, its occupants are exposed to many hazards that affect survival, one of which is fire. The fuel system is the major fire threat; however, cargo and other flammable fluids such as lubricating and hydraulic oils can also be a factor.

Now that truly crashworthy fuel systems exist in some U.S. military aircraft, and crashworthy hardware is available from many aerospace manufacturers, the fuel system designer is confronted with the problem of trying to determine how much fire safety can (or needs to) be obtained from any given fuel system design.

An evaluation technique has been developed which can allow a fuel system designer to rate a given fuel system design to determine the relative "Fire Hazard Level" for each component and/or hazardous area. Proposed crashworthy design changes can then be integrated into the original non-crashworthy design and the system can be re-evaluated to determine the "Fire Hazard Level" reductions.

For the evaluation to be performed, several assumptions must be made to establish a baseline or starting point. They are:

1. The only fire threat being evaluated is the one from the fuel system. (The cargo, oils, etc. are not included in this evaluation, although they, too, could be evaluated if they were included in the evaluation process to be discussed later.)
2. That the fire threat associated with the original, or non-crashworthy, fuel system design is the basis from which the fuel system improvements are to be measured. As an example, the overall fire threat associated with the original non-crashworthy fuel system is assumed to be 100%. Improvements in fuel system design are measured in percentage of reduction from the original 100% "Fire Hazard Level."
3. In order to evaluate the behavior of various fuel system designs, a crash environment that is typical of the serious, marginally survivable accident must be used as the basic reference point.
4. That the evaluator be familiar with accident reconstruction, fuel system behavior during crash situations, and that he have some formal accident investigation training such as that offered by Arizona State University's "Crash Survival Investigators School," a two-week concentrated course devoted exclusively to the study of human and system survival during the aircraft crash environment. (Editor's Note: The Crash Survival Investigator's School is currently owned and operated by Simula Technologies, Inc., which is located in Phoenix, Arizona.)

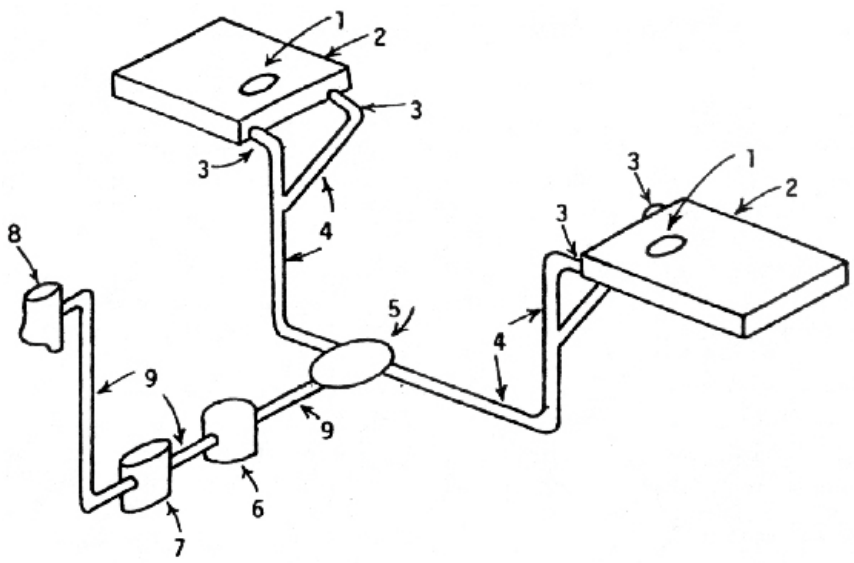
THIS DOCUMENT PROVIDED BY THE ABBOTT AEROSPACE
TECHNICAL LIBRARY
ABBOTTAEROSPACE.COM

DISCUSSION

The evaluation process is performed in the following manner:

1. The original non-crashworthy fuel system is defined, and the various components and/or hazardous areas are denoted, as shown in Figure 1.
2. Each identified component or hazardous area in the non-crashworthy fuel system is evaluated in accordance with the Rating System (defined later), to determine its relative "Fire Hazard Level."

NON-CRASHWORTHY FUEL SYSTEM



Item	Description	Item	Description
1	Fillers	6	Filter
2	Tanks	7	Pump
3	Outlets	8	Carburetor
4	Fuel Lines (Upper)	9	Fuel Lines (Lower)
5	Selector Valve		

Figure 1.
The non-crashworthy fuel system with the components and/or hazardous areas identified.

3. The non-crashworthy fuel system design is modified to incorporate various crashworthy hardware and/or design changes, and then re-evaluated in accordance with the Rating System to determine "Fire Hazard Level" reductions attributable to the improved design.

Note: The non-crashworthy fuel system can be upgraded by the addition of only one crashworthy item, or by the addition of many crashworthy items. Each upgraded system must be evaluated as a complete system to determine the "Fire Hazard Level" reduction attributable to separate design changes. The reason for the complete re-evaluation of each upgraded system is that the changing of one or more component and/or hazardous areas can, and usually does, influence the behavior of the remaining components and/or hazardous areas.

THIS DOCUMENT PROVIDED BY THE ABBOTT AEROSPACE
TECHNICAL LIBRARY
ABBOTTAEROSPACE.COM

RATING SYSTEMS (General)

The rating system evaluates the following four items:

1. The likelihood of fuel spillage occurring from the designated items (component and/or hazardous areas) during the serious, marginally survivable crash.
2. The likelihood of fuel spillage from the designated items catching fire.
3. The likelihood of an existing fire which started at a designated item functioning as an ignition source for other probable spillage in other designated areas. (The chain-reaction situation.)
4. The probable escape time available to occupants if a fire occurs at a designated Item.

RATING SYSTEM (Specific)

Failure of a Component to Cause Spillage

When rating the fuel system components and/or hazardous areas for the likelihood of fuel spillage during the serious, marginally survivable crashes, the following items should be included in the evaluation.

1. Vulnerability of the component and/or area during impact.
   (a) Location
   (b) Specific component or area design
2. Probability that a destructive impact will occur. Each designated area is rated in each specific system configuration. The rating is given in the form of a percentage of probable spillage occurrences. Example: If the designated Item will cause spillage during every serious crash, it is given a 100% rating, whereas if it will cause spillage in only one of our every four accidents it is given a rating of 25%.

Likelihood of Spillage Catching Fire

When rating the fuel system components and/or hazardous areas for the likelihood of fuel spillage catching fire, the following items should be included in the evaluation.

1. Availability of ignition sources.
   (a) Type
   (b) Available energy and duration
   (c) Location
2. Size of fuel spill.
3. Probable spillage paths.

Spillage occurring at each designated Item is rated in each specific system configuration. The rating is given in the form of percentages of probable ignition. Example: If the spillage will catch fire every time during the serious crash environment, it is given a 100% rating. If it will ignite in only one out of every four accidents it is given a rating of 25%.

Fire Starting Other Fires

When rating the fuel system components and/or hazardous areas for the likelihood of an existing fire serving as an ignition source for other spillage, the following items should be included in the evaluation.

1. Location of fire.
2. Size of fire.
3. Location of other ignitable material.
4. Possible spillage paths.
5. Possible flame spread paths.

THIS DOCUMENT PROVIDED BY THE ABBOTT AEROSPACE
TECHNICAL LIBRARY
ABBOTTAEROSPACE.COM

Each fire is rated in each specific system configuration. The rating is given in the form of points. If an existing fire is 90% to 100% likely to ignite surrounding spillage, a rating of 10 is given. If the likelihood of an ignition chain reaction is 80% to 90%, a rating of 9 is given. The point rating decreases at the rate of 1 point for each 10% decrease in likelihood of occurrence, as shown below.

RATING POINTS	LIKELIHOOD OF CHAIN-REACTION OCCURRENCE
10	90% - 100%
9	80% - 90%
8	70% - 80%
7	60% - 70%
6	50% - 60%
5	40% - 50%
4	30% - 40%
3	20% - 30%
2	10% - 20%
1	0% - 10%

Estimated Escape Time

When rating the fuel system components and/or hazardous areas for the probable escape time available to occupants if a fire occurs, the following Items should be included in the evaluation.

1. Location of initial fire relative to the occupants.
2. Growth potential of the fire.
   (a) Initial spillage quantity
   (b) Sustained spillage quantity
3. Egress considerations.
   (a) Location of occupants relative to escape routes
   (b) Complexity of the escape (doors, hatches, handles, cargo and other potentially delaying problems).

For a discussion of why 180 seconds is chosen as the maximum time duration, see Appendix 1.

HAZARD UNITS

"Hazard Units" are arbitrary numbers derived by the following formula:

$$(FCS \times LSCF) \times (FSOF + EET)$$

FCS = Rating in percent for each Item when evaluated for the likelihood of "Failure of a Component to Cause Spillage"
LSCF= Rating in percent for each Item when evaluated for the "Likelihood of Spillage Catching Fire"
FSOF= Rating in points for each fire when evaluated for the likelihood of "Fire Starting Other Fires"
EET = Rating in points for each fire when evaluated for "Estimated Escape Time" for occupants

FIRE HAZARD LEVEL

The "Fire Hazard Level" is 100% for the complete, non-crashworthy fuel system design. For a specific component and/or designated area, it is derived by the following formula:

$$FHA = \frac{\text{Component and/or area "Hazard Units"}}{\text{Total System "Hazard Units"}} \times 100$$

THIS DOCUMENT PROVIDED BY THE ABBOTT AEROSPACE
TECHNICAL LIBRARY
ABBOTTAEROSPACE.COM

SAMPLE PROBLEM

To assist the reader in understanding how the rating system works, assume that the fuel system depicted in Figure 1 was evaluated in accordance with the procedures defined under "Rating System" and that the totals derived are shown in Table 1.

Table 1.
Tabulation of points obtained from rating the typical fuel system shown in Figure 1.

Basic, Unmodified Fuel System							
Item	**Description**	**% FCS**	**% LSCF**	**Points FSOF**	**Points EET**	**Hazard Units**	**Fire Hazard Level**
1	Fillers	.50	.50	8	8	4.00	5.45
2	Tanks	.50	.80	10	10	8.00	10.90
3	Outlets	.90	.90	10	10	16.20	22.07
4	Fuel Lines (Upper)	.50	.90	10	10	9.00	12.26
5	Valve	.80	.30	8	8	3.84	5.23
6	Filter	.80	.75	10	7	10.20	13.90
7	Pump	.75	.75	10	7	9.56	13.02
8	Carburetor	.20	.75	10	6	2.40	3.27
9	Fuel Lines (Lower)	.80	.75	10	7	10.20	13.90
					TOTALS	73.4	100.00

It can be noted from the table that the non-crashworthy fuel system has a total "Fire Hazard Level" of 100%. Further, it can easily be seen that Item 3, the tank outlet area, is the largest contributor to the fuel system fire problem. Obviously, Items 2, 4, 6, 7, and 9 are also major contributors, whereas Items 1, 5, and 8 are of a much lesser hazard.

If, for example, Item 3 was modified so that it would greatly resist spilling fuel during a crash (like using crashworthy, high-strength fittings in the tanks; self-sealing breakaway valves at the coupling between the tank and the fuel line; and the fuel line was made flexible to accommodate fuel system displacement), the rating for Item 3 might be as follows:

Item	**Description**	**% FCS**	**% LSCF**	**Points FSOF**	**Points EET**	**Hazard Units**	**Fire Hazard Level**
3	Outlets	.10	.10	2	1	0.03	0.04

If all other Item ratings remained the same, which may or may not be the actual case, depending upon the influence on them due to the design change, the new "Fire Hazard Level" would be 77.94 or a 22.06-percent reduction in the original, non-crashworthy fuel system "Fire Hazard Level" of 100%.

This can be shown as follows:

Item 3, Outlet (original component design) "Hazard Unit" 16.20
Item 3, Outlet (crashworthy design) "Hazard Unit" .03
Total Original System "Hazard Units" 73.4
Component "Fire Hazard Level" = .03/73.4 x 100 = .04

Total non-crashworthy system "Fire Hazard Level" = 100.00%
Total crashworthy system "Fire Hazard Level" = 77.94%
"Fire Hazard Level" Reduction 22.06%

This Document Provided by the Abbott Aerospace
TECHNICAL LIBRARY
ABBOTTAEROSPACE.COM

CONCLUSION

In any given crash, there are many hazards to man's survival. Fire is usually one of the major threats.

The rating system presented provides a way for fuel system designers to evaluate an original non-crashworthy fuel system in terms of "Fire Hazard Level," and then evaluate an improved fuel system, to determine its "Fire Hazard Level" reduction.

APPENDIX 1

The length of time required for evacuation from a crashed aircraft can differ for a variety of reasons. Examples include the ratio of occupants to usable exits; ease of exit operation; interference problems such as cargo, fire, etc.; degree of occupant injury; and, obviously, the availability of rescue personnel.

Studies (conducted by the authors) of aircraft crash fire growth rates and of evacuation times used by survivors in some 3,500 air crashes, have shown that most evacuations fall into one of two categories. Either the occupants are out of the aircraft within a few seconds, up to a minute or so, or they are in the aircraft for a much longer period of time – in some cases, hours or days.

The growth rates of typical post-crash fires are such that they usually start out small, grow in intensity for several minutes, and then start to subside. An occupant's ability to survive these fires is usually predicated on the clothing they are wearing, the air they are breathing, the temperature to which they are being exposed, and the duration of their exposure.

A summary of actual crash data, as well as experimental crash test data, indicates that 3 minutes (180 seconds) is about as long as one can expect to survive in a major crash fire. In fact, survival time will be much less in many crashes, due primarily to the close proximity of the fuel to the occupants.

For further study of the subject, the reader is referred to the scientific literature, much of which is summarized in the U.S. Army Crash Survival Design Guide, USAAVSCOM TR 89-D-22 (A through E). This document, co-authored by the authors of this article, is the basic handbook in the field, and is available from the U.S. National Technical Information Service.